MIXED STORM AND TIDAL FACIES SUCCESSIONS OF MIXED GRAIN SIZE, SHALLOW MARINE SEDIMENT IN FORELAND BASIN UNITS: THE ALBIAN, VIKING FORMATION TOWNSHIPS 45 TO 54, RANGES 10W4 TO 21W4, ALBERTA, CANADA

By

JEREMY J. BARTLETT, M.Sc.

A Thesis

Submitted to the School of Graduate Studies

in Partial Fulfillment of the Requirements

for the Degree

Doctor of Philosophy

McMaster University

1994

DOCTOR OF PHILOSOPHY (1994) McMASTER UNIVERSITY

(Geology) Hamilton Ontario

TITLE: Mixed Storm and Tidal Facies Successions of Mixed Grain Size, Shallow Marine Sediment in Foreland Basin Units: the Albian, Viking Formation, Townships 45 to 54, Ranges 10W4 to 21W4, Alberta, Canada

AUTHOR: Jeremy John Bartlett, B.A. (The University of California, Berkeley)
M.Sc. (McMaster University)

SUPERVISOR: Professor R.G. Walker

NUMBER OF PAGES: 515

this thesis is dedicated
to the memories of

Ann Bartlett

and

John F. Prescott

"William James used to preach the "will to believe". For my part, I should wish to preach the will to doubt ... What is wanted is not the will to believe, but the wish to find out which is the exact opposite.."

B. Russell
Skeptical Essays

MIXED STORM AND TIDAL FACIES OF SHALLOW MARINE SEDIMENT

ABSTRACT

The siliciclastic, Lower Cretaceous, Albian, Viking Formation was deposited in the foreland basin of eastern central Alberta. Sediments in the area studied were formerly interpreted as "offshore bars" or lowstand shorefaces. It is shown in the first extensive, detailed core and well log study o the basinal portion of the formation that the sediments are sheet sand deposits laid down by a mixture of storm and tidal flows. The sediments divide into twenty facies ranging from grey shale to conglomerate but mostly consisting of bioturbated or crossbedded muddy sandstones and siltstones.

The facies assemble into six units: Mu, Epsilon, Delta, Gamma, Beta and Alpha, in stratigraphically ascending order. Unit boundaries are at points of rapid facies changes. There are no extensive discontinuities. Units Epsilon, Delta and Gamma are gradationally coarsening upward from basal bioturbated marine siltstones to heterolithic, sometimes glauconitic crossbedded or bioturbated marine sandstones. Unit Beta is consistently fine grained showing a slight coarsening upwards from bioturbated siltstones to crossbedded siltstones.

Datum to unit boundary isopachs and unit isopachs indicate post unit Mu, westward subsidence leading to accommodation of units Epsilon through Gamma. During deposition of units Alpha and Beta, subsidence returned to a more even basinwide pattern.

Unit isopachs of Epsilon, Delta and Gamma reveal prograding and aggrading "shoreface" wedges in the southwest of the study region. Details of the isopachs reflect fingers of irregular sand sheets. The facies of these sand sheets are interpreted to be finally deposited by storm enhanced flows in a tidally dominated

basin. Unit Beta provides evidence for a facies summary of a distal storm/wave dominated shallow shelf. In all cases, lateral facies changes appear random.

The units do not fit common sea level curve interpretations because the onset of transgression is located within the upper, coarser portion of the units rather than at the unit boundaries. Neither the units nor the formation can be correlated precisely to existing sea level curves. Combined with the evidence for tectonic control of unit geometries, this suggests periodic activity such as thrust loading of the cordillera west may control unit development in foreland basins.

ACKNOWLEDGMENTS

This thesis was financially supported by NSERC grants to my supervisor, Dr. R.G. Walker, whose comments and discussions are appreciated. Thanks are due to my parents. Thanks also to my friends for seeing me through life at McMaster. Jack Whorwood provided fine photographic productions. Len Zwicker created thin sections from some rather obnoxious `rocks'. Mark Birchard, Elizabeth Barr and Indraneel Raychaudhuri provided "field" assistance. Karen Downing and Floy Baird, at the former Texaco Canada, were immensely helpful as contacts supplying initial base maps, core and well log listings. Thanks also to Dave James formerly of Esso Canada for occasional comments and help. Finally thanks to all of the staff at the ERCB core laboratory in Calgary for their help.

TABLE OF CONTENTS

LIST OF FIGURES

LIST OF TABLES

CHAPTER 1

INTRODUCTION

In my beginning is my end ...

In my end is my beginning.

T.S. Eliot Four Quartets

1.1 SUMMARY

This thesis investigates the question: what processes distributed coarse sediment in gradationally based units offshore of lowstand "shorefaces"? The answer is pursued by interpreting facies assembled in stratigraphic packages referred to below as units. The study uses data from the Albian, Viking Formation in eastern central Alberta. Since the facies are grouped into related packages (units) prior to facies analysis, how they are packaged and the kinds of unit geometries and boundaries that develop in shallow marine foreland basin settings are investigated in order to provide a firm basis for the facies analysis. The facies analysis is the second step in the research. Building upon the unit analysis, the facies analysis provides information on the distributive mechanisms of gradationally based, coarse, crossbedded sediment in shallow marine settings.

1.2 INTRODUCTION

This research centers on the interpretation of marine sediments in which coarse to very coarse sand-bearing facies gradationally overly fine, very fine, silty, and muddy sediments and are apparently laterally separated by mudstones. In the literature, such deposits have been interpreted as lowstand shorefaces when the coarser sediments are undrlain by scarp shaped erosional surfaces (e.g., Plint (1988) and Plint et al. (1987)). When erosion surfaces are lacking and a linear pattern to the sediment accumulationis prsent and offshore bar interpretation has been assigned (Amajor, 1980). In contrast, Posamentier et al. (1992) intepreted western portions of the study area as representing lowstand shoreface deposits. However, oil and gas fields in the area are linear in the west and more irregular in the east. This observation, combined with preliminiary examination of the sediments preserved in the area, suggests that such interpretations merit re-examination. This study tests the existing hypotheses that the deposits in the area represent lowstand shorefaces or offshore bars. Implicit in this testing is consideration of processes alleged to have distributed medium and coarse sand across the shelf allowing the development of the gradational successions.

This thesis presents an investigation of this matter based on sedimentary facies observed in core and integrated with well log correlation and petrographic analysis. The facies study has been carried out in a sequence stratigraphic context. In order to better place the facies into a genetic framework, the study also considers the nature of marine sequences in foreland basin settings.

1.3 THE NATURE OF SMALL SCALE UNITS IN FORELAND BASINS

Before facies analysis can begin, sediments should be packaged into groups containing genetically related material. This essentially means grouping into packages without extensive internal unconformities. Such analysis of sedimentary successions has long been carried out although it is now more common and has come under the label of sequence stratigraphy, particularly as propounded by the Exxon school (e.g., Vail et al., 1977; Posamentier et al., 1989; Haq et al., 1988; Van Wagoner et al., 1990). Walker (1990) discusses the variety

of sequence divisions now available and some of their implications for facies modeling. In practice, the Exxon terminology dominates much of the discussion of sedimentary sequences, and it is increasingly being applied to the thinner units observed on the scale of outcrops. But, in part, because the foundations of sequence stratigraphy lie primarily in seismic section analysis (Clayton, 1977), there remain questions about its application to sediments at the outcrop scale. Events that occupy relatively thin stretches of the sedimentary record at the core or outcrop scale would not be observable on the scale at which sequence stratigraphy was initially generated.

In the decade following the publication of AAPG Memoir 26 (Clayton, 1977), Exxon terminology developed to included internal subdivisions of sequences and their classification depending on the extent of sea level drop (e.g., Type 1 and Type 2, Posamentier et al., 1988; Van Wagoner et al., 1988) but remained seismically oriented. Only recently have the published nomenclature and syntheses reached the point at which outcrop scale material is being incorporated into the models (Van Wagoner et al., 1990). This has been done using the "parasequence" which is

"a relatively conformable succession of genetically related beds or bedsets bounded by marine-flooding surfaces or their correlative surfaces" (Van Wagoner et al., 1990).

"Most siliciclastic parasequences are progradational (Van Wagoner et al., 1990)."

The parasequence is inherently smaller than the unconformity bounded sequence. In practice, parasequences form the most commonly observed units at the outcrop or core scale. Although it is now used as the fundamental building block of

sequences, the parasequence has undergone the least scrutiny and refinement due to its more recent development. Unconformities are implicitly not part of the parasequence; they are discussed only with regard to Type I and II sequences. There has been no investigation of whether unconformities at the scale of the parasequence behave as described for the larger scale, Type I and II sequences. Furthermore, the parasequence is defined in terms of rapid marine flooding surfaces, a boundary that carries a significant genetic interpretation. In examining facies successions, it may be inappropriate to include all material below a boundary in the regressive phase of sedimentation as implied in the parasequence model. Since the parasequences are inherently shallow marine, it is important to consider how much of the material contained within them is actually transgressively deposited or reworked. Is the parasequence boundary the point of onset of marine flooding or may this point lie below the rapid facies change? What is the most useful point for placement of the boundary? The concern has been discussed in the case of Type I and II scale sequences by Galloway (1989a) and Posamentier et al. (1988) the former favoring major flooding surfaces and the latter the "lowstand" unconformities. In the case of gradational sequences, such as those investigated here, a further question may be asked, can the transgressive/regressive turning point be located reliably enough that sea level curves can be accurately constructed at the core/outcrop scale?

Since the 'sequence" divisions of the facies are the foundation for their genetic grouping it is incumbent to consider whether the manner in which sediments are grouped in the foreland basin units described below differs from that prevalent in the literature. Most of the sequence geometries described in such works as Posamentier et al. (1988) and Van Wagoner et al. (1990) are drawn

from passive margin settings. Similarly, the published modeling of sediment and sequence distribution (e.g., Kendall et al., 1988; Jervey, 1988; Lawrence et al., 1990; Cross, 1990) are based on passive margin subsidence styles. The knowledge of sequences in foreland basins is comparatively limited. Therefore, the question may be asked, do sequence geometries developed in foreland basins differ from those described from passive margin settings?

1.4 QUESTIONS ABOUT FACIES INTERPRETATIONS

The above issues concerning sequence boundaries preclude examination of the sediment contained within a given facies succession contained within a "sequence" or unit. The successions of concern here are gradational, siliciclastic, shallow marine ones. Questions about coarse gradational marine sequences have long occupied facies modelers, and such shallow marine sediments still present many matters for consideration. Historically, many such sediments have been interpreted as various ridge forms (see Tillman et al. (1985), Johnson and Baldwin (1986) and Walker (1984a) for summaries). The mechanisms of sediment dispersal are debated because of the lack of extensive observation of the modern, shallow sea floor and its associated currents. One school of thought, in conjunction with the rise of sequence stratigraphy and the attendant re-emphasis on sea level change, reinterprets some such "shelf sandbodies" as "incised shoreface" deposits (e.g., Plint et al., 1986, 1987; Bergman and Walker, 1986, 1988); Plint, 1988). Both schools of interpretation rely heavily on the paleotopography of the deposits with incised shorefaces being defined on the basis of sharp-based, asymmetrical, 'sigmoid' scour fills.

Many of the gradational successions of the type with which this study is concerned contain crossbedding in their sandy, upper portions, evidence of

relatively strong current activity. Regardless of whether the sediment accumulated in a shelf or shoreface setting, this leads to the question, what processes were responsible for forming the crossbedding? Was this sediment regressive or reworked transgressively? Paleotopography may reflect distribution or accumulation mechanisms allowing discrimination between the shoreface and shelf alternative but the question remains what processes distributed the sediment? To what extent can different mechanisms be inferred or eliminated based on current knowledge of shelf processes and assumed bedform preservation styles? North American workers have tended to assign crossbedded sediments to storm or nearshore activity; by contrast, European workers have been more open to interpreting such effects as tidal (for summaries see Tillman et al., 1985 and Walker, 1984a). To what extent can details of the crossbedding establish or estimate the degree of interaction or influence of storm versus tidal events?

In addition to the cross bedded facies, many of the gradational sequences of marine sediments contain early diagenetic material (i.e., glauconitic and phosphates). The combination of these minerals with crossbedding poses something of a contradiction given the standard interpretation that glauconitic sediments represent conditions of slow sedimentation. How does this fit with an apparently high energy water column implied by coarse grained crossbedding? This is especially problematical for the regressive parasequence interpretation of such successions .

Finally, in addition to interpretation and extraction of environmental information from the sediments there is the more general question of the extent to which the facies and or sandbodies are laterally continuous. Do different facies

assemblages show different patterns or tendencies towards horizontal regularity? Can this even be ascertained?

1.5 THE STUDY LOCATION

To best answer the above questions, a study site was selected based on the following conditions:

1. The sediments were to be marine deposits suspected to lie offshore of postulated shorelines. There were to be no likely incised shoreface deposits in the central study area, but, if possible, the sediments were to be correlatable to a shoreline.

2. The density of data had to be sufficient to reveal sedimentological forms of interest and was to be 'three dimensional' in nature (i.e. offer complete penetration through facies successions of interest) with sufficient areal coverage to give a view of potential sequence geometry.

3. Measured sections were to be relatable to a marker usable as a datum for correlating sections. Location of the marker was to be accurate within 5 feet. This implied the use of subsurface data because of the difficulty of finding such markers in outcrop.

4. Given a subsurface site, there had to be a large amount of core to allow investigation of areal and lateral variations in facies.

The Lower Cretaceous, Upper Albian, Viking Formation of central Alberta met these criteria. Figure 1-1 shows the area of study as defined by oil and gas fields hosted by Upper Albian rocks; most of the fields are in Viking Formation reservoirs; the fields involved in this study are outlined. Figure 1-2 shows the exact study area which covers Townships 45 to 54, Ranges 10W4 to 21W4. This site was placed as close to the general center of the basin as possible

Figure 1-1. Lower Cretaceous Oil and Gas Fields of The Alberta Basin.

The figure is taken from Downing and Walker (1988) after Wallace-Dudley (1981). Most of the fields are Viking Formation reservoirs but not all. The approximate eastern extent of thrust faulting is shown in the southwest. The study area shown in more detail in figure 1-2 is outlined by the box.

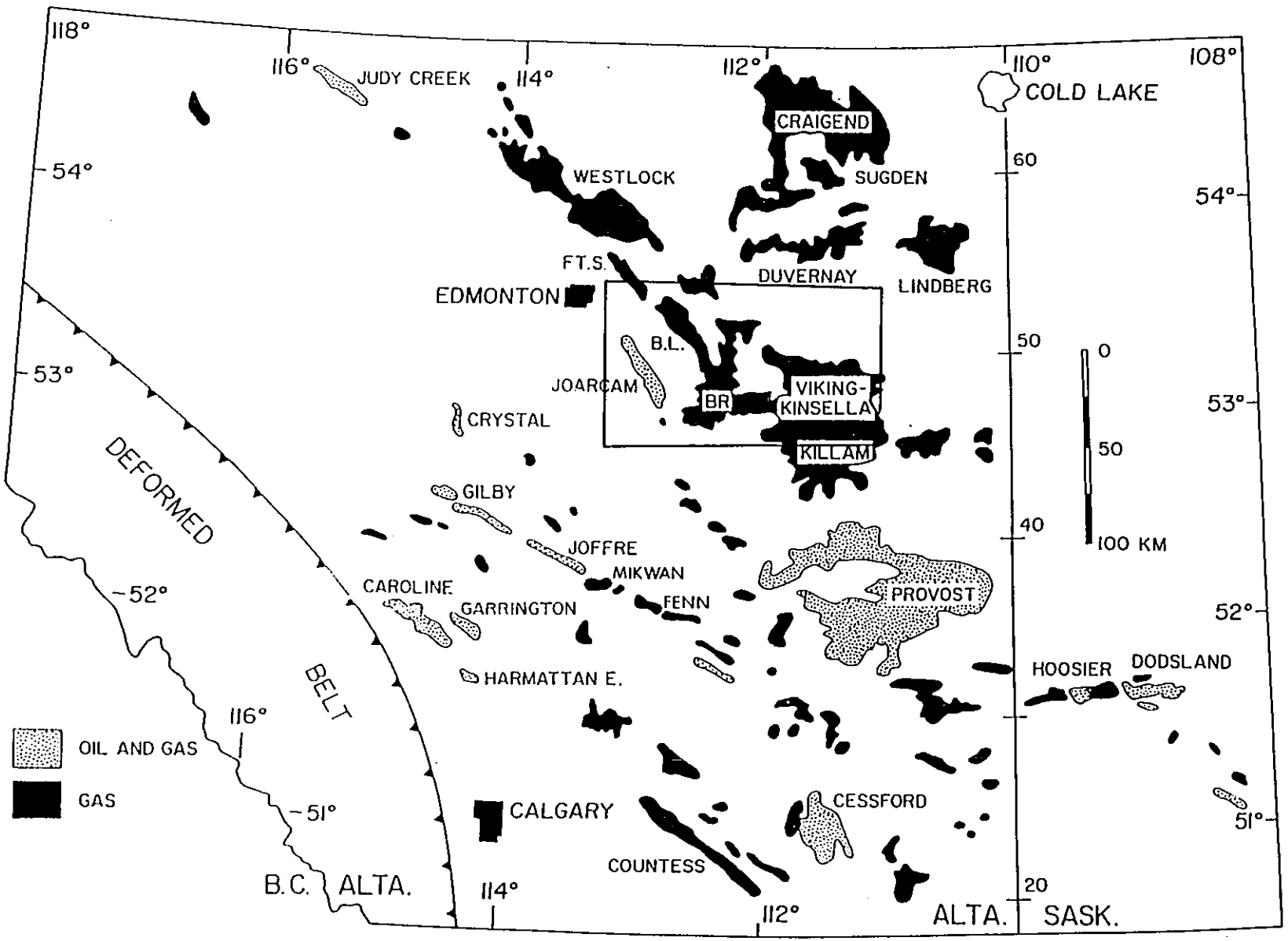
118°
116°
114°
112°
110°
108°
54°
53°
52°
51°
60
50
40
20
0
50
100 KM
JUDY CREEK
COLD LAKE
CRAIGEND
WESTLOCK
SUGDEN
FT.S.
EDMONTON
DUVERNAY
LINDBERG
B.L.
JOARCAM
BR
VIKING-
KINSELLA
CRYSTAL
KILLAM
GILBY
JOFFRE
MIKWAN
CAROLINE
GARRINGTON
FENN
PROVOST
HARMATTAN E.
HOOSIER
DODSLAND
DEFORMED
BELT
OIL AND GAS
GAS
CALGARY
CESSFORD
COUNTESS
B.C.
ALTA.
ALTA.
SASK.

Figure 1-2. Study Area and Data.

The study area discussed in this thesis is shown along with all the data locations. The townships are six mile squares. The small dots represent all examined well logs; the large dots represent cores examined. The large accumulation of points in the southwest is Joarcam Field.

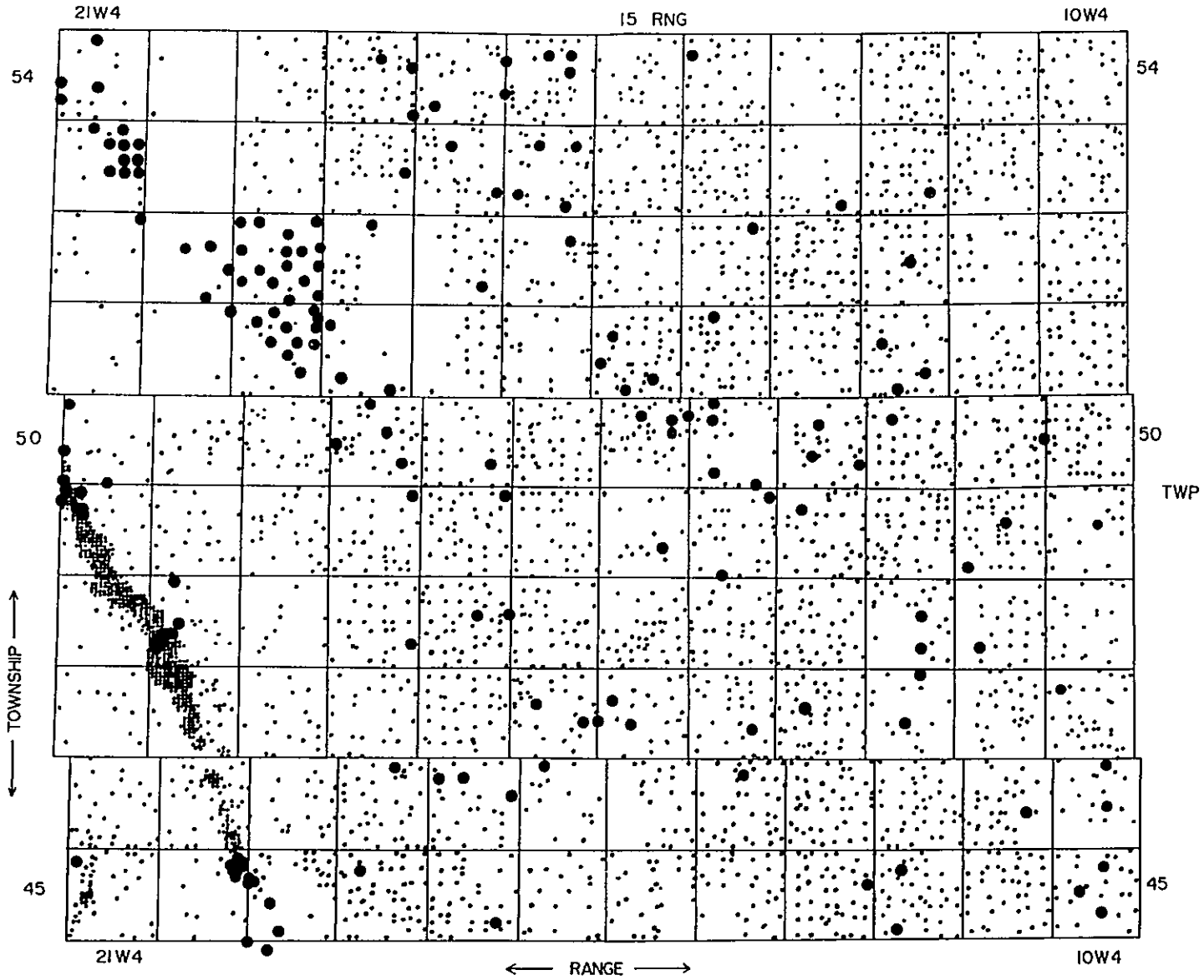
21W4
15 RNG
10W4
54
54
50
50
TWP
TOWNSHIP
45
45
21W4
RANGE
10W4

while maintaining a significant amount of core and log data. It lies away from postulated shorelines. Specifically, the site met the guiding criteria as follows:

1. As summarized in Chapter 2, previous work defined the site as suitably located in marine sediment offshore of possible shorelines.

2. Profuse drilling for oil and gas in the area, both at Viking Formation and deeper targets created a dense, `three dimensional', collection of core and well logs. The density of well logs is 1 to 2 points per square mile. This density is generally better than modern "ridge" sampling densities which vary between 0.3 to 7 datapoints per square mile (estimated from Swift et al. (1977) and Swift and Field (1981) for first and second order ridges, respectively). As visible in figure 1-2, compared to the well log density, the core density is more variable and generally less dense than sampling of modern "shelf ridges" off the Atlantic coast of the U.S. Nevertheless, interpretive capacities for the modern and ancient should be similar.

3. There are markers available in under- and overlying shales which serve as a datum for the correlated sections. Figure 1-3 shows an example of the Spontaneous Potential (SP) and Resistivity logs commonly run through the formation. (Few well logs of other types, such as gamma, are consistently available through the formation as much of the area was drilled before their development; consequently, correlations rely on SP and resistivity logs. The depths are given in feet which is true for all measurements in this thesis because most of the drilling in the area predates conversion to metric and the data is presented mostly in its original form. Metric equivalents are given in those instances where cores are now located in metres.)

4. Core is available over a wide area; cores range in diametre from rare 4" to common 3" with rare 2" and occasional 1".

As an added advantage, the region to be studied lies beyond the general limit of thrust related deformation in the Canadian Rockies. It is generally taken to be structurally undisturbed. This can be seen in figure 1-1 where the approximate limit of the thrust belt has been shown. However, despite its relatively undisturbed state, the area is not structurally planar. It preserves the form of the foreland basin developed in response to the latest phase of western orogeny. Figure 1-4 shows the current sub- sea level structure in topographic form which is matched in mesh diagram form in figure 1-5. The pattern is relatively smooth, but it is not completely simple. The changes in dip from steep in the west to shallow in the east probably exert some control on the distribution of fields and the field shape. This is worth noting because Beaumont (1984) inferred environment of deposition from map form of petroleum fields. The structural data alone strongly suggest that this must be avoided as local gradient is a powerful additional factor in fluid accumulation and migration. A simple comparison of figure 1-1 to either figure 1-4 or 1-5 shows, for example, that the broader, more irregular fields are located in the east where the lower structural gradient provides less concentrating pressure on the involved fluids. The "fluids" in these cases are also gas which may be related to the field pattern.

1.6 THESIS ORGANIZATION

The thesis presents investigation of the questions in sections 1.3 and 1.4 in the following manner. Chapter 2 presents a brief summary of previous work on the formation in a historical perspective with particular remarks on the relevance or absence of investigation of the questions

Figure 1-3. Typical Spontaneous Potential (SP) and Resistivity Well Logs.

The figure shows the SP and resistivity responses from well 10-11-53-18W4 from the center of the Beaverhill Lake fields. It contains most of the units discussed in the text and is typical of the Viking signature in the area.

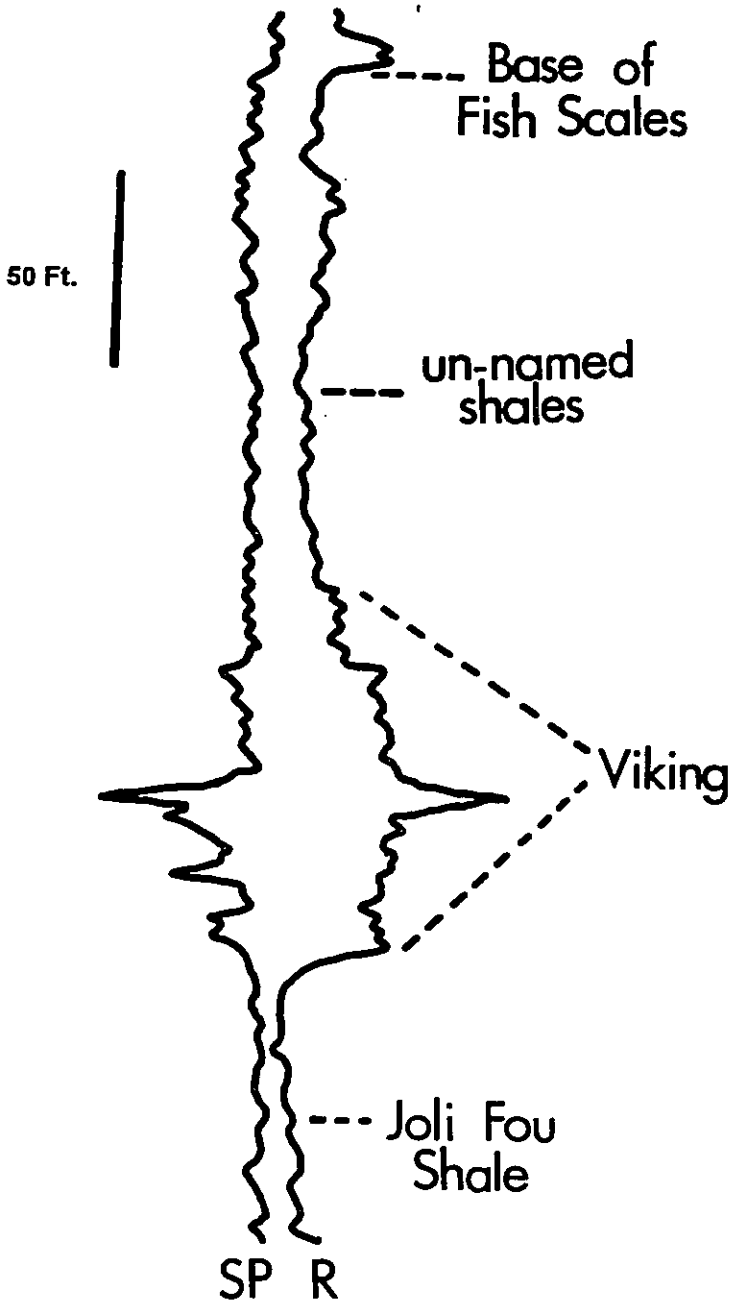
Base of
Fish Scales
50 Ft.
un-named
shales
Viking
Joli Fou
Shale
SP
R

Figure 1-4. Sub Sea-Level Structure Contour Map.

The contour map shows the current sub sea-level structure in the study area; it matches figure 1-1 for comparison and is based on the top of unit Alpha.

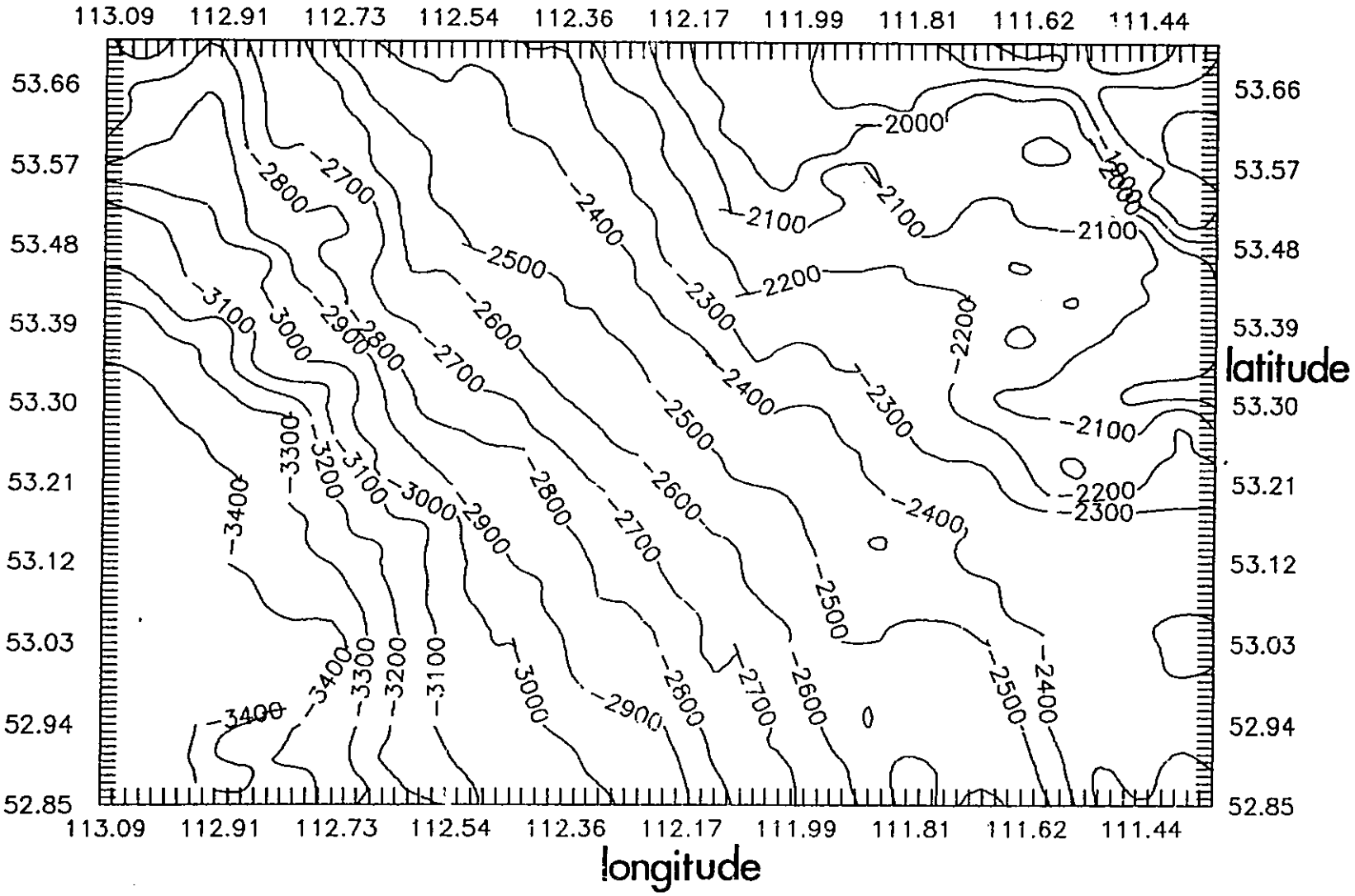
113.09
112.91
112.73
112.54
112.36
112.17
111.99
111.81
111.62
111.44
53.66
53.57
53.48
53.39
53.30
53.21
53.12
53.03
52.94
52.85
latitude
longitude
2000
2100
2200
2300
2400
2500
2600
2700
2800
2900
3000
3100
3200
3300
3400

Figure 1-5. Structural Mesh Diagram.

The mesh diagram presents the sub sea-level structure of figure 1-4 in more visible form. The view is from the southwest. The diagram is also based on the top of unit Alpha.

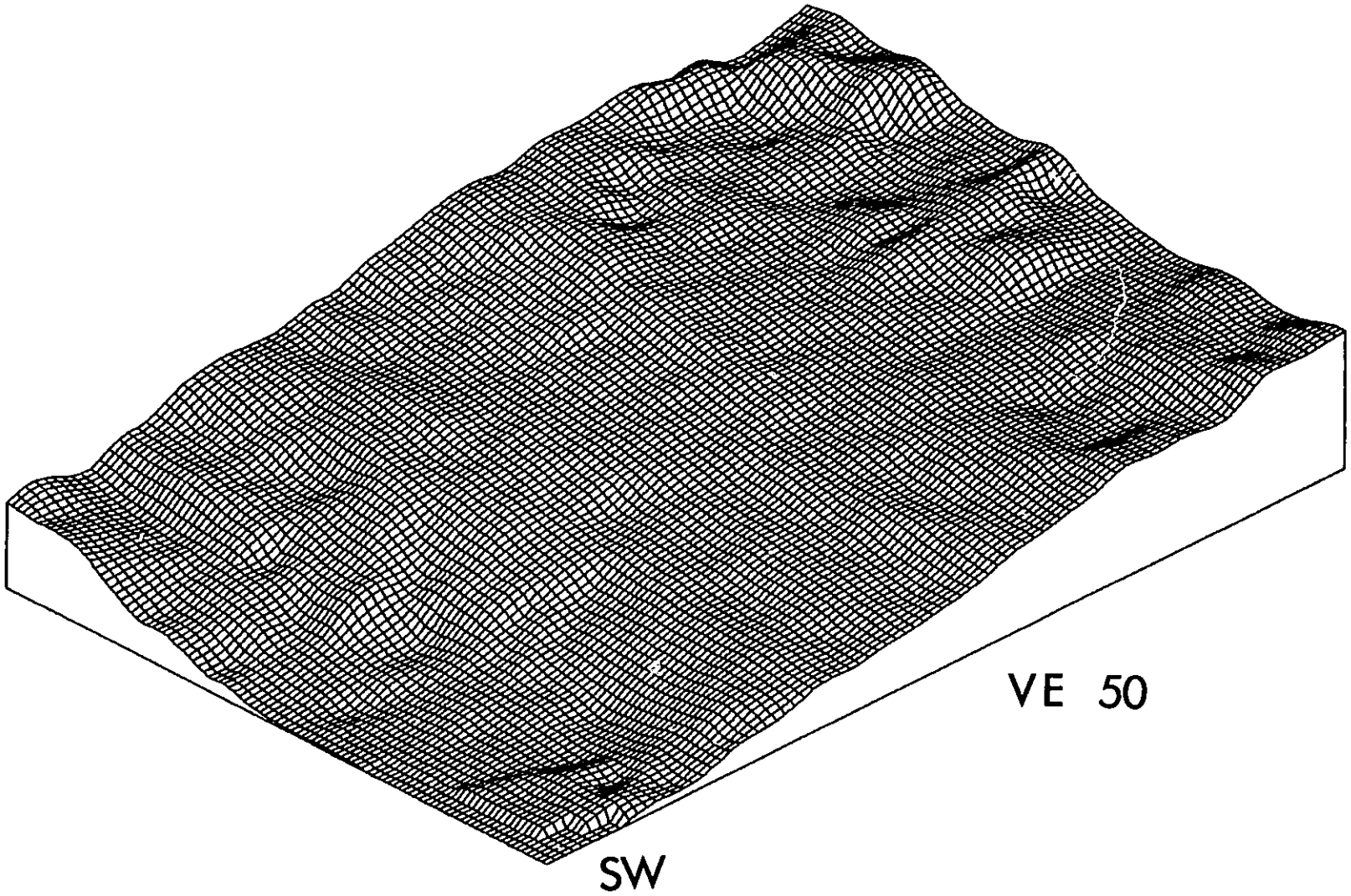
VE 50
SW

posed above. Chapter 3 presents the facies descriptions. Chapter 4 contains descriptions of the units correlated through the area; it includes the unit boundaries, the well log responses, and the facies compositions. It also has a summary of the petrographic investigation and bentonite geochemical analyses (NAA and XRF) that were carried out in an attempt to confirm or deny the core and well log correlations. The details of the petrographic investigation are described in Appendix B. Chapter 5 presents the three dimensional geometries of the units and includes a discussion of the implications of the geometries for the syn-depositional tectonics of the Viking Formation. Chapter 6 provides interpretations of the environments of deposition, facies by facies and unit by unit, in view of the sediment distribution discussed in chapters 4 and 5; it contains the facies summaries. A discussion and alternative interpretations of sea level histories related to the Viking unit can be found in chapter 7. Chapter 8 contains the conclusions of the study, and is followed by the appropriate references and appendices. Each chapter is headed by a brief summary of its contents.

CHAPTER 2

STRATIGRAPHIC SETTING AND PREVIOUS WORK

"It ain't necessarily so,
It ain't necessarily so,
De t'ings dat yo'li'ble
To read in de Bible,
It ain't necessarily so."

Ira Gershwin

2.1 SUMMARY

Biostratigraphically, the Viking Formation lies in the Upper Albian Stage of the Lower Cretaceous. In central Alberta, the Viking is a distinct unit correlated with the Paddy Formation to the northwest, the Pelican Formation to the northeast, the Bow Island Formation to the south and an unconformity over the Blairmore Formation to the west. It is underlain by shales of the Joli Fou Formation and overlain by an un-named package of shales.

The formation was deposited in the Western Interior Seaway in the western portion of the Alberta foreland basin. The precise paleogeography of the foreland basin is unknown although a reasonable palinspastic reconstruction (Bally et al., 1966) places the paleo-Rockies approximately 100 km to the west at the time of Viking deposition. The Viking Formation was laid down between what are generally described as the Columbian and Laramide orogenic episodes. These mountain building phases may have been related to major accretionary events on the west of the North American continent and/or changes in the angle and rate of subduction (e.g., van der Heyden, 1992).

Environmental interpretations generally describe most of the formation as marine but depending on the exact study area have ranged from estuarine through storm dominated shoreface and tidal ridges to turbidites. Historically, the environmental interpretations have moved from views based on simple sediment distribution to the consideration of gross facies characteristics and recently to discussion in terms of sequence development. Actualistic studies were applied to the Viking during the 1960's and 70's and now sequence stratigraphic studies have begun to appear. However, the basis for sequence divisions varies.

2.2 INTRODUCTION

There are two categories of previous work on the Viking Formation that are of prime interest: stratigraphic correlation and facies interpretation. Of the various approaches to stratigraphy, the biostratigraphic work is generally the earlier and has proven less contentious. The facies interpretations are more varied and complex. With the recent sequence stratigraphic studies, facies have begun to be integrated back into stratigraphy. However, the few sequences recently proposed have yet to be tied explicitly into the biostratigraphy.

2.3 LITHOSTRATIGRAPHY AND BIOSTRATIGRAPHY

2.3.1 Previous Work

Unlike the environmental interpretations, the gross stratigraphic correlations of the Viking Formation have been rather widely accepted, Early debate primarily concerned correlation of the Viking Formation to the northwest of Alberta. Because of the relatively inaccessible, subsurface occurrence of the formation, most biostratigraphic work has been micropaleontological, centered on foraminiferal zones in particular. Within the formation, a dearth of macrofaunal

remains restricts both biostratigraphic correlation and interpretation of environment of deposition. This absence of macrofauna may be due to the inherently limited amount of rock sampled by coring or a genuine lack of faunal remains caused by either initial absence or dissolution during burial.

Figure 2-1 shows a summary of the stratigraphic setting of the Viking drawn from the works of Glaister (1959), Oliver (1960) and Koke and Stelck (1985). Correlation of the formation throughout Alberta has been achieved using both litho-and biostratigraphy. I have not separated the two in this brief summary. The formation is Upper Albian in age, approximately 100 million years old (Tizzard and Lerbekmo (1975)) based on K/Ar dating of biotites and sanadine from bentonites. The ages ranged from 94 to 118 Ma. At this time the paleolatitude of the formation would have been roughly similar to it current latitude, lying at about 50° north of the equator (Parrish and Barron, 1986).

Most of the earliest work in the Viking was simply concerned with correlating the Formation as a whole across the Alberta basin. This began with the work of Slipper (1918) (in Stelck, 1958) following the discovery of natural gas in the formation near the town of Viking in eastern, central Alberta. Gammel (1955) summarized the general stratigraphic position of the formation in central Alberta; he considered the Viking to be a member of the Colourado Formation; the underlying Joli Fou shales had already been named and the overlying shales he merely described as the Upper Shale member. At this time, the Viking was correlated into the Bow Island Formation to the south, the Pelican Formation to the northeast and the Cadotte Formation to the northwest. The correlation into the Bow

Figure 2-1. Stratigraphic Setting of the Viking Formation.

The stratigraphic correlations shown here are drawn form Glaister (1959), Oliver (1960) and Koke and Stelck (1985). They represent an amalgamation of biostratigraphic and lithostratigraphic work.

The major undulatory lines represent accepted unconformities

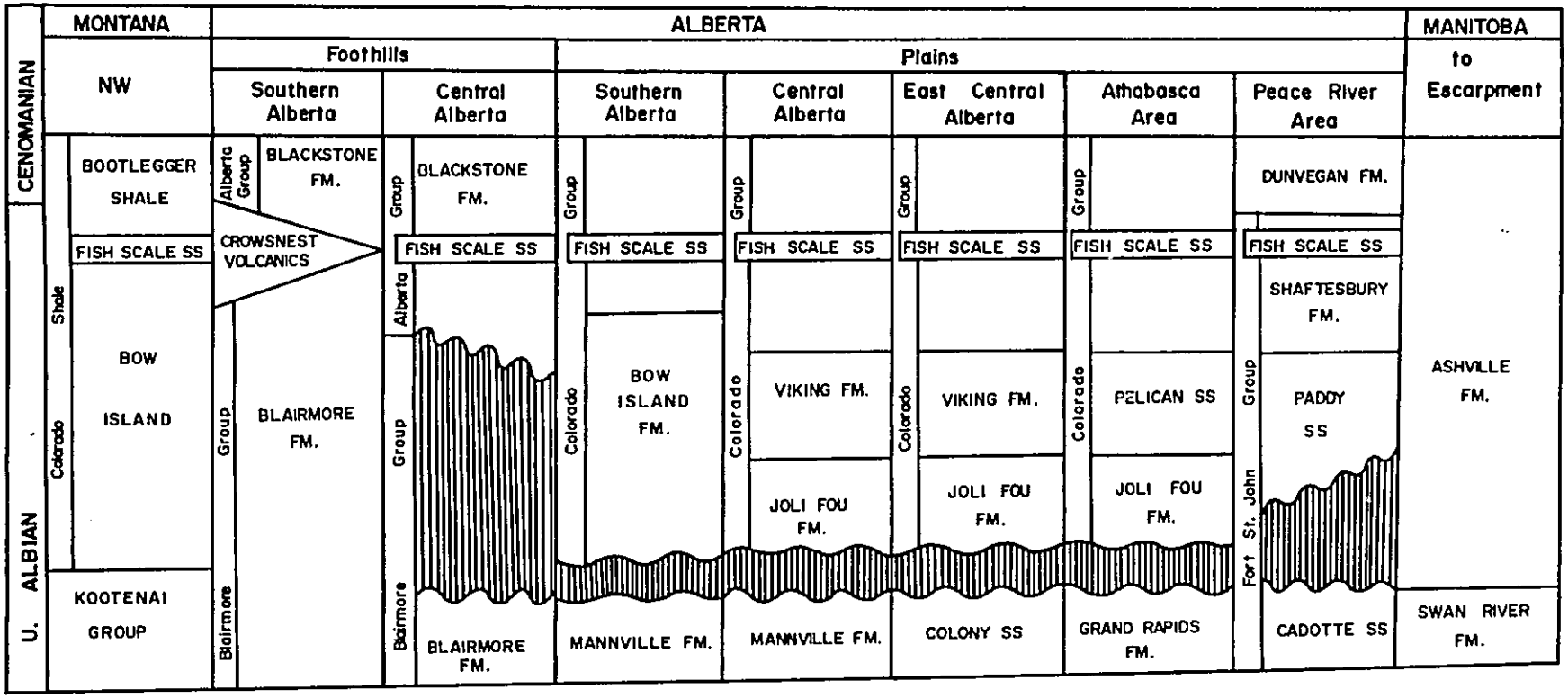

STRATIGRAPHY

after Glaister (1959)
Oliver (1960)
Koke & Stelck (1985)

Island is imprecise because the Bow Island is difficult to separate lithostratigraphically from the underlying formation, usually called the Mannville. The base of the Viking and the Joli Fou shales cannot be traced precisely southward into this gradational transition. The correlation into the Pelican to the northeast is essentially one which follows the shaling out of Viking Formation sands and muds into Pelican Formation silt.

Apart from a general "marine" interpretation, Gammel (1955) offered no opinion on environment of deposition. Stelck (1958) maintained most of Gammel's (1955) correlations, except that on biostratigraphic grounds, he correlated the Viking with the Paddy Sandstone rather than the Cadotte Sandstone to the northwest and raised it to formation status. He also added a correlation into an unconformity overlying the Blairmore Formation to the west and pointed out that the Joli Fou shales disappear to the west. Stelck (1958) placed the Viking in the Upper Albian, sandwiched between the *Miliammina manitobensis* foraminiferal zone in the overlying shales and the *Haplophragmoides gigas* foraminiferal zone in the Joli Fou. Details of the biostratigraphy, particularly the zonal species, are provided by Caldwell et al. (1978). Table 2-1 gives the molluscan and foraminiferal zone equivalencies of these authors.

The resolution of the biostratigraphic work is insufficient to clearly correlate unconformities reported from different locals as shown in Figure 2-1 or to allow basin wide correlation of sequences of the scale discussed in chapters bellow. For example, there is some question as to the behavior of the unconformity at the base of the Paddy "member" as reported by Leckie and Reinson (in press). These

authors would equate it with one at the base of the Joli Fou; however, it might be equivalent to the one described below in chapter 4 at the base of the Viking.

Following the biostratigraphic work of Stelck (1958), major regional lithological correlations were published by Glaister (1959) as part of a study of the entire Lower Cretaceous in both outcrop and subsurface. His correlations range from northern Montana to central Alberta. Well log picks generally used in the oil and gas industry are often marked on logs and closely follow his lithological criteria so it is worth noting in detail:

"*The top of the formation is placed at the top of a black chert-pebble stringer of chert-rich sandstone. The base of the formation is placed at the base of the sandstones or sandy shales.*" (Glaister, 1959)

Glaister did not subdivide the formation and made only limited environmental interpretations:

" *The Viking Formation consists of a marine succession of "salt and pepper" protoquartzites interbedded with gray siltstones and shales. In southern Alberta, the Viking and Joli Fou formations are not recognizable as two distinct units, and the entire succession is called the Bow Island formation which is correlated with parts of the upper Blairmore and Crowsnest formations in the Foothills area.* " (Glaister, 1959)

While maintaining Stelck's (1958) formational status for the Viking, Glaister (1959) included it as part of the Colourado Group making the formation roughly equivalent to the Ashville Formation in Manitoba.

The last contribution to the strictly lithological stratigraphy of the Viking was that of Oliver (1960) who correlated the Viking Formation to be roughly equivalent to the Paddy Formation to the northwest; his work

Table 2-1

Correlation of Selected Molluscan and Foraminiferal Zones (from Caldwell et al., 1978).

Molluscan Indices	Foraminiferal Subzones (Millammina manitobensis)
Neogastroplites muelleri *Neogastroplites cornutus*	*Haplophragmium swareni* *Haplophragmoides postis goodrichi*
Neogastroplites haasi	*Verneuilina canadensis*
Inoceramus comancheanus	*(Haplophragmoides gigas)*

Figure 2-2. Paleogeographic Setting of the Viking Formation.

This figure is taken from Koke and Stelck (1985) and shows the estimated extent of the Western Interior Seaway in the late Albian. The western boundary is more certain than the eastern.

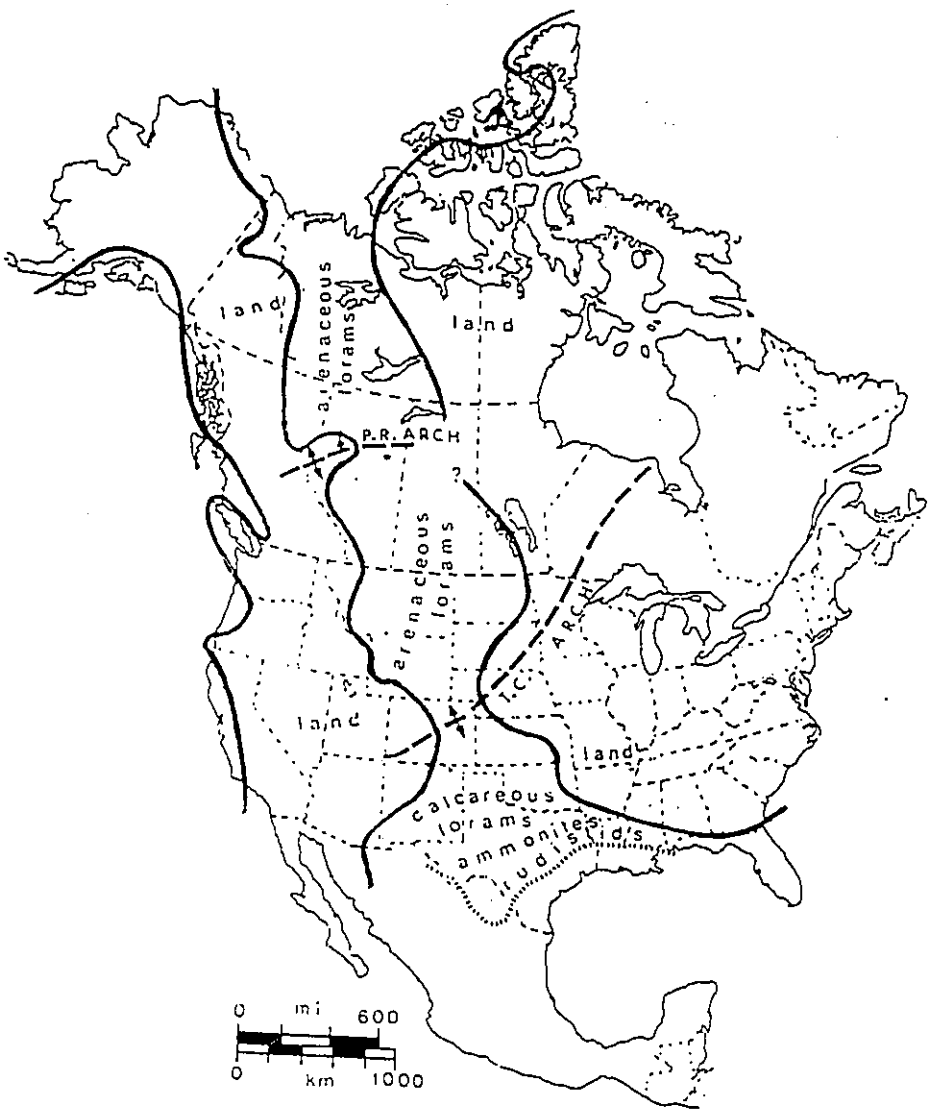
land
arenaceous forams
land
P.R. ARCH
arenaceous forams
T.C. ARCH
land
land
calcareous forams ammonites rudists
0 mi 600
0 km 1000

relied on log patterns and agrees with Stelck (1958) and Glaister (1959). Oliver (1960) placed an unconformity at the top of the Mannville Formation in the south which rose to the top of the Cadotte Formation to the northwest. Koke and Stelck (1985) and Stelck and Koke (1989), in their biostratigraphic work, have recently emphasized this unconformity at the base of the Joli Fou. The shales overlying this unconformity apparently mark the beginning of the formation of the Albian seaway connecting the Arctic and the Gulf (see figure 2-2)(Koke and Stelck (1985)).

2.3.2 Confirmation of Biostratigraphic Setting

Minor micropaleontological sampling of the basinal part of Viking was performed, in part to check the biostratigraphic location of the portion of the formation under study. The results suggests that the Viking Formation straddles the earlier subzones listed in Table 2-1. Five fifty-gram shale samples were taken from well 11-29-50-12W4 ranging from depths of 2010 to 2001 feet at equal intervals. The samples were crushed and disaggregated according to the procedure of Then and Dougherty (1983). Foraminifera recovered indicate that only the upper part of the formation, unit alpha (see chapter 4), contains foraminifera from the *Verneuilina canadensis* subzone (J. Wall, p. comm., 1988). The Viking may thus be considered to straddle the *Milammina manitobensis* and *Haplophragmoides gigas* zones, but probably lies mostly within the former.

2.4 TECTONIC SETTING

The Viking Formation is a foreland basin deposit (or alternatively a retroarc basin according to Dickenson's (1974) classification); this is widely recognized (e.g., Bally et al., 1966; Price, 1981, 1986). In general terms, the

Albian age Viking Formation was deposited between the major Columbian and Laramide tectonic events (e.g., Tankard, 1986). The foreland basin formed towards the end of the Jurassic when the western margin of the North American continent changed from a passive margin to a subduction margin. This led to "thin skinned" thrust deformation of the margin the extent of which was investigated in the classic work of Bally et al. (1966) using both seismic and borehole information. Bally et al. (1966) concluded that the basin underwent approximately 200 kilometres of shortening during two primary episodes of thrusting at the end of the Jurassic and the end of the Cretaceous periods. This conclusion is supported by Price (1981); however, Monger and Price (1979) have pointed out that the existence of varying angles of subduction of western plates, as summarized in greater detail by Riddihough (1982), means that there is some indeterminacy in the palinspastic reconstructions because of ensuing strike slip components in the faulting. More recently in conjunction with the development of accretionary tectonics, Brown et al. (1986) have interpreted up to 200 kilometres of shortening in the Late Jurassic alone due to the accretion of Terrane I of Monger et al (1982).

The reason for the intermittent occurrence of tectonic shortening has recently been attributed to the "docking" of exotic terranes from the western subducted plates with the edge of the North American Craton. Jones et al. (1978), Davis et al. (1978) and Coney et al. (1980) have described the western margin of the North American craton as being made up of a collage of terranes accreted beginning at times ranging from the Middle Triassic to Early Jurassic from central California to Alaska. The angle of subduction varied during this time but

while the Farallon Plate was being subducted in the Albian, at the time of Viking Formation deposition, was approximately orthogonal to the continental margin (Riddihough, 1982). The initial descriptions of the terranes present in western Canada (Monger, 1977) have been refined to the point where it appears that there were two major agglomerates of terranes that collided with the North American continent in the Mid-Jurassic and Late-Cretaceous respectively (Monger et al., 1977, 1982) corresponding to the major orogenic phases of the Columbian and Laramide orogenies. The accretionary terrane model of growth of the western margin of the continent has been questioned, however, by van der Heyden (1992) who discusses evidence for the theory that by the time of the Cretaceous the margin was a classic Andean type subduction zone. It should also be noted that Chamberlain and Lambert (1985) and Lambert and Chamberlain (1988) have argued that there were, in effect, no such terrane accretions in the immediate proximity of what is now the western part of Canada but that the terranes were emplaced far to the south and moved laterally into their current locations by strike slip faulting. There is little evidence for the transcurrent faulting required for this motion, however, and the notion is not commonly accepted. Regardless of the merits of the differing tectonic explanations, the Viking can be viewed as being deposited during a relatively orogenically quiescent period. However, there is possible minor tectonic activity during the Albian and might have influenced Viking deposition (see Chapter 5). For example, Monger and Price (1979) describe thrusts in eastern central British Columbia whose activity possibly dates to the early Cretaceous (minimum ages of 108 and 120 Ma). These thrusts may be signs of tectonic activity during Viking deposition or slightly predating it.

Van der Heyden (1992) also discusses tectonic activity in the mid Cretaceous roughly contemporaneous with the Viking.

Following compressional deformation there was a phase of extensional faulting in the Rockies:

> "*Late Mesozoic and early Tertiary thrusting was followed by late Tertiary normal faulting. Reflection data suggest that these normal faults, which are steep at the surface, also flatten at depth (listric normal faults) and may merge with older thrust faults.*" (Bally et al., 1966)

The throw on the Flathead Fault, interpreted as such a fault, west of the Lewis thrust, may reach 10,000 feet (Bally et al., 1966). Bally et al. (1966) interpret these normal faults as the product of intramontane basin formation occurring simultaneously with regional uplift that occurred in the Tertiary and describe them as being limited to the thrust belt in the Main Ranges. Investigation of these extensional features has not been thoroughly pursued by other researchers.

Because the shortening of the western margin of North America moved successively from west to east and was limited to the line of the modern foothills, the "Interior Plains" of the modern 'basin', where the Viking Formation exists, was relatively undisturbed (Bally et al., 1966). Deformation essentially stops where reverse thrusting is encountered at the triangle zone at the east of the foothills (e.g., Price, 1986).

2.5 INTERNAL STRATIGRAPHY

More debatable than the large scale geology described above is the internal stratigraphy of the formation. There has been little published in this field; the work that has been published has usually been a minor part of

environmental interpretations. Relatively recent work (Boreen and Walker, 1991, Pattison, 1992; Downing and Walker, 1988) has begun to place the various facies successions of the Viking Formation into an overall sequence stratigraphy. However, the correlation of the "sequences" defined in these studies into the eastern portion of the basin is still unclear. There is no evidence (see below) for the continuation of the erosional surfaces VE1 through VE4 of Boreen and Walker (1991) into the eastern portion of the basin. An Exxon style sequence stratigraphy has been proposed by Posamentier et al. (1992) for the basinal portion of the Viking Formation in the area covered by this thesis. Their proposed stratigraphy is based primarily upon well log correlations (discussed in more detail below) and postulates a series of regressive sequences containing lowstand shorefaces that are assembled into an overall regressive then transgressive package whose transition lies roughly in the center of the formation.

There is little hope of using previous lithostratigraphic work to add to postulated sequence stratigraphies. Glaister's (1959) first chert stringer, for example, would probably lie at different sequence levels depending on such factors as the extent of transgression of the formation and the degree to which the coarser material was available for final incorporation into the units. Furthermore, the fine grained nature of most of the basinal part of the Viking prevents the use of this lithostratigraphic definition.

2.6 PREVIOUS ENVIRONMENTAL INTERPRETATIONS

Because of its greater age as a field of study, there has been more speculation about the environments of deposition of the Viking sediments compared to development of their potential sequence stratigraphy.

The formation has almost as many environmental interpretations as workers who have published on it, and unfortunately few of the works discussed below build upon each other; they exist as independent and largely unrelated studies. It is thus impossible to discuss how the view of the formation has developed as a whole because there has been no such environmentally comprehensive research. Environmental interpretations vary to some degree because over the large area covered by the formation, there are b ound to be a variety of 'environments' preserved. Yet, in the area discussed in this thesis, there have been conflicting interpretations. Within the variety of interpretations, there is a component of the evolution and application of new ideas. Historically, interpretations move from those based mostly on sediment size distribution through the application of the turbidite model to a more generalized use of actualistic models in the 60's and 70's. The most recent studies have begun to incorporate the facies into sequence stratigraphy.

The published discussion of specific environments and processes of deposition began with the controversial assertion by Beach (1955) that all sandstones of the Viking were turbidites, a view contested by DeWeil (1956) who saw the formation as a "shallow water" deposit laid down on an almost flat basin floor preferably by "longshore currents in front of a shifting strandline ... never descending below the base of wave and current action ...". Beach, in a reply to DeWeil (1956) postulated possible tsunami distribution of the sediment, an idea he continued to cling to in later remarks (Beach, 1961). It is interesting to note that Beach's introduction of the turbidite interpretation only slightly post-dated the generation of the turbidite concept in the work of Kuenen and Migliorini

(1950). Beach's views were largely abandoned, however, and Glaister (1959) followed DeWeil (1956) adding, without explanation,

> *"fossil evidence indicates that the lower Colourado sea in southern Alberta was shallow, probably never more than 120 feet deep. As a result, slight fluctuations in sea-level shifted the strand line many miles."*

These early views of DeWiel and Glaister fit the central premise of sequence stratigraphy that sediment distribution largely reflects relative sea level. Such views continued with Jones' (1961) interpretation of most of the Viking Formation in southwestern Saskatchewan as a "nearshore" deposit. Jones (1961) described the formation as deposited "largely in a neritic and/or littoral environment" and included the possibility of "tidal flat" deposition based on the presence *linsen.* Given the general state of sedimentary knowledge of the time, this was a reasonable, although general, summary.

Since most of the early work on the Viking predates the development of modern facies analysis, there could be little consideration of the now traditional environmental indications given by sedimentary structures and trace fossils. Passing remarks such as those above on sedimentary structures were generally the only support offered for environmental interpretations at the time. Our current knowledge of facies now allows the dismissal of some early interpretations. For example, given our current understanding of sedimentary structures in turbidites (e.g., Walker, 1984) and reference to the facies described in chapter 3 and discussed in chapter 6 and onwards, we can confidently dismiss Beach's interpretations.

The early `nearshore' interpretations, although relying for the most part on very general criteria such as sediment distribution and presence of marine fossils,

are more reasonable. However, in light of current knowledge of sedimentary structures and shallow marine environments, they require refinement. Jones (1961) made the only reference to sedimentary structures, arguing that low angle stratification might be "foreshore stratification (as) ... described by Thompson (1937)". Given the juvenile state of actualistic environmental studies at the time, there was little more that could be expected.

As investigation of modern environments proceeded so did attempts to apply the results to the interpretation of Viking sediments; interpretations proliferated in step with the growing understanding and subdivision of modern environments. In some cases, interpretations successively contradict each other, in others the interpretations merely represent differentiation of the formation into its preserved sub-`environments'.

Following Stride's (1963) and Off's (1963) study of tidal ridges, Evans (1970) interpreted the Viking sediments of southern Saskatchewan as deposits of migrating tidal ridges. Although Evans presented detailed local correlations, there was no discussion the sediments in terms of sequences. The same portion of the Viking Formation has been re-analyzed by Pozzobon and Walker (1990) in terms of sequences (see below). Evans' work was soon followed by that of Tizzard and Lerbekmo (1975) who applied the recently published barrier island studies of Galveston Island (Davies et al., 1971) to the Viking Formation in southeastern Alberta. Although Tizzard and Lerbekmo take account of sedimentary structures, their detailed interpretation is confused. They could not decide whether to describe the sediments as `offshore bars' or barrier island deposits. Compare the following statements:

"It is concluded that the Viking in the ... area was a bar sand complex situated some distance from the shoreline, surrounded by open-marine seas; but the extent to which these sand bars may have been emergent, if they were at all, is uncertain..."

"Comparison of sedimentary structures and textures in the cores with published accounts of those occurring in Galveston Island has permitted recognition of lower, middle and upper shoreface facies.."

Despite this confusion, the work is typical of its time in its heavy reference to actualistic studies.

Apart from their introduction of newly emphasized environments to the Viking interpretations, Evans (1970) and Tizzard and Lerbeckmo (1975) were the first to introduce detailed sub-stratigraphy mentioning members within the Viking Formation However, they did not emphasize their subdivisions, and there was no real discussion of interpreted relative sea level history.

The recognition of internal members within the formation does become standard after this time, but, the members appear mostly as postulated local sand accumulations and are lithostratigraphic rather than allostratigraphic or `sequence stratigraphic' (e.g., Posamentier et al., 1988). Boethling (1977a,b) asserted that up to 15 different members exist in the Viking but presented no evidence for his claim. He viewed the Albertan portion of the formation as being "entirely marine" bar and sheet sands. He also introduced the possibility of the sands being "distributed by a relatively strong southward flowing cold boreal current with perhaps a northward flowing warm gulfian current having an influence in the more shallow areas." His guess at water depth is 30-150 feet. Most investigations by industry geologists are similar in their `informality' and also emphasize the "offshore" bar concept. Koldijk (1976) used typical industry alphabetic terminology to describe `members' of the formation crudely equivalent

to different sandbodies. He interpreted the coarser sediments in the Gilby field (see figure 1-1) as being the result of across shelf storm transport. Lerand and Thompson (1976) similarly refer to "shorelines, tidal flats, bays and shoals" and discuss the possibility of deposition around a series of "low shale islands" in the middle of the sea. Their work covered the Hamilton Lake/ Provost fields just south of the study area of this thesis (see figure 1-1). Reinson et al. (1983), in a very limited study of the Joffre area, generally interpreted the sands as nearshore systems but with some "tidally modified density current" deposits. Most of these publications contain no specific discussion of how the facies indicate the postulated environments. Furthermore, these works all lack detailed discussion of the generating mechanisms for their postulated members both from the point of view of sea level analysis and detailed environmental interpretation. In this sense, they are little different than the earliest works such as Jones (1961), making similar but slightly more knowledgeable interpretations of more specific areas.

The tendency to apply recently developed interpretations or models continued with the publications of the 1980's. At this point, sea level became a predominant part of the studies and recent environmental interpretations become less separable from their 'micro-stratigraphy' which was often interpreted as reflecting sea level fluctuations. This prominence reflects the introduction of the Exxon sea level curves by Vail et al. (1977).

The development of the incised shoreface model in the Cardium Formation (Plint et al., 1986, 1987, Bergman and Walker, 1986, 1987) fit neatly into the mental framework of sea level changes and the "incised shoreface"

concept was soon applied to the Viking. In this way, Downing and Walker (1989) described an incised deposit along the Joffre-Mikwan-Fenn fields interpreted as being a shoreface (see figure 1-1 for field locations). Raddysh (1988) argued for a scour in the Gilby field area in some way related to shoreface sedimentation. Power (1988a,b) also applied this idea, but, unusually, he applied it to interpretation of a gradational sequence in his study of the Joarcam field. Posamentier et al. (1992) have continued the application of the lowstand shoreface model from the Joarcam field basinward into the area covered in this study; their application is similar to that of Power (1988a) and is discussed in greater detail below and in following chapters.

The incised shoreface model is not the only interpretation to refer strongly to sea level changes. Pozzobon and Walker (1990) have recently re-evaluated the region studied by Evans (1970) and interpreted the Viking in this area as a "Nile delta like plume" which moved successively across a shallow ocean floor in response to a postulated transgression. A number of other authors have also presented their interpretations in the context of sea level changes without reference to incised shorefaces, but none have dealt with issues such as the precise location of sequence boundaries or their interpretation. For example, Leckie (1987) linked tidal flats and estuaries to lowstand and transgression in the Viking equivalent, the Paddy Formation. Leckie and Reinson (in press) correlated two interpreted major sequences from northwest to central Alberta. They described these sequences as containing "a series of coarsening upward units" and indicated "in south central Alberta, the Viking Formation consists of two to four ... cycles which constitute the regional `shelf shoreface'

progradational sequence". However, they did not offer any detailed evidence for the basis of the division of the subsequences. Leckie and Reinson's (in press) general conclusion is that the upper half of the Viking was deposited transgressively by tidal currents mostly in the form of tidal ridges. Ryer (1987), in his "offshore barrier-island/spit complexes" interpretation of the formation, also makes references to sea level change in southern Alberta although his views on environment of deposition mostly match the conclusions of Tizzard and Lerbekmo (1975) and Jones (1961). Hein et al. (1986) also referred to sea level changes and interpreted the Viking in western central Alberta in terms of one sea level cycle inducing shoreline progradation, incision, and reworking corresponding to the fall and rise of the cycle. The transgressive reworking was described as generating bar geometries in the coarser sediment; although these authors discuss a general regressive/transgressive cycle, there is little comment on the specific locations of sequence boundaries. Leckie (1986) maintained an essentially identical interpretation to that of Hein et al. (1986) for the nearby Caroline field. Reinson and Foscolos (1986) briefly interpreted the formation in the Provost area, south of this study area as a shoreface but did not offer any detailed reasoning for support, being primarily concerned with petrography.

Some portions of the Viking have now been interpreted as estuarine fills, notably the Crystal field (Reinson, 1983, Reinson et al., 1988, Pattison, 1992 and Pattison, 1990). Reinson's work ties the estuarine complex into two major sea level changes (the same as those of Leckie and Reinson, in press) at the base and top of a valley fill complex at the Crystal field.

Of special note, there are a few works which contain wholly or partially the same area studied in this thesis. These works are those of Amajor (1980) and Beaumont (1984). The work of Beaumont (1984) is discussed in chapter 7.

Amajor (1980), whose Ph.D. Thesis included most of the area I have examined, generally interpreted the sands as migrating tidal ridges. He did allow for other possibilities, however:

"Although deposits of semi-permanent currents are very poorly known, and consequently no compelling evidence in their favor is recognized here, the writer is of the opinion that they may have been significant sediment dispersal mechanisms during Viking deposition (p.277) (Amajor, 1980)

Deposition of these offshore sandbodies probably occurred mostly below normal wavebase in a subtidal tide-dominated offshore environment, in a manner fairly similar to that of the present day tidal sand ridges of the North Sea (p.299) (Amajor, 1980)."

Unfortunately, his interpretations suffer from a lack of data. He examined only approximately 8 cores in the area (as opposed to the approximately 200 on which the facies descriptions below are based) so he had comparatively very little information to work with. Furthermore, the criteria he used for selecting this data are strongly biased towards particular locations and his determinations of sandbody thickness flawed:

"In areas where discrete sandbodies are stacked vertically but separated by less than 30' of shale, mudstone or siltstone, isopach maps include the whole interval ... (p.15);"

"The resulting isopach and isolith maps were used as base maps for stratigraphic sections and core control (p. 16) ...

"they restricted the search for cored wells to the mapped sand units (p.17)." (Amajor, 1980)

More importantly, his conclusions are tenuous because they are based on a chronostratigraphy developed from postulated bentonite signatures in well logs that are, in fact, uncorrelatable over the area. On the basis of his own data and admission the bentonites used to subdivide the stratigraphy do not extend across the region:

"... bentonites E and C cannot be reliably picked in the electric logs of the area ... (Amajor, 1980)"

Perhaps the most fundamental problem with Amajor's (1980) proposed chronostratigraphy is that many of the correlations of well logs signatures are inconsistent; they correlate high resistivity to low resistivity responses even for the reputedly "extensive" bentonites. This situation is made worse by a complete lack of any core evidence for the bentonite picks despite the fact that bentonites may be observed locally in the core of the area (see below).

Although not necessarily incorrect, Amajor's (1980) environmental interpretations are also built on a weak foundation. This is partly a consequence of his paleogeography being dependent on the flawed stratigraphic approach described above but is also a function of his limited core examination. For example, regarding a barrier island interpretation for the "Upper Viking",

"Although this interpretation was generated from the cores of only one well, the writer believes ... it does provide an adequate amount of significant information (Amajor, 1990, p. 235)."

Lack of core examination is also a flaw in Beaumont's (1984) study although he acquired somewhat more data. He examined a maximum of 20 cores outside the Joarcam field (see figure 1-1) in unspecified locations. Beaumont

(1984) interpreted the sediments in terms of a transgressed delta in the Viking-Kinsella field region overlain by westwardly shingled "retrograding shelf sediments" in the form of sheet sands containing linear sand bodies. His idea of a relict delta derives from little but the shape of gas fields:

> "*During a profound regression at the beginning of Viking deposition, streams flowed across the former shelf surfaces depositing sand in deltas, as now evidenced by the irregular-shaped reservoirs of eastern Alberta*" (Beaumont, 1984).

The work of Posamentier et al. (1992) is particularly relevant to this study because the authors postulate the existence of lowstand shorefaces across the region where this study interprets none to exist. Figure 2- 3 is a reproduction of figure 7 of Posamentier et al. (1992) showing their well log correlation cross-section. This cross-section runs approximately diagonally across the western portion of the study area discribed above. The bold print and heavy lines are additions highlighting areas of concern. There are fundamental flaws in both the construction and interpretation of this cross-section which make the conclusions of Posamentier et al. (1992) untenable.

The construction flaws include a lack of datum and the failure to recognize markers below and above the Viking Formation signature that would have served as markers. On the top of figure 2-3 two examples of such markers have been drawn in heavy lines. Because the cross-section was not constructed using such markers their behavior cannot be followed across the length of the drawing and they have not been clearly reproduced in the well log responses. These over and underlying markers are important as discussed below in chapter 4 because they are essentially subparallel. Construction of cross-sections relative to

such markers therefore makes a strong case for topographic interpretation of the deposits between the markers. Such construction techniques were used in this study and are shown in foldouts 1 through 7 as covered in chapter 4. The general parallelism of markers above and below the Viking Formation suggests that the topography inferred by Posamentier et al. (1992) is incorrect. An examination of the cross-section reveals that by not using a datum the top of the Viking is allowed to dip down in regions where a "lowstand shoreface" is interpreted. Forexample, wells 7-7-49-18W4 and 13-8-49-18W4 at the left of the line marked 'region of comparison' may be compared to the correlations between wells 9-2-49-18W4 and 13-8-49-18W4 in foldout 4 (rear pocket; cross-section D-D'). This conveniently avoids the problem introduced by use of a reliable datum which is that most of the areas interpreted as "lowstand shorefaces" have a slight positive relief which is visible in the interval in foldout 4 (see chapter 4). More importantly than the lack of recognition of these markers is the fact that the cross-section of figure 2-3 was not constructed with a consistent datum outside the Viking. As can be seen there is no line which is flat across the cross-section. This has been highlighted across the figure in several locations with the phrase 'no continuous datum' where log signatures above and below the major response of the Viking Formation have not been incorporated into the study. Posamentier has stated that a datum was used internal to the Viking that varied depending on location (p.comm., 1989). An additional technical flaw is that the interpreted "sequences" are based on a single cross-section. There is no documentation or discussion of tying the correlations together in fence diagram or box form to confirm their internal consistency.

Figure 2-3. The Lowstand Shoreface Cross-Section of Posamentier et al. (1992).

The figure is a copy of the cross-section presented by Posamentier et al. (1992) in their figure 7. Areas of concern discussed in the text have been highlighted.

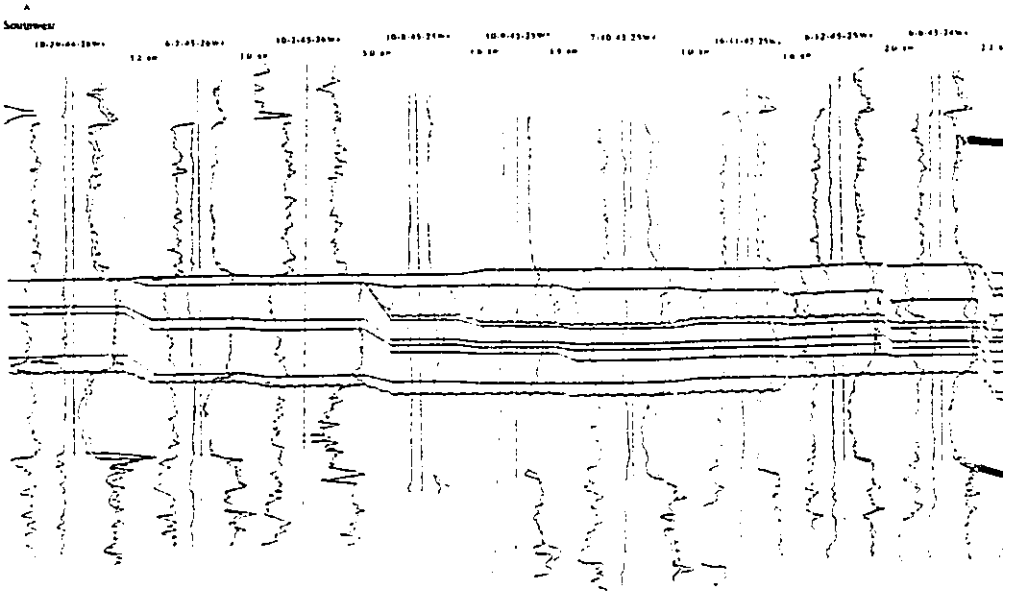

no continuous datum

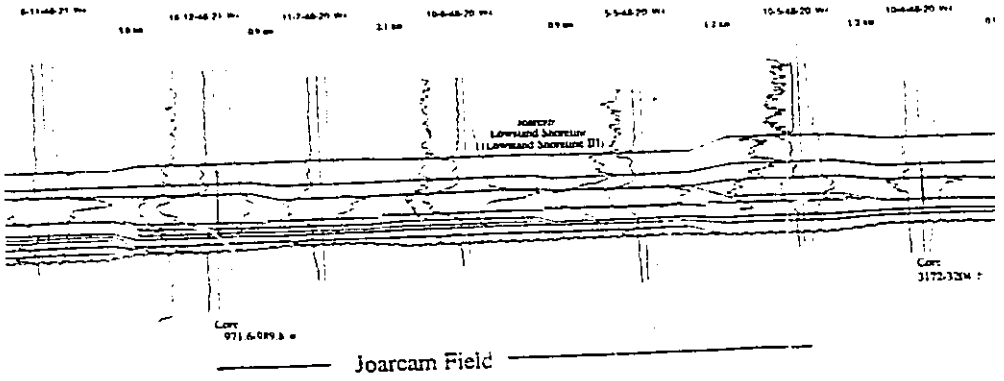

(b)

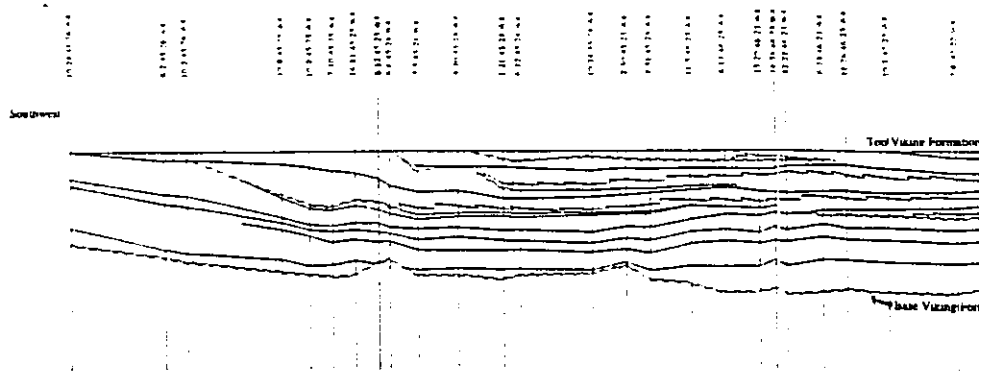

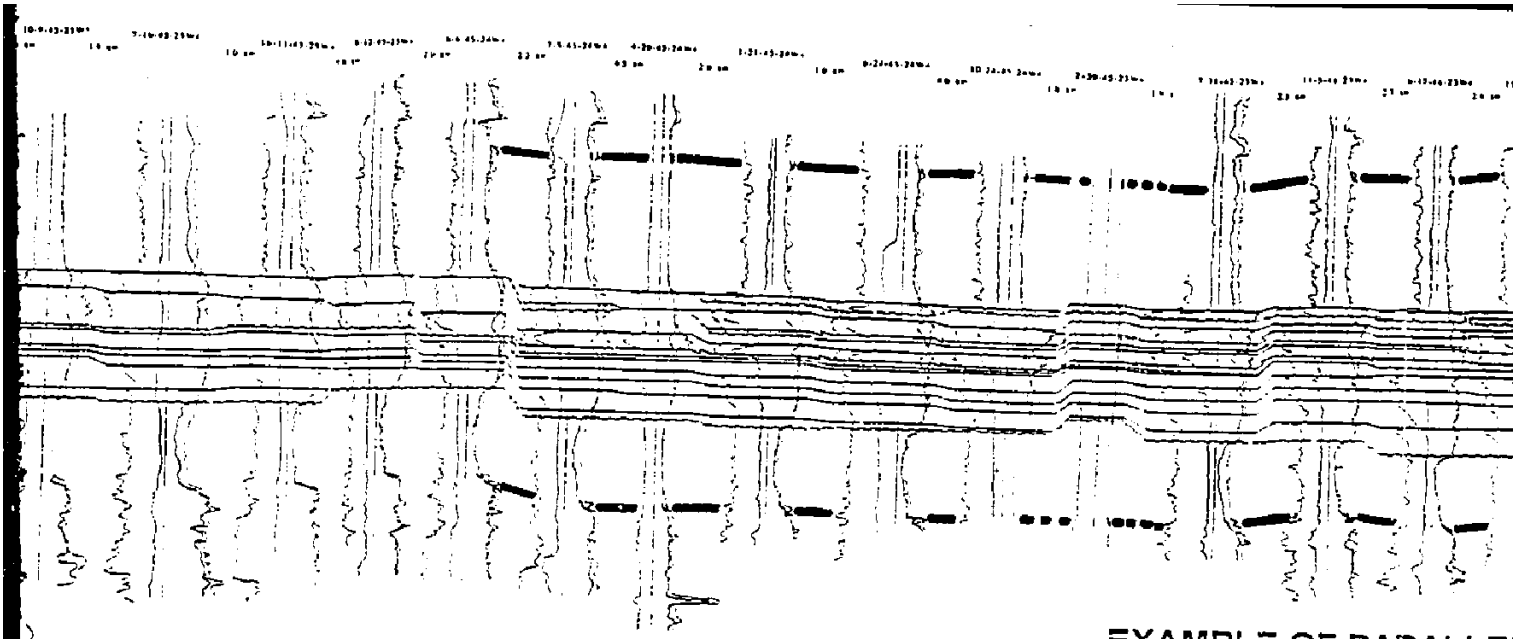

EXAMPLE OF PARALLEL
SUB- AND SUPER- VIKI

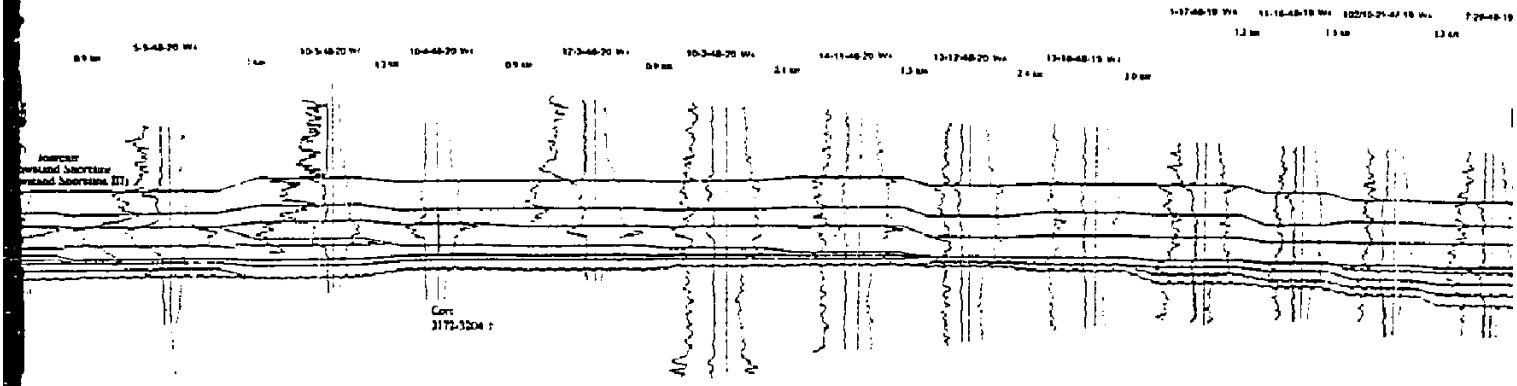

EXAMPLES OF LOCATIONS OF
MISSING UNCONFORMITIES

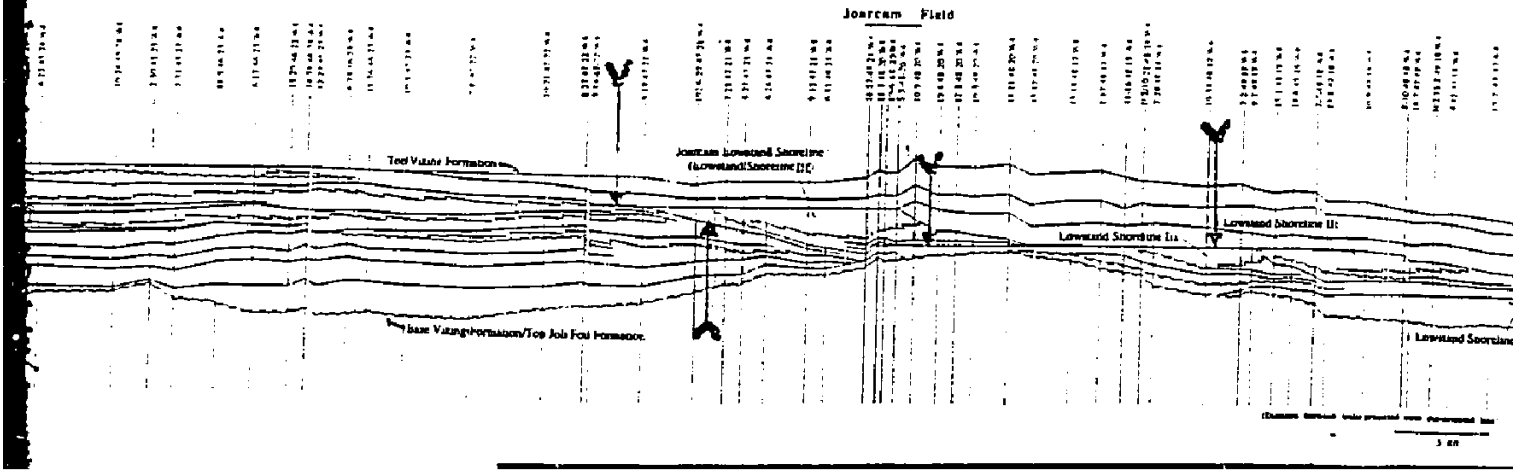

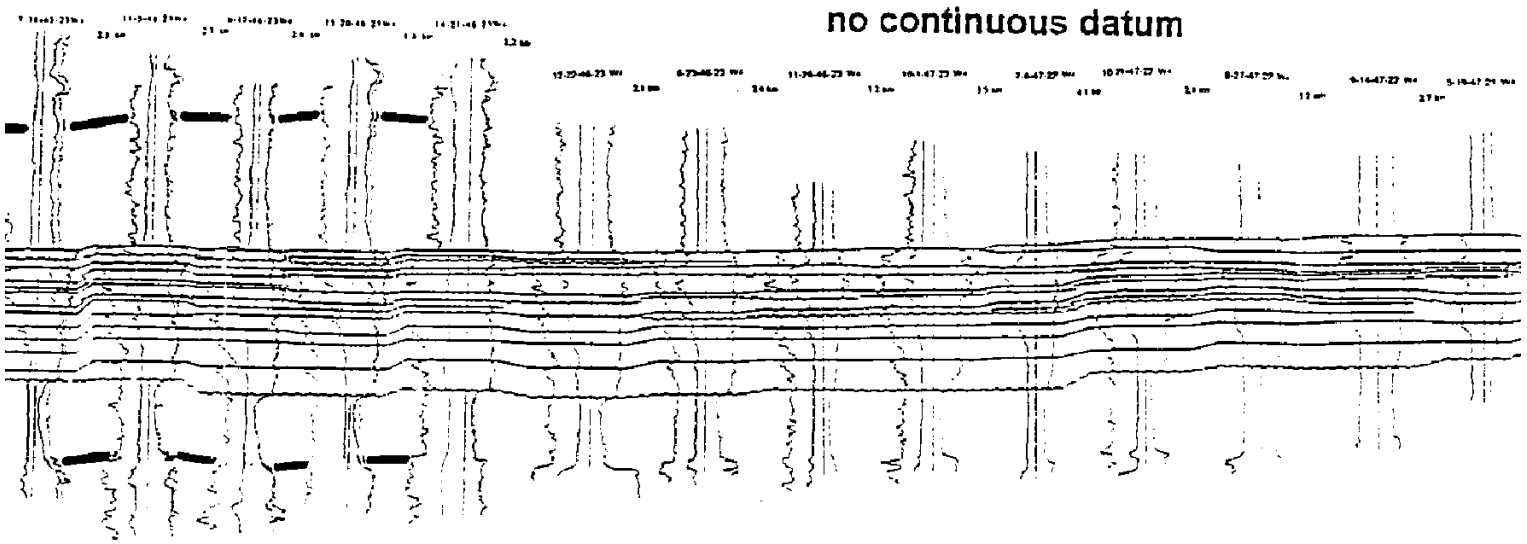

MPLE OF PARALLEL TRACKING OF
- AND SUPER- VIKING MARKERS

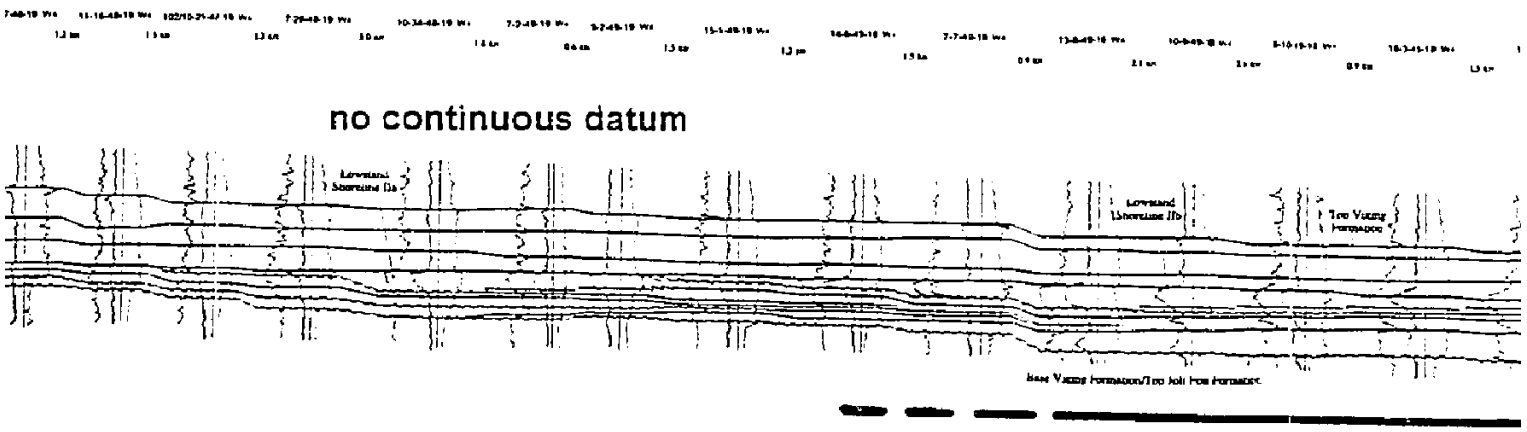

REGION OF COMPARISONS

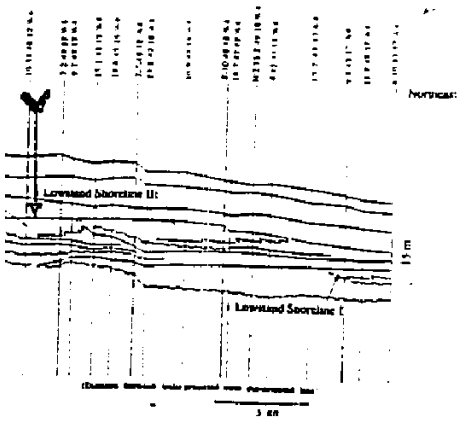

no continuous datum

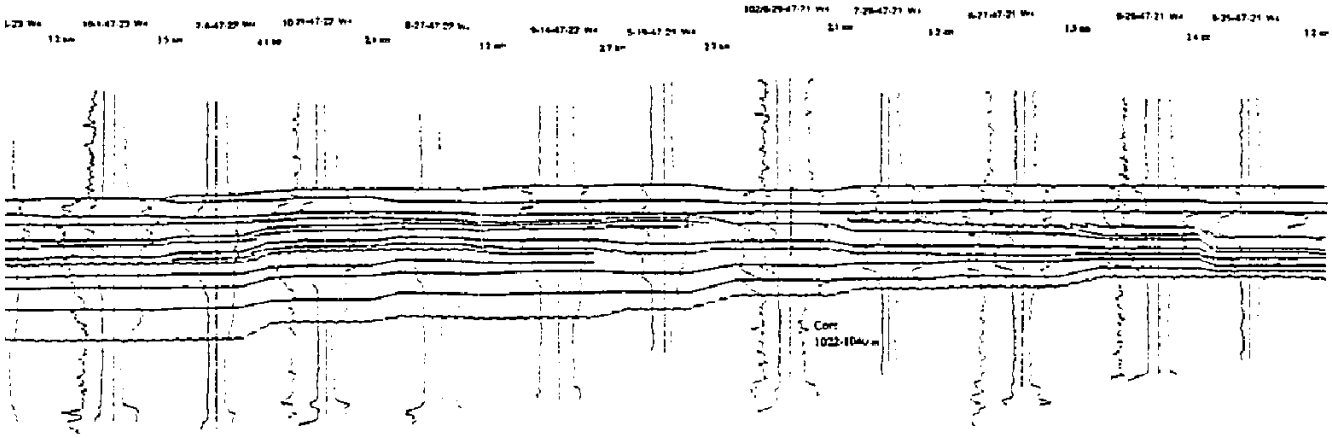

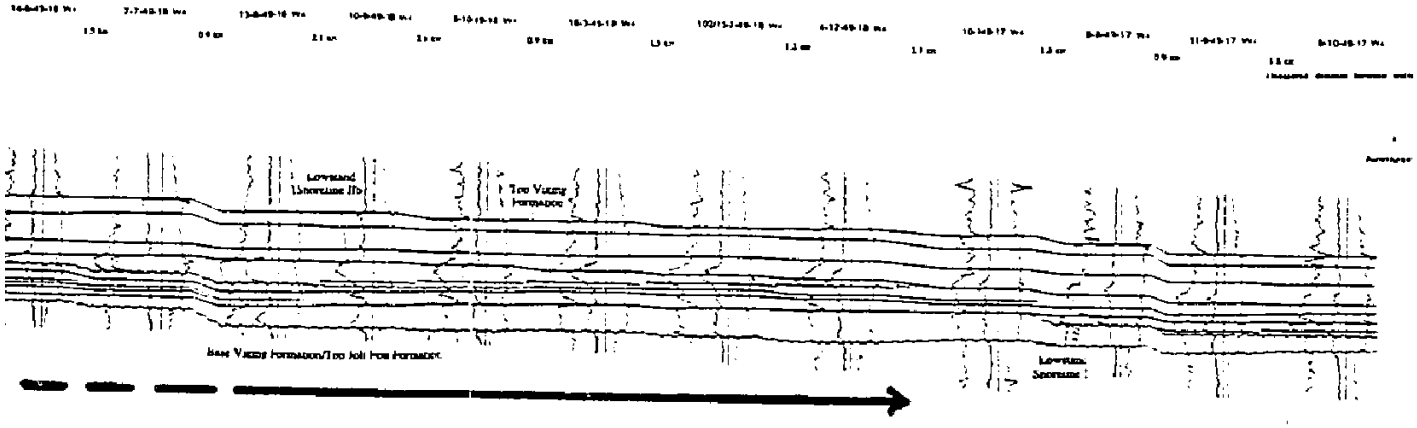

REGION OF COMPARISONS

The interpretive flaws in the Posamentier et al. (1992) model arise from inconsistencies and a sparcity of data. The sparcity of data is actually a lack of consideration of the sediment types in the region through which the authors have constructed their cross-section. As described below in chapter 3 and interpreted in chapter 6, the facies of the sediments are pronounced in their muddiness, particularly in the eastern portion of the study area. There are a number of problems with placing even the sandier portions of the sediments into "lowstand shorefaces". Since Posamentier et al. (1992) do not discuss the details of their facies interpretation (apparently having examined minimal core in the area) the reader is referred to the cited chapters for an discussion of the arguments against the lowstand shoreface model.

It also seems unlikely that in the basinal setting indicated by the cores in the study area that none of the sediment would be deposited during the transgressive phase of the sea level changes associated with the lowstand shorefaces. Yet this is the implications of Posamentier et al.'s (1992) argument. (Beaumont (1984) and Leckie and Reinson (in press) are the only authors to attribute significant amounts of sediment to deposition during transgression.)

The inconsistencies of the Posamentier et al. (1992) interpretation are pointed out in figure 2-3 by arrows and the label 'examples of locations of missing unconformities' on the summarized cross-section (b). These arrows point to horizons where, if the lowstand shorefaces drawn onto the diagram are correct, there should be subaerial erosion surfaces. Posamentier et al. (1992) have not accounted for such surfaces which are demanded by their own interpretation. This is a fundamental flaw in their work. Furthermore, examination of any of the

lithological cross-sections in foldouts 8-12 (rear pocket) reveals that there are no such unconformities or regional scouring in the area. Posamentier et al.'s (1992) lowstand shoreface interpretation is thus dismissable on the basis that observations fail to confirm its predictions.

Despite the detailed interpretations of specific locations in the Viking described above, there is still scope for further interpretation and extensive documentation of sediment distribution in the area of figure 1-2. Not only have there not been detailed basic facies studies of this region, but the issues enumerated in chapter 1 have not generally been considered anywhere in the formation. For example, in none of the existing work on the Viking, have any authors considered the possible complexities introduced into environmental interpretations by the presence of early diagenetic products such as phosphate and glauconite. This is a particularly important omission from work such as Power (1988b), Downing and Walker (1988) and Posamentier et al. (1992) because of the apparent contradiction between the diagenetic evidence for depositional environment and the interpreted sedimentary evidence. Diagenetic investigation (e.g., Reinson and Foscolos, 1986 and Longstaffe and Ayalon, 1987) have mentioned glauconite but dwell on the minerals associated with deeper burial alterations and do not discuss its possible epigenetic implications. The early diagenetic products, whether out of convenience or ignorance have been left unaccounted for.

Finally, no one has tried to tackle the question of the lateral extent and variation in facies patterns. The first step in improving on the existing and sometimes questionable nature of the earlier interpretations, is to take a much more detailed and comprehensive look at the rocks on which they are based.

CHAPTER 3

FACIES DESCRIPTIONS

Where is the Life we have lost in living?
Where is the wisdom we have lost in knowledge?
Where is the knowledge we have lost in information?

T.S. Eliot The Rock, 1934

3.1 SUMMARY

Twenty basic facies are described with subdivisions based on percentage of sand present. The facies were erected on the basis of sedimentary structures, trace fauna and sand content and are described in terms of diagnostic and secondary criteria. Facies range from grey shale to conglomerate, but are mostly forms of bioturbated or crossbedded muddy sandstones and siltstones. Interpretations follow in chapter 6.

3.2 INTRODUCTION

Facies are the fundamental building blocks of this investigation. This chapter contains descriptions of the facies defined in eastern central Alberta. Figure 3-1 is a legend of their symbolic representations as used in all figures in the thesis. Although particular facies show sedimentary structures indicative of certain bedforms or bedform types and others have suites of ichnofauna that place them within various ichnofacies, their full environmental interpretation benefits from consideration in light of 'higher order' observations such as vertical and lateral successions, so interpretations are withheld until chapter 6.

FIGURE 3-1

GRAPHICAL FACIES LEGEND

The legend overleaf displays the graphic presentation used for each facies with the appropriate facies number underneath

1. Grey Mudstone 2. Laminated Siltstone

3. Discontinuously Laminated Siltstone

4. Bedded Siltstone

5. Interbedded Siltstone 6. Bioturbated Mudstone

7. Bioturbated Siltstone 8. Bioturbated Sandstone

9. Mottled Siltstone 10. Lensoid Sandstone

11. Muddy Sandstone 12. Massive Sandstone

13. Crossbedded Sandstone 14. Tangential Parallel

15. Planar Parallel 16. Low Angle Parallel

17. Low Angle, Intersecting 18. Pebbly Sandstone

19. Pebbly Mudstone 20. Conglomerate

21. Diagenetic Clast Conglomerate 22. Slumped Siltstone

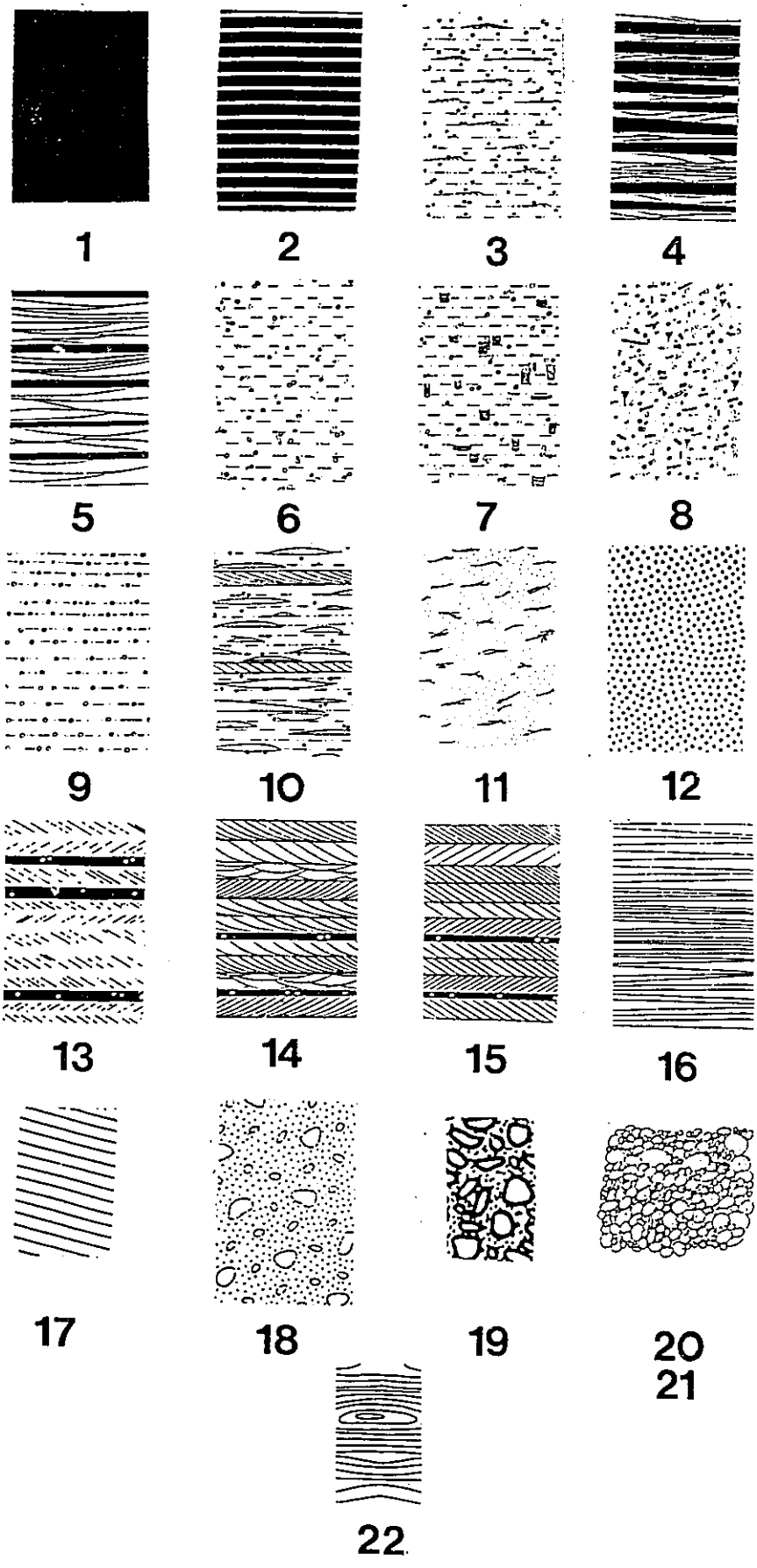
1
2
3
4
5
6
7
8
9
10
11
12
13
14
15
16
17
18
19
20
21
22

3.3 FACIES CONSTRUCTION AND PRESENTATION

The facies have all been erected using standard sedimentological and ichnological criteria (e.g., Walker, 1984c). They are defined on the basis of examining 169 cores within the area shown in Figure 1-2; and approximately 50 more cores examined to the northwest of the study area described in chapter one. Cores range in diametre from 1" to 4".

Each facies description is arranged in terms of primary (i.e. diagnostic) and secondary criteria; primary criteria are always present, secondary criteria may be. Additionally, a range of possible grain sizes is given; these are the sizes observed over all occurrences of a given facies, not the range for one. The facies are largely independent of maximum grainsize. If sediment thicknesses of the same aspect but distinctly different grainsizes occur directly on top of one another, then a facies may succeed itself. Such consideration of grain size based division of units is of potential importance when considering subtle basinal changes which might only be reflected in available or transportable grain size. The grain size divisions used here refer to measurements made with the CanStrat card whose categories are:

VERY FINE
- (lower) VFL ; 4 - 3.5 PHI
- (upper) VFU ; 3.5 - 3 PHI

FINE
- (lower) FL ; 3 - 2.5 PHI
- (upper) FU ; 2.5 - 2 PHI

MEDIUM
- (lower) ML ; 2 - 1.5 PHI
- (upper) MU ; 1.5 - 1 PHI

COARSE
- (lower) CL ; 1 - 0.5 PHI
- (upper) CU ; 0.5 - 0 PHI

VERY COARSE
(lower) VCL ; 0 - -0.5 PHI
(upper) VCU ; -0.5 - -1 PHI

Coarser grain sizes, from granules up were estimated from the apparent maximum and minimum axes visible on the side of the core. Burrow dimensions are based, where visible and appropriate, on circular cross sections or otherwise on the visible dimensions on the core side. The percentage of sand given for many facies is a visual estimate. All observations are from core washed clean of drilling mud which, surprisingly, obscured most cores examined. Most photographs were taken with the core faintly wet and illuminated by two tungsten lights from each side. Camera lens apertures were often set at f22 to insure adequate depth of focus.

In addition to grain size ranges, thickness statistics are provided. These are the number of units measured and the average thickness. Measurements are in centimetres. Some cores, usually 1" in diametre, were not included in the statistics because the facies present were difficult to determine due to small size and obscurement by formational swelling clays. Many facies occur as the first or last unit in a core; in these cases, their thicknesses were not included in the averages. This is particularly true for shales above and below the Viking. Units in such initial or terminating positions only contribute to the knowledge of minimum thickness and are inappropriate as parts of averages. Most of the facies contacts are gradational; thickness divisions are therefore somewhat arbitrary and should only be considered accurate to within 10cm. This estimate is based on remeasurement of a few cores in successive field seasons which gave a general agreement of plus or minus 10 centimetres.

No facies were defined using dominantly petrographic criteria, but diagenetic products such as glauconite and siderite are included in a secondary portion of facies descriptions because they can convey some environmental information. Relevant inferences that can be drawn from petrographic information are discussed in chapter 6.

3.4 FACIES DESCRIPTIONS

3.4.1 GREY MUDSTONE (n=68, avg=221cm); Figure 3-2A

Primary Criteria: This facies' dominant aspect is the massive appearance of the mudstone with only traces of silt laminae. No bioturbation is visible. The core breaks in a platy to blocky fashion.

Secondary Criteria: Samples, usually in the unnamed shales overlying the Viking, occasionally contain fish scales. The mud is usually relatively smectitic. In the structurally shallower cores examined, this facies can be very smectitic with dramatically swelling clay. The change to a less swelling and presumably more illitic clay appears to be depth controlled and is therefore ignored in the facies division. Bands of siderite may also occur, predominantly in shales above the Viking but also within the Joli Fou Formation. Bentonites are sometimes found. Occasionally pyritic streaks appear on bedding planes (*Gordia*?).

3.4.2 LAMINATED SILTSTONE (see subdivisions for statistics); Figure 3-2B

Primary Criteria: This facies is characterized by multiple silt to FU laminae typically less than 1mm to 5mm thick representing 5-50% of the beds (see subdivisions below). The laminae are often sharp based. Frequently, they show both colour and size grading and cross lamination. The cross lamination is mostly horizontal to sub-horizontal but may show short wavelength (10-20 cm

estimated) curvature and intersection. It is low angle, less than 15 °. Rarely, slumping or overturning of the laminae is visible.

Secondary Criteria: Portions of some units may be very rich in *Chondrites*. Infrequently, 1-2mm *Terebellina* and 3-5mm *Planolites* burrows appear, as may *Arenicolites anorexia* (see Appendix A) . Bentonites can be found. Extremely rarely, *Muensteria* occur. One example of *Conichnus* was seen. Plant material may be detected; in some cases, centimetre by several centimetre twig like fragments lie on bedding planes. Fish scales have also been observed. Glauconite occurs rarely in some laminae, and there is occasionally some sideritization.

Subdivisions were made on the basis of the percent of silt beds as follows:

A. Laminated: 5%-20% (n=417, avg=177cm)

B. Abundantly Laminated: 20%-30% (50% rarely)

(n=113, avg=171cm)

All subdivisions may be further modified on the basis of the grain sizes they contain. Those completely composed of FU sand and coarser (observed to granule size) over more than 10 cm thick were labeled as Coarse Laminated; those with only occasional beds of coarser sands had the modifier `with coarse material' added to the description. The coarse beds often exhibit cross stratification described by one of the subdivisions of Crossbedded Sandstone (below).

3.4.3 DISCONTINUOUSLY LAMINATED, SILTSTONE (n=37, avg=239); Figure 3-2C

Primary Criteria: This facies has common discontinuous laminae of VF-CL (rarely VCU) sand; the finer sizes are much more common. Sandy laminae form between 20-70% of the units and are accompanied by mudstone containing 2-6mm *Planolites*. The facies differs from the Mottled Siltstones (below) in that the laminae are more abundant and distinctly cross laminated. The cross laminae vary from approximately horizontal to 25° in dip, and they usually dip in the same direction. The lower angles are more abundant.

Secondary Criteria: Rarely, 180° opposing cross laminae occur and one poor example of climbing ripples was seen. Glauconite may be found in cross laminae and siderite may occur in the mudstones. Fusain may also be present. The *Planolites* traces are sometimes accompanied 2-3 mm *Terebellina*, 1 cm *Muensteria*, retrusive 1 cm *Teichichnus* and *Arenicolites*. The latter may permeate some units. Bentonites may also exist.

3.4.4 BEDDED SILTSTONE (see subdivisions for statistics) Figure 3-2D

Primary Criteria: Units of this facies are dominated by 10 to 90% silt or VFU sand generally in 2-3cm thick beds. Bed thickness may reach 20cm. The beds often show low angle lamination (less than 10°) frequently intersecting at different angles. There may also be parallel to low angle undulatory lamination. Some laminae are convex upward. When one direction of lamination dominates a single set, the lamination is tangential to the base of the bed at a low angle. Cross lamination abruptly abutting the base may also occur. The beds are invariably sharp based with either sudden or gradational tops. Colour grading from light base to dark top is common.

Figure 3-2

A. Grey Mudstone, Facies 1.
Well 11-11-51-12W4; depth: 1950 feet.
The core is 3" in diametre; scale bar is 3 cm.

B. Laminated Siltstone, Facies 2.
Well 10-18-61-4W5; depth: 2988 feet.
The core is 3" in diametre.

C. Discontinuously Laminated Siltstone, Facies 3.
Well A6-5-51-24W4; depth: 3326 feet.
The core is 3" in diametre; scale bar is 3 cm long.

D. Bedded Siltstone, Facies 4.
Well 15-24-45-20W4; depth: 3186 feet.
The core is 3" in diametre.

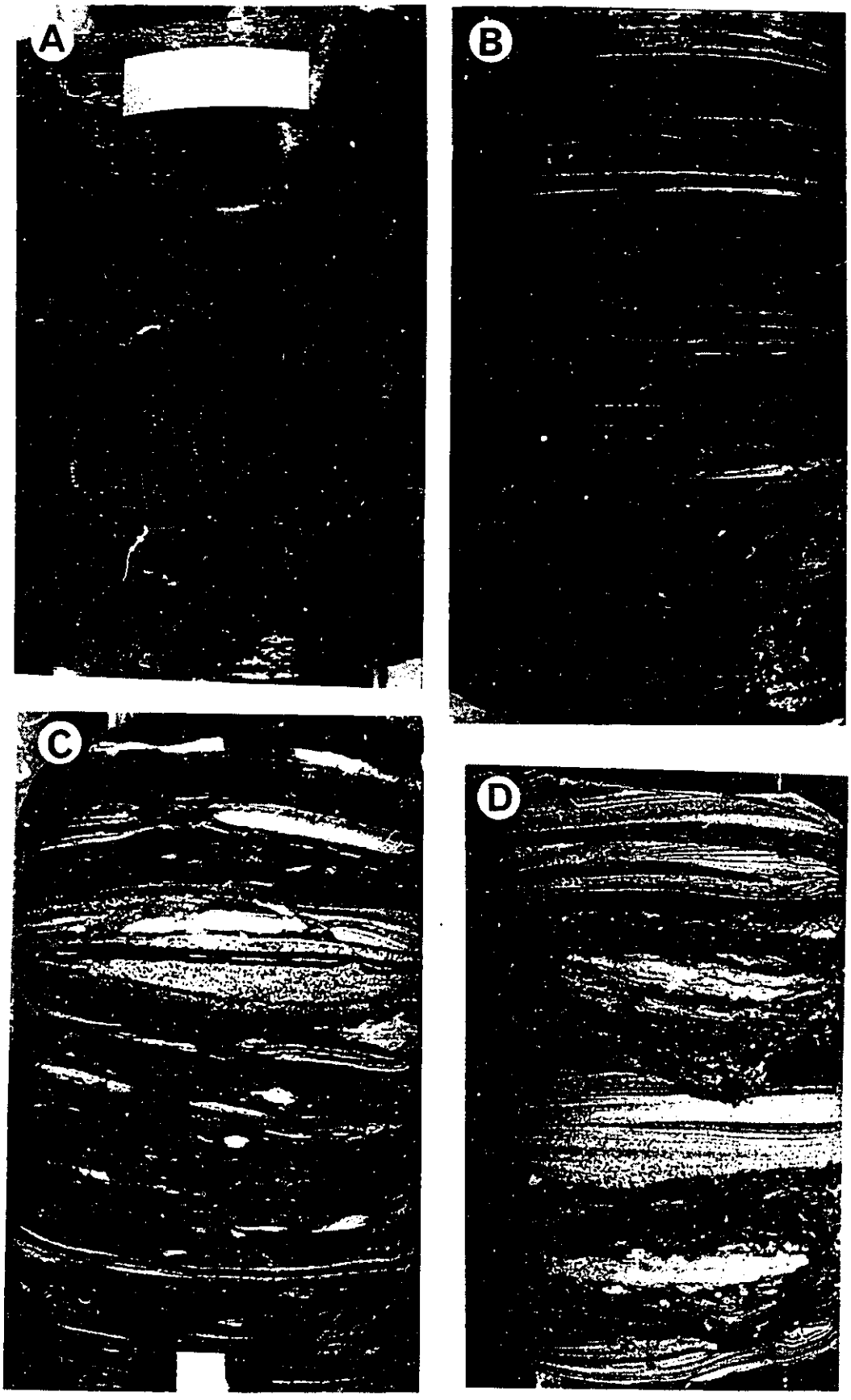
A
B
C
D

Secondary Criteria: Distinct burrows are rare to absent; *Planolites* (3-5mm) is the most common, but it may be augmented by *Chondrites*, and rare *Terebellina* (1-2mm). *Arenicolites anorexia* may be seen rarely. Portions may show indistinct bioturbation, but usually beds are more or less intact. Siderite and bentonite may sometimes be found. In some locations, fish scales and comminuted plant debris (fusain) may be common on bedding planes.

Subdivisions were made on the basis of the percentage of sand beds.

A. Bedded: 10-40% (n=119, avg=167cm)

B. Abundantly Bedded: 40-90% (n=19, avg=93cm)

The same grain size modifiers as applied to Laminated Siltstone also apply here with units bearing predominantly FU to granular material for more than 10 cm being labeled coarse bedded and those having occasional coarse material in the beds as 'with coarse pulses'. When coarser material occurs, it may either form the entire bed or lie at the base and be interlaminated upwards in decreasing amounts with the finer material. The coarser sands may be crossbedded. A gradational spectrum of such types is present.

3.4.5 INTERBEDDED SILTSTONE (n=25, avg=141cm); Figure 3-3A

Primary Criteria: In this facies, many thick (4-25cm) beds of sand showing low angle (inclined up to 10°) and intersecting laminae are interbedded with bioturbated mud and silt. The sand beds form approximately 30-80% of the facies and are composed of VF-ML size grains, predominantly VF. The base of the beds is sharp, and the tops are sometimes bioturbated.

Secondary Criteria: Individual unidirectional cross laminae sets may also occur with angles approaching 25°; where measurable, sets tend to have the same

orientation. The tops of sets may be reworked into concavo-convex, low angle, crosslamination. Sometimes no intersections of the laminae occur. The burrows visible in the bioturbated portion of the facies include retrusive *Teichichnus* (5 by 15mm), *Planolites* (3-5mm), *Muensteria* and *Chondrites* (<1mm). *Arenicolites anorexia* may be present. In some cases, *Chondrites* may be extremely common, and rarely is the only trace. Some examples have no bioturbation visible in the mudstones. Fusain may occur. Uncommonly, coarser (CU-VCL) grains may lie throughout a unit or may be concentrated in a single bed. Glauconite occurs in the laminae of the beds, sometimes abundantly, and mudstones may be sideritized.

3.4.6 BIOTURBATED MUDSTONE (n=24, avg=120cm); Figure 3-3B

Primary Criteria: This facies contains sufficient silt to reveal a completely bioturbated texture. Additionally, there are a few distinct *Terebellina* (1-2mm) and occasional *Planolites* (3mm).

Secondary Criteria: Very rare silt laminae may be seen. This facies is descriptively continuous with Pebbly Mudstone as some units contain scatterings of coarse (ML-VC) sand at about the 5% level.

3.4.7 BIOTURBATED SILTSTONE (n=199, avg=63cm); Figure 3-3C

Primary Criteria: This facies is composed of 40%-80% silt to VF-FL sand. The units commonly contain *Terebellina* (2-3mm), retrusive *Teichichnus*, *Planolites* (2-3mm) and rarely *Muensteria.* The number of distinct burrows is smaller and more consistent than for the Bioturbated Sandstone.

Secondary criteria: In some cases, remnant low angle parallel to undulatory lamination occurs. Bentonites may be found. *Arenicolites*

Figure 3-3

A. Interbedded Siltstone, Facies 5.
Well 11-2-58-5W5; depth: 3890 feet
The core is 3" in diametre.

B. Bioturbated Mudstone, Facies 6.
Well 1-1-45-20W4; depth: 3281 feet
The core is 3" in diametre.

C. Bioturbated Siltstone, Facies 7.
Well 4-4-49-14W4; depth: 2283 feet
The core is 3" in diametre.

D. Bioturbated Sandstone, Facies 8.
Well 8-30-47-16W; depth: 2183 feet
The core is 3" in diametre and the scale is 3cm long.

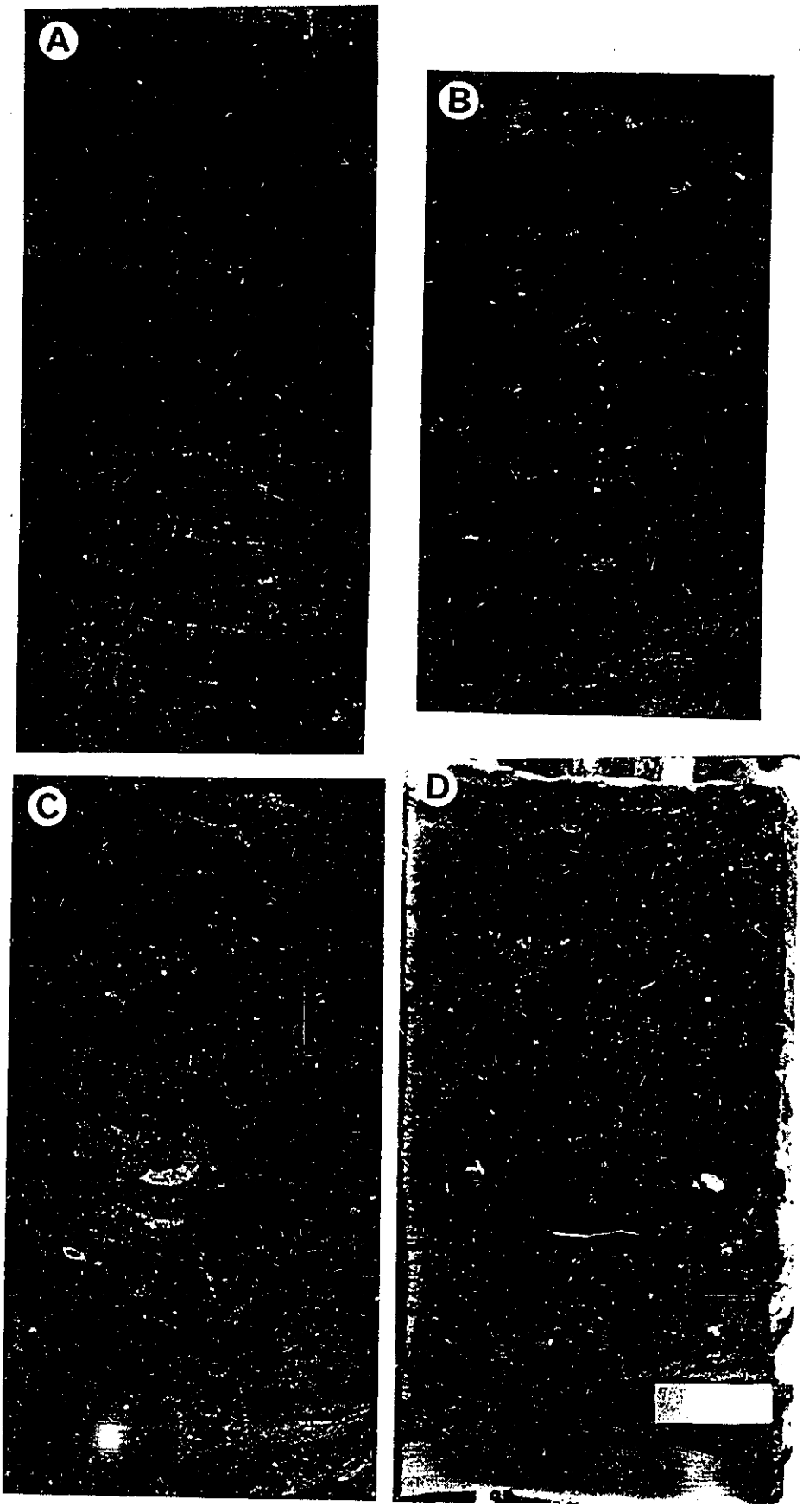
A
B
C
D

anorexia may also be observed in some samples, and one questionable *Asterosoma* was seen. Coarser material (ML-CU sand) may occur in some units.

3.4.8 BIOTURBATED SANDSTONE (n=273, avg=126cm); Figure 3-3D

Primary Criteria: Bioturbated Sandstone contains 50-95% VFU-FU sand (predominantly 70%+). This facies comprises sand rich rocks which, despite being almost completely bioturbated, contain an assortment of distinct burrows. Not all burrows are always present, but there is sufficient overlap among them that when combined with the generally bioturbated nature of the sand they are placed within one facies. The burrows include *Terebellina* (2-3mm), *Rosselia* (3-5cm), *Arenicolites anorexia, Planolites* (2-3 mm), *Paleophycus* (3-6mm), *Muensteria* (1cm), *Chondrites* and *Bergaueria* (2 by 3cm).

Secondary Criteria: *Skolithos* may be found in portions (usually the upper parts) of some units. Extremely rare retrusive *Teichichnus* and possible *Zoophycus* may also be found. Some portions of units may show remnant low angle indistinct to sub-parallel lamination or unidirectional high angle, planar based, cross lamination. Bentonites may be present as may siderite. Centimetre scale coal fragments also occur.

Units containing common coarser material (ML-CU sand to granules) are labeled, 'with coarse material'.

3.4.9 MOTTLED SILTSTONE (see subdivisions for statistics); Figure 3-4A

Primary Criteria: This facies is dominated by *Planolites* (2-10mm, with 3-6 mm most common) with 10%-50% VFL-MU sand distributed in mud.

Secondary Criteria: Some sharp based, 1-6 cm bedding may be partially preserved showing low angle undulatory, intersecting, laminae. Portions may be

smectitic or iron stained (siderite cementation?). *Chondrites* (1-0.5 mm) may occur along with rare *Terebellina* (1-2 mm). *Arenicolites anorexia* are visible in some units. Rare glauconite may be found as may bentonites. Occasionally, fusain and centimetre scale plant fragments are visible.

Subdivisions are made on the basis of the amount of sand as follows:

A Mottled: 10-35% VFL-ML (n=202, avg=129cm)

B Abundantly Mottled: 40-50% (70%) VFU-MU (n=112, avg=132cm)

3.4.10 LENSOID SANDSTONE (n=35, avg=84cm); Figure 3-4B

This facies has distinct but often semicontinuous, lensoid, 1-10 cm thick FU-ML sand beds which may be cross stratified and make up 40-70% of the units. These beds are separated by mud beds or laminae on the order of 1 cm thick. There are very commonly *Planolites* burrows (2-8 mm) in the mudstone. The facies is descriptively gradational with Mottled Siltstone as beds become indistinct.

Secondary Criteria: Rarely, high angle, 25° cross laminae may be seen in the sandstone beds. Retrusive *Teichichnus* may be observed, but it is uncommon. Siderite and bentonites may also occur as may scattered coarser (ML-VCU) grains. In some cases, coarser grains (ML-VCU) lie in isolated high angle crossbed sets (type uncertain). Coarse material may dominate the facies, in which case it is given a modifier 'coarse' or 'with coarse material' in a manner analogous to other facies.

3.4.11 MUDDY SANDSTONE (n=178, avg=95cm); Figure 3-4C

Primary Criteria: This facies is composed of 50%-90% VFU-CL sand with scattered granules in some units. The beds are usually

Figure 3-4

A. Mottled Siltstone, Facies 9.
Well 11-29-49-21W4; depth: (1015 metres); 3329 feet
The core is 3" in diametre; the scale bar is 3 cm long.

B. Lensoid Sandstone, Facies 10.
Well 10-21-51-19W4; depth: 2719 feet
The core is 3" wide.

C. Muddy Sandstone, Facies 11.
Well 11-23-51-19W4; depth: 2630 feet
The core is 3" in diametre.

D. Massive Sandstone, Facies 12.
Well 6-31-49-21W4; depth: 3289 feet
The core is 3" in diametre.

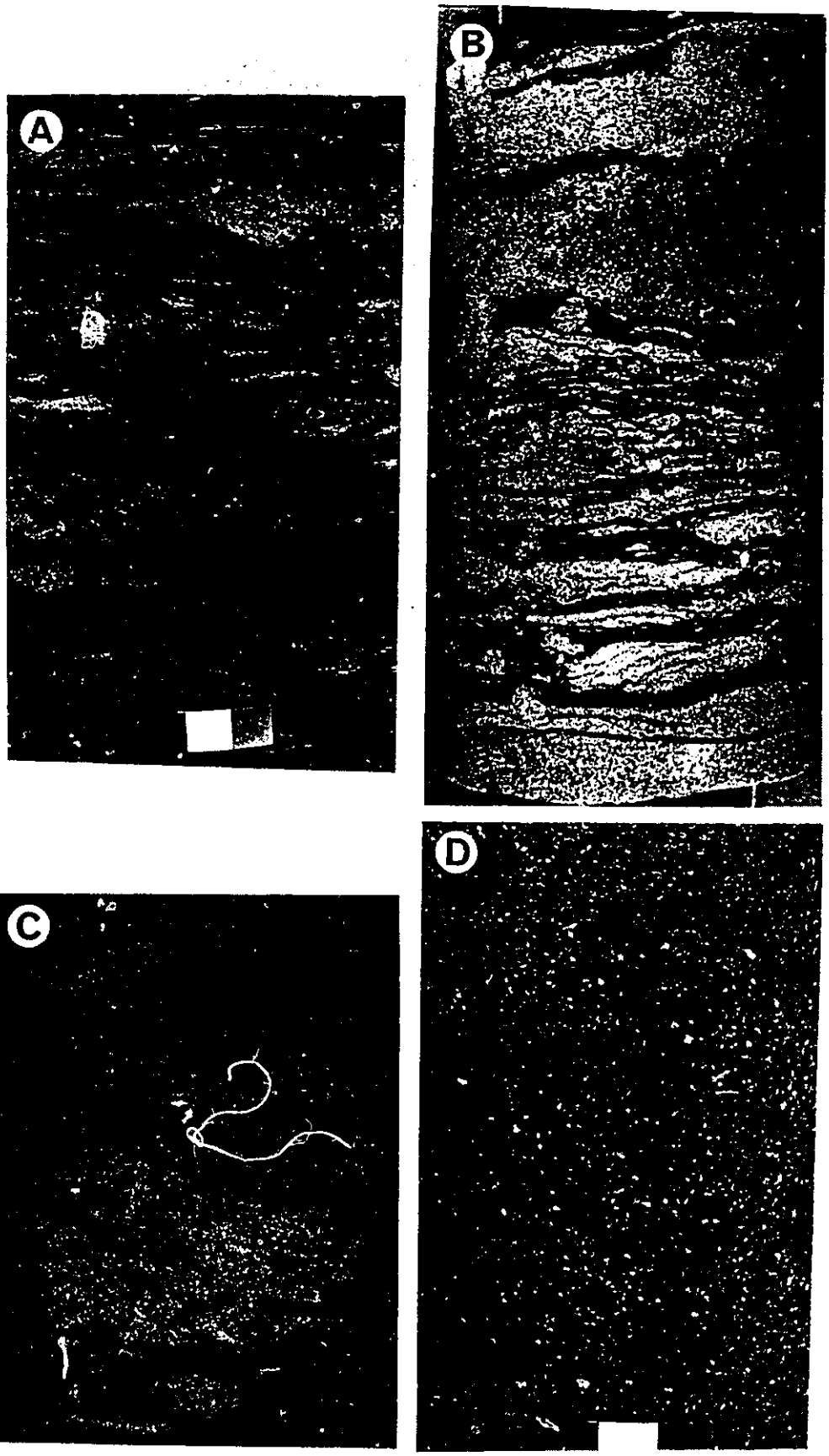
A
B
C
D

bioturbated to the point where no structure remains. Few distinct burrows are visible. The characteristic bioturbation takes the form of wisps or shreds of mud a few millimetres thick and centimetres long. A large portion of the mud in the facies occurs in such forms.

Secondary Criteria: Unidirectional high angle crossbeds may appear. Hints of low angle, 10° parallel lamination and crossbedding may be seen. Crossbedding may contain glauconite within crosslaminae. Alternatively, rare traces of glauconite may be found bioturbated within the facies or in *Arenicolites anorexia*. Sideritization (iron staining) is sometimes visible. Occasionally, *Skolithos* burrows along with abundant *Arenicolites anorexia* burrows appear. Rare accompanying burrows may include *Planolites* (3-4mm), *Chondrites*, *Rosselia* and *Muensteria*. Bentonites may occur.

3.4.12 MASSIVE SANDSTONE (n=35, avg=23cm); Figure 3-4D

Primary Criteria: Sedimentary structures are absent and burrows are extremely rare. Sand size varies from FL-VCU.

Secondary Criteria: Iron staining (sideritization?) may occur. In some cases, *Arenicolites anorexia* burrows occur pervasively, and *Muensteria* may be seen. Flat, centimetre size pieces of coal may also be found. As with many facies, granules and pebbles are also occasionally encountered along with rare sideritized mud clasts. Bentonites can be found. Very rarely, hints of low angle parallel or high angle cross bedding may be seen; however, when such lamination is more than sketchily visible the unit is placed in the crossbedded facies.

3.4.13 CROSSBEDDED SANDSTONE (see subdivisions for statistics)

Ideally, this facies would have been broken down into different facies each reflecting deposition from a major type of bedform. However, the condition of much of the core examined prohibits such a consistent subdivision. Many of units are poorly, or not, cemented and consequently badly preserved. Additionally, many pieces of core have been cut for large diametre permeability tests destroying the base of the sets. Frequently, the most that can be said of a sand is that it is crossbedded in some form. Subdivisions were made for those units that could be distinguished. Average set thickness has only an order of magnitude meaning.

Rarely, paleocurrent data can be obtained between successive cosets, or between isolated sets in core whose component pieces may be fit together. No core in the study was scribed so complete relative paleocurrents through units are unattainable. Paleocurrents were measured by taking the orientation of the steep cross-laminae with a card. There is some possibility, in the case of tangentially based crossbeds that the resulting relative paleocurrents might not correspond to genuine paleocurrents and instead merely reflect varying samples of orientations at the base of curved troughs. I do not think this is actually the case because the relatively flat nature of most set bases and the steepness of the cross-laminae in small sets suggests that there has not been much sampling of the sides of larger troughs. (This has implications also for the shape of the bedforms discussed in chapter 6.) The paleocurrents which were

Figure 3-5

Relative Paleocurrents (all crossbedding)

The figure shows the relative paleocurrents for all relatable sets within a core. The measurements are recorded in 10^{o} increments. Each rose is a separate set of relatable paleocurrents. Individual roses and separate cores cannot be related. The well number is above each rose. An R by the side of the rose indicates measurements from ripple cross stratification; the rest of the measurements are from crossbedding, usually tangential. The Greek letter at the hub of each rose indicates the unit from which the data is from.

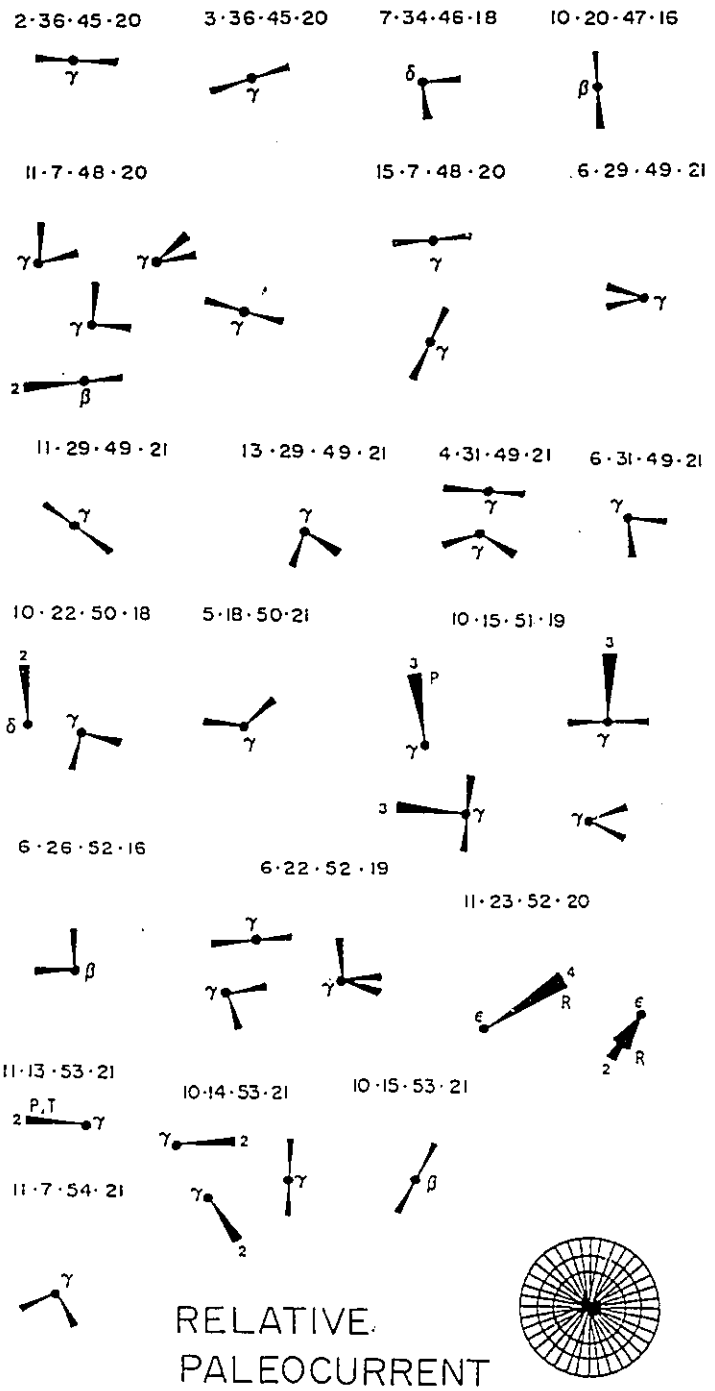
2·36·45·20
3·36·45·20
7·34·46·18
10·20·47·16
11·7·48·20
15·7·48·20
6·29·49·21
11·29·49·21
13·29·49·21
4·31·49·21
6·31·49·21
10·22·50·18
5·18·50·21
10·15·51·19
6·26·52·16
6·22·52·19
11·23·52·20
11·13·53·21
10·14·53·21
10·15·53·21
11·7·54·21
RELATIVE PALEOCURRENT DATA

Figure 3-6

Example of Divergent Paleocurrents

Well 4-32-56-24W4; depth: 2780 feet
The core is 3 inches in diametre and is slabbed across the right side.

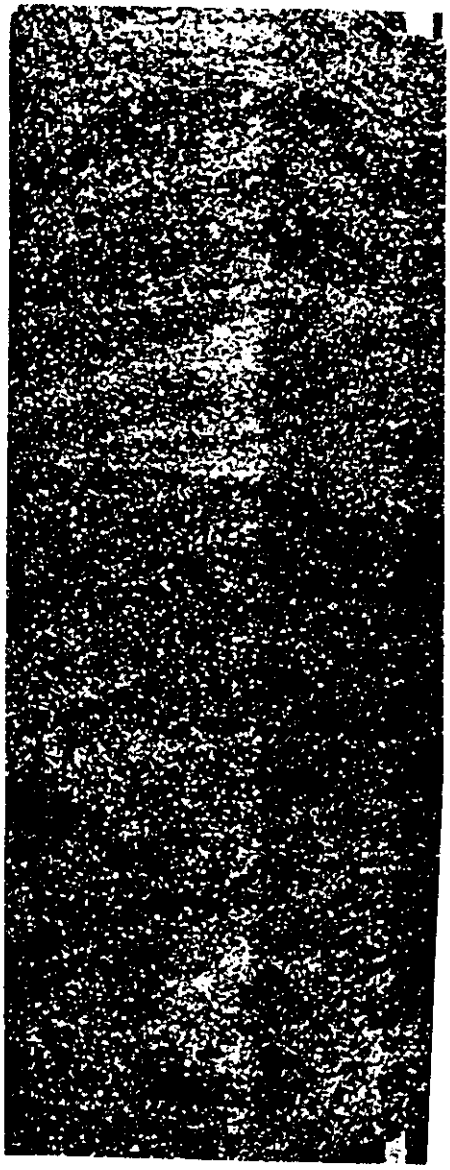

obtained are shown in figure 3-5. They are not absolute, in that their compass bearing is unknown. Furthermore, measurements are only relative within an isolated paleocurrent "rose"; they cannot be related between different wells or even within the same well were more than one rose is presented. There appears to be a slight tendency toward either unimodal or bimodal at 180° distributions, but possibilities may box the compass. Figure 3-6 shows a photograph of the rare occurrence of relatable sets showing different paleocurrents.

Crossbedded Sandstone: (n=135, avg=69cm); see below for figures.

Primary Criteria: FU-VCU sandstone occurs in this facies with cross laminae dipping in the range 25-30° . Some beds show grading from granules or VCU sand at the base up to MU-ML sand tops; others show inverse grading.

Secondary Criteria: In many cases, 1 to 10 centimetre beds of mudstone, which may be sideritized, separate sets or cosets. The mudstone beds may occupy up to 50% of the facies and may have sand laminae within them. *Arenicolites anorexia* and extremely rare *Rosselia* may occur in the sandstones; rare *Planolites* (3mm) may appear in the mudstones. Although most cross lamination is visible as the result of size variations in the sand, some are the result of the presence of fine mud cross laminae. However, there are no distinct couplets or bundle drapes (Visser, 1980). Reversing ripple cross lamination may be seen very rarely.

Tangential Parallel Crossbedded Sandstone: (n=125, avg=16cm); Figure 3-7A

Primary Criteria: Cross lamination and cross bedding in this facies show tangential curvature at the base which often increases in angle upward to 20° to 30°. The dip is unidirectional for a given set.

Secondary Criteria: The cross laminae may be enhanced by mud, sideritized mud, mud clasts (sometimes sideritized), and glauconite. In many cases, high angle cross stratification decreases in angle upward into low angle subparallel lamination typically going from 25° to 5° . This latter behavior is most visible when the facies occurs as a single set within another, often muddier, facies, but may be seen within cosets. Such cross stratification might reflect preservation of sigmoidal sets. There are occasionally stacked V-shaped 'kinks' in the cross lamination interpreted as *Arenicolites* burrows (see Appendix 1). Of the high angle crossbedding sets whose base is visible, this facies is most common.

Planar Parallel Crossbedded Sandstone: (n=50, avg=12cm); Figure 3-7B

Primary Criteria: The cross strata in this case may be traced to the base of the set where they meet the underlying strata abruptly without changing their angle.

Secondary Criteria: The set height may be as small as 5 cm. These smaller sets are just as common as the 10 to 20 cm scales sets and cosets. In some cases, the base is irregular and the laminae contain mud fragments. Some sets grade upwards into low angle sub-parallel lamination. Rare, 6 by 6 cm *Rosselia* and 3 by 4 cm *Bergaueria* may be seen in addition to *Arenicolites anorexia*. Heavy glauconite concentrations may occur in the cross laminae.

Figure 3-7
The crossbedded facies.

A. Tangential Parallel, Facies 14.
Well 2-18-48-20W4; depth 3214 feet
The scale bar is 3 cm long.

B. Planar Parallel, Facies 15.
Well 1-31-56-24W4; depth 2806 feet
The core is 3" in diametre; the scale bar is 3cm long.

C. Low Angle Parallel, Facies 16.
Well 6-3-58-25W4; depth 2518 feet
The core is 3" wide; the scale bar is 3 cm long.

D. Low Angle Intersecting, Facies 17.
Well 10-21-51-19W4; depth 2710 feet
The core is 3" in diametre; the scale bar is 3 cm long.

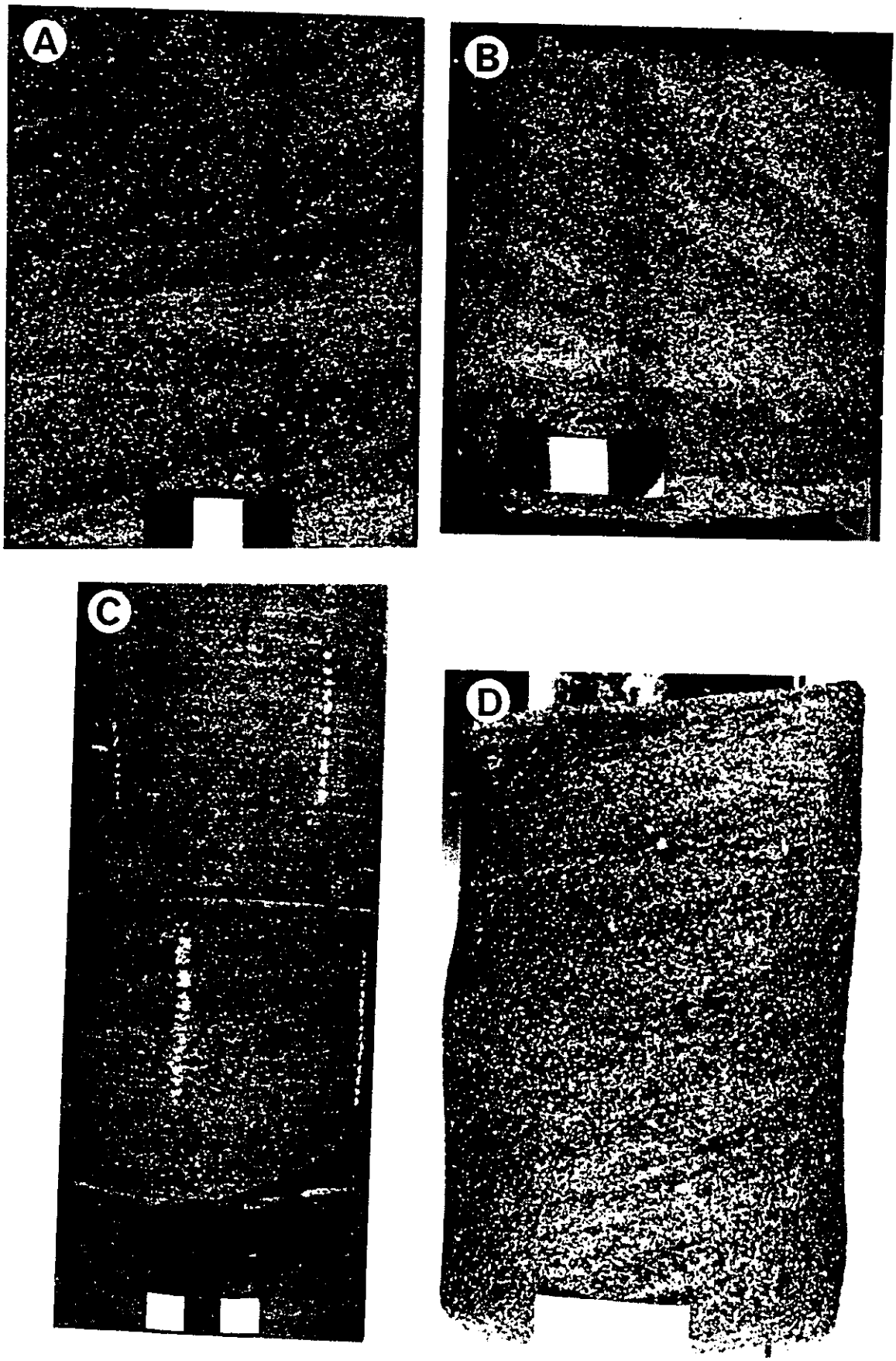
A
B
C
D

Low Angle Parallel Laminated Sandstone: (n=35, avg=22cm); Figure 3-7C

Primary Criteria: The laminations all lie within 5° of horizontal; subtle divergences may be present but usually are not visible.

Secondary Criteria: Grading may occur and V shaped laminae resembling the stacked V's of escape traces but interpreted as *Arenicolites anorexia* have been seen. Glauconite may occur abundantly in the cross laminae and units may show sideritization.

Low Angle Intersecting Crossbedded Sandstone: (n=28, avg=20cm); Figure 3-7D

Primary Criteria: The cross laminae in this facies have curved, tangential bases and steepen upwards but are overlain by the succeeding set of cross laminae dipping in a different orientation before the angle of dip reaches more than about 15°.

3.4.14 PEBBLY SANDSTONE (n=10,avg=82cm,); Figure 3-8A

Primary Criteria: This facies consists of abundant pebbles, or more commonly granules, within massive sand. The pebbles and granules are often circular (assumed spherical). The facies is very poorly sorted, and frequently contains some wisps of mud. There is no visible texture or structure.

Secondary Criteria: The maximum observed cross-sectional size is 20 by 18mm. Pebbles may come close to being clast supported, and the facies is obviously gradational with Conglomerate. There are rare hints of parallel bedding and imbrication; one example of faint crossbedding (type unknown) was seen. Siderite cementation can be very common. Mud lined *Arenicolites anorexia* may occur abundantly.

3.4.15 PEBBLY MUDSTONE (n=14, avg=24cm); Figure 3-8B

Primary Criteria: This facies is composed of 5%-50% coarse material (pebbles to sand) mixed into a matrix of mud and silt. The maximum apparent cross sectional axes visible in core for the pebbles are 15 by 10 mm. There are rarely any distinct burrows.

Secondary Criteria: The pebbles are sometimes siderite clasts, and large wood fragments may rarely be seen. Intense sideritization may also occur. Units are placed within this facies even if they only contain granule size material as long as the general aspect is similar. Occasionally, laminae of granules and pebbles may be made out within a unit.

3.4.16 CONGLOMERATE (n=16, avg=16cm)

This facies comprises predominantly pebbly material at least close to being clast supported. I make two subdivisions based on clast type: Rip Up Conglomerate and Chert Conglomerate (Figure 3-8C; 3-8D). This division is somewhat arbitrary as both clast types may occur together in varying proportions; the label is based on the predominant component.

Primary Criteria: The Rip Up conglomerate is composed of sideritic or phosphatic shale fragments usually on the order of 10 by 20 cm maximum apparent cross section. It is always close to being matrix supported. The chert conglomerate contains pebbles and granules (maximum size observed was 18 by 7 mm in core cross section) with intervening spaces commonly filled by matrix of sand. It is much more obviously clast supported. The matrix ranges from mud to VCU sand although there is an apparent dearth of material in the F range. The

Figure 3-8

A. Pebbly Sandstone, Facies 18.
Well 6-29-59-1W5; depth: 2772 feet
The core is 3" in diametre with a 3 cm scale bar.

B. Pebbly Mudstone, Facies 19.
Well 1-1-45-20W4; depth: 3283 feet
The core is 3" in diametre with a 3 cm scale bar.

C. Diagenetic Clast Conglomerate, Facies 21.
Well 14-32-448-20W4; depth: (1000 metres); 3280 feet.
The core is 3" wide. The scale bar is 3cm long.

D. Chert Conglomerate, Facies 20.
Well 10-18-61-4W5; depth: 3056 feet
The core is 3" in diametre with a 3 cm scale bar.

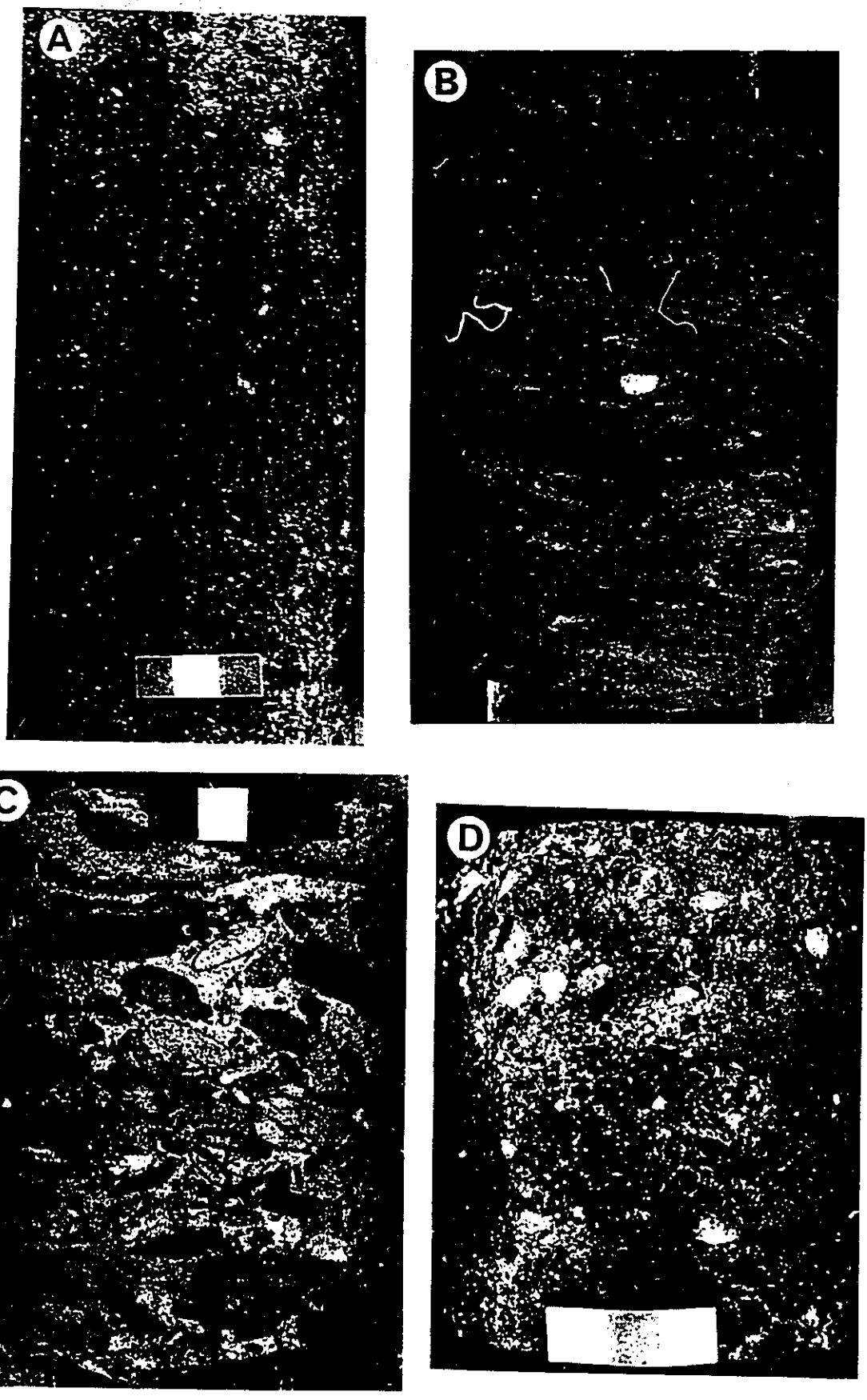
A
B
C
D

Figure 3-9.

Slumped Siltstone, Facies 22.
Well 10-1-52-19W4; depth: 2546 feet
The core is 3" in diametre.

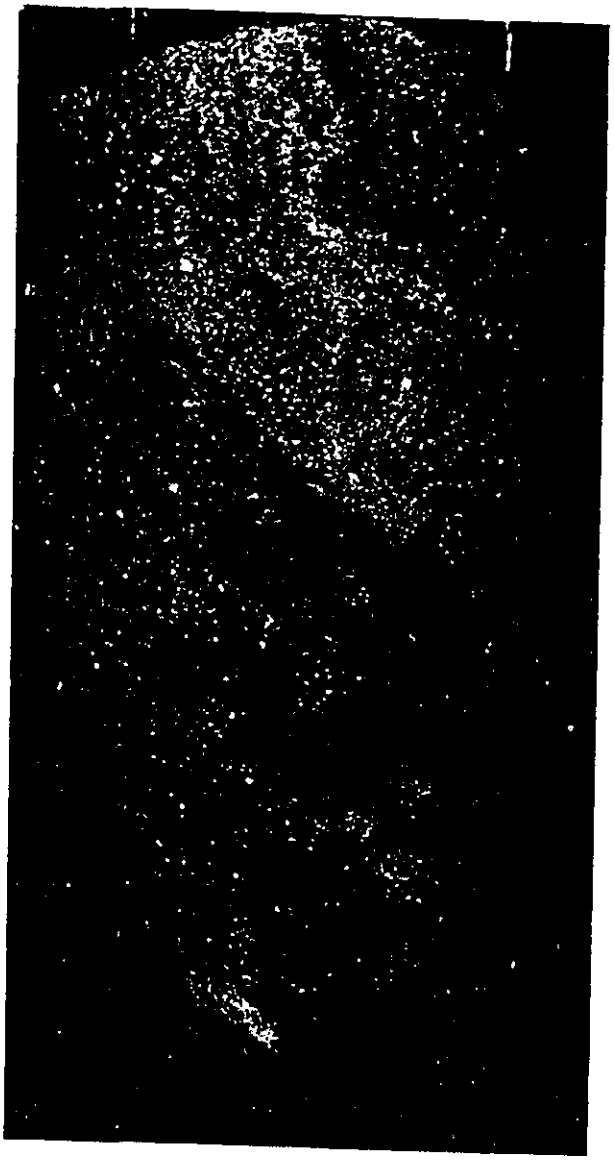

pebbles seem roughly spherical based on a the observation that most exposures at the side of the core are approximately circular. No structures or preferred clast orientation are visible although rare hints of parallel (?) bedding may be seen.

Secondary Criteria: Both forms of this facies are very rare within the area studied. Siderite cement is sometimes observed.

3.4.17 SLUMPED SILTSTONE (n=2, avg=26cm); Figure 3-9

Primary Criteria: This facies shows distinct slumping or contortion of laminae or equivalent warping of 'bands' of bioturbation. The facies is not common and occurs within other mudstone units.

CHAPTER 4

UNIT DESCRIPTIONS:

LOG CORRELATIONS, PETROGRAPHIC ANALYSES

AND FACIES COMPONENTS

"A curious and amusing implication of this model is that all of the "aberrant" kinds of thoughts listed ... are composed, at rock bottom, completely out of beliefs..."

D. Hofstatder
Godel, Escher, Bach: An Eternal Golden Braid

4.1 SUMMARY

The Viking Formation in east central Alberta may be divided into six units, five of which extend across the area studied. The units are defined on the basis of interactive examination of core and well logs. The unit boundaries are lithological rather than allostratigraphic; they are placed at the tops of gradational sequences at points of rapid facies changes which coincide with changes in the percentage of sand present. There are no visible, extensive discontinuities. The facies represented across the boundaries, as well as their expression in the well logs, change across the basin, so their correlation is a matter of tracking variations rather than matching a fixed signal. The units are petrographically homogenous chert (or quartz) arenites. The bentonites contained within them are also chemically indistinguishable (Appendix B). The homogeneity includes both mineralogic composition and diagenetic successions. Thus, confirmation of the unit correlations does not seem possible by petrographical means.

The units have been labeled Mu, Epsilon, Delta, Gamma, Beta and Alpha in ascending order. Areal distribution of the maximum grain size is usually random for each unit except in unit Gamma where there is a roughly eastward decrease. Mu is only a thin local accumulation in the south east part of the study area and its facies composition is uncertain. Epsilon, Delta and Gamma are composed primarily of mixtures of facies 8, 9, 10, 11, 13, 14, 15 and 16. Beta is composed mostly of facies 2, 4, 5, 6 and 7. Alpha is mostly mudstone (facies 1) with occasional laminae of coarser sediment, up to granule size and fairly frequent siderite concretions.

4.2 INTRODUCTION

As discussed in Chapter 1, most formations are now described in terms of units. Sequence boundaries may theoretically be placed anywhere within a sequence, but some locations are more practical than others. Galloway (1989a) argued that the boundaries should be placed at the point of maximum transgression. This location is arguably the most gradational of all within the sequences and is difficult to locate (see below). The "seismic stratigraphic" approach to locating sequence boundaries, as described by Vail et al. (1977) and Posamentier et al. (1988), is more practical in that it places sequence boundaries at unconformities interpreted as representing lowstands. The unconformities are inherently more readily located than the non-lithologically expressed gradational transition chosen by Galloway (1989a). Closely related to the seismic stratigraphic approach is the North American Stratigraphic Code's allostratigraphic approach which has been used to describe formations divided by unconformities in a manner analogous to the divisions of seismic stratigraphy.

In practice none of these three approaches applies to the units of the Viking Formation as studied in this work because the most practical unit boundaries do not fit any of the above schemes. Yet, the type of unit boundary present in the Viking may represent general unit behavior in the basinal marine sediments of foreland basins. The sediment packages in the Viking are, nevertheless usefully described as units because they extend over the entire study area. Furthermore, despite variation in the exact facies transitions from unit to unit laterally within a unit, the units themselves represent fundamental variations in conditions of deposition. The interpretation of unit boundaries is discussed more thoroughly in chapters 6 and 7. The differences between the Viking unit boundaries and sequence stratigraphic boundaries leads to variations in interpretations of the units themselves; these too are discussed in greater depth in chapters 6 and 7 after the unit boundaries, correlations and compositions have been described.

4.3 UNIT BOUNDARIES IN THE VIKING

4.3.1 Boundary Definitions

Unit boundaries in the Viking have been located at points of rapid facies changes which correspond to points of rapid change in sand content. These changes usually show up as marked deflections in spontaneous potential (SP) and/or resistivity logs across the formation at the tops of gradationally based patterns. This is a practical division in that such lithological points are more readily located than the point of maximum transgression. Moreover, unit boundaries have been so defined because there are no regionally extensive disconformities allowing for an allostratigraphic or seismic stratigraphic division.

However, these unit boundaries do not necessarily correspond to a fundamental point on a theoretical sea level curve such as onset of transgression or even the point of maximum flooding rate following the parasequence interpretation (Van Wagoner et al., 1990) [see chapter 7].

In more detail, the boundaries are marked by rapidly gradational, but not usually scoured, facies changes and rarely by thin granule or pebble layers. The gradations occur over the space of one to two decimetres but may be instantaneous. This style of unit boundary is similar for all the units except Alpha. The lack of regionally correlatable disconformities is the most significant observation from the point of view of currently popular sequence definitions.

4.3.2 Scoured 'Boundaries'

Although discontinuities are not widespread in the area of the Viking Formation studied, and cannot therefore be used as unit boundary criteria, they do exist. Such scours and sharp facies changes within coarsening upward successions are laterally equivalent to gradational changes in facies successionss. For example, in cross-section A-A' (foldout 1 in the rear pocket) compare the Delta-Gamma transition in well 6-8-51-18W4 to that in well 10-22-50-18W4. Because of the predominance of gradational transitions in most of the cores observed (see foldouts 8 through 12 for representative cross-sections) only the rapid change at the top of the coarser, sandier units can easily be traced laterally; this is particularly the case with well log correlations. There is no indication of where the scoured surface would be traced laterally if it were taken as a fundamentally important point such as a sequence boundary. The isolation of such scours strongly suggests that they reflect local processes rather than regional

Figure 4-1. Examples of Sharp, Scoured Contacts near Unit Boundaries

A. Core 10-19-52-19W4; depth: 2671 feet
Top of unit Delta; core is 3" in diametre

B. Core 10-23-50-15W4; depth: 2168.5 feet
Top of unit Delta; scale bar is 3 cm long

C. Core 4-4-49-14W4; depth: 2307 feet
Top of unit Delta; core is 3" in diametre

D. Core 10-29-50-14W4; depth: 2138 feet
Top of unit Beta; scale bar is 3 cm long

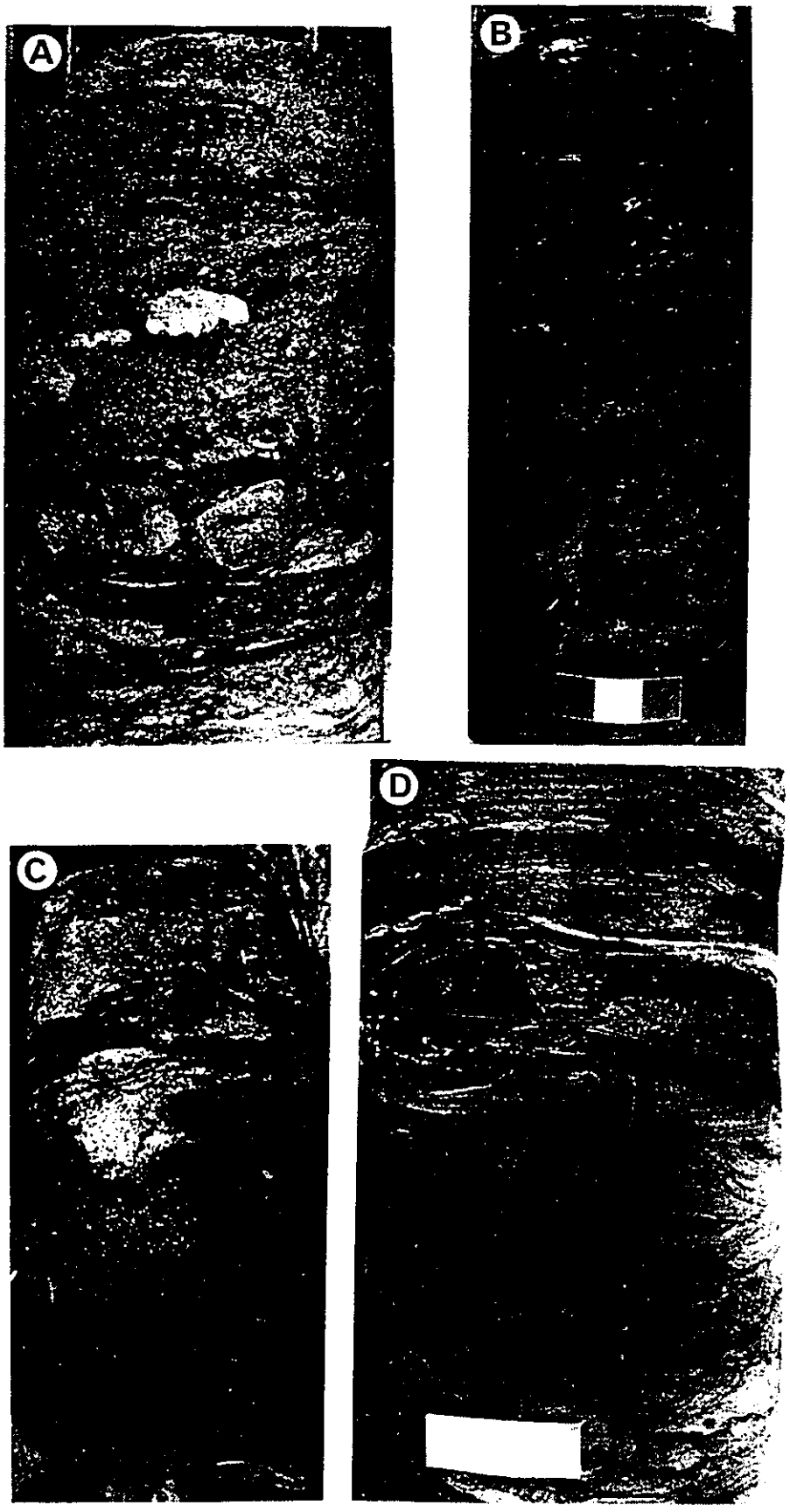
A
B
C
D

behavior that should be evident for classification as part of a sequence component.

Figure 4-1 shows examples of the rarer cases of scoured contacts that coincide with sequence boundaries. I emphasize that these are exceptions to the usual gradational style of unit boundary. Such sharp transitions are often marked by a veneer of coarse sediment ranging from sand to pebbles in size. The transition is usually from a bioturbated sediment (facies 9 or 11) into, ultimately, either similar but muddier facies or a laminated siltstone (facies 2). The coarse material on the scoured surface may be massive sandstone, crossbedded sandstone (usually an isolated set) or conglomerate. The conglomerate components are mixtures of chert and "autoconglomerate" visible in figure 4-1 a, b and d. The "autoconglomerate" comprises sideritized and phosphatized shale clasts. The sharp contacts may also have a large number of penetrating *Arenicolites anorexis* traces filled with the coarser overlying sediment. Other burrows may be present (see fig. 4-1 c ,d).

The entire variety of scoured/sharp transitions occurring is shown schematically in the core cross-sections in foldouts 8 through 12 (rear pocket). It must be emphasized that in all units, these are local scours correlating laterally into gradational boundaries. The boundary between unit Delta and Gamma comes the closest to being a discontinuity by virtue of having the most extensive occurrences of sharp scoured contacts; however, this boundary still has many cases of lateral equivalence to gradational units. For example, at the Delta-Gamma boundary in cross-section A-A' (foldout 8), well 11-23-52-20W4 shows muddy sandstone to crossbedded sandstone, well 6-8-51-18W4 shows mottled

siltstone to massive sandstone and well 10-33-51-19W4 shows a mottled siltstone to autoconglomerate transition.

4.3.3 Rapidly Gradational Unit Boundaries

The more typical transition between units is more difficult to display because of its comparatively extensive nature. The majority of transitions are like those that may be seen in figures 4-2 through 4-9 which show photographs and lithologs of typical cores through the units. The transition from Delta to Gamma in 10-21-51-19W4 (fig. 4-6) is a prime example of a rapidly gradational boundary. This same boundary correlates into the examples shown in figure 4-1 a,b and c. Further illustrations of the placement of unit boundaries may be seen in foldouts 8 through 12. Comparing the core photos of figures 4-2, 4-4, 4-6 and 4-8 to the lithologs for each core placed next to the appropriate well log in figures 4-3, 4-5, 4-7 and 4-9 should give a good impression of the graphic representation.

4.4 LOG UNITS

4.4.1 Resistivity and SP Correlation

The core based details of unit boundaries described above have been correlated primarily on the basis of their well log signatures. Both Spontaneous Potential (SP) and resistivity logs were used. The well log correlations show the extensive nature of the sediment packages in the Viking and are the justification for their description as units. This section concentrates on the well log signature of each unit with only minor reference to the core descriptions. The full core based unit descriptions are given in a later section. Representative correlations are visible in foldouts 1 through 7 in the rear pocket. The well logs are more useful than the

Figure 4-2. Core from Well 11-11-51-12W4 (three pages)

The core is three inches in diametre and two and a half feet tall. The depths are as tagged from 1990 feet to 1945 feet; the base is shown first to the left; top is up.

Tags to the side of the core mark the locations of unit boundaries. The core shows the top of unit Delta and the base of unit Beta coinciding; at this point unit Gamma has pinched out and does not have a physical representation. The upper portion of the core also contains the transition from unit Beta to Alpha. Unit Alpha occupies most of the core. The final page shows the transition from the slightly silty unit Alpha to the un-named shales overlying the Viking Formation.

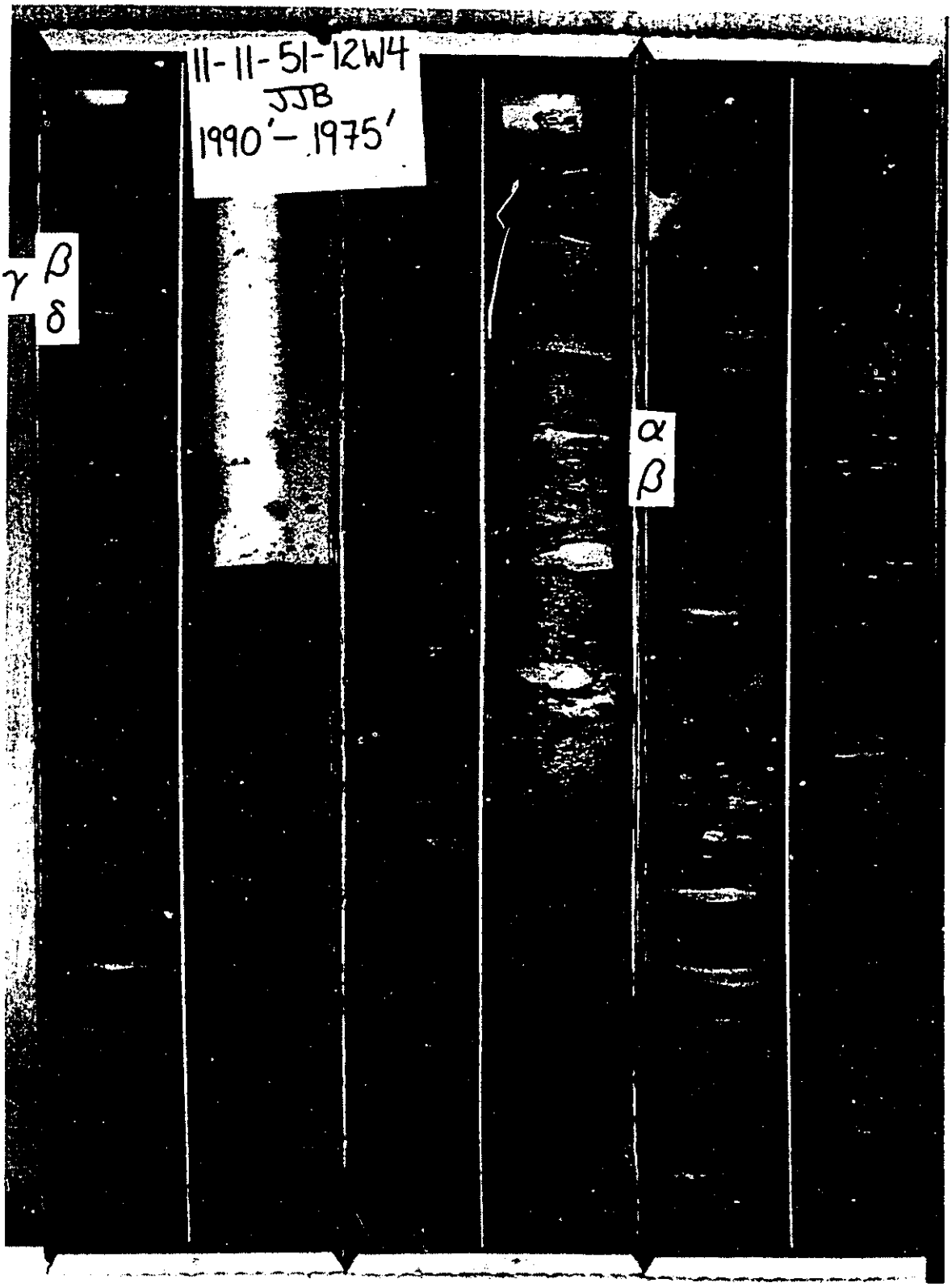
11-11-51-12W4
JJB
1990'-1975'
γ β
δ
α
β

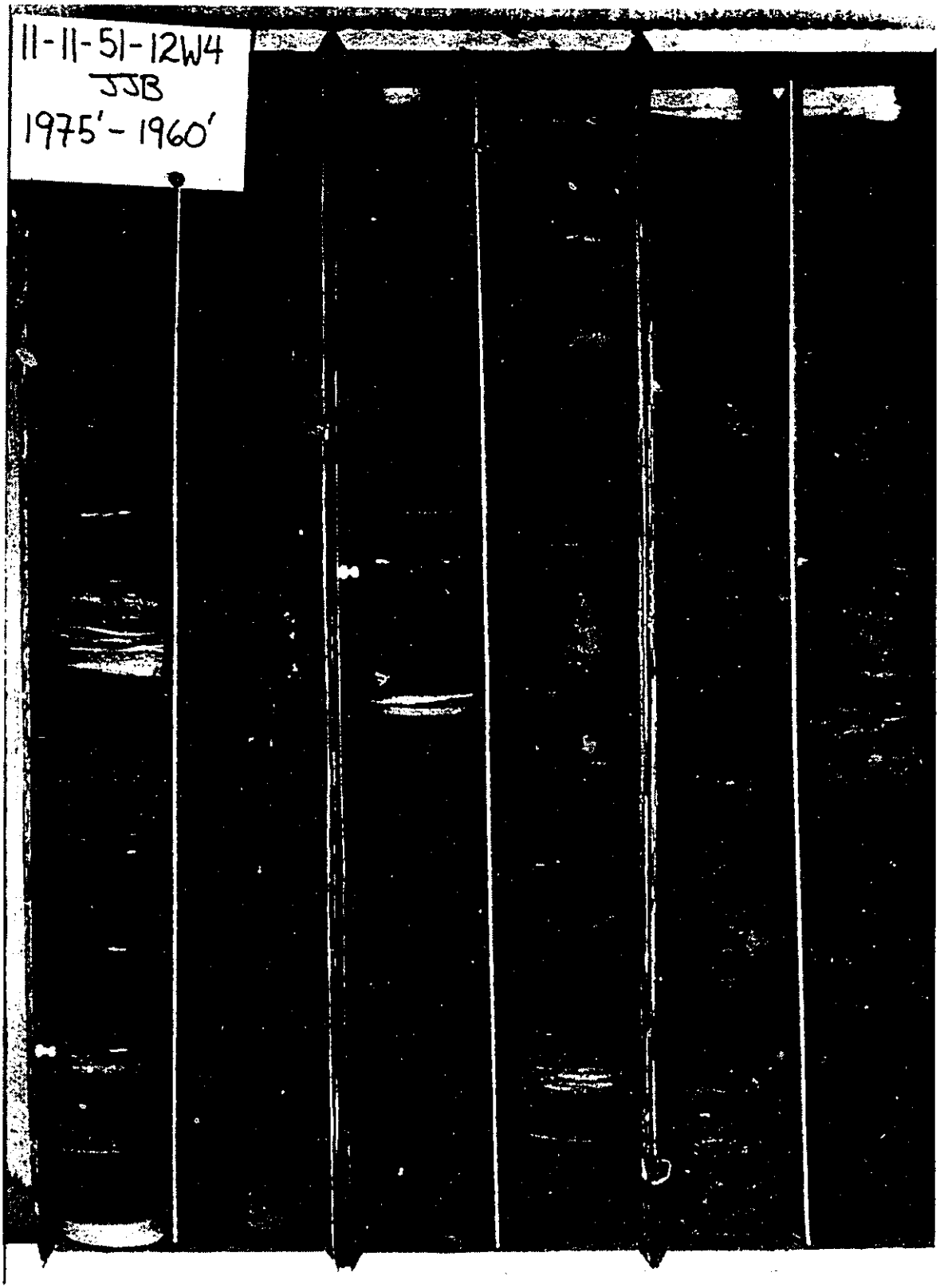
11-11-51-12W4
JJB
1975' - 1960'

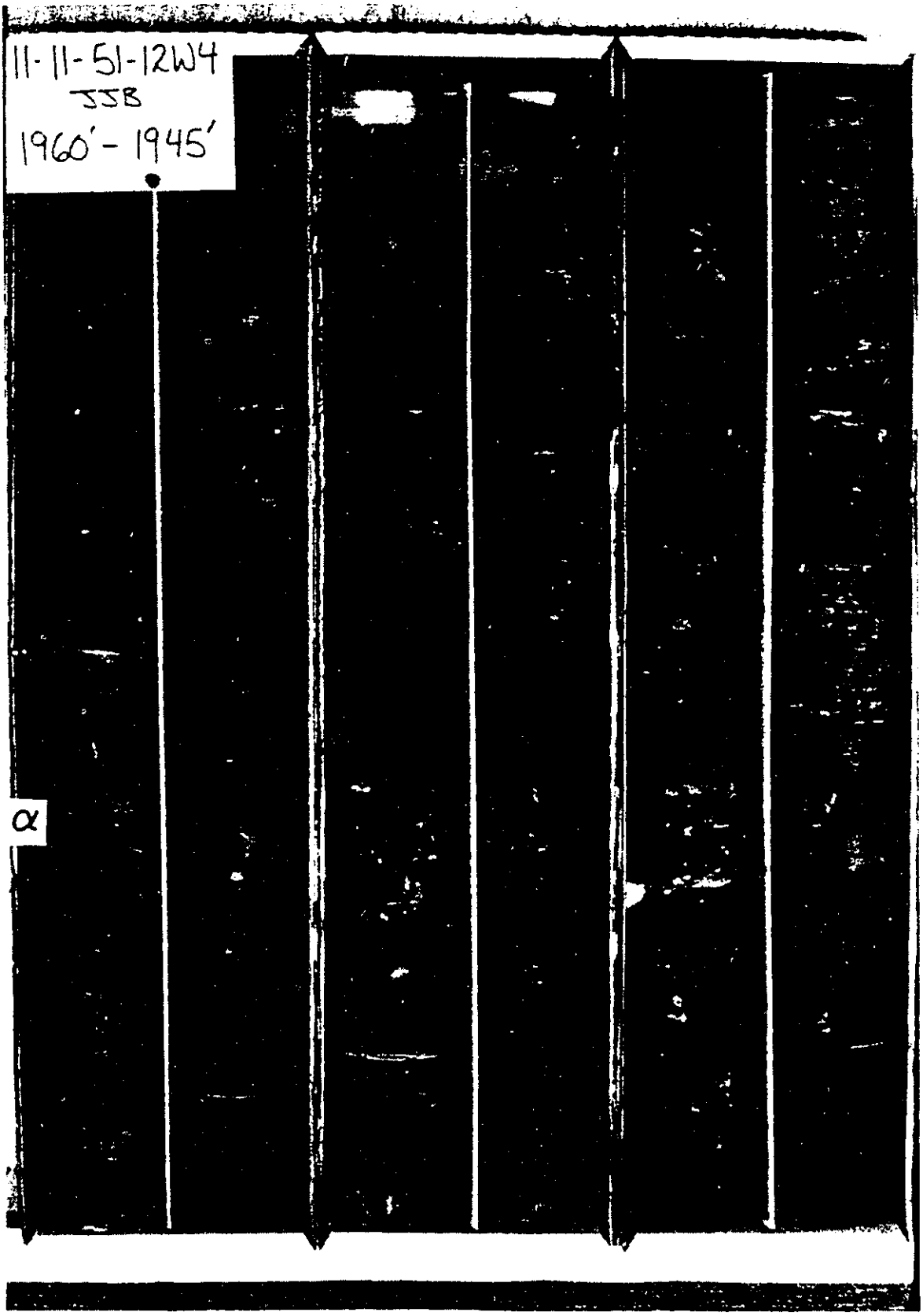
11-11-51-12W4
JJB
1960' - 1945'
α

Figure 4-3. Litholog of Core 11-11-51-12W4 Shown Against Its Resistivity and SP Logs.

The litholog uses the same facies scheme as shown in figure 3-1. Heavy straight lines mark unit boundaries. The trace on the left is the SP and that on the right is the resistivity.

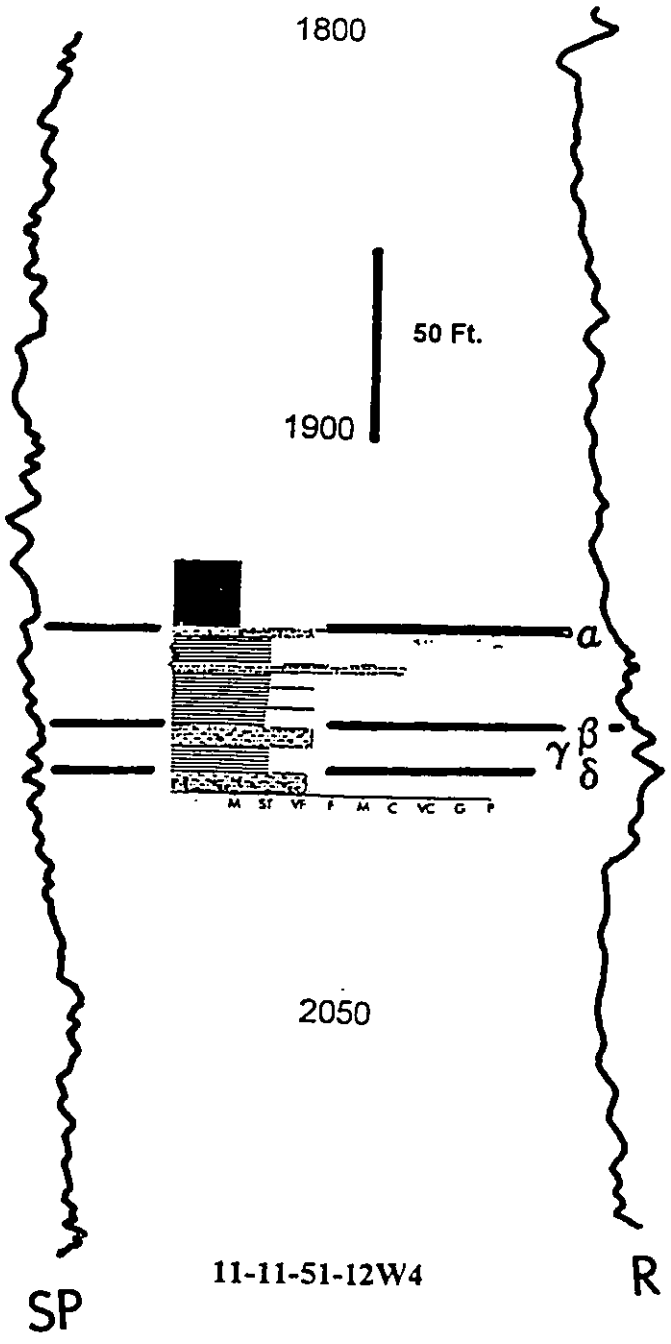
1800
50 Ft.
1900
α
β
γ
δ
M St VF F M C VC G P
2050
SP
11-11-51-12W4
R

Figure 4-4. Core from Well 10-22-50-18W4 (2 pages).

The core is three inches in diametre and two and a half feet tall. The depths are as tagged from 2560 feet to 2530 feet; the base is shown first to the left; top is up.

Tags to the side of the core mark the locations of unit boundaries. The core shows the rapid transition from unit Gamma to unit Beta. (The transition is not preserved intact, but other cores and log responses show changes occurring over the space of a few inches.) The core shows a typical assembly of facies for units Gamma and Beta.

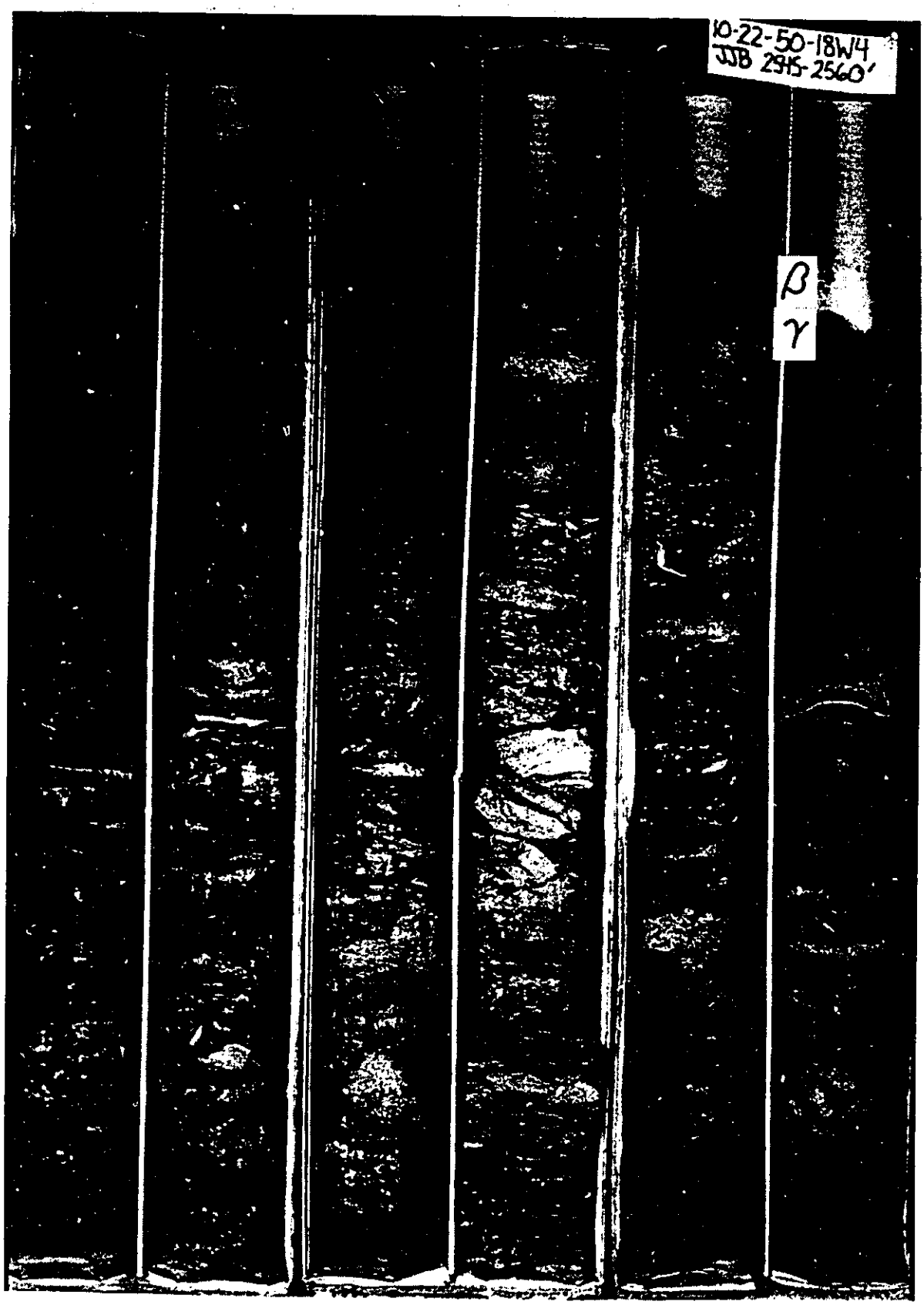
10-22-50-18W4
JJB 2915-2560'
β
γ

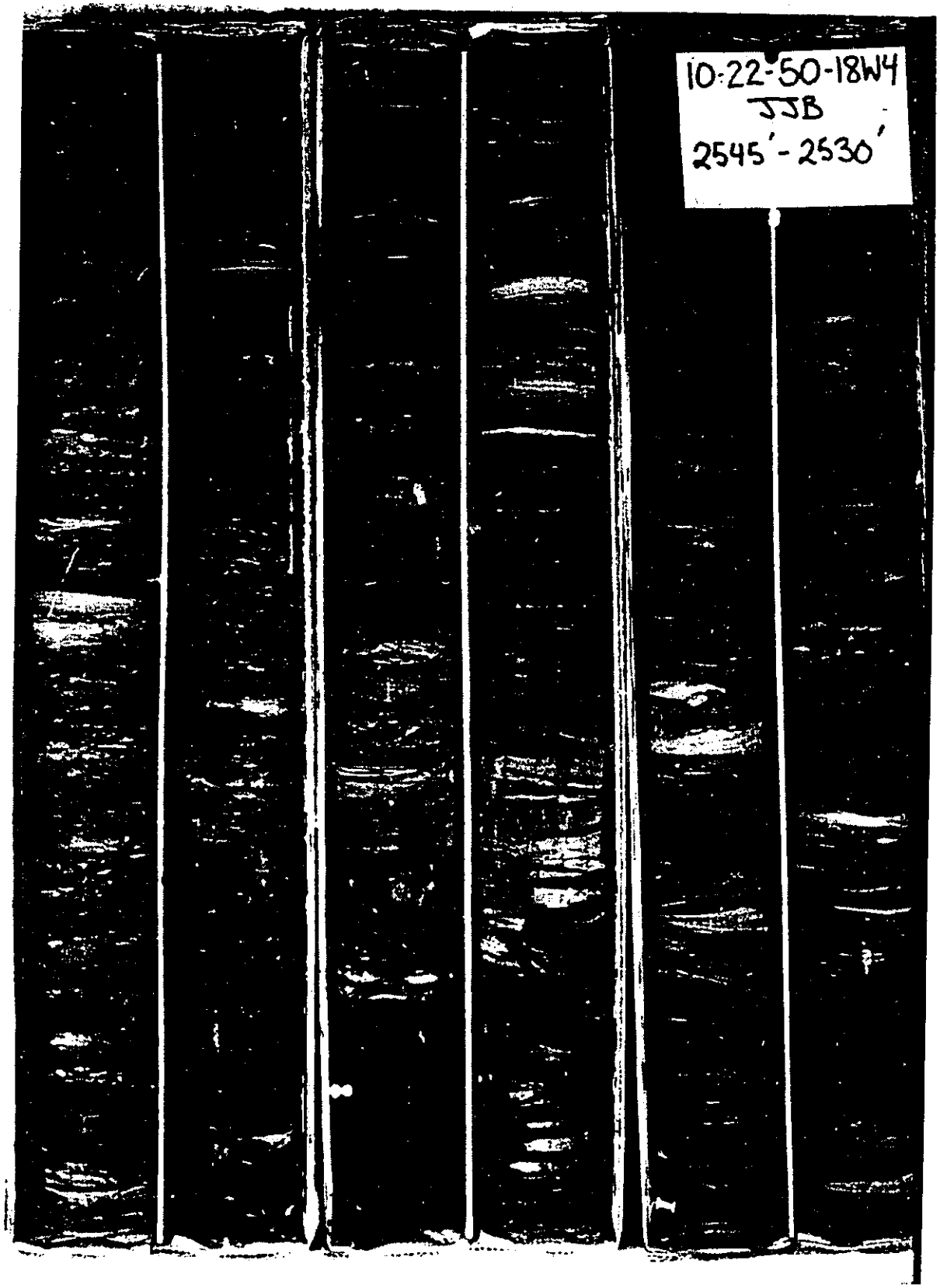
10-22-50-18W4
JJB
2545' - 2530'

Figure 4-5. Litholog of Core 10-22-50-18W4 Shown against Its Resistivity and SP Logs.

The litholog uses the same facies scheme as shown in figure 3-1. Heavy straight lines mark unit boundaries. The trace on the left is the SP and that on the right is the resistivity.

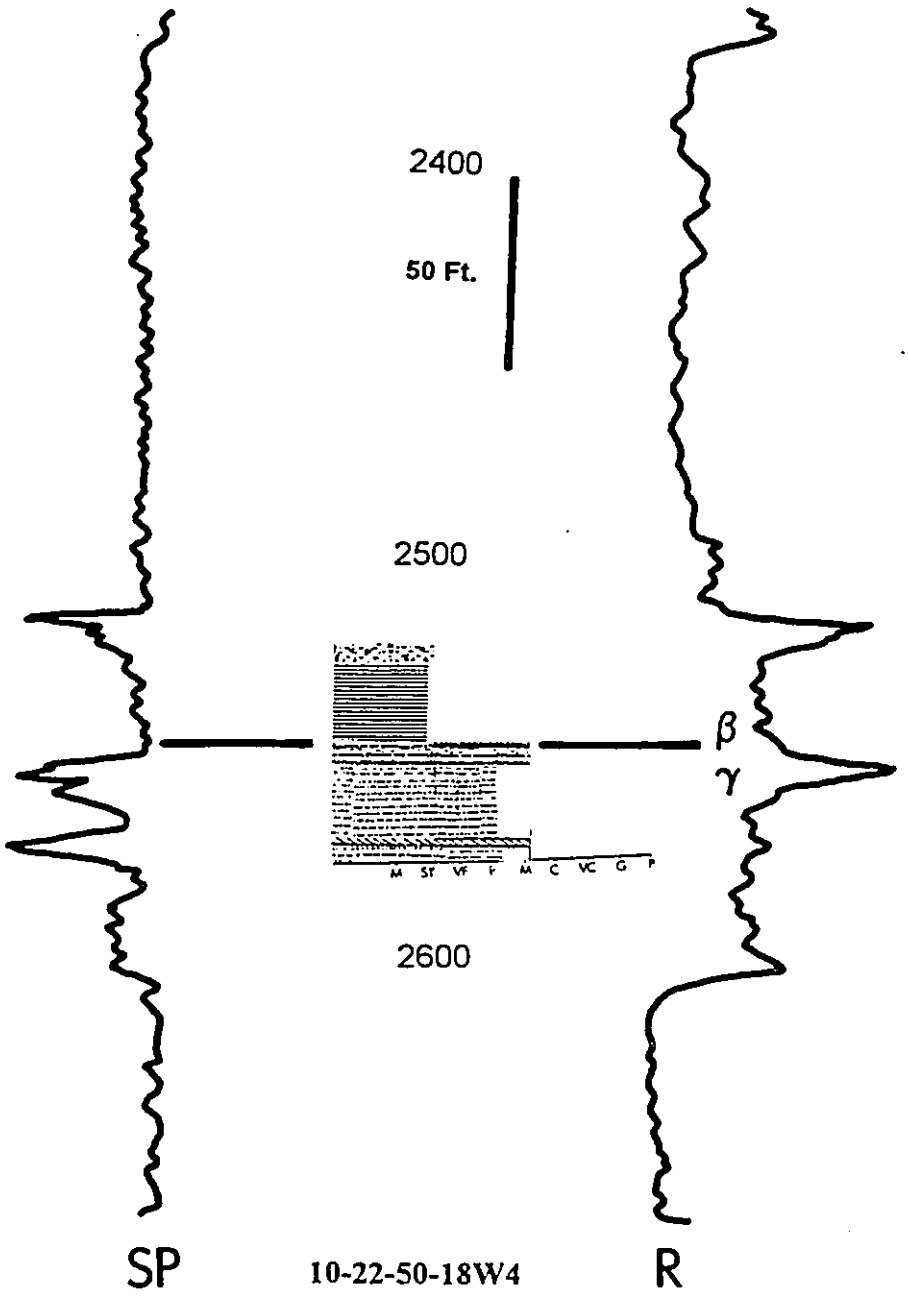
2400
50 Ft.
2500
β
γ
2600
SP
10-22-50-18W4
R

Figure 4-6. Core from Well 10-21-51-19W4 (4 pages).

The core is three inches in diametre and two and a half feet tall. The depths are as tagged from 2757 feet to 2705 feet; the base is shown first to the left; top is up.

Tags to the side of the core mark the locations of unit boundaries. The core shows a typical section through unit Delta and an example of the Delta to Gamma boundary. There is a complete record through gradational unit Gamma, and a good example of the Gamma to Beta boundary.

10-21-51-19W4
JJB
2750'-2757'

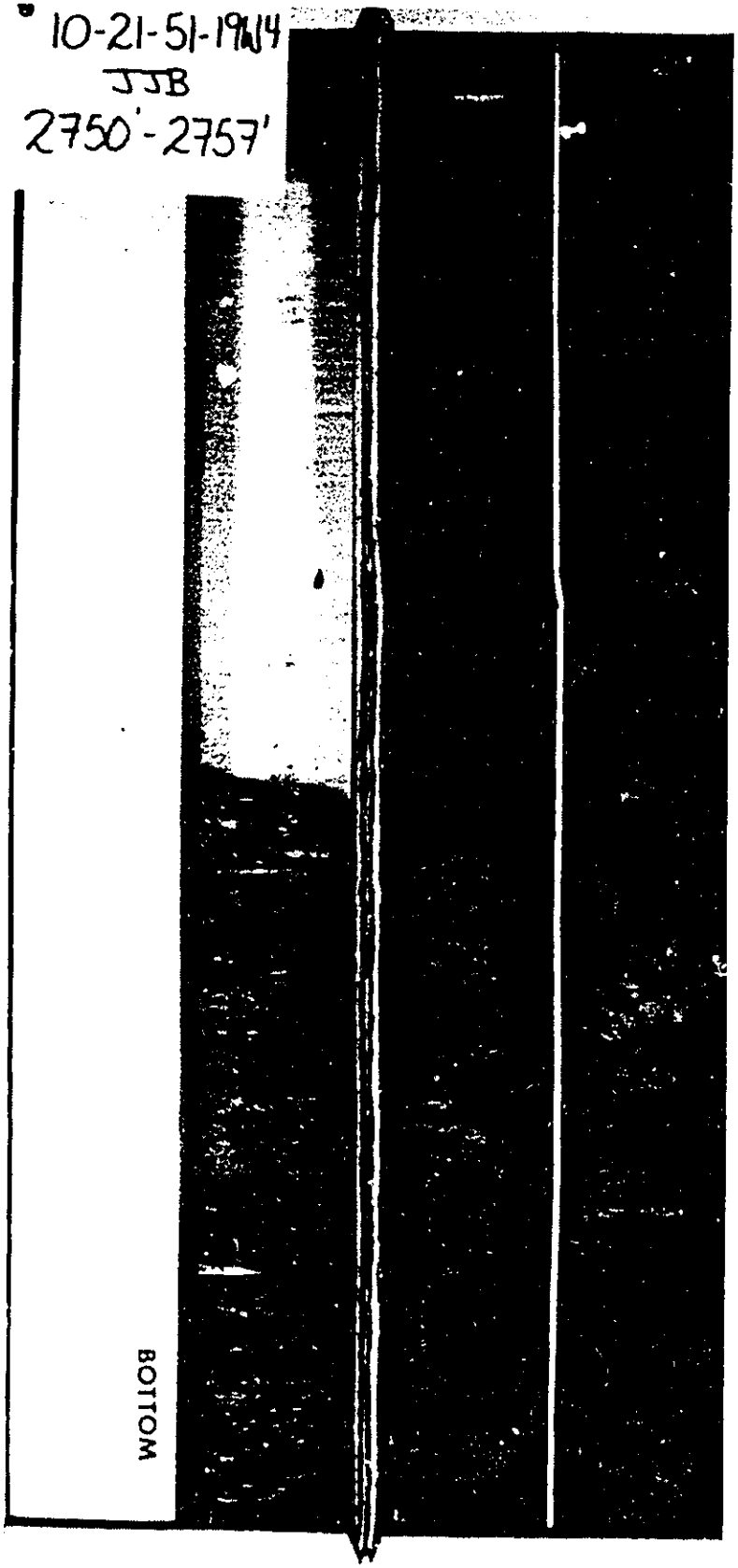

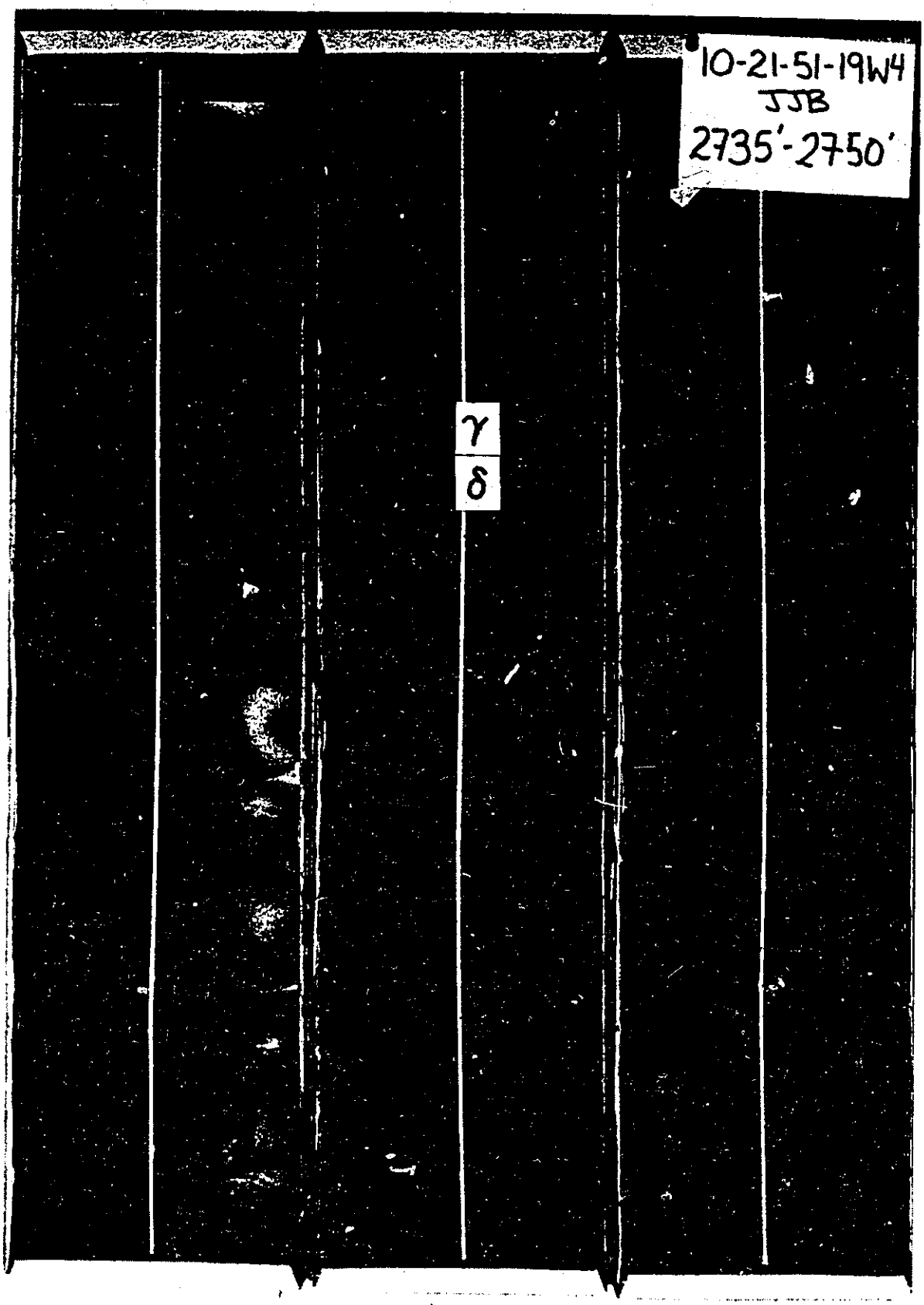
10-21-51-19W4
JJB
2735'-2750'
γ
δ

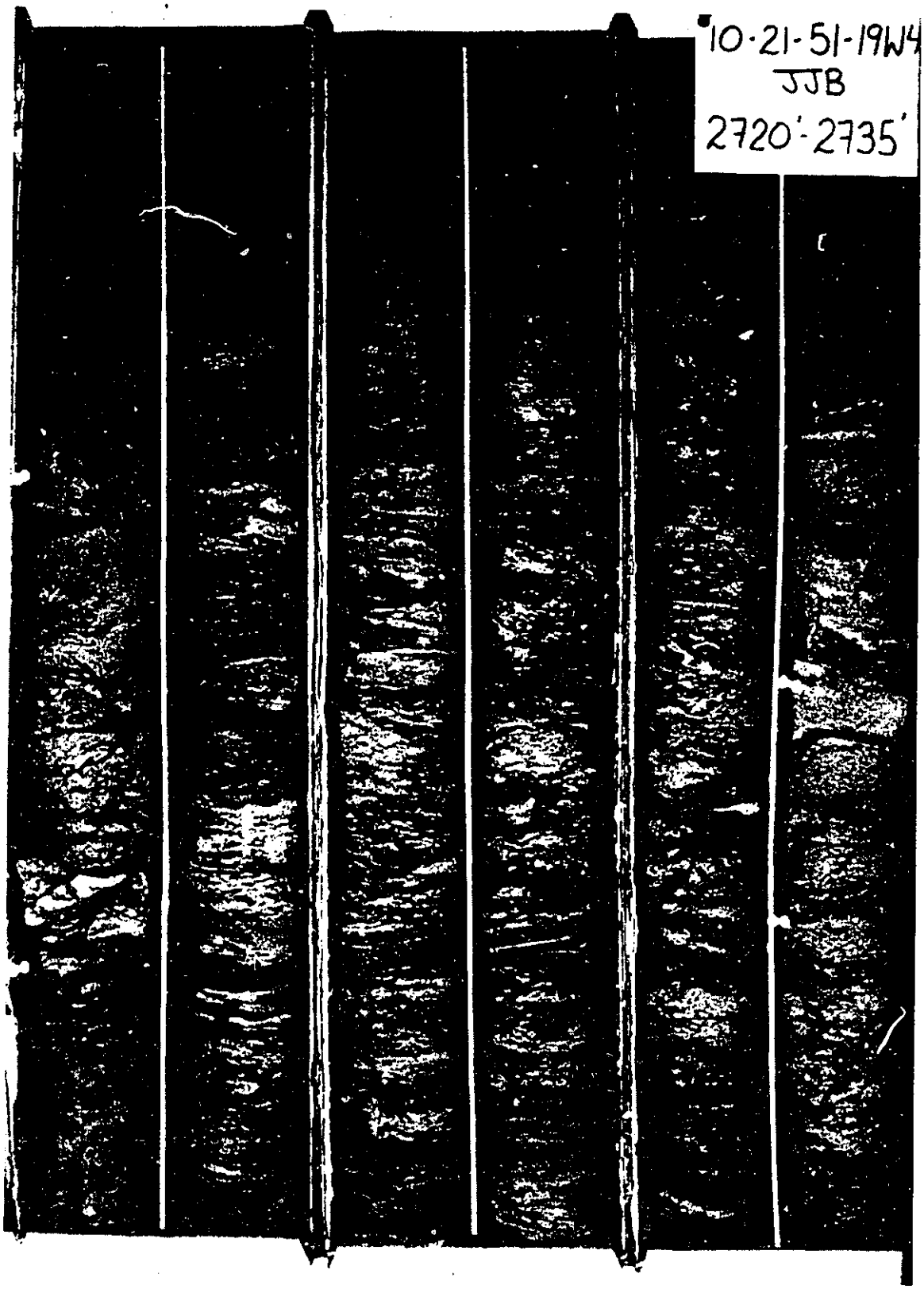
10-21-51-19W4
JJB
2720'-2735'

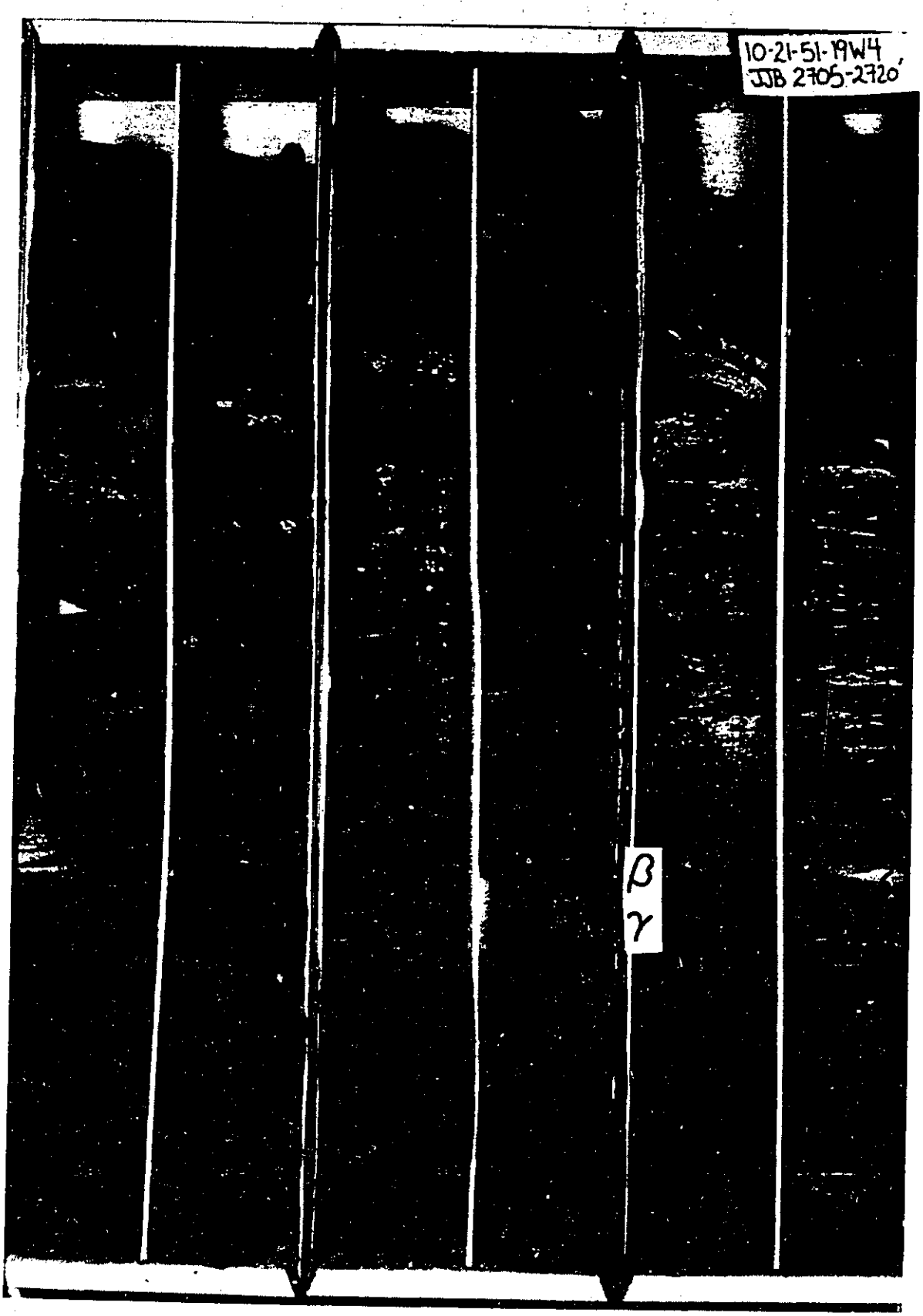
10-21-51-19W4
JJB 2705-2720'
β
γ

Figure 4-7. Litholog of Core 10-21-51-19W4 Shown against the Appropriate Well Log.

The litholog uses the same facies scheme as shown in figure 3-1. Heavy straight lines mark unit boundaries. The trace on the left is the SP and that on the right is the resistivity.

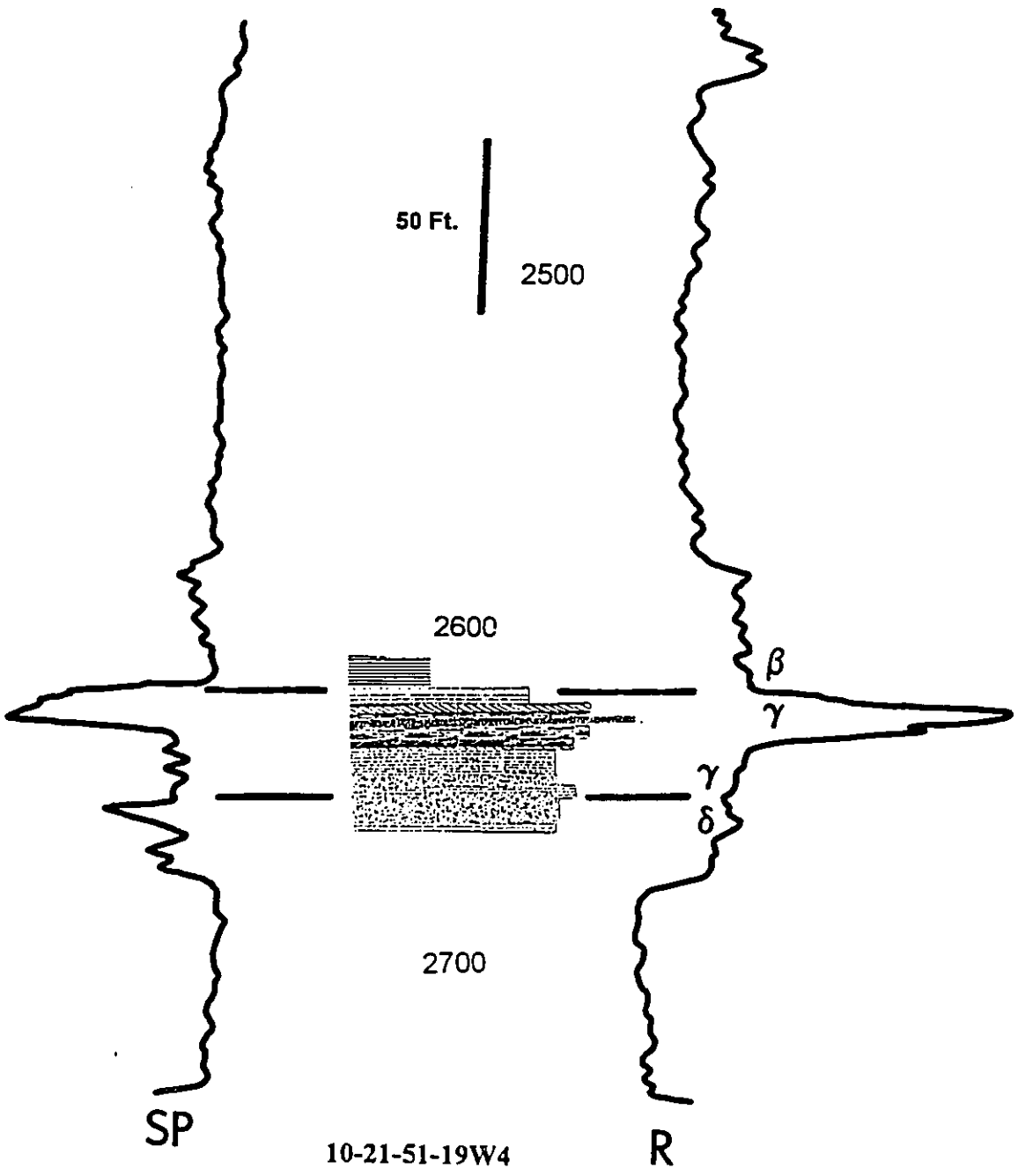
50 Ft.
2500
2600
β
γ
γ
δ
2700
SP
R
10-21-51-19W4

Figure 4-8. Core from Well 11-29-49-21W4 (2 pages).

The core is three and a half inches in diametre and two feet tall. The depths are as tagged on the boxes from 1015 metres (3329 feet) to 1001 metres (3283 feet). The base is shown at the bottom left; top is up.

Tags to the side of the core mark the locations of unit boundaries; in this case only the rapid change from Gamma to Beta is visible.

The core shows an excellent example of the gradational nature of unit Gamma even in its westernmost (toward the basin margin) occurrence. Of special note are the bentonites visible as large white discs of core in the second set of core boxes from the bottom (at approximately 1011 and 1010 metres).

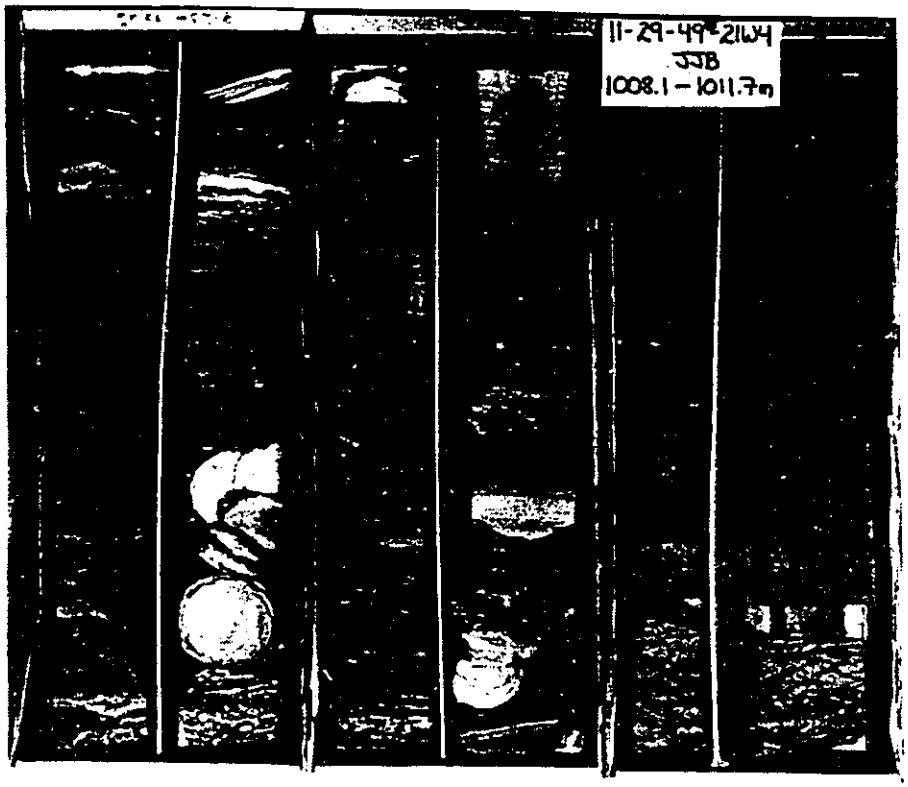
11-29-49-21W4
JJB
1008.1 – 1011.7m

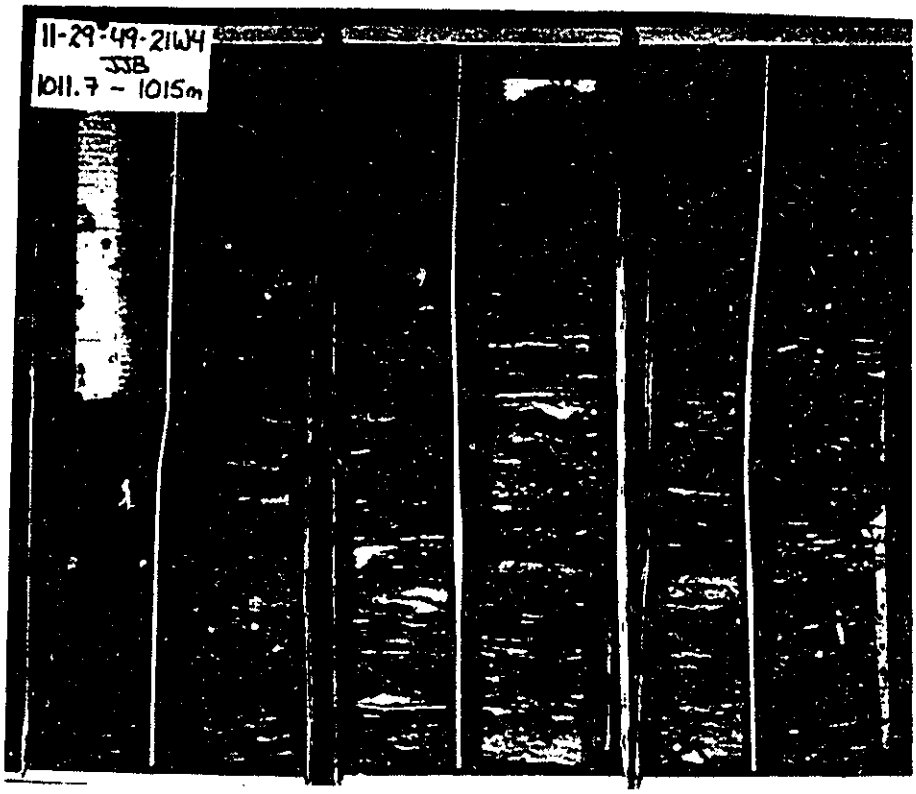
11-29-49-21W4
JJB
1011.7 – 1015m

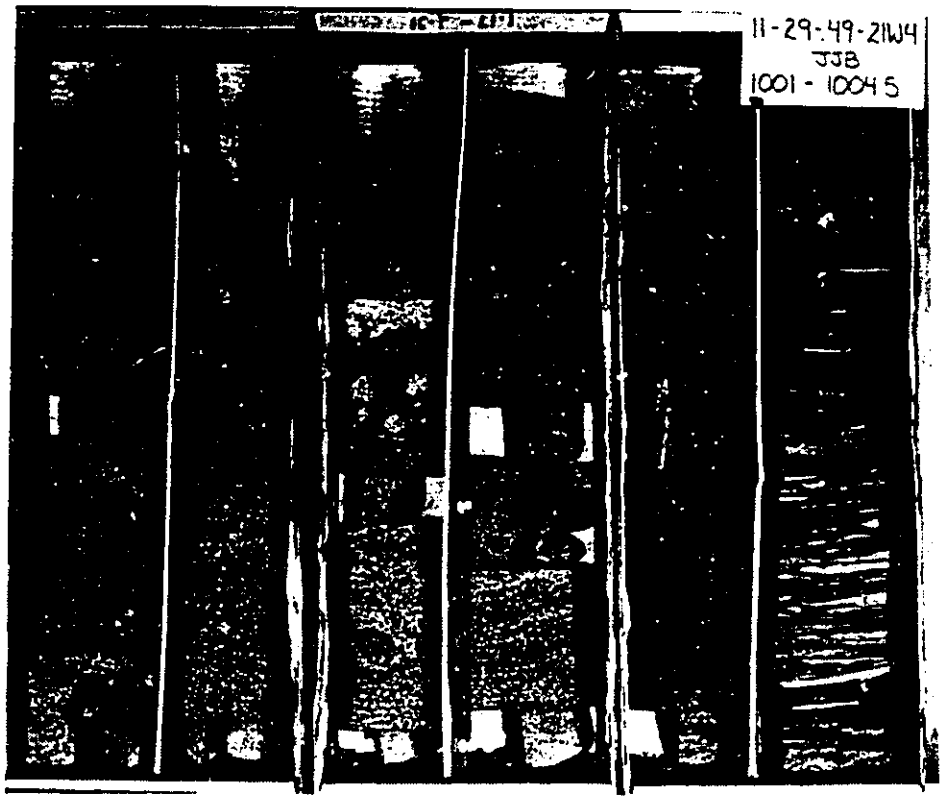
11-29-49-21W4
JJB
1001 - 1004.5


11-29-49-21W4
JJB
1004.5-1008.1

Figure 4-9. Litholog of Core 11-29-49-21W4 Shown against the Appropriate Well Log.

The litholog uses the same facies scheme as shown in figure 3-1. Heavy straight lines mark unit boundaries. The trace on the left is the SP and that on the right is the resistivity.

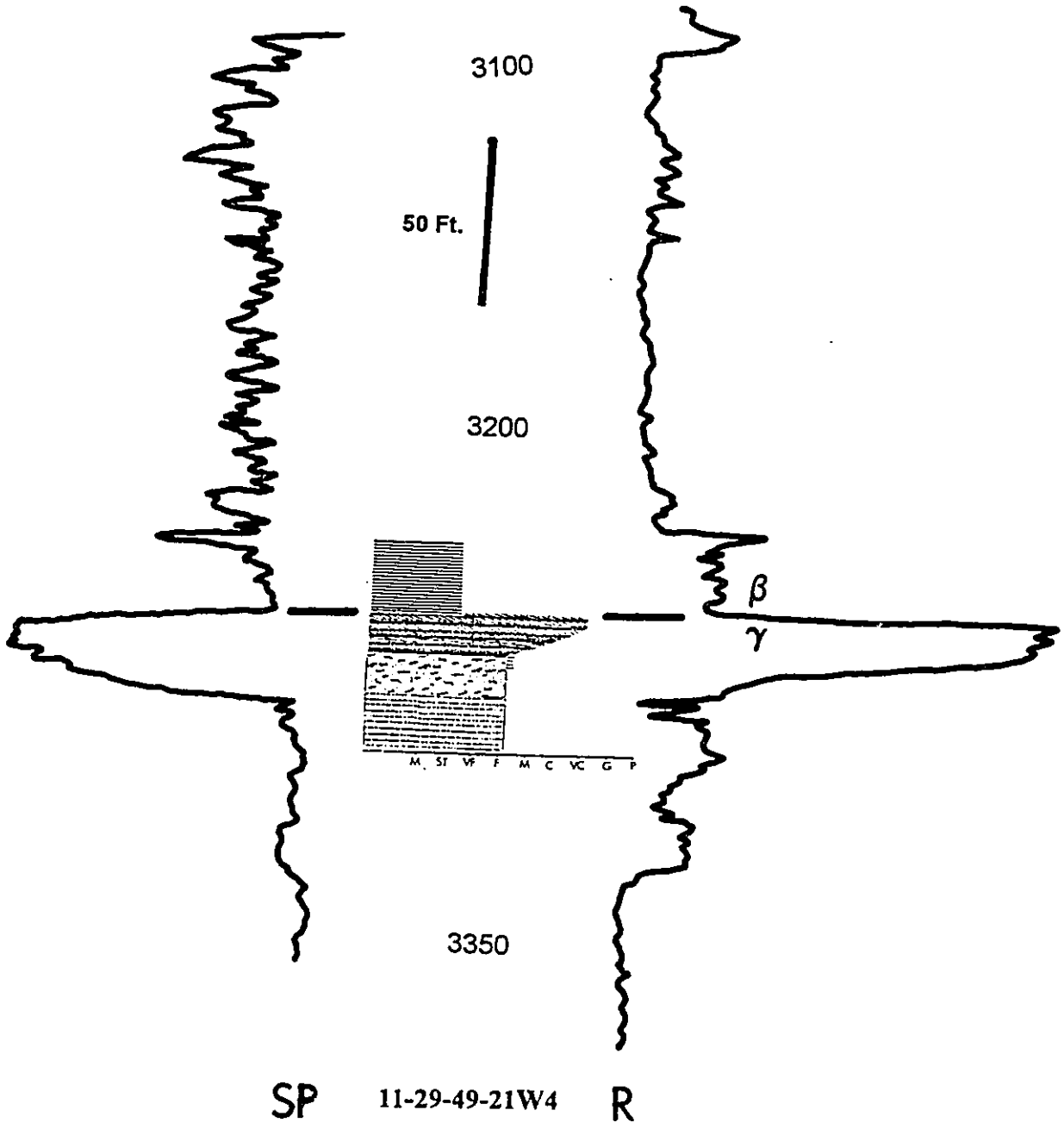
3100
50 Ft.
3200
β
γ
M SI VF F M C VC G P
3350
SP
11-29-49-21W4
R

core facies for regional correlation because they are less variable. Also the density of logs is greater than that of core, so the changes in their responses can be followed more smoothly than those in core. Although each core was compared to the appropriate well log, it can be difficult to correlate only the cores, so while the correlation process was interactive it did rely somewhat more on the well log signature once it had been related to the closest core. The log response often corresponds very closely to the sandiness of the facies as seen in core so the correlations are rather reliable lithologically.

The cross-sections are located in figure 4-10 which also shows the datapoints (wells) used in the study. The well log cross-sections do not have exactly the same wells as the core cross-sections because the latter were chosen to maximize the number of cores shown while the former were chosen to optimize the variation and transitions visible between well log signatures. Correlations were confirmed by successively closing boxes around the intersection of cross-sections shown in figure 4-10. While this does not prove the correlations it establishes their consistency. The correlations below stretch over a large enough region that iteratively correlating changing signatures was necessary. This was achieved by repetitively closing loops as cross-sections were constructed. The descriptions of well log units below can be followed on two typical cross-sections: A-A' (foldout 1), which is roughly parallel to depositional strike, and E-E' (foldout 5), which is roughly perpendicular to depositional strike.

4.4.2 Datum Location

The foldout cross-sections, both core and well log, have all been hung from the same datum. The chosen datum is visible in the log

Figure 4-10. Location of Cross-sections.

This figure shows all cross-sections present in the rear pocket. The entire study area is shown with small dots representing well logs through the Viking and large dots representing the presence of core at some point in the Viking. Each Township is a six mile square (36 square miles). The basin margin is to the west and strikes roughly northwest. (The dense pattern of drilling in the southwest is the Joarcam field.)

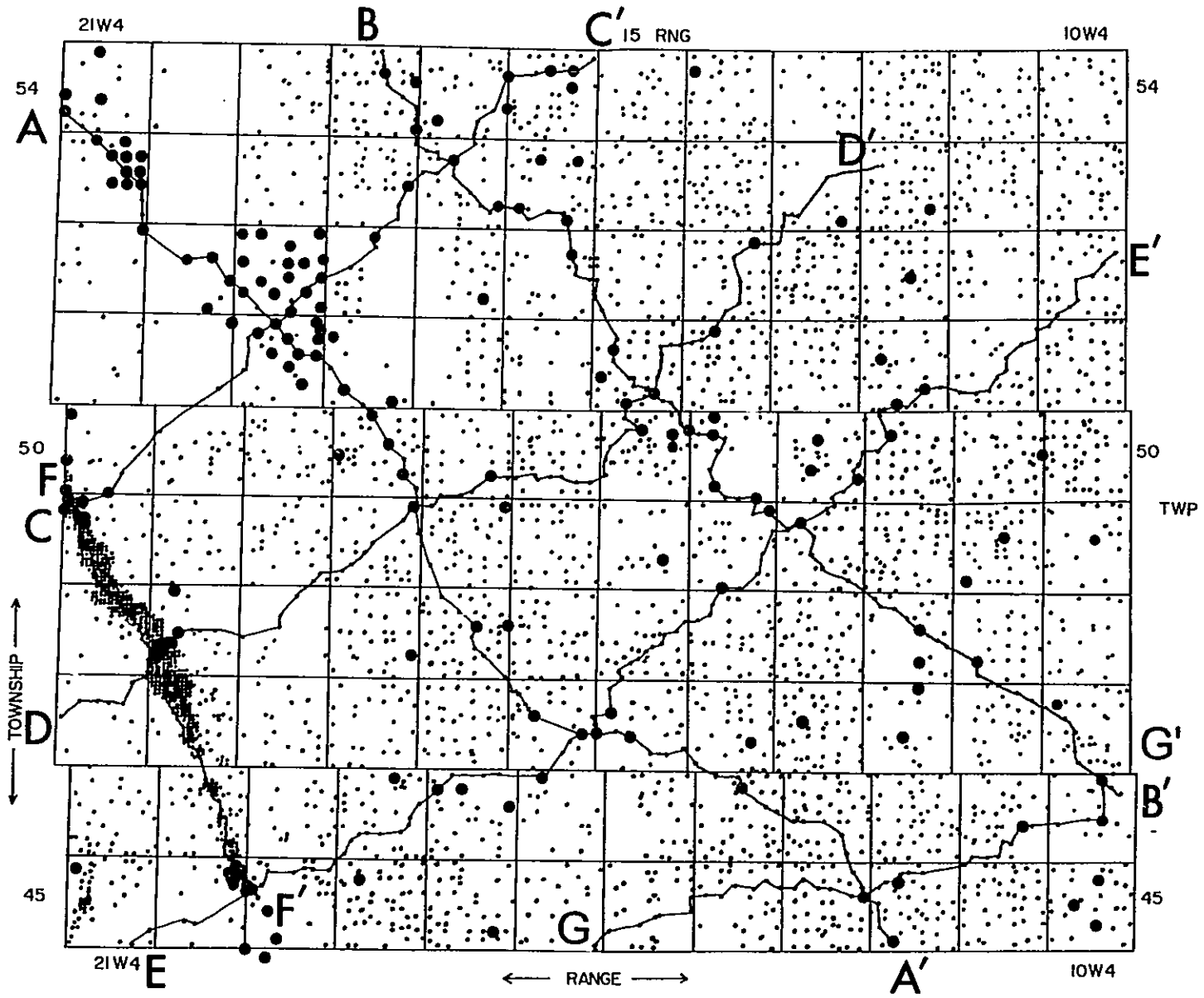
21W4
B
C′
15 RNG
10W4
54
A
D′
E′
50
F
C
TWP
TOWNSHIP
D
G′
B′
45
F′
G
21W4
E
RANGE
A′
10W4

sections and was labeled b (see for example A-A'); it is the central rightward deflection of a set of four deflections in the shales overlying the Viking which are located below the Base of Fish Scales marker. The two peaks above b tend to be very close; rarely they are almost or totally indistinguishable, so the indentation between them was taken as a marker named a. When the two signals merge the marker was taken as the peak and called a'. The rightward deflection below b was labeled c. b was taken as the datum because it is regionally more persistent in character than a or c.

The stratigraphic equivalent of these markers outside the study area is unknown; they could merely die out or onlap the formation elsewhere. Perhaps they mark a basinal record of sandier units known elsewhere in Alberta such as the Goodrich sandstone in the far northwest (see Koke and Stelck, 1985). The lithological nature of the log responses are also uncertain because they are rarely cored. When they are, the core is only 1" in diametre with significant losses in the relevant region. For example, core 4-4-48-14W4 visible in E-E' (foldout 12) penetrates this level with some unlocatable loss. Occasional siderite bands may be seen, and although their presence would account for the resistivity response observed, the response might equally well be due to changes in silt content or clay mineralogy.

Regardless of their behavior elsewhere in the basin the markers are quite serviceable as datums. This usefulness is implied by two observations. First, throughout the region, they form essentially parallel traces. Second, and more important, throughout the region, they are roughly sub-parallel to a marker in the Joli Fou shales underlying the Viking. This marker was picked as the most

rightward deflection in the resistivity log at a point approximately twenty feet above the base of the Joli Fou and was named z for reference; the general log response in the location of this pick rapidly deflects to the right and then gradually dies of upward in a series of serrated secondary deflections. Its character and location may be seen in the log cross-sections, for example A-A' (foldout 1) and E-E' (foldout 5). This marker in the Joli Fou was not taken as a datum for the cross-sections because it is less frequently penetrated by the logs; moreover, it can be harder to pick because it varies more in form than the responses in the shales overlying the Viking. The importance of the sub-parallel nature of the markers in the Joli Fou and the un-named shales relates to potential interpretation of the behavior of the Viking. It may be argued that if markers above and below a unit are parallel, then the behavior of markers within the unit may reflect depositional form. As will be seen in chapter 5 there are other basinal factors that confuse this issue in the case of the Viking, but the argument is generally valid and the best one for choosing the given datum. As discussed at length below this an important point for comparing the cross-sections presented here to that presented by Posamentier et al. (1992) which is not hung on a consistent datum. The approximately parallel nature of these under- and overlying markers strongly suggests that markers within the Viking are not valid as datums unless they too are sub-parallel to the shale markers.

4.4.3 Unit Names

Between the upper and lower markers, the core-based log correlations reveal six units in the area, generally bounded by rapid facies changes corresponding to rapid changes in the amount of sand distributed in the sediment.

In stratigraphically ascending order these are Mu, Epsilon, Delta, Gamma, Beta and Alpha. These may be seen in strike-parallel and strike-perpendicular form in cross-sections A-A' and E-E' (foldouts 1 and 5 respectively) that have already been used as examples. Their facies content and variation is discussed below. The variations in the units' log signatures are described in stratigraphically ascending order below.

4.4.4 Unit Mu

The first extensive, large log signature above the Joli Fou marker, z, is the base of the Viking; this also forms the base of both units Epsilon and Mu. The base of the Viking is marked almost everywhere in the study area by a pronounced increase (rightward deflection) in resistivity and a corresponding decrease (leftward deflection) in SP logs. The pick for the base of the Viking has been made in the center of this lower deflection. This agrees with the scanty core evidence from this level, such as core 8-14-47-16W4 in A-A' (foldouts 1 and 8), which show very rapid, arguably locally scoured, facies transitions. The greater resistivities within the Viking correspond to the presence of sandier and siltier facies.

The first unit above the base of the Viking, Mu, is unusual in that it can only be isolated as a separate signature in the southeast of the study area; it is also is the most debatable of the correlations. Mu has been designated on the basis of a locally distinct resistivity log deflection corresponding to an apparent sediment package shown by minor core control. The separation of the Mu log signature is best seen in foldouts 2 (B-B') and 7 (G-G'); G-G' shows the most pronounced Mu signatures. The minor evidence from cores through the package may be seen in

the southeast end of foldout 8 (cross-section A-A'). Where it can be separated from Epsilon, the overlying unit, Mu is best expressed as a single rightward deflection in the resistivity log which varies from zero to approximately ten feet thick; its signature is not usually separable on the SP recording but may show up as a subtle leftward deflection. On the basis of very limited core substantiation, and partly by analogy with the behavior of the overlying Epsilon unit, the boundary to Mu has been placed at the midpoint of the upper limb of the rightward resistivity deflection. The lower boundary is, of course the base of the Viking. Mu does not even occur ubiquitously in the southeastern part of the study area; for example, in cross-section G-G' (foldout 7) between wells 11-24-45-13W4 and 7-6-46-11W4 the signature disappears. I have correlated this as an onlapping onto an irregular base of Viking. However, this correlation is open to question. Local disappearances such as this might be due to minor extensional fault removal of section; some evidence for this is discussed below in chapter 5. The unit is hypothesized to amalgamate with the base of the Viking to the west and north where its signature disappears. A weak case might be made for amalgamation of Mu in the lower portion of unit Epsilon.

4.4.5 Unit Epsilon

The resistivity increase at the base of the Viking in the rest of the study area is generally part of the next unit, Epsilon. It may only last for a couple of feet or may be up to twenty feet thick with an overall, slightly serrated, high resistivity pattern. The unifying factor in assigning these variable thicknesses to the same unit is a general sustained high resistivity across most of the study area often followed by a rapid decrease (leftward response) before the onset of the

next unit, Delta. The base of unit Epsilon lies either at the pronounced rightward deflection at the base of the Viking or at the top of unit Mu where it is present. The ideal rapid decrease in resistivity marking the top of Epsilon may be seen in foldout 5 (E-E') in wells 11-9-45-20W4, 7-10-47-16W4 and 7-32-48-14W4, for example.

There are exceptions to this pattern of pronounced resistivity decrease at the top of Epsilon. In wells, 4-34-45-19W4 through 14-24-46-18W4 (E-E') the decreased resistivity is not present; instead there is an approximate continuation of the serrated response, yet the SP log shows a pronounced variation where an increased (rightward) response reflects the drop off in the sandier portion of the preceding package (based on comparison core evidence). There are even ambiguous cases such as 2-22-48-17W4 in cross-section A-A'; in this case, the location of the boundary of unit Epsilon is justified on the basis of rapid grain size and sand percent changes visible in cores that penetrate such log responses (see the same well in foldout 8).

As a rule, the leftward resistivity deflection of the unit boundary is most pronounced to the east in the basin interior and decays to the west at the basin margin as sand content of the unit increases. The pattern is visible in cross-section A-A' (foldouts 1 and 8) because of the decrease in sand content from the northwest to southeast.

4.4.6 Unit Delta

The next unit is Delta whose base everywhere coincides with the top of Epsilon; however, the log signatures are slightly more consistent than those of Epsilon. The well log signature of Delta is behaviorally very similar to Epsilon.

The resistivity signature rises from the generally rapid decrease marking the top of Epsilon to a minor decrease marking the top of Delta. However, it is usually the SP trace which shows a more pronounced response, decaying gradually upward (leftward deflection) and then very rapidly increasing. The top of Delta is located at the extremity of the decrease in the SP log based on comparison to core. Cross-section E-E' (foldout 7) shows this placement quite well. The thickness of Delta varies from approximately thirty feet in the west to five or ten feet in the east.

There are locations where the signature becomes indistinct, and consequently more debatable. I have correlated the pattern in the form of onlap onto the underlying unit top. This type of behavior is visible in section E-E' (foldout 7) between wells 4-32-45-19W4 and 6-6-48-18W4. The signatures of both Epsilon and Gamma decrease across this area so it is difficult to estimate their behavior. The correlations are based on tracking the decaying responses and the continued presence, although subtle, of a fall of in the resistivity through this area.

4.4.7 Unit Gamma

Unit Gamma, whose base usually coincides with Delta except in locations such as that in cross-section E-E' discussed above, is less extensive than the underlying units being confined mostly to the west. It correlates as a wedge dying to the east. Through most of its extent its signature is rather similar, however, to both Epsilon and Delta. The base begins at the generally pronounced decrease in resistivity and increase in SP taken as the top of Delta, except where Epsilon is exposed through Delta. The base of the unit may be locally scoured in such

cases; there is more evidence for this further into the basin (discussed below). Once again, the resistivity response gradually increases upward to a maximum reflecting increased sand content; the SP mimics the resistivity, decreasing upward to a minimum. In the western portion of the study area, the upper ten to twenty feet of the responses may show marked fluctuations. Generally these fluctuations cannot be traced extensively to indicate basin wide behavior. There are local exceptions, however, such as pronounced bentonite signatures which can be reliably correlated in the western portion of the study area particularly in the region of Joarcam field (see fig. 1-1). These bentonites are shown correlated by a dotted line in foldout 6 (F-F'); the responses are the two minor decreases in resistivity lying one on top of another approximately fifteen feet up in the unit. The geometry and significance of these bentonites is discussed in chapter 5. Unlike Epsilon and Delta, there are few case of local scours near the top of the unit further into the basin as may be seen in the core cross-sections (foldouts 8-12). In fact, Gamma is the most gradational of all units from bottom to top. In the context of the Exxon concept of unit stratigraphy this absence of detectable scour or disconformity in the coarser portion of the sediment package is particularly important for sea level interpretations discussed in chapter 7.

The top of Gamma is picked easily in the west of the study site where it lies just above the extreme deflections in the SP and resistivity logs. The unit becomes much more subtle further into the basin where the top is marked not so much at the top of an extreme deflection but just below a smaller decrease in the resistivity (or increase in the SP). This kind of signature may be seen in wells 4-34-45-19W4 through 10-36-46-17W4 in cross-section A-A' (foldout 1); such

picks can be locally difficult but do tie into the rare core control through such logs; see core 4-13-53-18W4 in cross-section C-C' (foldout 10) for example. In the basin, the lithological expression of the unit boundary locations appears to be somewhat different than at the western boundary of the study site. There seems to be more persistent scour at the base of the thinner unit in this eastern area; this can be seen in core cross-section A-A' (foldout 7) where thin units correlated as unit Gamma are underlain by a scour in cores 8-14-47-16W4 and 10-13-47-16W4.

At approximately the township 15W4 line, unit Gamma ceases to have any sedimentological expression, and the log signature merges with that of underlying unit Delta. This merger shows up in the perpendicular to strike cross-sections, C-C', D-D' and E-E'. As this point is approached the unit becomes increasingly difficult to pick on the log response both because of the thinner sediment package and its finer grainsize (and hence subdued log response).

4.4.8 Unit Beta

Unit Beta overlies unit Gamma where the latter exists and unit Delta in the eastern part of the study area. The log response of unit Beta is generally rather subdued compared to those of Gamma and the upper portions of Delta and Epsilon. This is because of the generally finer grainsize of the units contained within it (see the core cross-sections, foldouts 8 through 12, for evidence of this). Unit Beta's base is taken at the drop off in resistivity (SP increase) taken as the top of either Gamma or Delta. Following this peak, the unit's response is often rather static and columnar in form, although with numerous secondary serrations. It lacks the funnel characteristics of the lower units. Locally, there are sandier

accumulations within the unit; core 16-25-50-15W4 illustrates an example of laminated siltstone separating sandier bioturbated sandstones and siltstones. However, these accumulations do not seem to have any great lateral extent and cannot be correlated across the basin in the electrical logs. The top of Beta is usually marked merely by an abrupt decrease in the resistivity paralleled by a similarly abrupt increase in the SP trace. The top of the unit, using core data, lies at the point just before this decay. In some instances, there is an increase in resistivity forming a twin peak before the decay; for example see 16-26-49-21W4, 8-11-47-15W4 and 11-24-45-13W4 in foldout 1, A-A'. These peaks seem to correspond to the presence of much sandier, coarser, crossbedded units, sometimes overlying a scour. As with the scours discussed previously, such as that at the base of unit Gamma, these do not appear in every core through the unit. Consequently, they have not been taken as the location of the unit boundary, despite their proximity to it.

4.4.9 Unit Alpha

The last unit, Alpha, is barely classifiable as such considering its sedimentary composition and thinness; it does however, persist across the area as a correlatable response and has therefore been included in the unit compilations. Alpha's log signature is similar to that of Beta but more subdued. It starts as a stepped reduction in the resistivity which is matched by a stepped increase in the SP response and maintains a rather constant degree of resistance. The unit is on the order of ten feet thick across the region. The base is at the beginning of resistivity decrease taken as the top of Beta; the top, in turn, is at the next pronounced decrease in resistivity following a generally serrated trace. The top

of Alpha is also taken as the top of the Viking in the area. Often the drop off in resistivity is preceded by a minor increase in the resistivity; there is less often such a corresponding response in the SP log. In such cases, the unit boundary is placed at the extreme of the peak in a manner analogous to the underlying unit, Beta. The core support for such placement is infrequent; see core 11-28-53-17W4 in core cross-section C-C' (foldout 10) for example. This example also provides evidence for excluding a minor overlying resistivity peak from inclusion as part of the unit; compare the litholog to the well log correlation in foldout 3 (C-C').

In conclusion, each unit varies in signature across the basin in a manner that can only really be appreciated by close examination of the well log cross-sections presented in the foldouts. However, there is sufficient consistency of signatures that unit boundaries and the evolution of the unit signatures can be traced consistently across the region of figure 1-2.

4.5 UNIT PETROGRAPHY

4.5.1 The Goals of Petrographic Study

Ideally, the unit correlations made above would be confirmed by other means. Petrographic differences offered one way of doing this. The petrology presented in Appendix B was an attempt to discover petrographic differences between the units that might be used to check correlations; it was not intended as an in depth diagenetic study. Unfortunately, none of the categories investigated provided distinct elements for confirmation of the well-log correlations.

The investigation of potential petrographic correlations was divided into three categories. The first was the study of petrofacies (Dickinson and Rich,

1972, Ingersoll, 1978) using groupings of both established units and multivariate statistical analysis to attempt groupings. The second was examination of inter-unit diagenetic changes. The third was measurement of trace element composition of bentonites that are contained in the units in an attempt to use them as geochemical markers. The petrofacies analysis depends on the occurrence of provenance changes during deposition of the formation; the diagenetic analysis depends primarily on the previous existence of different fluid flow patterns between units since each unit undergoes essentially the same burial history. The bentonite analysis relies on the existence of different trace element compositions in each ash fall and their lateral preservation.

Most data is from the unit Gamma with lesser amounts from Epsilon, Delta and Beta. No data comes from Alpha which is usually only mudstone where cored.

4.5.2 Petrofacies Analysis

4.5.2.1 Techniques

The techniques used in the petrographic study were standard and are described in Appendix B. Thin section petrography was accompanied by X-ray diffraction (XRD) analysis of clay components of the units.

4.5.2.2 Classification of Petrographic Components

Petrographic components were counted following established classifications including divisions into undulatory and non-undulatory quartz (Basu et al., 1975). No division of polycrystalline quartz was attempted although chert was subdivided into lithic chert and chert (an original division, see Appendix B). Feldpars were divided into alkali (orthoclase, perthite and

microcline) or plagioclase. Tallies were kept of trace components (e.g., phosphatic clasts).

4.5.2.3 Petrofacies Results

The results of the petrographic investigation are presented fully in Appendix B. Standard plots and statistical analyses of the data indicate that the Formation is petrographically homogenous regardless of the manner of analysis. This is true of both the sand and clay fractions. According to Folk (1974) the sandstone portion would be categorized as a chert arenite.

4.5.3 Diagenetic History

In addition to the petrographic component analysis summarized above, an attempt was made to distinguish units on the basis of potentially different diagenetic histories. The investigation involved XRD, cathodoluminescence study of carbonate cements and quartz overgrowths and SEM examination. The details are also included in Appendix B.

As for the petrofacies investigation summarized above, there was no fundamental difference between units.

The diagenetic examination did reveal evidence for early, probably epigenetic, phosphatization and glauconitization of sediments which has important environmental implications for the sediments (discussed in Chapter 6).

4.5.4 Bentonite Geochemistry

4.5.4.1 Techniques

Bentonites were analyzed by X-Ray Fluorescence (XRF) and Neutron Activation Analysis (NAA); the same samples were used for both analyses. The elements analyzed by XRF were chosen to match those examined by Amajor and

Lerbeckmo (1980). Neither the XRF nor the NAA lead to any potential grouping of the bentonites that might confirm or deny the unit correlations based on the well logs and cores. This is particularly surprising for the XRF results because of the previous results of Amajor and Lerbeckmo (1980).

4.6 GRAIN SIZE DISTRIBUTIONS WITHIN UNITS

4.6.1 Introduction

Given the unit correlations described in section 4.4, maps of grain size distribution can be prepared for each unit. The grainsize data that offers the most potential information is the maximum size occurring within the unit. Such maps might yield clues to source direction, sediment migration direction or information useful in environmental interpretations. Such data can only be obtained from cores that fully penetrate the unit in question, so the data is somewhat limited.

The maximum grainsize distribution of each unit was geostatistically analyzed prior to mapping using the U.S.G.S. Statpac program (Grundy and Miesch, 1987). The primary purpose of this analysis was to check for areal structure because randomly distributed or apparently randomly distributed data cannot be contoured (Sharp, 1977). In checking for non-random distributions, multiple runs through each data set were made, including both isotropic and anisotropic analyses.

4.6.2 Maximum Grain Size Maps by Unit

Figure 4-12 shows the distribution of maximum grain size data points for unit Mu. There are too few points to draw a descriptive summary. Figure 4-13 shows the maximum grain size data distribution for unit Epsilon. No geostatistical structure was discernible for the data so it has not been contoured.

Figure 4-14 shows similar results for the maximum grain size of unit Delta. Figure 4-15 shows the maximum grain size distribution for unit Gamma and is the only one of the data sets to show geostatistical structure. Consequently it is the only map that has been contoured. Following Sharp (1987), the valid contour interval is 2.5 Phi units (derived from a irreducible variance or "nugget effect"). The base line for the contours was selected to provide the most contour lines on the map. The heavy arrows and accompanying question marks are intended to highlight the ambiguity in the regional slope of the contour lines. Part of the reason for this ambiguity lies in the distribution of the data. There is not any data available in a strip running northwest-southeast from latitude 53.37 to 53.48 on the western edge of the figure; this gap corresponds to the gap between the Joarcam and Ft. Saskatchewan-Beaverhill Lake Fields shown in figure 1-1. Although detailed trends in grain size distribution cannot be found, there is a general decrease to the east. Figure 4-16 shows the analogous map for unit Beta; the data was apparently randomly distributed and has not been contoured. The same is true of Figure 4-17 which shows the maximum grain size data for unit Alpha. In the case of unit Alpha, however, there are comparatively few data points, so there is less certainty about the reality of the apparent randomness; the lack of structure could reflect a paucity of data rather than an actually randomly distributed grain size pattern.

4.7 FACIES COMPONENTS OF THE UNITS

4.7.1 Techniques of Summarizing Units

The distribution of facies may be described either quantitatively or qualitatively. Currently most facies models rely on the latter technique.

Figure 4-12. Grain Size Data for Unit Mu.

The figure shows those core for which maximum observed grain sizes are available for unit Mu. The values are in Phi units.

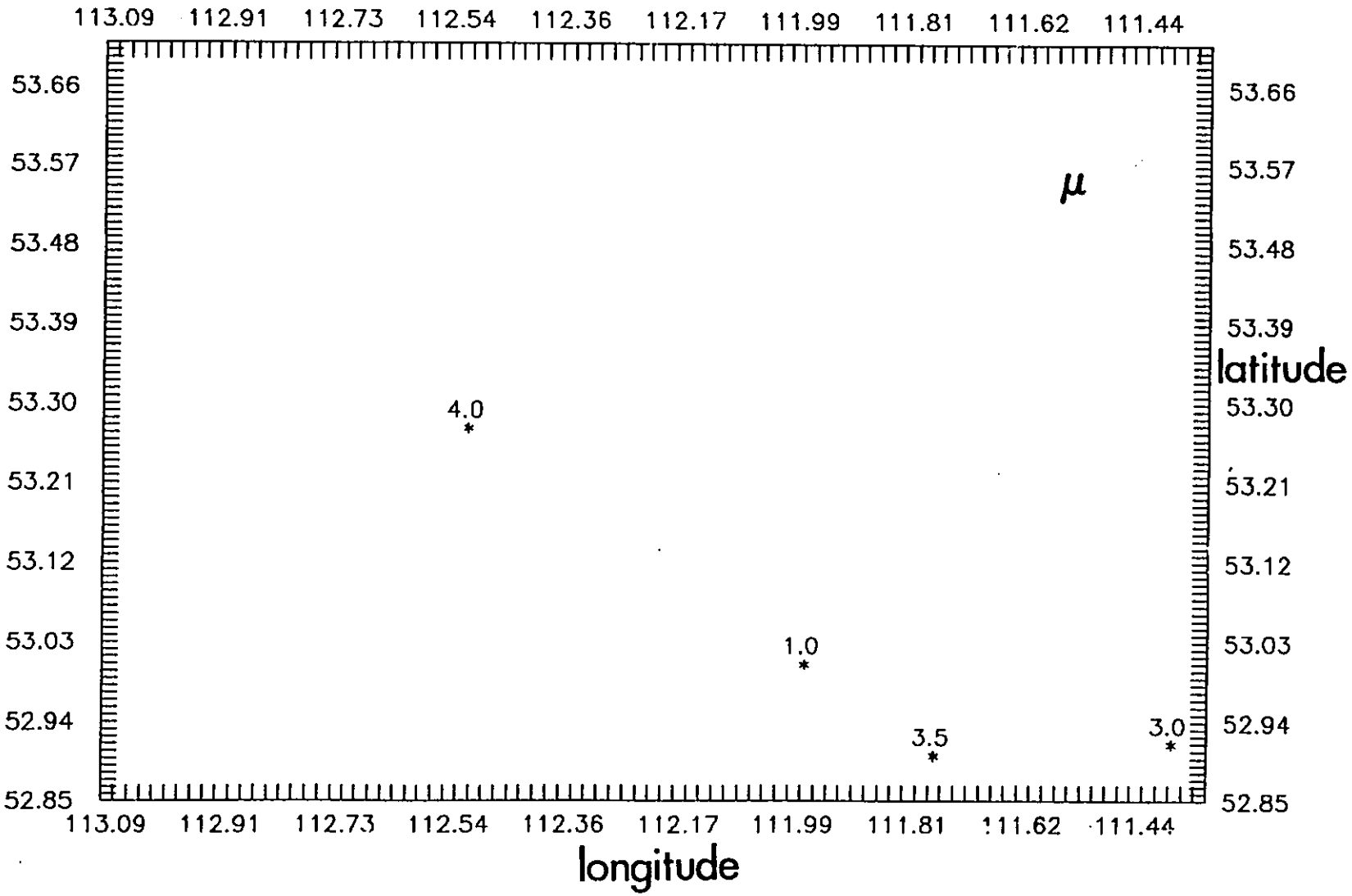
113.09 112.91 112.73 112.54 112.36 112.17 111.99 111.81 111.62 111.44
53.66
53.57
53.48
53.39
53.30
53.21
53.12
53.03
52.94
52.85
μ
4.0
1.0
3.5
3.0
latitude
longitude

Figure 4-13. Grain Size Data for Unit Epsilon.

The figure shows those core for which maximum observed grain sizes are available for unit Epsilon. The values are in Phi units.

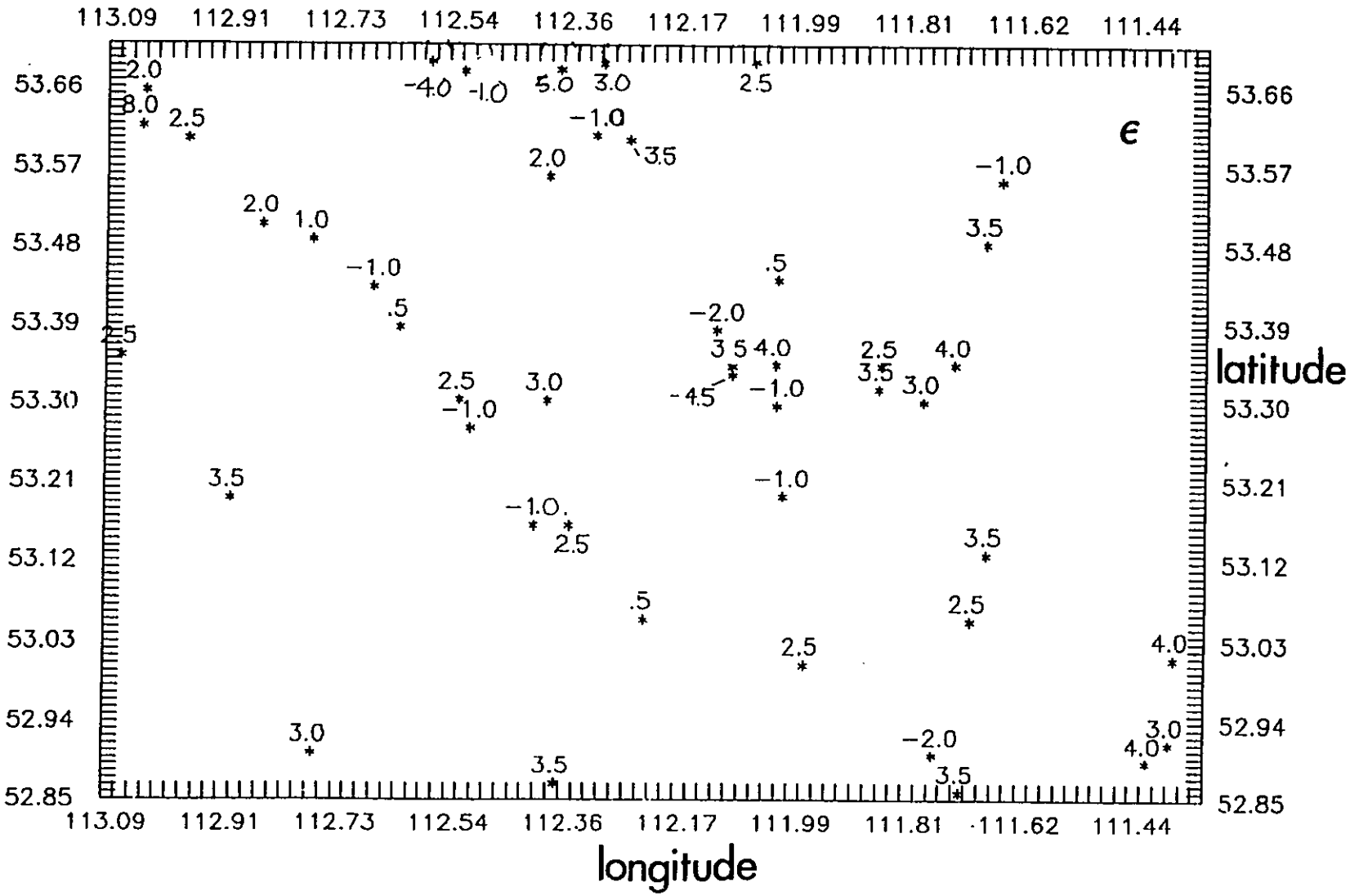
113.09
112.91
112.73
112.54
112.36
112.17
111.99
111.81
111.62
111.44
53.66
53.57
53.48
53.39
53.30
53.21
53.12
53.03
52.94
52.85
latitude
longitude
ϵ

Figure 4-14. Grain Size Data for Unit Delta.

The figure shows those core for which maximum observed grain sizes are available for unit Delta. The values are in Phi units.

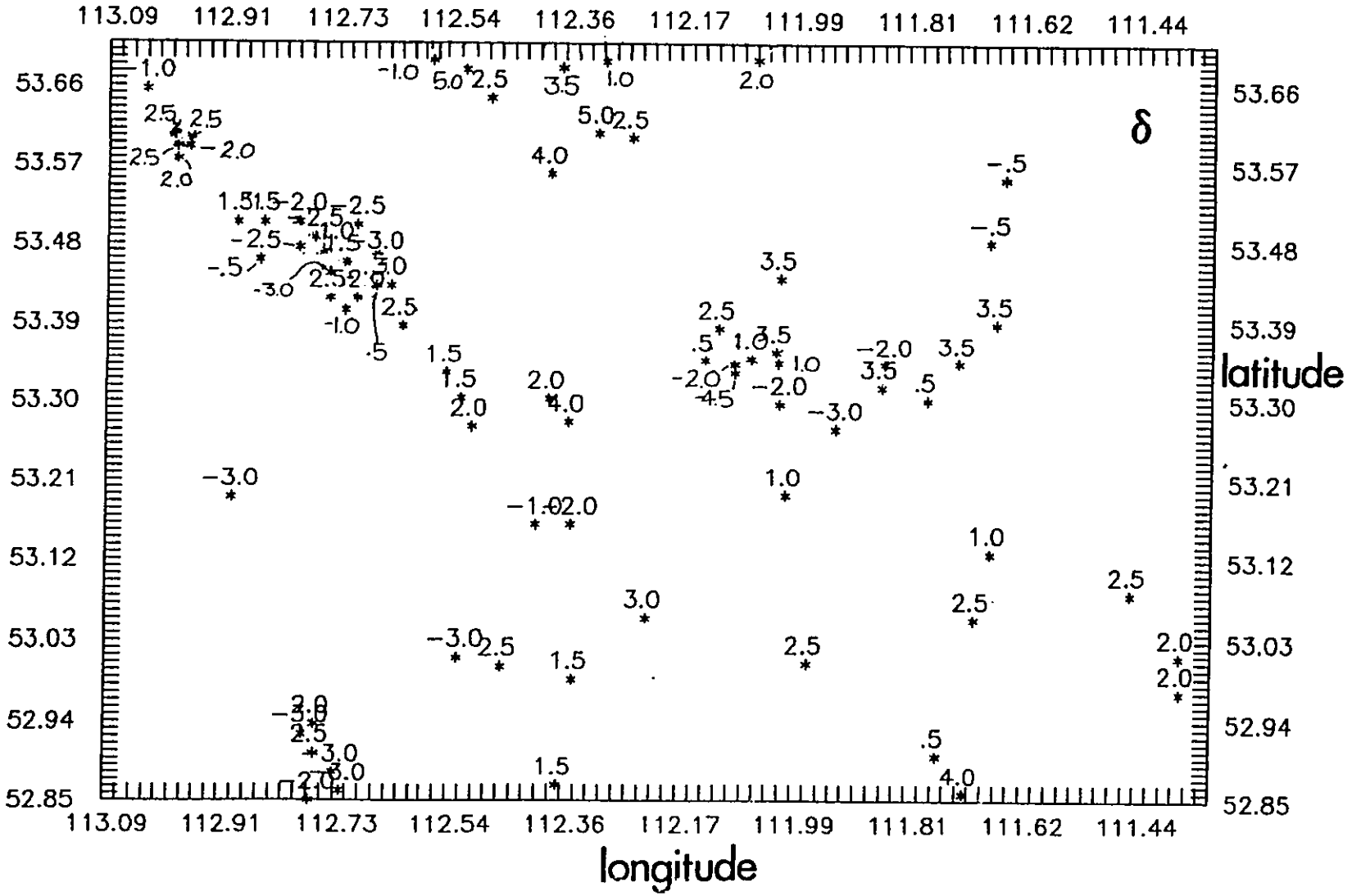
δ
113.09
112.91
112.73
112.54
112.36
112.17
111.99
111.81
111.62
111.44
53.66
53.57
53.48
53.39
53.30
53.21
53.12
53.03
52.94
52.85
latitude
longitude

Figure 4-15. Grain Size Data for Unit Gamma.

The figure shows those core for which maximum observed grain sizes are available for unit Gamma. As discussed in the text, the values have been contoured at 2.5 Phi unit intervals.

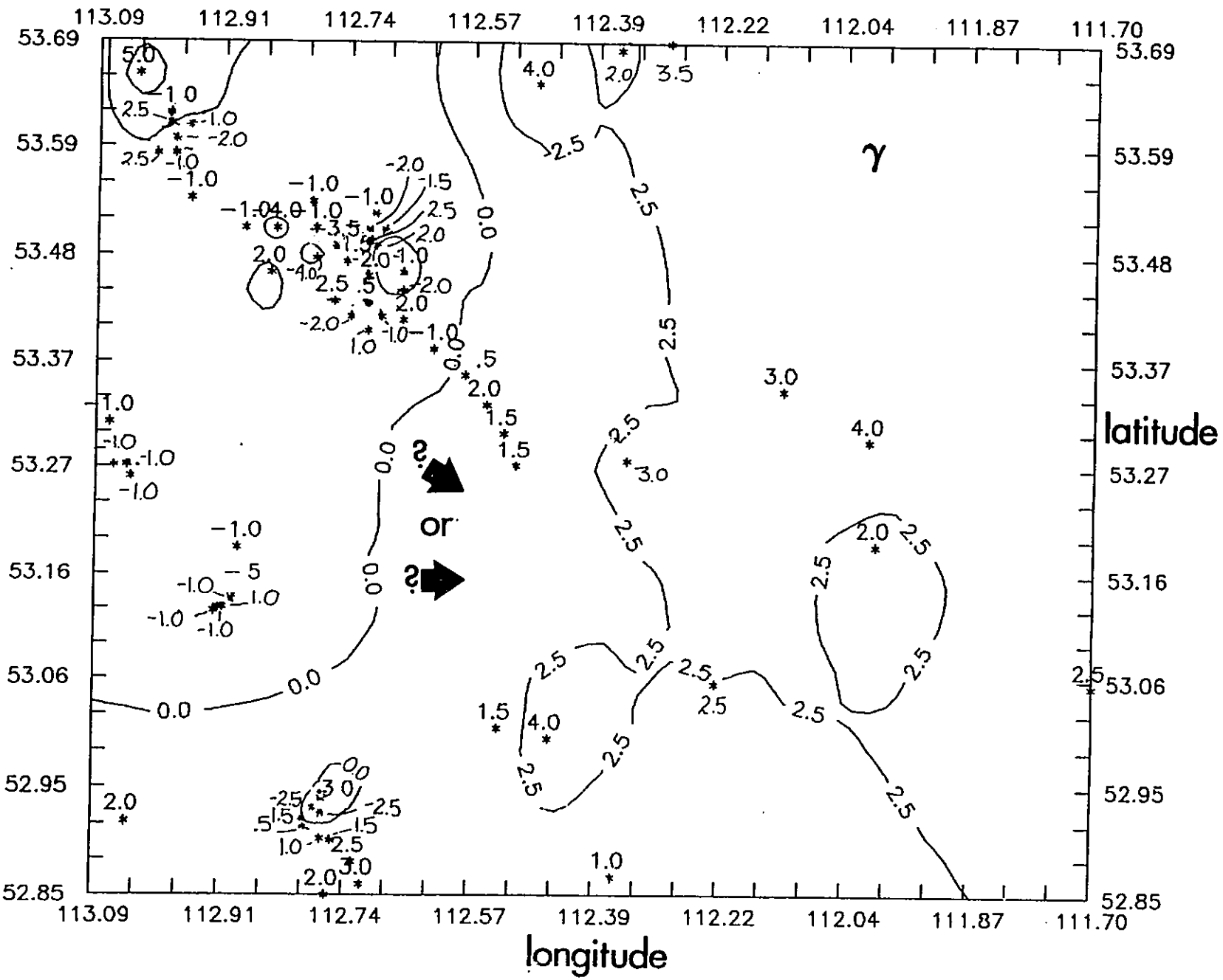
113.09
112.91
112.74
112.57
112.39
112.22
112.04
111.87
111.70
53.69
53.59
53.48
53.37
53.27
53.16
53.06
52.95
52.85
γ
or
?
?
latitude
longitude

Figure 4-16. Grain Size Data for Unit Beta.

The figure shows those core for which maximum observed grain sizes are available for unit Beta. The values are in Phi units.

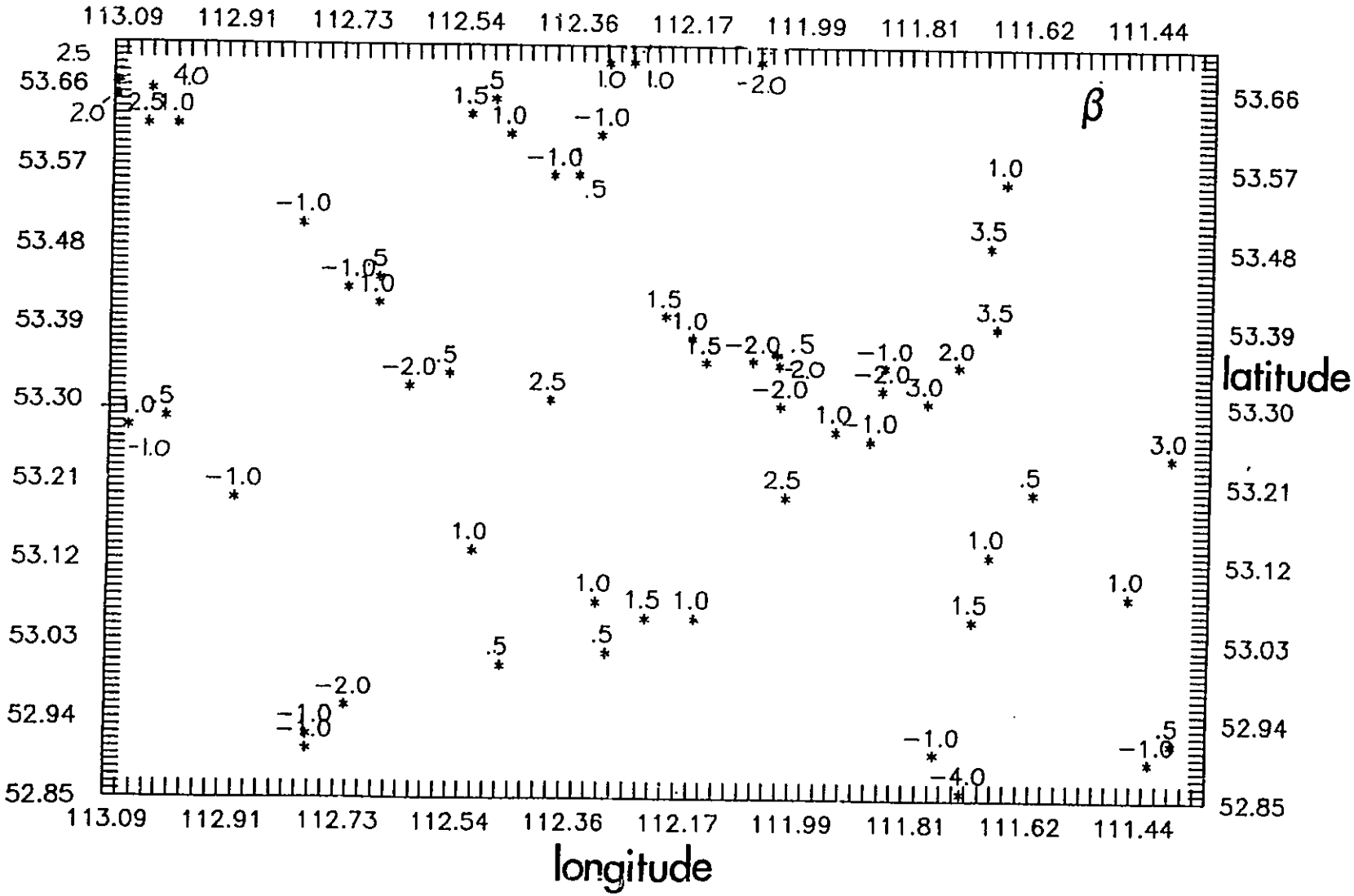
113.09 112.91 112.73 112.54 112.36 112.17 111.99 111.81 111.62 111.44
53.66 53.57 53.48 53.39 53.30 53.21 53.12 53.03 52.94 52.85
β
latitude
longitude

Figure 4-17. Grain Size Data for Unit Alpha.

The figure shows those core for which maximum observed grain sizes are available for unit Alpha. The values are in Phi units.

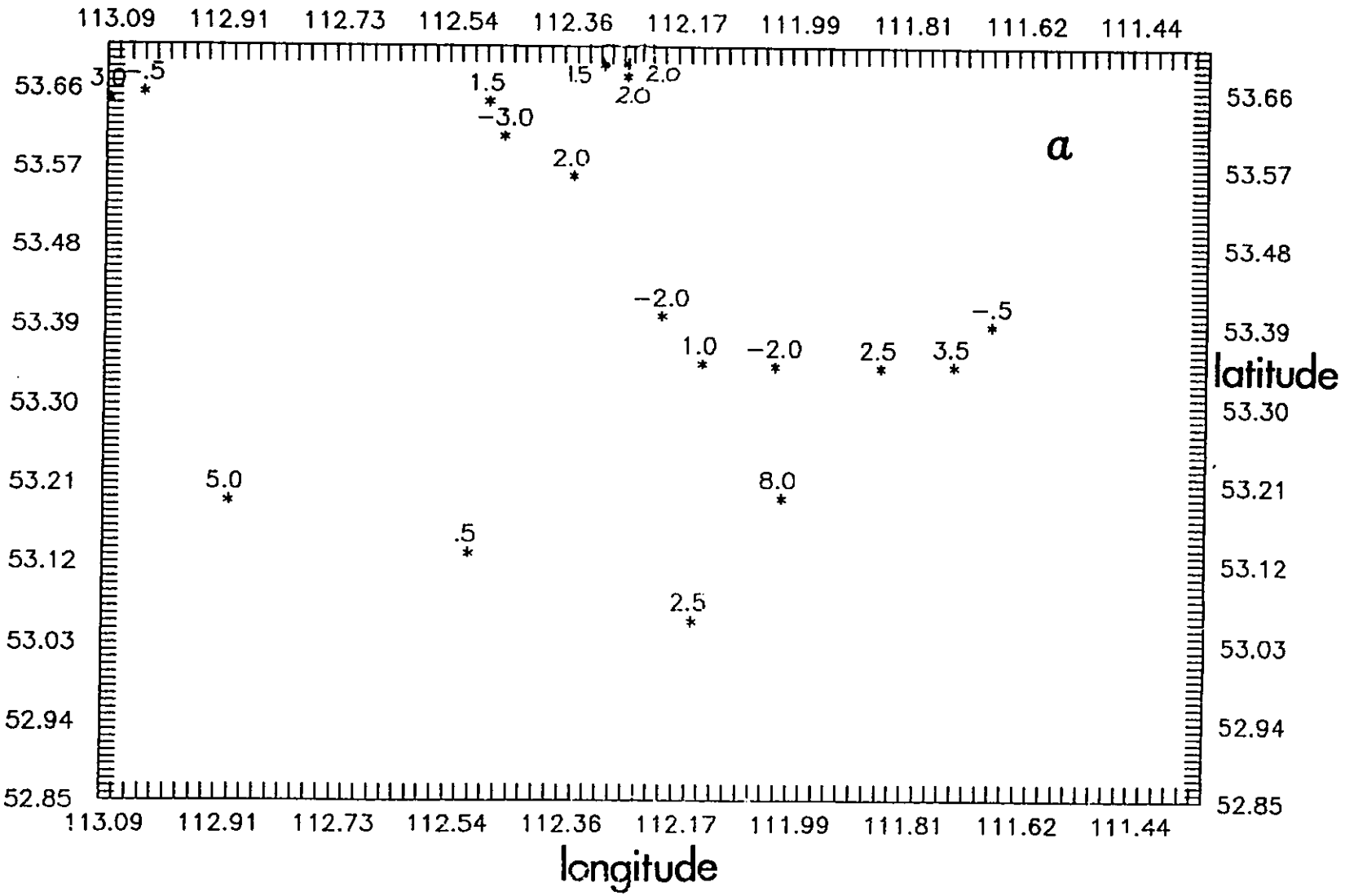
113.09
112.91
112.73
112.54
112.36
112.17
111.99
111.81
111.62
111.44
53.66
53.57
53.48
53.39
53.30
53.21
53.12
53.03
52.94
52.85
a
latitude
longitude
-.5
1.5
-3.0
2.0
2.0
-2.0
1.0
-2.0
2.5
3.5
-.5
5.0
8.0
.5
2.5

This is presumably because the quantitative description, in more than one dimension, of such natural non-parametric variables as facies is currently without a solid statistical foundation (Lin and Harbaugh, 1988). Consequently, for the most part, quantitative facies models have been limited to one-dimensional summaries of long vertical sections. An introduction to this type of summary along with discussions of some of the errors committed may be found in the works of Walker (1984c), Harper (1984), Carr (1982) and Powers and Easterling (1982). This approach cannot be taken with the Viking units because neither the core lengths nor the thicknesses of each unit contains sufficient repetition of states (facies) to allow for Markov chain construction. However, artificial stacking of neighboring sections may be used to a limited extent to investigate a given units facies structure.4.7.1.1 Artificial Stacking of Laterally Equivalent Sections

Artificial stacking as used in this investigation is the creation of a large vertical section by stacking of associated laterally equivalent sections. In order to artificially stack sections, the sections must therefore first be correlated into units or other related packages as described above. Criteria have not been set for the order in which measured sections should be artificially stacked. The best ordering for stacking might be thought to be proximity, but the choice of a nearest neighbor would still be dependent on an arbitrary starting point. This lack of criteria for stacking order leads to a restriction that in tallying the transitions the changes from the top of one section to the base of the next cannot be counted in the tallies. In the ideal case of an infinite number of sections through a unit of states A-B-C-D-E, the stacking limitation therefore will not allow recording the

E-A transition; its potential existence remains a matter of speculation. Section stacking thus allows investigation of elements of any type within a correlated package being stacked, but it does not allow developing the package into a closed system or cycle.

Most importantly, the act of artificial stacking does not in itself generate a traditional facies `model' or summary. Rather it provides an investigative tool for analyzing facies within a unit and between units; this is primarily because of a second complication in artificial stacking. This second complication is that the data across a unit may be non stationary. While stationarity is usually conveniently ignored in the analysis of single vertical sections, it is more obviously a problem in compiling laterally equivalent sections from within a unit. There is no guarantee that a section taken to be laterally equivalent with another necessarily has the same inherent probabilities of a succession of states (i.e., comes from exactly the same `environment' or contains the same mixture of environments). Consequently, stacking of laterally equivalent sections does not necessarily provide a simple statistical summary of the transition states of a single `environment'. It merely provides a statistical measure of the data from the unit in question. Although single environment summaries are usually the goal of Markov analysis of facies, the impossibility of obtaining this goal in inter-unit analysis does not mean that the technique is without use. Given similar distribution of core data from unit to unit, the summaries of different units may be compared. Such comparison provides information on the degree to which an assemblage of facies in one unit is more or less random than another assemblage

from a different unit. Such information is of potential interest in environmental interpretations as discussed in chapter 6.

The Markov analyses should not be considered apart from qualitative summaries of the facies, however, because the embedded Markov techniques that are used in facies analysis do not give any weight to the amount (i.e., thickness) of a particular facies present or the extent of a single facies (i.e., self similar transitions). Furthermore, the traditional display of only the non-random relationships may obscure the bulk of an "environment's" behavior if the environmental record consists predominantly of a random succession of facies states. The "non-random" relationships that arise from analysis of laterally equivalent sections are potentially useful in the construction of qualitative facies "models". They provide a check against the deterministic biases that can enter purely qualitative models.

A program to analyze adjacent sections in the manner described above is presented in Appendix C. The program is written in QuickBASIC as modified from Wells (1989).

4.7.1.2 Qualitative Facies "Models"

Because of the lack of quantitative methods capable of unambiguously summarizing facies distributions, description of the units ultimately requires qualitative, mostly impressionistic, descriptions. These are best made graphically where large amounts of data can be incorporated into a single `summary'. The most immediate form of graphic presentation is a simple presentation of the facies relationships in cross-section form as done in foldouts 8 through 12 for representative cross-sections through all of the units. Despite the relative detail of

such a scheme, its proximity to the original data lacks the summarizing simplicity so valuable in a model. The general facies composition of each unit needs to be summarized impressionistically which is best done in a series of vertical units. The representative vertical sections discussed below are from actual cores and are not idealizations.

4.7.2 Qualitative Facies Summaries

An examination of the cross-sections 8 through 12 in the rear pocket provides scope for a qualitative assessment of the facies compositions of the units. Note that the wells used in the construction of the core cross-sections are not exactly the same as those used in the construction of the well log cross-sections. This difference is due to the fact that some wells have less informative log signatures and more informative core and vice versa.

The facies compositions may be summarized briefly as follows. Mu is only a thin local accumulation in the south east part of the study area and its facies composition is uncertain. Epsilon, Delta and Gamma are composed primarily of mixtures of facies 8, 9, 10, 11, 13, 14, 15 and 16. Beta is composed mostly of facies 2, 4, 5, 6 and 7. Alpha is mostly mudstone, facies 1, with occasional laminae of coarser sediment, up to granule size and fairly frequent siderite concretions.

Units Alpha and Mu barely qualify as units; Alpha is mostly mudstone with rare coarser pulses or siderite concretions, and Mu is a local accumulation with comparatively sparse core information the implications of which are discussed in chapter 5.

The most important division is between units Epsilon, Delta and Gamma and unit Beta; the former are similar in their facies and differ from the latter in the presence of the coarser facies, particularly the abundant crossbedded sandstones and bioturbated sandstones. However, examination of foldouts 8 through 12 reveals that units Epsilon, Delta and Gamma do contain facies similar to those of Beta in their eastern portions.

Further examination of any of the core cross-section foldouts will show that there is not much possibility of correlating facies at a scale smaller than that of the unit. For example, in foldout 8, between cores 11-23-52-20W4 and 10-7-52-19W4 at the level of unit Gamma, there is almost no correspondence of facies and, on the detailed level, no precise correspondence of grain size. The best that can usually be done by way of intraunit correlation involves only one or two facies between one to three cores, covering perhaps ten miles. These tentatively correlatable facies are usually siltstone facies, and their physical correlation does not necessarily describe temporal correlation. The lateral variability of the facies throughout each unit is matched by the fluctuating appearance of the bentonites characterized above. For example, in cross-section C-C' (foldout 10), bentonites appear in six of the twelve cores at different levels; few of them can be demonstrably correlated and there are frequently cores between those bearing bentonites that have no signature at all of their existence.

Figures 4-18 through 4-23 show typical facies successions from the various facies assemblages characteristic of the units. Each litholog represents a core and is not an idealization.

Figure 4-18 shows the representative section of unit Alpha. Only one core was taken for Alpha because, as may be seen from an examination of the foldouts 8 through 12, there is relatively little variation in the unit across the area. Core 6-25-52-16W4 was chosen because it contains laminated siltstone, grey mudstone and occasional pulses of pebbly and granular material; these are the most common elements of unit Alpha. They do not have any apparent order.

Like unit Alpha, unit Beta does not have any striking regional variations. Consequently, only one core has been picked to represent typical facies associations; this core, 7-24-51-19W4 is shown in figure 4-19. Laminated and bioturbated siltstones are important facies in unit Beta; a perfect core would also contain some interbedded siltstone. The core also shows a common tendency in the unit to be slightly coarser upwards, passing from silts to very fine or even fine sands. There is often an accompanying fining upward portion to the unit at the base overlying the coarser sandstones of unit Gamma. This basal portion may contain a number of pulses of coarser sands and/or isolated crossbedded sets. Finally unit Beta may have one or two coarser crossbedded sandstones as isolated sets in the upper portions.

In general, the units from Gamma may be taken as somewhat representative of units Delta and Epsilon as well. This is because they seem to have essentially the same component facies and are consequently interpreted as being different realizations of the same overall "environment". Unit Gamma has been represented by a series of three cores because it shows fairly

Figure 4-18. Typical Facies Succession for Unit Alpha.

The litholog opposite shows a typical example of facies as they appear in unit Alpha. The example is taken from core 6-26-52-16W4 at depths between 2118 and 2148 feet. See Figure 3-1 for a legend for the facies.

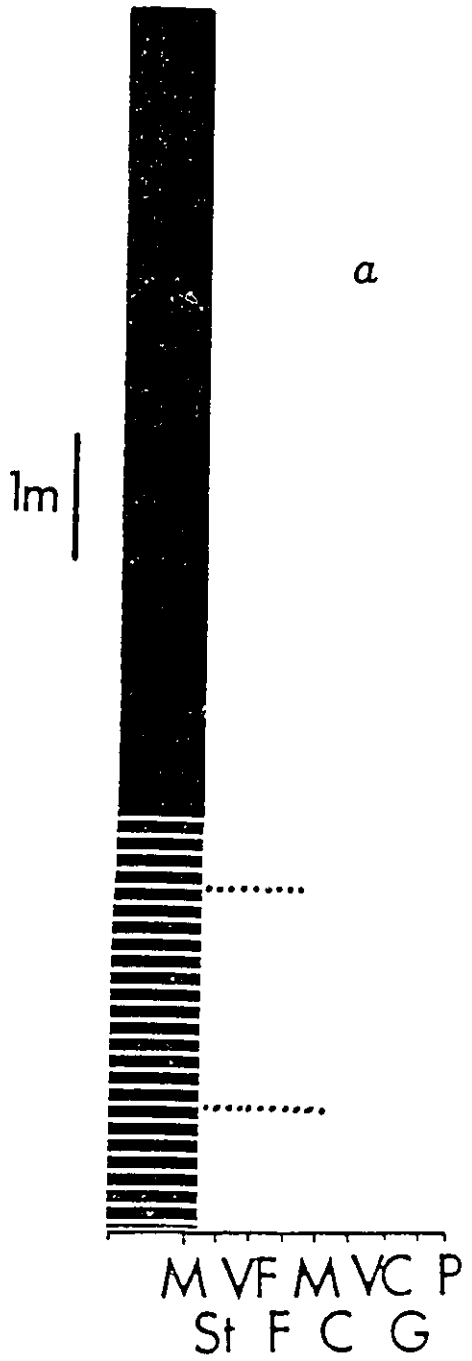
a
1m
M VF M VC P
St F C G

Figure 4-19. Typical Facies Succession for Unit Beta.

The litholog opposite shows a typical example of facies as they appear in unit Beta. The example is taken from core 7-24-51-19W4 at depths between 2515 and 2560 feet. See Figure 3-1 for a legend for the facies.

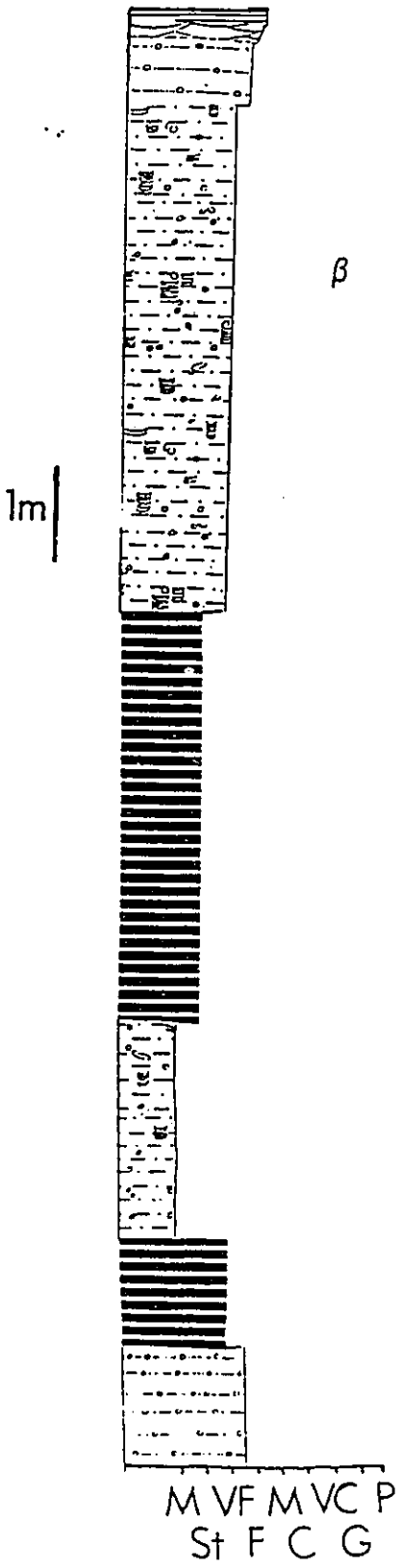
β
1m
M VF M VC P
St F C G

strong lateral variation in its distribution of facies. Figure 4-20 shows a core, from well 11-7-54-21W4, that has been taken to represent the proximal portion of unit Gamma. This core is typical of the sandier region in the northwest of the study area (see figure 1-2) in that there is no apparent grading of grain size or facies throughout the unit, and, in fact, there is some question as to where one unit begins and the other ends. In this particular case, part of the lower portion of the core may belong to unit Delta. Isolated coarse, crossbedded sandstone sets are frequent among mottled siltstones, muddy sandstones and occasional bioturbated sandstones. In the upper regions of the more westward portions of unit Gamma, there are often up to a metre or two of crossbedded sandstones of various forms with only minor mudstone/siltstone interbeds. The crossbedding is usually tangential parallel; rare examples of planar parallel occur as do both low angle intersecting and low angle parallel. Both of the latter often occur as part of the upper portions of tangential parallel sets while the planar parallel crossbeds usually seem to be isolated.

Figure 4-21 shows core 10-33-51-19W4 as representative of the intermediate portions of unit Gamma. The facies assemblage is essentially identical to that of the proximal section. The difference is primarily in the thickness of the section with fewer examples of sedimentary structures and a greater proportion of bioturbated sediment.

Core 2-22-48-17W4 shown in Figure 4-22 is representative of the distal portion of unit Gamma. There is a greater proportion of bioturbated sediment in the eastern region of the unit, represented here in the bioturbated sandstone. As with the intermediate section, above, the amount of crossbedding has decreased to

Figure 4-20. Typical Facies Succession for the Proximal Portion of Unit Gamma.

The litholog opposite shows a typical example of facies as they appear in the proximal portions of unit Gamma. The example is taken from core 11-7-54-21W4 at depths between 2600 and 2635 feet. See Figure 3-1 for a legend for the facies.

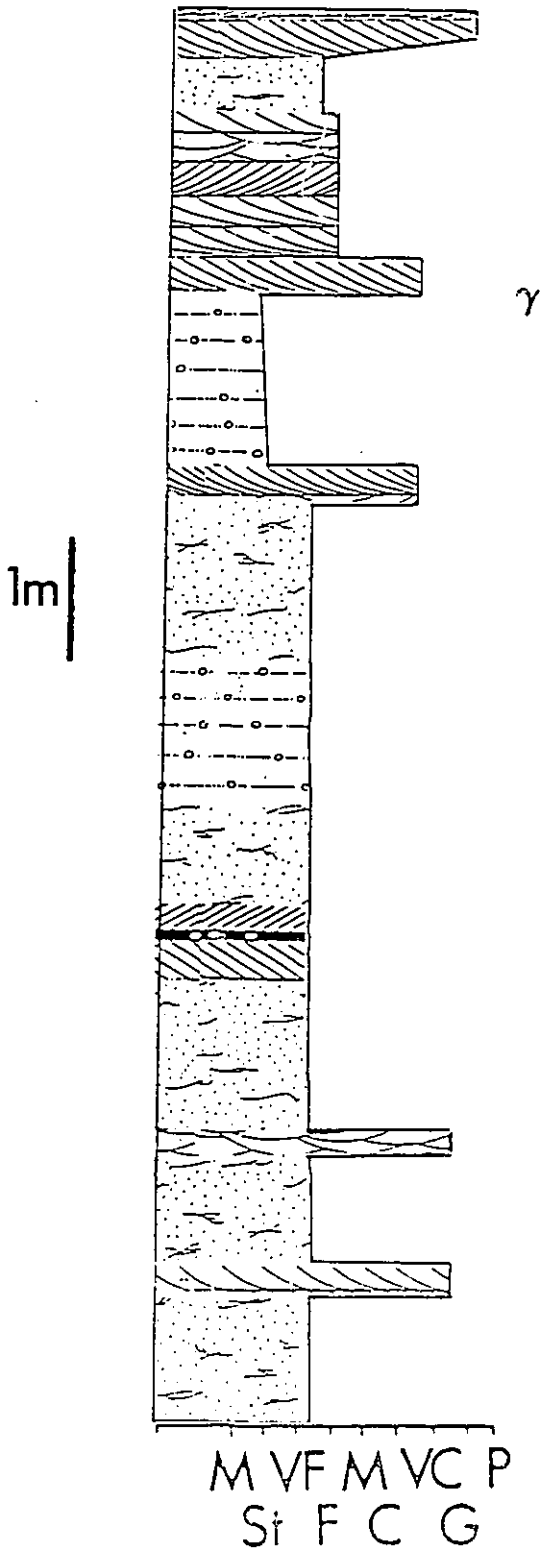
γ
1m
M VF M VC P
Si F C G

Figure 4-21. Typical Facies Succession for the Intermediate Portion of Unit Gamma.

The litholog opposite shows a typical example of facies as they appear in the intermediate portions of unit Gamma. The example is taken from core 2-22-48-17W4 between depths 2694 and 2664 feet. See Figure 3-1 for a legend for the facies.

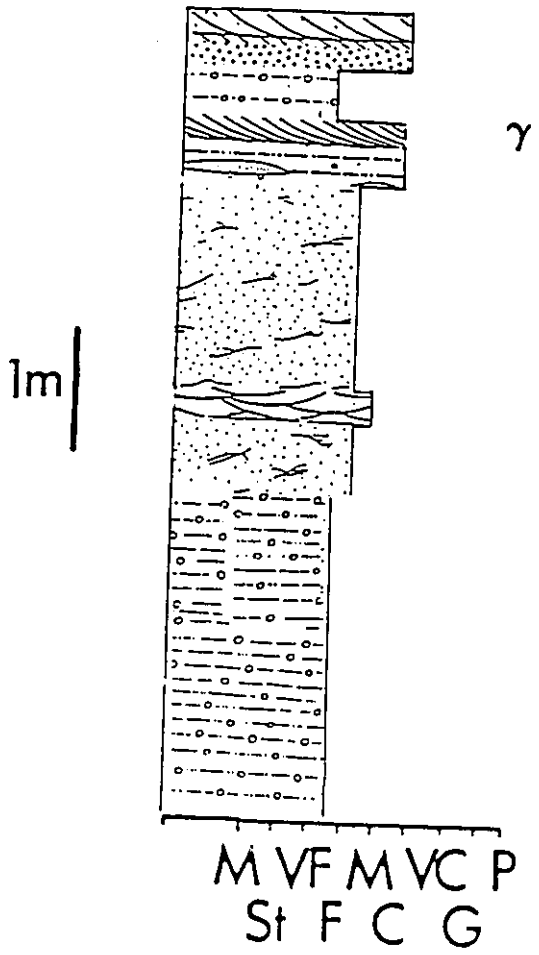
γ
1m
M VF M VC P
St F C G

Figure 4-22. Typical Facies Succession for the Distal Portion of Unit Gamma.

The litholog opposite shows a typical example of facies as they appear in the distal portions of unit Gamma. The example is taken from core 10-33-51-19W4 between depths 2635 and 2665 feet. See Figure 3-1 for a legend for the facies.

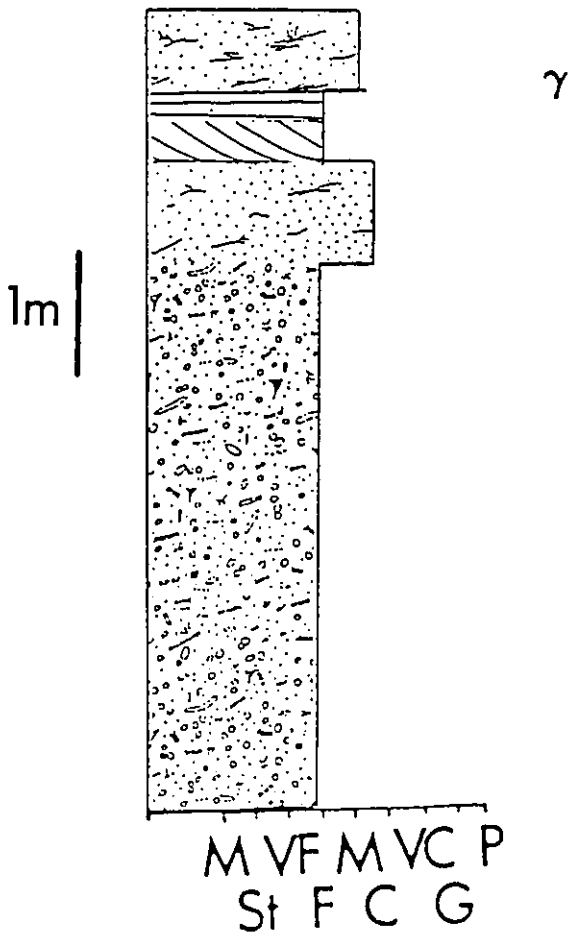
1m
M VF M VC P
St F C G

Figure 4-23. Typical Facies Succession for Unit Delta.

The litholog opposite shows a typical example of facies as they appear in unit Delta. The example is taken from core 11-23-52-20W4 between depths 2705 and 2717 feet. See Figure 3-1 for a legend for the facies.

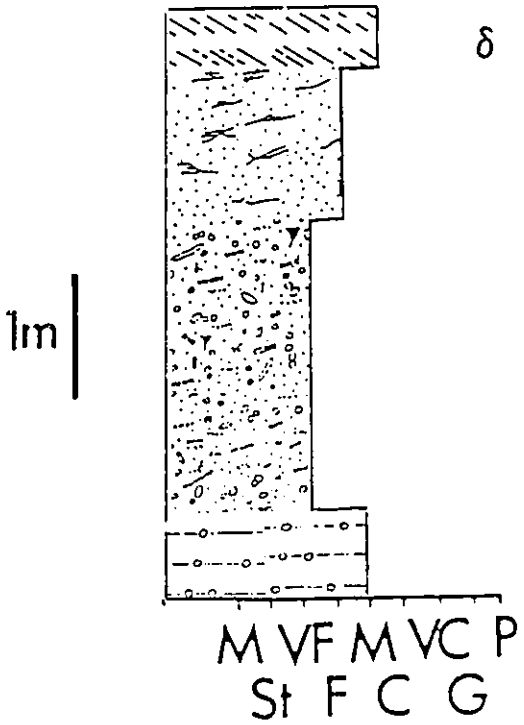
δ
1m
M VF M VC P
St F C G

the point where in many sections there may be none. Grain size still remains frequently fairly coarse.

Figure 4-23 shows the core from well 11-23-52-20W4 as representative of unit Delta. In fact, unit Delta has more variable expression, but as discussed above, is fairly similar to unit Gamma. As may be seen in foldouts 8 through 12 both units Delta and Epsilon are roughly similar to the intermediate and distal portions of unit Gamma. This may be seen in the almost identical nature of figures 4-23 and 4-22. Because of this descriptive similarity the three units are classified together for eventual environmental interpretations.

4.7.3 Quantitative Information on Facies Composition of the Units

The results of Markov analysis of artificially stacked data from across units Beta, Gamma, Delta and Epsilon are shown in figures 4-24 through 4-27 as a series of facies relationships diagrams. Units Alpha and Mu are not presented because their data was too limited. The locations of the cores used in the analyses may be seen in figures 4-13 through 4-16; a listing of the facies and location identification information is available on disk from the author. Only the relationships of the facies are described here; their interpretations are presented in chapter 6. The probability values for each transition have not been shown because the slight variations in the locations of the cores used between each unit sequence analysis set would not make intersequence numerical comparison valid.

Each facies relationship diagram should be considered both in terms of its relationships and in terms of those elements that are not present. The latter requires comparison to the qualitative facies summaries shown in foldouts 8 through 12 and described above. It is

Figure 4-24. Facies Relationships Diagram for Unit Beta.

The figure shows those facies transitions that have 90% confidence of being non-random. The calculations are based on the program in Appendix C. Arrows show the direction of the favored transitions.

SEQUENCE BETA

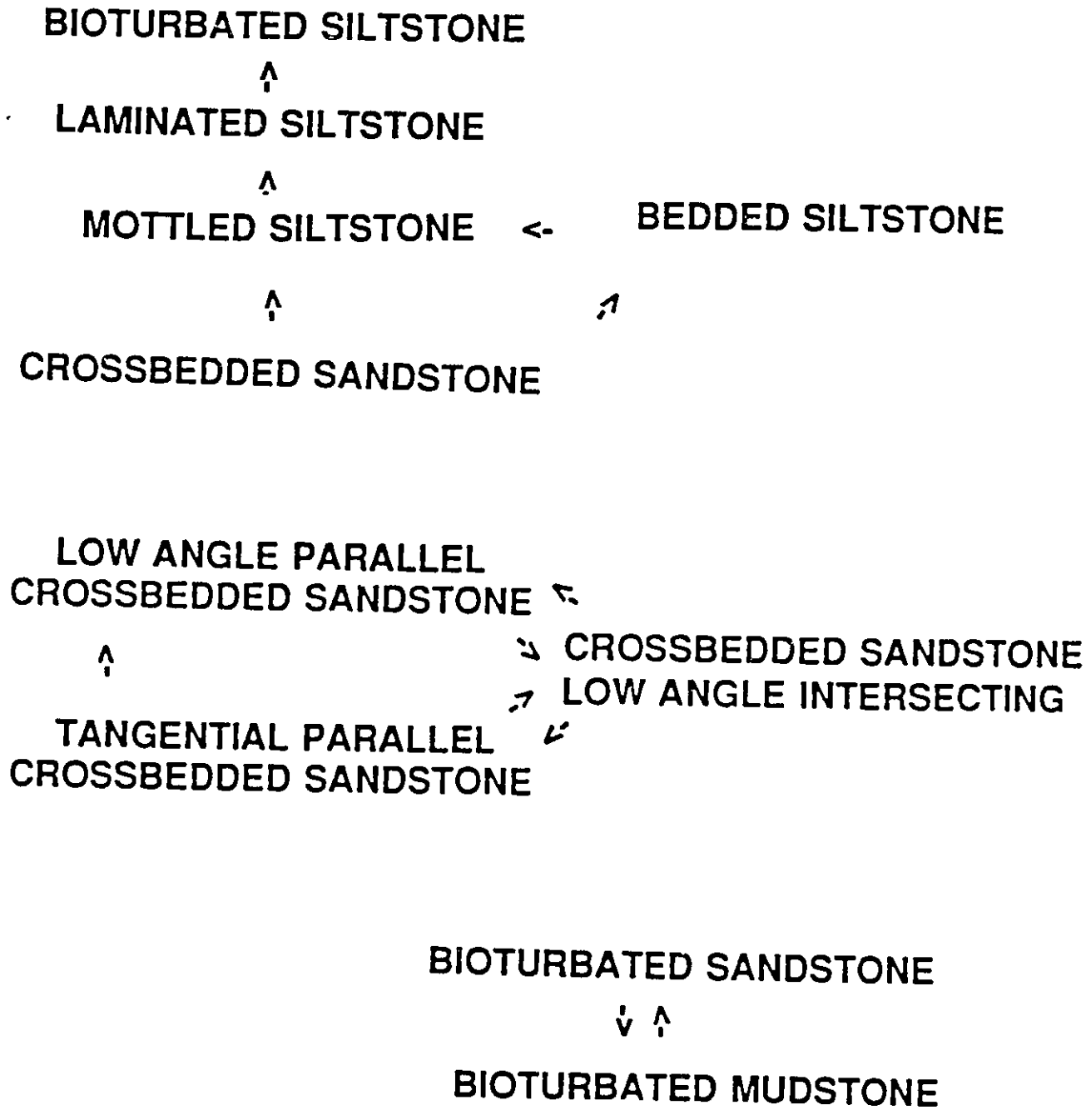

Figure 4-25. Facies Relationships Diagram for Unit Gamma.

The figure shows those facies transitions that have 90% confidence of being non-random. The calculations are based on the program in Appendix C. Arrows show the direction of the favored transitions.

SEQUENCE GAMMA

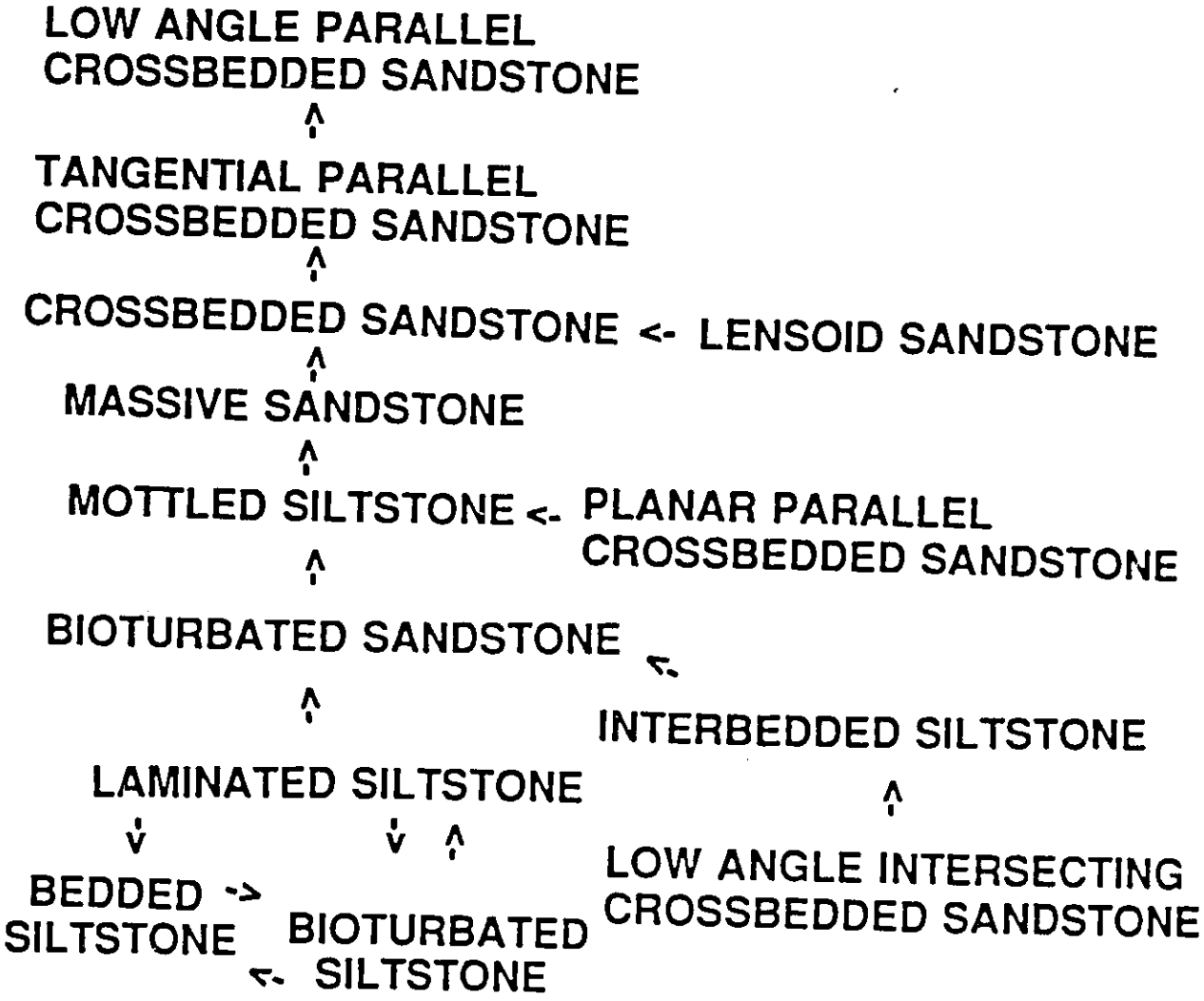

Figure 4-26. Facies Relationships Diagram for Unit Delta.

The figure shows those facies transitions that have 90% confidence of being non-random. The calculations are based on the program in Appendix C. Arrows show the direction of the favored transitions.

SEQUENCE DELTA

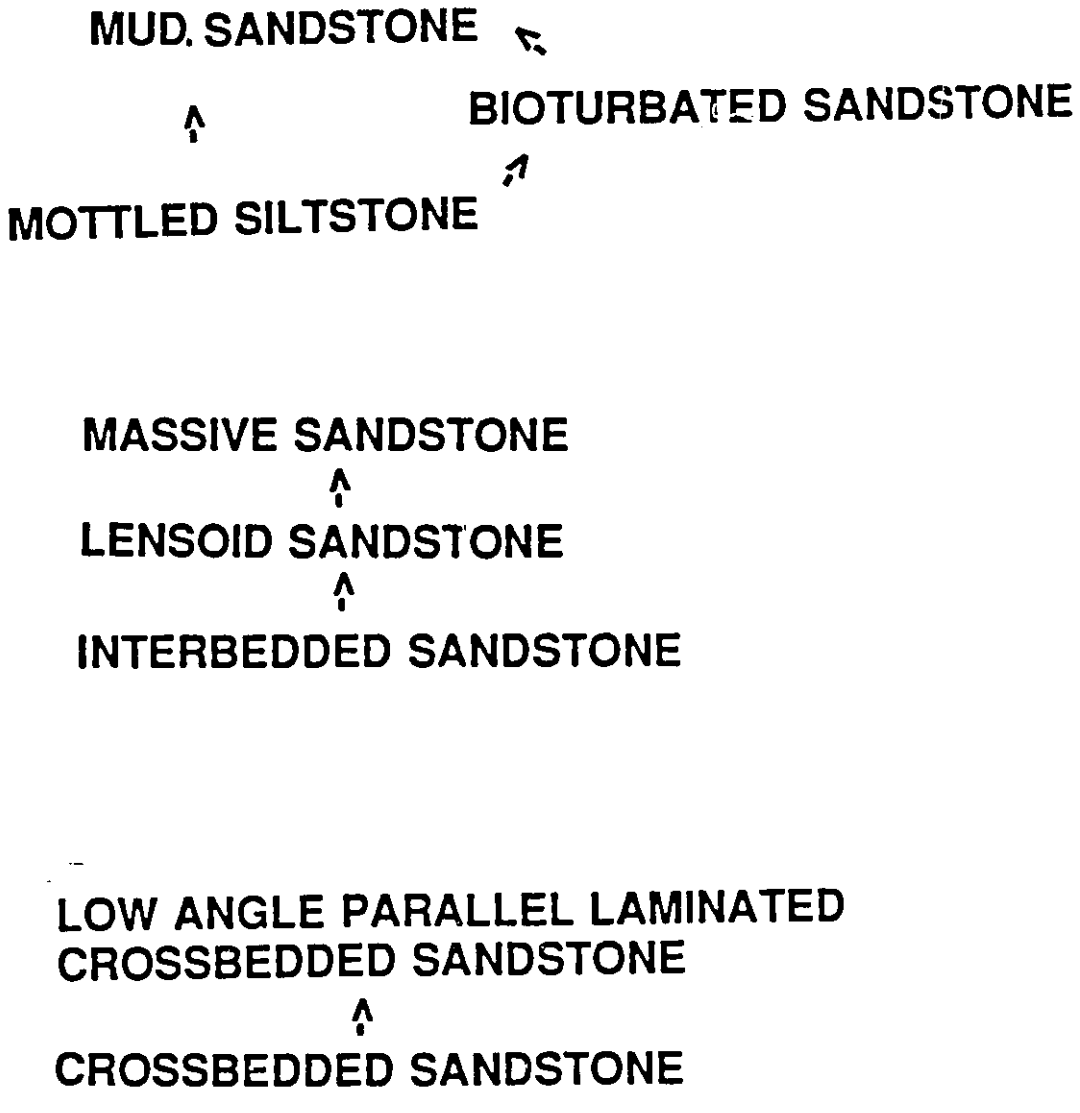

Figure 4-27. Facies Relationships Diagram for Unit Epsilon.
The figure shows those facies transitions that have 90% confidence of being non-random. The calculations are based on the program in Appendix C. Arrows show the direction of the favored transitions.

SEQUENCE EPSILON

MUDSTONE -> BIOTURBATED SILTSTONE

MOTTLED SILTSTONE -> BIOTURBATED SANDSTONE

PEBBLY MUDSTONE -> LAMINATED SILTSTONE

important to bear in mind that the absence of facies from a facies relationship diagram of "significant" transitions does not mean that the facies are necessarily insignificant in terms of their existence in the unit. Beyond the analysis of intraunit behavior, the relationship diagrams may also be compared to one another for a sense of comparative randomness.

In the most general terms, it can be seen that unit Gamma has the most continuous chain of facies relationships. Units Beta and Delta are somewhat similar each revealing a number of separate, `short' relationships such as the circuit between the various crossbedded sandstone facies in unit Beta. Unit Epsilon appears to have the least order to its facies with only three bi-state relationships. The regularity of the Gamma facies relationships reflects the succession from the finer grained facies into the coarser generally crossbedded facies so characteristic of the unit. The more prominent relationships in unit Beta do not reflect a grainsize increase because such an increase is not consistently present in the unit (see above and foldouts 8 through 12); they do however, show that the prominent facies in the unit have non-random relationships.

The relationships that are common between units are those between various forms of crossbedding and those between mottled siltstone and bioturbated sandstone. The former relationships appear in all but unit Epsilon and invariably involve higher angle cross-stratification (tangential parallel or planar parallel) being succeeded upwards by low angle cross-stratification. The relationship between mottled siltstone and bioturbated sandstone is absent only from unit Beta and inverted in the unit Gamma chain. These predominant relationships have implications for process interpretations discussed in chapter 6.

CHAPTER 5

UNIT GEOMETRY AND BASIN BEHAVIOR

Our fabled shores none ever reach,
No mariner has found our beach,
Scarcely our mirage now is seen ...
Yet still the oldest charts contain
Some dotted outline of our main.

H.D. Thoreau The Atlantides

5.1 SUMMARY

Operator and fault related errors in measurements of the six units, Alpha through Mu, described in chapter four are small enough that the unit geometries constructed from them may be used to judge general sediment accumulation. The combination of datum to unit boundary isopachs and unit isopachs reveals a pulse of foreland basin subsidence that began after deposition of the Joli Fou shale. Apart from possible minor eastward subsidence during the deposition of unit Mu, subsidence was initially greatest in the west where it allowed accommodation of a relatively large amount of sediment during the formation of units Epsilon through Gamma. The subsidence appears to have been hinged more or less at a stationary line across the southwest of the study area near Joarcam field. Following unit Gamma, during deposition of units Alpha and Beta, subsidence became more even across the basin. The Viking Formation, in the region studied reflects accommodation in a pulse of basin deformation.

In addition to this basin behavior, elements of Gamma's geometry reveal a net northeastern progradation superimposed on the units aggradational

component. The edge of the unit marks the onset of a correlative conformity. From the isopach maps of the units a reasonable argument can be made for depositional topography revealing shoreface wedges in the units Epsilon, Delta and Gamma in the southwest of the study region. Furthermore, it is likely that subtle sand 'ridges' appear in the isopachs of the same units possibly analogous to those seen the George's Bank area of the Atlantic coast.

The pronounced base of the Viking visible in logs may reflect long term scouring in a low accommodation basin center which correlates into a gradational base to the west due to greater accommodation. This might be a common occurrence in foreland basins.

5.2 INTRODUCTION: MEASUREMENTS OF UNIT BOUNDARIES

With the establishment of the unit correlations in chapter 4, the geometries of the units can be described. In particular, their geometries may be considered relative to those geometries described from sediments in passive margin basins. The forms of the units, provide information on the history of basin deformation. This history of basin deformation in turn provides some information on controls of sediment distribution.

The geometries of the units have been measured in two ways. The first is a standard isopach between the upper and lower boundaries of the appropriate unit; the second is an isopach from the datum b to the top of the unit in question. If there were no significant post- or syn-depositional deformation, then the former would give an idea of sediment distribution and the latter would portray the paleotopography of the unit boundary.

These different measurements are displayed in different ways; for each unit isopach both mesh diagrams and contour maps are shown. The datum to unit boundary isopachs are displayed only as mesh diagrams. In addition to the two measurements above, compressed versions of cross-sections in A-A' through G-G' (see foldouts 1-8 in the rear pocket and figure 4-10 for locations) are used to show the relationships of the geometries to each other.

The isopach maps were all generated using version 4.1 of Golden Software's Surfer program. The ASCII files used in this program were in turn all generated from files of the appropriate well log depth picks using simple FORTRAN programs. Copies of the files are available on disk from the author. To obtain the unit isopach files, the shallower depth files of an upper unit boundary were subtracted from the deeper files of a lower unit boundary. To obtain the datum to unit boundary isopach files, the deeper unit boundary files were subtracted from the datum file. This yields negative values and thus maintains a sense of relative geometry; in other words, this process creates the illusion of a currently horizontal datum and shows the relationship of the unit boundaries to it.

5.3 ERRORS IN MEASUREMENT AND ESTIMATION OF VALID DETAILS

5.3.1 Sources of Error

Before examining these different isopach displays, their accuracy was considered. The picks for unit boundaries and those for the markers in the over- and underlying shale have a number of potential sources of error. The sources of error include apparent extensional faulting, operator error in the picking of unit

boundaries on well logs, possibly undetected well deviation and horizontal mislocation of the well in the survey records.

5.3.2 Magnitudes of Errors

Undetected well deviation is probably a very minor to non-existent problem as is horizontal mislocation of the well in the survey data. Deviation in the well must be quite severe before it will create a comparatively noticeable extension in the well log signature and hence in the well log picks. (For example, it takes a 25° deviation to produce a 10% extension of a log.) The existence of operator error in the picks on well logs is almost certainly present, but there is no direct measurement for it. Likewise, there are certainly fault offsets in the well logs that would distort the local form of the unit (see below).

5.3.2.1 Fault Offsets

The existence of faulting was unexpected in this area and does not usually show up in pronounced form. However, it is present. Figure 5-1 shows an example of the type of correlation between well logs that indicates faulting. The parallel kinking of all correlation lines below a certain point in the central well indicates that material has probably been lost from the shales immediately overlying the Viking. This loss is interpreted to be due to faulting because of the lack of other suitable mechanisms and the presence of minor evidence in core for faulting (see below). The exact location of the fault offset is unknown because there are no pronounced markers that can be traced through the shales close enough to the location in question. Figure 5-1 shows the largest throw observed in any detected fault, of approximately twenty five feet. All of the examples observed suggest extensional faults because of apparent removal of material. The

Figure 5-1. Faulting Revealed by Well Log Correlation

Correlation of the SP (left side) and resistivity (right side) traces of the indicated wells reveals loss of section attributed to faulting in the un-named shales above the Viking.

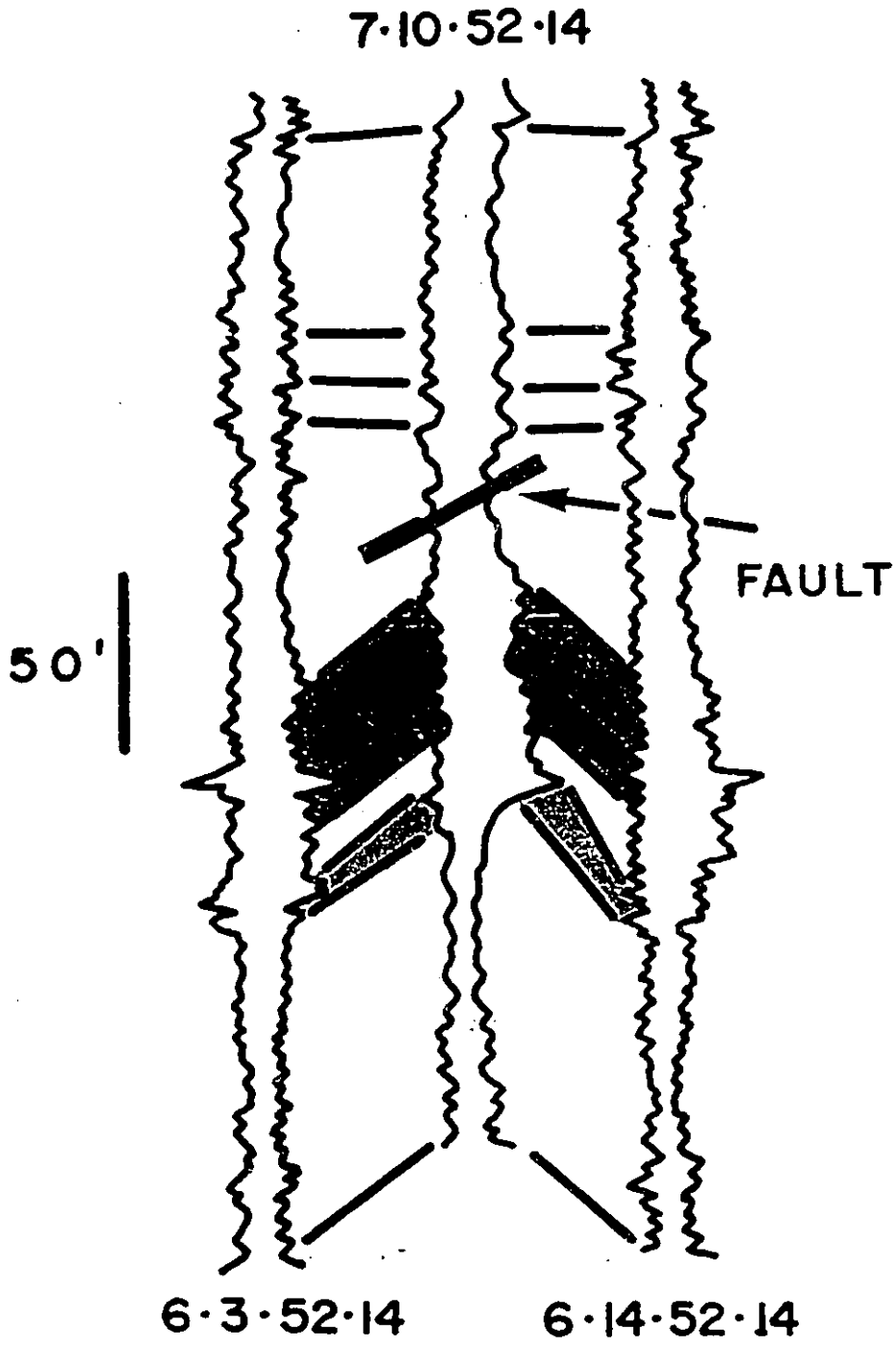
7·10·52·14
FAULT
50'
6·3·52·14
6·14·52·14

Figure 5-2. Extensional Faulting in Core

This figure shows minor extensional faulting with a throw on the order of three centimetres.

The scale bar i

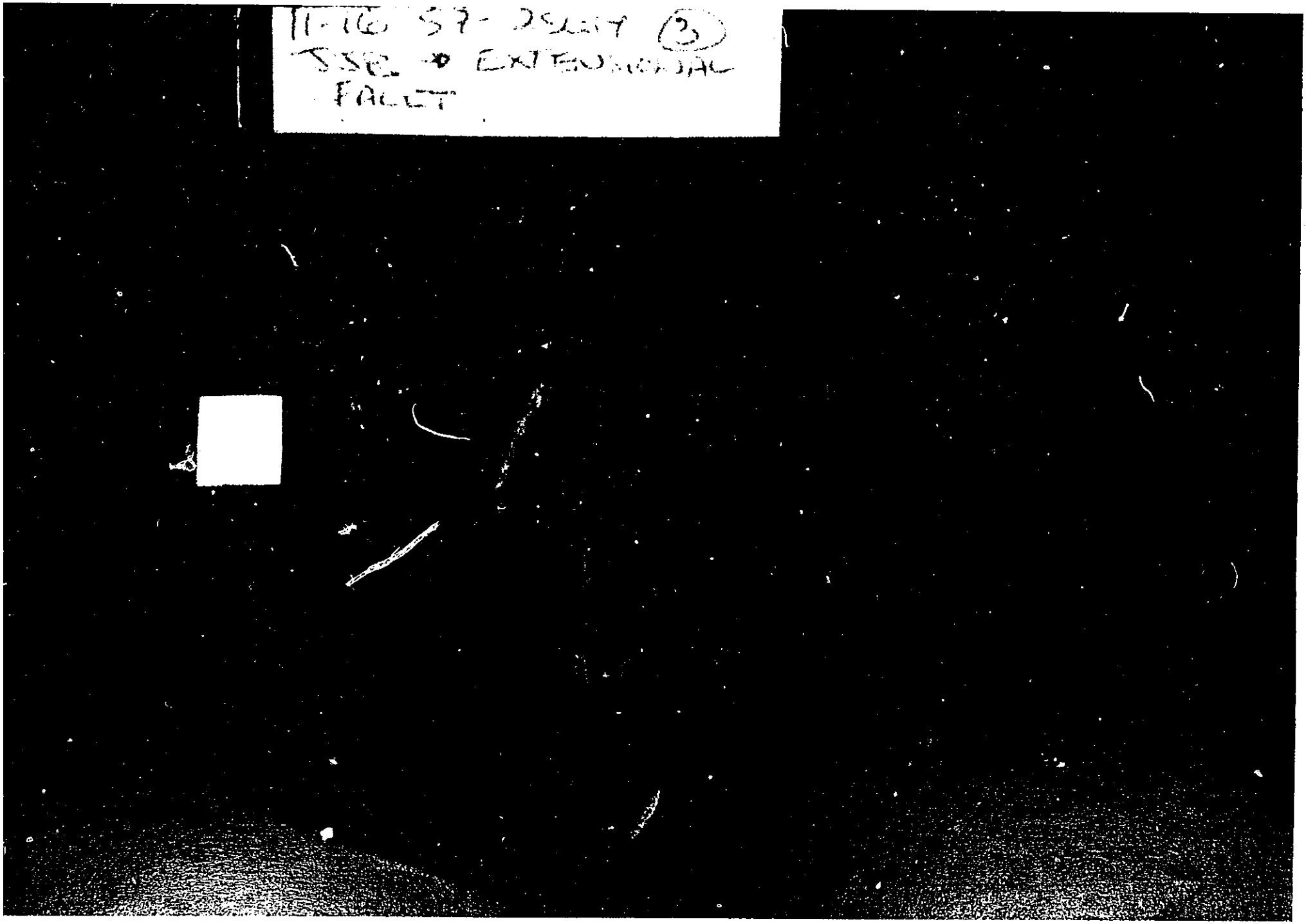
11-16 SP - DSLIT (2)
SSE - EXTENSIONAL
FAULT

Figure 5-3. Extensional Faulting in Core

This figure shows an approximately 1 cm. throw visible in an offset in the siderite nodule at the base of the unit.

The scale bar is 3 cm in length. Well 6-33-58-25W4; depth: 2590 feet.

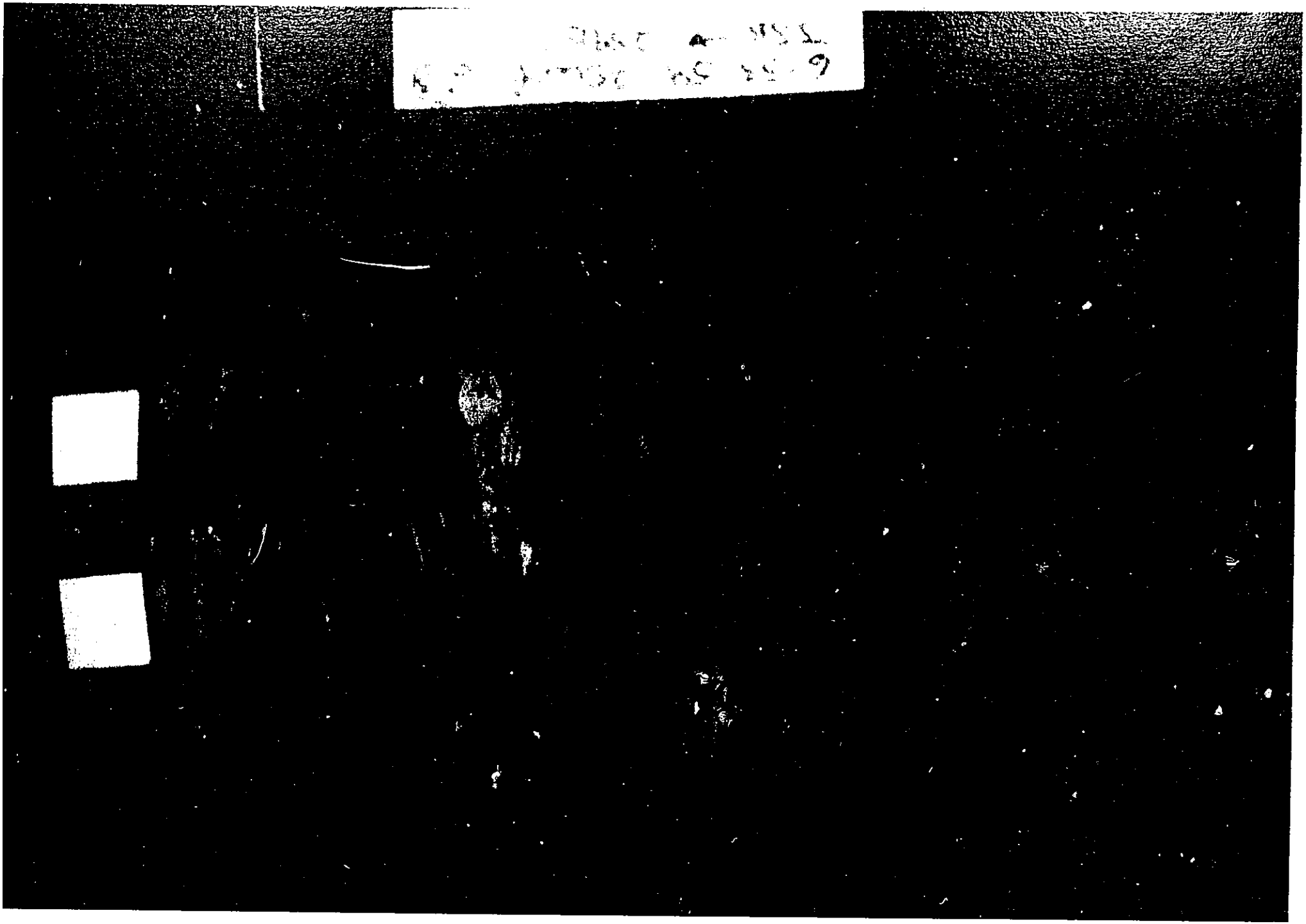

angle of the faulting could not be determined for any case because the spacing of the wells is so large that almost any angle down to less than a degree could be comfortably located within the intervening space. Furthermore, faults could not be mapped across the area.

The core evidence for extensional faulting is rare and rather subdued. Figures 5-2 and 5-3 show examples of the kind of minor faults that can be found; their offsets are on the order of centimetres. Comparing this to the example from figure 5-1 gives a possible range for the fault throws.

Obviously faulted sections such as that shown in figure 5-1 were restored prior to mapping the datum to unit boundary isopach value. This was done by matching the effected well log to an almost identical neighboring log so that the Viking Formation responses coincided. A given thickness was then added to the Viking unit depth picks in order to raise the markers a, b and c into coincidence with the neighboring, unfaulted log. This technique suffers from potential introduction of a slight planar bias to the isopachs; this introduction stems from the inherent assumption about the horizontal consistency in the local Viking responses. However, based on comparison to the apparently undisturbed parts of cross-sections this did not seem likely to be a real problem since the majority of correlations are approximately planar. This is apparent in the cross-sections A-A' through G-G' of foldouts 1 through 7.

Fault responses such as that shown in figure 5-1 are difficult to detect when the throw approaches five feet or less. Consequently, corrections were not made at a scale smaller that this. In the simplest approach, five feet may thus be

considered a rough limit of resolution imposed on the isopach maps. However, there are other means of estimating the map reliability.

5.3.2.2 Geostatistical Error Estimation

Beyond the kind of simple accuracy limitations such as the five feet restriction noted above, geostatistical analysis allows for a more encompassing estimation of error (e.g.,Journel and Huijbregts, 1978). It has the virtue of including otherwise immeasurable errors such as operator error in picking the well logs. Unfortunately, geostatistical analysis of the isopach map data over the area of figure 1-2 is rather difficult because the horizontal and vertical extent of variation is such that larger trends are difficult to remove and smaller ones are insufficiently repeated to adequately average out fluctuations. However, geostatistical results do provide a general feel for the accuracy of the contour maps presented and are worth presenting from this point of view.

The data from each unit isopach was analyzed geostatistically using the U.S.G.S. Statpac program (Grundy and Miesch, 1987). Data was entered in the form of latitude-longitude coordinates with either the unit thickness or datum to unit boundary thickness as the dependent variable. Only a punctual kriging approach turned out to be useful. For reasons that are not understood, trend removal prior to universal kriging gave much higher variations in the semi-variogram; in fact, the variations were higher than the simple general variation in the data by up to two orders of magnitude. This may reflect the relatively strong variation in unit thickness compared to simple geometrical trend surfaces. Because of this complication, kriged maps were not produced. The variogram analysis

Figure 5-4. Semi-Variogram of Unit Alpha Isopach

This figure shows the data points and fitted semi-variogram for the data from the isopach of unit Alpha. The program and interpretation are discussed in the text.

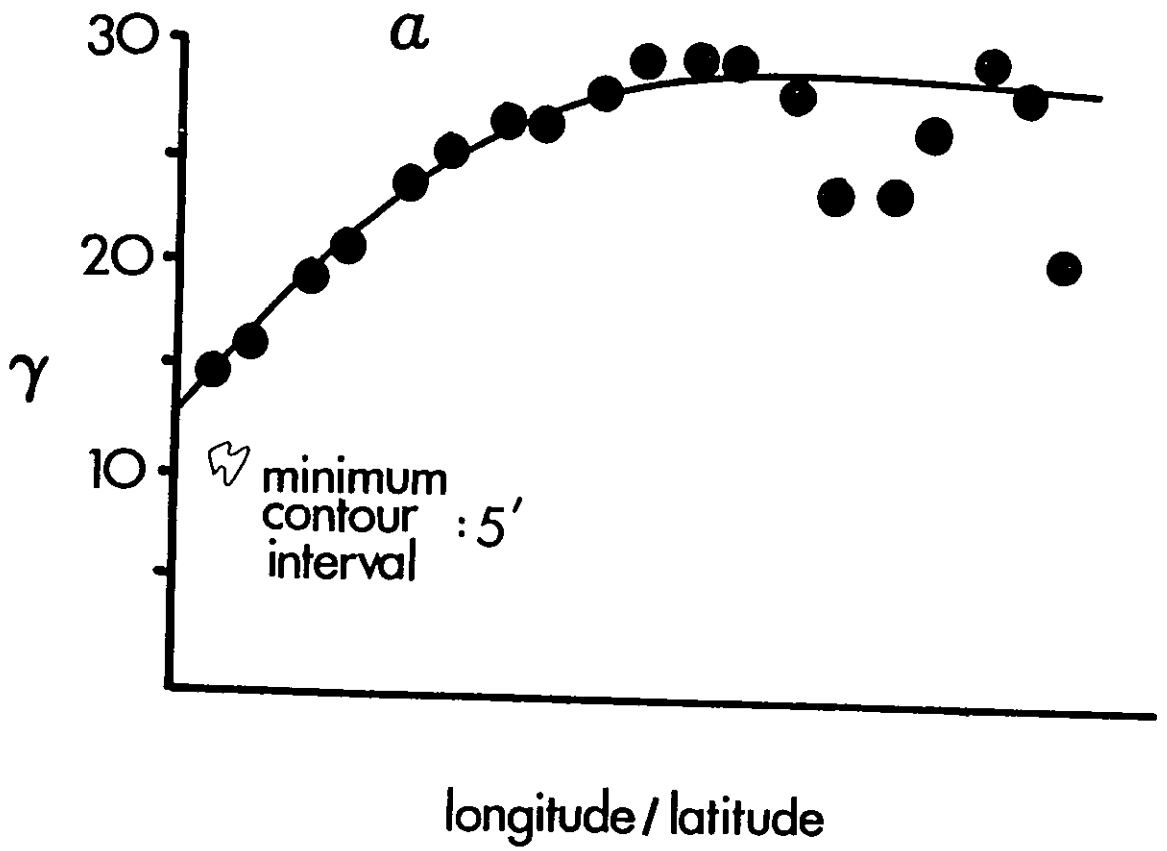
30
20
10
γ
a
minimum
contour
interval
: 5′
longitude / latitude

was limited to obtaining restrictions on the contour interval according to the scheme used by Sharp (1988). For the purposes of this investigation the isopach data are approximately isotropic, so simple, single variogram calculations were all that were employed. (Multiple variograms reflecting different sampling directions (anisotropy) did not appear to be vastly different from the isotropic ones.)

Because such a basic, reconnaissance approach was taken to a complex set of data, only simple efforts were made to fit models to the resulting variograms. In all cases, a simple spherical model was used. In most cases, the range was on the order of 0.8. Figure 5-4 shows an example semi-variogram for the unit isopach for Alpha. Since minimum contour intervals were the only goal of this analysis precise modeling of the variograms was not as important asestimation of the "nugget effect" or irreducible variance. The irreducible variances for all analyses were transformed into standard deviations that take the form of feet. These are shown in figure 5-5 for both the unit isopach (labeled isopach) and the datum to unit boundary (labeled marker) analyses. Following Sharp (1988), these values are the minimum contour interval that should be applied to the maps in order to maintain two thirds of the valid data within the appropriate contour intervals.

The minimum contour intervals correlate with the geometry of the various unit isopachs with smaller values corresponding to more tabular isopachs. The analysis of unit Alpha was the only one which had an ideal form for the variogram because Alpha is a relatively tabular unit and also has a relatively planar relationship to the overlying markers (see below). Consequently, there is

almost no trend to remove before processing the data. This is not the case for the other units when measured from the datum to their boundaries (the column labeled marker in figure 5-5); therefore, their analyses are noisier, as can be seen in the increased minimum contour interval. The exception to this trend of increased uncertainty with depth from the datum is the marker z in the Joli Fou. This is because the marker is more roughly parallel to the datum than the responses within the Viking. There is consequently a drop off in the level of uncertainty, but it remains higher than that of Alpha because of the decreased amount of data and some uncertainty in the picks made (operator error).

The unit isopach minimum contour intervals (the column labeled isopach in figure 5-5) fluctuate more but again reflect the general geometry of the units (see below). The more tabular isopachs tend to have the lower contour intervals.

Although these minimum contour intervals are in essence only semi-quantitative, they do provide a basis for the estimation of the validity of the forms shown in the mesh diagrams and contour maps below. Perhaps more importantly, they also serve as a warning not to take the contour intervals as precise measurements from which more detailed analyses might be derived.

5.4 UNIT ISOPACHS DESCRIPTIONS

5.4.1 Introduction

Of all the unit geometry maps, the unit isopachs are the simplest. The description of the isopachs revolves around their illustration in figures 5-6 through 5-11. Each unit isopach is described in ascending order. A mesh diagram and accompanying contour map are shown for each unit. The contour maps are contoured at the minimum interval indicated in figure 5-5 following the

analysis of the semi-variogram of the appropriate data. The data point locations for the generation of the maps and diagrams are shown in figure 1-2.

The unit isopachs have all been constructed using the same parametres in the Golden Software Surfer (V. 4.1) program. They are displayed in longitude latitude format with a vertical exaggeration of 2500 times (corresponding to a display scale of .0025 in the program). The gridding algorithm used was inverse distance squared weighing of eight nearest neighbor sampling. The grid was of dimensions seventy two by thirty six and was scaled with one x unit being equal to 1.4 y units for display in order to approximate the longitude latitude distortion at the latitude of the study site. More precise correction was not made because the results were only for display purposes, and the fine detailing would not have been noticeable. Prior to final printing, the isopach grids were smoothed using the program's spline option with a tension factor of 2.5.4.2 Unit Mu Isopach

As discussed in chapter 4, unit Mu is the most tenuous of the correlated units. It appears to have accumulated only in the southeast corner of the region studied, because it either disappears or amalgamates with unit Epsilon in other locations. This can be seen quite clearly in figure 5-6; the flat areas of the mesh diagram are those regions were unit Mu does not appear to exist. The degree to which the isolated 'mounds' in the figure represent genuine sediment accumulation as opposed to regions were the signature of the unit is merely more distinct is likewise unknown. These mounds, for the most part reflect several wells so the effect is more than just an isolated variation in a well pick. This may be seen by comparing the data points of figure 1-2 to figure 5-7, the contour map

Figure 5-5. Minimum Contour Intervals from Isopach Semi-Variograms

The columns opposite are the minimum estimated valid contour intervals that could be used for maps of either the unit isopachs (the isopach column) or the unit boundary to datum isopachs (the marker column). The values are derived from the irreducible variance to meet the criterion proposed by Sharp (1988). The unit corresponding to the appropriate value is shown in the far left column with z being the marker in the Joli Fou shales.

	ISOPACH	MARKER
α	5′	6′
β	7′	10′
γ	12′	10′
δ	9′	16′
ϵ	6′	22′
μ	3′	23′
Z	13′	15′

Figure 5-6 Mesh Diagram Isopach of Unit Mu

View form the northeast of the isopach of unit Mu. Vertical exaggeration of 2500 times. Each grid square is approximately 1 mile square.

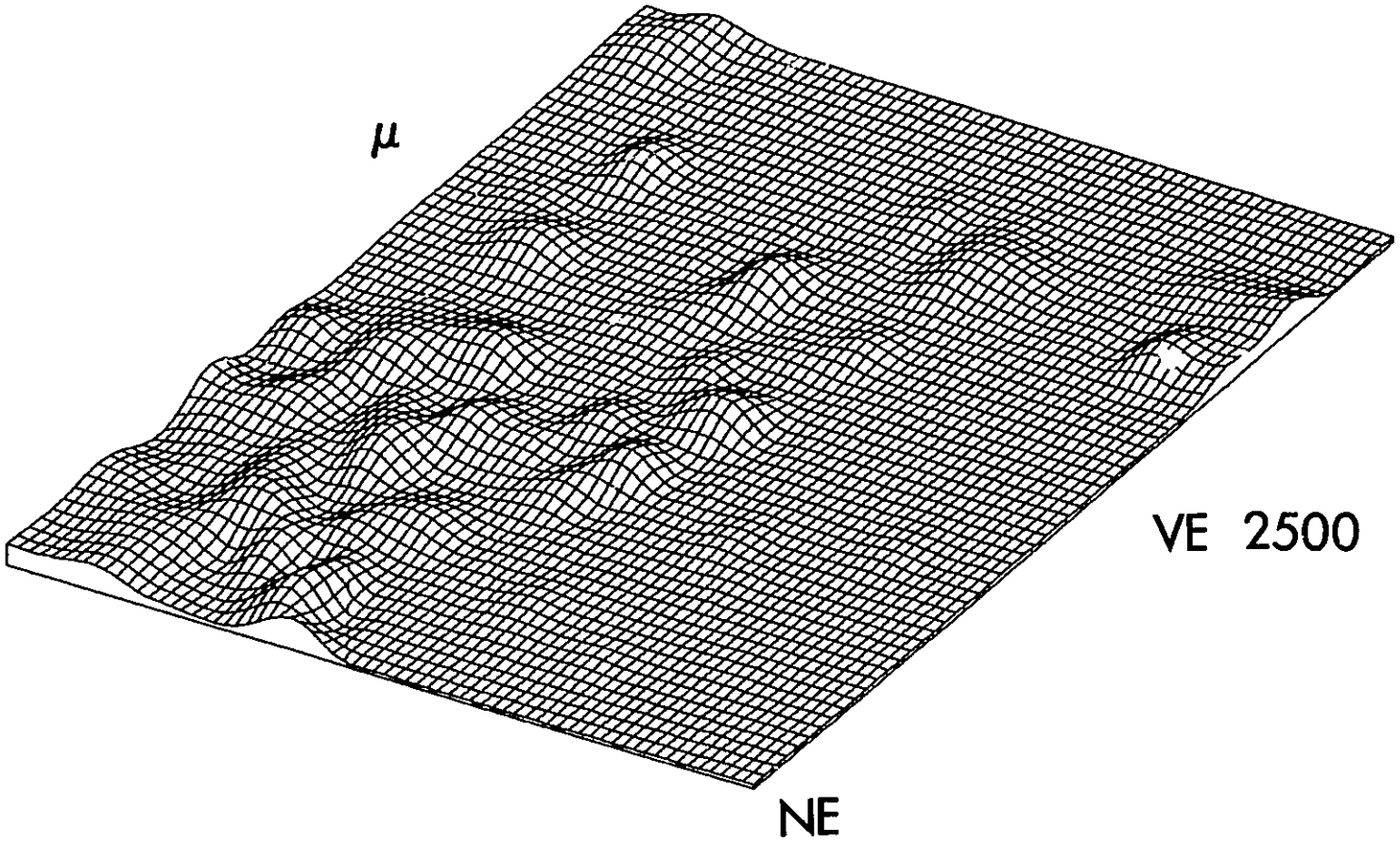
μ
VE 2500
NE

Figure 5-7 Contour Map of Unit Mu Isopach

The contours in the map are based on the minimum estimated contour interval from geostatistical analysis (see figure 5-5).

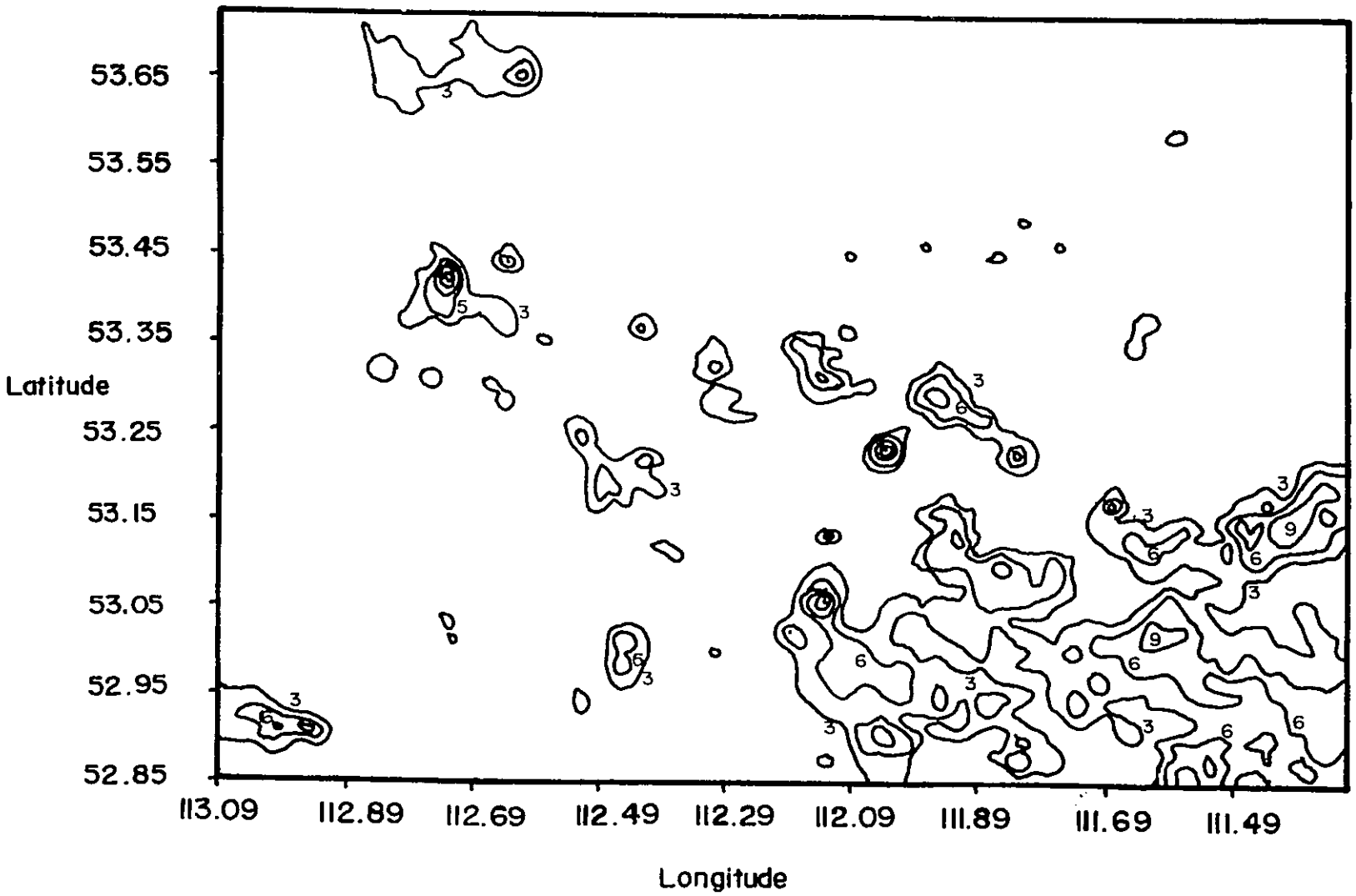
53.65
53.55
53.45
53.35
Latitude
53.25
53.15
53.05
52.95
52.85
113.09
112.89
112.69
112.49
112.29
112.09
111.89
111.69
111.49
Longitude

corresponding to the mesh diagram of figure 5-6. There are a few unlabelled pinpoint dots on the map which are isolated well points, but the more varied contours include several wells. The contour map, figure 5-7, shows the overall thinness of Mu which reflects its uncertain nature.

5.4.3 Unit Epsilon Isopach

The isopach data for unit Epsilon is displayed in figure 5-8 in mesh diagram form and figure 5-9 in contour map form. In the most general sense, unit Epsilon thins to the east in a crudely planar fashion. The most notable accumulation of sediment is in the southwest corner of the map; this appears as a high in the mesh diagram which is about eighteen to twenty four feet thick in the contour map. Comparison of figure 5-9 to figure 1-2 reveals that this thickness lies to the southwest of the Joarcam field. The next largest feature of the isopach is the development of somewhat linear thick and thin patches sub parallel to this large, southwestern accumulation. The mesh diagram shows this trend fairly clearly; it can be observed in the contour map by following the twelve foot contour in the center of the figure. This bulge has rough dimensions of fifteen by sixty miles as estimated from the twelve foot contour intervals. As with all the following estimations of accumulation sizes, the result is rather inaccurate because it depends on a loose estimate of the point of closure for the isopach; moreover, this point may not even be the best point for defining such `bodies'. Despite these vagaries the effort is useful for relative comparison.

As with all of the maps here, the smallest scale irregularities (bumps) cannot be taken as real. They do not show up clearly in the cross-sections and almost certainly are artifacts of the inverse distance square gridding algorithm.

Figure 5-8 Mesh Diagram Isopach of Unit Epsilon

View form the northeast of the isopach of unit Epsilon. Vertical exaggeration of 2500 times. Each grid square is approximately 1 mile square.

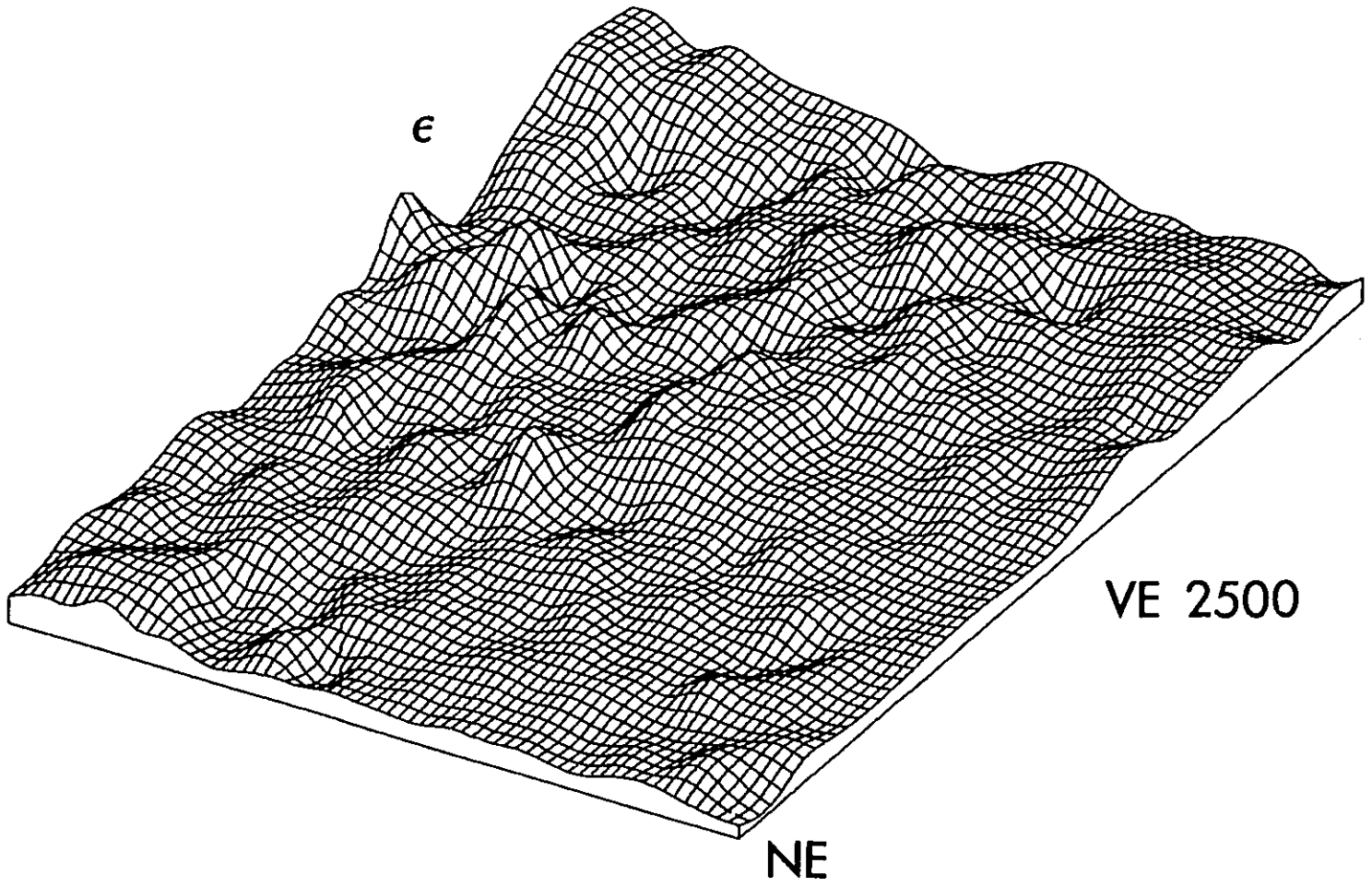
ϵ
VE 2500
NE

Figure 5-9 Contour Map of Unit Epsilon Isopach

The contours in the map are based on the minimum estimated contour interval from geostatistical analysis (see figure 5-5).

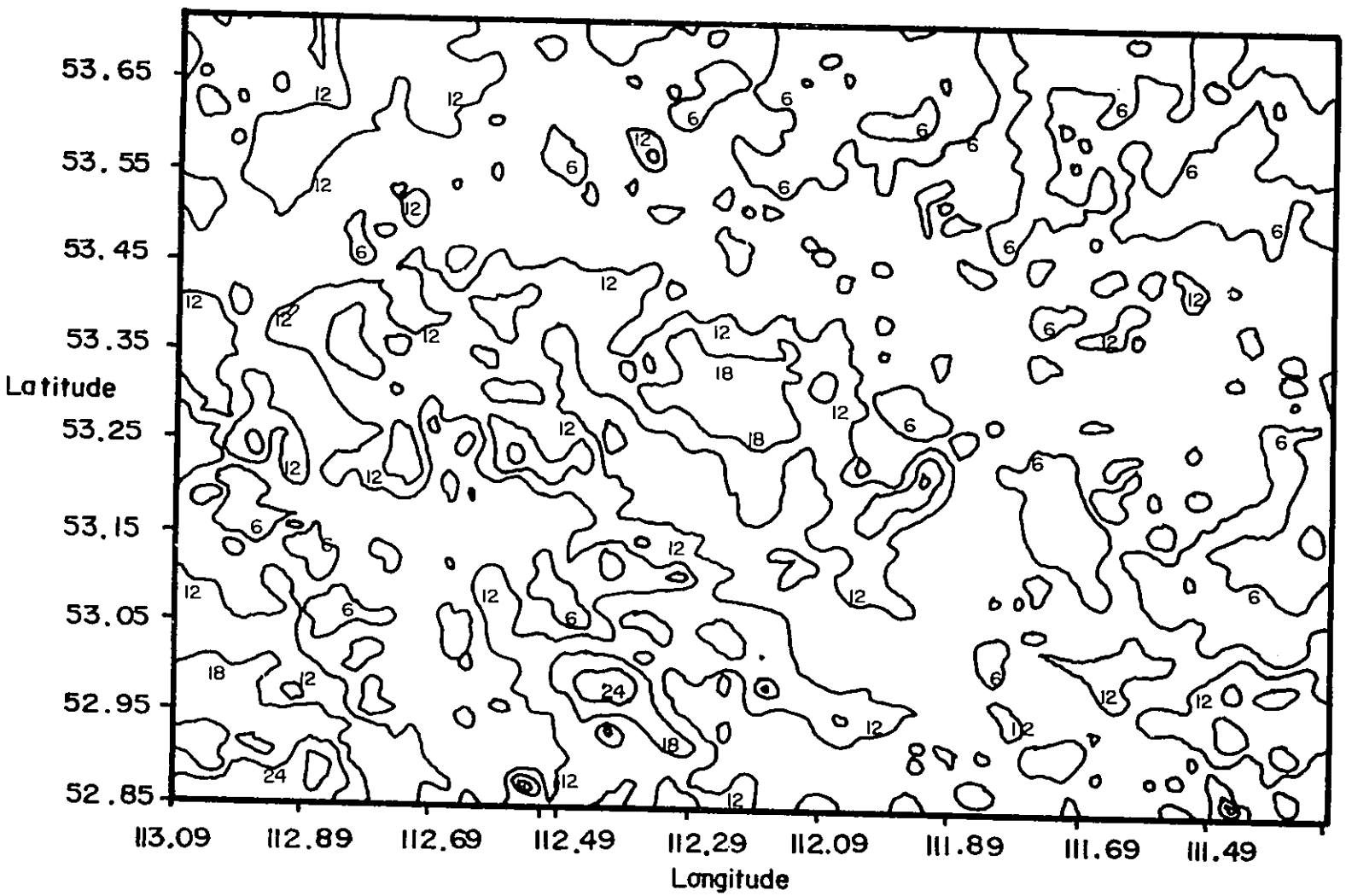
53.65
53.55
53.45
53.35
Latitude
53.25
53.15
53.05
52.95
52.85
113.09
112.89
112.69
112.49
112.29
112.09
111.89
111.69
111.49
Longitude

5.4.4 Unit Delta Isopach

Unit Delta is in many ways similar to unit Epsilon. This similarity may be seen in the mesh diagram of figure 5-10 and the accompanying contour map of figure 5-11. Delta has a first order, roughly planar pattern of thinning to the east identical to that of unit Epsilon. On the whole, unit Delta is only slightly thicker than Epsilon, but Epsilon has a more pronounced thickening in the central region of the study area. Like Epsilon, Delta's largest accumulation is also in the southwest of the study area. This unit thins in a region more or less identical to that of the thinning in unit Epsilon. Delta has less pronounced thickening and thinning away from this southwestern accumulation, but there is still a trend toward lineation sub-parallel to it. This may be seen in the nine and eighteen foot contour interval in the lower left and central-right regions of figure 5-11. The size of this 'lineation' is about ten by sixty miles based approximately on the eighteen foot contour interval. The inaccuracy inherent in the measurement makes precise comparison impossible but there is a rough relationship between these northwest-southeast trends in the two units. Comparison of the maps of figures 5-9 and 5-11 suggests that apart from the large accumulation in the southwest, the thicker areas of unit Delta tend to overly the thinner regions of unit Epsilon.

5.4.5 Unit Gamma Isopach

The isopachs of unit Gamma are shown in mesh diagram form and contour map form in figures 5-12 and 5-13 respectively. The most striking aspect of these figures is the wedge like nature of the unit. The thickest part of the unit has moved slightly from the southwest corner of

Figure 5-10 Mesh Diagram Isopach of Unit Delta

View form the northeast of the isopach of unit Delta. Vertical exaggeration of 2500 times. Each grid square is approximately 1 mile square.

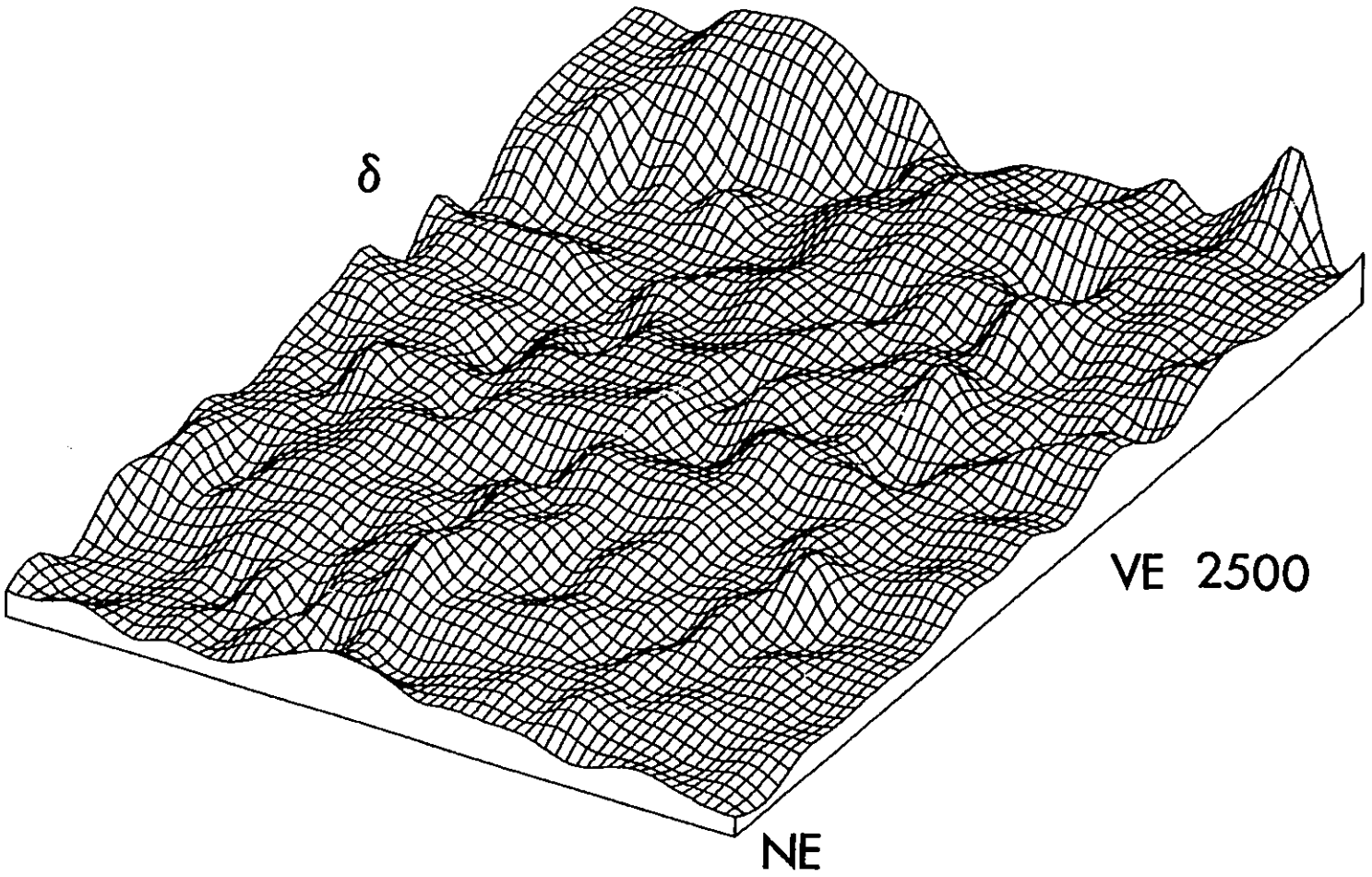
δ
VE 2500
NE

Figure 5-11 Contour Map of Unit Delta Isopach

The contours in the map are based on the minimum estimated contour interval from geostatistical analysis (see figure 5-5).

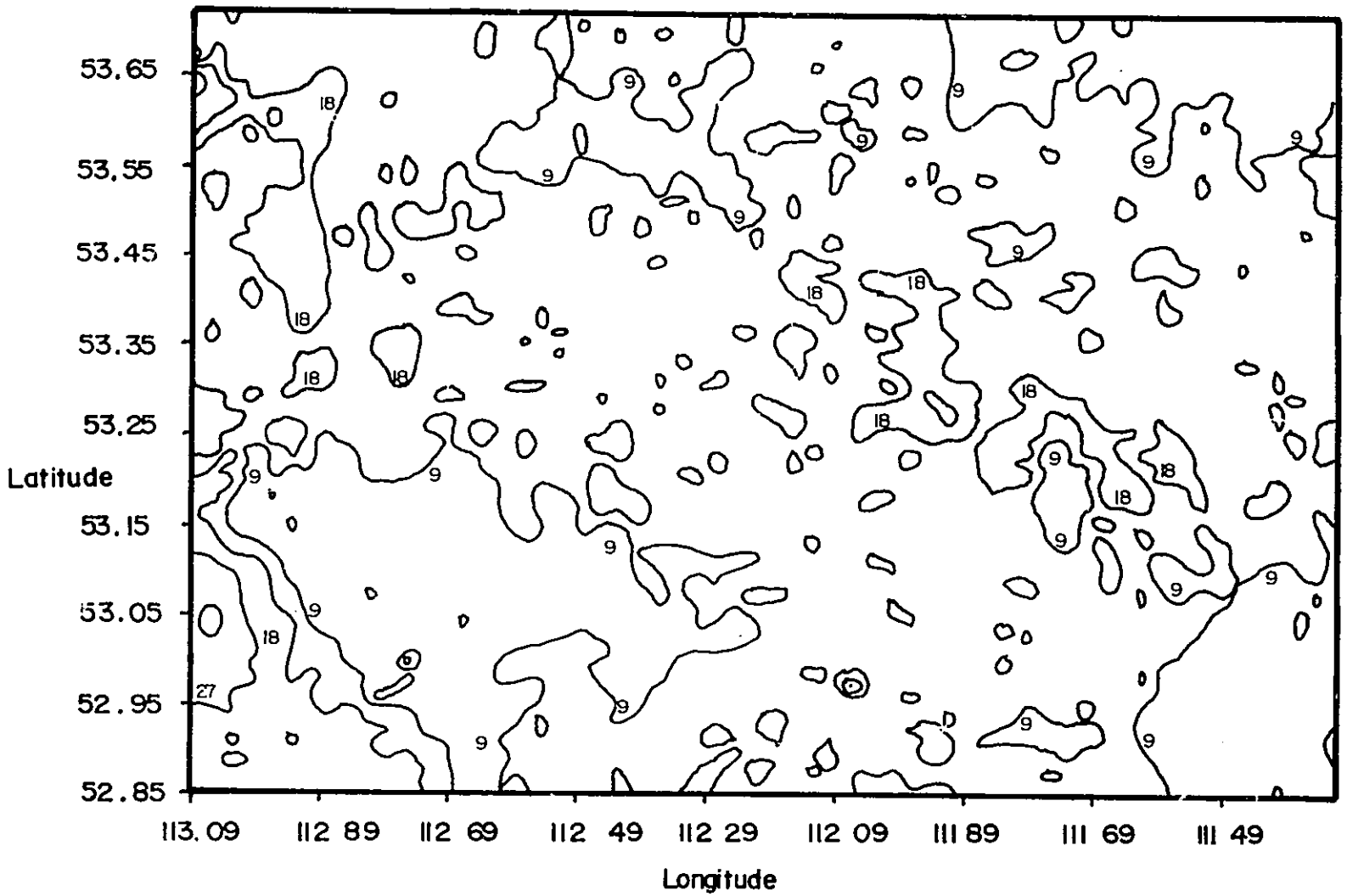
53.65
53.55
53.45
53.35
53.25
53.15
53.05
52.95
52.85
Latitude
113.09
112 89
112 69
112 49
112 29
112 09
111 89
111 69
111 49
Longitude

the study area to the center of the western edge. However, the entire western portion of the package now has considerable thickness, on the order of twenty feet as seen in figure 5-13. The flat portion of figure 5-12 in the eastern half of the diagram represents an area of zero thickness; the unit has no depositional record in this location apart from a few questionable 'mounds'. Following the pattern on units Delta and Epsilon, unit Gamma still appears to have northwest-southeast trends in thickness superimposed on the overall eastward thinning. These trends are weaker than those in Delta and may be seen in the twenty four foot contour interval in figure 5-13; the mesh diagram shows some suggestion of this trend as well. The lobe that lies off the westernmost accumulation and primarily constitutes the 'trend' measures about ten by thirty miles and is about twenty feet thick at a maximum crudely based on the twenty four foot contour level. As for the other maps, the smallest scale features probably are artifacts of the gridding algorithm.

5.4.6 Unit Beta Isopach

Unit Beta's isopach returns to the much more subdued planar pattern shown previously in units Delta and Epsilon. The measurements of unit Beta are portrayed in mesh diagram form in figure 5-14 and in contour map form in figure 5-15. The difference between the planar patterns of units Delta and Epsilon and Beta is primarily that Beta does not have a large accumulation of material in the southwest of the diagram. Instead, unit Beta's thickest region lies roughly in the center of the study site. Superimposed on the isopach thick are rough northwest-southeast elongations; the trends are visible in figure 5-14. These elongations appear to be on the order of ten by twenty miles using the approximately forty

Figure 5-12 Mesh Diagram Isopach of Unit Gamma

View form the northeast of the isopach of unit Gamma. Vertical exaggeration of 2500 times. Each grid square is approximately 1 mile square.

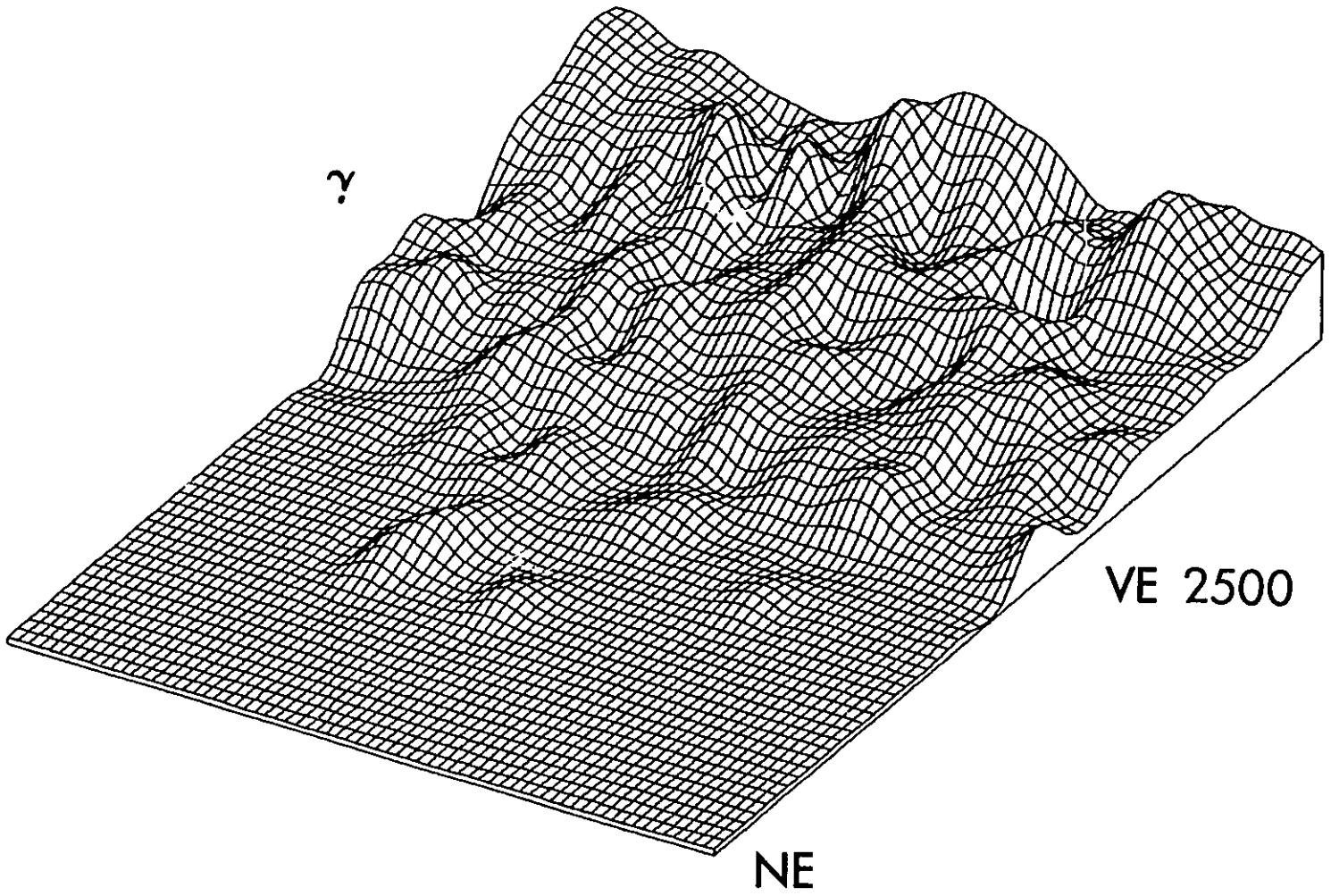
?
VE 2500
NE

Figure 5-13 Contour Map of Unit Gamma Isopach

The contours in the map are based on the minimum estimated contour interval from geostatistical analysis (see figure 5-5).

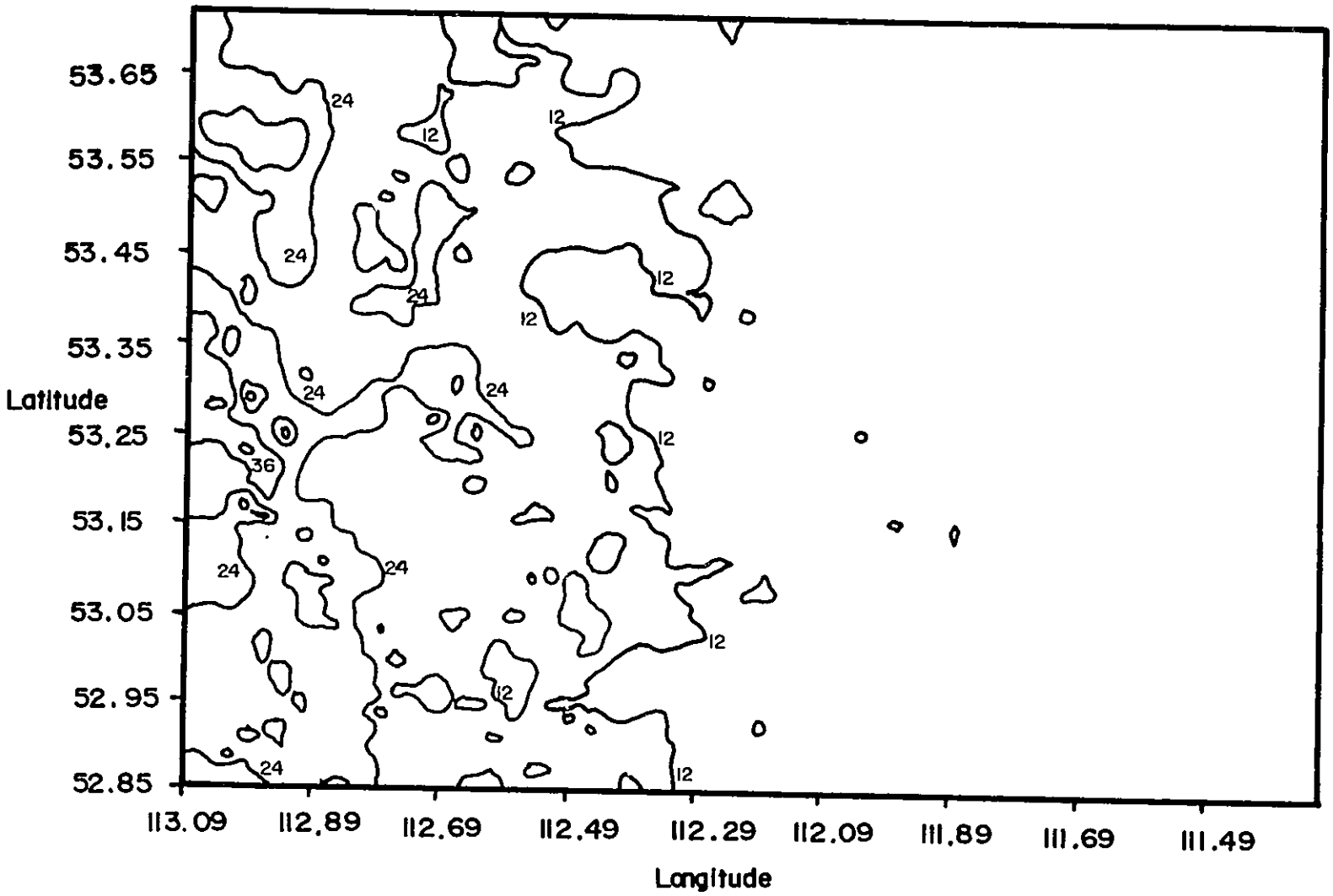
53.65
53.55
53.45
53.35
Latitude
53.25
53.15
53.05
52.95
52.85
24
12
36
113.09
112.89
112.69
112.49
112.29
112.09
111.89
111.69
111.49
Longitude

foot contour level, but they are much more irregular than those of units Delta and Epsilon. It is useful to compare figure 5-15 to figure 5-13. The thicker portions of unit Beta appear to overly the thinner portions of unit Gamma. This may be seen most clearly by examining the location of the accumulations defined by the thirty five and thicker contours.

5.4.7 Unit Alpha Isopach

Unit Alpha's isopach information is shown in figures 5-16 and 5-17. The former is a mesh diagram and the latter a contour map. Of all the unit isopachs, Alpha's is most nearly planar. There is a mildly thicker portion, again trending northwest-southeast, but this is only five feet thicker than the rest of most of the unit. This thicker portion of the unit, defined by approximately the twenty foot contour, roughly coincides with the thicker portion of Beta's isopach as may be seen by comparing figure 5-17 and 5-15. Apart from this trend, there is not any noticeable thinning of the unit from west to east.

5.5 DATUM TO UNIT BOUNDARY ISOPACHS

5.5.1 Introduction

The datum to unit boundary isopachs have all been displayed using only mesh diagrams. This is because, as is discussed below, their more detailed form is less important than that of the unit isopachs. The required information can be gathered from examination of their gross geometry alone which is best done by means of the mesh diagrams. Since the point of primary interest in these displays is in the southwest corner of the study area, the point of view has been change from that used in the unit isopach figures; the view is now from the southwest for figures 5-18 through 5-25. The other notable change from that of the unit

Figure 5-14 Mesh Diagram Isopach of Unit Beta

View form the northeast of the isopach of unit Beta. Vertical exaggeration of 2500 times. Each grid square is approximately 1 mile square.

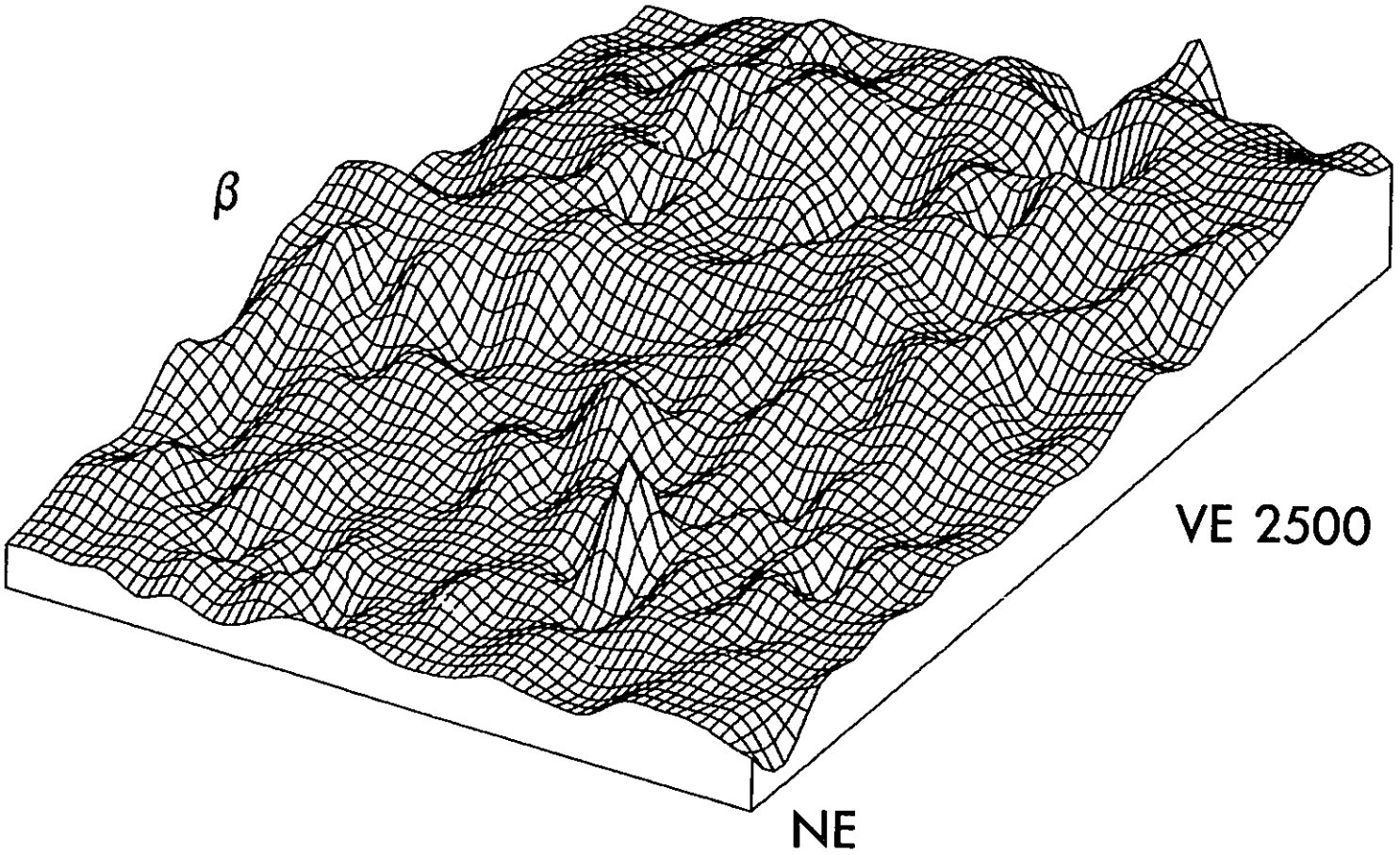
β
VE 2500
NE

Figure 5-15 Contour Map of Unit Beta Isopach

The contours in the map are based on the minimum estimated contour interval from geostatistical analysis (see figure 5-5).

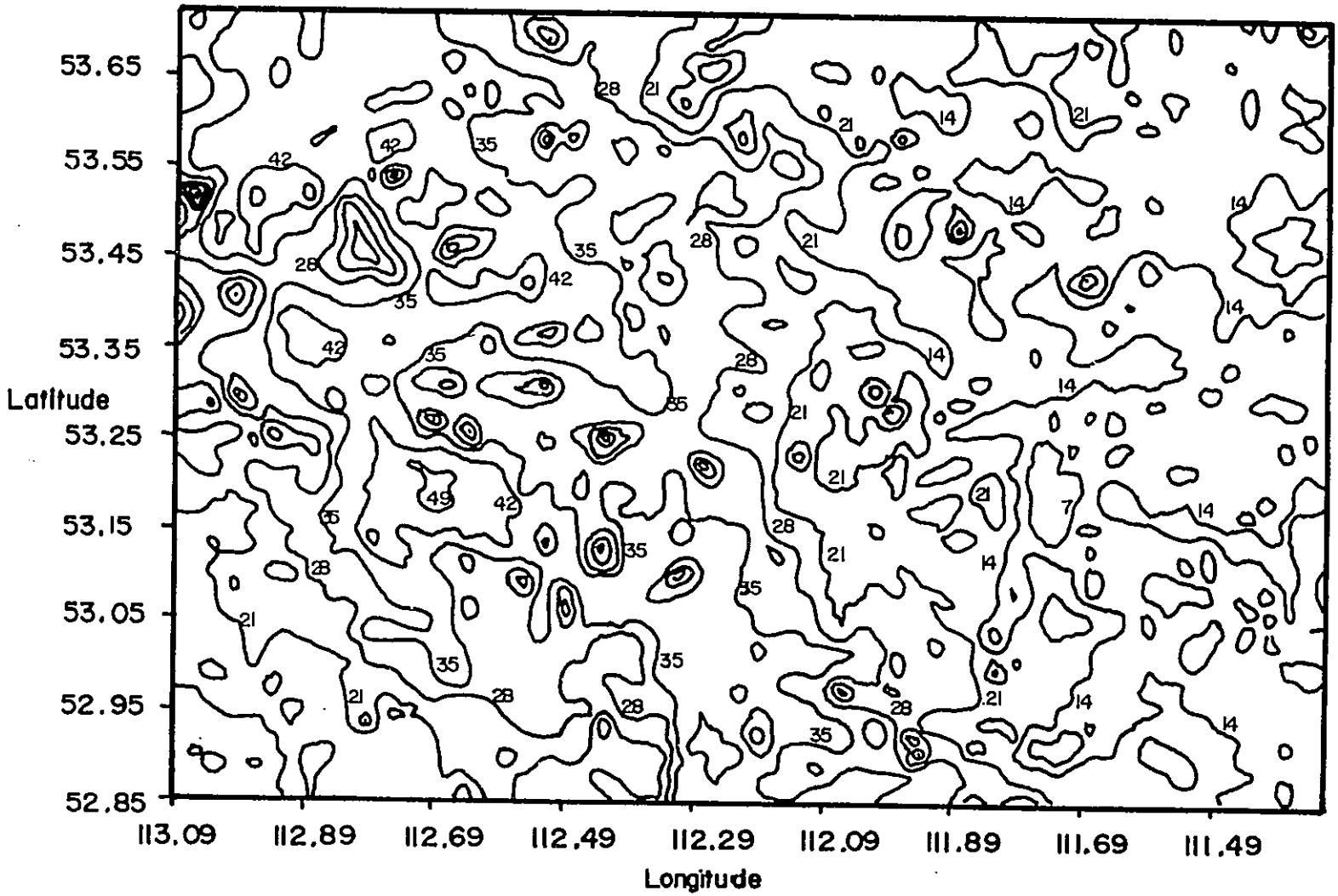
53.65
53.55
53.45
53.35
Latitude
53.25
53.15
53.05
52.95
52.85
113.09
112.89
112.69
112.49
112.29
112.09
111.89
111.69
111.49
Longitude

Figure 5-16 Mesh Diagram Isopach of Unit Alpha

View form the northeast of the isopach of unit Alpha. Vertical exaggeration of 2500 times. Each grid square is approximately 1 mile square.

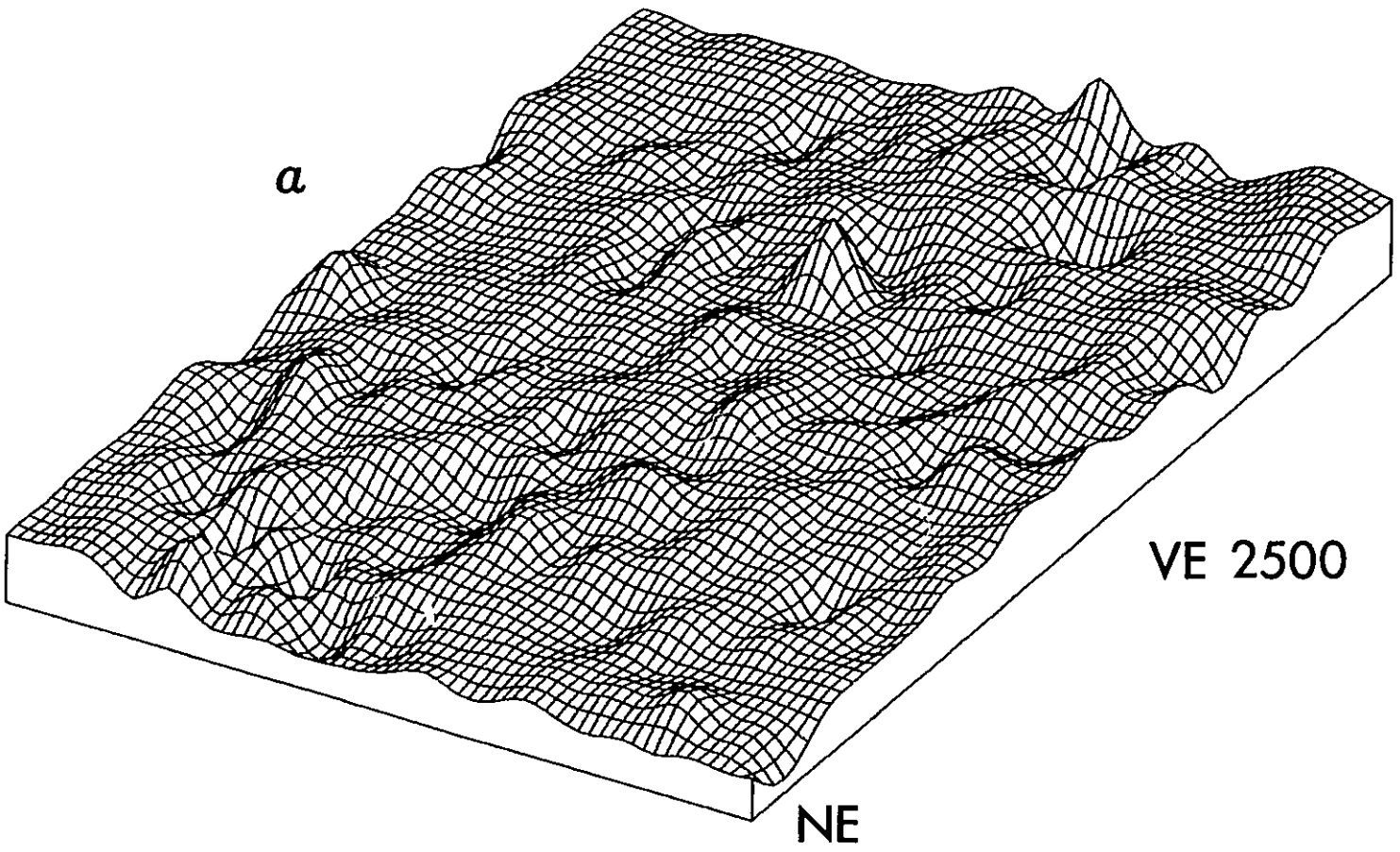
a
VE 2500
NE

Figure 5-17 Contour Map of Unit Alpha Isopach

The contours in the map are based on the minimum estimated contour interval from geostatistical analysis (see figure 5-5).

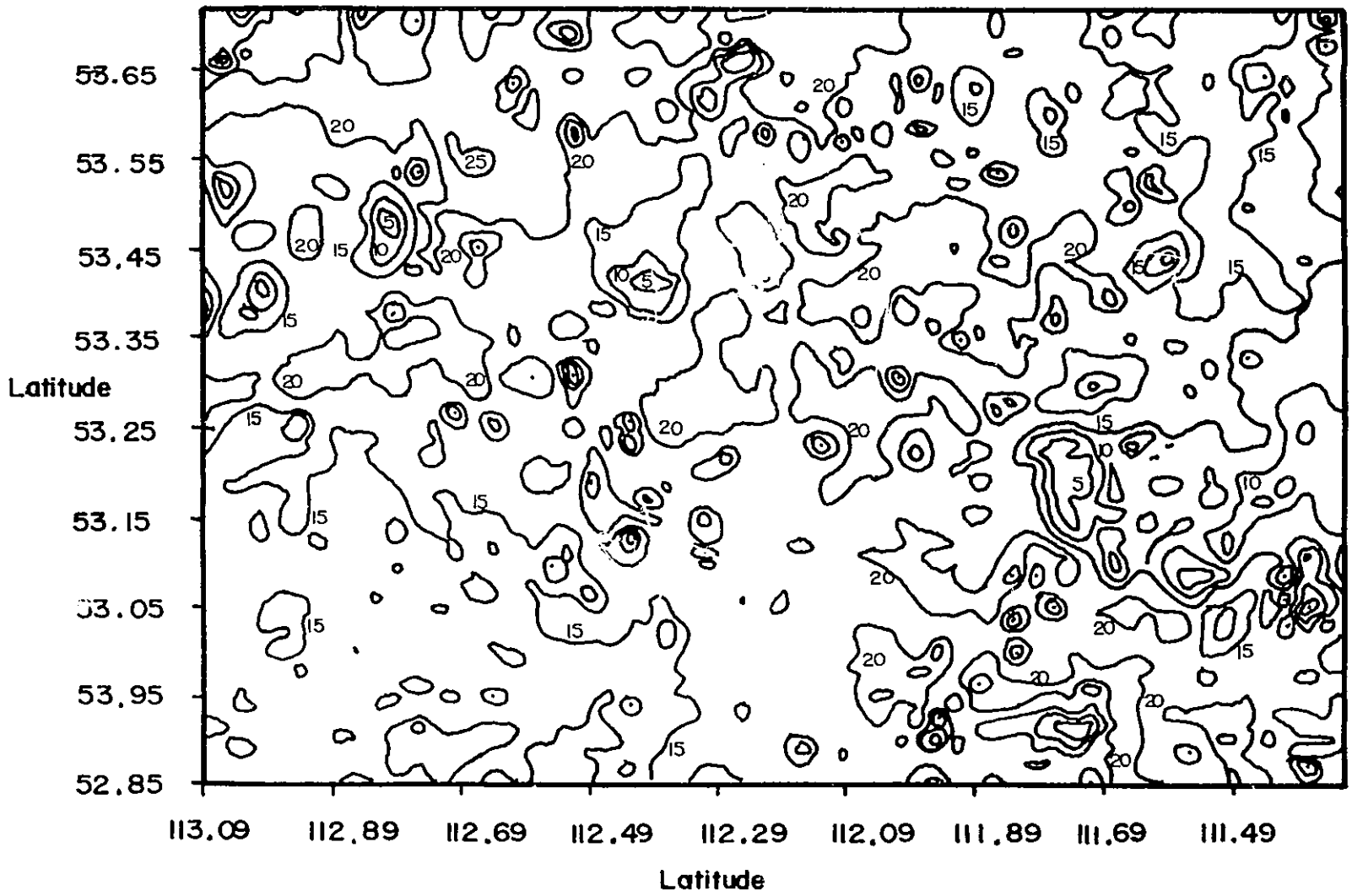
53.65
53.55
53.45
53.35
Latitude
53.25
53.15
53.05
53.95
52.85
113.09
112.89
112.69
112.49
112.29
112.09
111.89
111.69
111.49
Latitude

boundary isopachs is that the marker, z, in the Joli Fou shales and the Base of the Viking are included in the isopachs. This is because their geometries relative to those of the boundaries internal to the Viking offer important information about the structural behavior of the basin during the time of Viking deposition.

As for the mesh diagrams of the unit isopachs, the datum to unit boundary isopachs have all been constructed using the same parametres in the Golden Software Surfer (V. 4.1) program. They are displayed in longitude latitude format with a vertical exaggeration of 800 times (corresponding to a display scale of .0025 in the program). The gridding algorithm used was inverse distance squared weighing of eight nearest neighbor sampling. The grid was of dimensions seventy two by thirty six and was scaled with one x unit being equal to 1.4 y units for display in order to approximate the longitude latitude distortion at the latitude of the study site. Prior to final printing, the isopach grid was smoothed using the spline option of the program with a tension factor of 2.

5.5.2 Datum to the Joli Fou marker, Z, Isopach

The most notable aspect of the isopach from the datum, b, to the marker in the Joli Fou, z, is that the geometry is essentially planar. This may be seen in figure 5-18. There is a very slight tilt to the west-southwest. The source of the minor undulations on this 'surface' are not isolatible and many of them certainly reflect errors of the kind described in section 5.3. However, there are some of these forms that continue throughout the isopachs right up to that of the top of unit Alpha. Such matching of patterns is particularly obvious along the eastern edge of the diagrams. This may be incidental mapping of the smaller fault offsets described in section 5.3; see section 5.7.2 for a discussion.

5.5.3 Datum to Base of Viking Isopach

The isopach that reflects the relative orientation of the surface represented by the base of the Viking has a greatly different form to that of z, the marker in the Joli Fou shales beneath the formation. This form is shown in figure 5-19. The base of Viking has a pronounced tilt to the west-southwest relative to the datum, b. The direction of this inclination is consistent with that currently existing in the basin as the result of foreland basin subsidence. The gradient of this surface, although extreme in the mesh diagram, is actually only approximately 1 in 10,000 at its steepest. Gradients of successive unit boundaries become less pronounced as one proceeds up the stratigraphic column (see below). Because z is roughly parallel to b, this tilt in the base of the Viking is also relative to the marker in the Joli Fou although just slightly less pronounced due to the latter's minor western tilt.

5.5.4 Datum to Top of Unit Mu Isopach

Figure 5-20 shows the relative surface represented by the isopach of b to the top of unit Mu. Not surprisingly it essentially mimics that of the base of the Viking. This is because of the very thin nature of the unit. The minor peaks at the edge of the figure and the one in the southern central portion could not be matched with particular data points; hence specific sources of errors could not be determined; they may reflect gridding algorithm artifacts. Their anomalous appearance might be due to projection of one or more minor errors into the grid used for map generation.

Figure 5-18 Mesh Diagram of Datum to Joli Fou Marker

The view of this diagram is from the southwest; vertical exaggeration is 800 times; Each grid square is approximately 1 mile square.

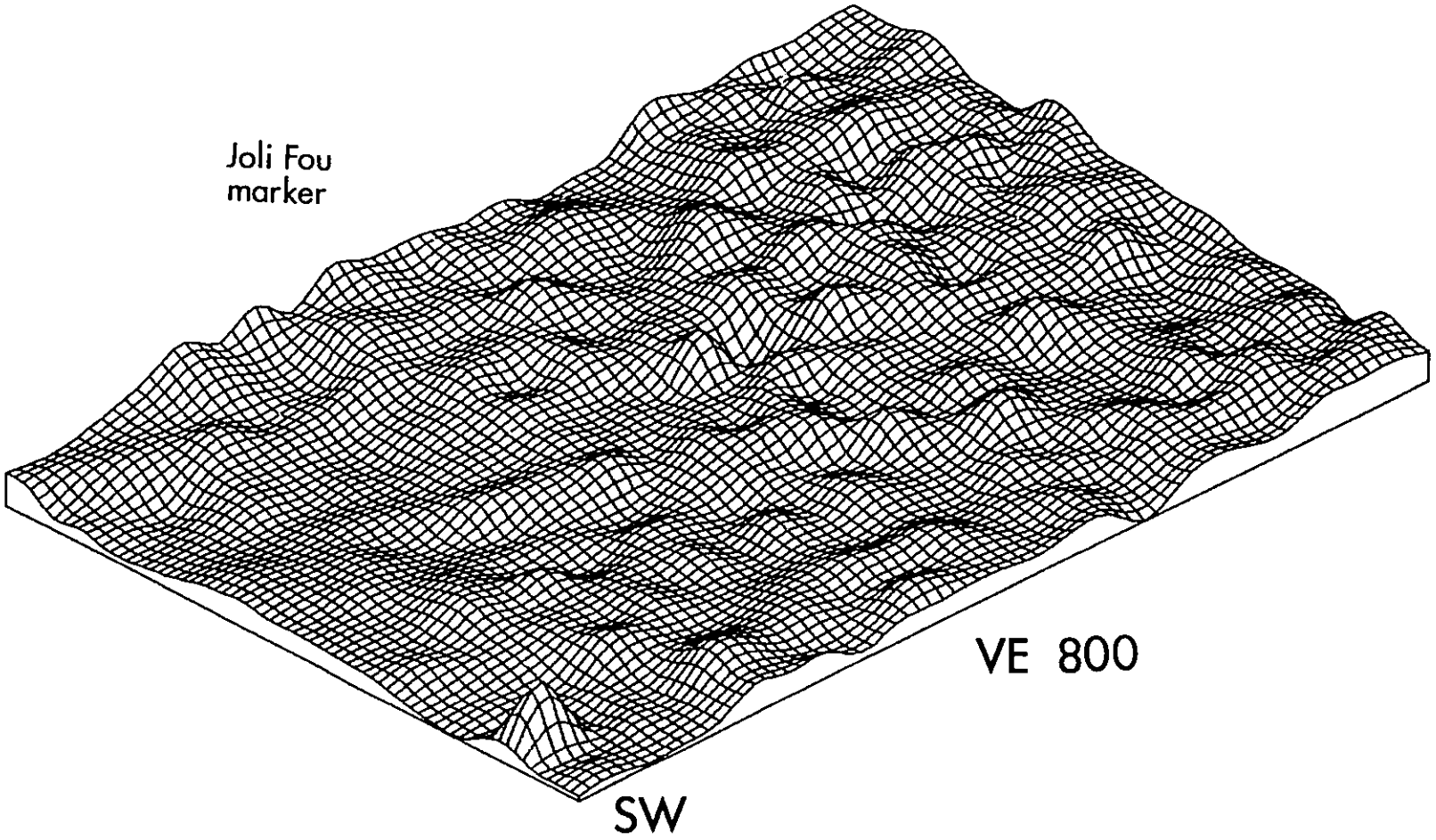
Joli Fou
marker
VE 800
SW

Figure 5-19 Mesh Diagram of Datum to Base of Viking

The view of this diagram is from the southwest; vertical exaggeration is 800 times; Each grid square is approximately 1 mile square.

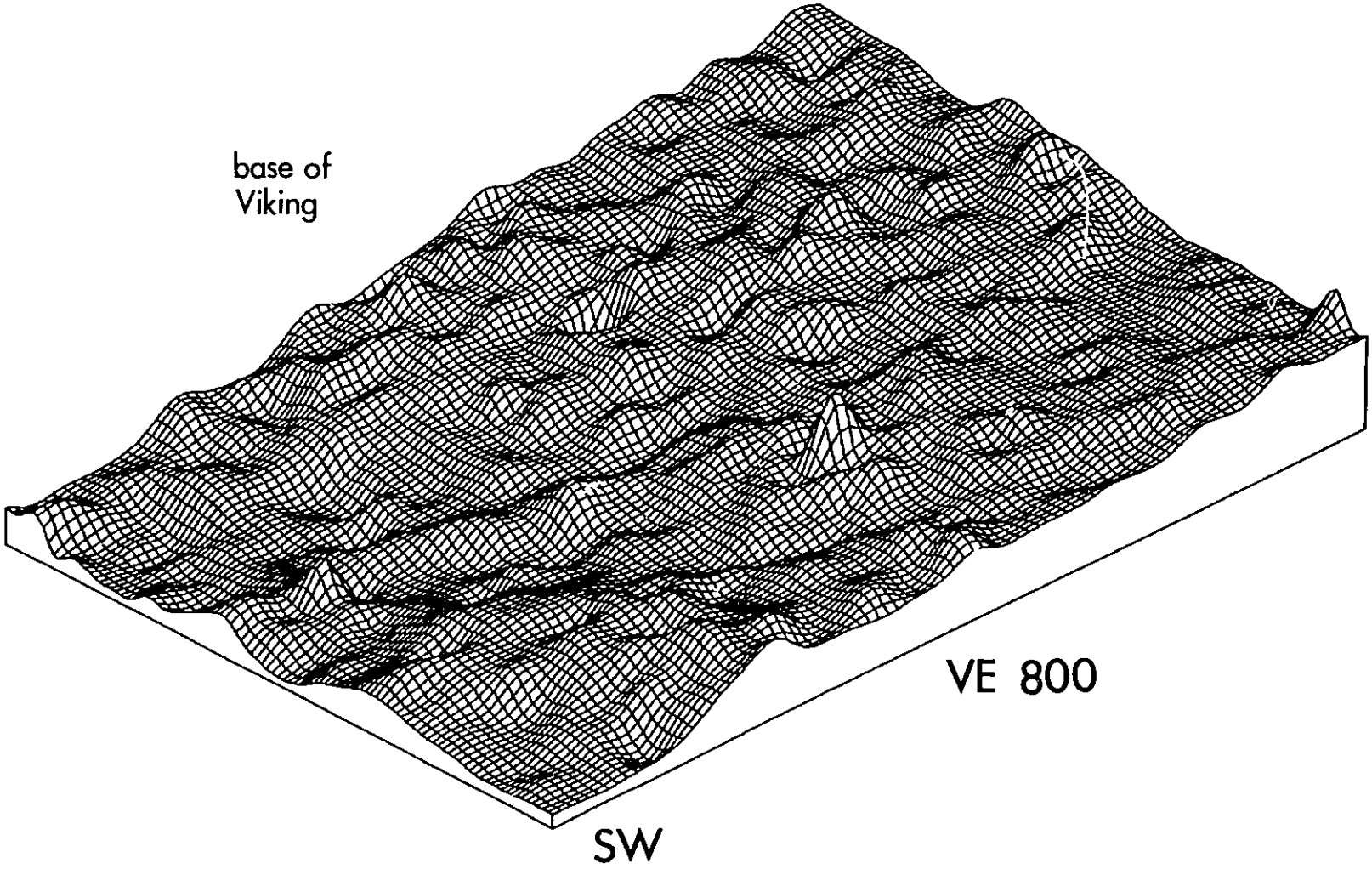
base of
Viking
VE 800
SW

5.5.5 Datum to Top of Unit Epsilon Isopach

Figure 5-21 portrays the isopach from b to the top of unit Epsilon. It too still shows a strong west-southwest tilt in the relative surface. The tilt is less pronounced than those of boundaries below.

5.5.6 Datum to Top of Unit Delta Isopach

The decrease in the degree of west-southwest tilting continues with the diagram of unit Delta's boundary visible in figure 5-22. The tilting is much decreased relative to that at the base of the Viking and the unit boundary is now almost planar relative to the datum.

Some of the undulations in this surface are similar to undulations in other unit to datum isopachs. This shows up particularly well in the comparison of Epsilon and Delta. The most easily spotted examples of identical form lie in the northeast corner and along the northern edge of figure 5-21 and 5-22.

5.5.7 Datum to Top of Unit Gamma Isopach

Figure 5-23 shows the map of the relative surface generated by the isopaching of the interval from b to the top of unit Gamma. The sense of western tilting is now gone to be replaced by a slight eastward `tilt' along the western edge. As discussed below (section 5.7.3), this local `tilt' almost certainly corresponds to the addition of the sediment wedge of unit Gamma shown in figures 5-12 and 5-13.

5.5.7.1 Datum to Gamma Bentonites Isopach

There is one feature within unit Gamma whose form is of particular interest; these are the bentonite traces discussed in chapter 4 that

Figure 5-20 Mesh Diagram of Datum to Top of Unit Mu

The view of this diagram is from the southwest; vertical exaggeration is 800 times; Each grid square is approximately 1 mile square.

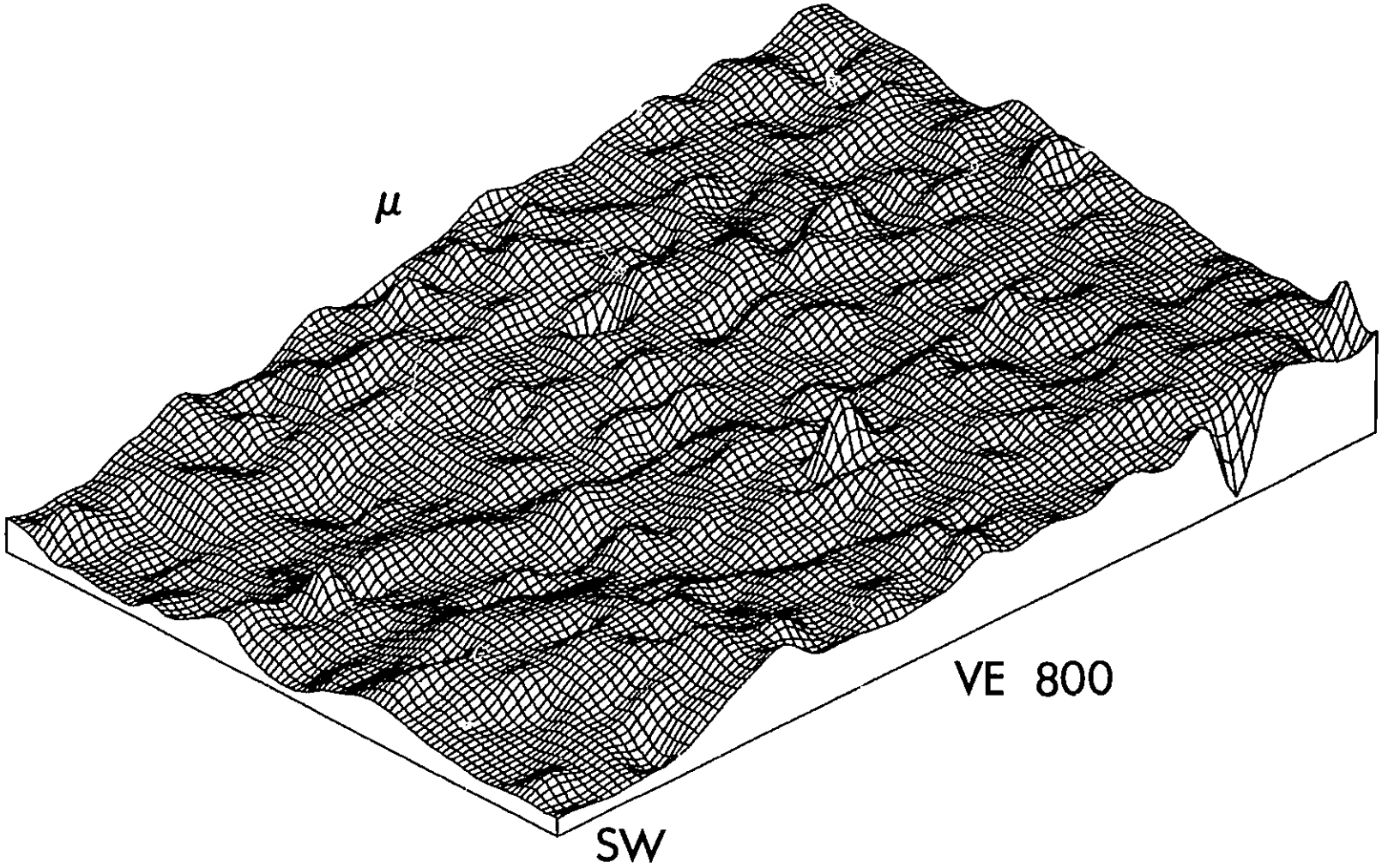
μ
VE 800
SW

Figure 5-21 Mesh Diagram of Datum to Top of Unit Epsilon

The view of this diagram is from the southwest; vertical exaggeration is 800 times; Each grid square is approximately 1 mile square.

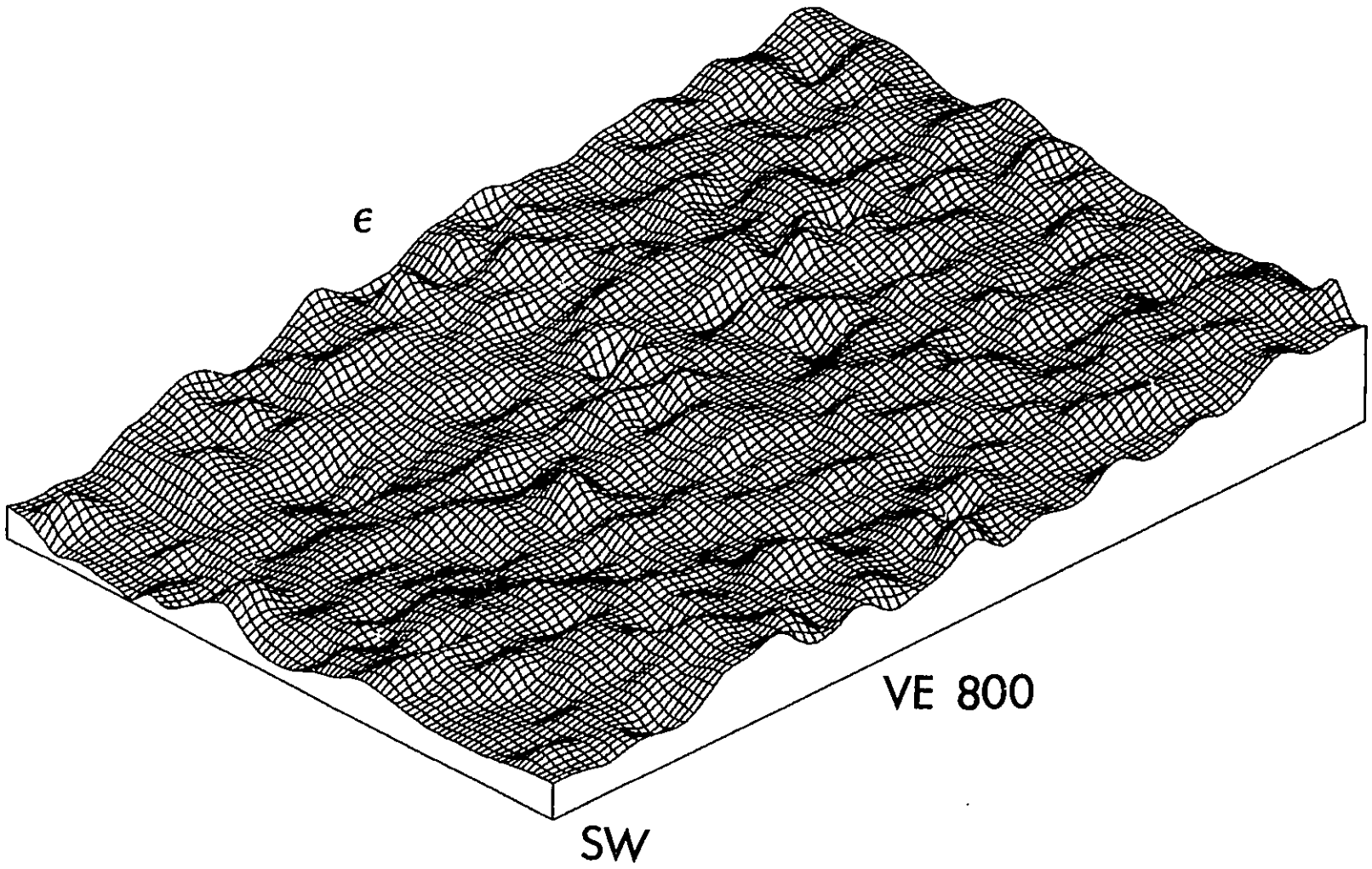
ϵ
VE 800
SW

Figure 5-22 Mesh Diagram of Datum to Top of Unit Delta

The view of this diagram is from the southwest; vertical exaggeration is 800 times; Each grid square is approximately 1 mile square.

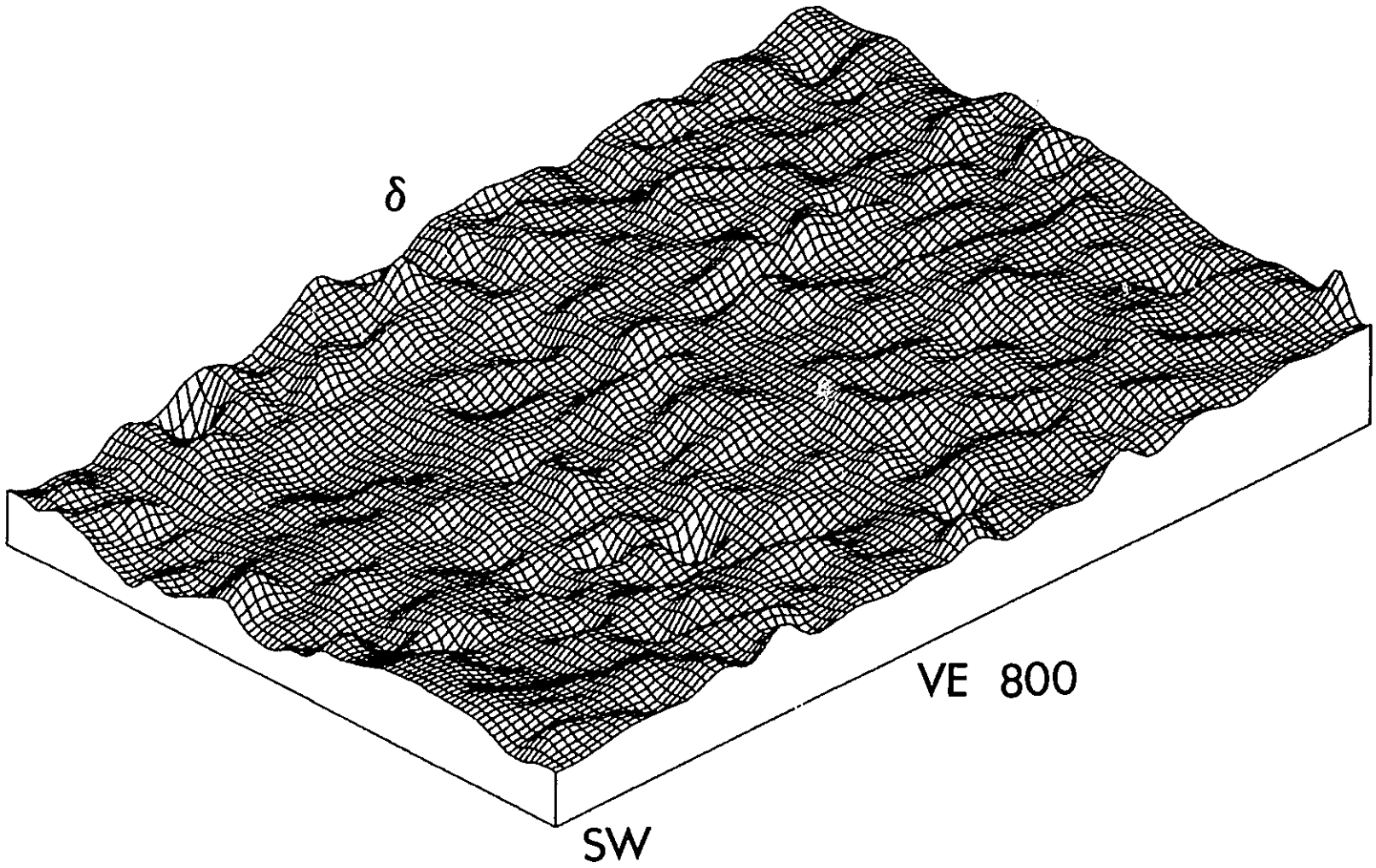
δ
VE 800
SW

Figure 5-23 Mesh Diagram of Datum to Top of Unit Gamma

The view of this diagram is from the southwest; vertical exaggeration is 800 times; Each grid square is approximately 1 mile square.

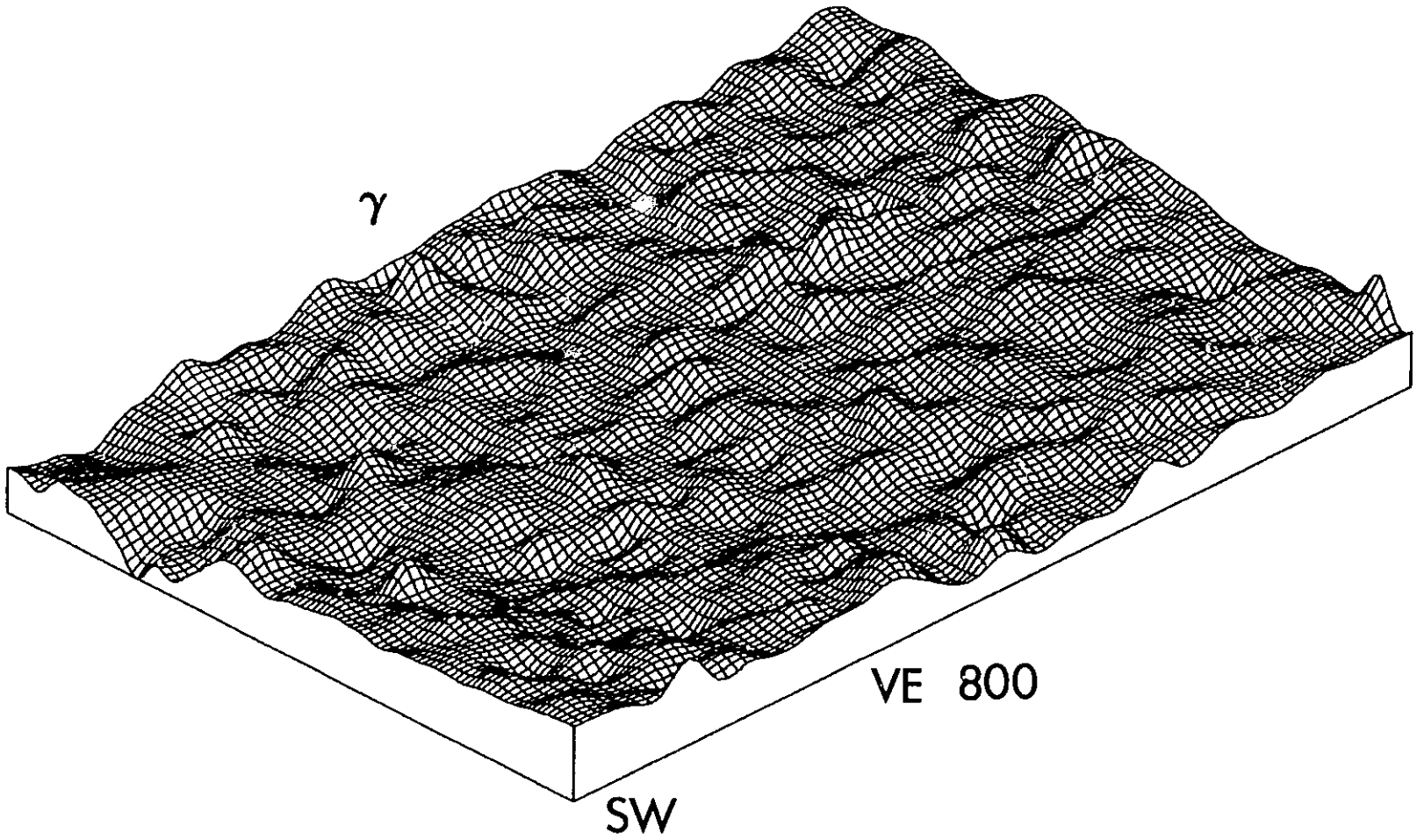
γ
VE 800
SW

lie in unit Gamma near the Joarcam field. Figure 5-24 shows a mesh diagram of the datum to first bentonite response made in the same way as the isopachs for the unit tops. The image is that of an inclined plane dipping roughly northeast.

5.5.8 Datum to Top of Unit Beta Isopach

Figure 5-25 shows the mesh diagram of this isopach. The tilt has now vanished and essentially returned to the planar pattern first seen in the image of the interval to the marker in the Joli Fou shales. The similarities to other isopachs in the form of minor undulations can still be seen in this figure.

5.5.9 Datum to Top of Unit Alpha Isopach

Figure 5-26 is much like that of figure 5-25. It shows the relative surface represented by the isopach from the datum to the top of unit Alpha. There are many similarities in the micro undulations to those of the view of the top of unit Beta. The boundary as a whole is quite undeniably planar relative to the overlying datum.

5.6 DATUM TO UNIT BOUNDARY CROSS-SECTIONS: RELATIVE GEOMETRIES

5.6.1 Introduction

Ideally, the relationships between all these geometries discussed above would be shown in three dimensions; however, this is not possible. The next best thing is to display the complete cross-sections along lines A-A' through G-G' in condensed, `stick figure' form. This condensation involves taking every well along the cross-sections and recording the appropriate unit boundary or other pick as a point on a vertical line representing it location. When all the wells have been properly located,

Figure 5-24 Mesh Diagram of the Time Line Formed by the Joarcam Bentonites

The diagram is viewed from the northeast at a vertical exaggeration of 2500 times. The dimensions of the field of view are approximately 18 miles west by 24 miles north.

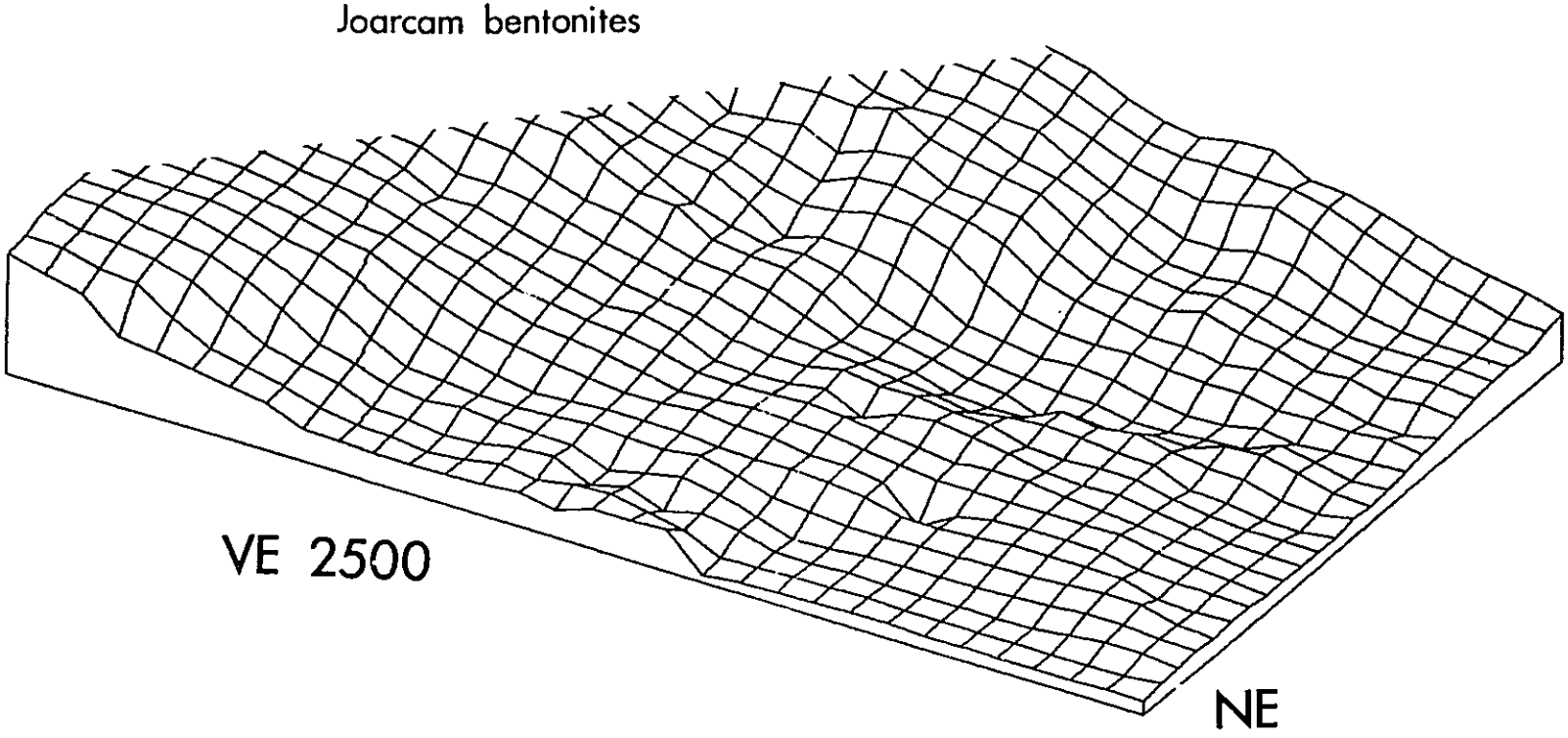
Joarcam bentonites
VE 2500
NE

Figure 5-25 Mesh Diagram of Datum to Top of Unit Beta

The view of this diagram is from the southwest; vertical exaggeration is 800 times; Each grid square is approximately 1 mile square.

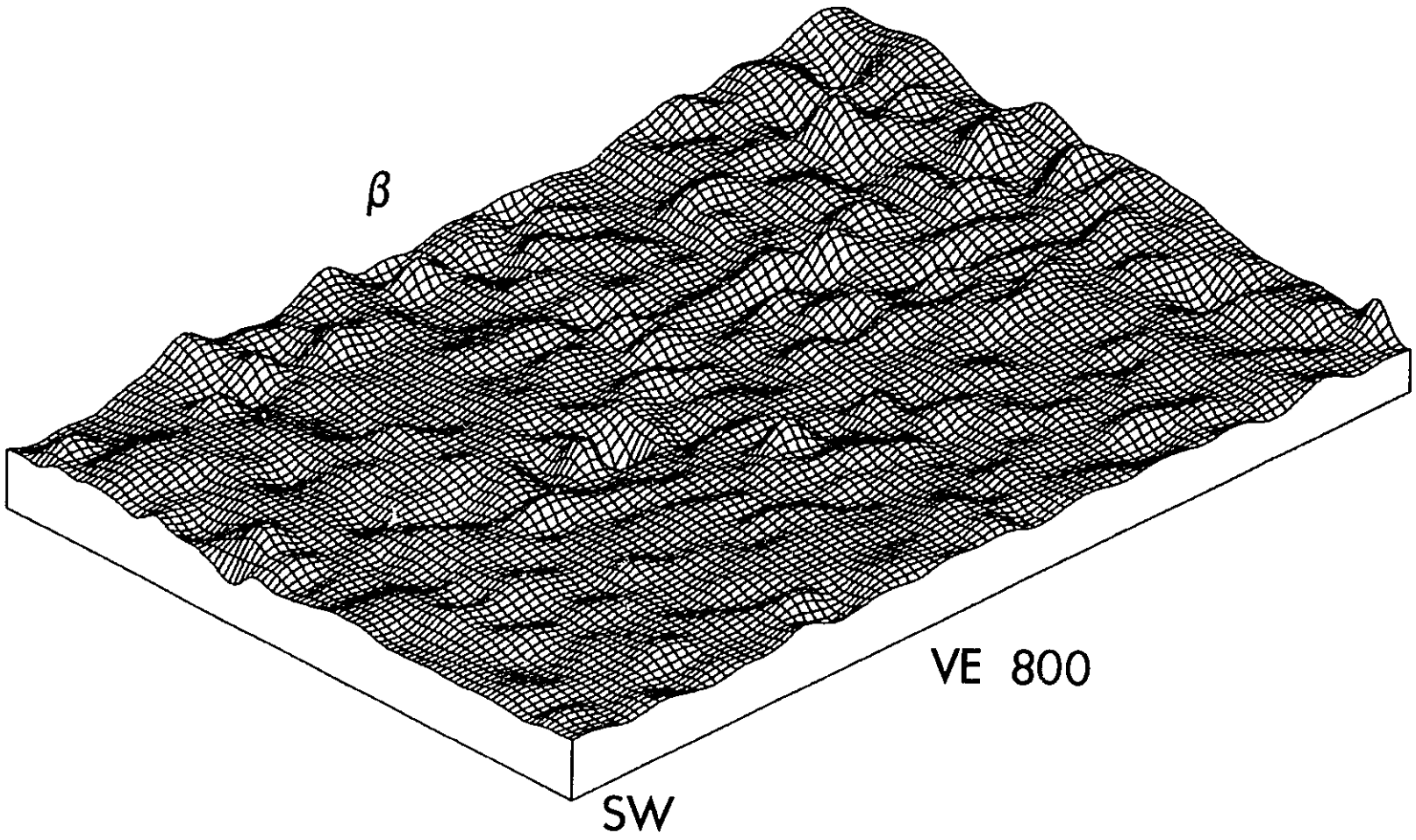
β
VE 800
SW

Figure 5-26 Mesh Diagram of Datum to Top of Unit Alpha

The view of this diagram is from the southwest; vertical exaggeration is 800 times; Each grid square is approximately 1 mile square.

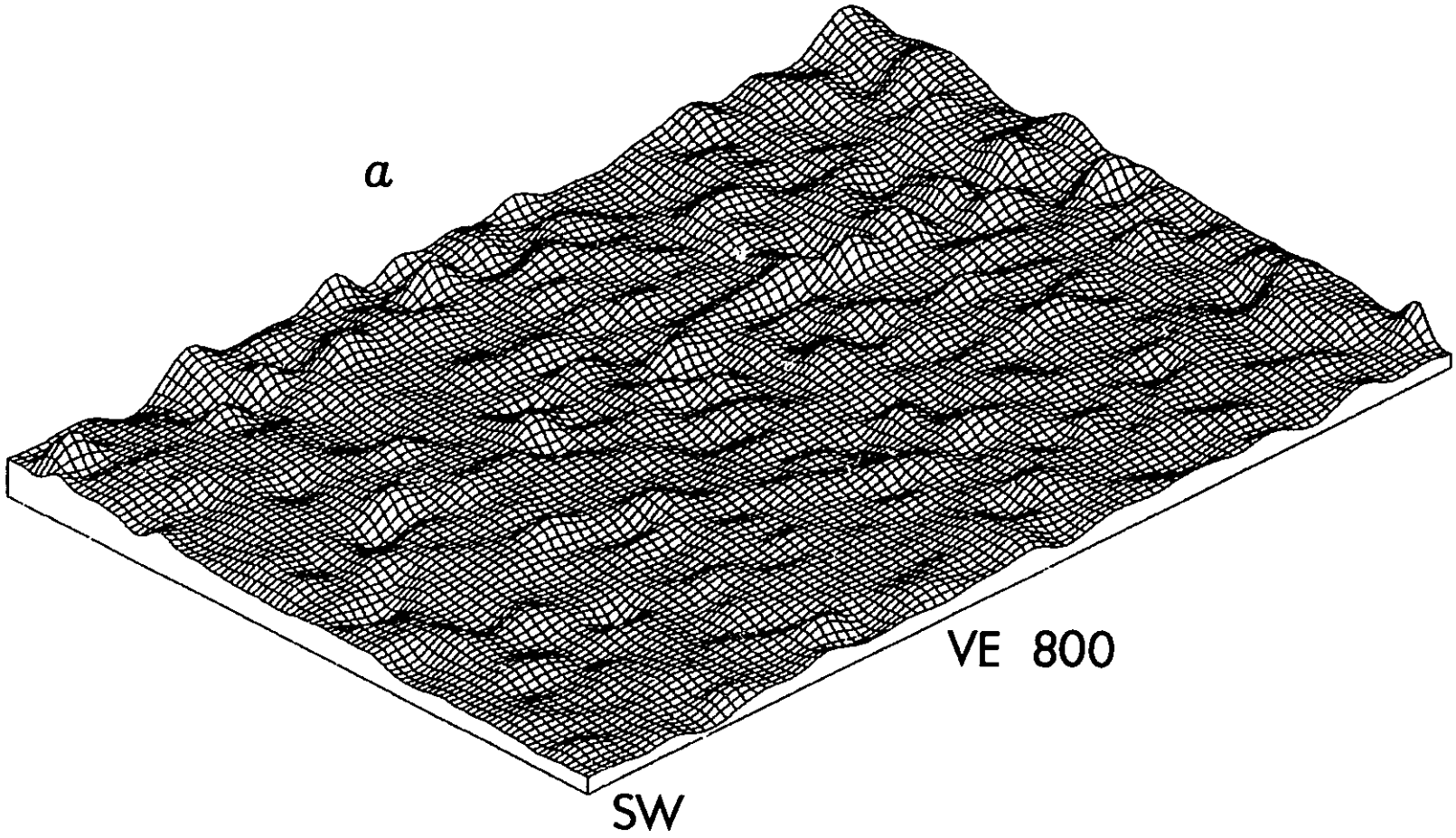
a
VE 800
SW

the correlated picks are joined by lines to show a cross-section through the formation without the clutter of the original well log signatures. Although the well log signatures leading to the correlations are not visible, this second hand display allows incorporation of more data into the space available.

These condensed cross-sections are shown separately in a step by step description of what is essentially a resulting fence diagram. The locations of the cross-sections are shown in figure 4-10.

5.6.2 Condensed Cross-Section A-A'

Figures 5-27 and 5-28 both show versions of the condensed form of cross-section A-A'. Figure 5-27 uses z, the marker in the Joli Fou as a datum, and figure 5-28 uses b as a datum. Because z is essentially parallel to b, there is very little difference in the two diagrams. Therefore, the rest of the diagrams are hung from b which allows more data to be incorporated in the diagrams due to the fact that z is sometimes not penetrated (about one third of the wells).

The diagrams show the successive decrease in the post z tilt of the unit boundaries to a form roughly parallel with the datum at the time of deposition of unit Alpha. This summarizes the evidence shown separately in the mesh diagrams above (section 5.5). The importance of this cross-section (and others below) is that it establishes that the decrease in westward tilting of the unit boundaries relative to the datum is not due purely to the addition of sediment filling in the initial extreme tilt of the base of the Viking. This is because the cross-section does not reveal a downlapping (or onlapping) relationship. The relative tilt of the boundaries to the west is primarily a function of other forces (see section 5.7.3 below). It should be noted that even though cross-section A-A'

is roughly parallel to the strike of the basin margin and the tilting pattern, it is sufficiently deviated from parallel that the tilting of the units appears.

The other feature to note in this cross-section is the superimposition of many of the smaller fluctuations from unit boundary to unit boundary; this is typified by the set of three spikes at the far right of figure 5-28 which run through all the correlation lines. These identical spikes are the type of response that is visible in the mesh diagrams in section 5.5 as a similarity in the form and location of minor `mounds'. Note that they do not occur in the markers to either side of the datum, and when they occur they usually do so throughout the Viking Formation. They are discussed below in section 5.7.2.

5.6.3 Condensed Cross-Section B-B'

Figure 5-29 shows the condensed cross-section B-B'. The tilting of the lower unit boundaries is not so apparent in this figure for two reasons. The first is the orientation of B-B' which is approximately perpendicular to the dip of the tilt. The other is that further into the basin (to the east) the tilt is not as extreme as in the west. This may be seen in the mesh diagrams of the tilted unit boundaries in section 5-5. In other words, the tilt is not planar but curved. The general matching of small offsets may been seen in this cross-section as in A-A'.

5.6.4 Condensed Cross-Section C-C'

Figure 5-30 shows cross-section C-C' in summarized form. The location of C-C' is parallel to the dip of the unit boundary tilts and to the wedge of sediment represented by unit Gamma. Consequently, the tilting of the lower boundaries is more prominent in this cross-section. There are fewer matching

Figure 5-27 Condensed Cross-Section A-A', Lower Datum

The figure shows cross-section A-A' plotted against the Joli Fou marker with all well-log responses deleted and only the correlation lines remaining. The cross-section is viewed from the west.

Figure 5-28 Condensed Cross-Section A-A', Upper Datum

The figure shows cross-section A-A' plotted against the upper datum in the un-named shales. The well log responses are removed and only the correlation lines shown. The view is again from the west.

Figure 5-29 Condensed Cross-Section B-B', Upper Datum

The figure shows cross-section B-B' plotted against the upper datum in the un-named shales. The well log responses are removed and only the correlation lines shown. The view is from the west.

Figure 5-30 Condensed Cross-Section C-C', Upper Datum

The figure shows cross-section C-C' plotted against the upper datum in the un-named shales. The well log responses are removed and only the correlation lines shown. The view is from the west.

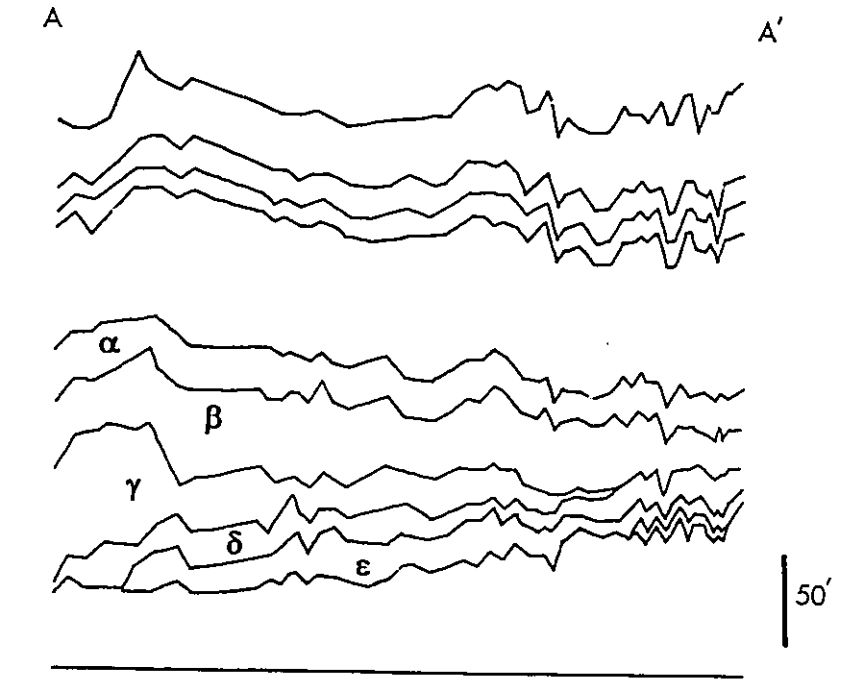
A
A'
α
β
γ
δ
ε
50'

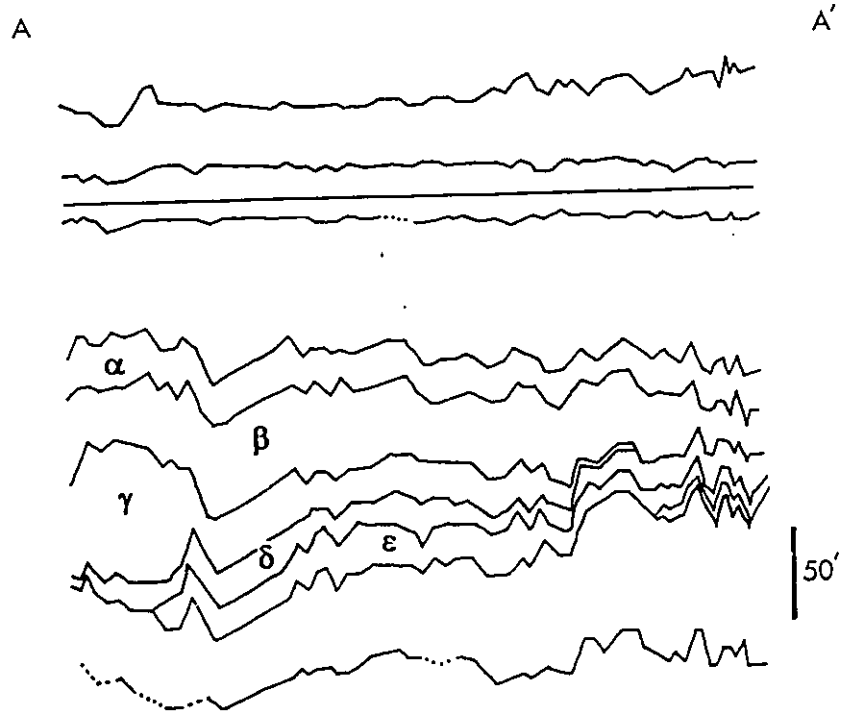
A
A'
α
β
γ
δ
ε
50'

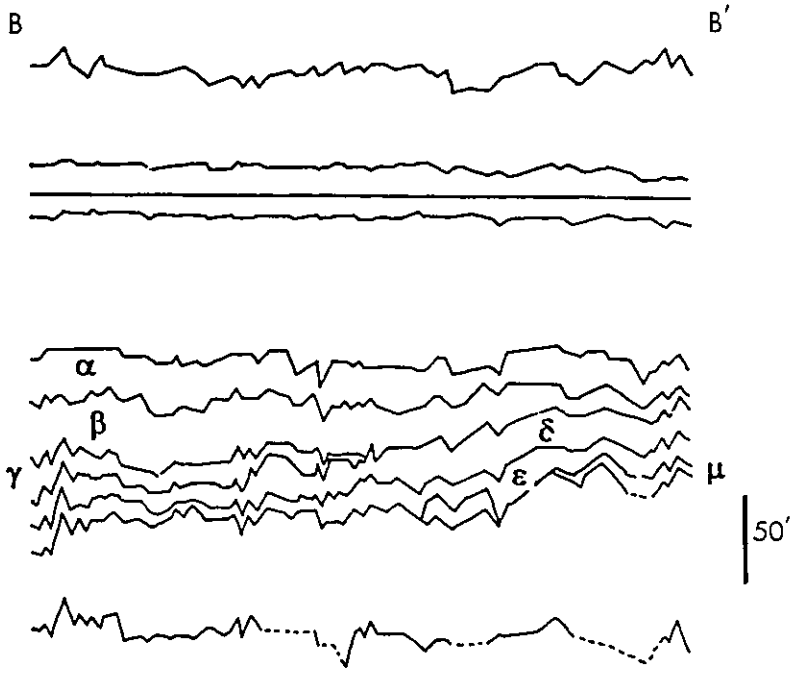
B
B'
α
β
γ
δ
ε
μ
50'

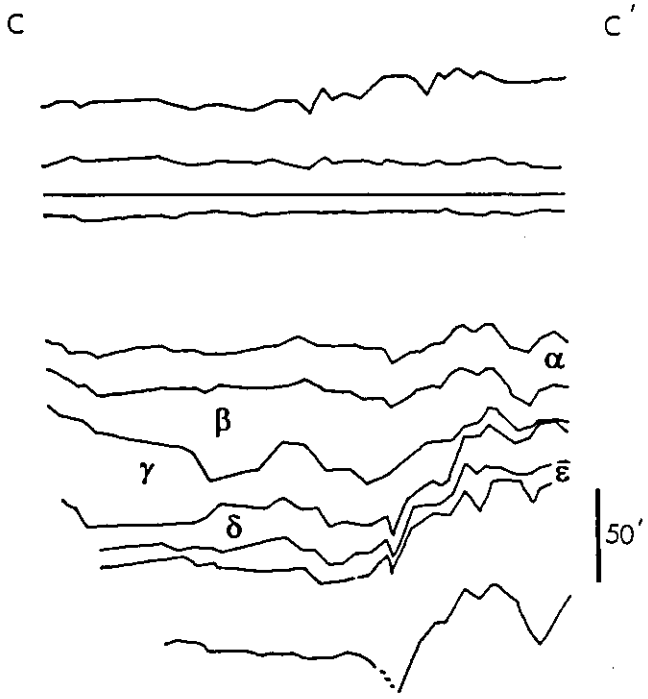
C
C'
α
β
γ
δ
ε̄
50'

offsets here; this may be due to the lower density of wells in part of the cross-section (see figure 4-10) which would make for a smoother appearance.

The other feature of note here is the relationship between the unit thicknesses. Gamma's wedge form may be seen as partially filling in over the tilted unit Delta and partially as a positive `topography' in its own right. Following Gamma, unit Beta seems to fill in the small `basin' created by Gamma. This filling relationship was noted in the offset pattern of sediment thicknesses in the isopach maps of the units Epsilon, Delta, Gamma and Beta in described in section 5.4.

5.6.5 Condensed Cross-Section D-D'

The stick figure form of cross-section D-D' is visible in figure 5-31. The orientation is essentially identical to that of C-C', but it extends further to the northeast, into the basin. All three main features, unit boundary tilting, matching offsets and compensation of thickness according to underlying unit form, are visible here but in less pronounced form than other cross-sections.

5.6.6 Condensed Cross-Section E-E'

Figure 5-32 shows the condensed version of E-E'. It does not show anything not already discussed in the other cross-sections, but like D-D' does show all the important features rather well because of its extensive length. The `fill' like form of unit Beta is particularly evident here.

5.6.7 Condensed Cross-Section F-F'

Figure 5-33 shows the condensed version of F-F'. This is the least informative of the cross-sections because of the lack of penetration to the Joli Fou marker. This lack is due to its location sub-parallel to the

Figure 5-31 Condensed Cross-Section D-D', Upper Datum

The figure shows cross-section D-D' plotted against the upper datum in the un-named shales. The well log responses are removed and only the correlation lines shown. The view is from the west.

Figure 5-32 Condensed Cross-Section E-E', Upper Datum

The figure shows cross-section E-E' plotted against the upper datum in the un-named shales. The well log responses are removed and only the correlation lines shown. The view is from the west.

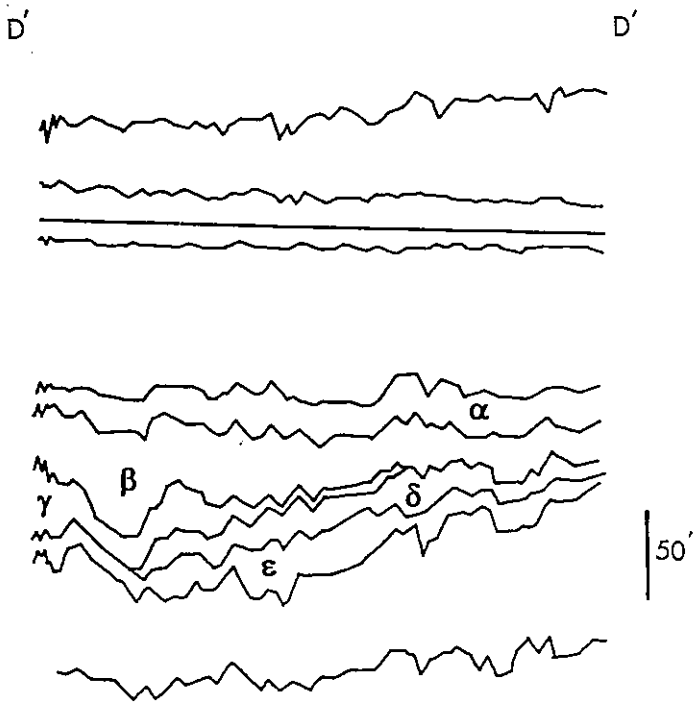
D'
D'
α
β
γ
δ
ε
50'

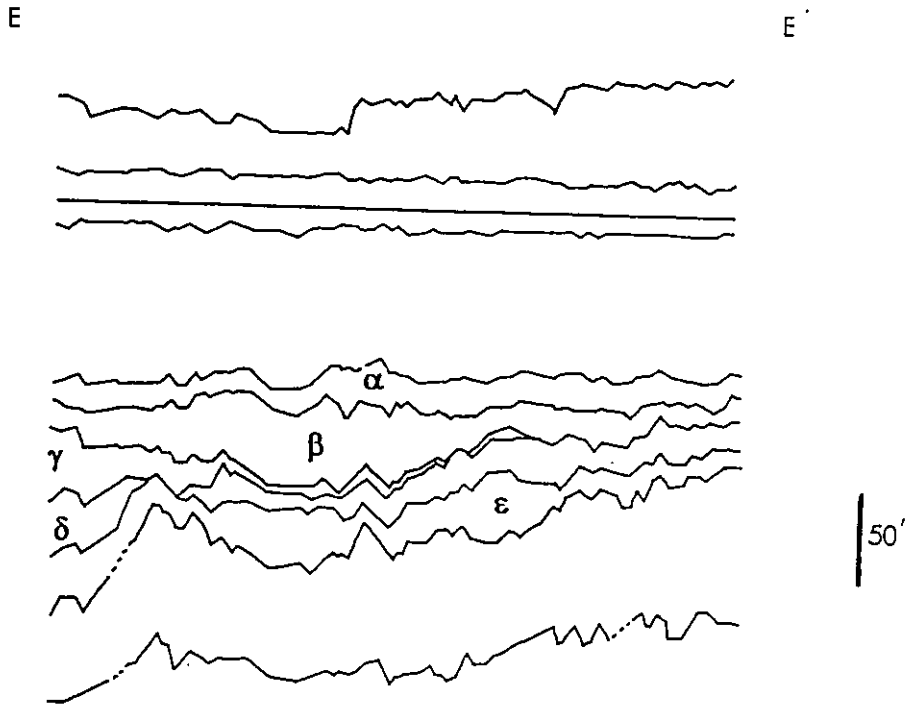
E
E'
α
β
γ
δ
ε
50'

Joarcam field where most drilling stops at the base of the Viking, or shallower. Nevertheless the cross-section gives an idea of the difference in extent between units Epsilon and Delta and the overlying units Gamma, Beta and Alpha. The apparent onlap of unit Delta onto a high in Epsilon is somewhat questionable as indicated in the discussion of the correlations in chapter 4. However, the pattern is consistent with that of a local high which also appears in A-A', D-D' and, to some extent, E-E'.

5.6.8 Condensed Cross-Section G-G'

Figure 5-34 is the condensed view of cross-section G-G'. It is rather short given its location (figure 4-10) and is most useful for its portrayal of the basinal unit relationships where unit Gamma does not appear to have been deposited. The lack of unit Gamma does not significantly alter any of the general observations made for the other cross-sections. Of note here is that unit Beta seems to have maintained its geometry of filling in the basin to roughly horizontal form, in essence compensating for the absence of Gamma.

5.7 INTERPRETATIONS OF UNIT GEOMETRY

5.7.1 Introduction

Consideration of the geometries described above leads to conclusions of varying importance on a number of subjects including the degree of extensional faulting in the area, the nature of basin subsidence during the deposition of the units, the direction of the sediment supply, and topographically related information on the environment in which the sediment was deposited.

Figure 5-33 Condensed Cross-Section F-F', Upper Datum

The figure shows cross-section F-F' plotted against the upper datum in the un-named shales. The well log responses are removed and only the correlation lines shown. The view is from the west.

Figure 5-34 Condensed Cross-Section G-G', Upper Datum

The figure shows cross-section G-G' plotted against the upper datum in the un-named shales. The well log responses are removed and only the correlation lines shown. The view is from the west.

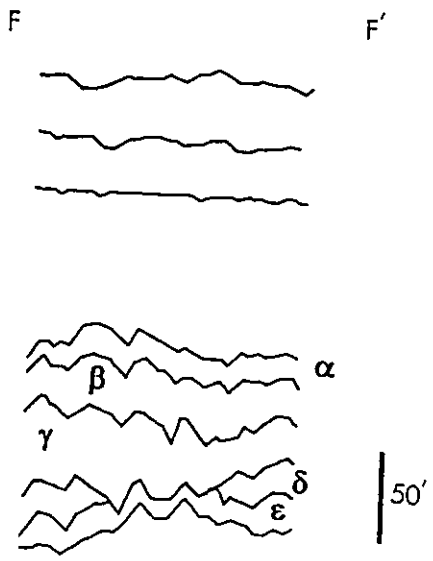
F
F'
α
β
γ
δ
ε
50'

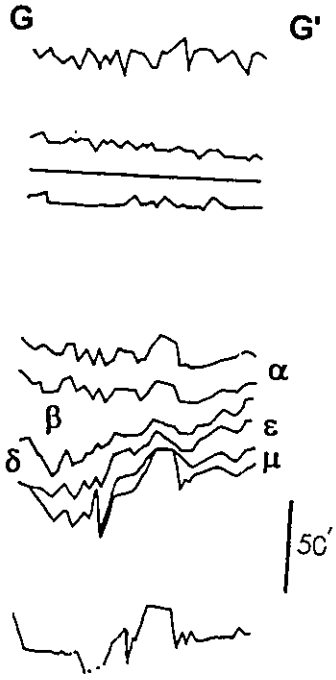
G
G'
α
β
ε
δ
μ
50'

5.7.2 Potential Fault Mapping

The faults discussed in section 5.3 cannot easily be mapped or followed in the diagrams of either section 5.4 or 5.5. However, the matching small scale offsets that appear in the condensed cross-sections of section 5.6 are most reasonably interpreted as indications of faulting in the shales surrounding the Viking. If extensional faulting existed at some point in the shales between the datum and the top of the Viking, then the relative loss of material in vertical section would cause the underlying markers to be elevated relative to their neighbors. This is exactly what most of the matching offsets in the markers correspond to, so given the evidence provided in section 5.3, the interpretation of the offsets as extensional faults follows. The stratigraphic extent of the faults is unknown. Furthermore, their relative dating is not possible. There are sufficient offsets in the Base of Fish Scales marker above the datum that the faults probably extend at least to this level. It is conceivable that they could lie much higher in the section. Therefore, the case cannot be made that they date from the time between deposition of the Viking and the datum; they may just as likely be a relatively recent Quaternary phenomenum.

The report of normal faulting in the late Cretaceous, Cardium section at Seebe Dam site by Wright and Walker (1979) and the discussion of extensional faulting in the Main Ranges of the Rockies by Bally et al. (1966) suggest that recent dates of faulting are more likely than Cretaceous ones. I suspect that the faults are probably Tertiary in age, coeval with those described by Bally et al. (1966) and possibly reflect the northern extent of extensional faulting in the Basin and Range province of central western North America.

Since the matching offsets in the condensed cross-sections probably correspond to the matching minor `topography' on the unit boundary mesh diagrams, it is very likely that some of these small undulations in the unit surfaces correspond to fault related offsets. The continuity of the mounds is unknown and indeterminate though, and such an interpretation still leaves no knowledge of the exact fault locations or orientations. Nevertheless, a case can be made for a tendency towards a northwest-southeast trend in some of the minor undulations in the mesh diagrams. If this tendency is real, it would be roughly parallel to the basin margin which seems a reasonable orientation for development of such faulting if it reflect relaxation of a compressional foreland basin stress regime.

5.7.3 Basin Fill and Deformation: Subsidence Patterns

5.7.3.1 Accommodation History

The most important and definitive information to be gained from the examination of the cross-section and isopach geometries above is an interpretation of the manner in which the basin subsided and filled with sediment. This interpretation stems primarily from the geometry of the unit boundaries. In essence, the interpretations allows a detailed accommodation history (Jervey, 1989) to be developed. Only the tectonic (i.e. subsidence) aspects of this history are interpreted here; the discussion of relative sea level interpretations is located in chapter seven because that discussion relies on further evidence. Associated with this history is the possibility of comparing the units to the geometries developed in locations of different subsidence patterns, most notably passive margins.

Figure 5-35 Accommodation History of the Basinal Viking

The figure schematically shows the tectonically controlled accommodation of the Viking units as described over the study area. The diagram is broken into eight stages in which each of the successive markers such as the Joli Fou marker of the unit boundaries is drawn relative to the marker in the overlying shales as it was later deposited. See the text for a complete description of each stage. The diagrams are not to any scale. Light arrows indicate pronounced sediment input and dark, straight arrows locations of possible pronounced subsidence. The curved arrow indicates the location of a relatively stable tectonic `hinge'.

The explanation of the manner in which the unit boundary geometries developed is summarized in figure 5-35 and involves the initial warping of the basement around the time the Viking first began to be deposited. This initial warping subsequently decreased in magnitude until the basin returned to its initial form at the end of Viking deposition. The details of this history are discussed successively in stratigraphically ascending order.

5.7.3.2 Matching Starting and Ending Basin Geometry

The key to revealing the behavior of the basin during Viking deposition is the positioning of the marker in the Joli Fou shale relative to the datum in the unnamed shales above the formation. Since both of these markers lie in the same environment, apparently marine shales, it is reasonable to assume that their subparallel geometry reflects similar basin shape at the time of deposition. This relationship is shown in step one of figure 5-35.

Given this relationship, the differing forms of the unit boundary plots implies either a variation in the geometry of the basin or in depositional topography. Because the southwestern tilt in many of the unit boundary isopachs denies the possibility of primary control by depositional processes, it is likely that the shape of the unit boundaries, at least in the cases of the base of the Viking through the top of unit Delta, reflects primarily the behavior of the basin. It is almost inconceivable that a depositional setting could exist tilted down to the sediment source in the west and contain the relatively sandy facies shown in chapters 3 and 4. On the contrary, at the time of each unit's formation a slight westward rise would be expected towards the source of the sediment.

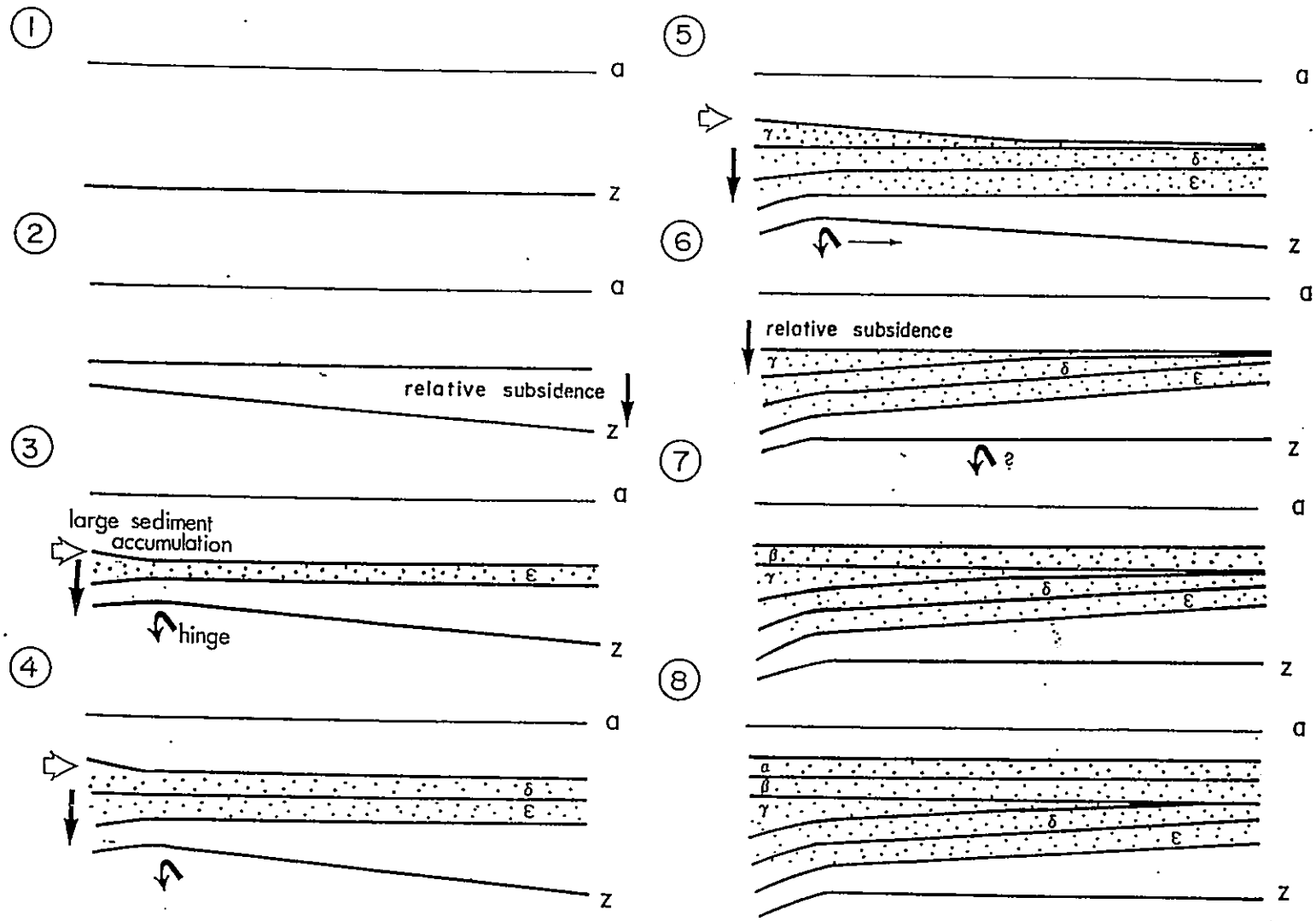
1
a
z
2
a
relative subsidence
z
3
a
large sediment accumulation
ε
hinge
z
4
a
δ
ε
z
5
a
γ
δ
ε
6
z
a
relative subsidence
γ
δ
ε
7
z
?
a
β
γ
δ
ε
8
z
a
α
β
γ
δ
ε
z

5.7.3.3 Stepped `Bulge' Development: Syn-Formational Subsidence

In order to generate the westward tilting geometry of the base of the Viking, the basin must have either locally risen in the east or sunk in the west prior to and just after the time of formation of the base of the Viking. The fact that the base of the Viking throughout the cross-sections and mesh diagrams described above has an abrupt well log response over the Joli Fou shales strongly suggests a component of uplift prior to deposition of the Viking. Such an uplift would have raised the Joli Fou shales into a higher energy regime than that in which they were deposited leading to scouring of the pre-Viking ocean floor. Unfortunately this implication cannot be supported by facies analysis because of the paucity of core at the depths of concern.

Although this pattern suggests local uplift, there was almost certainly greater regional subsidence throughout Viking deposition to the west. This is an interpretation of the fact that compared to the signatures described in chapter 4, the formation has an apparently gradational base in well log signatures and is generally thicker to the west (Boreen, 1990; Davies, 1990; Hein et al., 1986). This pattern was noted by Amajor (1980) who states:

> "Saskatchewan workers place a break at the base of the Viking based on physical evidence (Jones, 1961; Evans, 1970; Simpson, 1975) whereas Albertan workers ... indicate no significant break (Amajor, 1980)."

The loss of the abrupt base to the Viking to the west suggests that uplift took the form of an eastern upwarping parallel to the axis of the foreland basin. This type of behavior is not unexpected given the models of foreland basin behavior put forward by such workers as Tankard (1986a) and Quinlan and Beaumont (1984).

Following the major change in basin subsidence that apparently led to the abrupt base to the Viking Formation in the study area, there was continued local relative subsidence to the east allowing for accumulation of unit Mu. Although it is the most tentative of the stages, this has been shown in step two of figure 5-35.

Steps three and four in figure 5-35 show the development of units Epsilon and Delta. They seem to have been deposited in a basinal setting in which uplift had ceased and a more typical westward subsidence/accommodation had returned. This relative subsidence in the west/southwest is interpreted to account for accommodation of the relatively large accumulations of sediment in the southwest corner of the isopach maps combined with the units' continued western tilt relative to the datum The similar location of both the accumulations in units Epsilon and Delta and the relatively planar nature the unit further into the basin suggests that the subsidence was hinged in the areas of the Joarcam field (figure 1-1); this hinge is shown in figure 5-35 by the curved arrow on the left (western) side.

The extent to which this hinge existed during deposition of unit Gamma is uncertain. This stage of development of the formation is shown in step five of figure 5-35. The relative geometries of units Gamma and Delta described in section 5.6 suggest that subsidence in the west continued during at least the initial part of unit Gamma's deposition; the lack of sediment present in the eastern half of the study area during this time may imply that the subsidence/accommodation increased to such an extent that sediment was only just able to fill the basin without prograding past the hinge. The argument that subsidence continued during the onset of unit Gamma is based on the assumption that a westward

dipping slope that would otherwise have to have existed at the top of Delta would not allow deposition of the kind of sandy facies interpreted in chapter six and described in chapter 4. If the geometry were interpreted as reflecting an oceanic trough existing at the time of deposition one would expect to find turbidite or pelagic facies. Since the relative geometry of the base of unit Gamma does dip westward, the base is therefore assumed to have subsided into this position after deposition. The top of the unit is a different matter, however. It does not show a westward tilting; moreover, its thickest accumulation extends more eastward than those of the underlying units Delta and Epsilon. This suggests that accommodation potential (i.e. subsidence) decreased in the west allowing the sediment introduced into the basin to be spread further to the east. An argument could be made that the hinge line may have migrated eastward allowing the preservation of the Gamma wedge while preventing the accumulation of sediment further into the basin thus creating the point of the correlative conformity at the edge of the wedge. This has been shown in steps five and six of figure 5-35 as an arrow next to the curved arrow of the hinge and a questioned subsidence. However, this view is speculative. Alternatively, it may be that the magnitude of subsidence decreased at this time in the area leading to the basinward thinning of unit Gamma. Regardless of these alternatives, there is little doubt that by the end of unit Gamma the subsidence had returned to approximately what it was at the time of deposition of z, the marker in the Joli Fou shales. This can be seen in the geometry of the upper boundary of unit Beta.

5.7.3.4 The Cessation of Deformation

Step 7 in figure 5-35 shows the probable development of the basin at the time of deposition of unit Beta. The relatively planar nature of both unit Beta and unit Alpha relative to the overlying datum and the marker in the Joli Fou shales implies that the basin has returned to a pattern of subsidence and accommodation similar to that which existed prior to deposition of the lower part of the Viking (units Mu, Epsilon, Delta and Gamma). The interpreted accommodation history shown through figure 5-35 ends in step eight with a cross-section sketch which accounts for the form of such cross-sections as described in section 5.6.

5.7.3.5 Changes in Unit Geometries as a Function of Decompaction

The exact form of each unit summarized in figure 5-35 will vary if decompaction of the sediments is taken into account; however, the general conclusions will not change because they are based primarily on the wedge form of the Joli Fou interval and unit Gamma (see discussion below). Decompaction calculations would change the exact form of the unit geometries because each unit has differing percentages of shale present laterally. As may be seen in foldouts 8-12 (discussed in chapter 4), the eastern portions of the units are generally muddier than the western regions.

Decompaction of the sediments has not been taken into account for a couple of reasons. First, since the overall picture doesn't change, the calculations are qualitatively unnecessary. Second, there is some question as to exactly how much decompaction is to be accounted for. This uncertainty arises from lack of knowledge of the exact depth of burial, given post burial uplift, and doubt over the manner in which, if at all, decompaction is to be carried out for the kind of

muddy sandstones that dominate much of the Viking in the region studied. There is no criterion for choosing among the different decompaction curves (e.g., Dzevanshir et al., 1986; Baldwin and Butler, 1985; Magara, 1980) available.

There is evidence that there should be comparatively little decompaction of the Viking Formation facies because compaction of the muds seems to have occurred primarily at the surface. This evidence takes the form of approximately circular sub-horizontal burrows, particularly *Terebellina* traces some of which may be seen in the figures of chapter 3; it is the preservation of the circular form which indicates relatively little deformation of the sediment has occurred since creation of the trace essentially at the surface.

Without carrying out a series of estimated decompaction calculations, it can be said, qualitatively, that decompaction would have the following effects on unit geometries. The wedge of the Joli Fou shales would become more pronounced in its westward tilt because of the greater volume of shale in its eastern side. Unit Mu would be more or less still volumetrically irrelevant. Units Epsilon and Delta would become more planar, possibly developing westward rather than eastward tilts depending on the degree of decompaction; like the Joli Fou wedge, this too would be due to the larger amounts of shales in the eastern portions of the units. Unit Gamma would remain more or less unchanged because of the lack of a presence in the east. Units Beta and Alpha would similarly remain approximately tabular given their more or less homogenous distribution of facies.

Thus it can be said that the overall subsidence patterns interpreted from the undecompacted data do not change when qualitative decompaction is

considered. The initial westward uplift remains by virtue of the wedge geometry of the Joli Fou/base of the Viking. This may persist longer than interpreted into unit Epsilon and Delta if decompaction is extreme enough; however, the wedge form of unit Gamma persists through decompaction suggesting that westward accommodation returned due subsidence in that direction.

The geometries of the units can therefore be interpreted as showing that the deposition of the Viking Formation corresponds to a phase of tectonic deformation along the west of the North American continent.

5.7.3.6 Possible Causes of Deformation

The interpretation in the literature that the west of the North American continent has been assembled from a "collage" of accreted exotic terranes was discussed above in chapter 2. Until recently most authors interpreted the accretion of these terranes to have occurred either in the late Jurassic or the Late Cretaceous, roughly corresponding with the major Columbian and Laramide orogenies, respectively. Only the Bridge River terrane located in central, southern British Columbia (Monger et al., 1982) had been reported to have accreted in the Early Cretaceous (Monger et al., 1982) between the major "Terrane I" and "Terrane II" emplacements which made it a possible candidate for causing deformation of the foreland basin. However, in view of the recent work of van der Heyden (1992) it seems that terrane docking did not occur at the time of Viking Formation deposition.

5.7.4 Sediment Migration Direction

Given the general western source of sediment implied by the facies distributions and grain size characteristics described in chapter four and the

geometries of the unit isopachs described above, it appears that the simplest direction of sediment input for the Viking units in the study area of figure 1-2 was from the west-southwest. This is almost certainly the direction of the progradational component of the units. The bentonite geometry from within unit Gamma shown in figure 5-24 supports this. It forms an isochronous surface whose inclination implies northeastward progradational component. However, uncertainty about local sediment sources as opposed to the net component of progradation, arises from the possibility that sediment moved along the edge of a wedge of deposition while contributing to its progradation perpendicular to the direction of sediment motion. Sediment may have been derived from a point to the northwest of the study site and been moved to the southeast on the sea floor. While this was occurring much of the material may have been deposited along the front of the sediment wedges prograding to the northeast. This ambiguity is reflected in the grain size map of unit Gamma in chapter four (figure 4-39) whose geostatistically derived contours are indecisive on the issue; either case could be supported.

Interpretation of the issue of source direction is not helped by the relative paleocurrent data of chapter 3 either (see figure 3-5). Although there is a tendency to bipolar relationships between crossbeds, the absence of absolute directional information means this cannot be related to progradation direction. Furthermore the presence of a wide spread in possible relative directions of sediment motion, from 90° to 180° suggests that the relatively instantaneous record of a single paleocurrent would not reliably indicate progradational

direction in this case. So although the net progradation component was from the southwest the actual source (or sources) must remain debatable.

5.8 A Comparison to Passive Margin Sequences

The general pattern of subsidence interpreted in figure 5-35 agrees with the overall form to be expected in the fill of a foreland basin. Here the greatest subsidence is toward the basin margin rather than toward the basin center as in passive margin settings. There is little new about this. To date most sequences have been described in sequence stratigraphic terms from passive margin settings (see chapter one for a synopsis). For example, neither Vail et al. (1977), Posamentier et al. (1988) nor Van Wagoner et al. (1990) discuss the possibility that foreland basin geometries might differ significantly from those of passive margin. The parasequence geometry is not discussed relative to basin type (Van Wagoner et al., 1990); it is defined in terms of a vertical succession. The different subsidence patterns of foreland basins, particularly the likelihood of migrating forebulges (e.g., Quinlan and Beaumont, 1984 and Tankard, 1986) imply that different geometries are possible.

At the scale of this investigation, however, no clear differences are discernible in unit structure although there are suggestions of variations to be expected at the parasequence scale across larger areas. The lack of unconformities or clear disconformities does not allow comparison to the Type I and Type II sequences. The evidence for basin warping discussed above suggests that smaller scale successions, or parasequences, may deviate from the simple downlapping pattern characteristically used to describe them. It may be that parasequences onlap toward the center of the basin where a foreland bulge

has existed. Or alternatively they may show preferential onlapping or downlapping relationships in upper versus lower portions of the formation as a whole (i.e., Sequence) depending on the position of the foreland bulge at the time of formation. The difference in orientations of units Mu and Gamma is a weak example of such a possibility.

CHAPTER 6

ENVIRONMENTAL INTERPRETATION OF FACIES AND UNITS

" `When I use a word, ' Humpty Dumpty said, in rather a scornful tone, `it means just what I choose it to mean - neither more nor less.'
`The question is,' said Alice, `whether you can make words mean so many different things.'
`The question is,' said Humpty Dumpty, `which is to be master - that's all.' "

L. Carroll
Through the Looking Glass and
What Alice Found There

6.1 SUMMARY

Both early diagenetic and trace fossil information indicate that the Viking Formation sediments, in the area studied, were deposited under relatively slow sedimentation rates and partly transgressively. The energy of flow fluctuated irregularly. The flows molding the sediments of units Epsilon through Gamma, inclusive, were primarily storm enhanced tidal currents located on the inner shelf, the shelf being divided into inner and outer based on the presence of "geostrophic flow" components. These successions record the facies elements of tidal sand sheets whose upper portions are transgressively deposited. Units Beta, and to some extent Alpha, bear the imprint of storm/wave dominated processes on the outer shelf. In no unit is there strong evidence for preferential lateral equivalence of particular facies. The lateral preservation of processes appears to be random.

6.2 INTRODUCTION

The previous chapters contain descriptions of the sediments of the Viking Formation and their distributions with only minimal remarks about the mechanisms responsible for distributing the sediment. This chapter contains additional detailed information on the sediments that has direct bearing on their interpreted environment of deposition. These details are followed by interpretations of the individual facies described in chapter three and by environmental interpretations of the facies successions of each unit.

6.3 INTERPRETATION OF ADDITIONAL DETAILED INFORMATION

6.3.1 Sources of Additional Information

In addition to the facies descriptions provided in chapter three, there are a number of more specific criteria that carry information on environment of deposition. These include sediment isopachs as described in chapters 4 and 5, petrographic details as described in Appendix B, particular trace fossils and, finally, details of some of the less common primary sedimentary structures. Many of these latter details are not actually included in the generalized facies descriptions. Relevant details from each category are described and discussed successively before interpretation of the general facies descriptions.

6.3.2 "Paleotopography"

6.3.2.1 The Use of Unit Isopachs

Unlike the results from other formations, (e.g.,Plint et al., 1986, 1987, Bergman and Walker 1986) isopaching of the intervals from the datum to unit boundaries as presented in chapter 5 has not proven useful for detailed paleotopographic mapping in this area of the Viking Formation. This is because

of the strong effect of subsidence on the unit geometries discussed in section 5.7.3. Although this approach was not productive, the more traditional isopachs of the units do offer some indication of gross depositional topography. They too are not pure paleotopographic images because they are also influenced by subsidence; however, some of the smaller features of the isopachs may be reasonably argued to be depositional in nature. These smaller scale features are probably depositional because it would be difficult to create small scale subsidence capable of accounting for the sediment accumulations; only local syndepositional faulting of the 'basement' would allow such accumulation and there is no strong and pervasive evidence of such activity.

6.3.2.2 "Shoreface" Wedges

The most prominent of the smaller features that may be interpreted as dominantly depositional forms are the wedges of material visible in units Epsilon, Delta and Gamma in the southwest corner of the region as described in section 5.5. The sense of progradational component discussed in chapter five implies these wedges probably, in part, reflect the distal portion of shoreline progradation which in this area is primarily aggradational. Although the terminology is rather confused, on geometric grounds, the wedges may be described as "shorefaces" (see below for a more involved discussion of environmental details).

6.3.2.3 Shelf "Ridges"

The only other features of the isopach maps that lend themselves to environmental interpretation are the northwest-southeast thickness trends described for units Epsilon, Delta and Gamma in section 5.5. These trends are lower order features than the wedge geometries. Although these trends are on the

order of tens of miles in dimensions, they are comparatively thin, usually on the order of twenty or less feet which is the order of the unit thickness. The northwest to southeast linear trend in the middle of unit Beta appears to be passive infilling over underlying accumulations in unit Gamma and so is not discussed here. The thicknesses of these trends is not equivalent to a simple sand thickness; marine siltstones account for the majority of the units's thicknesses in these locations. Only the upper foot to five feet of these thick trends is occupied by sandy facies (see cross-sections A-A' through E-E', foldouts 8-12). Other authors (e.g., Brenner and Davies (1974), Brenner (1978) and Seeling (1978)) have interpreted similar units in other formations as entirely sandy bars ("offshore bars") which, although inappropriate because it ignores the large silt/clay thickness, has played a significant role in the development of the "offshore bar" facies model (e.g., Walker, 1984a). In the case of the Viking, the space between the thicker part of the trends seems to be void of the sandier facies as determined by relatively subdued resistivity and SP log responses. There is little core in these intervening regions to confirm this directly, but the lack of core is circumstantial evidence for a lack of reservoir quality sands. Because there is little sand between the thicker accumulations in the west and the northwest trends in the center of the study area (i.e., the Beaverhill Lake - Fort Saskatchewan trend in figure 3-1), it seems very likely that there was a distributive process responsible for the pattern. It is difficult to imagine a subsidence dominated mechanism that would generate such sediment patterns given the information available on the tectonic history of the area. These isopach trends may therefore reasonably be interpreted as subtle shallow marine `ridges' or fingers of sand.

Figure 6-1 Unit Gamma Compared to Modern Ridge Forms

The diagram shows cross-sectional views through the thickest portions of unit Gamma and a number of modern ridge form examples. (see Walker 1984 for references containing dimensions). The black portions illustrate the smallest range of sizes. The lighter forms show the maximum sizes.

SAND BODY COMPARISON

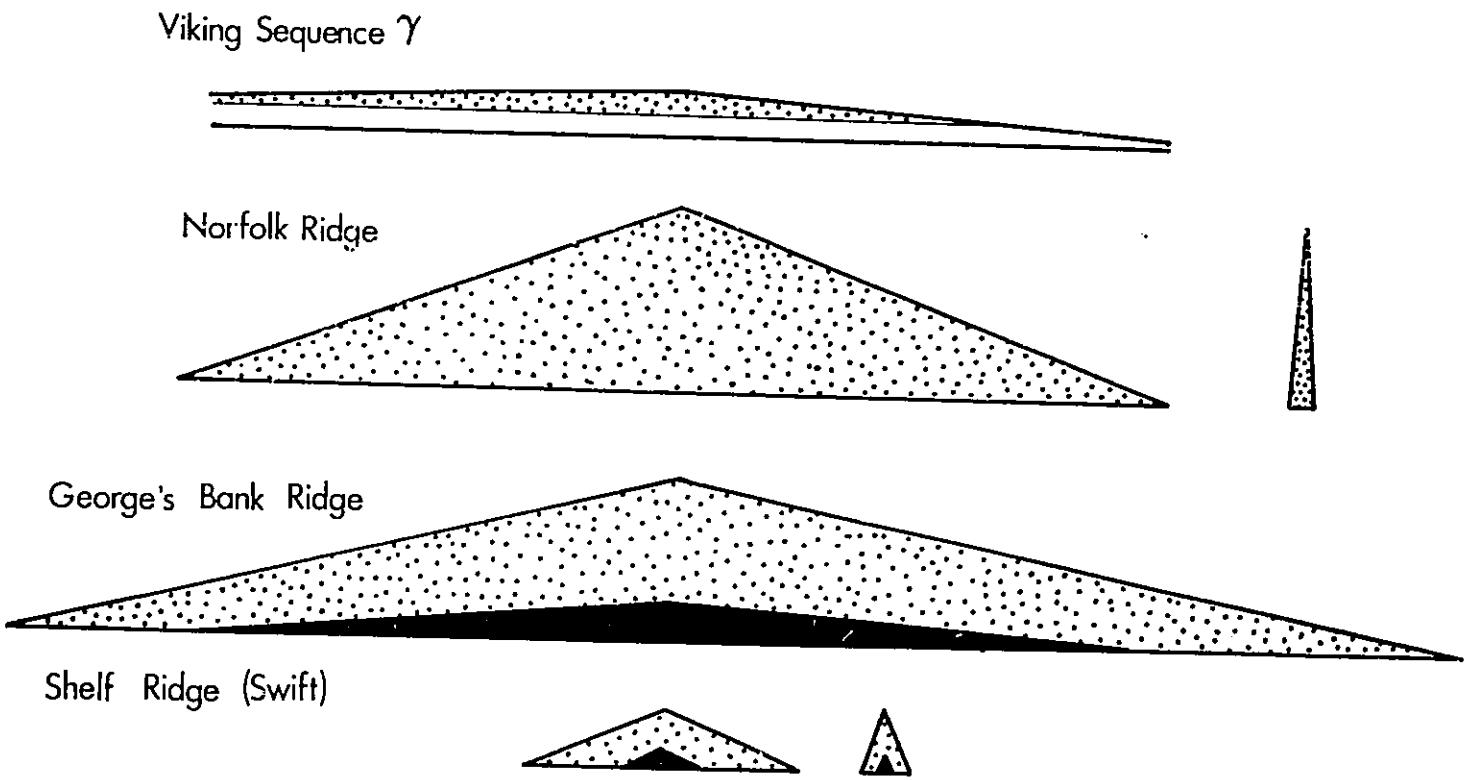

The type of `ridges' may be estimated by comparison to those measured from modern marine settings. Figure 6-1 shows a comparison of the unit Gamma wedge from the Viking Formation to the Norfolk tidal ridges in the North Sea, the Georges Bank ridge off the Atlantic coast and the shelf ridges described off the east coast of the U.S. The modern ridges are shown as `lateral' and `frontal' profiles. If Belderson's (1987) conclusion that there are fundamental differences in size between tidal ridges and the shelf ridges described by Swift and co-worker (e.g.,Swift et al., 1973) is accepted, then tidal ridges as a class can be dismissed as being the primary cause of the sediment accumulations in the Viking Formation. The Viking Formation accumulations are much too small to fit the tidal ridge outline as shown for the Norfolk ridges. This size analysis is a strong argument against interpreting the Viking sediments as "Tidal Ridges" as has been done by such workers as Amajor (1980) and Leckie (1986).

On the other hand, the size of the Viking Formation accumulations is sufficient to place them in either a mixed storm-tidal setting such as may have created the George's Bank type of accumulation or in the storm dominated setting interpreted to have formed the shelf ridges described by Swift and co-workers. Purely on the basis of scale the case of George's Bank or North Sea sheet sands type distributions are more likely than that of the Swiftian shelf ridge because the latter would require multiple ridges reworked into a broader assemblage. There is no good evidence for such reworking in the units described in chapters three and four or in the sediment distribution indicated in the isopach maps. Furthermore, the sparse core information available for the shoreface attached ridges (Rine et al., 1986) does not seem to closely match the facies of the Viking units.

Although, in most cases, sedimentary structures in the modern cores are not very clear, neither their x-radiographs nor their interpreted facies seem to have as much high angle crossbedding as occurs in the Viking. The best case for a ridge analogy is thus the Georges Bank. However, even this example is thick by comparison to the Viking units. It would thus seem more appropriate to described the Viking as being composed primarily of sheet sands with irregular distributions. However, conclusions about depositional mechanisms responsible for the generation of the sheet pattern must rely primarily on analyses of the facies supported by additional details below.

6.3.2.4 Paleogradient and Depth Variation

One other fairly significant piece of information to be derived from the unit geometries is that the ocean floor upon which the sediments were deposited was almost flat. Comparison of unit Gamma to the datum as used to generate the map in figure 5-23 yields a general gradient of 1/10,000. This is the maximum such gradient for all units; the others are flatter. Given that the basinal shales were almost certainly depositionally flatter that the coarser sediments of the Viking, the maximum paleogradient that could be expected at any time would probably have been no greater that 2/10,000. Subsidence would have been unlikely to increase this given its generally greater magnitude in the west towards the shoreline. Provided that these assumptions are realistic, the depths in the eastern part of the study area would only be on the order of 45 metres greater than those at the western edge (where depths may have been on the order of 20 metres, see below).

6.3.3 Petrological Information

6.3.3.1 Description

Most of the petrographic information important for environmental interpretation has already been presented in the petrographic section of chapter four and Appendix B as descriptions of early diagenetic products. Consequently, this section mostly contains interpretations of data from those sections.

Glauconite is the most abundant early diagenetic mineral of interest; it may be observed in locations varying from cross-laminae to chert grains. The glauconite is also accompanied by phosphatic material ranging from probable altered fecal pellets to bone fragments. The Viking is not rich in phosphatic alterations, but such products, nevertheless, have environmental implications.

6.3.3.2 Interpretation: Slow Sedimentation

Glauconitic and phosphatic alterations imply relatively slow sedimentation under a fairly nutrient rich water column. This inference is based on studies of the modern ocean floor (e.g.,Hein et al., 1974 and Odin and Matter, 1981) as well as on studies of condensed sedimentary units (e.g.,Goodman, 1922). In fact, the presence of glauconite has been incorporated by Van Wagoner et al. (1990) and Posamentier et al. (1988) into "sequence stratigraphy" as an indication of slow sedimentation at unit boundaries.

In the case of the Viking Formation, the implications of the glauconite are slightly more debatable than those of the phosphates and bone material. A semi-reducing environment is required to allow precipitation of the mixed state iron incorporated in the glauconite (e.g.,Harder, 1978, Odin, 1985 and Odin and Matter, 1981). Modern joint glauconitic and phosphatic accumulations occur in

regions of mixed oxygenation levels (not anoxic but not normally oxygenated either) (Burnett, 1980). Furthermore, the presence of iron in silicate form means that there was sufficiently low CO_2 to prevent formation of siderite (e.g., Allen et al., 1986). The early textural nature of the glauconite implies that this chemical environment existed either at the sediment surface, under shallows depths of the deposited sediment (a matter of a few metres depth) or within the sediment during shallow burial (a matter of a few tens of metres depth). Obviously the first two settings carry stronger environmental implications because both reworking and interaction with surficial water is possible at such depths.

The argument that the glauconite formed at relatively surficial burial depths depends, in part, on information from the facies and, in part, on the absence of other diagenetic products. It is quite apparent (see below) from the nature of the bioturbation through most of the units that there was abundant organic matter deposited within the sediment. Given such abundance, it seems likely that there would have been a rather shallow reducing environment generated by organic decay. Accompanying this reduction, there would have been relatively large amounts of CO_2 generated. Had the iron been released at the relatively greater depths of a few metres, it seems likely that it would have been primarily reduced iron and furthermore, that it would have combined with CO_2 to form siderite or other iron rich carbonates. To form glauconite at depths on the order of a few tens of metres or more would depend on the presence of micro-environments such as might be present in the crevices of grains (e.g.,Hughes and Whitehead). While this mechanism of formation is quite conceivable for a substrate such as chert grains which are seen altered in the

Viking, it is more difficult to explain the widespread glauconitization of varying substrates over areas as comparatively large as whole cross-laminae in this manner. While micro-environments may well have played a role in the formation of glauconite it appears to have been secondary to an overall environmental state that existed at very shallow depths in the sediment column.

Formation of the glauconite at the immediate surface is unlikely. There are two reasons for this conclusion. The first is that according to the interpretations offered below for the sedimentary structures and facies, the water was probably only tens of metres deep (20 to 50 metres). If these interpretations are correct, then following modern analogs, glauconite would not be expected to present since it "predominates only at depths exceeding 60 m and distant from fresh water input (Porrenga, 1967)" (also see Odin, 1985 and Odin and Matter, 1981). There is some uncertainty about this argument, however, as the deeper projected depth ranges for the Viking sediments are close to those at which glauconite occurs in modern sediments. The second argument against the surficial formation of the glauconite is that it would be expected to degrade under the comparatively energetic conditions implied by the presence of crossbedding (again see the interpretations below). Such intermittent high energy conditions would be expected to lead to chemical degradation of the glauconite (Odin and Matter, 1981; Giresse and Odin, 1973) because an active water column would be expected to be relatively oxidizing. Furthermore, the lack of distinct pelloidal forms in the glauconitic cross laminae (see chapter 4) suggests that the material was not reworked but formed *in situ*. Reworked glauconite would be expected to take the form of well rounded, fairly durable pellets (e.g., Light, 1952).

The glauconite is best interpreted as having formed at depths of a few metres in relatively unconsolidated material. If the iron were mobilized closer to the surface, there would be greater 'aeration' of the sediment column by oxidized waters allowing for the mixed reduction states of iron present in glauconite. A near surficial location would also allow diffusion of CO_2, generated from the decay of organic material, into the water column thus preventing competition for the iron by carbonate phases.

6.3.4 Ichnological Information

6.3.4.1 Types of Information to Be Gained

The information to be gained from specific traces involves the condition of the substrate, the nature of the water column and the relative rates of sediment supply. In most cases, this information is best incorporated as part of the individual facies interpretations; however, there are some observations which are relevant to unit boundaries and regional sedimentary behavior.

6.3.4.2 Traces and Unit Boundaries

The trace fossils of greatest interest for the detection of unconformities are those that would occupy firmgrounds developed at scoured horizons. As the description of the unit boundaries in chapter four revealed, however, there are no signs of such traces in the Viking Formation in the region studied. Moreover, there is no consistent evidence of clustering of traces at a particular horizon that might by used as strong evidence of a relative slowdown in sedimentation. As with the local scours described in chapter 4 under unit boundaries, there are local accumulations of traces, but they do not extend across significant portions of the basin. Such occasional clusters are particularly noticeable in *Arenicolites*

Figure 6-2. Tillman's (1985) Depth Based Shelf Division.

Figure 6-3. The Wave-Dominated Shelf Classification of Walker (1984).

SHELF SUBDIVISIONS

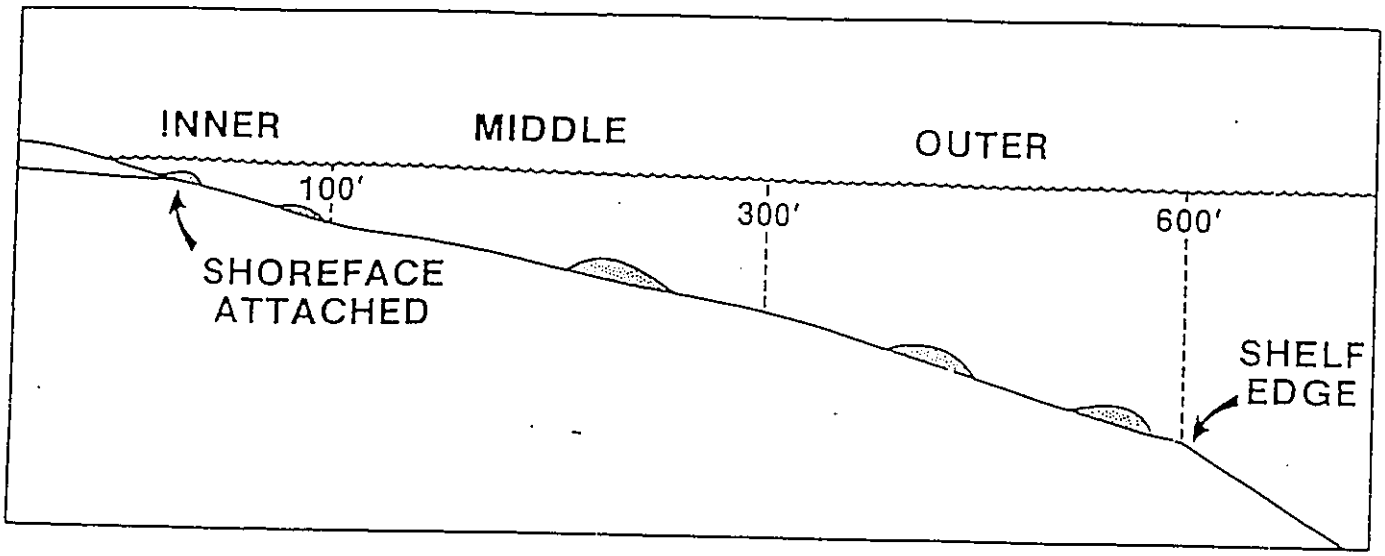

Figure 1. Subdivisions of the shelf where sand may accumulate.

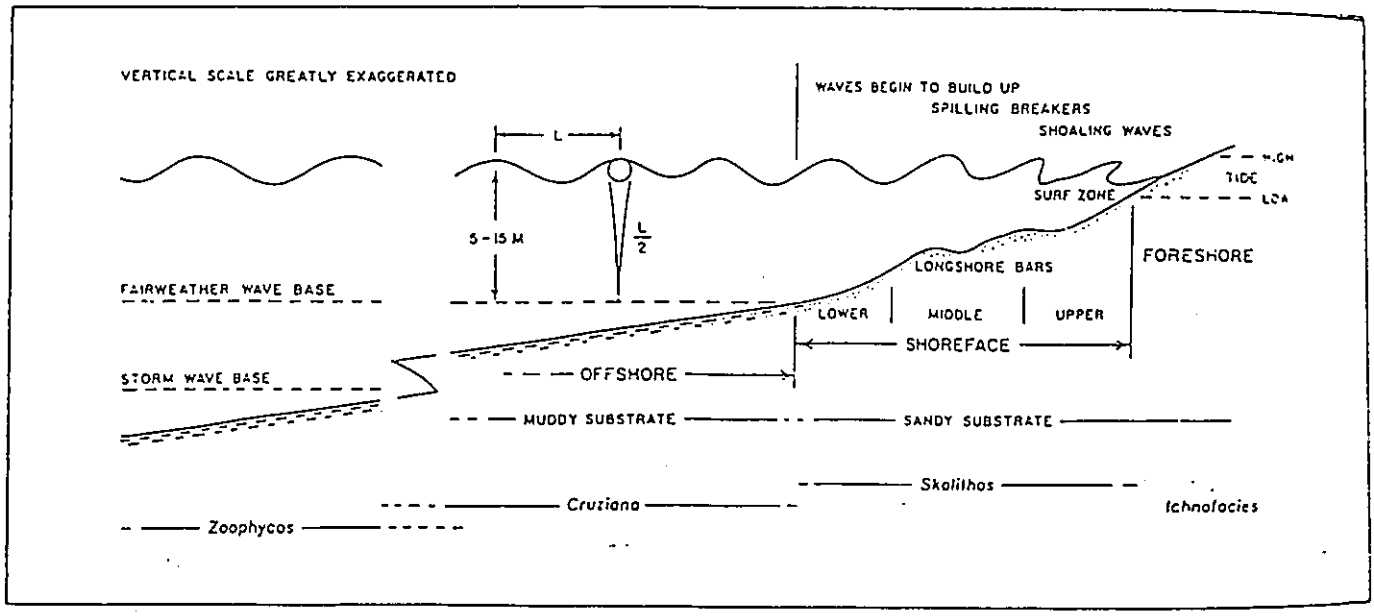

anorexis traces (see figure A-1b in appendix A and well 10-11-50-18W4 and 10-22-50-18W4 from unit Delta in foldout 8, A-A'). The absence of ichnological indicators of firm- or hardgrounds is thus negative evidence for the lack of pronounced scouring on the ocean floor. This absence does not contradict the interpretation of slow sedimentation derived from the diagenetic products.

6.3.5 Shelf Terminology

Before considering the environmental information to be gleaned from details of the sedimentary structures present in the Viking Formation it is appropriate to discuss the classification of the environments which may have generated them.

There are a number of classification schemes for shelf sediments in the geological literature, but there does not appear to be a general classification applicable or adaptable to all circumstances. Perhaps the simplest scheme is that of Tillman (1985), Figure 6-2, which simply categorizes the shelf into inner, middle and outer based on depth. Few geologists use this scheme, perhaps partly because of the inherent difficulty of determining paleodepth. One of the most influential schemes is that based on 'wave-dominated' shelves in which sediments are characterized as nearshore, within fairweather wavebase, between fairweather and storm wavebase or below storm wavebase. Figure 6-3 shows this scheme according to Walker (1984). There are subtle variations on this latter scheme depending on the author, but the framework may be found in all facies oriented texts covering shelf sediments (e.g., Johnson and Baldwin, 1987; Walker, 1984). In fact, the fairweather wavebase concept is the most common basis for discussing 'shelf' sediments because of the ubiquitous presence of waves. It is

used in discussions of shelf sediments even when these are not interpreted as storm-dominated but merely as having some signs of wave activity (see for examples Tillman et al., 1985).

The acceptance of the fairweather wavebase concept itself seems to have arisen gradually from informal modification of the meaning of the term. Wavebase was originally used around the turn of the century to describe the entire shelf and shelf break profile in terms of a response to wave action. Dietz (1963) presents an excellent summary of this earlier work. Dietz himself (1963) used "surf base" to account for the nearshore concave up profile of the shoreface which is more nearly what fairweather wavebase is applied to today. This 'geomorphic' view of shelves, coeval with the "peneplanation" view of erosion, contained the inherent assumption that "*at wave base, by any definition there is an abrupt transition from agitation to quiet water*" (Dietz (1963)). The relation of modern use of fairweather wavebase to this older usage is not entirely clear but may have been given its initial impetus by Hobday and Reading (1972) who discussed the development of erosion features in shelf sediments as a function of alternation between fairweather and storm events. It is after Hobday and Reading (1974) that fairweather wavebase entered the literature as a behavioral property of wave populations and hence a concept useful in categorizing shelf sediments (see the textbooks above). Hobday and Reading's (1972) use of the term may merely reflect an assumption of land-based geologists that storms (and hence waves) are binary in nature (i.e., either there's a "storm" or there's not). This assumption seems to have been reinforced by the alternation of sandstone and mudstone beds that may be found in cores of modern sediment and almost any sedimentary rock

sequence (for examples see Tillman et al. (1985), Moslow and Rhodes (1986), and Aigner (1985)). The work of Hamblin and Walker (1979) was further influential in advancing the fairweather wavebase concept, particularly as it played an important role in the related debate over the nature of hummocky cross stratification. The most extensive explanation for the use of fairweather wavebase is given by Walker (1985):

> " ... *wavelength L is a function of wind velocity, and we can THEREFORE (my emphasis) distinguish between fairweather and storm waves. Clearly, storm wave base will increase as the intensity of the storm increases, whereas we may be able to define a little more precisely the fairweather wave base. IF we DEFINE STORM WINDS (my emphasis) as gale force of greater (7 on the Beaufort scale), our maximum fairweather winds can be taken at about 50 km/hour ... Using the L/2 criterion, the depth at which such waves can just feel bottom is about 20m. They will not be able to move sand at this depth, so effective fairweather wave base for sand transport must be less than 20m. ... The coastal sand environments include the upper and lower shoreface, and the "lower shoreface [is an environment] where normal waves do not reach and sediment is moved only during storms" (Reineck and Singh, 1973, p. 305). Thus the lower shoreface/transitional boundary is roughly equivalent to or slightly deeper than "normal wave" base and it varies from "2 to 20m ..." [Reineck and Singh, 1973] ... Thus, evidence from modern oceans suggests that fairweather wave base is shallower than 20m ... If we ASSUME (my emphasis) that for the sandy part of the sequence, stratigraphic thickness roughly approximates depth of deposition ... , then fairweather wavebase must approximate the mud-sand contact ... I will define the base of the lower shoreface at the point where sands pass seaward into muds.*" (Walker, 1985)

This argument depends on a number of assumptions and arbitrary divisions of probably continuous natural populations (winds and waves) stemming from the non-sequitur the because wavelength is a function of wind velocity, a fairweather and storm wave may be distinguished. The relevant points

have been emphasized above in the quoted text. Few geologists working with marine sediments have questioned the concept of fairweather wavebase. An interesting exception is Aigner (1985); he summarized his views as:

> "In shallow-marine rock sequences, "wave base" has long been inferred to control sedimentation ... Hamblin & Walker (1979) first proposed a distinct zonation of storm-generated facies types with hummocky cross-stratification being formed between "fair-weather" and "storm wave base" ... However, on modern shelves, the depth of wave reworking shows strong seasonal variations: wave base during winter storms may be twice as deep as during the summer ... Thus there seems to be a continuous spectrum of conditions, and the terms "fair-weather" and "storm wave base" are probably rather artificial categories ..."

In summary it may be said that, with rare exceptions, geologists have assumed fairweather wavebase to be a fact of long term wave population behavior. The concept is definitely not one that has arisen from oceanographic work on wave populations or from the geological proposition and testing of specific hypotheses.

Some of the problems with the explanation of fairweather wavebase are as follows. Firstly, the existence of multiple wave populations interacting over the shelf bottom has not been taken into account; such multiple populations will have an averaging effect on the depths of interaction with sediment. Secondly, the shape of the shoreface is not necessarily due to "fairweather" activity which can be very shallow. For example, Shipp (1984) describes fairweather wavebase as being at the toe of the shoreface, but does not offer any long term measurements to confirm this. There are several factors that could account for the shape of the "shoreface"; it could well be shaped by an average wave climate not a "fairweather" regime. Even if the "toe of the shoreface" corresponds to a "fairweather wavebase", it is difficult to equate such a geomorphic feature with a

point in a stratigraphic column. Thirdly, Walker's (1985) assumption that winds divide neatly into storm and fairweather and that waves automatically follow such a division does not necessarily follow. Generation of waves is a complex matter, and the modifications waves undergo as they travel from their point of origin into other areas which contain waves generated at other points and times makes the idea of a simple separation into fairweather and storm very unlikely. Terms such as swell·and sea waves with a recognition of a gradation are probably more appropriate. Even more important is a focus on the variation on behavior of the sediment at the sea floor which might be attendant on different kinds of wave activity. Fourthly, currently available wave data has apparently either not been collected over a sufficiently long time or in an adequate manner to allow investigation of the existence of fairweather wavebase. Histograms of wave studies are short term (a few days), and long term data is often summarized in terms of significant height and/or significant period which does not clearly reveal the lower energy waves of crucial interest. Finally, the evidence from stratigraphic sections presented in the literature is that fairweather wavebase does not exist or is not preserved and is therefore not descriptively useful. For example, figure 6-4 shows a summary section through an ideal gradational -based wave dominated shoreface succession (from Walker and Plint 1992). It is typical of many wave dominated sections. It continuously coarsens and thickens upward and the wave influenced structures become steadily larger upwards; there is a continuum of smaller to larger wave ripples into HCS and sometimes into swaley cross stratification. Those structures that are not wave produced in the upper reaches of such sections are associated with nearshore processes such as ridge and

Figure 6-4. An Ideal Section through a Wave Dominated Shoreface Succession from Walker and Plint (1992).

The sequence shows typical bioturbated siltstones going to wave rippled and thin HCS beds to thicker HCS beds and Swaley Cross stratification.

"Normal," gradational-based shoreface succession

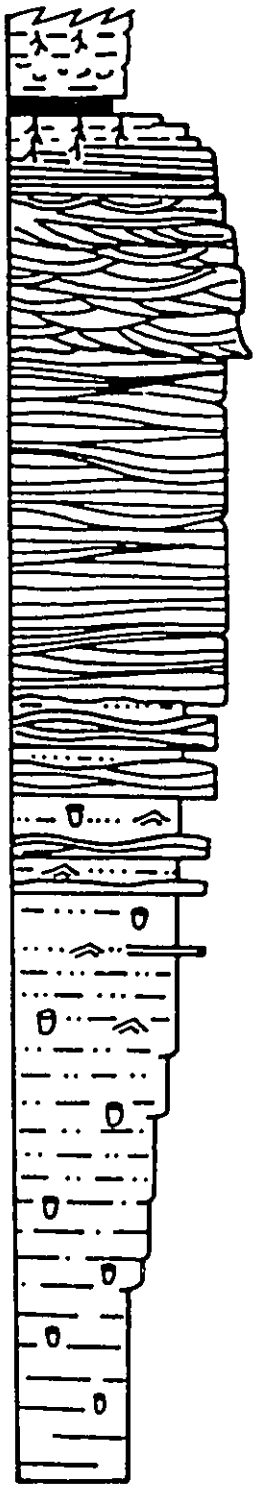

Coastal plain

Coal / Backshore

Beach

Breaker zone – ridge & runnel / rip channels

Shoreface – Swaley cross-stratification

Lower shoreface – inner shelf transition – Hummocky cross-stratification

Mid-shelf – bioturbated sandy siltstone

Outer shelf – bioturbated mudstone

10

m

0

Figure 6-5. A Shelf Classification without Fairweather Wavebase.

The shelf is divided into nearshore, inner and outer based on the presence of breakers, coastal jets, the "friction dominant zone" (Swift and Niedoroda, 1985) and "geostrophic" flow. The divisions reflect only those dominant processes reported in the literature (see text for details).

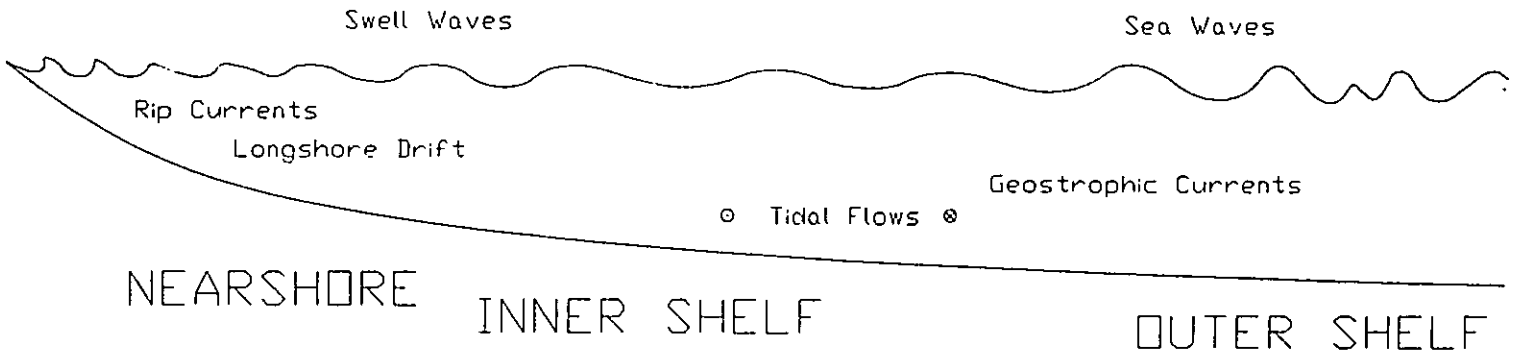
Swell Waves
Sea Waves
Rip Currents
Longshore Drift
Geostrophic Currents
⊙ Tidal Flows ⊗
NEARSHORE
INNER SHELF
OUTER SHELF

runnel and rip channel flow. This gradational behavior does not clearly present a point at which fairweather wavebase may be located. There are sufficient problems both with the explanation of the fairweather wavebase concept and with stratigraphic `evidence' for it that pending the proposal and testing of an adequate hypothesis regarding its existence, the idea is better disregarded in so far as classification and interpretation of shelf sediments are concerned.

Figure 6-5 presents a shelf classification scheme that does not include fairweather wavebase because of its debatable existence. This scheme is based on processes summarized in Tillman et al. (1985), Walker (1984a), McKnight and McClean (1986) and Davis (1987). Three shelf regimes are proposed. These divisions are the nearshore, inner and outer shelf. Across the shelf, waves have been labeled as either sea or swell waves (e.g., Kinsman, 1984); either may occur. Swell waves are taken to be relatively regular trains of waves usually approaching an area from a distance. Sea waves are taken to be assemblages of waves whose heights and directions are relatively random. Sea waves might impinge on the nearshore, but their dominance would depend on the energy level of swell waves. The nearshore corresponds to what many workers call the shoreface or upper to middle shoreface based on geomorphological terminology. This division is taken to be the area where shoaling waves are the controlling process. Within this region are the accompanying processes of rip currents, longshore drift with or without the effects of nearshore bars. Apart from the products of ebb tide deltas there would not be much tidal signature here; this conclusion is based on the work of Davis et al. (1972). Seaward of the nearshore is the inner shelf. This portion lies seaward of the effects of shoaling waves but before the zone of geostrophic

flow. Depth is shallow enough here that the Ekmann spiral is inhibited and the "friction dominated zone" is prevalent (Swift and Niedoroda, 1985). Shore normal flow is apparently possible in this zone through the activity of coastal jets (Csanady, 1982; Swift and Niedoroda, 1985). Tidal signatures may also be preserved here because they are no longer overwhelmed by the activity of breakers.

Seaward still comes the last division of the outer shelf. This is where "geostrophic" and ocean current flows become possible. Apart from this development, the processes are very similar to those of the inner shelf. The primary division is thus that of the shelf from the nearshore and is based on the point at which waves begin to shoal.

6.3.5 Primary Sedimentary Structure Details

The facies descriptions defined in chapter three may be used to place the sediments of the Viking within the classification of the above section. In conjunction with the facies descriptions, there is further information to be derived from details of sedimentary structures that is useful in such placement. The additional details of sedimentary structures mostly involve facets of the coarse, crossbedded facies or facies containing coarser material. This probably reflects the decreased possibility these sediments had of being bioturbated.

Exceptions to this are shown in Figures 6-6 and 6-7 which portray very fine grain size sandstones and siltstones. In particular, the figures show examples of the kind of unidirectional component, ripple cross-lamination that may be observed in facies such as Bedded Siltstone. This cross-lamination is not as common as the more randomly intersecting laminae shown in figure 3-2d as

Figure 6-6 "Unidirectional" Ripple Cross-Lamination in Bedded Siltstone

The photograph shows a piece of three inch diametre core with a two centimetre scale bar from well 10-20-47-16W4 from a depth of 2586 feet. The toesets are tangential parallel, and there is a preserved topset which is subhorizontal on the left and merges with the toesets to the right.

Figure 6-7 "Unidirectional" Ripple Cross-Lamination in Bedded Siltstone

The photograph is of a three inch diametre core from well 7-18-51-15W4 at a depth of 2203 feet; the scale bar is three centimetres long. The ripple cross-lamination shows possible breaks in activity marked by clay drapes included possible evidence for climbing ripple cross-lamination at the lower far right.


10-20-47-16W4
STORM BED
12

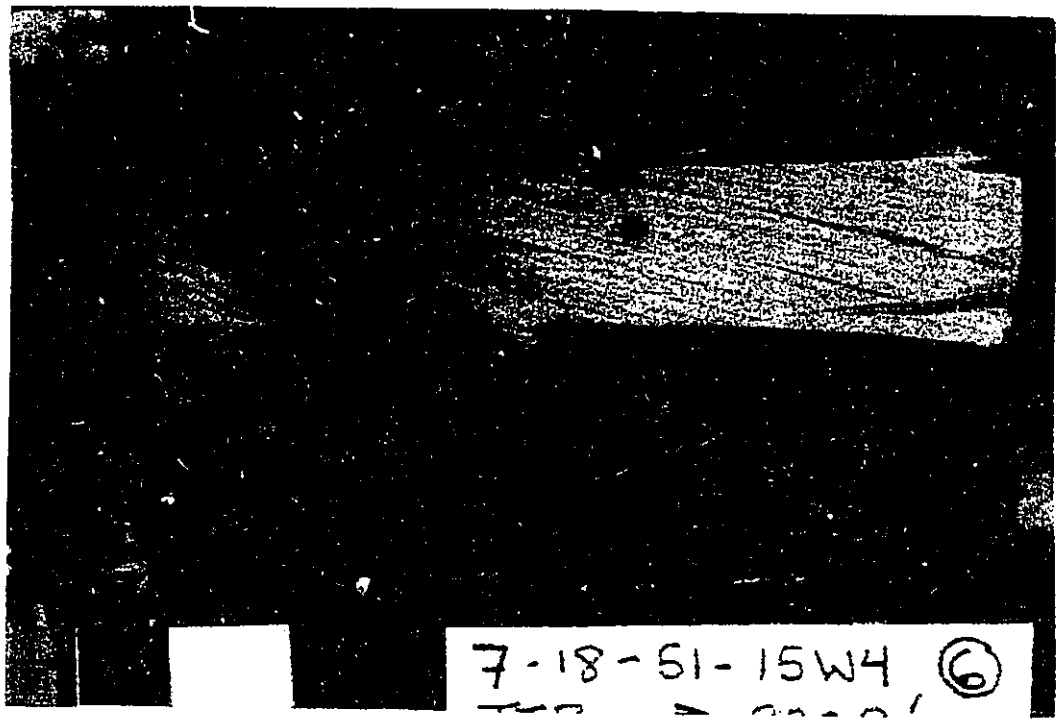
7-18-51-15W4
6

representative of the facies; however, it offers important clues about the processes distributing and reworking the sediment.

The cross-lamination in figure 6-6 is interpreted to result from a unidirectional current which gradually died out releasing its load to drape the initial ripple form; this is the change from lateral to vertical accretion visible in the cross-lamination. When taken in the context of the facies from which it comes (Bedded Siltstones; see below) such stratification is likely to indicate either deposition from shore parallel, "geostrophic" flow (e.g., Swift and Niedoroda, 1984, Swift et al., 1983, Swift et al., 1979) or from shore normal, "coastal jets" (e.g., Hayes, 1967 in Walker, 1984a; Leckie and Krystinik, 1989). Because paleocurrents cannot be determined from the cores, a decision between these options cannot be made. The possibility of tidal currents generating such stratification is ruled out on the basis of the much more common existence of wave rippled sediments in the facies (see below).

The ripple cross-lamination of figure 6-7 differs from that of figure 6-6 in that it suggests deposition from pulses of flow with relatively abrupt endings. The abrupt endings are implied by the constant form of the cross-lamination within an individual set. The pulsed nature of the flow is suggested by the mud drapes. The evidence for subcritical climbing of the cross-lamination at the right of the photograph, nevertheless, leads to the conclusion that overall sediment was being supplied to this location. This kind of "unidirectional" stratification is also interpreted to be created by unidirectional storm flows. Tidal flows are again ruled out because of the fact that only a few of the beds in the facies show this kind of cross-lamination; if tidal flows were capable of working the sediment in

Figure 6-8A Mixed Grain Size, Low Angle, Wave-Worked, Crossbedding, Core Surface View

This figure shows the exterior of a three inch diametre core from well 6-20-57-21W4 from a depth of 2050 feet. The scale bar is three centimetre long. The low angle intersecting laminae range in grain size from silt to Upper Medium sand (1 Phi).

Figure 6-8B Mixed Grain Size, Low Angle, Wave-Worked, Crossbedding, Slab View.

This is a photograph of the same piece of core as in figure 4a above but showing a slabbed view without any apparent distortion caused by curvature of the core.

one bed into such stratification, they should have accounted for a much larger proportion of the stratification given their 'daily' presence. This is not the case for intermittent storm flows whose activity would not be expected to predominate over that of other forms of wave activity.

Figure 6-8 shows a particularly informative example of the more predominant form of cross-stratification in the Bedded Siltstone facies. In this case, not only do the constantly intersecting laminae give no sense of preferred paleocurrent direction, but the coarser sediment has been intimately intermixed with the finer sediment. This kind of cross-stratification seen in core without the coarser material is often interpreted as HCS (e.g., Walker, 1983). There is no reason that this should not be the case here although it is a semantic matter at what point such intersecting laminae are labeled as wave ripple cross-lamination versus HCS. This cross-stratification is interpreted to represent reworking of the sediment, more or less in place, by sea waves. Whether the current that reworked the sediment was related to that which transported it to the site of deposition is indeterminate because of the lack of transportation indicators. The lack of beds showing reworking from another type of cross-lamination to the low angle intersecting type would seem to imply, however, that the sea waves were intimately related to the transporting current and remained as the imprinting agent after the decay of the transporting current. Neither flume (e.g., Arnott and Southard, 1990) nor computer models (e.g., Rubin, 1987) of sedimentation are of much help in resolving this issue; the former suffer from serious scale problems and the latter have not been attempted yet for the various wave current combinations possible. Moreover, arguments that have been made for the *in situ*

Figure 6-9A Mixed Grain Size, "Unidirectional", Ripple Cross Lamination with a Top `Lag'.

The photograph is from well 2-35-45-20W4 at a depth of 3166 feet and shows a three inch diametre core with a three centimetre scale bar. The cross laminae are planar parallel and consist of alternations of very fine sand to silt with up to medium upper sand (1 Phi). The upper few millimetres of the bed are subhorizontal laminae of a mixture of the same grain sizes.

Figure 6-9B Sketch of Core from Figure 6-5A

The sketch highlights the features of the cross lamination of interest in figure 6-5a.

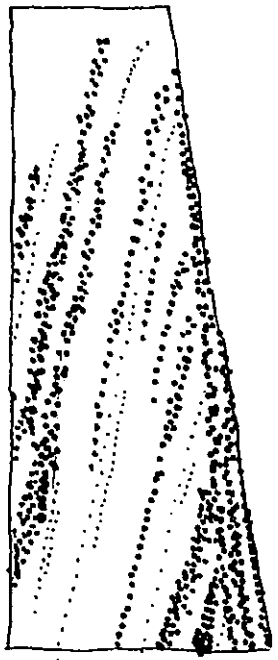


SSB → 3166

development of HCS from pure oscillatory currents (e.g., Arnott and Southard, 1990) suffer from the logical flaw of accounting for the introduction of the sediment into the relevant location. This sediment supply problem is also not addressed by the argument of Duke (1990) that paleocurrent evidence for shore normal and shore parallel flows actually are all part of shore parallel flows. If the sea wave interpretation is correct, then the multidirectional nature of the crosslamination implies that the internal structure of such beds mimics the multidirectional nature of paleocurrents on the soles of "distal storm beds" as described by Gray and Benton (1982) and described from two dimensional outcrop by deRaaf et al. (1977).

Signs of the type of flow responsible for transporting sediment onto the shelf may be shown in figure 6-9. It may be that this type of stratification represents the rare event where a unidirectional transporting current outlasted associated wave activity or flowed into an area of decreased wave activity, so HCS/wave ripple cross-lamination was therefore not created. Thus while there appears to be a fundamental difference between the behavior of mixed grain size sediment in this form of stratification and that shown in figure 6-8, they may be part of the same spectrum. Regardless of the causal relationships between the two types of stratification in neither was activity repeated sufficiently or sustained long enough to segregate the different sand size fractions. This is further evidence in support of intermittent storm activity as opposed to daily wave and/or tidal flows.

Not all sedimentary structure details are related to wave or storm processes. Figures 6-10A and B show much more distinctly heterolithic

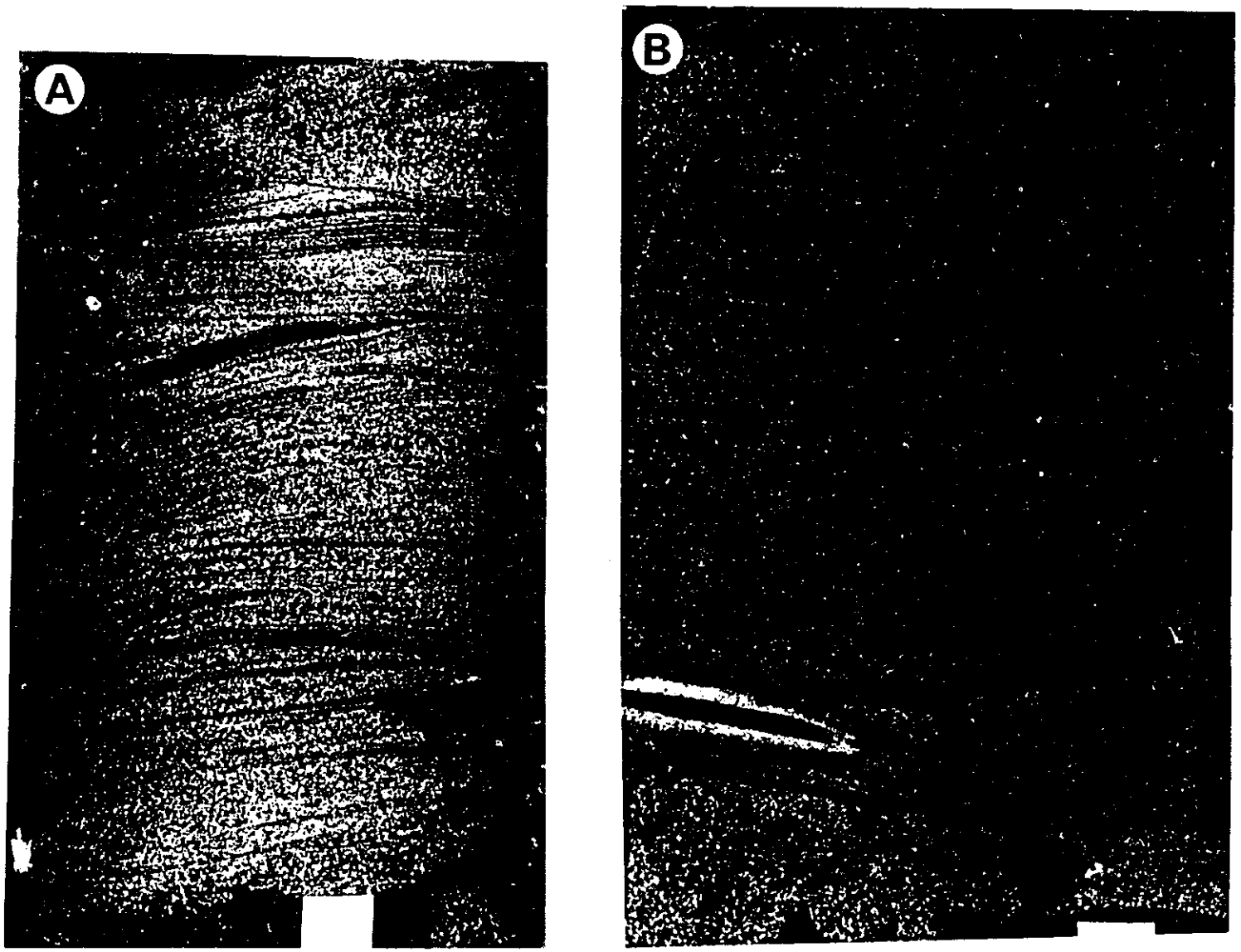
A
B

Figure 6-10A Draped Toeset Wedge

The core in the photograph is three inches in diametre and comes from well 11-7-48-20W4 from a depth of 3203 feet. The portion of particular interest is the lower right were a `triangular' wedge is overlain by heterolithic mudstone bearing *Planolites* burrows.

Figure 6-10B Draped Crossbedding

The figure shows medium to granular sandstone draped by thin laminae of siltstone and mudstone with possible descending ripple cross laminae and forms in the upper left of the lower piece. The core is three inches in diametre from well 10-18-61-4W5 at a depth of 3060 feet.

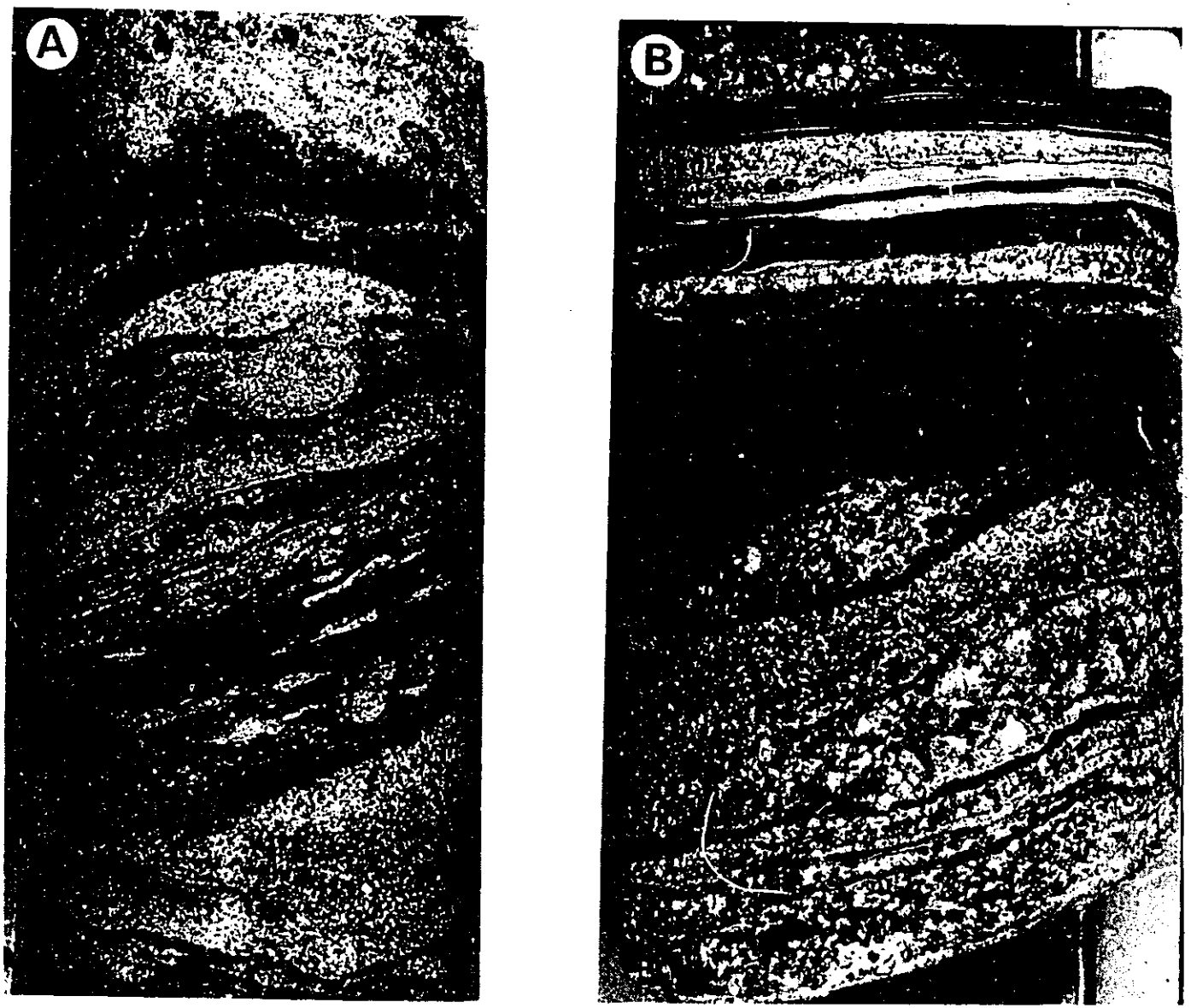
A
B

crossbedding whose clear mud/sand separation implies a different process of deposition. Figure 6-10A shows a triangular wedge of medium to coarse sandstone at the lower right of the core which is interpreted to be the toeset of an advancing bedform. This toeset is draped by alternating mudstone and sandstone laminae containing *Planolites* traces. The lack of mudstone drapes within the toeset implies that the bedform creating it moved under fairly continuous high energy conditions which were suddenly terminated allowing for the draping of the form by muds. However, this period of draping was not uniformly quiescent; it was punctuated by times of higher energy allowing movement of medium to coarse sand. These laminae of draping sands may conceivably have been worked off the top of the bedform. The presence of a bedform requiring high energy flows followed by much lower energy flows is interpreted be the result of a storm enhanced tidal flow followed by a non-enhanced tidal flow allowing draping of the bedform with alternating coarse and fine sediment. A tidal interpretation of these structures is partially predicated on a relative absence of wave produced structures (see the discussions of units Epsilon, Delta and Gamma below). If there were more signs of wave induced structures, it would be difficult to distinguish between tidal and storm related flows. However, pure tidal flow is unlikely to have resulted in the rapid variation between very sandy crossbedding and very muddy crossbedding. Pure tidal flow would probably have led to either more gradual lithological changes and/or development of grain size changes/mud laminae internal to the toeset. This is the reason behind interpreting a necessary 'boosting' flow in the form of storm activity to move relatively large, homogeneously sandy bedforms. Such boosting activity by storm currents has

been put forward as explanation for the transport of modern sediment in the North Sea (Stride, 1988). Furthermore, swell waves alone would not create crossbedding in such coarse sediments; it has been widely reported (Clifton, 1973; Clifton et al., 1971; deRaaf et al., 1977; Dupre, 1984; Komar et al., 1972; Luternauer, 1986; Yorath et al., 1979) and is the author's observational experience that in coarser sediments swell waves form relatively two dimensional wave ripples that are incapable of creating such crossbedding. Although this particular core is not from within the study area covered by this thesis, the presence of such tidal indicators and the lack of drastic formational changes between cores from this area (10-18-61-4W5) and the study site suggest that tidal flows would also be active in the area of figure 1-2.

Additional evidence for tidal activity in the basin is shown in figure 6-10B. In this case, very coarse to granular sands alternate with mud and silt drapes in moderate angle, 20°, crossbedding also interpreted to be a preserved toeset. At the center of the core, the top of the toeset is marked by a probable descending ripple form encased in mud. The delicate and alternating cross-laminae in this bed are unlikely to have been created by storm activity which could not turn on and off rapidly enough; such internal grain size variations probably reflect tidal currents. Adequate evidence from both the rock record (Klein and Ryer, 1978; Kreisa and Moiola, 1986; McCrory and Walker, 1986) and theoretical studies (Slater, 1985; Ericksen and Slingerland, 1990) demonstrates the existence and feasibility, respectively of tidal flows in the epeiric sea of the Western Interior of North America. Although the numerical models cannot predict detailed tidal velocity and range distributions and, in particular, may predict only microtidal

domains at the time of interest (the Albian) (e.g., Ericksen and Slingerland, 1990), the possibility of tidal flow at any point in the basin allows for amplification of the flow due to local topography which may have occurred in the case of the Viking. Such local details are not accounted for in the large scale, numerical models, so the absence of large tidal fluctuations in these models does not rule out their actual occurrence.

A tidal interpretation of crossbedding is also put forward for the structure shown figure 6-11A which has very regular fluctuations in sand size, from fine and medium to very coarse, combined with decreasing upward thicknesses of the cross-laminae. Although this not a classical tidal signature it is interpreted to be tidal because it seems unlikely that such a regular decrease in cross-laminae thickness could have been generated by successive storm flows. Similar behavior may be seen in sediments with classical tidal indicators such as the Lower Greensand of England (Allen and Narayan, 1964; Narayan, 1971). Although the core shown in figure 6-11Aa is not from within the exact study area, as with figure 6-10A, its presence in the Viking basin contributes to the tidal interpretation.

Figure 6-11B shows an example of the typical type of mud drape in crossbedded sandstones of the Viking. On its own, it is somewhat ambiguous, although for the reasons outlined in the discussion of figure 6-10B, a tidal interpretation might be favored. This kind of mud drape is so interpreted partly on the strength of the rarer evidence presented above and on very rare examples such as that shown in figure 6-11C. Figure

Figure 6-11A Bimodal Grain Size Crossbedding Showing Gradations in Crossbedding Thickness

The figure shows core from well 11-16-57-25W4 from 2786 feet which is three inches in diametre. The crossbedding is tangential parallel and alternates between fine and medium to very coarse (3 Phi and -1 Phi). Both thickness and angle decrease upward.

Figure 6-11A Bimodal Grain Size Crossbedding Showing Gradations in Crossbedding Thickness

The figure shows poorly sorted sediment ranging from medium to granular in size in crossbedding. The crossbedding is best delineated by three mudstone drapes in the lower half of the core each about two millimetres thick. The core is from well 11-19-56-24W4 at a depth of 2812 feet; the core is three inches in diametre and the scale bar is three centimetres long.

Figure 6-11C Crossbedding with Delicate Mud Couplets

The crossbedding is in fine to medium grain size sandstone (3 to 1 Phi) but is of unknown type. The crossbedding is best defined by very thin mud couplets that occur throughout the core. The core is two inches in diametre and comes from well 5-7-48-20W4 at a depth of 3221 feet.

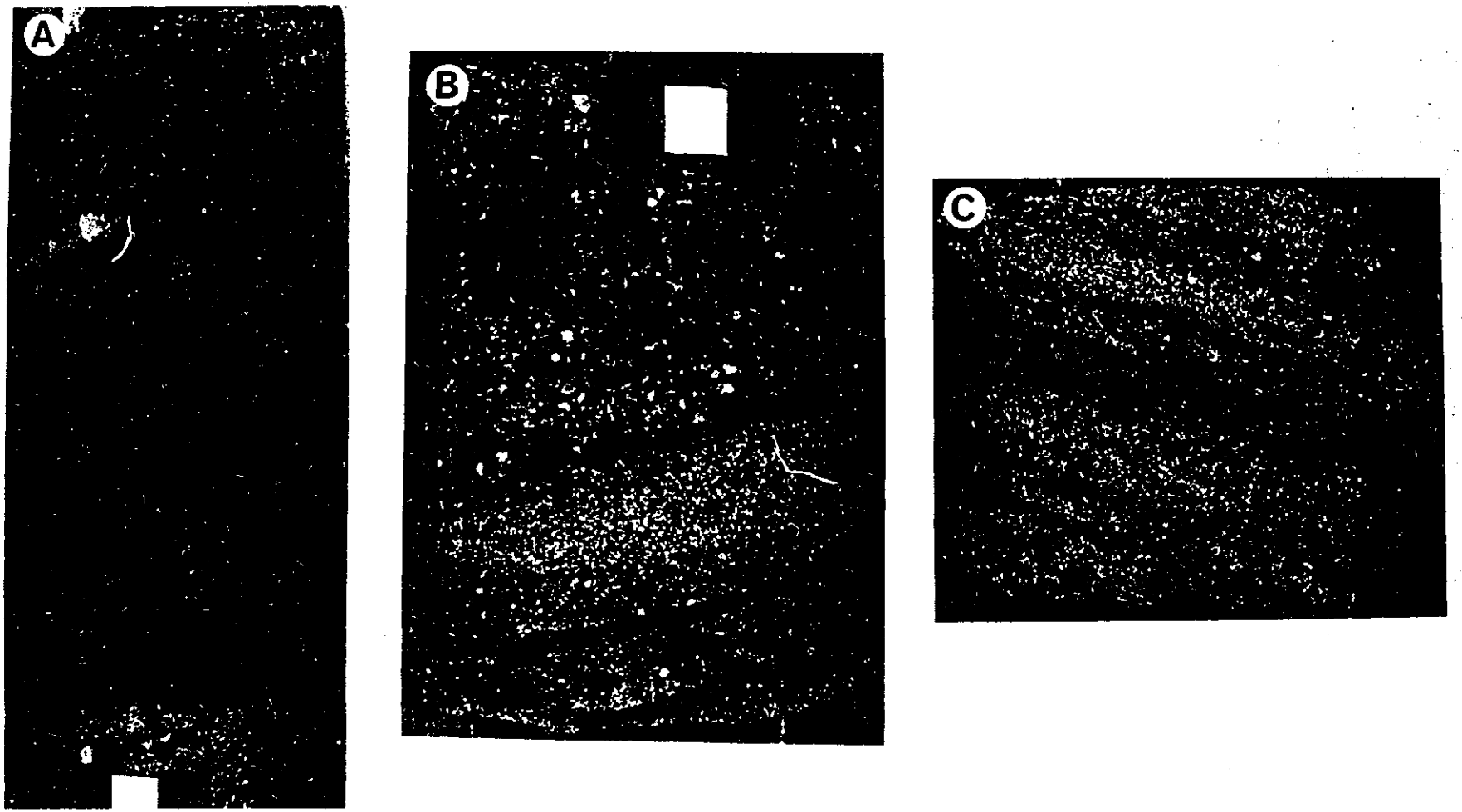
A
B
C

6-11C is the best example of mud couplets in the study area and is one of the few cases that is arguably a classic tidal indicator following Visser (1980).

In terms of the shelf classification delineated in section 6.3, the structures above indicate that the Viking was deposited outside the nearshore zone. There are no examples of the continuous low angle and high angle wave crossbedding and crosslamination that would be expected in the nearshore zone (e.g., Clifton et al., 1971; Davidson-Arnott and Greenwood, 1976). This is true of both the storm and tidal features, and is primarily indicated by the absence of swell wave reworking combined with abundant buildups of mudstone between and within the various crosslaminated beds. While the features interpreted above are not commonly visible, their existence helps to put the more generalized individual facies into an environmental context.

6.4 INDIVIDUAL FACIES INTERPRETATIONS

6.4.1 Introduction

Each of the individual facies contains different information on its general environment of deposition. In some cases, the general environment is similar to that of other facies with minor differences providing a more complete view of the environment. In other cases, there are fairly distinct implications that can be drawn from a particular facies that do not show up in other facies.

6.4.2 Grey Mudstone

The featureless nature of this facies makes its interpretation relatively mundane. Its context in the units and the presence of foraminifera and fish scales support an interpretation as a relatively deep marine mudstone deposited under quiescent conditions. Its close lateral and vertical association with facies such as

the crossbedded sandstones when considered with the evidence of the unit geometries (see above) would seem to restrict depths of deposition to a maximum of around 50 metres. In all probability Grey Mudstone was relatively organic rich when deposited and hence probably supported a diverse infauna; however, due to its homolithic nature, bioturbation is not readily apparent.

It is conceivable that thinner occurrences of the facies may merely represent chance accumulations of mud in settings that on average were relatively high energy (see the interpretation of crossbedded sandstones below). Such accumulations have been documented in modern high energy settings (e.g., Stride et al., 1982). However, the thicker accumulations underlying, within and above the Viking almost certainly represent periods of relatively deep marine sedimentation somewhere in an outer shelf setting. Although muds may accumulate in almost any location from the shore outwards (McCave, 1984), the presence of Grey Mudstone in successions whose grain size and associated facies are interpreted to indicate deepening water implies an outer shelf setting.

6.4.3 Laminated Siltstone

Laminated Siltstone is interpreted to be a mixture of storm deposited and wave reworked sediments laid down in comparatively distal settings of the inner to outer shelf. The facies is similar to the "sand-streaked muds" lithotype of de Raaf et al. (1977). The fundamental evidence for the process of deposition is the sharp-based occasionally graded nature of the laminae combined with their thinness. Sea wave reworking of the sediment is taken to be the dominant recorded process because of the lack of any preferred direction paleocurrent

indicators and the facies' association with Bedded Siltstone which has a strong wave/storm signature (see below).

The preservation of the laminae in the Laminated Siltstones likely reflects a local predominance of physical over biological reworking of the sediment rather than an anaerobic state in the water column or sediment. This inference is supported by the apparently random lateral relationships between this facies and facies such as Bioturbated Siltstone (see chapter 4 and below) and by the occurrence of bioturbated patches within the Laminated Siltstones and visa versa. These relationships indicate that the basin did not become anoxic. As with Grey Mudstone, thinner occurrences of this facies associated with coarser grain size facies may represent chance accumulations reworked by relatively weak waves in a generally higher energy setting.

6.4.4 Discontinuously Laminated Siltstone

Although this facies is not very common within the study area discussed, its presence warrants interpretation. Despite an appearance similar to Laminated Siltstone, Discontinuously Laminated Siltstone reflects preservation of a related but different balance of processes. The tendency of the cross-laminae to dip in the same direction despite being at relatively low angles implies a component of unidirectional flow in the depositing current. The generally low angle to the laminae is interpreted to reflect deposition from storm flows rather than either in situ reworking by waves or simple unidirectional flows. This interpretation is based on an argument of elimination. Unidirectional flows would be expected to produce either flat laminae or high angle crossbedding (Harms et al., 1982; Boguchwal and Southard, 1990; Southard and Boguchwal, 1990) and *in situ*

wave reworking is interpreted to produce relatively random intersections of laminae or small scale occurrences of high angle crosslamination (de Raaf et al., 1977; Newton, 1968) ((also see interpretation of Bedded Siltstone below). A weak combination of these two end members might produce the described features; the unidirectional component might produce the preferred orientation while the wave component restricted bedform growth. The flows would have to have been comparatively weak with identical directions. Unfortunately, the storm flow interpretation does not eliminate deposition by one or the other of shore normal flow or "geostrophic" flow in the sense of Swift (Swift and Niedoroda, 1985). Locating the facies in the shelf division presented above is difficult without paleocurrent information. The relatively consistent paleocurrents suggest distal shore normal flow on the inner shelf; "geostrophic" flow would be more likely to alternate direction depending on set up or drawdown conditions (e.g., Walker, 1984a).

6.4.5 Bedded Siltstone

As for Laminated Siltstone, the sharp-based sometimes graded nature of the beds in this facies is taken as evidence for deposition from waning storm currents. This facies roughly corresponds to the lenticular lithotype of de Raaf et al. (1977). The apparently randomly intersecting, low angle cross-laminae are interpreted to be the final product of sea waves rather than swell waves or "unidirectional" current interaction with the sediment, as discussed above for figures 6-6 through 6-8. Even given the thin nature of the beds (20 cm or less), if calculations of the maximum amount erosion and transportation possible for storm related flows are correct (e.g., Kachel and Smith, 1986), then the

approximate five centimetre limitation imposed on 'new' bed generation implies that both transportation and amalgamation has occurred in the thicker beds. The transportation of the sediment cannot be assigned with certainty to either "geostrophic", coastal jet, or random wave drift because of the lack of absolute paleocurrent information and sedimentary structures strongly indicative of transportation. Perhaps all played a role, but it seems likely that coastal jets, at least, must have been present to transport sand in such quantities from the western shoreline. The comparative thinness of the bedding and the large amounts of mudstone definitely place the facies outside of the nearshore zone (see the argument above). The *Planolites* and *Terebellina* traces that occur in this facies suggest a relatively high energy setting conducive to such *domichnia.* The facies probably lies in the outer portions of the inner shelf

6.4.6 Interbedded Siltstone

Interbedded Siltstone is essentially identical in interpretation to Bedded Siltstone as far as physical processes are concerned. The physical process is similarly interpreted to be reworking by sea waves in the outer inner shelf; the laminations are too small and variable to fall into the category of HCS. The presence of thicker beds and the lesser amount of mudstone might be taken at face value as indicating a more energetic, shore proximal location on the sea floor. However, in the case of the Viking, as discussed below under unit Beta's environmental summary, this is not the case. Interbedded Siltstone units do not necessarily occur in the more westward, shore proximal, cores. The thicker accumulations of sediment in Interbedded Siltstone compared to Bedded Siltstone are therefore interpreted to reflect random higher local rates of sedimentation.

Such locally higher rates could conceivably have been encouraged by small scale topography no longer or not resolvable on the core cross-sections. This interpretation is supported by the types of trace fauna observed most commonly in the two facies. In contrast to Bedded Siltstone, Interbedded Siltstone commonly contains more *fodichnia* such as *Teichichnus* and *Muensteria.* Such feeding traces would be encouraged by a higher rate of sedimentation that allowed organic material to accumulate in the sediments.

6.4.7 Bioturbated Mudstone

This facies is interpreted to reflect relatively quiescent settings in comparatively deep water. Biological processes dominate the physical although the latter were certainly present. The sedimentation rate is interpreted to have been relatively slow although organic rich. The completely bioturbated nature of the sediment implies sufficient organic material to support feeding activity in the muds while the presence of traces such as *Planolites* and *Terebellina* implies that the accumulation and or reworking of the sediment was slow enough that stable burrows could exist with occupants relying on surface feeding for their existence. Large accumulations of this facies probably, therefore reflect conditions in the outer shelf.

6.4.8 Bioturbated Siltstone

Bioturbated Siltstone represents fluctuating physical conditions in a situation where biogenic activity dominated physical processes. Large thicknesses of this facies probably represent the border between inner and outer shelf. Despite the general absence of physical structures a mixture of physical conditions is implied by the mixture of *spreiten* generating *fodichnia*

(*Teichichnus, Muensteria*) and burrow generating *domichnia* (*Planolites, Terebellina*). The latter traces imply slower sedimentation rates with high enough energy flows to supply nutrients while the former probably indicate relatively higher sedimentation rates burying nutrients in the sediment. Such fluctuations probably reflect variable wave interaction with the ocean floor like that presented for Bedded Siltstone.

6.4.9 Bioturbated Sandstone

This facies almost certainly represents high energy conditions in the inner shelf. This interpretation is supported both by the greater grain size and decreased mudstone content compared to Bioturbated Siltstone and Mudstone and by the types of traces generally occurring in the facies. The rarity of *spreiten* producing *fodichnia* and the predominance of *domichnia* such as *Rosselia, Terebellina, Arenicolites anorexis* and *Paleophycus* suggests that the water column was fairly continuously energetic. Not only were there sufficient suspended nutrients to support organisms likely to create such traces, but insufficient amounts of the nutrients were deposited along with mud to sustain a large community of deposit feeders. Tidal currents are interpreted as the primary physical agents responsible for this state. This inference partly relies on the presence of occasional crossbeds in the facies and the intimate association with tidally interpreted facies (see below, units Epsilon through Gamma). Additionally, tidal currents are more likely to have maintained a frequent high energy level below the nearshore setting; something storm flows would not be expected to do. It is the occasional presence of mudstone beds and *fodichnia* which place the facies outside of the nearshore zone (see references above).

6.4.10 Mottled Siltstone

The grain sizes and the associations of this facies with facies such as Bioturbated Sandstone imply that the facies reflects a somewhat higher energy setting than that of Bioturbated Siltstone, but one with a large proportion of mud available for transportation and deposition. The dominance of the facies by *domichnia* such as *Planolites* must be interpreted as above to reflect relatively continuous high energy water column conditions. Like Bioturbated Sandstone, this continuous high energy is taken as being tidally caused. However, compared to Bioturbated Sandstone, the muddier nature of this facies places it in the outer portion of the inner shelf. The lack of *fodichnia* in such a muddy facies is attributed to a combination of frequent reworking of the mud and existence of the mud in forms such as pellets that might not have carried a high enough organic content to support a large infaunal community.

6.4.11 Lensoid Sandstone

Lensoid Sandstone is interpreted to be have been deposited by storm enhanced tidal flows in the middle part of the inner shelf. The facies lies descriptively between classical *linsen* and *flaser* bedding (Reineck and Wunderlich, 1968) and the presence of relatively clean sandstone beds and possible bedforms within mudstone provides a case for arguments identical to those presented in the discussion of figures 6-10 a and b. The tidal interpretation is linked to that presented for the Crossbedded Sandstones (below) because of the occurrences of such facies/structures within Lensoid Sandstone units.

6.4.12 Muddy Sandstone

This facies, like Massive Sandstone below, contains relatively little information that allows for direct environmental interpretation. The facies is essentially interpreted by association with facies such as Crossbedded Sandstone to have been deposited in the inner portion of the inner shelf. This interpretation is further supported by the proportion and size of the sand grains within the facies. The sediment is almost certainly bioturbated, but the relatively clean state of the sand has prevented trace preservation.

6.4.13 Massive Sandstone

The Massive Sandstone facies cannot be definitely interpreted because of the lack of information it provides. It is most likely to have been deposited on the inner shelf in a manner identical to the crossbedded sandstones with which it is generally associated and whose grain size characteristics are similar. It may have lacked either the initial heterogeneity or subsequent diagenetic enhancement to reveal any crossbedded structure. There is no evidence in any of the other facies in the Viking to support interpretation of Massive Sandstone as being the result of any form of mass flow process, so it is not construed as evidence for operation of shelf turbidity currents.

6.4.14 Crossbedded Sandstone

Crossbedded Sandstone is broken down into its recognized subfacies for interpretation. The generic facies whose sets are not clearly divisible into any of the distinct subfacies are assumed to fall into the same general environment of deposition.

6.4.14.1 Tangential Parallel Crossbedded Sandstone

Tangential Parallel Crossbedded Sandstone is probably the deposit of relatively small 3-d dunes (Ashley et al., 1990) reworking and partly transporting sediment in the proximal to middle inner shelf. The general steepness of the crossbedding (25°) suggests that most of the trough has been preserved and that some of the above grade bedform might have been. Such small scale troughs seem unlikely to have been generated by bedforms larger than a metre or so high. As discussed above, swell waves are dismissed as a causal mechanism because they are incapable of making such crossbedding in coarse material. Because of the common mudstone interbeds and occasional mudstone drapes in the crossbedding, along with the details in figures 6-9 and 6-10 also discussed above, tidal flows are interpreted to have been the dominant depositing mechanism. Such flows are inferred to have been effective in the movement of sediment generally only when boosted by storm or wave currents. However, the extent of this influence is sometimes debatable. In cases where the crossbedded sandstone is relatively thick without mudstone interbeds, it may well be that such accumulations reflect a more predominant tidal flow; indeed, the facies in such cases are similar to those cored by Houboult (1968) in the Flemish Banks of the North Sea. It is conceivable that local topographic variations that are not now detectable in cross-section may have influenced the balance of such flows. The lack of distinctly bi-modal paleocurrent patterns as shown in figure 3-5 for all crossbedding could be attributed to influence of storm flows at an angle to a predominant tidal flow. This would fit an interpretation of coastal jets crossing shore parallel tidal flow. However, the possibility of the crossbedded sandstones

being deposited in relatively distal settings on the inner shelf would allow for relatively circular tidal "ellipses" (e.g., Houboult, 1968; Stride, 1963) with implication of relatively varied migration directions for bedforms. The more compelling evidence for intermittent, storm enhanced, activity is the common interbedding of mudstone with the crossbeds or the presence of isolated crossbeds within mudstone combined with the implications of slow sedimentation generated by the presence of glauconite (see above). The slow sedimentation and thickness of the mud would appear to rule out deposition of the mud over a single tidal cycle. A further case for storm enhanced generation of the crossbeds is made by the presence of Low Angle Intersecting and Parallel Crossbedding shown by Markov analysis to preferential succeed some crossbeds (see chapter 4). This is discussed under of Low Angle Intersecting Crossbedding below.

6.4.14.2 Planar Parallel Crossbedded Sandstone

Planar Parallel Crossbedded Sandstone probably reflects deposition from small 2-d dunes (Ashley et al., 1990). Its interpretation is essentially identical to that of the Tangential Parallel above. However, the presence of an abrupt base to the crossbedding indicates a lack of a trough and hence implies that the crossbedding represents essentially the preservation of a starved bedform. Preservation of such crossbedding with mudstone interbeds strongly supports a relatively long term energy fluctuation that would not be expected if tidal flows alone were moving the sediment.

6.4.14.3 Low Angle Parallel Crossbedded Sandstone

This facies is interpreted to deposited as the result of storm waves and currents although it might possibly be the trough deposits of large bedforms.

However, its preferential succession from higher angle crossbedding, as shown by the Markov analysis of chapter four, would not be expected if the latter were the case. It might also reflect the highest energy tidal flows possible, but the general paucity of the facies in comparison to the high angle crossbeds indicates conditions for its creation were not regularly available and hence probably not tidal. If the storm enhanced tidal interpretation of the high angle crossbeds is correct, then it is not unreasonable to extend this interpretation to the lower angle crossbedding. It is possible that the fact that low angle parallel crossbedding tends to succeed high angle crossbedding and not *vice versa* indicates decay of tidal current strength during a storm flow. This would leave the wave activity as the dominant flow which tends to produce horizontal lamination (e.g., Arnott and Southard, 1990).

6.4.14.4 Low Angle, Intersecting Crossbedded Sandstone

Low Angle, Intersecting Crossbedded Sandstone is interpreted as the result of swell wave or small amplitude sea wave reworking of sediment in the inner shelf. Unlike Low Angle Parallel, Low Angle Intersecting Crossbedding may preferentially succeed or precede high angle crossbedding in Markov analysis (see chapter 4). This indicates that its generating flow does not have a particular relationship to that responsible for the high angle crossbedding. Consequently, by analogy with examples of swell wave cross-stratification (Sharp, 1984; Sherman and Greenwood, 1984; Short, 1984), the crossbedding is interpreted to represent periods of high energy swell waves reworking sediment on the inner shelf.

6.4.15 Pebbly Sandstone

Pebbly Sandstone suffers from the same lack of diagnostic information as Muddy and Massive Sandstone. Most examples of this facies are located to the northwest of the study area. However, there are isolated, enigmatic occurrences in some cores such as 10-7-52-18W4 in A-A' (foldout 8). The grain size and associated facies place Pebbly Sandstone in the inner shelf. But the processes responsible for its deposition are speculative. The presence of mud and traces such as *Arenicolites anorexis* in the facies indicate a marine setting of fluctuating energy levels. The associations with Crossbedded Sandstone and Muddy Sandstone suggest that the same storm enhanced tidal processes were generally operating during this facies deposition. The coarse, pebbly fraction of the units is interpreted to have been storm supplied since there is no other data that might suggest a shoreline having reached the area and to be transgressed and reworked to leave a lag.

6.4.16 Pebbly Mudstone

Pebbly Mudstone is interpreted to reflect storm current sedimentation on both the inner and outer shelf. The mixture of lithologies requires a short term, extreme fluctuation from average flow conditions in order to transport the coarser material into a generally mudstone setting. Tidal flows are almost certainly incapable of doing this and storm flows can probably only accomplish it incrementally. The evidence of pebbly laminae in distal sediments (e.g., 11-5-45-12W4 in unit Alpha of A-A', foldout 8) strongly supports the inference that storm flows were capable of transporting pebbly sediment across the ocean floor away from shorelines.

6.4.17 Conglomerate

The chert dominated Conglomerate facies is comparatively rare in the study area, but important because of the energy levels required to move this size of material. The comparatively poor sorting of the Conglomerate argues against nearshore deposition by comparison to the few modern coarse systems described (Bluck, 1967) and the author's experience. Thicker occurrences to the northwest of the study area may represent transgressed, reworked shoreline systems that might have acted as sources for the sediments in the location discussed here (see chapter five). The few examples of chert conglomerate occurring in this area are inferred to be storm flow deposits, possibly tidally winnowed. Such winnowing is well known from modern tidal settings (Belderson and Stride, 1966; Stride, 1963) and has been documented for local beds in the ancient record (Phillips, 1984). The Chert Conglomerate situation is analogous to that of Pebbly Sandstone.

6.4.18 Diagenetic Clast Conglomerate

Diagenetic Clast Conglomerate is interpreted to be a mixture of locally derived rip up (auto-) conglomerate and storm imported clasts. The presence of phosphatic and glauconitic material strongly suggest that the sideritic mudstone and chert clasts do not reflect processes such as shoreline retreat (e.g., Plint et al., 1986) but instead represent development of a lag on the seafloor. As may be seen in foldouts 8 (A-A') and 10 (C-C'), and as discussed in Chapter 4, Diagenetic Clast Conglomerate may occur as the lateral equivalent to a number of different facies, most commonly at the uppermost portion of unit Delta. Therefore, the facies cannot be taken as corresponding directly to basin wide events. It is

interpreted to be due to local scouring by storms and/or tidal flows during the lower phases of sea level. Such scouring has been reported from modern shelves (Barrie and Bornhold, 1989; Belderson and Stride, 1966; Donovan and Stride, 1961; Stride, 1963).

6.4.19 Slumped Siltstone

This facies is interpreted as a product of tectonically related deformation of uncemented sea floor sediments. There is no data that would suggest the presence of a significant slope on the sea floor that would allow gravity slumping. Furthermore,

there is no data strongly suggesting tectonic activity in the immediate area that might have caused the slumping, so such activity is inferred to have occurred within the rising Cordillera to the west. These sediments thus help to confirm an element of tectonic activity during deposition of the formation.

6.5 ENVIRONMENTAL VARIATIONS RECORDED WITHIN UNITS

6.5.1 Fundamental Groupings

As discussed in chapter four, the fundamental divisions between units on a facies composition basis is between the group Epsilon, Delta and Gamma and the group Beta and Alpha. The latter are generally finer grained and composed of the wave/storm dominated facies while the former are made up primarily of the coarser, tidally dominated facies. The information available on unit Mu is too limited to allow such inferences.

6.5.2 Units Beta and Alpha: Storm Dominated Shelf Deposits

Assembling the individual facies interpretations of the units comprising units Alpha and Beta (see chapter four and foldouts 8-12) reveals that the units are storm/wave dominated.

The stacked Markov analyses show there is no clear vertical pattern present in the facies of unit Alpha that might be interpreted as progradational. Nor is any pattern visible in the lithological cross sections.

Examination of the lithological cross sections in foldouts 8 through 12 shows that of all the units Beta has the most pronounced tendency to have facies that are identical laterally, although not consistently so. Despite this tendency toward laterally consistent facies successions, there is no regular variation in the storm deposits of the kind that has been reported by Brenchly (1985) and Brenchly et al. (1985) for shallower units with occurrences of HCS. In unit Beta, the succession of facies indicates a general aggradation and minor progradation from the outer shelf to the outer reaches of the inner shelf followed by a transgression to the outer shelf. (See chapter seven for a discussion of the details of the locations of the points of transgression for each unit.) This appears in the preferred relationships even of the artificially stacked Markov analyses (see figure 4-24). Some of the preferred transitions are aggradational and others are interpreted as related to flow processes. A transgressive component appears in the siltstone facies (mottled to laminated) overlying the crossbedded sandstone. These facies show a transition from inner to outer and distal shelf settings. The phase with the greates progradational component is the laminated to bioturbated portion of the transitions. The environment changes from distal to inner/outer

shelf. The increase in percent of silt and a slight grain size change also suggests a progradational component to the aggradation.

6.5.3 Units Epsilon, Delta and Gamma: Storm Enhanced Tidally Dominated Units

Consideration of the vertical units presented in chapter four for these units (figures 4-20 through 4-23) and foldouts 8 through 12 in light of the individual interpretations delimits units Epsilon through Gamma as tidally dominated. The coarsening upward nature of these units suggests that the successions have a prograding, regressive component. This is largely confirmed by the interpretation of the individual facies; there is a movement from the outer, inner shelf to the inner shelf. However, as discussed in chapter seven, the upper portions are likely transgressive. This is a common occurrence for tidal sandstones (Nio, 1976). It is also possible that units Epsilon and Delta display a more transgressively dominated facies assemblage. This may be indicated by the greater occurrences of local scours, such as sometimes occur at the boundary between the two units, and may also be reflected in a more varied (random) distribution of the facies within the units.

There is a slightly more regular relationship between the facies in unit Gamma compared to those of units Beta and Alpha; this apparent relationship appears as a more pronounced coarsening upward pattern. This pattern appears despite a detailed lack of exact lateral correlation between facies in the lithological cross sections of foldouts 8 through 12. The Markov analyses of chapter four (figures 4-24 through 4-27) tend to support this impression through the greater number of preferred transitions expressed in unit Gamma in

comparison to unit Beta. It is difficult to relate such summaries precisely to lateral variation. There almost certainly remains a random component in the detailed lateral facies relationships, as may be seen in the less deterministic Markov chains for units Epsilon and Delta. The more random assemblages shown for units Epsilon and Delta may in part be due unit Gamma possessing a more pronounced progradational geometry. A steeper paleotopography may have existed during the deposition of unit Gamma effecting the distribution or impact of the distributary mechanisms; Epsilon and Delta may have had flatter topographic expressions allowing a more dispersed and potentially random, interaction between the sediment and water currents. Differences in the number of cores used to compile the summaries doubtless also have some impact on the relative randomness of the successions. The apparent randomness of the facies transitions in the units Epsilon through Gamma is reflected in the grain size distributions shown in figures 4-13 through 4-15. Gamma is also the only unit that has a pronounced trend in grain size; units Epsilon and Delta appear to have randomly distributed grain sizes, as indicated by geostatistical analysis.

The sheet geometry of the sandstones discussed above (section 6.3.2.3) combined with the facies distribution shown in foldouts 8 through 12 indicates that despite the random components of the detailed lateral relationships, on a general level, the units preserve sand ribbons with crossbedded sand preferentially located in the thicker accumulations. The bioturbated facies occur between these fingers and further into the basin. Tidal sheet sands may thus be simplistically summarized as depositing coarsening upward successions going from bioturbated, sandy mudstones to crossbedded, muddy sandstones whose sets

reflect small, single bedforms even if the sand sheet is continuous. Figure 4-21 is a typical example of the vertical profile.

Preferential transitions between facies also have some processes related interpretations. In almost all units with crossbedded facies, there is a preferred transition from high angle to low angle crossbedding. Sometimes this occurs within a single set, but the transitions recorded in the Markov analysis are between sets. This suggests a change in flow regimes and may indicate either waning flow or loss of a pronounced unidirectional component flow and change into a more wave dominated flow. In either case, the evidence is interpreted as support for an initial combined flow interpretation for the high angle crossbedding. The preferential transitions from bioturbated silts/muds to sands that occur for these units may reflect that bioturbation preferentially occurred in the areas between the thicker portions of the sand ridges where sand deposition was potentially slower.

By comparison with examples of modern tidal sheet sands, it may be estimated that peak surficial tidal velocities in the basin may have been on the order of 100 cm/s (Stride et al., 1982). This figure is approximate because of the possible differences in water depth between the North Sea and the Western Interior Seaway in the vicinity where the sediments studied were deposited. There are a number of differences between the modern North Sea example of tidal sand sheets which dominates the literature and the sediments of the Viking Formation. Most notable are the grain sizes of the sediment and the apparent thickness of the bedforms responsible for the crossbedding. On the whole, the Viking is somewhat coarser than the sheet sands of the North Sea which tend to

occur in fine sand (McCave, 1971) although the entire spectrum of sizes may be present (Stride et al., 1985). Conversely, the bedforms of the Viking were probably smaller than those emphasized in most studies (Mann et al., 1981; McCave, 1971; Stride, 1970) although they would fall in the lower end of reported spectra. It may be that the Viking sediments do not fit into the sheet sands as currently described but more accurately reflect accumulations of "sand ribbons" (Kenyon, 1970a; Kenyon and Stride, 1970) or "sand patches" (Kenyon, 1970b). The smaller bedforms usually associated with such divisions of the tidal sand spectrum match more closely those inferred from the crossbedding of the Viking. It is possible that migration of such ribbons during regression and ensuing transgression could produce a sheet like geometry as preserved in the Viking while distributing sediment roughly parallel to the basin margin from the northwest. Such a basin margin parallel distribution would agree with the transport paths determined from modern examples (Kenyon and Stride, 1970).

CHAPTER 7

VIKING UNITS AND INTERPRETATION OF SEA LEVEL HISTORY

These are much deeper waters than I had thought.

Arthur Conan Doyle (Sherlock Holmes)
Reigate Squires

7.1 SUMMARY

The units of the Viking Formation do not fit standard sea level curve based unit interpretations because the point of transgression is located within the upper, coarser portion of the units rather than exactly at the unit boundaries. The abrupt lithological changes at the unit boundaries do not necessarily reflect rapid transgressions; the transgressions were relatively slow. There are no distinct maximum flooding surfaces. The formation as a whole may correlate with formations in other areas of the Western Interior Seaway and hence represent a global sea level change. However, this is not the case for the units. The evidence for tectonic control of unit geometries suggests that the units reflect periodic tectonic activity such as thrust loading of the cordillera to the west.

7.2 INTRODUCTION

Current sea level interpretations based on siliciclastic sequence stratigraphy, regardless of the nature of the sequence classification used (Galloway, 1989a, Posamentier et al., 1988, Van Wagoner et al., 1990) all assume that particular points on the sea level cycle, such as the onset of transgression and the maximum flooding surface can be located accurately within the stratigraphic column. The locations are all placed at distinct lithological breaks. Even when

such particular points are not attached to the breaks, a rate change is often inferred. For example, Walker (1990) in his discussion of the various approaches to "sequence stratigraphy" discusses abrupt lithological changes as reflecting starts and stops in the velocity of sea level change. While it is reasonable that abrupt changes may correspond to basic changes in the direction of sea level change, it is possible that such changes do not necessarily correspond to fundamental points on a sea level curve.

In the portion of the Viking Formation examined, the interpretation of the sediments provided in chapter six suggest that the units do not fit this standard interpretation. There is little doubt that as an entire formation, the Viking Formation represents a regressive period of sedimentation preceded and followed by marine transgression. However, the locations of lesser regressions and transgressions within the units that comprise the formation are not immediately clear. This is particularly so for units Epsilon, Delta and Gamma.

7.3 LOCATING POINTS OF THE SEA LEVEL CYCLE

7.3.1 The Location and Rate of the Transgression

Although it was a matter of great debate in the study of modern/recent shelf sediments (see Walker, 1984; Tillman et al., 1985 and Johnson and Baldwin, 1986) the discussion of transgressively deposited and/or reworked sediment appears to have been largely left out of sequence stratigraphic models, perhaps largely because many sequences do not have large transgressive components. Particular facies successions have been described as partly transgressive, but usually only the thinnest veneer of sediment, immediately

associated with a trangressive erosion surface is considered as transgressive *per se.*

Interpretations of the Viking Formation have paralleled this state of affairs. Emphasis has been on regressive or lowstand sedimentation. Even recent studies with strong sequence stratigraphic emphases (Downing, 1988 and Power, 1988b) have interpreted the sediment as having minimal transgressive signatures. Only Beaumont (1984) has previously attributed significant portions of the Viking units to transgressive deposition. However, he did so in a manner which disagrees with the interpretations environmental and unit geometries discussed above and which does not adequately account for sediment distribution. His concept of shelf sequences retrograding during transgression does not allow for initial introduction of sediment onto the shelf. Additionally, his interpretation includes no mechanism to explain how coarsening upward sequences would imbricate laterally to produce a high in the middle of the basin and a low towards the basin margin which would be the source of the sediment. Consequently, the transgressive interpretation he puts forward for the equivalent of entire sequences is not accepted.

Descriptively the Viking unit boundaries described in chapter 4 are coincident with the "parasequence" division of Van Wagoner et al. (1990); however, the parasequence concept involves the interpretation of such boundaries as marine flooding surfaces essentially equivalent with the onset of transgression or a major increase in the rate of transgression (see figure 39 of Van Wagoner et al., 1990). Up until the parasequence boundary the sediments are considered to

be regressive. This is not interpreted to be the case either for the Viking unit boundaries.

The abrupt lithological changes in the Viking units Delta and Gamma and probably Epsilon are not interpreted to reflect fundamental points on sea level curves such as the onset of transgression or the onset of regression (i.e., point of maximum flooding). For these units, the point of onset of transgression appears to be located somewhere in the upper portion of the units within the coarser, usually crossbedded, sandstones.

This interpretation is based on three lines of argument. First, the existence of glauconite within the units suggests conditions of slow sedimentation under at least partially transgressive conditions (see chapter 6). The occurrence of glauconite is a condition commonly taken as indicative of a condensed horizon correlative with maximum flooding (e.g., Weimar, 1992); this has also been incorporated into "sequence stratigraphy" as described by Posamentier et al. (1988) and Van Wagoner et al. (1990). However, in "sequence stratigraphy", glauconitic horizons are considered as part of correlative conformities beyond the parasequence or sequence boundaries and are not discussed in terms of occurrences in areas of sudden lithological changes. Second, the environmental interpretation of the sediments in chapter 6 implies that transgression had started before the deposition of mud over the coarser sediment. Transgression led to distribution of the sediment from the nearshore environment further onto the shelf for reworking. Finally, there is rare evidence from some of the cores that the maximum grain size occurs within the middle portion of the crossbedded facies rather than being distributed generally throughout the upper portion of the units.

Figure 7-1 Lithologs of Core 10-21-51-19W4 and Alternative Sea Level Interpretations.

The figure shows a litholog through core from well 10-21-51-19W4 from depths 2705 - 2755 feet. The log shows facies successions through units Delta and Gamma. The left hand litholog is labeled according to the parasequence boundary definitions of Posamentier et al. (1988) and Van Wagoner et al. (19). That on the right gives the alternative interpretation discussed in the text. See figure 3-1 for a legend for the facies scheme. S marks the location of unit boundaries; T marks the location of the onset of transgression; M marks the possible location(s) of the "Maximum Flooding Surface".

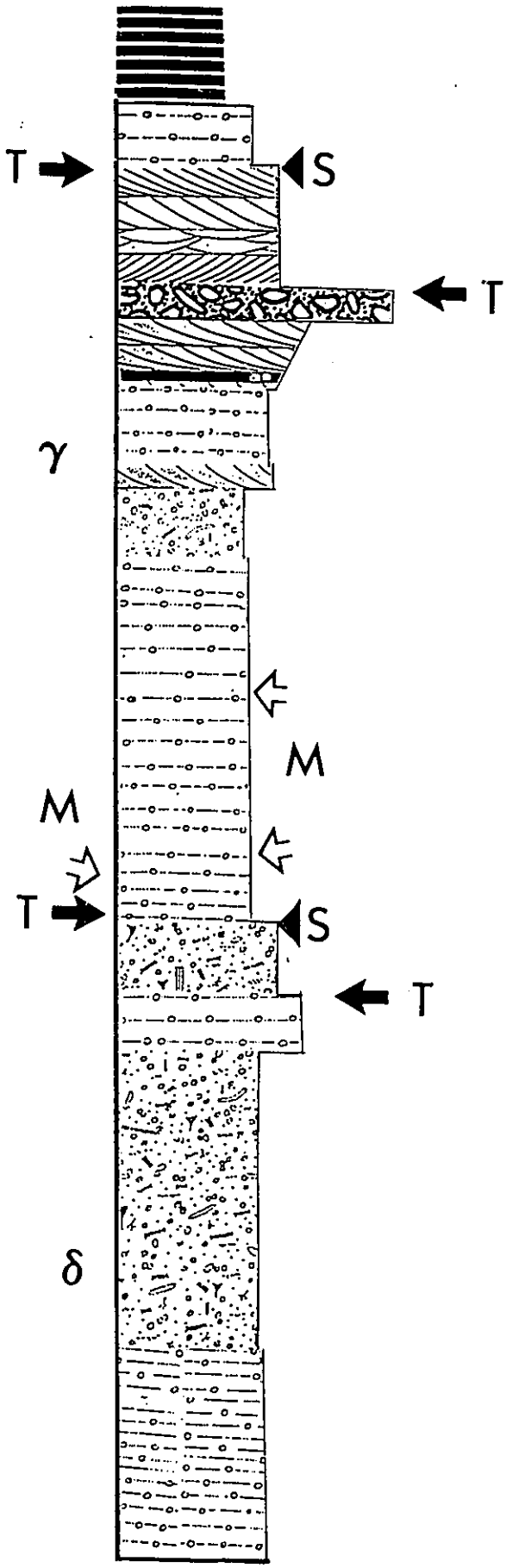
T
S
T
γ
M
M
T
S
T
δ

Such an example is shown in figure 7-1. This figure shows the litholog of core 10-21-51-19W4 through both units Delta and Gamma. In both cases, the coarsest part of the unit occurs on the order of a metre below the most abrupt facies changes taken as the unit boundaries. These points of coarsest grain size might be taken as the points of maximum regression (equivalent to the start of transgression) following the simple logic that the coarsest material represents higher energy and hence probably shallower settings. They have beenlabeled T in the figure. The location of the maximum flooding 'surface' is discussed in the next section. This argument alone is not conclusive because relatively random high energy events could deposit such coarser material without a fundamental change in base level having occurred. However, it is consistent with the additional inferences drawn above. Were such coarse intervals ubiquitous across the formation, they would provide lithological markers for unit boundaries just as valid as the rapid facies changes described above.

As may be seen in any of the vertical profiles in chapter 6 or foldouts 8 through 12, unit Beta differs from the other units in that it has no accumulations of material indicative of transgressive reworking. In this case, the onset of transgression and the unit boundaries are usually almost coincident. Nevertheless, the boundary is sometimes underlain (see chapter 6) by isolated sets of crossbedded sandstone or coarse sand interbedded with wave or storm current worked finer sands. Very rarely, these coarser beds are a few decimetres below the unit boundary. However, the transgression is still placed below the unit boundary for reasons similar to those discussed above for units Epsilon through Gamma. Unit Beta also has glauconite and phosphatic material intermixed with

the coarser sediment. As for the other units, isolated scours occur below the coarser material. The appearance of unit Beta is much closer to the Cardium Formation sequences described by Plint et al., (1987) and Bergman and Walker (1986). Unlike the case for the Cardium Formation, no subaerial exposure is interpreted to have occurred because of the lack of an extensive disconformity (see chapters 5 and 6 and foldouts 8 through 12). Because of the paucity of transgressive material, timelines are compressed near the unit boundary. The unit becomes close to the purely regressive parasequence model. This is not surprising if the environmental interpretation of the facies is correct because much less sediment would be expected to accumulate in distal shelf settings leading to thinner amounts of sediment between events on a sea level curve. Unit Beta is therefore interpreted as showing similar responses to sea level variation as the underlying units but in a more distal environmental setting.

As for the location of the first sign of transgression, the interpretation of rates of sea level change from rates of lithological change differs from existing interpretations associated with current sequence stratigraphic approaches. The common interpretation, that rapid change in one means rapid change in the other (e.g., Van Wagoner et al., 1990 and Walker, 1990), need not necessarily be so. In the eastern Viking Formation it appears that rapid lithological (or facies) changes correspond to slow transgression.

The widespread distribution of the coarser sediment across the area studied, in the form of discontinuous sheets, supports reworking during a relatively slow transgression. Intermittent reworking is further supported by both the signs of slow sedimentation rates and the occurrence of small amounts of

coarser material in the overlying mudstones discussed in chapter 6. Relatively rapid transgression would be expected to leave sediment in more isolated distributions (e.g., Plint et al. (1987); Bergman and Walker (1986); Walker (1990)). As transgression continued, it is likely that the source of coarser material was eventually overrun. Without further supply, the coarser material already on the shelf was then buried in mud as the currents became less capable of keeping finer sediment mobile. It is also possible that with transgression the shape of the seaway changed sufficiently to shut off tidal flow or decrease them sufficiently to cease the effective distribution of coarser material. The rapid change in facies thus could actually reflect a gradual decrease in capability of relevant ocean currents, in this case predominantly tidal, to move sediment. Interpretation of the rate of transgression for unit Beta is more ambiguous. Without correlation to more proximal deposits for comparison the rate could be interpreted as similar to that for the underlying units or as a more abrupt or intermittent (i.e., stillstand to transgression) event.

In some locations coarse material has not accumulated, most notably in units Delta and Epsilon where the units are capped by only thin accumulations of coarse sediment, including autoconglomerate, on top of local scours. They are interpreted as locations where the cover of sediment was breached on the sea floor and the semi-lithified substrate exposed. Once this substrate had been exposed, continued erosion would become possible. Such local scouring has been documented in areas of the North Sea and English channel (e.g., Donovan and Stride, 1961). The accumulation of a sedimentary cover in other locations prevented such scouring of the ocean floor from being widespread. In most of the

eastern portion of the Viking Formation there is thus no inference of either a renewed transgression following stillstand (Walker, 1990) or an increased rate of transgression (Van Wagoner et al., 1990) at unit boundaries or within the units.

7.3.2 The Point of Maximum Flooding

Like the point of onset of transgression, the point of maximum flooding is not located at abrupt lithological breaks. The point of maximum flooding is equivalent to the point of onset of regression. however, the flooding surface is more commonly referred to in the literature than the onset of regression (e.g., Posamentier et al., 1988; Van Wagoner et al., 1990; Walker, 1990; Wiemer, 1992) so that use is continued here. Locating the point of maximum flooding presents even greater problems than locating of the point of onset of transgression. Walker (1990) has pointed out that "*without chemical or micropaleontological analysis, we cannot easily determine from cores exactly where the maximum flooding surface (MFS) occurs*". Even this may be rather optimistic. Bartlett (1987) studied the Cardium example cited by Walker (1990) at the stratigraphic points that Walker (1990) takes to be the point of maximum flooding (i.e., at the lithological change from conglomerate to mudstone). Bartlett's (1987) results, which relied primarily on measurement of foraminiferal accumulations, did not show any signs of a maximum flooding surface at the indicated locations or at any overlying point. This suggests that either the "chemical and micropaleontological" means of analysis is invalid or the location of the assumed MFS is wrong. It is most likely that the MFS cannot be detected by chemical and micropaleontological means, in any practical sense. Furthermore, such a point is probably some distance above any abrupt transition

from coarse to fine sediment. There is a further point that can be made about the behavior of the MFS. Bartlett's (1987) investigation and Walker's statement both assume that the MFS is characterized by relatively condensed sedimentation that would be mirrored in the chemical characteristics of the sediment and a potential increase in the proportion of micropaleontological remains preserved. This is consistent with the kind of response predicted for the correlative conformity of sequence stratigraphy. In the existing sequence stratigraphic models, the correlative conformity largely develops during regression when the previously deposited muddy shelf sediments have not yet been buried by the more distal portions of the newly regressing parasequences (e.g., Van Wagoner et al., 1990). The correlative conformity is described as being muddy and characterized by diagenetic products such as glauconite and phosphate, indicative of slow sedimentation. While glauconite and phosphate occur within the units, and are interpreted to be indicative of overall slow sedimentation, this slow sedimentation is interpreted to have occurred in more proximal settings during transgression, not in distal settings during regression (see above). This condition implies that the condensed sedimentation postulated to exist at the MFS may not be there; in this case it is associated with the transgressive phase of sedimentation. This implies that if the correlative conformity is located on the basis of the signs of slow sedimentation rather than being the basinward equivalent of the MFS, then the units described above behave as correlative conformites. The correlative conformity would thus have to be defined as potentially occurring in sandier, shallower facies than previously acknowledged. Similar behavior has recently been reported for an interval in the

Upper Cretaceous Mancos Shale where crossbedded ironstones have formed a transgressive condensed deposit (Chan, 1992).

In the parasequence model the MFS would be located above the most abrupt lithological/facies change which in the eastern Viking Formation would correspond to placing it at the unit boundary. If the interpretation of the facies successions provided in chapter 4 is accepted, then this location would not be sedimentologically reasonable. It would imply that following the deposition of the coarse sediment no material was deposited until the regression began. It is much more likely that when coarse sediment motion and supply ceased finer material was still being deposited. In this scenario, there would be no lithological indicators of the turn around from transgression to regression to be found. This is the reason Walker (1990) has stated that locating the MFS would be very difficult in core. It seems likely that only in relatively large scale sequences where internal geometries can be traced via internal markers (e.g., Galloway, 1989b) can the maximum flooding surface be located. This makes Galloway's (1989a) proposal for sequence divisions inapplicable to thinner units such as those of the Viking. Consequently, the MFS point has not been delineated with any accuracy on lithologs of the formation. The ambiguity of locating the MFS has been shown in Figure 7-1 by the spread of arrows on the right above the postulated point of onset of transgression. In summary, the grain size variation of the facies successions/units is, broadly speaking, offset from the sea level cycle. During regression coarse sediment is held in the shallower environments. Upon transgression, the flow mechanisms operating in deeper water (e.g., tidal flows)

Figure 7-2 Sea Level Curve from the Viking Formation

The figure shows a qualitative interpretation of sea level fluctuations recorded in the sediments of the Viking Formation in the area described in the thesis. Particular aspects are discussed in the text. The horizontal axis is arbitrary distance from the basin margin, and the vertical axis is unscaled time.

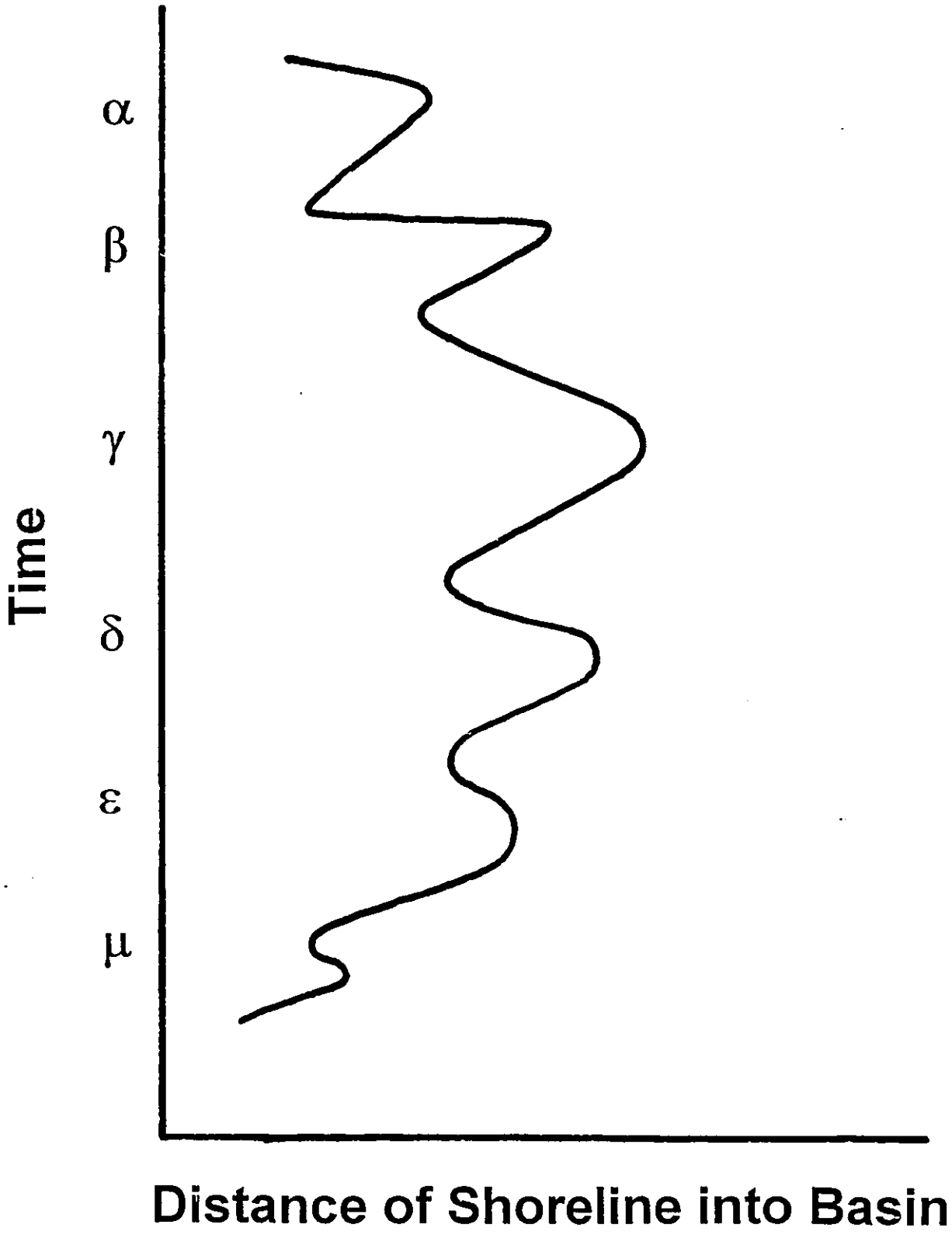
α
β
γ
δ
ε
μ
Time
Distance of Shoreline into Basin

have access to this sediment and are capable of distributing it more broadly over the shelf, particularly in a slow transgression.

7.4 Sea Level History Inferred from the Viking

Figure 7-2 shows an inferred sea level curve for the Viking Formation which includes all the interpretations attached to the units in sections 7.3.2. Both the onset of transgression and regression on the curve have been smoothed to reflect potential ambiguity in the timing of these events. To a certain extent the smoothing may also reflect genuine sea level behavior. The steepness of the regressive and transgressive branches of the curves reflects the inferred velocity of the transgression or regression once it had been initiated. The curve for unit Alpha is quite ambiguous because its ubiquitously fine grain size facies allow little interpretation. The rapid transgression in the upper portion of unit Beta is drawn to reflect the very thin or absent nature of the transgressive sediments in the unit. However, as discussed in section 7.3.2, this may reflect the distal nature of the sediments, and the curve could conceivably be much steeper. Likewise, the curves for units Gamma, Delta and Epsilon are drawn primarily to reflect the quantity of sediment present in the portions of the unit attributed to transgression and regression respectively. Since these units contain a greater transgressive signature, the curves are steeper. The curves are qualitative.

7.5 MATCHING THE VIKING TO OTHER SEA LEVEL CURVES

It is impossible in practice to definitively fit the individual units of the Viking to a global sea level curve and difficult to do so for the formation as a whole. The difficulty does not relate only to whether such curves as that of Haq

et al. (1988) are in fact global, but also to the technical problems associated with accurately dating sediments as old as those of the Viking. Ignoring statistical measurements of inaccuracy and merely examining the range of the K/Ar age dates of 96 to 108 Ma (Tizzard and Lerbeckmo, 1975) there are approximately six sea level cycles reported on the Haq et al., (1988) curve for this time range. Even if a very optimistic view is taken of the age dating results and the average value of approximately 98 Ma taken, there exist two closely spaced sea level cycles at this time. The argument put forward by Haq et al. (1988) is that each of these cycles would generate a "sequence" which would theoretically be composed of parasequences similar to the units defined in the Viking. The curves are not purported to be accurate enough to discern these "parasequence" scale events (Posamentier, p. comm., 1989), so following this argument, a wide variety of potential sea level fluctuations might have accounted for the formation as a whole. Moreover, if this particular sea level curve (Haq et al., 1988) is valid, then two major sequences on the scale of the Viking Formation would be expected in the rough timespan occupied by the Viking. The absence of a second "sequence" implies that either major sea level fluctuation generate "parasequences" or that one of the sea level fluctuations did not extend into the entire Western Interior basin perhaps due to tectonic events.

The matter is even more complicated when sea level curves from other authors are examined. General correspondence of the Viking Formation to an overall regression can be found but evidence for correlation of the sub-sequences is not available. Within the time span allowable for Viking deposition, Weimer (1988) reports two major unconformities interpreted as two sea level curve

fluctuations, neither, either or both of which could correspond to the overall Viking regression. Kauffman (1977) describes only one sea level cycle in the time corresponding to possible Viking deposition. The optimum correlation of the entire formation would be with his regression, R5. However, the correlation varies depending on the timescale used. If Kauffman's (1977) revisions of the absolute dating of the Albian are accepted, then the upper Albian and the Viking would correspond to his transgression, T5. However, if the Van Hinte standard scale is used, then the Viking does correspond to Kauffman's (1977) regression, R5. Given the overall nature of the Viking, the latter seems more likely.

There is a great deal of local variation in the ages and number of sub-sequences occurring across the Western Interior Seaway. Their equivalence or lack thereof can probably only be resolved by detailed correlation of the type exemplified in the cross-sections in foldout 1 through 7.

Biostratigraphic correlation of these purported sea fluctuations across even the relatively `local' Western Interior basin is more ambiguous than overall "sequence" (i.e., formation) correlation. This is partly because of the lack of macrofauna in the Viking combined with the unzoned state of most of the Albian in the U.S. (Kauffman, 1977), but is also due to contradictory sea level correlations. Given that the Viking lies between the *Miliammina manitobensis* (above) and *Haplophragmoides gigas* (below) foraminiferal zones (see chapter two) which correspond almost to the boundary between the *Neogastropolites haasi* and *Inoceramus comancheus* molluscan indices (Caldwell et al., 1978), a biostratigraphic correlation would place the Viking as equivalent to T5 transgression of Kauffman (1977). This biostratigraphic correlation would imply

local control over not only the sequence developments but the deposition of the whole formation given that the Viking should correspond to a regression/transgression peak on a correlative sea level curve. Contrary evidence is provided by Weimar (1992). He reports that the Muddy Sandstone in the Colourado area of the Rockies immediately overlies the *Haplophragmoides gigas* zone which would strongly suggest that the formation is equivalent to the Viking Formation.

7.6 EUSTATIC VERSUS TECTONIC CONTROLS ON UNITS

The uncertainty over the "eustatic" correlation of the formation raises the issue of the causal mechanisms of sea level change. Problems in the mechanisms for generating eustatic fluctuation have been discussed elsewhere (e.g., Pitman, 1978) and will not be reviewed here. The most feasible method of global fluctuation, the variation in the volume of polar ice, may have just begun weakly operating in the Albian (Matthews, 1984). However, the argument for glacial eustacy at this time remains highly speculative and cannot be definitely assigned as a cause for the formation scale regression.

A better case for a causal mechanism can be made for the units within the eastern Viking Formation. As the interpretation of the unit geometries in chapter five revealed there is a strong case to be made for tectonic control of the shape of the unit packages. In fact, if the correlations of chapter four are correct it is inconceivable that these geometries could have been generated by simple sea level fluctuations involving a relatively static basin margin. There is circumstantial evidence that the basin was tectonically active during Viking Formation deposition. Such evidence includes deformations of the Slumped

Siltstone facies discussed in chapter six. Sandstone dikes have also been described in the formation and attributed to seismic disturbance of the basin (Leckie, 1987). The necessity of basin deformation for accommodation of the unit geometries has been discussed in chapter 5 and will not be reiterated here. Given evidence for tectonic activity, it is much more likely that in addition to the geometries of the units that tectonic activity was actually responsible for the generation of the units themselves.

CHAPTER 8

CONCLUSIONS

We shall not cease from exploration.
And the end of all our exploring
Will be to arrive where we started
And to know the place for the first time.

T.S. Eliot Four Quartets

8.1 SUMMARY

Existing sequence stratigraphic terminology does not readily apply to the units of the eastern Viking Formation because fundamental points on sea level curves such as the onset of transgression are contained within the units rather than at the unit boundaries. The gradational units contain major transgressive components and behaviorally may be characterized as correlative conformities. Their existence implies that the correlative conformity of current sequence stratigraphy can extend into relatively shallow settings and be composed of strongly transgressive components.

The coarser material of the units was initially supplied to the "shelf" during regression, but substantial parts were moved and reworked during transgressive phases. The environment of deposition preserved within the units of the Viking is generally tidally-dominated but with storm enhancement of the transport. These transgressive sediments record a laterally, comparatively random assemblage of muddy crossbedded sandstones and bioturbated sandy siltstones that were distributed in a ragged sheet across the ocean floor. The facies successions show no regular lateral relationships. The sediments are

heterolithic from the scale of cross-laminae to bedding with sedimentary structures indicating intermittent flow.

8.2 INTRODUCTION

Chapters five, six and seven all contain discussions of the aspects of facies investigations and unit behavior that were raised in chapter one. The answers to the questions contained in these chapters are summarized collectively here.

8.3 SMALL SCALE, DISTAL MARINE UNITS IN FORELAND BASINS

8.3.1 Unit Definitions

The most useful point for unit boundary placement in distal marine units is lithostratigraphic. The potential MFS of Galloway (1990) is undetectable in thin units. In the case of gradational, marine units that were never subaerially exposed or shallow enough to develop regional scours or discontinuities there are no sequence stratigraphic boundaries. On the whole, existing sequence stratigraphic nomenclature (e.g., Type I and Type II of Posamentier et al., (1990)) does not apply to units as described in the eastern portion of the Viking Formation because such units lack extensive disconformities. This also means that the less interpretive allostratigraphic nomenclature of the North American Stratigraphic Code (North American Commission on Stratigraphic Nomenclature, 1983,) cannot be applied.

As currently construed, the parasequence model does not apply either. While the lithostratigraphic divisions of units described in this study, descriptively correspond to the "parasequence" (Van Wagoner et al., 1990), the interpretive aspects of the parasequence model do not conform to the information

contained within the units. This is because the onset of transgression and maximum flooding are offset from the locations implied in the model.

The evidence from these Viking units suggests that the parasequence as currently construed requires refinement to become a general foundation for sequence stratigraphic interpretations. The need for refinement may arise because the current parasequence appears to be based on the relatively proximal deposits of finer grained storm dominated units which does not account for a full range of means of distributing sediment. The impact of tidal components in a transgressive setting has been argued above to be such that if the parasequence terminology is to be retained to describe the resulting units, then the possibility of a pronounced transgressive component needs to be included in the definition.

Furthermore, in the existing sequence stratigraphic nomenclature, the parasequence and the correlative conformity are separated with the correlative conformity assigned to the distal portions of the parasequence equivalent strata in the realm of the mud dominated sedimentation (e.g., Van Wagoner et al., 1990, figure 20a and b). The conclusion to be drawn from consideration of the arguments presented above is that the correlative conformities can extend into intermittently, high energy environments containing sandy deposits. Furthermore, the correlative conformity is not formed only during the regressive phase of sedimentation, as implied in the discussion and illustration of Van Wagoner et al. (1990); The correlative conformity may be transgressive, as illustrated in the case of units Epsilon through Gamma by the uppermost coarse sediments. It may thus be concluded that in cases where sediment is intermittently mobile under conditions of transgression, parasequences will

develop a transgressive component and beneath the sequence (i.e., "parasequence") boundary. This transgressive component will reflect sedimentation at a correlative conformity. Because the maximum flooding surface lies above the unit boundary, such correlative conformities are probably predominantly transgressive. This is the reverse of the existing model which is centered around regressive events.

Such units correspond to correlative conformities; however, they are implicitly much shallower than the correlative conformity is usually taken to be. This implies that correlative conformities can occur in shallow enough settings that relatively high energy events can be recorded and a record of sea level fluctuation can be deciphered. The existing model of the correlative conformity is one of condensation of units in a manner that does not allow clear separation of sea level fluctuations. Correlative conformities can develop for individual units at the parasequence scale.

8.3.2 The Units Sea Level History

At the scale of units described in the chapters above, there is insufficient information within the units to allow for precise location of points such as the onset of transgression and the maximum flooding surface (i.e., the onset of regression). This lack of information means that sea level curves cannot be accurately located in such small scale units. However, this does not disallow the construction of sea level curves; it merely means that there is uncertainty about the precise correlation of the curve to the stratigraphy. Correlation of sea level curves, between sections and between formations is still theoretically possible based on the number of undulations in the curve.

The abrupt lithological changes taken as boundaries for the units Gamma, Delta and Epsilon do not reflect fundamental points on sea level curves such as the onset of transgression or the onset of regression (i.e., point of maximum flooding). Although the point of transgression cannot be located accurately, the sedimentological interpretation and early diagenetic evidence implies that it lies within the coarser portion of the unit with the uppermost portion.

The most important point to be made about coarse sandstone facies, as typified by the Viking Formation, is that they are not necessarily completely regressive. As discussed in chapters six and seven, a significant portion of the coarse sediment was reworked and deposited during transgressive conditions. Coarseness of material does not automatically correlate with water depth. Although ultimately the introduction of coarser material onto the Albian seafloor required a lowering of sea level to bring material to a source to the west of the area studied here, sediment in the upper portions of the units was transgressively reworked.

Unit Beta's sedimentological and early diagenetic evidence suggests a sea level history geometrically much closer to the parasequence model but still fundamentally equivalent to that of units Epsilon through Gamma. Unit Beta is closer to the ideal regressive parasequence because it is largely lacking in transgressively deposited or reworked material, so the onset of transgression is placed close to the unit boundary.

In most of the eastern portion of the Viking Formation there is thus no inference of either a renewed transgression following stillstand (Walker, 1990) or

an increased rate of transgression (Van Wagoner et al., 1990) at unit boundaries or within the units.

8.3.3 Foreland Basin Unit Geometries

As the interpretation of the unit geometries in chapter five revealed there is a strong case to be made for tectonic control of the shape of the unit packages. The Viking Formation itself may, however, correspond to a eustatic event. The pattern suggested by the geometries of the eastern Viking Formation units is that foreland bulge migration may create a characteristic basinward onlapping of units. The more distal portions of such units may be more abruptly based than their proximal equivalents due to the upwarping and consequent migration of the foreland bulge. The expectation is that other foreland basin, distal marine units should show an abrupt onlap like pinching into the basin in an area where they take on characteristics of correlative conformities.

The question of whether unit geometries developed in foreland basins differ from those of passive margin basins cannot be clearly answered over the area covered in this study because onlap or offlap relationships were not observed. The relatively planar, distal portions of units appear to be similar between the two types of basins. However, the tectonically influenced geometries discussed above could influence the manner of onlap and offlap of the units when seen at a larger scale. The foreland basins may conceivably have more varied downlap relationships because of the greater potential for warping of the basement onto which they were deposited.

8.4 FACIES SUMMARIES

8.4.1 Tidally Dominated Sheet Sands

The two prior hypotheses were tested 1) that sediments in the area reflect deposition in offshore bars or 2) lowstand shorefaces. It is concluded that "offshore bar" and shoreface sediments are not present. Sediment was apparently distributed offshore of the paleoshoreline during Viking Formation time by a combination of processes summarized as storm enhanced tidal flow. This distributive mechanism relies on an initial transgression, however, to allow the sediment to enter the distributive realm. The transgressive regressive cycle attributed to the Viking Formation units described here strongly suggests that such sea level variation is the precursor to developing coarsening upward successions in a marine environment. Large amounts of coarse sand are not known to be distributed out onto modern shallow marine settings ("shelves") and it is unlikely that any distributive mechanism would exist in the past that has not currently been observed.

The particular features of the crossbedding and their associated trace fauna indicate the storm enhanced tidal flow distributive mechanism. The crossbedding is characteristic of a predominantly unidirectional flow but on the basis of its heterolithic nature apparently moved intermittently enough that regular unidirectional flow was insufficiently powerful to entrain the coarser sediment. Details of the crossbedding that are indicative of this process include potential sigmoid cross-bedding, very rare potential mud couplets, mud draped (heterolithic) crossbedding, and heterolithic toesets. The epigenetic products visible in the Viking Formation, glauconite and phosphate. are commonly associated with relatively slow sedimentation. Their occurrence in the Viking in association with sedimentary structures such as high angle crossbedding, usually indicative of high energy flows, is interpreted to be the result of intermittent high

energy flows stirring sediment in an otherwise comparatively calm sea floor. As discussed in chapter 4, the trace fossil evidence supports this interpretation.

Simple storm and wave distribution of the sediment can be eliminated on the basis of knowledge of wave ripple behavior known from modern coarse sediment. The conclusion that tidal processes were primarily responsible for the crossbedding arises mostly by the process of elimination. Pure wave activity is eliminated by reference to modern shelf and sediment studies combined with reliable studies of ancient sediments. Deep ocean current activity is eliminated on the basis of estimated depth of deposition as judged from cross-section gradients and ichnological evidence.

The sediment in these storm-enhanced tidally dominated sediments is distributed in subparallel, broad flat and somewhat ragged sheet sands. The thicker accumulations of coarser sediment occur closest to the likely transgressed source of material and are on the order of only a few metres thick. Accumulations finger out away from the source and into the basin and become thinner. There is no apparent lateral relationship between facies on the scale of the core sampling although more proximal successions may be more predictable in their vertical successions.

The vertical succession of sediment characterizing these sheet sands is generally one of gradual coarsening upward, occasionally with the very coarsest material occurring a few metres below the uppermost part of the succession, which is marked by a relatively sudden lithological change to muddier sediment. The facies typically contain diagenetic indications of slow sedimentation such as phosphatic and particularly glauconitic accumulations and alteration. The facies

in the lower reaches of the succession are mottled silts and bioturbated sands; these are overlain by a variety of crossbedded sands, predominantly tangentially crossbedded. The crossbedding shows tendencies to evolve into a lower angle upwards. The more proximal the facies succession is to the shoreline the more preferred are the apparent vertical transitions and the closer they appear to this general summary. More distal succession, while having similar facies components may have less preferred vertical transitions.

8.4.2 Distal Storm/Wave Dominated Successions

Only unit Beta contains a storm/wave dominated facies package. The facies are dominated by distal, outer to inner shelf units that build up a package with a moderate aggradational component. The facies show some lateral equivalence but no predictable lateral relationships. The vertical successions of the distal storm dominated sediments appear to show greater preferred relationships compared to those of the tidally dominated packages. The vertical succession are quite characteristic of previously storm/wave dominated packages with grey mudstone being succeeded by laminated silts which in turn are followed by thicker bedded siltstones with low angle intersecting cross-laminae. There is frequent bioturbation of the *Cruziana* ichnofacies.

8.5 General Conclusion

The general conclusion is that the coarse sediments of the Viking Formation in the eastern portion of the Alberta basin predominantly represent tidally dominated sheet sands that were transgressively reworked across the basin floor. Reworking of these sediments created coarsening upwards successions whose upper portions were transgressive. Distal facies successions may be

comparatively more random in the tidally dominated systems than in comparable settings in storm dominated settings. Geometry of the units themselves probably shows a pronounced tectonic overprint indicative of syndepositional foreland basin warping.

REFERENCES

Allen, J.R.L. and Narayan, J., 1964, Cross-Stratified Units, Some with Silt Bands, in the Folkestone Beds (Lower Greensand) of Southeast England, Geol. en Minj., V. 43, pp. 451-461.

Amajor, L.C., 1980, Chronostratigraphy, Depositional Patterns and Environmental Analysis of Subsurface Lower Cretaceous (Albian) Viking Reservoir Sandstones in Central Alberta and Part of Southern Saskatchewan, Ph.D. Thesis, University of Alberta, Dept. of Geol., 602pp.

Amajor, L.C. and Lerbekmo, J.F., 1980, Subsurface Correlation of Bentonite Beds in the Lower Cretaceous Viking Formation of South-Central Alberta, Bull. Can. Petrol. Geol., V. 28, pp. 149-172.

Amieux, P., 1982, La Cathodoluminescence: Methode d'Etude Sedimentologique des Carbonates, Bull. Centres Rech. Expl. Prod. Elf. Aq., V. 6., pp. 437-483.

Arnott, R.W. and Southard, J.B., 1990, Exploratory Flow-Duct Experiments on Combined-Flow Bed Configurations and Some Implications for Interpreting Storm-Event Stratification, J. Sed. Pet., V.60, pp. 211-219.

Ashley, G.M. and SEPM Bedforms and Bedding Structures Panel, 1990, Classification of Large-Scale Subaqueous Bedforms: a New Look at an Old Problem, J. Sed. Pet., V. 60, pp. 160-172.

Baldwin, B. and Butler, C., 1985, Compaction Curves, AAPG Bull., V. 69, pp. 622-626.

Bally, A.W., Gordy, P.L. and Stewart, G.A., 1966, Structure , Seismic Data, and Orogenic Evolution of the Southern Canadian Rocky Mountains, Bull. of Can. Petrol. Geol., V. 14, pp. 337-381.

Barrie, J.V. and Bornhold, B.D., 1989, Surficial Geology of Hecate Strait, British Columbia Continental Shelf, Can. J. Ear. Sci., V. 26, pp. 1241-1254.

Bartlett, J.J., 1987, An Analysis of Sequence Boundaries of the Event Stratigraphy of the Cardium Formation, Alberta, MSc. Thesis, McMaster University, 185 pp.

Basu A., Young, S.W., Suttner, L.J., James, W.C. and Mack, G.H., 1975, Re-Evaluation of the Use of Undulatory Extinction and Polycrystallinity in Detrital Quartz for Provenance Interpretation, Jour. of Sed. Pet., V. 45, pp. 873-882.

Beach, F.K., 1961, Viking Deposition, Discussion, J. Alta Soc. Petrol. Geol., V. 9, pp. 352-355.

Beach, F.K., 1955, Cardium a Turbidity Current Deposit, J. Alta Soc. Petrol. Geol., V. 3, pp. 123-125.

Beaumont, E.A., 1984, "Retrogradational Shelf Sedimentation: Lower Cretaceous Viking Formation, Central Alberta" in Siliciclastic Shelf Sediments, SEPM Spec. Pub. 34, Tillman, R.W. and Siemers, C.T., eds., Tulsa, OK, pp. 163-178.

Belderson, R.H., 1987, "Offshore Tidal and Non-Tidal Sand Ridges and Sand Sheets: Differences in Morphology and Hydrodynamic Setting" in Shelf Sands and Sandstones, C.S.P.G. Memoir 11, Knight, R.J. and McLean, J.R., eds., pp. 293-302.

Belderson, R.H. and Stride, A.H., 1966, Tidal Current Fashioning of a Basal Bed, Mar. Geol., V. 4, pp. 237-257.

Bell, D.L. and Goodell, H.G., 1967, A Comparative Study of Glauconite and the Associated Clay Fraction in Modern Marine Sediments, Sed., V. 9, pp. 169-202.

Bergman, K.M. and Walker, R.G., 1987, The Importance of Sea Level Fluctuations in the Formation of Linear Conglomerate Bodies: Carrot Creek Member, Cretaceous Western Interior Seaway, Alberta, Canada, J. Sed. Pet., V. 57, pp. 651-665.

Bergman, K.M. and Walker, R.G., 1986, "Cardium Formation 9. Conglomerates at Carrot Creek Field: Offshore Linear Ridges or Shoreface Deposits?" in Modern and Ancient Shelf Clastics, Moslow, T.F. and Rhodes, E.G., eds., SEPM Core Workshop No. 9, Tulsa, OK, pp.217-268.

Bice, D.C., 1985, Quaternary Volcanic Stratigraphy of Managua, Nicaragua: Correlation and Source Assignment for Multiple Overlapping Plinian Deposits, G.S.A. Bull., V. 96, pp 553-566.

Blatt, H., 1967a, Original Characteristics of Clastic Quartz Grains, Jour. of Sed. Pet., V.37, pp.401-424.

Blatt, H., 1967b, Provenance Determinations and Recycling of Sediments, Jour. of Sed. Pet., V.37, pp.1031-1044.

Blatt, H., Middleton, G.V. and Murray, R.C., 1980, Origin of Sedimentary Rocks, Prentice-Hall, 2nd ed., 634pp.

Blatt, H. and Christie, J.M., 1963, Undulatory Extinction in Quartz of Igneous and Metamorphic Rocks and Its Significance in Provenance Studies of Sedimentary Rocks, Jour. of Sed. Pet., V. 33, pp. 559-579.

Bluck, B.J., 1967, Sedimentation of Beach Gravels: Examples from South Wales, Jour. of Sed. Pet., V.37, pp. 128-156.

Boethling, F.C.Jr., 1977a, Increase in Gas Prices Rekindles Viking-Sandstone Interest, Oil and Gas Jour., Mar. 21, pp. 196-200.

Boethling, F.C.Jr., 1977b, Typical Viking Sequence: a Marine Sand Enclosed with Marine Shales, Oil and Gas Jour., Mar. 28, pp. 173-176.

Boggs, S., Jr., 1968, Experimental Study of Rock Fragments, Jour. of Sed. Pet., V. 38, pp. 1326-1339.

Boguchwal, L.A. and Southard, J.B., 1990, Bed Configurations in Steady Unidirectional Water Flows. Part 1. Scale Model Study Using Fine Sands, J. Sed. Pet., V. 60, pp. 649-657.

Borchardt, G.A., Aruscavage, P.J. and Millard, H.T.Jr., 1972, Correlation of the Bishop Ash, A Pliestocene Marker Bed, Using Instrumental Neutron Activation Analysis, J. Sed. Pet., V. 42, pp. 301-306.

Boreen, T.D., 1990, Sedimentology, Stratigraphy and Depositional History of the Lower Cretaceous Viking Formation at Willesden Green, Alberta, MSc. Thesis, McMaster University, Geol. Dept., 190 pp.

Brenchley, P.J., 1985, Storm Influenced Sandstone Beds, Mod. Geol., V. 9, pp. 369-396.

Brenchley, P.J., Romano, M. and Gutierrez-Marco, J.C., 1986, "Proximal and Distal Hummocky Cross-Stratified Facies on a Wide Ordovician Shelf in Iberia" in Shelf Sands and Sandstones CSPG Memoir 11, McKnight, R.J. and McClean, J.R., eds., Calgary, pp. 241-256.

Brenner, R.L., 1978, Sussex Sandstone of Wyoming -Example of Cretaceous Offshore Sedimentation, AAPG Bull., V. 62, pp. 1223-1244.

Brenner, R.L. and Davies, D.K., 1974, Oxfordian Sedimentation in Western Interior United States, AAPG Bull., V. 58, pp. 407-428.

Brown, R.L., Journeay, J.M., Lane, L.S., Murphy, D.C. and Rees, C.J., 1986, Obduction, Backfolding and Piggyback Thrusting in the Metamorphic Hinterland of the Southeastern Canadian Cordillera, J. of Structural Geol., V. 8, pp. 255-268.

Burnett, W.C., 1980, Apatite-Glauconite Associations off Peru and Chile: Paleo-Oceanographic Implications, Quart. J. Geol. Soc. London, V. 137, pp. 757-764.

Caldwell, W.G.E., North, B.R., Stelck, C.R. and Wall, J.H., 1978, "A Foraminiferal Zonal Scheme for the Cretaceous System in the Interior Plains of Canada" in Western and Arctic Canadian Biostratigraphy, Stelck C.R. and Chatterton, B.D.E., eds., G.A.C. Spec. Pap. 18, pp. 493-575.

Carr, T.R., 1982, Log-Linear Models, Markov Chains and Cyclic Sedimentation, J. Sed. Pet., V.52., pp. 905-912.

Chamberlain, V.E. and Lambert, R. St J., 1985, Cordillera, a Newly Defined Canadian Microcontinent, Nature, V. 314, April, pp. 707-713.

Chan, Marjorie, A., 1992, Oolitic Ironstone of the Cretaceous Western Interior Seaway, East-Central Utah, J. Sed. Pet., V. 62, pp. 693-705.

Clifton, H.E., 1973, Pebble Segregation and Bed Lenticularity in Wave-Worked versus Alluvial Gravel, Sed., V. 20, pp. 173-187.

Clifton, H.E., Hunter, R.E. and Phillips, R.L., 1971, Depositional Structures and Processes in the Non-Barred, High-Energy Nearshore, J. Sed. Pet., V. 41, pp. 651-670.

Coney, P.J., Jones, D.L. and Monger, J.W.H., 1980, Cordilleran Suspect Terranes, Nature, V. 288, November, pp. 329-333.

Conolly, J.R., 1965, The Occurrence of Polycrystallinity and Undulatory Extinction in Quartz in Sandstones, Jour. of Sed. Pet., V.35, pp.116-135.

Cross, T.A., ed., 1990, Quantitative Dynamic Stratigraphy, Prentice Hall, New Jersey.

Csanady, G.T., 1982, Circulation in the Coastal Ocean, Boston, Reidel, 280 pp.

Davidson-Arnott, R.G.D. and Greenwood, B., 1976, "Facies Relationships in a Barred Coast, Kouchibouguac Bay, New Brunswick, Canada" in Beach and Nearshore Sedimentation SEPM Special Publication 24, Davis, R.J. Jr., ed., Tulsa, OK, pp. 149-168.

Davies, D.K., Ethridge, F.G. and Berg, R.R., 1971, Recognition of Barrier Environments, AAPG Bull., V. 55, pp. 550-565.

Davies, S.D., 1990, The Sedimentology, Stratigraphy and Depositional History of the Lower Cretaceous Viking Formation at Caroline and Garrington, Alberta, Canada, MSc. Thesis, McMaster University, Geol. Dept., 207pp.

Davis, G.A., Monger, J.W.H., and Burchfiel, B.C., 1978, "Mesozoic Construction of the Cordilleran "Collage", Central British Columbia to Central California" in Pacific Coast Paleogeography Symposium 2: Mesozoic Paleogeography of the Western United States, D.G. Howell and K.A. McDougall, eds., pp. 1-32.

Davis, J.C., 1986, Statistics and Data Analysis in Geology, 2nd edition, John Wiley and Sons, Toronto, pp.646.

Davis, R.A., Jr. (ed.), 1987, Beach and Nearshore Sediments and Processes, SEPM Reprint Series Number 12, pp. 1-222.

Davis, R.A., Jr., Fox, W.T., Hayes, M.O. and Boothroyd, J.C., 1972, Comparison of Ridge and Runnel Systems in Tidal and Non-Tidal Environments, J. Sed. Pet., v.42, pp.413-421.

Decker, J. and Helmold, K.P., 1985, The Effect of Grain Size on Detrital Modes: a Test of the Gazzi-Dickinson Point-Counting Method - Discussion, Jour. of Sed. Pet., V.55, pp.618-619.

Deitz, R.S., 1963, Wave Base, Marine Profile of Equilibrium and Wave-Built Terraces - a Critical Appraisal, Bull. G.S.A., V. 74, pp. 971-990.

deRaaf, J.F.M., Boersma, J.R. and van Gelder, A., 1977, Wave-Generated Structures and Sequences from a Shallow Marine Succession, Lower Carboniferous, County Cork, Ireland, Sed., V. 24, pp. 451-483.

DeWiel, J.E.F., 1956, Viking and Cardium not Turbidity Current Deposits, J. Alta Soc. Petrol. Geol., V.4, pp. 173-177.

Dickinson, W.R., 1974, "Plate Tectonics and Sedimentation" in Tectonics and Sedimentation S.E.P.M. Spec. Pub. No. 22, W.R. Dickinson, ed., pp. 1-27.

Dickinson, W.R., 1970, Interpreting Detrital Modes of Graywacke and Arkose, Jour. of Sed. Pet., V.40, pp695-707.

Dickinson, W.R., Beard, L.S., Brakenridge, G.R., Erjavec, J.L., Ferguson, R.C., Inman, K.F., Knepp, R.A., Lindberg, F.A and Ryberg, P.T., 1983, Provenance of North American Phanerozoic Sandstones in Relation to Tectonic Setting, Geol. Soc. of Am. Bull., V.94, pp. 222-235.

Dickinson, W.R. and Suczek, C.A., 1979, Plate Tectonics and Sandstone Composition, AAPG Bull., V.63, pp. 2164-2182.

Dickinson, W.R. and Rich, E.I., 1972, Petrologic Intervals and Petrofacies in the Great Valley Sequence, Sacramento Valley, California, Geol. Soc. Am. Bull., V. 83, pp. 3007-3024.

Donovan, D.T. and Stride, A.H., 1961, Erosion of a Rock Floor by Tidal Sand Streams, Geol. Mag., V. 98, pp. 393-398.

Downing, K.P. and Walker, R.G., 1988, Viking Formation, Joffre Field, Alberta: Shoreface Origin of Long Narrow Sand Body Encased in Marine Mudstones, AAPG Bull., V. 72, pp. 1212-1228.

Duke, W.L., 1990, Geostrophic Circulation or Shallow Marine Turbidity Currents? the Dilemma of Paleoflow Patterns in Storm-Influenced Prograding Shoreline Systems, J. Sed. Pet., V. 60. pp. 870-883.

Dupre, W.R., 1984, Reconstruction of Paleo-Wave Conditions during the Late Pliestocene from Marine Terrace Deposits, Monterey Bay, Calif., Mar. Geol., V.60, pp. 435-454.

Dzevanshir, R.D., Buryakovskiy, L.A. and Chilingarian, G.V., 1986, Simple Quantitative Evaluation of Porosity of Argillaceous Sediments at Various Depths of Burial, Sed. Geol., V. 46, pp. 169-175.

Ericksen, M.C. and Slingerland, R., 1990, Numerical Simulations of Tidal and Wind-Driven Circulation in the Cretaceous Interior Seaway of North America, Bull. Geol. Soc. Am., V. 102, pp. 1499-1516.

Eslinger, E. and Pevear, D., 1988, Clay Minerals for Petroleum Geologists and Engineers, SEPM Short Course Notes No. 22., Tulsa OK.

Ethridge, F.G., 1977, Petrology, Transport, and Environment in Isochronous Upper Devonian Sandstone and Siltstone Units, New York, Jour. of Sed. Pet., V.47, pp. 53-65.

Evans, W.E., 1970, Imbricate Linear Sandstone Bodies of Viking Formation in Dodsland-Hoosier Area of Southwestern Saskatchewan, Canada, AAPG Bull., V. 54, pp. 469-486.

Foscolos, A.E., Reinson, G.E. and Powell, T.G., Controls on Clay-Mineral Authigenesis in the Viking Sandstone, Central Alberta. I. Shallow Depths, Can. Min., V. 20, pp. 141-150.

Frey, R.W. and Pemberton, S.G., 1984, "Trace Fossil Facies Models" in Facies Models, 2nd ed., Walker, R.G., ed., GAC, Toronto, pp. 189-207

Galehouse, J.S., 1971, "Point Counting" in Procedures in Sedimentary Petrology, R.E. Carver ed., Wiley Interscience, New York, pp.385-408.

Galloway, W.E., 1989a, Genetic Stratigraphic Sequences in Basin Analysis I: Architecture and Genesis of Flooding-Surface Bounded Depositional Units, AAPG Bull., V. 73, pp. 125-142.

Galloway, W.E., 1989b, Genetic Stratigraphic Sequences in Basin Analysis II: Application to the Northwest Gulf of Mexico Cenozoic Basin, AAPG Bull., V. 73, pp. 143-154.

Gammel, H.G., 1955, The Viking Member in Central Alberta, J. Alta Soc. of Petrol. Geol., V.3, pp. 63-69.

Giresse, P. and Odin, G.S., 1973, Nature Mineralogique et Origine des Glauconies du Plateau Continental du Gabon et du Congo, Sed., V. 20, pp. 457-488.

Glaister, R.P., 1959, Lower Cretaceous of Southern Alberta and Adjoining Areas, Bull. A.A.P.G., V. 43, pp. 590-640.

Graham, S.A, Ingersoll, R.V. and Dickinson, W.R., 1976, Common Provenance for Lithic Grains in Carboniferous Sandstones from Ouachita Mountains and Black Warrior Basin, Jour. of Sed. Pet., V.46, pp.620-632.

Gray, D.I. and Benton, M.J., 1982, "Multidirectional Paleocurrents as Indicators of Shelf Storm Beds" in Cyclic and Event Stratification, Einsele, G. and Seilacher, A., eds., pp. 350-353.

Griffiths, J.C., 1967, Scientific Methods in Analysis of Sediments, McGraw Hill, Toronto, pp.175-199.

Griffiths, J.C. and Rosenfeld, M.A., 1954, Operator Variation in Experimental Research, Jour. of Geol., V.62, pp. 74-91.

Grundy, W.D. and Miesch, A.T., 1987, Brief Descriptions of STATPAC and Related Statistical Programs for the IBM Personal Computer, U.S.G.S Open File Report 87-411-A, 35pp.

Hamblin, A.P. and Walker, R.G., 1979, Storm-Dominated Shallow Marine Deposits: the Fernie-Kootenay Transition, Southern Rocky Mountains, Can. J. Earth Sci., V.16, 1673-1690.

Hantzschell, W., 1975, "Trace Fossils and Problematica" in Treatise on Invertebrate Paleontology, Part W, Miscellanea, Supplement 1, Teichert, C., ed., Univ. of Kansas Press and Geological Society of America, pp. 269.

Haq, B.U., Hardenbol, J. and Vail, P.R., 1988, "Mesozoic and Cenozoic Chronostratigraphy and Eustatic Cycles" in Sea Level Changes: an Integrated Approach SEPM Special Publication 42, Wilgus, C.K., Hastings, B.S., Kendall, C.G.St.C, Posamentier, H.W., Ross, C.A and Van Wagoner, J.C., eds., Tulsa, OK, pp. 71-108.

Haq, B.U., Hardenbol, J. and Vail, P.R., 1987, Chronology of Fluctuating Sea Levels Since the Triassic, Science, V.235, pp. 1156-1167.

Harms, J.C., Southard, J.B. and Walker, R.G., 1982, Structures and Sequences in Clastic Rocks, SEPM Short Course No. 9., Tulsa, OK.

Harper, C.W.Jr., 1984, "Improved Methods of Facies Sequence Analysis" in Facies Models, 2nd edition, Walker, R.G., ed., G.A.C., pp. 11-13.

Harrell, J. and Blatt, H., 1978, Polycrystallinity: Effect on the Durability of Detrital Quartz, Jour. of Sed. Pet., V. 48, pp. 25-30.

Hayes, J.R., 1962, Quartz and Feldspar Content in South Platte, Platte and Missouri River Sands, Jour. of Sed. Pet., V.32, pp. 793-800.

Hein, F.J., Dean, M.E., DeIure, A.M., Grant, S.K., Robb, G.A. and Longstaffe, F.J., 1986, The Viking Formation in the Caroline, Garrington and Harmattan East Fields, Western South-Central Alberta: Sedimentology and Paleogeography, Bull. Can. Petrol. Geol., V. 34, pp. 91-110.

Heinberg, C. and Birkelund, T., 1984, Trace-Fossil Assemblages and Basin Evolution of the Vardekloft Formation (Middle Jurassic, Central East Greenland), J. Palcont., V. 58, pp 362-397.

Hobday, D.K. and Reading, H.G., 1972, Fairweather versus Storm processes in Shallow Marine Sandbar Sequences in the Late PreCambrian of Finnmark, North Norway, J. Sed. Pet., V.42, pp. 318-324.

Houbolt, J.J.H.C., 1968, Recent Sediments in the Southern Bight of the North Sea, Geol. en Minj., V. 47, pp. 245-273.

Houghton, H.F., 1980, Refined Techniques for Staining Plagioclase and Alkali Feldspars in Thin Section, Jour. of Sed. Pet., V.50, pp.629-631.

Hughes, A.D. and Whitehead, D., 1987, Glauconitization of Detrital Silica Substrates in the Barton Formation (upper Eocene) of the Hampshire Basin, southern England, Sed., V.34, pp. 825-835.

Ingersoll, R.V., 1978, Petrofacies and Petrologic Evolution of the Late Cretaceous Fore-Arc Basin, Northern and Central California, Jour. of Geol., V.86, pp. 335-352.

Ingersoll, R.V., Bullard, T.F., Ford, R.L. and Pickle, J.D., 1985a, The Effect of Grain Size on Detrital Modes: a Test of the Gazzi-Dickinson Point-Counting Method-Reply to Discussion of Lee J. Suttner and Abhijit Basu, Jour. of Sed. Pet., V.55, pp.617-618.

Ingersoll, R.V., Bullard, T.F., Ford, R.L. and Pickle, J.D., 1985a, The Effect of Grain Size on Detrital Modes: a Test of the Gazzi-Dickinson Point-Counting Method-Reply to Discussion of John Decker and Kenneth P. Helmold, Jour. of Sed. Pet., V.55, pp.620-621.

Ingersoll, R.V., Bullard, T.F., Ford, R.L., Grimm, J.P., Pickle, J.D. and Sares, S.W., 1984, The Effect of Grain Size on Detrital Modes: a Test of the Gazzi-Dickinson Point-Counting Method, Jour. of Sed. Pet., V. 54, pp.103-116.

Jervey, M.T., 1988, "Quantitative Geological Modeling of Siliciclastic Rock Sequences and Their Seismic Expression" in Sea Level Changes: an Integrated Approach Wigus, C.K., Hastings, B.S., Kendall, C.G.St.C, Posamentier, H.W. Ross, C.A. and Van Wagoner, J.C., eds., SEPM Spec. Pub. 42, Tulsa, OK, pp.47-70.

Johnson, H.D. and Baldwin, C.T., 1986, "Shallow Siliciclastic Seas" in Sedimentary Environments and Facies, Reading, H.G., ed., Blackwell Scientific, Palo Alto, pp. 229-282.

Jordon, T.E., 1981, Thrust Loads and Foreland Basin Evolution, Cretaceous Western United States, AAPG Bull., V. 65, pp. 2506-2520.
Joreskog, K.G., Klovan, J.E. and Reyment, R.A., 1976, Geological Factor Analysis, Methods in Geomathematics 1, Elsevier Pub. Co., New York, pp.178.

Jones, D.L., Silberling, N.J. and Hillhouse, J.W., 1978, "Microplate Tectonics of Alaska- Significance for the Mesozoic History of the Pacific Coast of North America" in Pacific Coast Paleogeography Symposium 2: Mesozoic Paleogeography of the Western United States, D.G. Howell and K.A. McDougall, eds., pp. 71-74.

Jones, H.L., 1961, Viking Deposition in Southwestern Saskatchewan with a Note on the Source of the Sediments, J. Alta Soc. Petrol. Geol., V. 9, pp. 231-244.

Journel, A.G. and Huijbregts, C., 1978, Mining Geostatistics, Academic Press, London, 600pp.

Kachel, N.B. and Smith, J.D., 1986, "Geological Impact of Sediment Transporting Events on the Washington Continental Shelf" in Shelf Sands and Sandstones, CSPG Memoir 11, Knight, R.J. and McLean, J.R., eds., pp. 145-162.

Kauffman, E.G., 1977, Geological and Biological Overview: Western Interior Cretaceous Basin, Mount. Geol., V. 14, pp. 75-99.

Kendall, C.G.St.C and Lerche, I., 1988, "The Rise and Fall of Eustacy" in Sea Level Changes: an Integrated Approach Wigus, C.K., Hastings, B.S., Kendall, C.G.St.C, Posamentier, H.W. Ross, C.A. and Van Wagoner, J.C., eds., SEPM Spec. Pub. 42, Tulsa, OK, pp. 3-18.

Kenyon, N.H., 1970a, Sand Ribbons of European Tidal Seas, Mar. Geol., V. 9, pp. 25-39.

Kenyon, N.H., 1970b, The Origin of Some Transverse Sand Patches in the Celtic Sea, Geol. Mag., V. 107, pp. 389-394.

Kenyon, N.H. and Stride, A.H., 1970, The Tide-Swept Continental Shelf Sediments between the Shetland Islands and France, Sed., V. 14, pp. 159-173.

Kinsman, B., 1984, Wind Waves, Their Generation and Propagation on the Ocean Surface, Dover Publications, Inc., N.Y., 676pp.

Klein, G.dV. and Ryer, T.A., 1978, Tidal Circulation Patterns in Precambrian, Paleozoic and Cretaceous Epeiric and Mioclinal Shelf Seas, G.S.A.Bull., V. 89, pp. 1050-1058.

Koke, K.R. and Stelck, C.R., 1985, Foraminifera of a Joli Fou Shale Equivalent in the Lower Cretaceous (Albian) Hasler Formation, Northeastern British Columbia, Can. J. Earth Sci., V. 22, pp. 1299-1313.

Koldijk, W.S., 1976, "Gilby Viking `B' a Storm Deposit" in The Sedimentology of Selected Clastic Oil and Gas Reservoirs in Alberta, Lerand, M.M., ed., C.S.P.G., pp. 62-77.

Komar, P.D., Neudeck, R.H. and Kulm, L.D., 1972, "Observations and Significance of Deep-Water Oscillatory Ripple Marks on the Oregon Continental Shelf" in Shelf Sediment Transport, Process and Pattern, Swift, D.J.P., Duane, D.B. and Pilkey, O.H., eds., Dowden, Hutchinson and Ross, Strousburg, PA, pp. 601-619.

Kreisa, R.D. and Moiola, R.J., 1986, Sigmoidal Tidal Bundles and Other Tide-Generated Sedimentary Structures of the Curtis Formation, Utah, G.S.A.Bull., V. 97, pp. 381-387.

Kuenen, P.H. and Migliorini, C., 1950, Turbidity Currents as a Cause of Graded Bedding, J. Geol., V. 58, pp. 91-127.

Lambert, R. St J. and Chamberlain, V.E., 1988, Cordilleria Revisited, with a Three-Dimensional Model of Cretaceous Tectonics in North America, J. of Geology, V. 96, pp. 47-60.

Lawrence, D.T., Doyle, M. and Aigner, T., 1990, Statigraphic Simulation of Sedimentary Basins: Concepts and Calibration, AAPG Bull., V. 74, pp. 273-295.

Leckie, D.A., 1987, Late Albian Sea Level Fluctuations: Effects on the Viking and Boulder Creek Formations and Paddy/Cadotte Members, (abstr.), CSPG Reservoir, V.14, No. 10, pp. 1-2.

Leckie, D.A., 1986, Tidally Influenced, Transgressive Shelf Sediments in the Viking Formation, Caroline, Alberta, Bull. Can. Petrol. Geol., V. 34, pp. 111-125.

Leckie, D.A. and Reinson, G.E., in press, "Effects of Middle to Late Albian Sea Level Fluctuations in the Cretaceous Interior Seaway, Western Canada" in Evolution of the Western Interior Basin:, G.A.C. Spec. Paper.

Leckie, D.A. and Krystinik, I.F., 1989, Is There Evidence for Geostrophic Currents Preserved in the Sedimentary Record of Inner to Middle-Shelf Deposits?, J. Sed. Pet., V.59, pp. 862-870.

Lerand, M.M. and Thompson, D.K., 1976, "Provost Lake -Hamilton Field Pool" in Joint Convention on Enhanced Recovery, Core Conference, Calgary, Alberta, Clack, W.J.F. and Huff, G. eds., CSPG-Petrol. Soc. Can. Instit. of Mining. pp. B1-B34.

Lewis, D.W., 1964, "Perigenic"; a New Term, Jour. of Sed. Pet., V. 34, pp. 875-890.

Lin, Cunshan and Harbaugh, J.W., 1988, Graphic Display of Two and Three Dimensional Markov Computer Models in Geology, Van Nostrand Reinhold, Co., NY., 180 pp.

Lindholm, R.C. and Finkelman, R.B., 1972, Calcite Staining: Semiquantitative Determination of Ferrous Iron, Jour. of Sed. Pet., V.42, pp.239-242.

Longstaffe, F.J. and Ayalan, A., 1987, "Oxygen Isotope Studies of Clastic Diagenesis in the Lower Cretaceous Viking Formation, Alberta: Implications for the Role of Meteoric Water" in Diagenesis of Sedimentary Sequences, G.S.C. Spec. Pub. 36, pp. 277-296.

Luternauer, J.L., 1986, "Character and Setting of Sand and Gravel Bed Forms on the Open Continental Shelf off Western Canada" in Shelf Sands and Sandstones CSPG Memoir 11, Knight, R.J. and McClean, J.R., eds., pp. 45-56.

MacEachern, J.A., Bechtel, D.J. and Pemberton, S.G., 1992, "Ichnology and Sedimentology of Transgressive Deposits, Transgressively-Related Deposits and Transgressive Systems Tracts in the Viking Formation of Alberta" in Applications of Ichnology to Petroleum Exploration A Core Workshop, SEPM Core Workshop No. 17, pp. 251-290.

Mack, G.H., 1978, The Survivability of Labile Light-Mineral Grains in Fluvial, Aeolian and Littoral Marine Environments: the Permian Cutler and Cedar Mesa Formations, Moab, Utah, Sed., V. 25, pp. 587-604.

Mack, G.H., 1984, Exceptions to the Relationship Between Plate Tectonics and Sandstone Composition, Jour. of Sed. Pet., V.54, pp. 212-220.

Magara, Kinji, 1980, Comparison of Porosity-Depth Relationships of Shale and Sandstone, J. Petrol. Geol., V. 3, pp. 175-185.

Mann, R.G., Swift, D.J.P. and Perry, R., 1981, Size Classes of Flow-Transverse Bedforms in a Subtidal Environment, Nantucket Shoals, North American Atlantic Shelf, Geo. Mar. Let., V. 1, pp. 39-43.

Matthews, R.K., 1984, "Oxygen-Isotope Record of Ice-Volume History: 100 Million Years of Glacio-Eustatic Sea-Level Fluctuations" in Interregional Unconformities and Hydrocarbon Accumulation, AAPG Memoir 36, Schlee, J.S., ed., pp. 97-107.

McCave, I.N., 1984, "Erosion, Transport and Deposition of Fine-Grained Marine Sediments" in Fine Grained Sediments: Deep-Water Processes and Facies, Spec. Pub. Geol. Soc. London, No. 15, Stow, D.A.V. and Piper, D.J.W., eds., pp. 35-69.

McCave, I.N., 1971, Sand Waves in the North Sea off the Coast of Holland, Mar. Geol., V. 10, pp. 199-225.

McConchie, D.M. and Lewis, D.W., 1978, Authigenic, Perigenic and Allogenic Glauconites from the Castle Hill Basin, North Canterbury, New Zealand, New Zealand Jour. of Geol., V. 21, pp. 199-214.

McCrory, V.L.C. and Walker, R.G., 1986, A Storm and Tidally Influenced Prograding Shoreline - Upper Cretaceous Milk River Formation of Southern Alberta, Sed., V. 33, pp. 47-60.

McKnight, R.J. and McClean, J.R., eds., 1986, Shelf Sands and Sandstones, CSPG Memoir 11, Calgary, 347 pp.

Miesch, A.T., 1976, Interactive Computer Programs for Petrologic Modeling with Extended Q-Mode Factor Analysis, Comp. and Geosci., V. 2, pp. 439-492.

Minnis, M., 1984, An Automatic Point-Counting Method for Mineral Assessment, AAPG Bull., V.68, pp. 744-752.

Misko, R.M. and Hendry, H.E., 1979, The Petrology of Sands in the Uppermost Cretaceous and Palaeocene of Southern Saskatchewan: a Study of Composition Influenced by Grain Size, Source Area and Tectonics, Can. Jour. of Ear. Sci., V.16, pp. 38-49.

Monger, J.W.H., 1977, Upper Paleozoic Rocks of the Western Canadian Cordillera and Their Bearing on Cordilleran Evolution, Can. J. Earth Sci., V.14, pp. 1832-1859.

Monger, J.W.H., Price, R.A. and Tempelman-Kluit, D.J., 1982, Tectonic Accretion and the Origin of the Two Major Metamorphic and Plutonic Welts in the Canadian Cordillera, Geology, V. 10, pp. 70-75.

Monger, J.W.H. and Price, R.A., 1979, Geodynamic Evolution of the Canadian Cordillera - Progress and Problems, Can. J. Earth Sci., V. 16, pp 770 791.

Monger, J.W.H., Tichards, T.A. and Paterson, I.A., 1978, The Hinterland Belt of the Canadian Cordillera: New Data from Northern and Central British Columbia, Can. J. Earth Sci., V. 15, pp. 823-830.

Moslow, T.F. and Rhodes, E.G.,eds., 1986, Modern and Ancient Shelf Clastics: a Core Workshop, SEPM Core Workshop No. 9, pp. 1-457.

Narayan, J., 1971, Sedimentary Structures in the Lower Greensand of the Weald, England and Bas-Boulonais, France, Sed. Geol., V. 6, pp. 73-109.

Newton, R.S., 1968, Internal Structure of Wave-Formed Ripple Marks in the Nearshore Zone, Sed., V.11, pp. 275-292.

North American Commission on Stratigraphic Nomenclature, 1983, North American Stratigraphic Code, AAPG Bull., V. 67, pp 841-875.

Odin, G.S., 1985, "Significance of Green Particles (Glaucony, Berthierine, Chlorite) in Arenites" in Provenance of Arenites, G.G. Zuffa ed., NATO

Advanced Sciences Institute Series, Series C: Vol. 148, D. Reidel Pub. Co., pp. 279-307.

Odin, G.S., 1972, Observations Nouvelles sur la Structure de la Glauconie en Accordeon ("Vermicular Pellets"); Description du Processus de Genese de ces Granules par Neoformation, Sed., V.19, pp. 285-294.

Odin, G.S. and Matter, A., 1981, De Glauconiarum Origine, Sed., V. 28, pp 611-641.

Odom, I.E., 1975, Feldspar-Grain Size Relations in Cambrian Arenites, Upper Mississippi Valley, Jour. of Sed. Pet., V. 45, pp. 636-650.

Odom, I.E., Doe, T.W. and Dott, R.H., 1976, Nature of Feldspar-Grain Size Relations in Some Quartz Rich Sandstones, Jour. of Sed. Pet., V. 46, pp. 862-870.

Off, T., 1963, Rythmic Linear Sand Bodies Caused by Tidal Currents, AAPG Bull., V. 47, pp. 324-341

Oliver, T.A., 1960, The Viking - Cadotte Relationship, J. Alberta Soc. of Petrol. Geol., V.8, pp. 247-253.

Parrish, J.T. and Barron, E.J., 1986, Paleoclimates and Economic Geology SEPM Short Course No. 18, Tulsa, OK, 162 pp.

Pattison, S.A.J., 1992, "Recognition and Interpretation of Estuarine Mudstones (Central Basin Mudstones) in the Tripartite Valley-Fill Deposits of the Viking Formation, Central Alberta" in Applications of Ichnology to Petroleum Exploration A Core Workshop, SEPM Core Workshop 17, pp. 223-250.

Pattison, S.A.J., 1990, Valley-Fill Sediments at Crystal and Viking Formation Allostratigraphy, Tech. Rep. 90-1, McMaster Univ. Dept. of Geol.

Payton, C.E., ed., 1977, Seismic Stratigraphy -Applications to Hydrocarbon Exploration, AAPG Memoir 26, Tulsa, OK.

Pemberton, S.G., MacEachern, J.A. and Frey, R.W., 1992, "Trace Fossil Facies Models: Environmental and Allostratigraphic Significance" in Facies Models, Response to Sea Level Change, R.G. Walker and N. James, eds., GAC, pp.47-72.

Phillips, R.L., 1984, "Depositional Features of Late Miocene, Marine Cross-Bedded Conglomerates, California" in Sedimentology of Gravels and Conglomerates CSPG Memoir 10, Koster, E.H. and Steel, R.H., eds., CSPG, Calgary, pp. 345-358.

Pitman, W.C.III, 1978, Relationship between Eustasy and Stratigraphic Sequences of Passive Margins, Bull. Geol. Soc. Am., V. 89, pp. 1389-1403.

Plint, A.G., 1988, "Sharp-Based Shoreface Sequences and 'Offshore Bars' in the Cardium Formation of Alberta: Their Relationships to Changes in Sea Level" in Sea Level Changes an Integrated Approach Wigus, C.K., Hastings, B.S., Kendall, C.G.St.C, Posamentier, H.W. Ross, C.A. and Van Wagoner, J.C., eds., SEPM Spec. Pub. 42, Tulsa, OK, pp.

Plint, A.G., Walker, R.G. and Bergman, K.M., 1987, Cardium Formation 6: Stratigraphic Framework of the Cardium in Subsurface: Reply, Bull. Can. Petrol. Geol., V.35, pp. 365-374.

Plint, A.G., Walker, R.G. and Bergman, K.M., 1986, Cardium Formation 6: Stratigraphic Framework of the Cardium in Subsurface, Bull. Can. Petrol. Geol., V.34, pp. 213-225.

Posamentier, H.W., Jervey, M.T. and Vail, P.R., 1988, "Eustatic Controls on Clastic Deposition II - Sequence and Systems Tract Models" in Sea Level Changes: an Integrated Approach Wigus, C.K., Hastings, B.S., Kendall, C.G.St.C, Posamentier, H.W. Ross, C.A. and Van Wagoner, J.C., eds., SEPM Spec. Pub. 42, Tulsa, OK, pp. 109-124.

Potter, P.E., 1986, South America and a Few Grains of Sand, Jour. of Geol., V. 94, pp. 301-319.

Potter, P.E., 1984, South African (sic) Modern Beach Sand and Plate Tectonics, Nature, V. 311, pp. 645-648.

Power, B.A., 1988a, Coarsening Upward Shoreface and Shelf Sequences: Examples from the Lower Cretaceous Viking Formation at Joarcam, Alberta, Canada" in Sequences, Stratigraphy, Sedimentology: Surface and Subsurface, C.S.P.G. Memoir 15, pp. 185-194.

Power, B.A., 1988b, Depositional Environments of the Lower Cretaceous (Albian) Viking Formation at Joarcam Field, Alberta, Canada, MSc. Thesis, McMaster University, Geol. Dept., 165pp.

Powers, D.W. and Easterling, R.G., 1982, Improved Methodology for Using Embedded Markov Chains to Describe Cyclical Sediments, J. Sed. Pet., V. 52, pp. 913-923.

Pozzobon, J.G., 1987, Sedimentology and Stratigraphy of the Viking Formation, Eureka Field, Southwestern Saskatchewan, MSc., McMaster University, Geol. Dept.

Pozzobon, J.G. and Walker, R.G., 1990, Viking Formation (Albian) at Eureka, Saskatchewan: a Transgressed and Degraded Shelf Sand Ridge, AAPG Bull., V. 74, pp. 1212-1227.

Price, R.A., 1986, The Southeastern Canadian Cordillera: Thrust Faulting, Tectonic Wedging, and Delamination of the Lithosphere, pp. 239-254.

Price, R.A., 1981, "The Cordilleran Foreland Thrust and Fold Belt in the Southern Canadian Rocky Mountains", in Thrust and Nappe Tectonics, Spec. Pub. of Geol. Soc. London, Price, N.J. and McClay, K., eds., 9, pp. 427-448.

Quinlan, G.M. and Beaumont, C., 1984, Appalachian Thrusting, Lithospheric Flexure and the Paleozoic Stratigraphy of the Eastern Interior of North America, Can. J. Earth Sci., V.21, pp. 973-996.

Raddysh, H.K, 1988, "Sedimentology and `Geometry' of the Lower Cretaceous Viking Formation, Gilby A and B Fields, Alberta" in Sequences, Stratigraphy Sedimentology: Surface and Subsurface, James, D.P. and Leckie, D.A., eds., CSPG Memoir 15, pp. 417-430.

Raychaudhuri, I., Brekke, H.G., Pemberton, S.G. and MacEachern, J.A., 1992, "Depositional Facies and Trace Fossils of a Low Wave Energy Shoreface Succession, Albian Viking Formation, Chigwell Field, Alberta, Canada, in Applications of Ichnology to Petroleum Exploration A Core Workshop, SEPM Core Workshop 17, pp. 291-318.

Reineck, H.E. and Wunderlich, F., 1968, Classification and Origin of Flaser and Lenticular Bedding, Sed., V. 11, 1968, pp. 99-104.

Reinson, G.E., 1983, Facies Analysis and Reservoir Geometry of the Crystal Viking Field, Tp. 45 and 46, Rg. 3 and 4W5 Central Alberta, G.S.C. Open File Rep. 1193, 168pp.

Reinson, G.E. and Foscolos, A.E., 1986, Trends in Sandstone Diagenesis with Burial, Viking Formation, Southern Alberta, Bull. Can. Pet. Geol., V. 34, pp. 126-152.

Reinson, G.E., Clark, J.E. and Foscolos, A.E., 1988, Reservoir Geology of Crystal Viking Field, Lower Cretaceous Estuarine Tidal Channel-Bay Complex, South-Central Alberta, AAPG Bull., V. 72, pp. 1270-1294.

Reinson, G.E., Foscolos, A.E. and Powell, T.G., 1983, "Comparison of Viking Sandstone Sequences, Joffre and Caroline Fields" in Sedimentology of Selected Mesozoic Clastic Sequences, McLean, J.R. and Reinson, G.E., eds., CSPG Corexpo '83, pp. 101-118.

Riddihough, R.P., 1982, One Hundred Million Years of Plate Tectonics in Western Canada, Geoscience Canada, V.9, pp.28-34.

Rine, J.M., Tillman, R.W., Stubblefield, W.L. and Swift, D.J.P., 1986, "Lithostratigraphy of Holocene Sand Ridges from the Nearshore and Middle Continental Shelf of New Jersey, U.S.A., in Modern and Ancient Shelf Clastics: a Core Workshop, SEPM Core Workshop No.9, Moslow, T.F. and Rhodes, E.G., eds., pp. 1-72.

Rubin, D.M., 1987, Cross-bedding, Bedforms, and Paleocurrents, SEPM Concepts in Sedimentology and Paleontology, V.1., Tulsa, OK, 187 pp.

Ryer, T.A., 1987, Stratigraphy, Sedimentology and Paleoenvironments of the Viking Formation, Southern Alberta (abstr.), CSPG Reservoir, V. 14, No. 6, pp. 1-2.

Schwab, F.L., 1986, "Sedimentary Signatures of Foreland Basin Assemblages: Real or Counterfeit?" in Foreland Basins, Special Publication of the International Association of Sedimentologists, No 8, pp. 395-410.

Seeling, A., 1978, The Shannon Sandstone, a Further Look at the Environment of Deposition at Heldt Draw Field, Wyoming, Mountain Geologist, V. 15, pp. 133-144.

Sharp, W.E., 1987, Two Basic Rules for Valid Contouring, Geobyte, V. 3, November, pp. 11-15.

Sherman, D.J. and Greenwood, B, 1984, Boundary Roughness and Bedforms in the Surf Zone, Mar. Geol., V.60, pp. 198-218.

Shipp, R.C., 1984, Bedforms and Depositional Sedimentary Structures of a Barred Nearshore System, Eastern Long Island, New York, Mar. Geol., V. 60, pp. 235-259.

Short, A.D., 1984, Beach and Nearshore Facies: Southeastern Australia, Mar. Geol., V. 60, pp. 261-282.

Simpson, F., 1975, "Marine Lithofacies and Biofacies of the Colourado Group (Middle Albian to Santonian) in Saskatchewan" in The Cretaceous System of Western Interior North America, Caldwell, W.G.E., ed., G.A.C. Spec. Paper Number 13, pp. 553-587.

Slater, R.D., 1985, A Numerical Model of Tides in the Cretaceous Seaway of North America, J. Geol., V. 93, pp. 333-345.

Sloss, L.L., 1963, Sequences in the Cratonic Interior of North America, G.S.A. Bull., V.89, pp. 1389-1403.

Smith, J.V. and Stenstrom, R.C., 1965, Electron-Excited Luminescence as a Petrologic Tool, Jour. of Geol., V.73, pp. 627-635.

Stelck, C.R., 1958, Stratigraphic Position of the Viking Sand, J. Alta. Soc. Petrol. Geol., V. 6, pp. 2-7.

Stelck, C.R. and Koke, K.R., 1987, Foraminiferal Zonation of the Viking Interval in the Hasler Shale (Albian), Northeastern British Columbia, Can. J. Earth Sci., V. 24., pp. 2254-2278.

Stockmal, G.S. and Beaumont, C., 1987, "Geodynamic Models of Convergent Margin Tectonics: the Southern Canadian Cordillera and the Swiss Alps" in Sedimentary Basins and Basin Forming Mechanisms, Beaumont, C. and Tankard, A.J., eds., CSPG Memoir 12, pp. 393-411.

Stockmal, G.S., Beaumont, C. and Boutilier, R., 1986, Geodynamic Models of Convergent Margin Tectonics: Transition from Rifted Margin to Overthrust Belt and Consequences for Foreland Basin Development, AAPG Bull., V. 70, pp. 181-190.

Stride, A.H., 1988, Indications of Long Term Episodic Suspension Transport of Sand Across the Norfolk Banks, North Sea, Mar. Geol., V. 79, pp. 55-64.

Stride, A.H., 1970, Shape and Size Trends for Sand Waves in a Depositional Zone of the North Sea, Geol. Mag., V. 107, pp. 469-477.

Stride, A.H., 1963, Current-Swept Sea Floors Near the Southern Half of Great Britain, Quat. J. of the Geol. Soc. London, V. 119, pp.175-199.

Stride, A.H., Belderson, R.H., Kenyon, N.H. and Johnson, M.A., 1982, "Offshore Tidal Deposits: Sand Sheet and Sand Bank Facies" in Offshore Tidal Sands, Processes and Deposits, Stride, A.H., ed., Chapman and Hall, New York, pp.95-125.

Suttner, L.J. and Basu, A., 1985, The Effect of Grain Size on Detrital Modes: a Test of the Gazzi-Dickinson Point-Counting Method-Discussion, Jour. of Sed. Pet., V.55, pp.616-617.

Swie-Djin, N., 1976, Marine Transgressions as a Factor in the Formation of Sandwave Complexes, Geol. en Minj., V. 55, pp. 18-40.

Swift, D.J.P. and Niedoroda, A.W., 1985, "Fluid and Sediment Dynamics on Continental Shelves" in Shelf Sands and Sandstone Reservoirs, Tillman, R.W., Swift, D.J.P. and Walker, R.G., eds., SEPM Short Course no. 13., pp. 47-134.

Swift, D.J.P., Figueiredo, A.G., Freeland, G.L. and Oertel, G.F., 1983, Hummocky Cross Stratification and Megaripples: a Geological Double Standard, J. Sed. Pet., V. 53, p. 1295-1317.

Swift, D.J.P. and Field, M.F., 1981, Evolution of a Classic Ridge Field, Maryland Sector, North American Inner Shelf, Sed., V. 28, pp. 461-482.

Swift, D.J.P., Freeland, G.L. and Young, R.A., 1979, Time and Space Distribution of Megaripples and Associated Bedforms, Middle Atlantic Bight, North American Atlantic Shelf, Sed., V. 26, pp. 389-406.

Swift, D.J.P., Nelson, T., McHone, J., Holliday, B., Palmer, H. and Sheldon, G., 1977, Holocene Evolution of the Inner Shelf of Southern Virginia, J. Sed. Pet., V. 47, pp. 1454-1474.

Tankard, A.J., 1986, Depositional Response to Foreland Deformation in the Carboniferous of Eastern Kentucky, AAPG Bull., V. 70, pp. 853-868.

Then, D.R. and Dougherty, B.J., 1983, "A New Procedure for Extracting Foraminifera from Indurated Organic Shale" in Current Research, Part B, G.S.C. Paper 83-1B, pp. 413-414.

Thomas, M.B. and Oliver, T.A., 1979, Depth-Porosity Relationships in the Viking and Cardium Formations of Central Alberta, Bull. Can. Pet. Geol., V. 27, pp.209-228.

Tillman, R.W., 1985, A Spectrum of Shelf Sands and Sandstones in Shelf Sands and Sandstone Reservoirs SEPM Short Course 13, R.W. Tillman, D.J. Swift and R.G. Walker eds., pp. 1-47.

Tillman, R.W., Swift, D.J.P. and Walker, R.G., 1985, Shelf Sandstones and Sandstone Reservoirs, SEPM Short Course Notes No. 13., Tulsa, OK

Tizzard, P.G. and Lerbekmo, J.F., 1975, Depositional History of the Viking Formation, Suffield Area, Alberta, Canada, Bull. Can. Petrol. Geol., V. 23, pp. 715-752.

Vail, P.R., Mitchum, R.M.Jr., Thompson, S., III, "Global Cycles of Relative Changes of Sea Level" in Seismic Stratigraphy - Applications to Hydrocarbon Exploration, AAPG Memoir 26, Tulsa, OK, pp.83-98.

Van Wagoner, J.C., Mitchum, R.M., Campion, K.M. and Rahmanian, V.D., 1990, Siliciclastic Sequence Stratigraphy in Well Logs, Cores and Outcrops: Concepts for High-Resolution Correlation of Time and Facies, AAPG Methods in Exploration Series, No. 7, Tulsa, OK pp. 1-55.

Van Wagoner, J.C., Posamentier, H.W., Mitchum, R.M. Jr., Vail, P.R., Sarg, J.F., Loutit, T.S. and Hardenbol, J., 1988, "An Overview of the Fundamentals of Sequence Stratigraphy and Key Definitions" in Sea Level Changes: an Integrated Approach Wigus, C.K., Hastings, B.S., Kendall, C.G.St.C, Posamentier, H.W. Ross, C.A. and Van Wagoner, J.C., eds., SEPM Spec. Pub. 42, Tulsa, OK, pp. 39-46.

Van der Plas, L. and Tobi, A.C., 1965, A Chart for Judging the Reliability of Point Counting Results, Amer. Jour. of Sci., V. 263, pp. 87-90.

Visser, J.N.J., 1980, Neap-Spring Cycles Reflected in Holocene Subtidal Large Scale Bedform Deposits, Geology, V.8, pp. 543-546.

Walker, R.G., 1990, Facies Modeling and Sequence Stratigraphy, J. Sed. Pet., V. 60., pp. 777-786.

Walker, R.G., 1986, Cardium 7: Progress Report Compiling Data from Outcrop and Subsurface in Southern Alberta, McMaster Geology Department Technical Memo. 86-3.

Walker, R.G., 1985, "Geological Evidence for Storm Transportation and Deposition on Ancient Shelves" in Shelf Sands and Sandstone Reservoirs SEPM Short Course No. 13, Tillman, R.W., Swift, D.J.P., and Walker, R.G., eds., pp. 243-302.

Walker, R.G., 1984a, "Shelf and Shallow Marine Sands" in Facies Models, Walker, R.G., ed., G.A.C. Publications, Toronto, pp. 141-170.

Walker, R.G., 1984b, "Turbidites and Associated Coarse Clastic Deposits" in Facies Models, Walker, R.G., ed., G.A.C. Publications, Toronto, pp. 171-188.

Walker, R.G., 1984c, "General Introduction: Facies, Facies Sequences and Facies Models" in Facies Models, Walker, R.G., ed., G.A.C. Publications, Toronto, pp. 1-10.

Walker, R.G., 1983, Cardium Formation 3. Sedimentology and Stratigraphy in the Garrington-Caroline Area, Alberta, Bull. C.S.P.G., V. 31, pp. 213-230.

Walker, R.G., 1982, Hummocky and Swaley Cross Stratification in Clastic Units of the Front Ranges, Foothills and Plains from Field B.C. to Drumheller, Alberta: IAS 11th International Congress on Sedimentology Field Excursion Guidebook, 21A, pp. 205-212.

Walker, R.G. and Plint, A.G., 1992, "Wave and Storm-Dominated Shallow Marine Systems" in Facies Models, Response to Sea Level Change, R.G. Walker and N.P. James eds., GAC, Toronto, pp. 219-238.

Wallace-Dudley, K.H., 1981, Gas Pools of Western Canada (Map 1558A) and Oil Pools of Western Canada (Map 1559A), Geol. Surv. Canada.

Weimer, R.J., 1992, "Presidential Address: Developments in Sequence Stratigraphy: Foreland and Cratonic Basins", AAPG Bull., V.76, pp. 965-982.

Weimer, R.J., 1988, "Record of Sea-Level Changes, Cretaceous Western Interior, USA" in Sea Level Changes: an Integrated Approach SEPM Special Publication

42, Wilgus, C.K., Hastings, B.S., Kendall, C.G.St.C, Posamentier, H.W., Ross, C.A and Van Wagoner, J.C., eds., Tulsa, OK, pp. 285-288.

Wells, N.A., 1989, A Program in BASIC for Facies by Facies Markov Chain Analysis, Computers and Geosciences, V. 15, pp. 145-156.

Wright, M.E. and Walker, R.G., 1981, Cardium Formation (Upper Cretaceous) at Seebe, Alberta - Storm Transported Sandstones and Conglomerates in Shallow Marine Depositional Environments below Fair-weather Wavebase, Can. J. Earth Sci., V. 18, pp. 795-809.

Yen, F. and Goodwin, J.H., 1976, Correlation of Tuff Layers in the Green River Formation, Utah Using Biotite Compositions, J. Sed. Pet., V. 46, pp. 345-354.

Yorath, C.J., Bornhold, B.D. and Thomson, R.E., 1979, Oscillation Ripples on the Northeast Pacific Continental Shelf, V. 31, pp. 45-58.

Young, S.W., 1976, Petrographic Textures of Detrital Polycrystalline Quartz as an Aid to Interpreting Crystalline Source Rocks, Jour. of Sed. Pet., V. 46, p.595-603.

Zuffa, G.G., 1980, Hybrid Arenites: Their Composition and Classification, Jour. of Sed. Pet., V.50, pp. 21-29.

APPENDIX A

Arenicolites anorexis

A.1 SUMMARY

The trace fossil *Arenicolites anorexia* occurs in type form in the Albian, Viking Formation. The trace is a narrow diametre, mud-lined, U-tube whose arms are in close proximity to each other and whose length is ten to one hundred times the tube diametre. Rarely, funnels may be seen at the top of the tubes. The trace is interpreted to have been created by a sessile surface feeder living under conditions of relatively slow sedimentation in an energetic water column. The trace may be placed within the *Diplocraterion ichnocoenoses.*

A.2 DESCRIPTION

Throughout the Viking Formation, there exists a dramatic but previously unanalyzed trace fossil. This trace appears to fit no existing ichnospecies description although it is analogous to similar traces described from other locations.

Figures A-1 through A-3 show the typical and defining characteristics of this ichnospecies. The traces are long U-shaped tubes visible when filled with sand. Only one possible example was seen of a mud filled form. The base of the traces is rarely visible; figure A-3 shows an example which has protrusive *spreiten.* In plan view (figure A-2b), the tubes vary from being clearly separated by up to 2 or 3 mm to being joined in a 'dumbbell' or 'double barrel' pattern. The tubes often appear to be supported by a thin mud lining which is visible in figure A-1[a-c]. This lining is not visible in the cases where the traces occur in mudstone/siltstone facies so its existence in such cases is unknown. Rarest of all characteristics is

Figure A-1. Vertical Views of *Arenicolites anorexis.*

A-1a. Mud-Lined Trace in Crossbedded Sandstone.

The figure is from well 15-24-45-20W4 at a depth of 3170 feet. The core is three inches in diametre and the scale bar is 3 centimetres long.

A-1b. Clustering of *Arenicolites anorexis* Traces.

The figure shows a clustering of the traces in muddy sandstone from well 10-22-50-18W4 at a depth of 2568 feet. The core is three inches in diametre.

A-1c. Thin Section Cut through a Tube Wall.

The figure shows a photograph of a standard thin section as cut through a tube. The cut reveals a slightly greater concentration of clay along the tube walls but no other structures. The example comes from well 10-22-50-18W4 at a depth of 2568 feet.

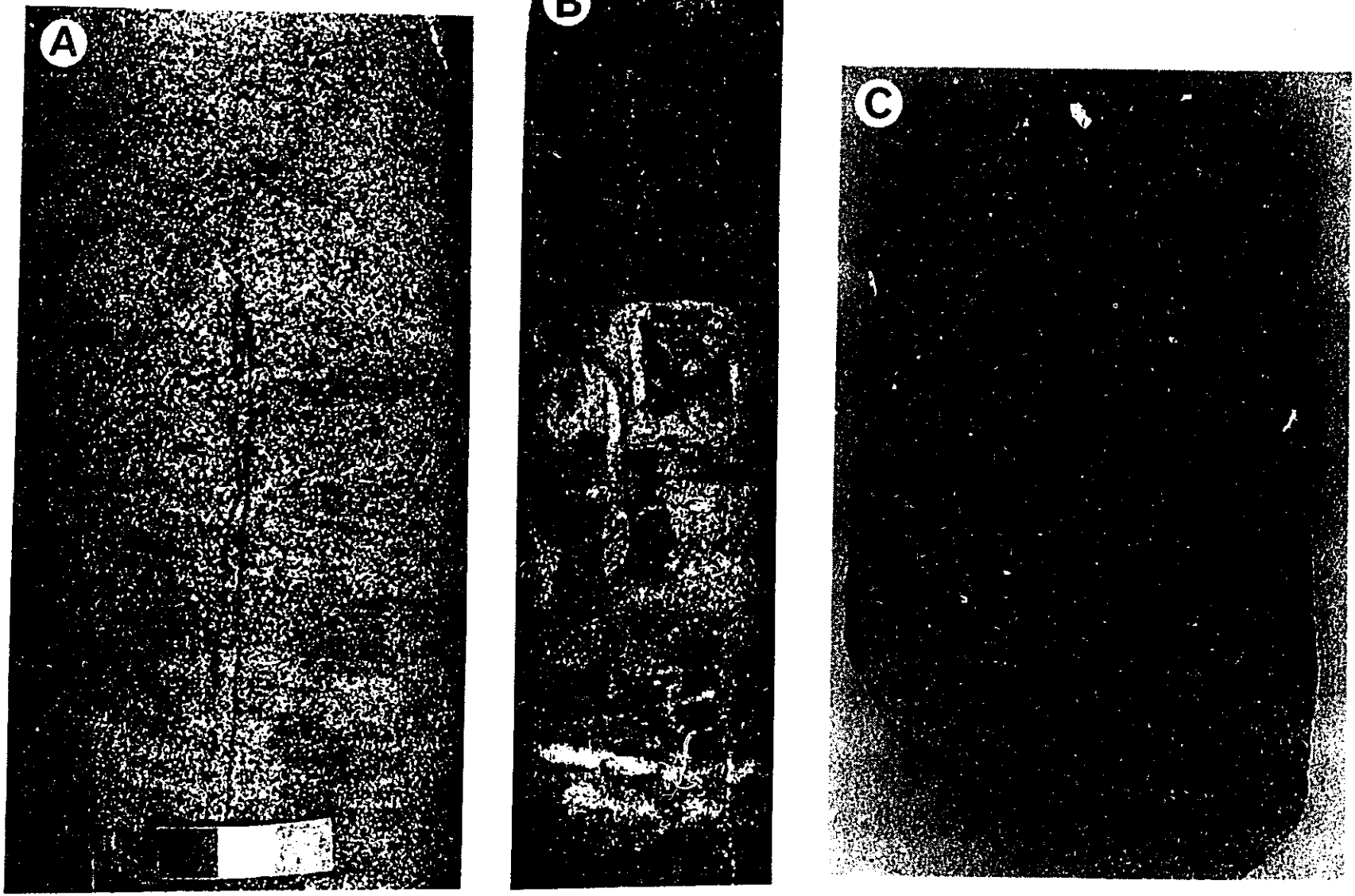
A
B
C

Figure A-2. Horizontal Views of *Arenicolites anorexis*.

A-2a. Horizontal View of *Arenicolites anorexis* Tubes in Funnels.

The figure shows two separate traces each with two U-tube openings within interpreted collapse funnels at the top of the traces. The photograph is of three inch core from well 4-20-57-26W4 at a depth of 2968 feet (905 metres). The scale bar is three centimetres long.

A-2b. Horizontal View of *Arenicolites anorexis* Tube Patterns.

The photograph is of the horizontal upper surface of a three inch core from well 11-13-59-26W4 at a depth of 2804 feet.

A-2c. Off Axis View of *Arenicolites anorexis* Funnel Fill.

The figure shows the funnel and interior tubes of an *Arenicolites anorexis* trace in three inch core from well 7-17-59-26W4 at a depth of 2653 feet. The scale bar is three centimetres long.

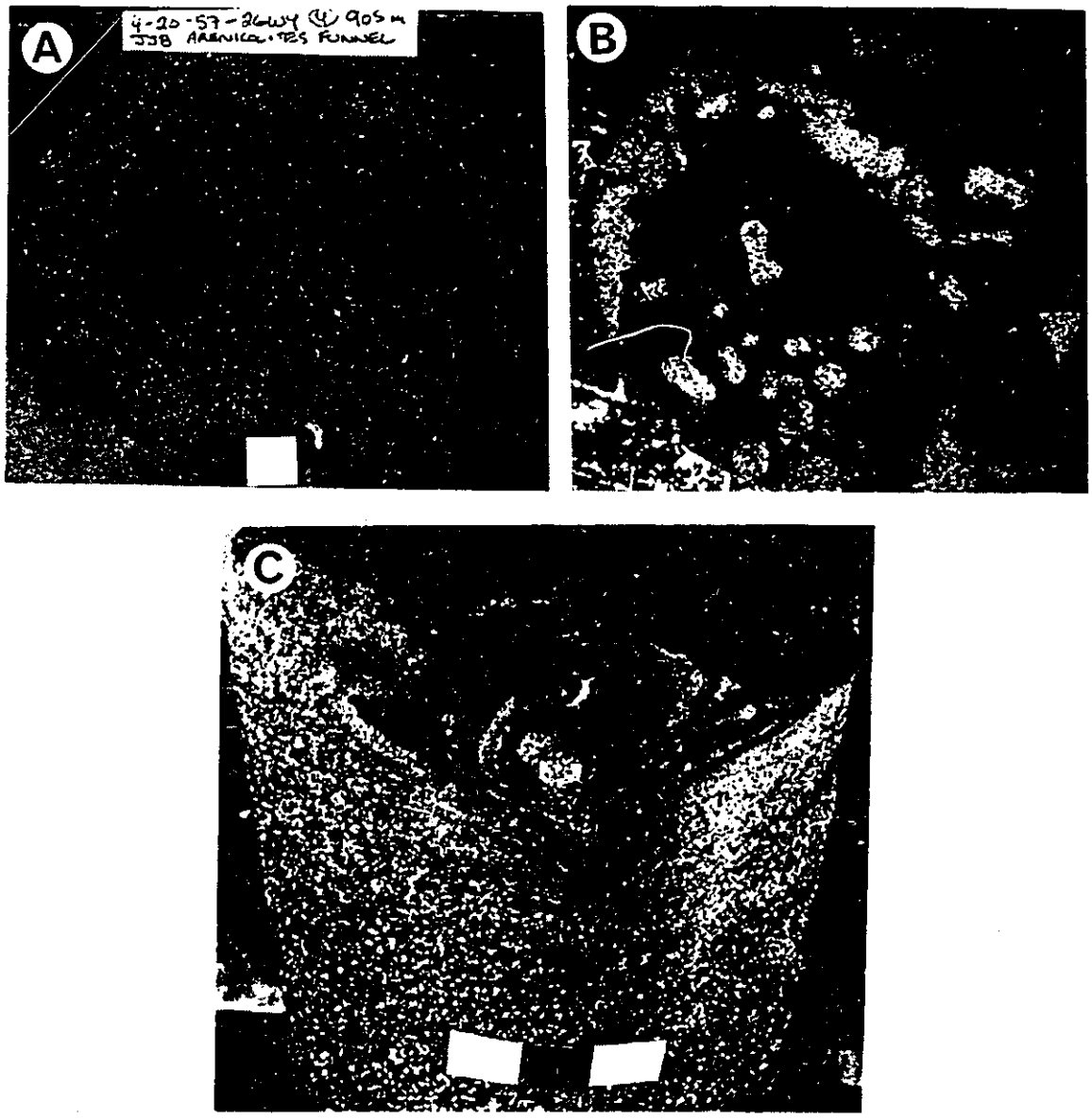
A
4-20-57-26WY ⑭ 90S m
338 ARNICOL. TES FUNNEL
B
C

Figure A-3. Base of *Arenicolites anorexis* with Possible Protrusive *Spreiten.*

The figure shows the base of a U-tube from well 6-27-59-24W4 at a depth of 2424 feet (at the base of the Viking Formation). The scale bar is three centimetres long and the core is three inches in diametre.

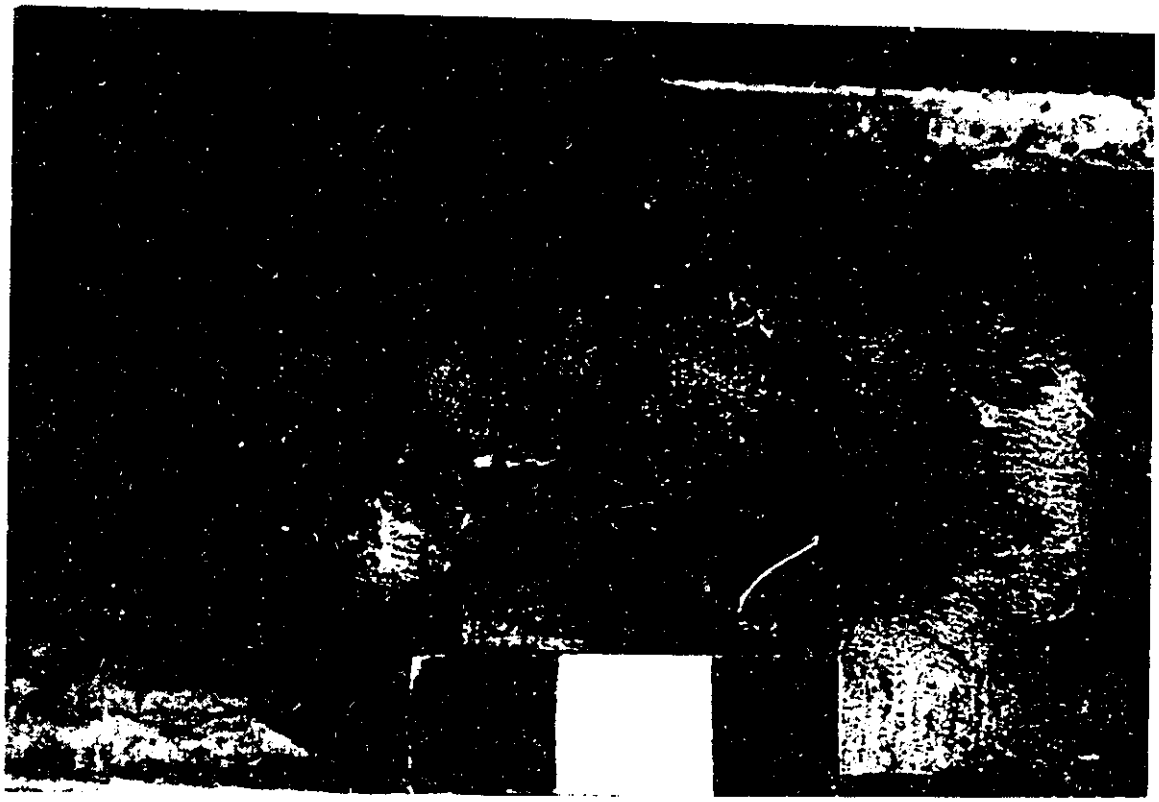

the evidence shown in figures A-2a and A-2c for funnel structures at the tops of the tubes. The largest measured diametre of the funnels is the 4 cm example shown in figure A-2c. The amount of lost material from the top of this example is unknown, so it represents a minimum value.

Figure A-4 shows a statistical summary of tube diametres. The average is approximately 5 mm, but the range is from 1 to 15 mm. Maximum tube lengths could not usually be accurately measured from the sides of cores because the tubes and core are not exactly parallel; moreover, irregularities in the direction of the tubes means that they disappear into and out of the cylinder of the core surface. Usually, a single set of tubes can be traced 10 to 20 cm. The maximum length measured was 95cm, but it is not impossible that lengths may exceed this maximum because in many cases core pieces could not be fit together to demonstrate greater extents.

The traces may occur in almost any facies and in varying concentrations ranging from a single, isolated trace to many superimposed forms as in figure A-1b. However, geographically, the traces tend to occur in the western half of the study area in association with the thicker, and overall, sandier portions of the units.

A.3 NOMENCLATURE

According to the Treatise on Invertebrate Paleontology (Hantzschell, 1975), *Arenicolites* species are characterized by U-shaped tubes with a funnel at one end of the tube. According to this definition, the traces described above fit into the *Arenicolites* genera (confirmed by S.G. Pemberton, p. comm., 1987). The species name *anorexis* was chosen to emphasis their very long and narrow form.

Figure A-4. Burrow Tube Diametre Histogram.

The figure shows a histogram for the dimensions of the tubes of the traces as seen on the horizontal surface of cores. The x-axis shows the diametre in millimetres and the y-axis gives the number of tubes having that diametre. One hundred and eighty eight observations were used to generate the graph.

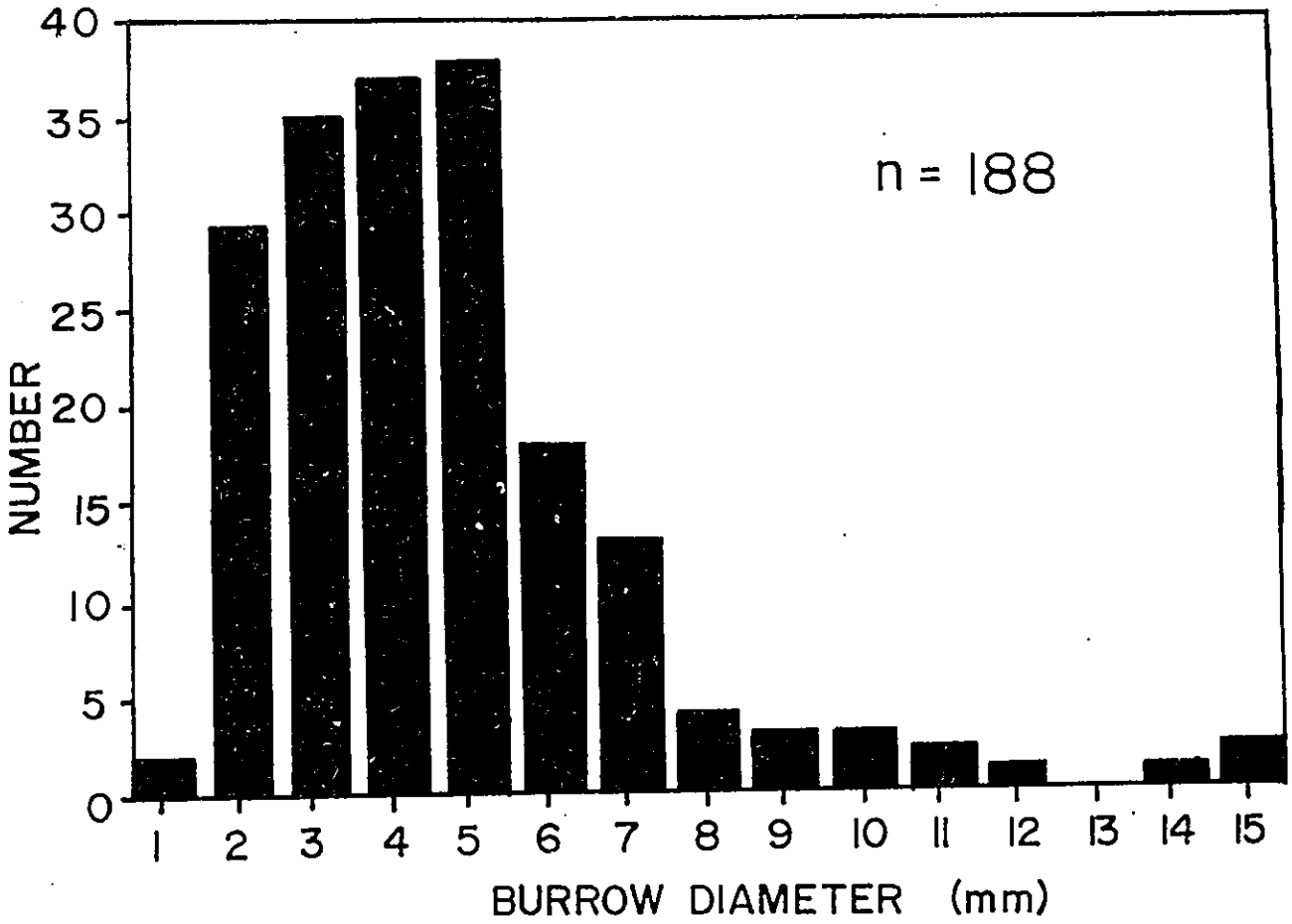
40
35
30
25
20
15
10
5
0
NUMBER
n = 188
1
2
3
4
5
6
7
8
9
10
11
12
13
14
15
BURROW DIAMETER (mm)

A.4 INTERPRETATION

No definite conclusions can be drawn regarding the type of creature responsible for these traces. However, it seems likely that only one species was responsible for the traces regardless of size. The histogram of burrow tube dimensions in figure A-4 strongly suggests a single population; the unimodal form of the histogram suggests that there were not two different species creating different size burrows. If, as seems likely, the individuals responsible for creating the burrows were relatively stationary, and maintained a constant rate of trace generation as they aged, then the histogram of the tube dimensions shown in figure A-4 may be taken to indicate the average size of the adult which would appear to be approximately 5 to 6 mm in diametre.

Some environmental information that can be inferred from the burrow description. Features of the tube construction provide the strongest evidence about conditions in which the burrowing organisms lived. The lining of the tubes implies an element of durability that suggests the traces were burrows. Maintenance of a burrow indicates a relatively long term residence in an area of slow or only occasional sediment motion and/or accumulation. This interpretation is strengthened by the presence of funnels at the tops of the tubes which imply stationary feeding activity. The occasional lining of the funnels with *spreiten* suggests that the animal may have fed off of material that collapsed into the funnel rather than simple suspension filtering. This feeding strategy would require that an overall slow sedimentation be accompanied by flows of sufficiently high energy and nutrient content to feed the stationary organisms.

The type of *spreiten* observed also provide evidence on the nature of sediment accumulation. The general lack of retrusive *spreiten* suggests that the seafloor was not experiencing rapid sedimentation during the organism's lifetime. It is difficult to judge whether denudation of the seafloor was regularly occurring by examination of the traces alone. This is because the narrowness of the tube spacing makes the existence of protrusive *spreiten* a speculative matter; their generation and/or detection in such small dimensions is problematic. [However, there is no interpretation of pervasive denudation, either laterally or temporally, based on the other aspects of the sediments discussed in the body of the thesis.] The lithology of the Viking Formation has implications for the interpretation of the traces. As discussed in chapter 6, the heterolithic nature of many of the facies of the Viking suggests that this transport occurred through intermittent high energy events rather than a state of constant intermediate energy. The timing between fluctuations in the energy level of any portion of the 'environment' is unknown, but the presence of the *Arenicolites anorexis* traces suggests that timing between major fluctuations capable of moving large amounts of bedload may have been relatively long (i.e., longer than tidal cycles).

Although there are no traces described that correspond precisely to this ichnospecies, an analogous trace has been described by Heinberg and Birkelund (1984) from the middle Jurassic Vardekloft Formation of Central East Greenland. Heinberg and Birkelund (1984) describe the trace *Diplocraterion habichi* located in this formation as being 0.5 to 1 metre long with tube diametres averaging 5 millimetres and having occasionally preserved funnels at the top of the U-tube. In, fact the *Diplocraterion habichi* label has been applied to this trace in recent

studies of the Viking Formation by MacEachern et al. (1992), Raychaudiri et al. (1992) and Pemberton et al. (1992). These authors do not provide a clear justification for their use of the *Diplocraterion* label. There are even cases where the same trace has apparently been labelled as both *Diplocraterion* and *Arenicolites* by Pemberton et al. (1992). *Diplocraterion habichi* differs from the *Arenicolites anorexis* described here only by virtue of having slightly greater tube separation and consequent preservation of retrusive and protrusive *spreiten* that places it in the *Diplocraterion* genera. Heinberg and Birkelund note that the trace probably reflects activity of a suspension feeder living in a setting where "physical reworking appears to have been frequent"; furthermore,

> "the long tubes may ... be interpreted as a protective shelter against unstable conditions in the sea floor, with high water agitation, but low rate of sedimentation."

The environment of deposition of the sediments containing these traces is interpreted by Heinberg and Birkelund (1984) to be that of an "offshore bar regime of relict sand". Descriptively the sediments are rather similar to the Viking sediments although somewhat thicker and sandier; they are also locally glauconitic. Considering both the description of *Arenicolites anorexis* and the interpreted depositional regime of the Viking sediments in comparison to those of the *Diplocraterion ichnocoenosis* defined by Heinberg and Birkelund (1984), it is reasonable to place the *Arenicolites anorexis* traces into this *ichnocoenosis*. The traces seem to be the product of creatures that thrived under conditions of slow sediment accumulation.

APPENDIX B

UNIT PETROGRAPHY

B.1 Petrofacies Analysis

B.1.1 Techniques

The majority of data for petrographic study come from standard thin sections stained for potassium and calcium feldspars according to Houghton (1980), and for carbonate cement type and iron content according to Lindholm and Finkelman (1972). Although the exact lighting used by the latter for classification of the calcite by iron content was not duplicated, a relative assessment of the degree of incorporation of iron into the calcite is possible. Dolomite was distinguishable using this staining process because it is iron bearing and thus takes a blue stain.

Point count data was taken by the Glagolev-Chayes method (Galehouse, 1971) using a mechanical point counter set so the smallest step, or number of steps, in the device was larger than the largest grain encountered in all traverses. In a few cases, this meant only 40 or so points could be collected, but generally 500 or more were possible. In many cases, 1000 or more points were tallied. The error for the common components was estimated using the chart of Van der Plas and Tobi (1965). Matrix, pore space and cements were tallied during the same traverse as the framework.

I used the Q_MRF point counting method rather than the QRL method (Dickinson, 1970; Dickinson and Suczek, 1979). Chert components are included as rock fragments, R. I did this to account for compositional variation with grain

size which is important because of lateral grain size changes at the same proposed unit level. The QFL approach essentially ignores this information (see Ingersoll et al., 1984; Suttner and Basu, 1985; Ingersoll et al., 1985a; Decker and Helmold, 1985; Ingersoll et al., 1985b). Consequently, it may also ignore grain size control of subtle provenance indicators (e.g.,Conolly, 1965). Nevertheless, for rock fragments, separate tallies were kept of the exact mineral under the cross hair in accordance with Dickinson's technique; this was invariably non-undulatory quartz. In practice, the extreme mineralogical maturity of the rocks means there is no real difference between methods. The rock fragment percentage is usually near zero, and transferring counts to the various component categories based on minerals contained in the few fragments present would be insignificant. Even following the QRF approach, little information can be gained from the very rare, possible, non sedimentary rock fragments present; because of their grain size insufficient texture is preserved (e.g.,Boggs, 1968). I also used the QRF approach because it has been adopted by previous workers so its employment aids in comparison.

Most provenance variations concentrate on the coarser, silt and up, fraction of sediments, but because the Viking Formation is encased in marine shales and is rather muddy in the area studied it is also appropriate to consider possible variations in clay mineralogy throughout the units. Clay mineralogy was studied by standard, oriented sample, X-Ray Diffraction analysis (XRD). XRD was done with copper radiation and scanning was done at 2^{o} per minute. Samples were oriented and both air dried and glycolated following procedures detailed in Eslinger and Pevear (1988). Results indicated further treatments were

not necessary. Approximately the same amount of material was used to generate each pattern, so peak heights indicate relative amounts of clays.

B.1.2 Classification of Petrographic Components

The sandstone components were divided into several categories. Most of these are conventional, but there are exceptions. The extreme mineralogical maturity (Folk, 1974) of the sands, mostly monocrystalline quartz and chert, which is typical of foreland basin settings (Dickinson and Suczek, 1979), makes distinguishing potential petrofacies difficult. This means that many standard indicators such as Q_MFL_T and K/F, (Graham et al., 1976) or proportions of quartz types that include polycrystalline quartz (Basu et al., 1975) are rather hopeless as detailed petrofacies criteria because of the small amount of index minerals present. For example, Schwab (1986) was unable to find secular variations in foreland basin fill using the QFL approach. Figure B-1 shows a typical example of the medium grain size sandstone of the formation illustrating the problem.

Attempts to subdivide polycrystalline quartz type following the approach of Basu et al. (1975), Blatt (1967a) or Young (1976), likewise, would be useless because only trace amounts of such materials are present. Moreover, the above subdivisions of polycrystalline quartz summarize material of metamorphic and igneous origin; it is very likely that some of the rare polycrystalline quartz grains encountered in this study actually come from coarse veins in chert. Inclusion of such grains would further complicate any such approach. Consequently, polycrystalline quartz, which typically occurs as less than 1% of the rock

Figure B-1. Typical Varieties of Chert.

(6-25-53-21W4, 2730 feet depth, medium to coarse sand, unit Gamma.; plane light, white scale bar is 1mm; 3 seconds exposure of ISO 1600 film.)

The clasts labeled LC are almost certainly chert grains but in point counting were arbitrarily separated from the more obviously quartzose grains, examples labeled C. Quartz is also abundant, and the cement is dolomite (see text).


LC
C

(or 5-10 points per thin section), was not placed into established subcategories. Monocrystalline quartz was divided into undulatory and non-undulatory following the 5° stage rotation criterion of Basu et al. (1975) (which negates Blatt and Christie's (1963) objections).

I made one unconventional division hoping it might prove useful in erecting petrofacies in such mature sandstones. I subdivided chert into two categories, lithic chert and chert. This is essentially a crystal size subdivision and is completely arbitrary although consistent for one operator. Figure B-1 shows examples of the division. Those grains clearly composed of microcrystalline quartz were assigned to the chert category; those grains whose crystal size was so small that they could be argued, in the extreme, to be lithic fragments were assigned to the lithic chert category. The subdivision is most apparent under crossed nicols. The categories are part of a spectrum as in large granules and pebbles veins of `chert' may be seen running through `lithic chert' grains. In such cases, the grain was classified as chert.

Feldspars were divided into alkali or plagioclase on the basis of staining and microstructure such as twinning. Alkali feldspar was categorized as having a faint stain, slightly rougher surface texture than quartz, occasional fracture and partial alteration. Where completely altered feldspars were observed, which was rare, they were assigned to the plagioclase category only if remnant or pseudomorphed twinning was visible. Alkali feldspars were placed into either an "orthoclase", "perthite" or "microcline" categories depending on, respectively, a lack of twinning, perthitic or antiperthitic structure and cross hatch twinning. The amount of sanidine in the orthoclase category and the amount of anorthoclase in

the microcline category is unknown. No further subdivision could be reliably made because of general inability to examine such criteria as optic sign although observations. Ideally, SEM point counting would have been done (Minnis, 1984), but this equipment was not available.

Many miscellaneous components were tallied individually; among the more common are phosphatic material including bone fragments or more rarely but locally abundant, phosphatized fecal pellets. Also common was glauconite either replacing clay matrix or chert. Opaque minerals were not examined in detail and were placed in one class; the majority appear to be pyrite. Rock fragments, always sedimentary when identifiable were noted individually but occur only in traces.

B.1.3 Point Counting Results; Traditional

The point counting results are tabulated in percentage of component form in Table B-1. Figure B-2 shows QRF diagrams for the very fine to fine, medium to coarse and very coarse up grain sizes based on the tabulated percentages. Figure B-3 summarizes the chert subdivisions made in the same standard triangle diagram approach. Some thin sections, represented by crosses, are separable from others using the approximate 95% confidence ellipses. The ellipses were estimated by following the results of Van der Plas and Tobi (1965). I plotted the 95% confidence range for each component in turn and fit a rough ellipse to the resulting three pairs of points. The grain size trend in the samples is marked on the side of the plot. The feldspar point count data is shown in Figure B-4 as plagioclase versus alkali feldspar percents. The ratio is roughly 2:1, but is highly variable.

ANOVA was carried out on the point count data (Griffiths and Rosenfeld, 1954; Griffiths, 1967) to check reliability. Since all data was acquired by one operator, inter operator variation was not a factor. Twelve thin sections were measured in separate traverses three times over eight months to check for such variation. Their results are shown in figure B-5. They show no significant difference between transects but a potential difference between sections at the 10% level. This suggested there may have been differences between samples that could be used to discriminate units petrographically but actually corresponds to the grain size effect visible in figure B-3.

B.1.4 Point Counting Results; Multivariate

Multivariate analyses of the point count data were carried out using a variety of measured components listed in Table B-1. The variety ranged from all inclusive using either micron or phi sizes to attempts to include only particular components such as locally present phosphate and glauconite. The analyses here were carried out using the commercially available STATGRAPHICS PC software. Only a typical result is presented here under cluster analysis.

Various approaches to cluster analysis (Davis, 1986) produce arbitrary numbers of clusters that can be made to fit the number of units observed. However, regardless of the exact technique used or the number of reasonable end result clusters chosen (this was varied from 2 to 7), most, typically 90+% of the datapoints fall within one cluster. Such end results based on a euclidian distance nearest neighbor analysis with division into five clusters are shown in Figure B-6, where for convenience the resulting cluster is projected onto the CHT versus PHI axes. Note the letters A-E denote clusters <u>not</u> units.

Table B-1

Tabulation of Point Count Data

The following tabulation is in percentage form. Each thin section is identified by a well number and its components tabulated. The category NUMB is the total number of point counts; PART is the number of counts comprising the components tabulated (it excludes pore space, matrix and cement). SEQ is the postulated sedimentary unit location of the sample. PHI is the representative phi grain size estimated from hand sample. SIZE is the representative size in mm. The other columns are the actual components and are as follows:

PQTZ = polycrystalline quartz
MQTZ = non-undulatory quartz
UQTZ = undulatory quartz
SAND = sedimentary rock fragments
FELD = feldspars
GLAU = glauconite
PHOS = phosphatic fragments (pellets, bones and teeth)
OPAQ = all opaque grains
LCHT = lithic chert
CHT = chert

The percentage of components is calculated relative to PART, the total of grain components.

row	SMPL ID	PQTZ	MQTZ	UQTZ	SAND	FELD	GLAU	PHOS	OPAQ	SIZE	CHT	LCHT	NUMB	PART	SEQ	PHI
1	10-30-51	0.5	17.6	10.8	0.5	0.9	1.8	0.0	0.	0.177	49.0	18.9	288	218	C	2.5
2	6-8-51-1	3.0	14.9	49.3	0.3	1.2	1.2	0.4	0.	0.250	20.2	9.5	1008	767	B	2.0
3	9-18-50-	2.4	12.5	41.2	0.2	1.1	3.6	2.7	1.	0.210	23.5	11.5	1003	762	C	2.0
4	6-8-51-1	1.8	18.7	46.7	0.0	3.0	1.5	0.0	0.	0.177	16.0	12.0	822	657	D	2.5
5	6-8-51-1	1.8	11.7	23.1	0.7	0.4	1.5	0.0	0.	1.190	38.1	22.3	320	268	D	0.0
6	10-33-51	2.0	10.1	33.0	0.4	3.0	4.9	0.5	2.	0.250	29.9	14.7	894	703	C	2.0
7	6-8-51-1	1.5	17.8	38.0	0.1	1.7	0.7	0.4	0.	0.250	24.7	15.0	1007	816	C	2.0
8	6-8-51-1	0.4	33.9	34.0	0.0	4.1	2.7	0.2	0.	0.297	12.4	12.2	1000	801	E	1.8
9	10-33-51	0.4	9.1	14.5	0.0	1.2	0.0	1.7	0.	0.500	50.7	22.4	302	237	C	1.0
10	10-22-50	1.9	23.1	20.6	0.3	3.2	8.0	0.0	5.	0.297	22.8	15.5	929	687	D	1.8
11	6-23-52-	3.6	30.1	19.4	0.2	2.9	3.6	1.0	0.	0.210	22.7	16.4	1038	791	C	2.0
12	6-8-51-1	2.7	30.5	33.4	0.4	2.9	1.5	0.0	0.	0.105	18.9	9.5	570	474	E	3.5
13	6-22-52-	3.3	13.5	15.3	0.5	2.8	0.5	0.5	1.	0.354	41.7	21.4	267	212	C	1.5
14	6-9-52-1	2.7	28.8	21.2	0.5	1.4	0.4	0.2	0.	1.000	30.6	14.1	1012	802	D	0.0
15	10-11-50	1.6	27.4	23.1	0.1	0.2	0.9	0.6	0.	1.500	33.2	12.5	1026	838	D	-0.5
16	6-25-53-	2.1	23.1	23.5	0.0	0.0	0.0	0.0	0.	0.595	36.8	14.5	302	234	C	1.0
17	5-8-54-1	2.5	14.0	7.0	0.0	1.0	0.0	0.5	0.	0.420	63.5	11.5	260	199	B	1.5
18	10-21-51	1.5	29.0	27.6	0.0	1.0	0.5	0.1	1.	1.410	29.3	10.2	930	724	C	-0.5
19	6-23-52-	1.5	22.3	20.2	0.0	0.6	0.9	0.0	0.	1.000	41.7	12.8	430	333	C	0.0
20	10-13-52	3.4	5.9	10.9	0.0	0.0	0.0	0.8	1.	1.410	60.6	17.6	135	117	B	-0.5
21	6-21-59-	1.0	8.7	9.6	1.0	0.0	2.9	0.0	1.	1.680	56.6	19.2	151	100	?	-0.5
22	6-9-52-1	4.2	10.4	16.7	2.1	0.0	0.0	6.3	0.	1.410	45.7	14.6	57	45	C	-0.5
23	6-22-52-	6.6	4.7	17.0	0.0	0.9	0.0	0.0	0.	1.410	48.2	22.6	122	106	C	-0.5
24	11-2-56-	3.5	2.7	3.5	0.0	0.0	0.0	0.0	8.	1.410	60.2	22.1	124	140	?	-0.5
25	10-29-49	2.9	12.7	20.2	0.0	0.3	0.0	6.2	0.	0.500	44.3	13.4	493	288	B	1.0
26	10-33-51	0.0	2.9	14.3	0.0	0.0	0.0	0.0	0.	0.210	65.7	17.1	63	35	D	2.0
27	10-29-45	0.4	4.0	11.9	0.0	0.0	0.0	2.9	1.	1.000	62.1	17.3	350	265	B	0.0
28	6-25-62-	1.0	5.6	8.2	0.7	0.1	0.0	2.9	0.	0.354	67.8	13.6	1020	744	?	1.5
29	10-27-52	0.7	15.5	20.3	0.2	0.9	0.0	2.4	0.	0.707	41.0	19.0	557	448	C	0.5
30	10-20-47	2.0	22.0	28.1	0.0	0.5	0.0	1.9	0.	0.500	35.2	10.0	1014	765	B	1.0
31	6-29-49-	2.6	19.5	36.3	0.0	0.5	0.5	0.2	1.	0.297	28.5	11.4	785	579	C	1.8
32	2-35-45-	2.5	13.8	22.9	0.0	0.4	1.9	0.4	2.	0.149	39.3	16.8	1007	719	C	3.0
33	10-13-47	0.7	20.6	27.1	0.0	1.9	0.0	25.3	0.	0.210	17.5	6.5	1001	552	B	2.0
34	11-24-45	0.6	27.3	34.8	0.0	1.3	0.0	1.0	2.	0.707	22.6	10.2	1023	758	B	0.5
35	1-1-45-2	1.2	34.5	35.6	0.1	1.6	0.4	0.2	0.	0.177	16.1	10.3	998	803	C	2.5
36	10-36-52	2.1	20.7	30.2	0.0	0.5	0.1	0.0	0.	0.354	30.1	16.3	1001	796	C	1.5
37	11-33-50	1.1	9.5	16.1	0.0	0.3	0.0	1.4	0.	0.210	46.9	24.4	429	342	C	2.0
38	10-22-50	4.0	6.6	13.6	0.0	0.0	0.0	1.7	0.	0.420	50.5	23.6	359	296	C	1.3
39	10-22-50	2.3	26.1	29.6	0.0	0.0	0.4	0.0	0.	0.297	27.3	14.1	627	529	C	1.8
40	13-29-49	1.9	20.8	24.8	0.1	0.5	0.4	0.1	0.	0.707	35.7	15.7	1002	742	C	0.5
41	14-13-53	2.3	26.6	28.1	0.0	5.7	0.1	1.5	0.	0.707	26.0	9.7	1000	722	B	0.5
42	10-21-52	0.7	16.9	29.2	0.0	0.4	13.2	0.5	0.	0.297	29.7	9.4	1000	628	D	1.8
43	10-7-52-	1.1	27.8	35.7	0.0	1.7	1.3	0.0	0.	0.177	21.7	10.3	1000	699	D	2.5
44	10-15-46	0.4	34.8	34.0	0.0	2.4	1.9	0.0	1.	0.149	15.3	10.6	997	884	B	2.8
45	7-34-46-	0.1	37.2	33.6	0.0	3.6	1.0	0.3	8.	0.149	5.8	10.5	896	610	?	2.8
46	10-21-51	2.1	15.4	23.7	0.0	1.3	18.8	0.4	4.	0.841	22.8	11.3	255	184	C	0.3
47	10-22-48	3.7	29.1	33.3	0.0	2.1	2.5	0.0	0.	0.210	17.8	11.2	1000	794	C	2.5
48	11-24-46	1.1	31.7	17.1	0.0	1.3	0.8	15.9	6.	0.074	12.3	14.1	1025	473	B	4.0
49	7-14-46-	0.3	11.7	7.0	0.0	0.3	0.1	70.6	1.	0.149	2.1	6.6	1000	223	?	2.8
50	7-28-50-	1.9	29.6	24.0	0.0	15.1	0.3	0.0	0.	0.210	18.2	10.3	982	853	B	2.0
51	11-19-56	3.9	26.0	18.7	0.2	1.7	0.1	0.2	0.	0.420	24.4	24.8	961	824	?	1.3
52	6-26-52-	0.4	38.4	12.6	0.0	0.8	0.0	24.1	0.	0.420	13.4	10.3	371	192	?	1.3
53	6-24-30-	11.2	27.9	30.7	0.0	7.0	0.0	0.0	0.	0.177	5.8	17.4	320	258	?	2.5
54	16-11-57	2.5	29.1	17.4	0.0	11.1	0.0	0.0	2.	0.177	23.2	14.4	641	388	?	2.5
55	1-11-53-	0.8	34.1	32.8	0.0	1.2	0.0	0.0	0.	0.177	16.8	14.3	349	244	?	2.5
56	13-3-56-	2.9	32.5	27.9	0.3	0.3	0.3	0.0	0.	0.210	25.8	10.0	449	379	?	2.0
57	10-30-54	0.7	35.1	23.8	0.0	2.5	0.0	6.0	5.	0.177	19.1	7.8	291	251	?	2.5
58	2-11-56-	2.9	26.7	20.0	0.0	0.0	8.1	0.0	5.	0.125	23.8	13.3	350	299	?	3.0
59	3-19-58-	0.8	37.2	29.5	0.0	0.0	0.0	0.0	2.	0.125	12.0	18.6	301	253	?	3.0
60	6-2-50-1	1.8	38.1	34.8	0.0	0.9	0.0	1.4	1.	0.177	14.2	8.3	300	214	?	2.5
61	11-6-49-	1.9	35.7	34.2	0.0	0.7	0.0	0.0	0.	0.125	14.5	12.6	301	268	?	3.0
62	13-14-45	1.9	35.5	34.4	0.0	1.5	0.0	0.4	0.	0.149	16.9	9.4	374	266	?	2.8

Figure B-2. QRF Diagrams for All Thin Section Samples by Grain Size.

All data for samples with currently postulated unit assignments is shown plotted on a standard QRF diagram. Postulated units are symbolized as shown in the legend. The grain size range used for each plot is shown; these sizes are the predominant size observed in hand sample examination. The samples plot as Quartz or Chert Arenites according to Folk's classification (1974).

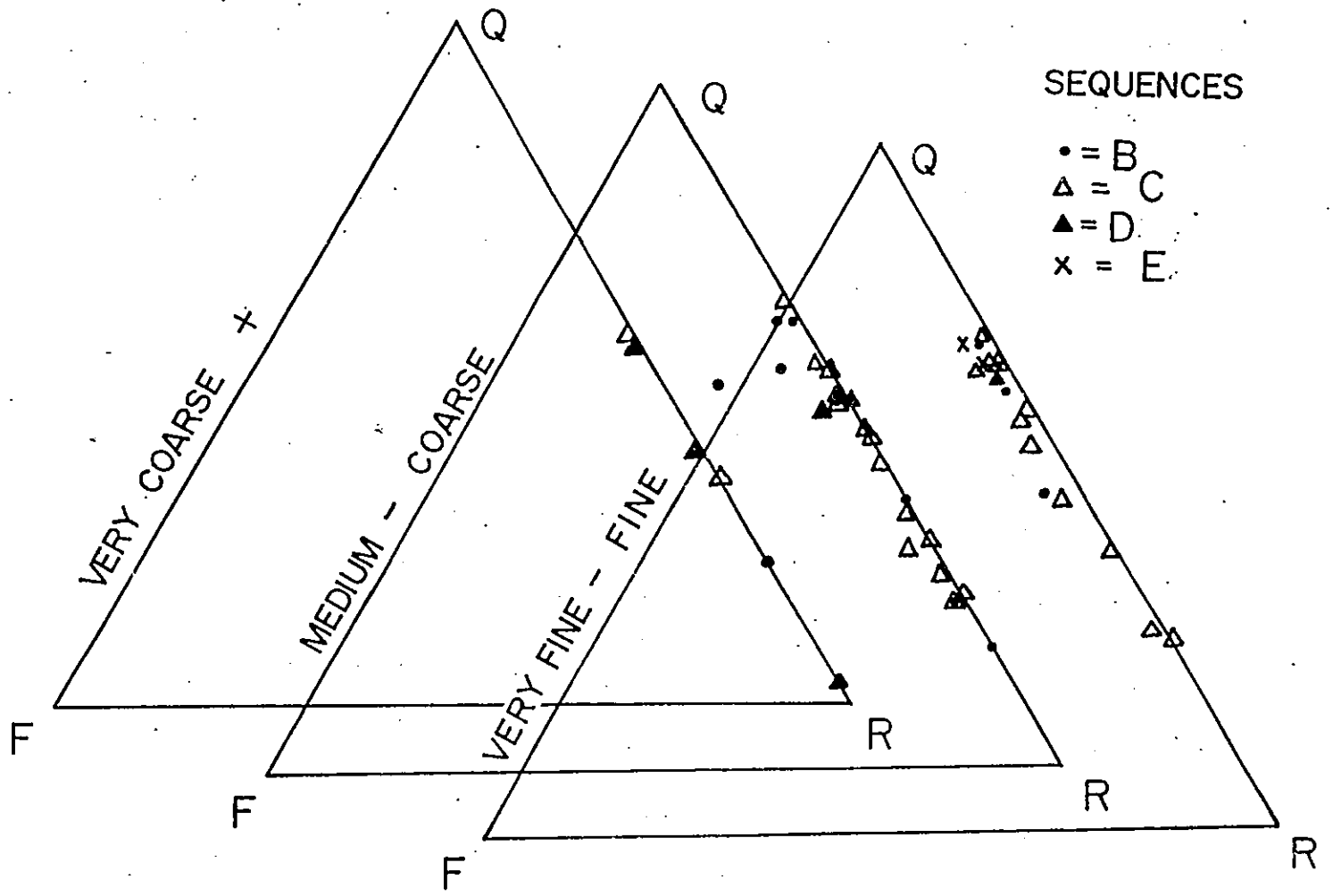
Q
Q
Q
SEQUENCES
• = B
△ = C
▲ = D
× = E
VERY COARSE +
MEDIUM - COARSE
VERY FINE - FINE
F
F
F
R
R
R

Figure B-3. Quartz, Chert and Lithic Chert Ternary Plot.

The diagram shows a plot of relative percentages of the total quartz component exclusive of chert, chert component and lithic chert component. The ellipsoids or partial ellipsoids around each data point are approximate zones of 95% confidence based on Van der Plas and Tobi (1965). The grain size range marked to the side indicates the trend in grain size that mimics the trend in composition.

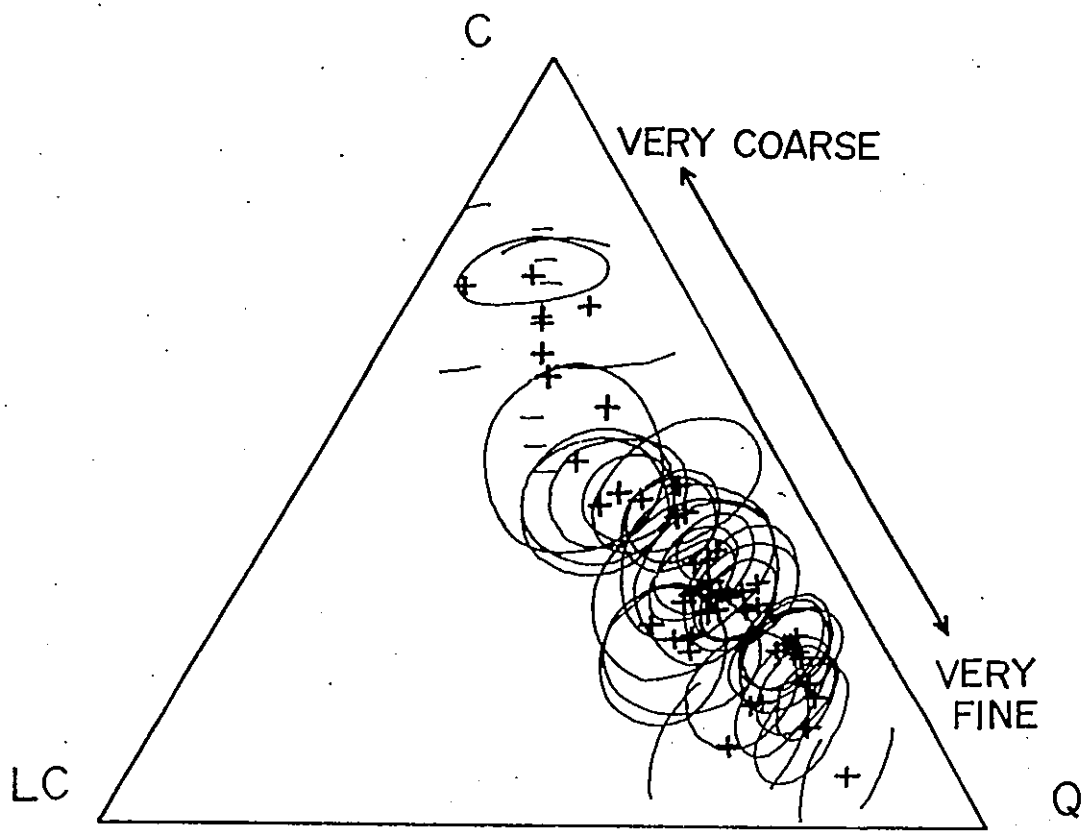
C
VERY COARSE
VERY
FINE
LC
Q

Figure B-4. Alkali Feldspar versus Plagioclase Feldspar.

The figure shows plots of number of feldspars counted in each class for all samples bearing feldspars. Regression (i.e. ratio) lines are not plotted because they would be statistically insignificant. There are no separations visible on the basis of units which are shown by symbol in the legend.

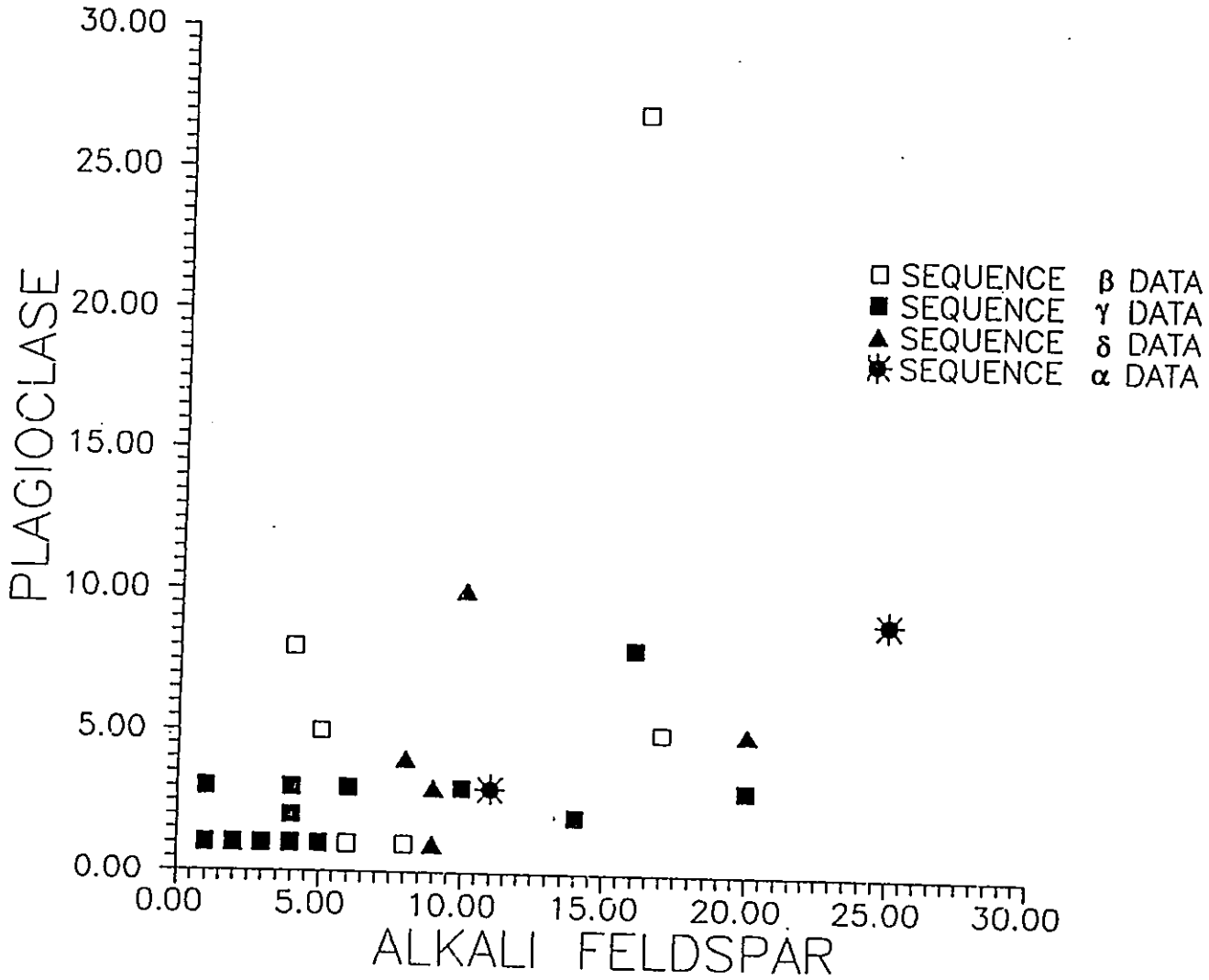
30.00
25.00
20.00
15.00
10.00
5.00
0.00
PLAGIOCLASE
0.00
5.00
10.00
15.00
20.00
25.00
30.00
ALKALI FELDSPAR
SEQUENCE β DATA
SEQUENCE γ DATA
SEQUENCE δ DATA
SEQUENCE α DATA

Figure B-5. Analysis of Variance Table for Thin Section Petrography.

Source	Sum of Squares	D.F.	Mean of Squares	F	%
Among Slides	31.36	4	7.84	1.023	>10
Among Transects	200.5	4	50.14	6.55	<.5
Error	122.64	16	7.665		
Total	354.46	24			

2 WAY ANOVA

B.1.5 X-Ray Diffraction Results

The results of the XRD analysis of the clays from below, within and above the Viking Formation are shown collectively in Figure B-7. The small, persistent peak at approximately 12.5 degrees 2 theta suggests minor amounts of kaolinite (since there is no 14 Angstrom peak revealing chlorite) and the small persistent peak left in the 8.5 degree region after glycolation suggests minor illite. This could also be illitic glauconite; the two cannot be separated on the basis of XRD. The major component of all samples is a K rich Smectite as determined from the approximate 12 angstrom air dried peak and 17 angstrom glycolated peak (Eslinger and Pevear, 1988).

B.1.6 Discussion of Petrographic Component Analysis: Traditional Petrography

Figure B-2 shows that Q_MRF plots do not allow unit discrimination. No separation of units occurs in any of the grain size fractions. The only trend apparent is a weak one of increasing lithic component, including chert, with grain size. This result disagrees with that of Reinson and Foscolos (1986) who suggest the possibility of dividing units into litharenites and feldspathic litharenites.

The division of chert particles into lithic and ordinary also fails to detect inter-unit variations. Figure B-3 shows that despite separation of some thin sections using the approximate 95% confidence ellipses, the results as a whole show no groupings. The separation of individual samples is merely a function of grain size with coarser samples having more chert than total quartz and slightly more ordinary than lithic chert. The sample trends follows the grain size trend on the side of the plot very well. This grain size pattern is in keeping with that observed for

Figure B-6. Cluster Analysis Example.

The figure shows the results of a nearest neighbor, euclidian distance approach to finding five clusters of data. The five end clusters are labeled A through E, but, essentially, one cluster, A, (circled in the figure) represents all the data. The plot here is in terms of Cht versus Phi, but the results are the same regardless of axes used or variable combinations.

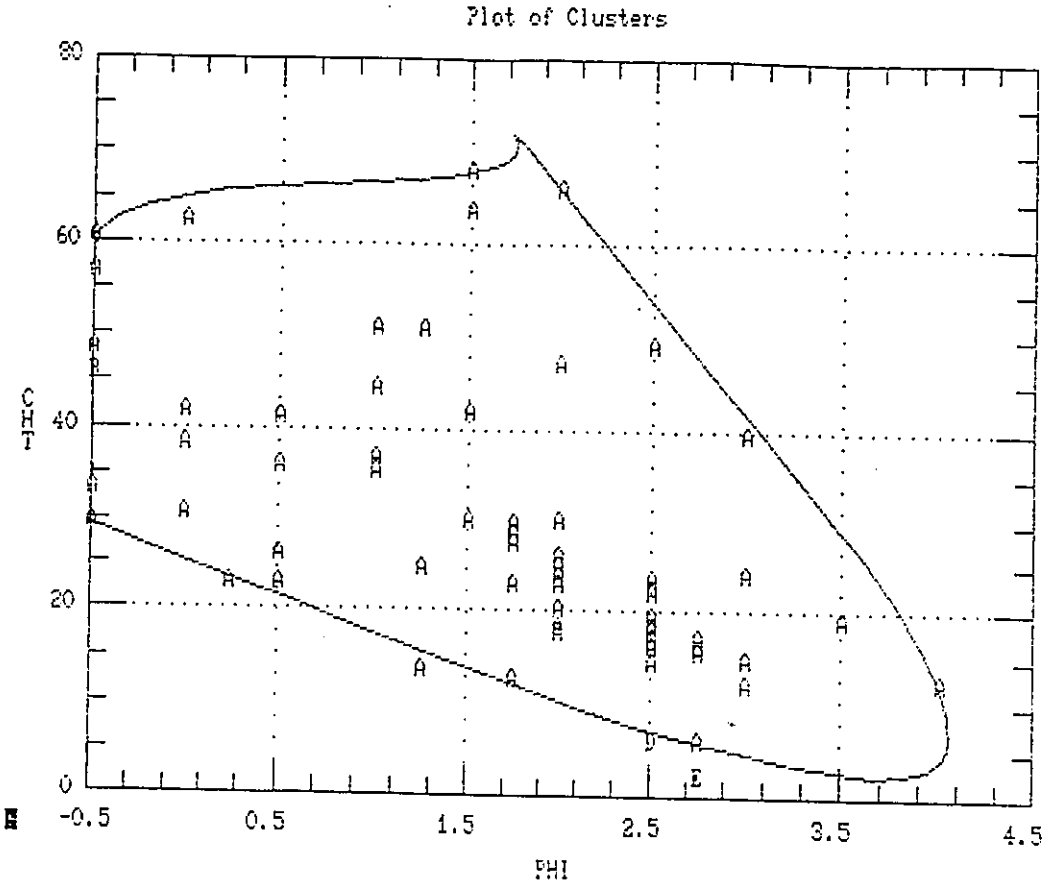
Plot of Clusters
80
60
40
20
0
CHT
-0.5
0.5
1.5
2.5
3.5
4.5
PHI

Figure B-7. X-ray Diffraction Patterns for Clays of the Joli Fou, Viking and Overlying Shales.

The diffraction patterns are for air dried and glycolated samples from the shales overlying the Viking Formation, the Viking Formation itself and the underlying Joli Fou shales. The well numbers are the locations of the samples. The vertical scale is relative intensity of the peaks, and the horizontal scale is in degrees 2 theta. The scanning was done at 2· per minute using Cu radiation.

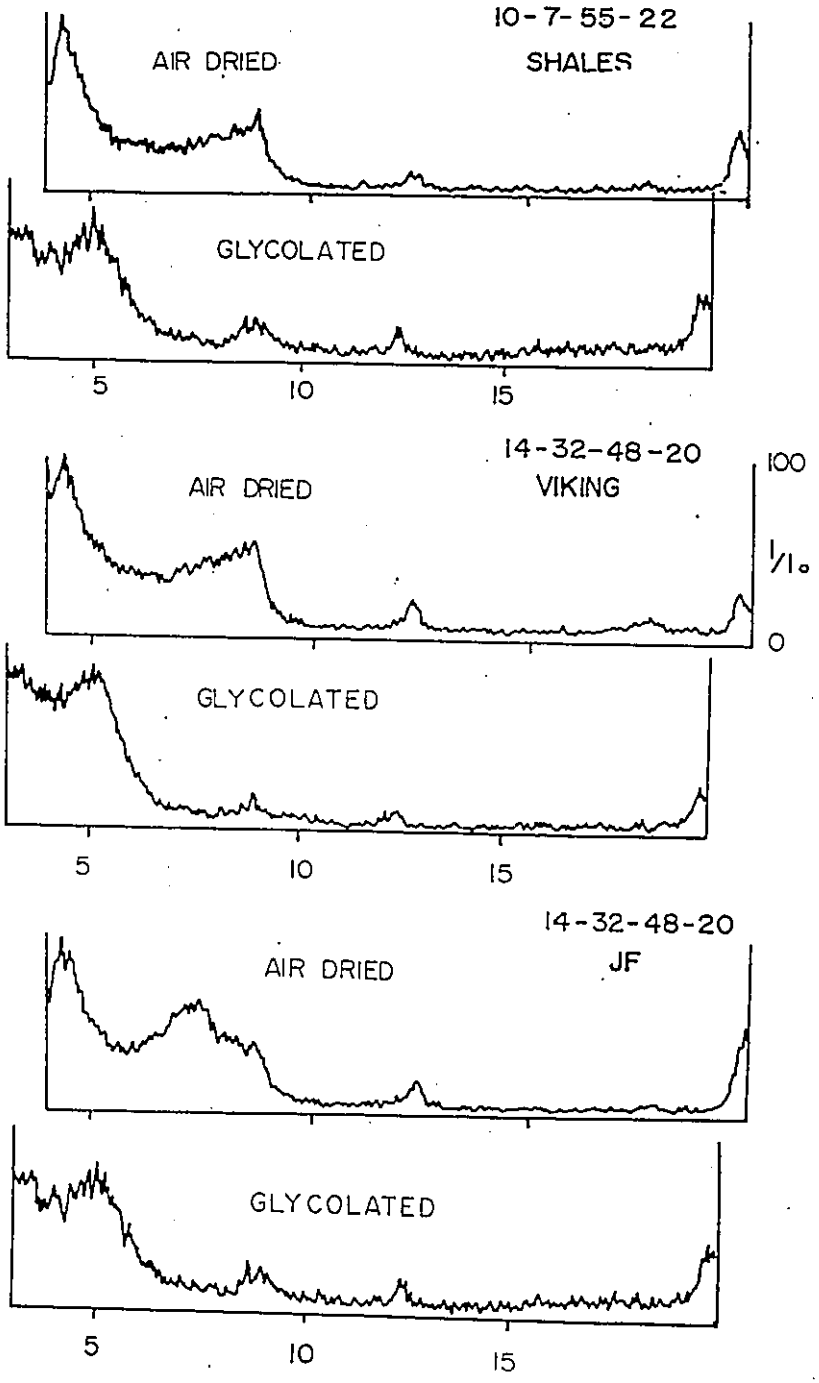
10-7-55-22
SHALES
AIR DRIED
GLYCOLATED
5
10
15
14-32-48-20
VIKING
AIR DRIED
100
1/10
0
GLYCOLATED
5
10
15
14-32-48-20
JF
AIR DRIED
GLYCOLATED
5
10
15

metamorphic and igneous polycrystalline quartz (Hayes, 1962; Ethridge, 1977; Harrell and Blatt, 1978) and with one of the few studies including chert (Misko and Hendry, 1979).

The ratio of alkali to plagioclase feldspars displayed in Figure B-4 is also inconclusive. No groups distinguishing units are apparent in the scattered data. The only general observation is a trend towards increasing feldspar content with finer grain size, visible as a slight movement of samples off the QR axis in Figure B-2. Such an increase is consistent with other petrographic studies (Odom, 1975; Odom et al., 1976).

The lack of feldspathic litharenites in the study area suggests that if such divisions reflect provenance variations rather than 'spot' accumulations of volcanic material then source input was relatively local and cannot be used for regional correlation. It is unlikely that the feldspars are merely accumulations derived solely from ash falls common in the formation (now bentonites) because there are plutonic feldspars in the alkali portion.

The general difficulty of making precise provenance determinations for mature, probably multicycle sandstones must be acknowledged (Blatt, 1967b). This problem is even more acute in the case of the Viking Formation in the study area because the sediments have passed through the foreshore and apparently undergone extensive exposure on the seafloor, implied by the presence of glauconite. So while the work of Potter (1984, 1986) suggests that Holocene beaches preserve provenance signatures the longer time frame involved here makes it more likely that mineralogical maturation has occurred analogous to that studied by Mack (1978) in the ancient littoral zone. There is no way of knowing

precisely to what extent the proportion of feldspars represent that of the original provenance(s) despite their relatively fresh appearance. Not only could transport have altered this ratio but volcanic contamination by "extrabasinal" material (Zuffa, 1980) may have altered feldspar ratios. Nevertheless it is not unreasonable to infer that there were both silicic plutonic and volcanic sources based on the presence of perthite and microcline in the feldspar population and the presence of bentonites indicating explosive silicic volcanism.

B.1.7 Discussion of Petrographic Results: Multivariate Analysis

The failure of standard plots to distinguish groups in the data leaves the approach of multivariate statistics. The methods tried also fail to reveal criteria for separating units. The lack of relevant clusters should be readily apparent in Figure B-6 where essentially all samples group together. Since this is true regardless of the exact clustering technique adopted, I conclude that there are no clusters present in the data that reflect the units.

B.1.8 Discussion of XRD Results

Qualitatively, there is no real difference between the XRD patterns of the clays in Figure B-7. It is a little surprising that no significant variations are apparent between the clays of the Viking and the enclosing shale given the possibility of differential transport of illite, kaolinite and smectites in offshore directions (e.g.,Blatt et al., 1980); therefore, smectite appears to have been the dominant detrital clay. Although sampling here is minimal, the obviously smectitic nature of the clays throughout the cores observed during cleaning implies a mineralogically homogenous clay component; thus, clay mineralogy does not seem to offer a useful criterion for unit separation.

B.2 Diagenetic History

B.2.1 Techniques

Paragenesis for each unit was primarily constructed by classical examination of thin section textural relationships. Additionally, Cathodoluminescence, X-ray diffraction (XRD) and SEM were employed. Gold coated SEM samples, scanned at 15Kv proved ineffective for EDX analysis. Generally, the only elemental peak obtainable was Au; sometimes a small neighboring Si peak was detectable when spot focusing was applied to a chert grain. Carbon coating was found in many cases to lead to such poor conduction across the looser samples that rapid charge build up destroyed resolution. The exception to this was a sample of phosphatized shale from well 14-32-45-20W4 discussed in chapter 6.

Cathodoluminescence was employed to examine carbonate cements and quartz overgrowths.

B.2.2 Unit Paragenesis

Figure B-8 summarizes the general diagenetic unit of events (paragenesis) for the Viking Formation in the region under study. Table B-2 shows the paragenetic series for each unit.

The earliest mineralization includes pyritization, glauconitization and phosphatization. Their relative timing could not be discerned. Examples of these may be seen in figures B-9, B-10, B-11, and B-12. Phosphatization occurs as shale rip ups, rims on

Table B-2

Diagenetic Variation by Unit

	UNIT							
	Beta	Gamma		Delta		Epsilon (1 thin section)		
DIAGENETIC COMPONENT								
Glauconite	*		*		*		*	
Dolomite	*		*		*			
Clay Lining	*		*					
Quartz Overgrowths		*		*		*		*
Calcite	*		*		*			
Siderite		*		*		*		

Figure B-8. General Diagenetic Unit.

The vertical axis shows the minerals forming and the horizontal axis gives their relative time of formation. The textural evidence is illustrated in the following figures.

Relative Timing

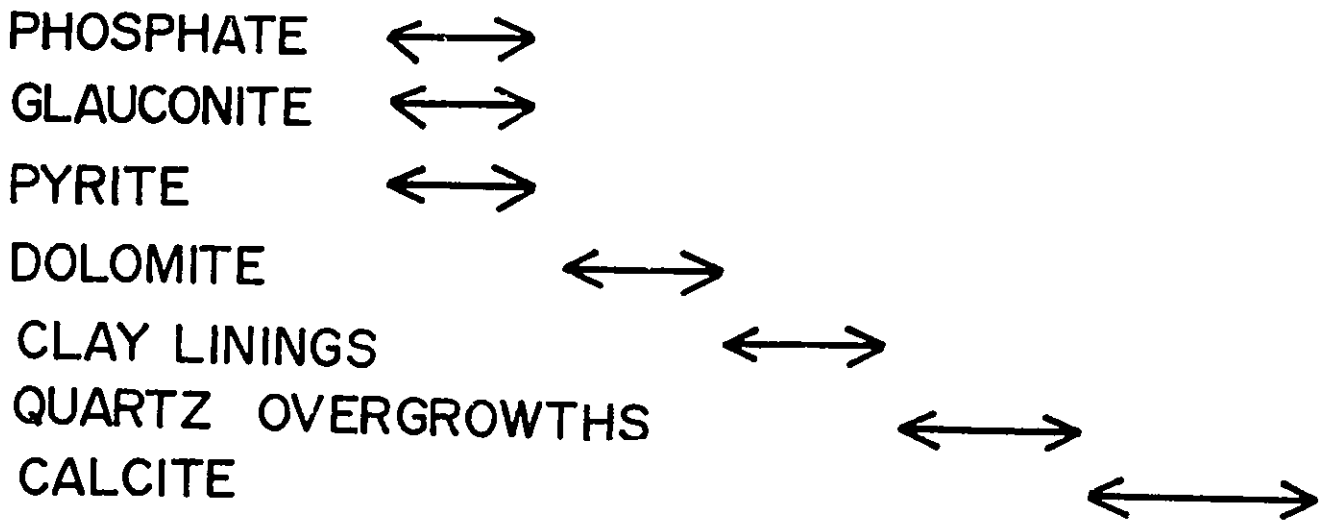

Figure B-9. Phosphatic Bone in Chert Arenite.

(6-22-52-19W4, 2649.6 feet depth, medium sand to granules, unit Gamma., white scale bar is 1mm; plain light 5 seconds exposure with ISO 1600 film.)

This is a typical occurrence of a bone fragment (labeled B) within the Viking sandstones. The fragment is isotropic. In addition compactional straight and concavo-convex contacts may be seen in the framework. These are typical of the deeper sandstones in the study area where no cement or matrix is present.

Figure B-10. Pyritic and Phosphatic Bone and Teeth Fragments.

(10-13-47-16W4, 2620 feet depth, fine sand, unit Beta, white scale bar is 1mm; 5 seconds exposure with ISO 1000 film.)

Calcium phosphate bone fragments (B), indicated by pink stain partially visible in the lower right, and pyritized bone and teeth fragments (PR) associated with quartz arenite at the top of unit Beta. The sandstone is cemented by ferroan calcite stained purple (see text). The textural relation is taken to indicate change in composition of phosphatic components and pyritization prior to calcite precipitation.

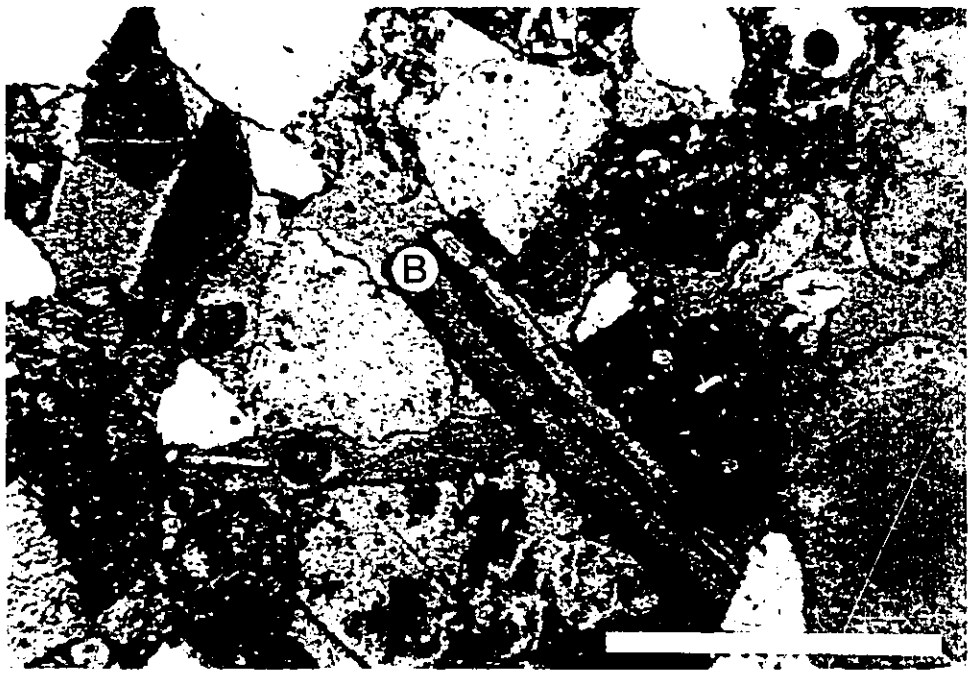
B

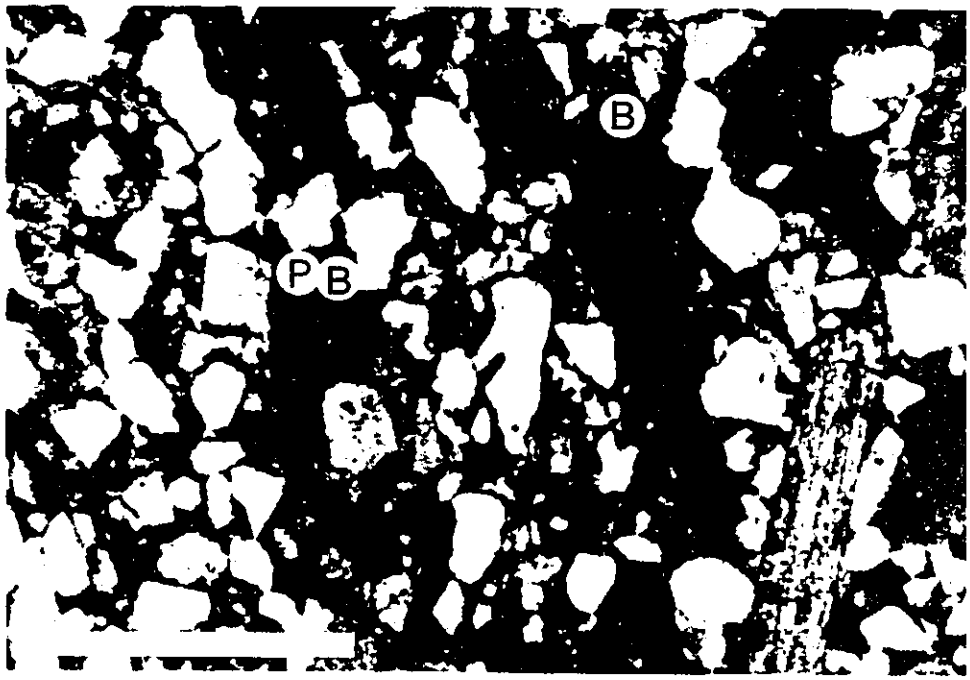
B
P
B

Figure B-11A. Phosphatized Fecal Pellets.

(7-14-46-11W4, 2134 feet depth, fine sand, unit Gamma, white scale bar is 1mm; plane light, 3 seconds exposure of 1000 ISO film.)

Phosphatic alteration of fecal pellets predates, on textural evidence the introduction of non-ferroan calcite, stained weakly pink. The fecal pellets appear relatively undeformed indicating very early alteration. The pellets occur in low angle (5·) cross bedding suggesting possible surficial alteration prior to final deposition.

Figure B-11B. Phosphatized Fecal Pellets under Crossed Nicols.

(7-14-46-11W4, 2134 feet depth, fine sand, unit Gamma, white scale bar is 1mm; crossed nicols, 20 seconds exposure of 1000 ISO film.)

This photograph is identical to the previous and shows the isotropic nature of the phosphatized pellets along with the calcite cement.

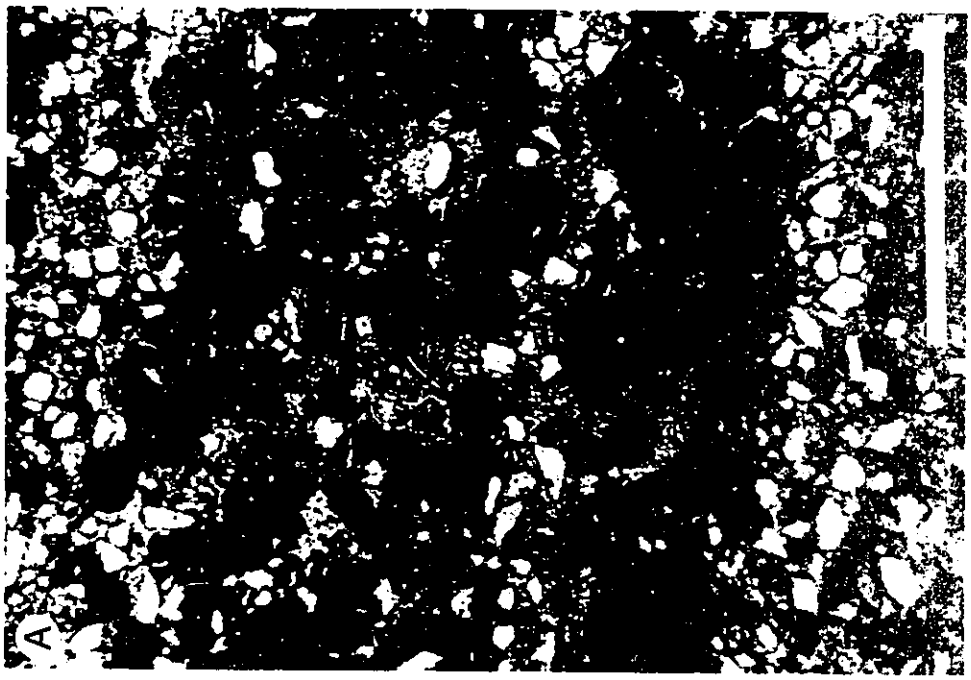
A

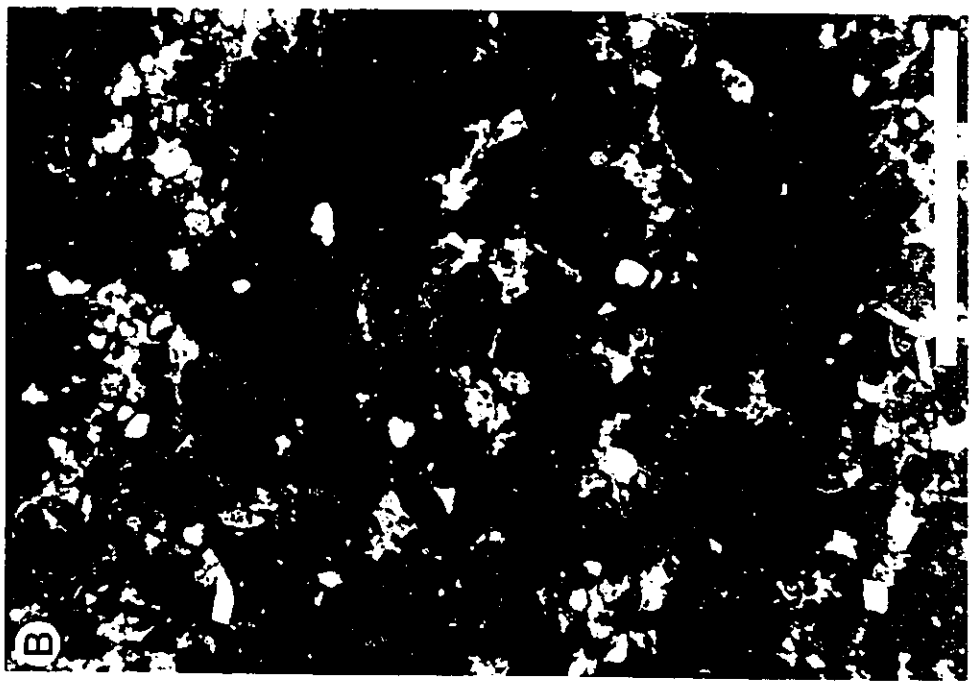
B

Figure B-12A. Glauconitized and Pyritized Matrix in a Quartz Arenite.

(10-21-51-19W4, 2110 feet depth, medium to granular sand, unit Gamma, white scale bar is 1mm; plane light, 7 seconds exposure of ISO 1000 film.)

The intimate association of glauconite, the light green/yellow material (G), and pyrite, the small opaques (P), implies coeval formation of their precursors. A few examples of glauconitized chert grains (GC) are visible. Compactional contacts are less pronounced here than in Figure 1.

Figure B-12B. Glauconitized and Pyritized Matrix in a Quartz Arenite under Crossed Nicols.

(10-21-51-19W4, 2110 feet depth, medium sand to granules, unit Gamma, white scale bar is 1mm; crossed nicols, 20 seconds exposure of ISO 1000 film.)

The coarse, micaceous nature of the glauconite may be seen in the extinction pattern in the center and left of the photograph. On the right, poorly visible remnant chert texture may be seen in a completely glauconitized grain (GC).

Figure B-13. Glauconitization of Chert.

(10-29-49-18W4, 2910.6 feet depth, medium sand to pebbles, unit Gamma, white scale bar is 1mm; plane light, 7 seconds exposure of ISO 1000 film.)

The yellow colouration in the interior of this chert granule is intermediate in the degree of alteration that may be observed. Colouration may vary from this straw yellow to bright lime green and may be located anywhere from around grain edges, in small interior patches to occurrence complete alteration (see figures 5-5A and B).

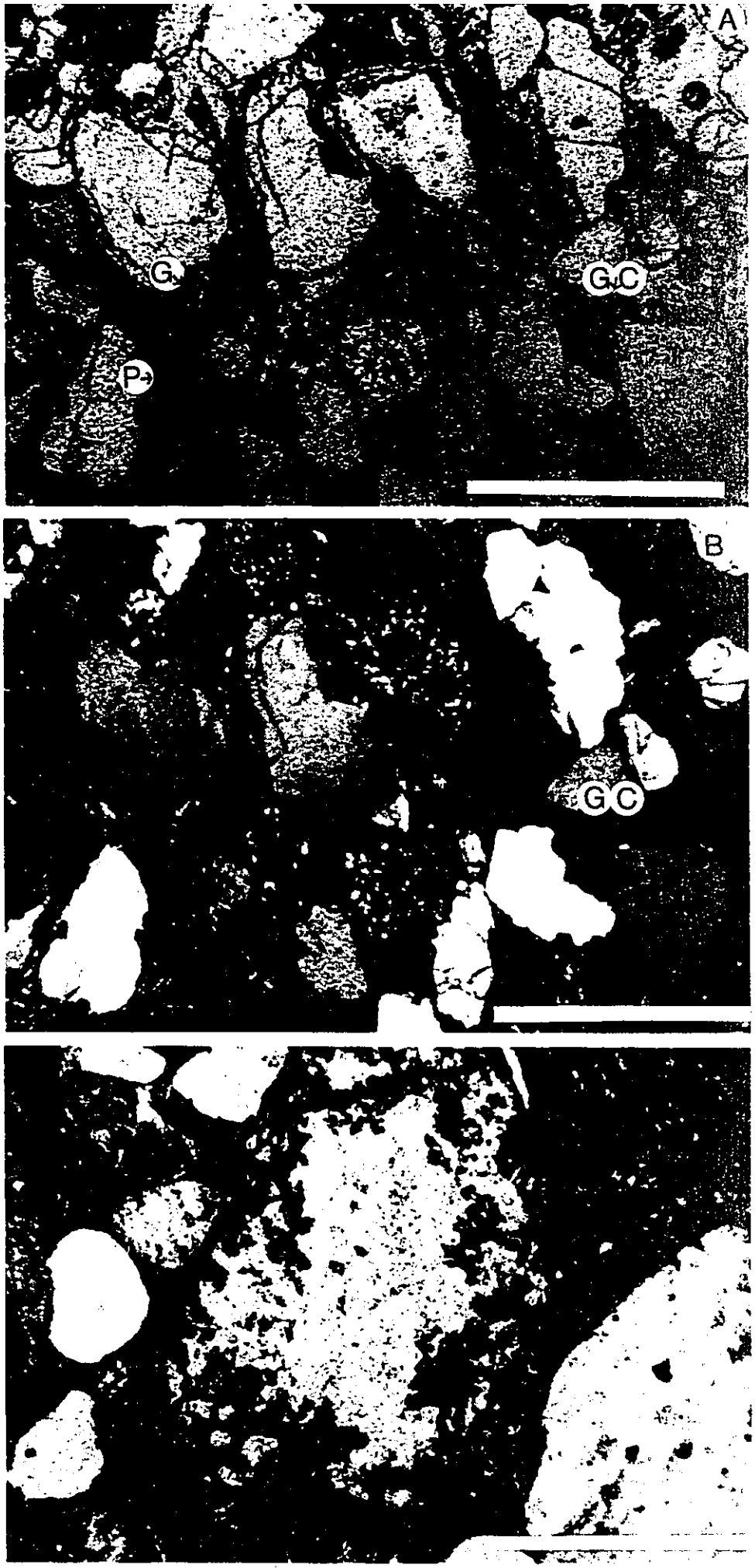
A
G
GC
P
B
GC

chert grains (?), bone and teeth fragments (figures B-9 and B-10) and as replacement of fecal pellets (Figure B-11, A and B). Pyritization takes several forms varying from alteration of bone and teeth fragments (Figure B-10) to associated precipitation with glauconite (Figure B-12, A and B).

Glauconite occurs as either alteration of clay laminae, pellets or, to varying degrees, as internal alteration of chert grains. Figures B-12, A and B show the mostly the former, although an extreme case of chert alteration can be seen, and Figure B-13 shows the latter. Hughes and Whitehead (1987) and Odin (1972) have reported similar occurrences of glauconite in chert and postulate that microscopic semi-reducing environments occur within the grains that allow for such formation. There are slight differences in the glauconitization of the Viking chert in that it is not restricted to inward growth from rims and may occur isolated within a grain. The glauconite is now mostly of the illitic variety (Odin, 1985; Odin and Matter, 1981; Giresse and Odin, 1973) as X-ray diffraction studies reveal (see Figure B-14). Rarely, smectitic varieties may be observed as very small swelling patches preserved within calcite cemented zones. This implies that most of the conversion is significantly post burial and that initially the glauconite was smectitic regionally as would be expected if the bulk clay mineralogy (Figure B-7) were mimicked by the glauconite (Bell and Goodell, 1967).

Following the above products are the cements and overgrowths of burial diagenesis. Most later diagenetic stages are additive rather than subtractive; there is very little dissolution of feldspar or quartz/chert etching. The occasional feldspar alterations observed include clay

Figure B-14. X-Ray Diffraction Patterns for Glauconite and Residue.

The diffraction patterns were obtained at a scanning rate of 2 degrees per minute under Cu K_ radiation. Prior to scanning the sample was separated in a Franz Isodynamic Separator following the separation criteria of Hughes and Whitehead (1987). However, 4 runs rather than 1 were made at each stage. (Samples were run at 0.3 amps, 10· side tilt and 20· forward tilt for 4 runs then at 0.5 amps, 5· side tilt and 25· forward tilt for 4 runs.) The vertical axis is relative intensity and the horizontal axis is degrees 2 theta.

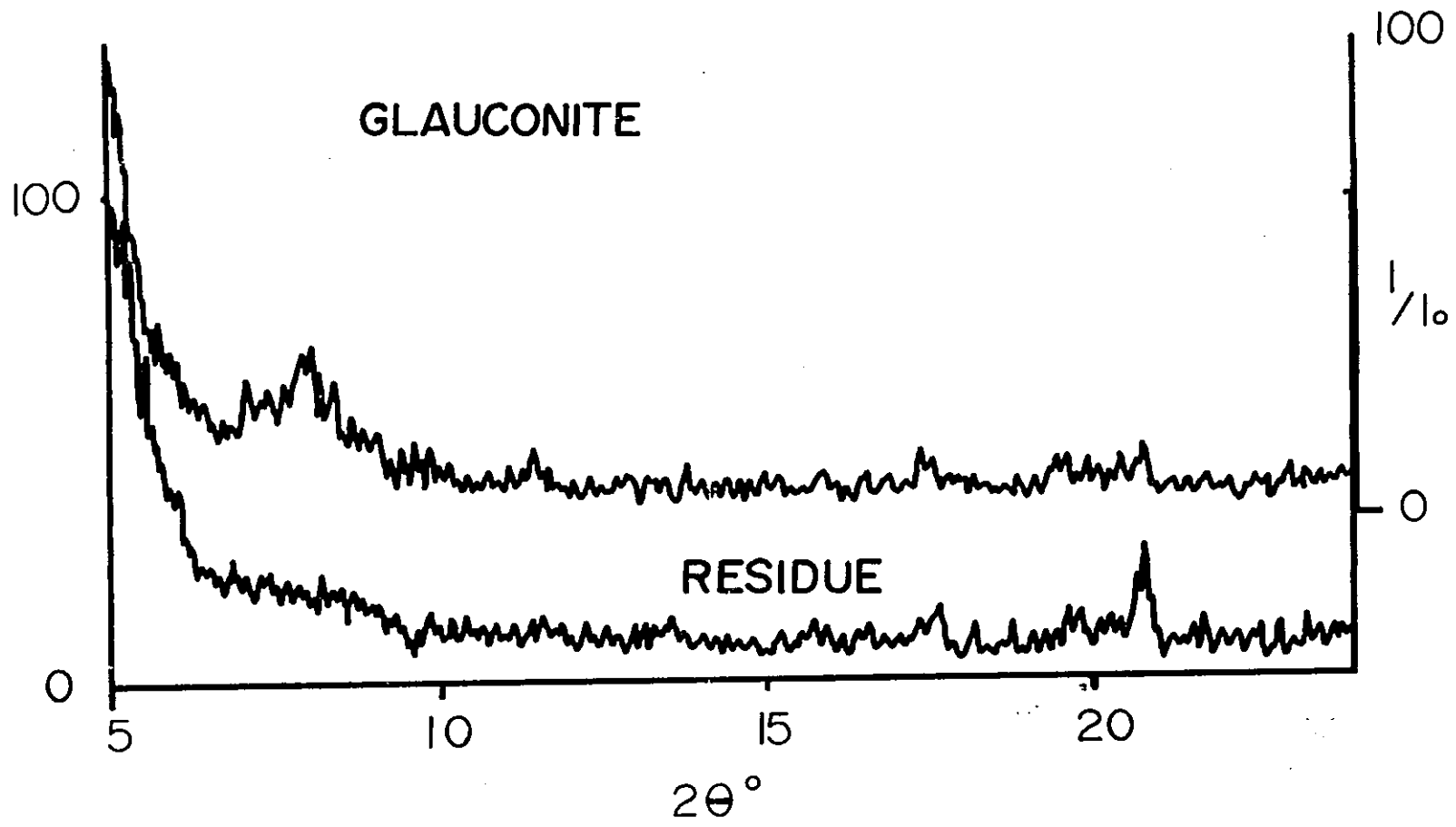
GLAUCONITE
RESIDUE
100
0
100
I/Io
0
5
10
15
20
2θ°

(kaolinite??) alteration of alkali feldspars, particularly those in the orthoclase class, sericitization of plagioclase and calcification of plagioclase. The timing of these events is difficult to place and may have been continuous except for calcification which seems directly related to precipitation of late calcite cement (see below).

Figures B-15 A and B show dolomite cement which is the next product. Blue staining (Figure B-15 A) reveals a high iron content which is confirmed by inhibition of intrinsic and extrinsic luminescence (Amieux, 1982; Smith and Stenstrom, 1965 (Figure B-15 B). There are no signs of quartz overgrowths.

Clay linings and bridging of pore spaces are observed at a stage post dating dolomite precipitation. Figures B-16 A and B show the textural evidence for this timing. In many cases, the two products are not together, so timing is inferred on the basis of the examples like those shown. The poorly crystalline nature of the clays under SEM is suggestive of smectite (figures B-16 C and D).

The next stage of diagenesis is the development of quartz overgrowths (visible as non-luminescing areas in figures B-18 A and B) probably associated with the beginning of greater compaction of the sands as judged by style of grain contacts. Increasingly concavo-convex contacts are visible in the figures.

Quartz overgrowths were followed by the precipitation of calcite cement, seen post-dating dolomite in Figure B-17 and B-18 and also shown in figures B-19 A and B. Staining indicates the calcite is moderately ferroan, containing in the vicinity of 1.5% FeO (Lindholm and Finkelman, 1972). The orange-red colour of the luminescence in figures B-18, B-19, B-20, B-21 and B-22 suggests a rather

Figure B-15A. Dolomite Cement

(6-23-52-19W4, 2643.4 feet depth, fine to medium sand, unit Gamma, white scale bar is 1mm; plane light, 3 seconds exposure of ISO 1600 film.)

Sparry dolomite cement has filled the porespace in this example. Compactional (non-tangential) grain contacts are rare suggesting early formation. The blue stain taken implies that the dolomite is highly ferroan. This is in agreement with the lack of luminescence in Figure 4-7B.

Figure B-15B. Dolomite Cement under Cathodoluminescence.

(6-23-52-19W4, 2643.4 feet depth, fine to medium sand, unit Gamma, white scale bar is 1mm; cathodoluminescence, 120 seconds exposure of ISO 1600 film at 0.5mA, 25mT and 20% focus.)

There is no luminescence of the dolomite in this example which is characteristic of all occurrences in the region studied. Also note that none of the quartz grains show evidence of overgrowths.


A

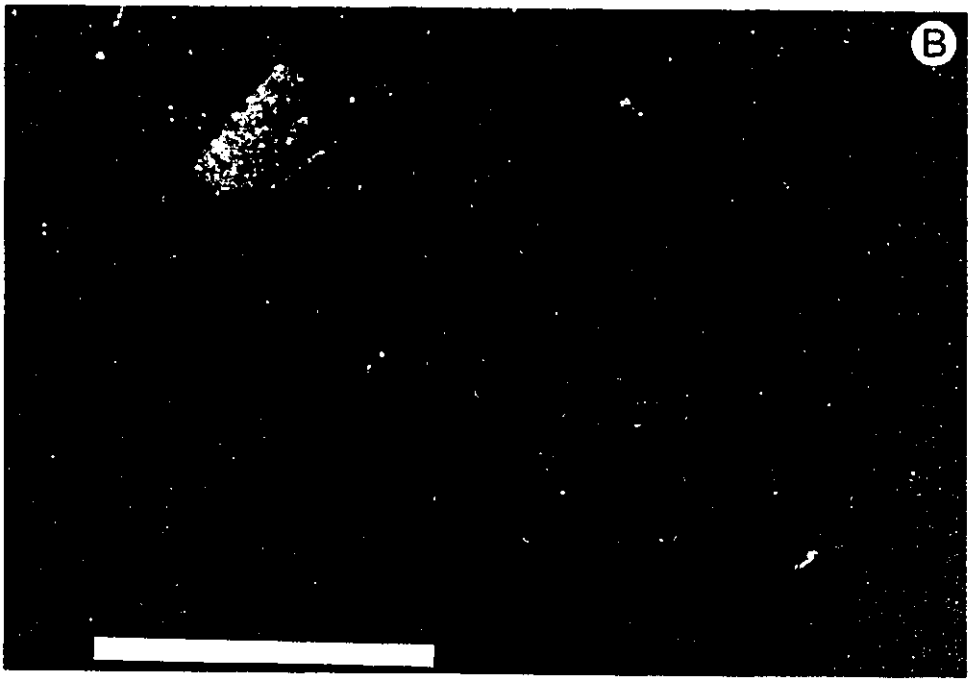
B

Figure B-16A. Clay Overgrowth on Dolomite in Thin Section.

(10-13-52-19W4, 2579 feet depth, coarse sand to granules, unit Beta, white scale bar is 1mm; plane light, 5 seconds exposure of ISO 1000 film.)

This photograph shows one of the rare examples of textural relationships between interstitial clay rims and bridges and other diagenetic products. Here clay, Cl, may be seen partially coating dolomite crystals. The dirty nature of the clay in thin section (brown colour, no form under high power) suggests smectite or smectite-illite forms.

Figure B-16B Clay Overgrowth on Dolomite under SEM.

(10-13-52-19W4, 2579 feet depth, coarse sand to granules, unit Beta; SEM, 15KV, see micron bar for scale, the magnification is not accurate for the photograph.)

Poorly formed clays may be seen coating the surface of the dolomite crystal in this example; the situation is identical to that in thin section above. The following figures, 5-8 C and D, show close ups of the clays on the surface (at 1) and at the junction of the dolomite with the chert grain below (at 2).

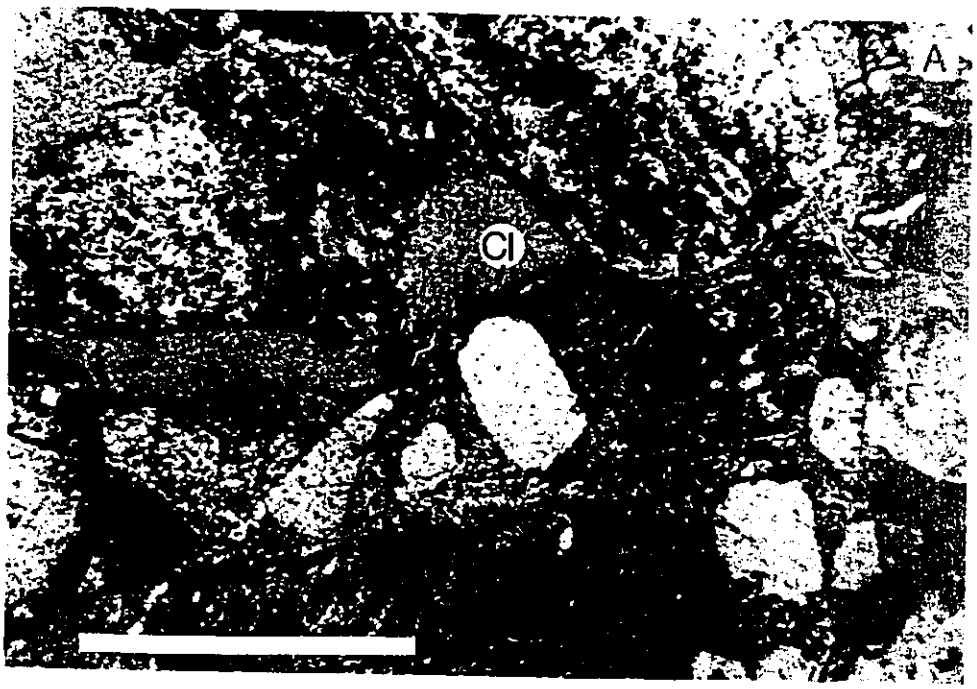
A
Cl

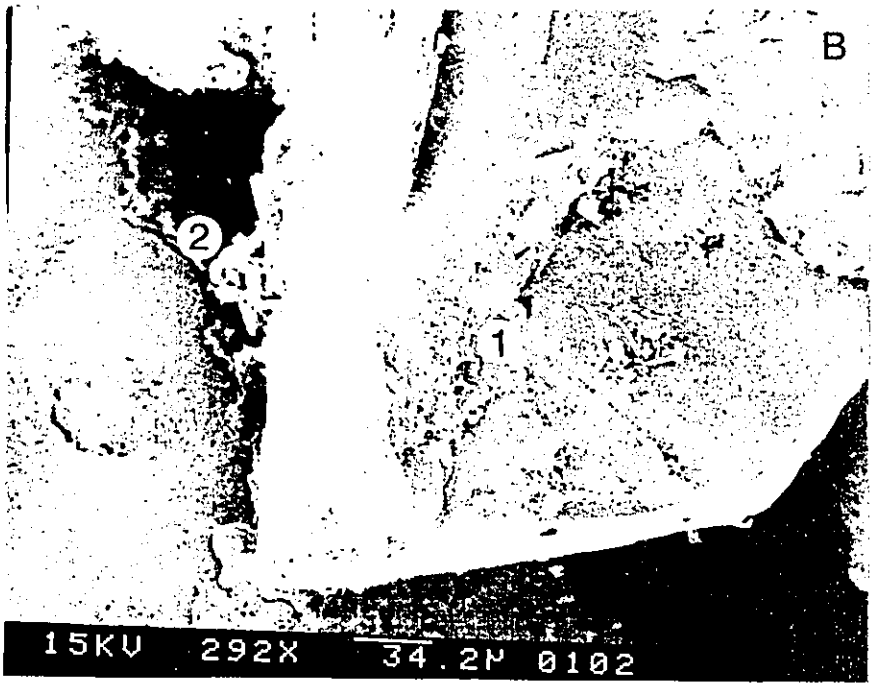
B
2
1
15KV 292X 34.2µ 0102

Figure B-16C. Detail of Clay Overgrowths on Dolomite under SEM.

(10-13-52-19W4, 2579 feet depth, coarse sand to granules, unit Beta; SEM, 15KV, see micron bar for scale, magnification is not accurate.)

This photograph is a detail of point 1 in Figure 8B. It reveals the poorly crystallized nature of most of the material which is strongly suggestive of smectites or illite-smectites. The exceptions are the well formed crystals at the bottom of the photograph which were the only such example spotted. These may be booklets of kaolinite.

Figure B-16D. Detail of Clay Overgrowth at Dolomite-Chert Junctions under SEM.

(10-13-52-19W4, 2579 feet depth, coarse sand to granules, unit Beta; SEM, 15KV, see micron bar for scale, magnification is not accurate.)

The form of the clay here is again typical of the smectite spectrum. Also present is an apparent case of framboidal pyrite in the center of the photograph (FP). Its presence suggests that there are different phases of pyrite formation in the Viking although the most visible seems to be that of early diagenesis shown in figures 5-5 A and B associated with glauconitization.

Figure B-17. Ferroan Calcite after Isolated Ferroan Dolomite.

(10-27-52-19W4, 2629.5 feet depth, medium to very coarse sand, unit C, white scale bar is 1mm; plain light, 10 second exposure of ISO 1000 film.)

Isolated spars of dolomite (D), stained light blue, are surrounded by sparry ferroan calcite stained dark purple. The apparent gradation in colour between dark blue and purple in the calcite seems to be an aberration of the staining procedure (over etching ??) as there is no corresponding zonation visible in cathodoluminescence photographs. The texture suggests that ferroan calcite post dates dolomite. Note that there are more signs of compaction in the form of straight to concavo-convex grain contacts here as compared to samples cemented by dolomite only (e.g.,Figure B-7 A and B).


C
15KV 5.78KX 1.73µ 0103

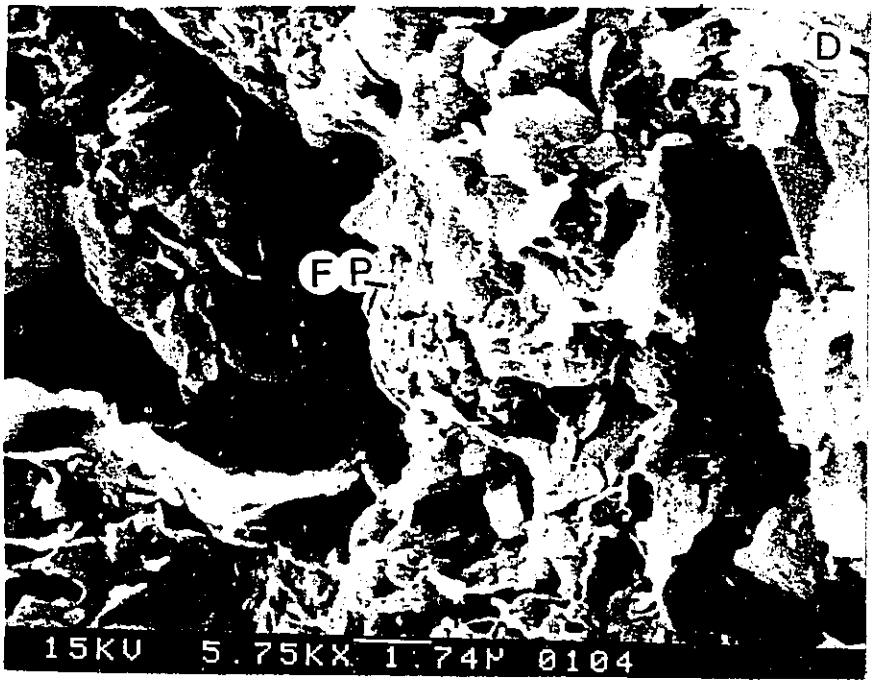
D
F
P
15KV 5.75KX 1.74µ 0104

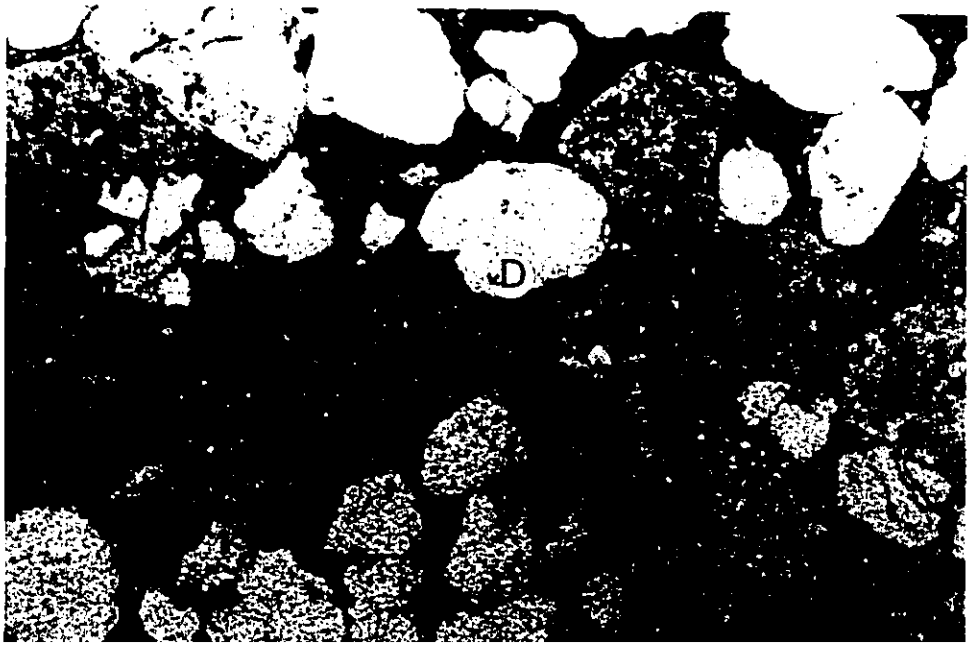
D

Figure B-18A. Mildly Ferroan Calcite Post Dating Quartz Overgrowths in Thin Section.

(10-11-50-18W4, 2585.5 feet depth, medium sand, unit Delta, white scale bar is 1mm; plain light, 3 seconds exposure of ISO 1000 film.)

The ferroan calcite is stained maroon indicating intermediate amounts of iron. Many of the quartz grains appear to have *in situ* quartz overgrowths (angular and connected), that texturally pre date the calcite. This is confirmed under cathodoluminescent examination (see Figure 10B).

Figure B-18B. Mildly Ferroan Calcite Post Dating Quartz Overgrowths under Cathodoluminescence.

(10-11-50-18W4, 2585.5 feet depth, medium sand, unit Delta, white scale bar is 1mm; cathodoluminescence, 120 seconds exposure of ISO 1600 film, 20% focus, 30mT, .5mA.)

Variations in luminescence confirms the presence of quartz overgrowths, the overgrowths showing no luminescence while most of the quartz grains are a dull blue. The calcite luminesces orange red despite the indication of some iron content by the staining technique. However, there is no indication of any zonation in the calcite. There appears to have been some compaction as judged by straight contacts even when the illusory contacts of the overgrowths are accounted for.


A

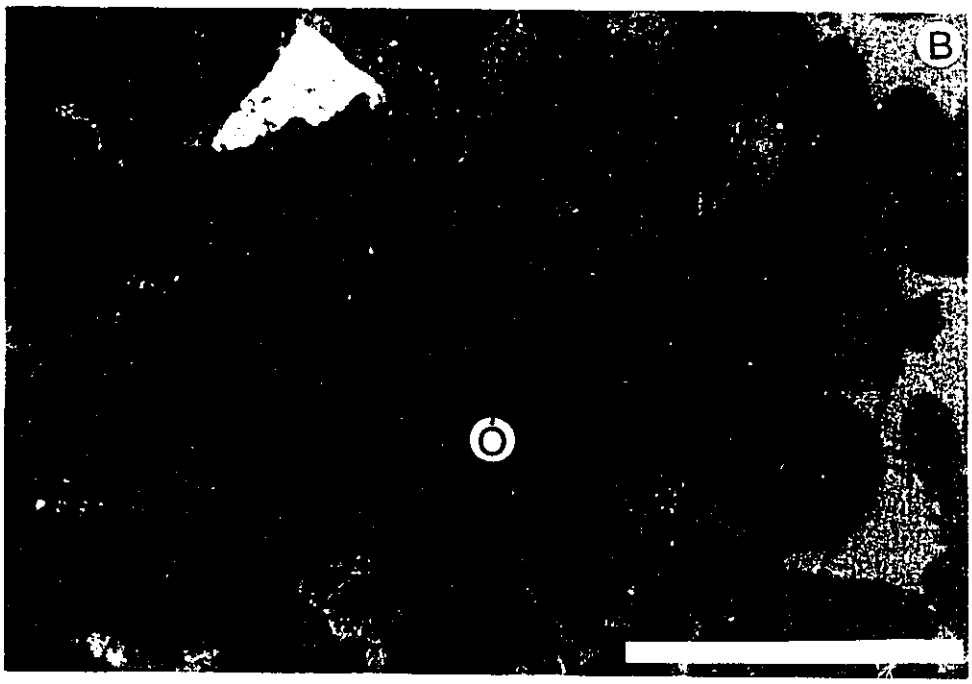
B

Figure B-19A. Contemporary Calcite and Siderite (?).

(10-29-45-18W4, 2922 feet depth, medium to very coarse sand, unit Beta, white scale bar is 1mm; plain light, 10 seconds exposure of ISO 1000 film.)

The pore space here has been completely filled by moderately ferroan calcite, reddish purple stain, and siderite rhombs (S). The relationship between the siderite and the calcite is uncertain.

Figure B-19B. Contemporary Calcite and Siderite (?).

(10-29-45-18W4, 2922 feet depth, medium to very coarse sand, unit Beta, white scale bar is 1mm; crossed nicols, 20 seconds exposure of ISO 1000 film.)

This crossed nicols photograph shows more clearly the presence of siderite in rhombic form either abutting against chert grains or apparently floating in the calcite. The intensity of the stain gives the calcite a false red colour in the photograph.


A
S

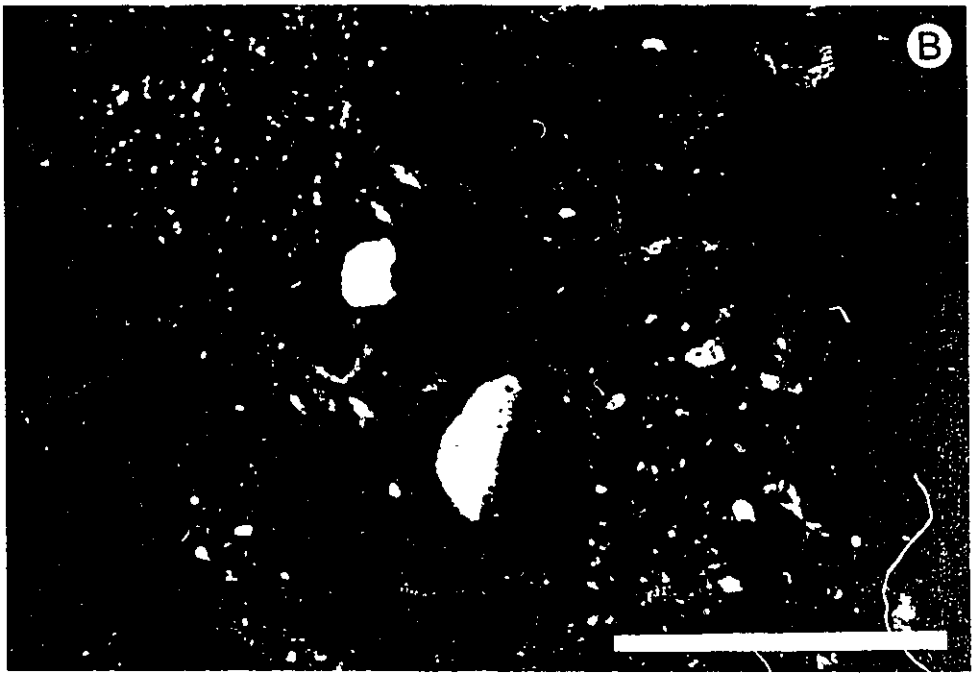
B

Figure B-20. Possible "Zoned" Sparry Calcite Cement Postdating Quartz Overgrowths under Cathodoluminescence.

(10-20-47-16W4, 2584 feet depth, medium to coarse sand, unit Beta, white scale bar is 1mm; cathodoluminescence, 120 seconds exposure of ISO 1600 film at 30% focus, .5mA and 38mT.)

This photograph is the only example of possible zonation in the calcite that was observed. The evidence is moreover, very tenuous. The variation in intensity of luminescence across the photograph is due to distortion of the ion beam which occurs at the 30% focus control setting and is irrelevant from the point of view of mineralogical variations. There is possibly a difference between a yellow orange and red orange calcite at the far left of the slide where the yellower patches are apparently randomly oriented relative to the grains. Quartz overgrowths occur prior to the calcite.

Figure B-21A. Unzoned Sparry Calcite Cement under Crossed Nicols.

(11-24-45-13W4, 2638 feet depth, lower medium sand, unit Beta, white scale bar is 1mm; crossed nicols, 10 seconds exposure of ISO 1600 film.)

The sparry calcite fills only part of the pore space but does so completely.

Figure B-21B. Unzoned Sparry Calcite Cement under Cathodoluminescence.

(11-24-45-13W4, 2368 feet depth, lower medium sand, unit Beta, white scale bar is 1mm; cathodoluminescence, 30 seconds exposure of ISO 1600 film at 20% focus, 0.4mA and 35mT.)

The unzoned nature of the orange red calcite may be clearly seen as may its postdating relationship with minor quartz overgrowths (QO). Some quartz overgrowths are irregular enough that they may either be inherited of partially dissolved. The degree of compaction is similar in both cemented and uncemented portions of the rock. Although not very clear at this scale, calcite has abrupt crystal boundaries; there is no evidence of dissolution of the calcite.

A
B
QO

Figure B-22A. Unzoned Sparry Calcite under Crossed Nicols.
(10-21-51-19W4, 2748.5 feet depth, medium to granular sand, unit Gamma, white scale bar is 1mm; 10 seconds exposure of ISO 1600 film.)
The calcite here shows features identical with that illustrated in figures 23, but it occurs at a different unit.

Figure B-22B. Unzoned Calcite under Cathodoluminescence.
(10-21-51-19W4, 2748.5 feet depth, medium to granular sand, unit Gamma, white scale bar is 1mm; 120 seconds exposure of ISO 1600 film at 20% focus, 35mT and .4mA.)
The only difference between this case and that of Figure 13B is that there are no quartz overgrowths present.


A

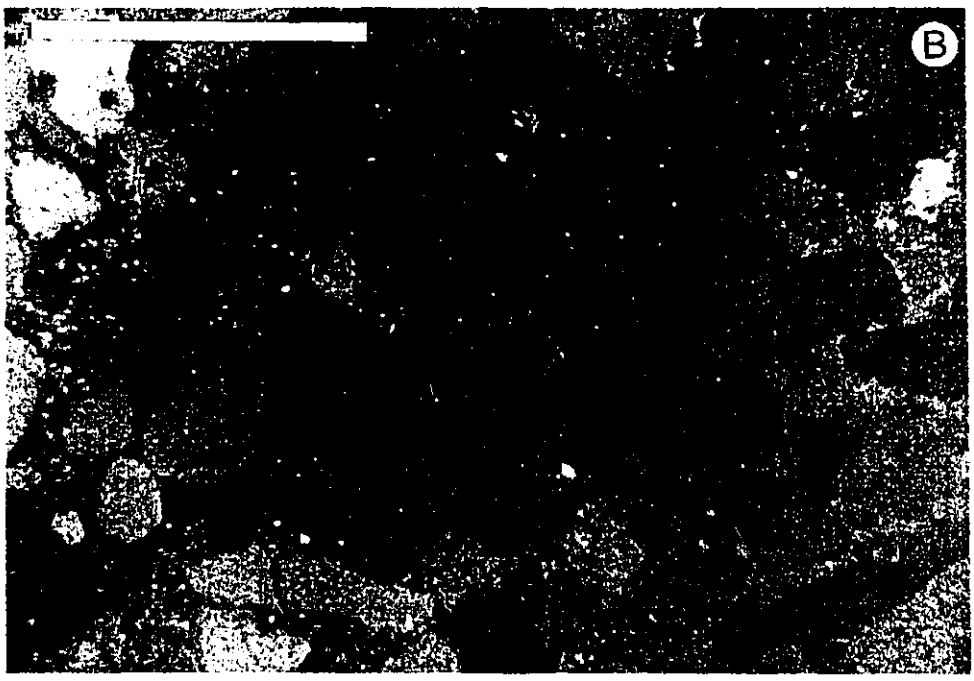
B

high relative proportion of Mn and that the iron is relatively reduced (Amieux, 1982). The calcite may fill in occasional fractured grains.

The last stage of diagenesis, perhaps penecontemporaneous with calcite precipitation is the formation of siderite rhombs shown in figures B-19 A and B. These are difficult to interpret texturally as they may be seen either attached to grains enclosed by calcite, floating in calcite or penetrating grains and calcite. They seem on the whole to have thus crystallized after the calcite perhaps locally replacing it.

The photomicrographs of figures B-17 through B-22 show that at no unit level is there an appreciable difference in the calcite cement, and moreover, that there exists no clear zonation of the cement allowing correlation of the host sands via 'cement stratigraphy'. Additionally, they do not suggest any dissolution of calcite; this is contrary to the mechanism of secondary porosity development proposed by Reinson and Foscolos (1986) to account for variations in porosity in calcite cemented zones in the region of the Viking that they studied. The straight form of the dolomite crystals, as illustrated in figures B-23 A-C is further evidence against dissolution of carbonate phases.

B.2.3 Diagenetic Variation

Consideration of units Epsilon, Delta, Gamma and Beta reveals no discernible differences in paragenesis; see Table B-1. Differences can be found from thin section to thin section because few samples display complete preservation of the diagenetic history; however, when that history is reconstructed for each unit, there are no distinct mineralogical responses.

Figure B-23A. Straight Edged Dolomite in Thin Section.
(6-22-52-19W4, 2656.4 feet depth, medium sand to granules, unit Gamma, white scale bar is 1mm; 2 seconds exposure of ISO 1600 film.)
The dolomite crystal (D) may be seen to have distinct edges intruding into the porespace. The well developed edges suggest that the patchy distribution is due to original precipitation patterns and not dissolution.

Figure B-23B. Straight Edged Dolomite under Crossed Nicols.
(6-22-52-19W4, 2656.4 feet depth, medium sand to granules, unit Gamma, white scale bar is 1mm; 5 seconds exposure of ISO 1600 film.)
The patchy distribution of the dolomite is clearer in this photograph due to its high birefringence.

Figure B-23C. Straight Edged Dolomite under Cathodoluminescence.
(6-22-52-19W4, 2656.4 feet depth, medium sand to granules, unit Gamma, white scale bar is 1mm; 120 seconds exposure of ISO 1600 film at 20% focus, .4mA and 35mT.)
The non-luminescing nature of the crystals suggest, along with the blue stain, that they are iron rich.


A
D
B
C

B.3 Bentonite Geochemistry

B.3.1 Techniques

Bentonites were analyzed by X-Ray Fluorescence (XRF) and Neutron Activation Analysis (NAA); the same samples were used for both analyses. XRF was used to quantify the Si, Al, Ca, K, Ti, Rb, Sr, Zr, Mg, Fe, Na, Mn, P, Nb and Y signatures. The elements analyzed by XRF were chosen to match those examined by Amajor and Lerbeckmo (1980). NAA was used to determine the signatures for the elements Nd, Sm, Eu, Tb, Yb, La and Ce. The heavy rare earth elements examined by NAA were chosen on the advice of Dr. Westgate at the University of Toronto following the reasoning that they would be least likely to mobilize and would offer the best chance of reflecting the original volcanic signature (Westgate p.comm. 1988). I did not analyze the bulk bentonite because in many cases there was obvious contamination from the surrounding sediments; for example, foraminifera tests can be found within the bentonites along with comparatively large amounts of quartz sand and silt. To remove this visible contamination, I disaggregated the samples and settled them in distilled water to separate material coarser than silt. The clay left in suspension was then dried and ground to pass through a 200 mesh sieve for analysis.

b.3.2 Results

Amajor and Lerbeckmo (1980) reported an ability to divide the bentonites into significant groups on the basis of the ratios of Ca/Sr and Rb/K. My results are shown compared to theirs and to those of Pozzobon (1988) in figure B-24. My data points have been labeled according to the postulated units containing the sample.

Figure B-24. Plot of XRF Data from Bentonites in All Viking Units.

The plot shows the ratio of calcium to strontium (in ppm) against the ratio of rubidium to potassium (in ppm) as derived from XRF analysis of the bentonite samples described in the text. The plot shows division according to Amajor and Lerbeckmo (1980) for bentonites elsewhere in the Viking and includes both their data and data from Pozzobon (1988) taken from the Viking in western Saskatchewan.

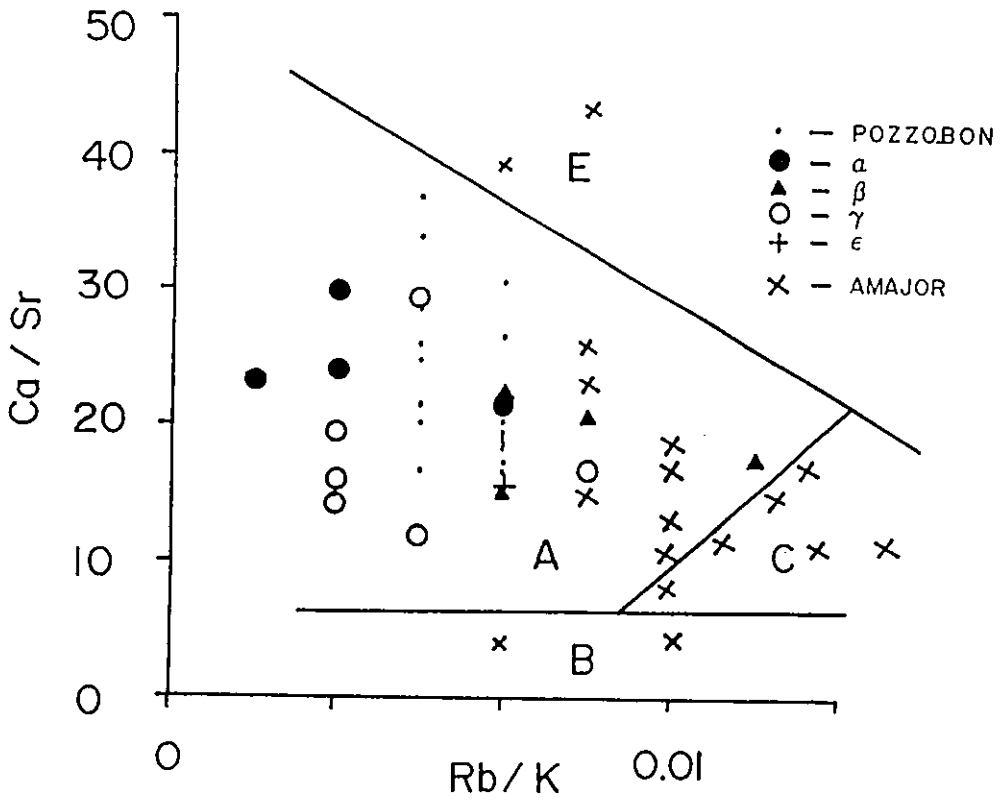

BENTONITE XRF DATA

(Plotted following Amajor and Lerbeckmo , 1980)

Figure B-25. Stick Plot of NAA Data from Bentonites in All Viking Units.

The figure shows the neutron activation analysis results for individual bentonites sampled from a variety of units. The postulated unit for each sample is indicated by shape code shown at the base of the plot. The abscissa shows the element analyzed; the ordinate shows the concentration present. The symbol enclosing or underlining each element marks the concentration scale to be used. Each sample is connected by lines to produce a `characteristic' pattern.

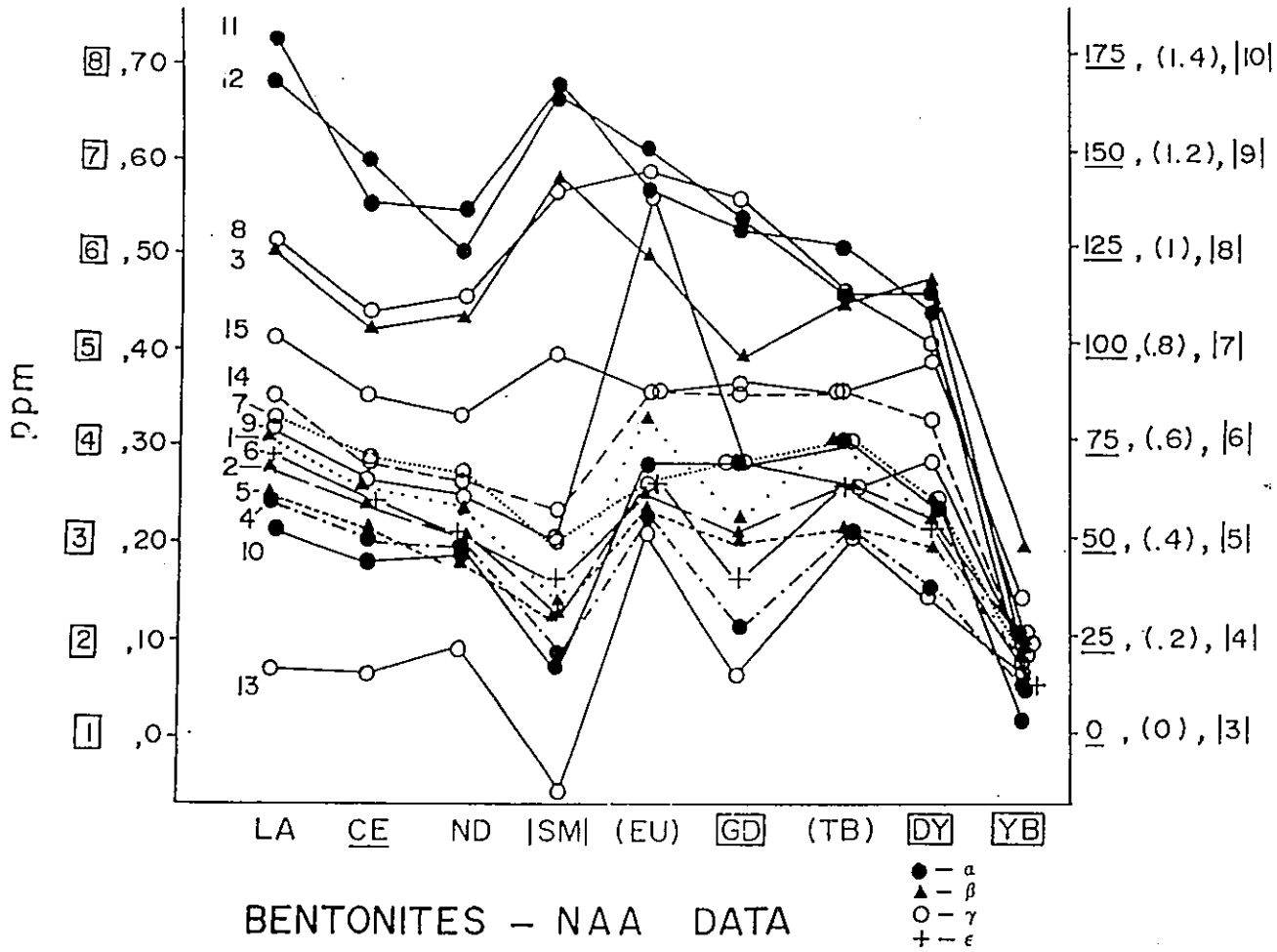
ppm
[8] ,70
[7] ,60
[6] ,50
[5] ,40
[4] ,30
[3] ,20
[2] ,10
[1] ,0
175 , (1.4), |10|
150 , (1.2), |9|
125 , (1), |8|
100 ,(.8), |7|
75 , (.6), |6|
50 , (.4), |5|
25 , (.2), |4|
0 , (0), |3|
11
12
8
3
15
14
7
9
1
6
2
5
4
10
13
LA CE ND |SM| (EU) GD (TB) DY YB
● – α
▲ – β
○ – γ
+ – ε
BENTONITES – NAA DATA

The results of the analysis are shown in figure B-25. Because of the relatively small sample size available, I have not run statistical analyses of these results; they would not be significant. The presentation is consequently only qualitative.

B.3.3 Discussion

Neither the XRF nor the NAA lead to any potential grouping of the bentonites that might confirm or deny the unit correlations based on the well logs and cores. This is particularly surprising for the XRF results because of the previous results of Amajor and Lerbeckmo (1980). Amajor and Lerbeckmo (1980) do not indicate what size fraction they analyzed, so I assume that they examined the entire bentonite sample. If so, it might be argued that they, in fact, measured a component in the larger sizes which I did not analyze because of the process of removing visible contamination. However, even if this were the case, the bentonites cannot be tagged over the entire formation because the results of Pozzobon (1988) from Saskatchewan fall, as do mine, into a fairly homogenous zone; they definitely do not following the groupings of Amajor and Lerbeckmo (1980) despite the fact that Pozzobon (1988) analyzed the bulk sample.

The NAA results tell a similar story and probably indicate extensive contamination even down to the clay size fraction. It is usually the case that volcanic events carry a fairly individual elemental tag (e.g., Bice, 1985; Borchardt et al., 1972; Yen and Goodwin, 1976), so it is surprising to see the relatively similar pattern generated by a variety of bentonites in figure B-25. To me this suggests that the samples are as contaminated in the fine size range as they are in the coarser and that the analysis in fact only shows a general pattern for the background sediment. The only hope for correlating

bentonites in the area of study thus seems to be by well logs in areas of high data density and pronounced resistivity signatures. Perhaps individual mineral component analysis such as sanidine or biotite might prove useful in the future.

APPENDIX C

MARKOV CHAIN ANALYSIS PROGRAM

The program listed below is written in QuickBasic V.4 and is designed to calculate significant transitions between non-parametric states (facies) using Markov chain analysis. The core of the program is taken from Wells (1989) modified as appropriate to account for changeover to QuickBasic. As such it will require minor modifications to run under other versions of BASIC.

Either embedded or standard Markov analysis may be chosen. For the embedded option the iterative, quasi-independence technique of Powers and Easterling (1982) is used. The calculation of the significant states is done using the binomial probability approach of Harper (1984).

The programming changes include both technical and theoretical variations. The technical alterations include modification of output control to allow for variable size matrix printing and automatic reading of data from a file of one of several given formats. This was done in a manner that allows any number of facies and their measurements which removes the restriction of 10 states (facies) or less imposed by Wells' code. Furthermore, users need no longer precalculate the number of transitions between states; this calculation has been made part of the program. All the user need enter is the measured sections in codified form along with the facies names. I also made a minor alteration to Wells' convergence criterion. Wells (1989) uses a fixed convergence criterion of 0.1 in his coding of the Powers and Easterling (1982) technique for row and column factor calculations. I have restored this to the original criterion of 0.1*(the ith - 1

factor) [see the cited article for details]. The program may be used to measure all transitions or to account for different sections at different locations.

The primary theoretical alteration is the option to compile transitions from sections postulated to be horizontally equivalent; this requires ignoring the transitions between tops and bases of the sections while compiling the internal transitions into one matrix. Furthermore the calculations have been encoded to ignore transitions between covered (or in the case of core unrecovered) intervals.

Data and facies names may be entered either from the keyboard or ASCII files. If automatic data entry is to be used, the data should be put into ASCII files in one of the following formats:

FACIES

or X, Y, ID, FACIES (X, Y = coordinates, ID = section identification)

IN ALL CASES, THE FACIES MUST BE INTEGER VALUES.

To run the program after compiling it with the QuickBASIC compiler the files INPUT.DAT and FACIES.DAT must be present in the same directory even if they are unused and/or empty. Theses two files should be created before execution on an independent editor capable of producing ASCII files.

FACIES.DAT must contain all the facies names to be used with each name on a separate line. Any number of potential irrelevant names may be included as the program will sift through the recorded transitions and select only those facies that are present in a particular analysis. This enables the user to prepare a file of all facies of interest in a given study even if not all of them occur in a particular set of data entered for analysis.

INPUT.DAT has two format options. In both options the facies code number must be entered as a simple integer. Covered interval code numbers may also be entered.

The program will prompt for this value when run. In the first format option, only the facies code number is entered with one code number per line. The file is thus constructed to represent the successions of states observed in a given section. The transitions are calculated continuously and are interrupted only by the presence of a covered interval. In the second option, the data must be entered in the following format:

x-location, y-location, identification, facies number code

Only one such entry is made per line. This option is used when sections from different locations are being jointly analyzed in horizontal artificial stacking. The location values are used by the program to keep track of when it is has to ignore transitions between different locations. The identification code is for the user's benefit in referring to the location; it might, for example be a well L.S.D. number. The facies number code is used exactly as in the first format option for the calculation of transitions between states.

The program is executed by typing MARK2 at the appropriate prompt.

PROGRAM LISTING

```
  '   Powers & Easterling's Markov Analysis
  ' J. Bartlett incorporating and modifying Neil Wells (1989)
  '
  OPEN "INPUT.DAT" FOR INPUT AS #1
  OPEN "FACIES.DAT" FOR INPUT AS #2
  PRINT " DO YOU WANT TO ANALYZE FOR EMBEDDED MARKOV CHAINS
(Y OR N)"; : INPUT EMB$
  PRINT " "
  PRINT "TYPE 3 FOR FULL PRINT-OUT OF MATRICES AND FAVORED
TRANSITIONS;"
  PRINT "     2 FOR A SELECTION OF NON-RANDOM TRANSITIONS ONLY;"
  PRINT "     1 FOR BINOMIAL PROBABILITIES OF SELECTED CELLS ONLY."
  INPUT Z4
  PRINT "WHAT FORM OF OUTPUT DO YOU WANT?"
  PRINT " (If your choice will include printer output turn the printer"
  PRINT "  on NOW)"
  PRINT " "
  PRINT "   1. SCREEN"
  PRINT "   2. PRINTER"
  PRINT "   3. BOTH"
  PRINT "  "
  PRINT " (IF YOU WISH TO USE THE PRINTER TURN IT ON.)"
  PRINT " "
  PRINT "WHICH NUMBER"; : INPUT CHOI
  IF CHOI <> 2 THEN SCR$ = "Y" ELSE SCR$ = "N"
  IF CHOI <> 1 THEN PR$ = "Y" ELSE PR$ = "N"
  IF EMB$ = "N" OR EMB$ = "n" GOTO 11
  PRINT "HOW MANY ITERATIONS DO YOU WANT"; : INPUT IT
11 PRINT "DO YOU WANT TO READ DATA FROM INPUT.DAT (Y OR N)"; :
INPUT AN$
  IF AN$ = "N" THEN 90
  IF AN$ = "n" THEN 90
  PRINT "TITLE"; : INPUT T$
  PRINT "HOW MANY FACIES "; : INPUT N
  PRINT "WHAT IS THE FACIES CODE FOR A COVERED INTERVAL"; : INPUT
CI
20 DIM T(IT): DIM U(IT): DIM X(IT, N): DIM Y(IT, N)
  DIM MAX(N): DIM N3(N): DIM F(N): DIM G(N): DIM F$(N)
  DIM A(N, N): DIM B(N, N): DIM C(N, N): DIM D(N, N): DIM E(N, N)
```

```
  FOR C = 1 TO N: F(C) = 0: G(C) = 0: MAX(C) = 0: N3(C) = 0: NEXT C
  FOR C = 1 TO IT: T(IT) = 0: U(IT) = 0: NEXT C
  IF CHECK$ = "Y" GOTO 140
  PRINT "DO YOU WANT THE FACIES NAMES READ FROM FACIES.DAT"; :
INPUT FAC$
  IF FAC$ = "Y" THEN 21
  IF FAC$ = "y" THEN 21
  GOTO 22
21 FOR K = 1 TO N
   INPUT #2, FS(K)
  NEXT K
  GOTO 23
22 FOR R = 1 TO N: FOR C = 1 TO N: A(R, C) = 0: NEXT C: NEXT R
  PRINT "TYPE EACH FACIES NAME FOLLOWED BY ENTER"
  FOR I = 1 TO N: INPUT FS(I): NEXT I
23 PRINT "HOW MANY OBSERVATIONS ARE THERE"; : INPUT NUM
  PRINT "CHOOSE ONE OF THE FOLLOWING FORMATS FOR DATA
READING:"
  PRINT "   1.  FACIES"
  PRINT "   2.  X,Y,ID.,FACIES (ignores transitions between"
  PRINT "                      different locations)"
  PRINT " WHICH NUMBER"; : INPUT WHICH
  PRINT " READING DATAFILE; PLEASE WAIT."
  IF WHICH = 1 GOTO 50
  '--------------------
  ' An input scheme for facies with locations
  FOR K = 1 TO NUM
    INPUT #1, LNG, LAT, WELLS, FACIES
    IF K = 1 GOTO 40
    IF LAT <> PLAT OR LNG <> PLONG THEN GOTO 40
    IF FACIES = CI OR PFACIES = CI THEN GOTO 40
    FOR I = 1 TO N
        FOR J = 1 TO N
         IF EMBS = "Y" OR EMBS = "y" THEN
          IF I = J GOTO 30
         END IF
         IF (PFACIES = I) AND (FACIES = J) THEN A(I, J) = A(I, J) + 1
30     NEXT J
    NEXT I
40  PLAT = LAT: PLONG = LNG: PFACIES = FACIES
  NEXT K
  GOTO 110
```

```
  ' -----------------
50 ' A facies only input routine
  FOR K = 1 TO NUM
    INPUT #1, FACIES
    IF K = 1 GOTO 70
    IF FACIES = CI OR PFACIES = CI THEN GOTO 70
    FOR I = 1 TO N
        FOR J = 1 TO N
         IF EMB$ = "Y" OR EMB$ = "y" THEN
          IF I = J GOTO 60
         END IF
         IF (PFACIES = I) AND (FACIES = J) THEN A(I, J) = A(I, J) + 1
60     NEXT J
    NEXT I
70  PFACIES = FACIES
  NEXT K
  GOTO 110
90 PRINT "DO YOU WISH TO INPUT TRANSITION DATA ON KEYBOARD, Y
OR N"; : INPUT B$
  IF B$ = "Y" THEN 100
  IF B$ = "y" THEN 100
  PRINT "THERE ARE NO MORE ALTERNATIVES! START AGAIN."
  STOP
100 PRINT "TITLE "; : INPUT T$
' Dimensioning routine
  PRINT "HOW MANY FACIES "; : INPUT N
  DIM MAX(N): DIM N3(N): DIM F(N): DIM G(N): DIM F$(N)
  DIM A(N, N): DIM B(N, N): DIM C(N, N): DIM D(N, N): DIM E(N, N)
  DIM T(IT): DIM U(IT): DIM X(IT, N): DIM Y(IT, N)
  FOR C = 1 TO N: F(C) = 0: G(C) = 0: MAX(C) = 0: N3(C) = 0: NEXT C
  FOR C = 1 TO IT: T(IT) = 0: U(IT) = 0: NEXT C
  PRINT "TYPE EACH FACIES NAME FOLLOWED BY ENTER";
    FOR I = 1 TO N: INPUT F$(I): NEXT I
    PRINT "INPUT DATA BY ROWS (ONE CELL ENTRY AT A TIME FOLLOWED
BY ENTER"
    PRINT "";
    FOR R = 1 TO N: FOR C = 1 TO N: INPUT A(R, C): NEXT C: NEXT R
' ------------------------------------------------
110 ' end input routine; start analysis
    IF PR$ = "Y" THEN
     LPRINT "MARKOV ANALYSIS ": LPRINT T$: LPRINT
    END IF
```

```
' calculating row totals F(R), column totals G(C), & grand total T

   FOR R = 1 TO N
    FOR C = 1 TO N
     F(R) = F(R) + A(R, C)
     G(C) = G(C) + A(R, C)
    NEXT C
    T = T + F(R)
   NEXT R

' check for zero row or column totals; rearrange matrices if found
    DIM TAG(N): DIM ASEC(N,N): DIM GS(N): DIM FS(N): DIM FSS(N): GOTO
112
111  REDIM TAG(N)
' tag row and columns to be deleted
112  FOR I = 1 TO N
     IF F(I) = 0 THEN TAG(I) = I
     IF G(I) = 0 THEN TAG(I) = I
    NEXT I
' remove overwritten row totals from total
    FOR I = 1 TO N
     IF TAG(I) = I THEN T = T - F(I)
    NEXT I
' count number of removals
    E = 0
    FOR I = 1 TO N
     IF TAG(I) <> 0 THEN E = E + 1
    NEXT I
    IF E = 0 THEN 113
' remove any tallied values from relevant totals
    FOR I = 1 TO N
     IF G(I) = 0 AND F(I) <> 0 THEN
      FOR J = 1 TO N
       G(J) = G(J) - A(I,J)
      NEXT J
     END IF
    NEXT I
    FOR J = 1 TO N
     IF F(J) = 0 AND G(J) <> O THEN
      FOR I = 1 TO N
       F(I) = F(I) - A(I,J)
```

```
      NEXT I
     END IF
    NEXT J
' transfer valid row and columns to smaller arrays
    REDIM ASEC(N - E, N - E)
    C = 0
    FOR J = 1 TO N
     R = 0
     IF TAG(J) = 0 THEN
      C = C + 1
      FOR I = 1 TO N
         IF TAG(I) = 0 THEN
          R = R + 1
          ASEC(R, C) = A(I, J)
         END IF
      NEXT I
     END IF
    NEXT J
' transfer valid row & col. totals to smaller arrays
    REDIM FS(N - E): REDIM GS(N - E)
    QU = 0
    FOR I = 1 TO N
     IF TAG(I) = 0 THEN
         QU = QU + 1
         FS(QU) = F(I)
         GS(QU) = G(I)
     END IF
    NEXT I
' transfer valid facies names to a smaller array
    XE = 0
    REDIM FS$(N - E)
    FOR I = 1 TO N
     IF TAG(I) = 0 THEN
      XE = XE + 1
      FS$(XE) = F$(I)
     END IF
    NEXT I

' redimension standard arrays and write manipulated arrays into
 them
    N = N - E
    ERASE A, F, G, F$
```

```
    REDIM A(N, N): REDIM F(N): REDIM G(N): REDIM F$(N)
    FOR I = 1 TO N
     F(I) = FS(I)
     G(I) = GS(I)
     F$(I) = FS$(I)
     FOR J = 1 TO N
      A(I, J) = ASEC(I, J)
     NEXT J
    NEXT I

' repeat the procedure to check against minor elimations leading to new 0 sums

    GOTO 111

' printing matrix #,

113 IF PR$ <> "Y" THEN 129
   IF Z4 < 3 THEN 140
   LPRINT "NUMBER OF FACIES "; N
   LPRINT : LPRINT "FACIES:": LPRINT
   FOR I = 1 TO N: LPRINT USING "##"; I; : LPRINT "  "; F$(I): NEXT I
   IF N < 10 THEN Q = 1: M = N: P = 1: L = N: GOTO 120
   L = 10
   P = L - 9
120 LPRINT : LPRINT : LPRINT "TRANSITIONS MATRIX; "; T$: LPRINT
   LPRINT " #";
   FOR C = P TO L: LPRINT "    "; : LPRINT "#"; : LPRINT USING "##"; C; : NEXT
C
   LPRINT
   FOR R = 1 TO N
    LPRINT USING "##"; R;
     FOR C = P TO L
      LPRINT "    "; : LPRINT USING "###"; A(R, C);
     NEXT C
      IF N - L = 0 THEN LPRINT "    "; : LPRINT USING "####";  F(R) ELSE LPRINT
" "
   NEXT R
   LPRINT
   LPRINT "  ";
   FOR C = P TO L: LPRINT "    "; : LPRINT USING "###"; G(C); : NEXT C
   IF N - L = 0 THEN
    LPRINT "    "; : LPRINT USING "####"; T
```

```
   END IF
   P = L + 1
   L = L + 10
   IF N - L <= -10 THEN GOTO 140
   IF N - L <= 0 THEN L = N: GOTO 120
   GOTO 120

' Screen printing matrices

129 IF SCR$ <> "Y" THEN 140
   PRINT "NUMBER OF FACIES "; N
   PRINT : PRINT "FACIES:": PRINT
   FOR I = 1 TO N: PRINT USING "##"; I; : PRINT "  "; F$(I)
   NEXT I
   IF N < 10 THEN Q = 1: M = N: P = 1: L = N: GOTO 130
   L = 10
   P = L - 9
130 PRINT : PRINT : PRINT "TRANSITIONS MATRIX; "; T$: PRINT
   PRINT " #";
   FOR C = P TO L: PRINT "    "; : PRINT "#"; : PRINT USING "##"; C; : NEXT C
   PRINT
   FOR R = 1 TO N
    PRINT USING "##"; R;
    FOR C = P TO L
     PRINT "    "; : PRINT USING "###"; A(R, C);
    NEXT C
    IF N - L = 0 THEN PRINT "    "; : PRINT USING "####"; F(R) ELSE PRINT "  "
   NEXT R
   PRINT
   PRINT "  ";
   FOR C = P TO L: PRINT "    "; : PRINT USING "###"; G(C); : NEXT C
   IF N - L = 0 THEN
    PRINT "    "; : PRINT USING "####"; T
   END IF
   P = L + 1
   L = L + 10
   IF N - L <= -10 THEN GOTO 140
   IF N - L <= 0 THEN L = N: GOTO 130
   GOTO 130

' start of iterations for row and column factors
' first iteration only, I=1, row factors X(I,R) & total of row factors
```

```
140 IF EMB$ = "n" OR EMB$ = "N" THEN 230
   PRINT "ITERATING ROW AND COLUMN FACTORS; PLEASE WAIT."
   I = 1
   FOR R = 1 TO N
    X(I, R) = F(R) / (N - 1)
    T(I) = T(I) + X(I, R)
   NEXT R

' column factors Y(I,C) and total of column factors U(I)
' H=counter: if all differences <0.01 then H=0 in line 180

150 H = 0
   FOR C = 1 TO N
    Y(I, C) = G(C) / (T(I) - X(I, C))
    U(I) = U(I) + Y(I, C)
    IF I = 1 THEN 160
    IF ABS(Y(I, R) - Y(I - 1, R)) <= .01 * Y(I, R) THEN 160
    H = H + 1
160 NEXT C

' row factor iterations beyond first iteration (I>1)
' row factors, row factor totals, difference between iterations, and
' check against failure to converge (causes abandonment of program)

   I = I + 1
   FOR R = 1 TO N
    X(I, R) = F(R) / (U(I - 1) - Y(I - 1, R))
    T(I) = T(I) + X(I, R)
    IF ABS(X(I, R) - X(I - 1, R)) <= .01 * X(I, R) THEN 170
    H = H + 1
170 NEXT R
   IF I < IT THEN 180
   PRINT IT; " ITERATIONS, NO CONVERGENCE YET": PRINT " "
   PRINT "WHAT NEW TOTAL OF ITERATIONS SHOULD BE TRIED"; : INPUT
IT
   REDIM T(IT): REDIM U(IT): REDIM X(IT, N): REDIM Y(IT, N): GOTO 140
180 IF H > 0 THEN 150

' printing row and column factors

181 IF PR$ <> "Y" THEN 202
```

```
   IF Z4 < 3 THEN 230
   LPRINT
   LPRINT
   LPRINT : LPRINT "ROW & COLUMN FACTORS; "; T$
   IF N < 10 THEN M = N ELSE M = 10
   Q = 1
190 LPRINT : LPRINT "Row Totals";
   FOR R = Q TO M: LPRINT USING "#######"; F(R); : NEXT R
   IF N - M = 0 THEN LPRINT "totals" ELSE LPRINT " "
   FOR G = 1 TO I
    LPRINT "      "; G; "r";
    FOR R = Q TO M
     LPRINT USING "###.##"; X(G, R);
    NEXT R
    IF N - M = 0 THEN LPRINT "   "; : LPRINT USING "###.##"; T(G) ELSE LPRINT
" "
    IF G = I THEN 200
    LPRINT "      "; G; "c";
    FOR C = Q TO M
     LPRINT USING "###.##"; Y(G, C);
    NEXT C
    IF N - M = 0 THEN LPRINT "   "; : LPRINT USING "###.##"; U(G) ELSE LPRINT
" "
   NEXT G
200 Q = M + 1
   M = M + 10
   IF N - M <= -10 THEN 230
   IF N - M <= 0 THEN M = N: GOTO 190
   GOTO 190

' printing row and column factors to screen

202 IF SCR$ <> "Y" THEN 230
   IF Z4 < 3 THEN 230
   PRINT
   PRINT
   PRINT : PRINT "ROW & COLUMN FACTORS; "; T$
   IF N < 10 THEN M = N ELSE M = 10
   Q = 1
210 PRINT : PRINT "Row Totals";
   FOR R = Q TO M: PRINT USING "#######"; F(R); : NEXT R
   IF N - M = 0 THEN PRINT "totals" ELSE PRINT " "
```

```
   FOR G = 1 TO I
    PRINT "      "; G; "r";
    FOR R = Q TO M
     PRINT USING "###.##"; X(G, R);
    NEXT R
    IF N - M = 0 THEN PRINT "   "; : PRINT USING "###.##"; T(G) ELSE PRINT " "
    IF G = I THEN 220
    PRINT "      "; G; "c";
    FOR C = Q TO M
     PRINT USING "###.##"; Y(G, C);
    NEXT C
    IF N - M = 0 THEN PRINT "   "; : PRINT USING "###.##"; U(G) ELSE PRINT " "
   NEXT G
220 Q = M + 1
   M = M + 10
   IF N - M <= -10 THEN 230
   IF N - M <= 0 THEN M = N: GOTO 210
   GOTO 210

' calculating expected and difference
' B=expected, C=difference, D=chi-square,

230 FOR R = 1 TO N
    FOR C = 1 TO N
     IF EMB$ = "y" OR EMB$ = "Y" THEN
        B(R, C) = X(I, R) * Y(I - 1, C)
     ELSE
        B(R, C) = F(R) * G(C) / T
     END IF
     C(R, C) = A(R, C) - B(R, C)
     D(R, C) = C(R, C) ^ 2 / B(R, C)
     IF EMB$ = "y" OR EMB$ = "Y" THEN
      IF R = C THEN 240
     END IF
     X2 = X2 + D(R, C)
     IF EMB$ = "y" OR EMB$ = "Y" THEN 250
240   IF R <= C THEN 280
250   IF R < C THEN 280
     IF A(R, C) - A(C, R) <> 0 THEN GOTO 260
     E(R, C) = 0: GOTO 270
260   E(R, C) = (A(R, C) - A(C, R)) ^ 2 / (A(R, C) + A(C, R))
270   X3 = X3 + E(R, C)
```

```
    IF A(R, C) OR A(C, R) <> 0 THEN 280
    Z0 = Z0 + 1
280 NEXT C
  NEXT R

' printing of four matrices

  IF PR$ <> "Y" THEN 411
  IF Z4 < 3 THEN 550
  FOR Z = 1 TO 4
   LPRINT : LPRINT : LPRINT : ON Z GOTO 290, 300, 310, 320
290 LPRINT "EXPECTED VALUES": GOTO 330
300 LPRINT "DIFFERENCE MATRIX": GOTO 330
310 LPRINT "SEQUENCE CHI-SQUARE MATRIX": GOTO 330
320 LPRINT "ASYMMETRY CHI-SQUARE MATRIX": GOTO 330
330 IF N < 10 THEN M = N ELSE M = 10
  Q = 1
340 LPRINT " "
  LPRINT " #    ";
  FOR C = Q TO M: LPRINT USING "#######"; C; : NEXT C: LPRINT
  LPRINT " "
  FOR R = 1 TO N
   LPRINT USING "##"; R;
   LPRINT "    ";
   FOR C = Q TO M
    IF EMB$ = "Y" OR EMB$ = "y" THEN
      IF R = C THEN 390
    END IF
    ON Z GOTO 350, 360, 370, 380
350   LPRINT USING "####.##"; B(R, C); : GOTO 400
360   LPRINT USING "####.##"; C(R, C); : GOTO 400
370   LPRINT USING "####.##"; D(R, C); : GOTO 400
380   IF EMB$ = "Y" OR EMB$ = "y" THEN 381
    IF R <= C THEN 390
381   IF R < C THEN 390
    LPRINT USING "####.##"; E(R, C); : GOTO 400
390   LPRINT "   - ";
400 NEXT C
   LPRINT " "
  NEXT R
  Q = M + 1
  M = M + 10
```

```
    IF N - M <= -10 THEN 410
    IF N - M <= 0 THEN M = N: GOTO 340
    GOTO 340
410 NEXT Z

' DF=chi-square degrees of freedom; DOF= asymmetry degrees of freedom

    DF = (N - 1) ^ 2 - N
   LPRINT : LPRINT "sequence chi-square sum ="; X2, DF; "degrees of freedom"
    DOF = (N * (N - 1) / 2) - Z0
   LPRINT : LPRINT "asymmetry chi-square ="; X3, DOF; " degrees of freedom"

' printing of four matrices to screen

411 IF SCR$ <> "Y" THEN 550
   IF Z4 < 3 THEN 550
   FOR Z = 1 TO 4
    PRINT : PRINT : PRINT : ON Z GOTO 420, 430, 440, 450
420  PRINT "EXPECTED VALUES": GOTO 460
430  PRINT "DIFFERENCE MATRIX": GOTO 460
440  PRINT "SEQUENCE CHI-SQUARE MATRIX": GOTO 460
450  PRINT "ASYMMETRY CHI-SQUARE MATRIX": GOTO 460
460  IF N < 10 THEN M = N ELSE M = 10
   Q = 1
470  PRINT "  "
    PRINT " #     ";
    FOR C = Q TO M: PRINT USING "########"; C; : NEXT C: PRINT
    PRINT " "
    FOR R = 1 TO N
     PRINT USING "##"; R;
     PRINT "     ";
     FOR C = Q TO M
      IF EMB$ = "y" OR EMB$ = "Y" THEN
         IF R = C THEN 521
      END IF
      ON Z GOTO 480, 490, 500, 510
480    PRINT USING "####.##"; B(R, C); : GOTO 530
490    PRINT USING "####.##"; C(R, C); : GOTO 530
500    PRINT USING "####.##"; D(R, C); : GOTO 530
510    IF EMB$ = "Y" OR EMB$ = "y" THEN 520
      IF R <= C THEN 521
520    IF R < C THEN 521
```

```
     PRINT USING "####.##"; E(R, C); : GOTO 530
521   PRINT "   - ";
530   NEXT C
     PRINT " "
    NEXT R
    Q = M + 1
    M = M + 10
    IF N - M <= -10 THEN 540
    IF N - M <= 0 THEN M = N: GOTO 470
    GOTO 470
540 NEXT Z

' DF=chi-square degrees of freedom; DOF= asymmetry degrees of freedom
    DF = (N - 1) ^ 2 - N
   PRINT : PRINT "sequence chi-square sum ="; X2, DF; " degrees of freedom"
    DOF = (N * (N - 1) / 2) - Z0
   PRINT : PRINT "asymmetry chi-square ="; X3, DOF; " degrees of freedom"

550 IF Z4 < 2 THEN 651
   IF PR$ <> "Y" THEN 601
   LPRINT : LPRINT : LPRINT "PRINCIPLE SUCCESSION FOR EACH FACIES"
   LPRINT "binomial probabilities listed at right give probability"
   LPRINT "(confidence level = 1 - level of significance)"
   LPRINT " of the observed frequency occurring by chance": LPRINT
    N2 = N - 1
   FOR R = 1 TO N
    MAX(R) = C(R, 1):  N3 = 1
    FOR C = 1 TO N2
     IF MAX(R) > C(R, C + 1) THEN 560
      MAX(R) = C(R, C + 1)
      N3 = C + 1
560  NEXT C
     N3(R) = N3
     C = N3
    FOR J = 1 TO N
     IF J = N3 THEN 570
     IF MAX(R) = C(R, J) THEN LPRINT F$(R); " EQUALLY TO ";  F$(J); " &"
570  NEXT J
   LPRINT F$(R); " to "; F$(N3);
   LPRINT "   (CONF. < .95;";
   GOSUB 690
   LPRINT "   BP=  "; : LPRINT USING "#.####"; BP; : LPRINT ")"
```

```
   NEXT R
   LPRINT : LPRINT
   LPRINT "Other Significant Favored Transitions";
   LPRINT "   Significantly Disfavored Transitions": LPRINT
   LPRINT "(conf. >ca. 0.95 & <20% probability of selection by chance)"
   LPRINT "(NB: binomial probabilities between .1 and .2 don't mean much)"
   LPRINT
   FOR R = 1 TO N
    FOR C = 1 TO N
     IF EMB$ = "Y" OR EMB$ = "y" THEN
      IF R = C THEN 600
     END IF
     IF C = N3(R) THEN 600
     GOSUB 690
     IF BP > .2 THEN 600
     IF C(R, C) > 0 THEN 580
     LPRINT "                                ";  FS(R); " to "; FS(C)
     LPRINT "                                ";
     GOTO 590
580  IF C(R, C) < 0 THEN 600
     LPRINT FS(R); " to "; FS(C)
590  LPRINT "      BP= "; : LPRINT USING "#.####"; BP
600  NEXT C
   NEXT R

' screen output

601 IF SCR$ <> "Y" THEN 651
   PRINT : PRINT : PRINT "PRINCIPLE SUCCESSION FOR EACH FACIES"
   PRINT "binomial probabilities listed at right give probability"
   PRINT "(confidence level = 1 - level of significance)"
   PRINT " of the observed frequency occurring by chance": PRINT
    N2 = N - 1
   FOR R = 1 TO N
    MAX(R) = C(R, 1):  N3 = 1
    FOR C = 1 TO N2
     IF MAX(R) > C(R, C + 1) THEN 610
      MAX(R) = C(R, C + 1)
      N3 = C + 1
610  NEXT C
     N3(R) = N3
     C = N3
```

```
    FOR J = 1 TO N
     IF J = N3 THEN 620
     IF MAX(R) = C(R, J) THEN PRINT F$(R); " EQUALLY TO "; F$(J); " &"
620  NEXT J
    PRINT F$(R); " to "; F$(N3);
    PRINT "   (CONF. < .95;";
    GOSUB 690
    PRINT "   BP=  "; : PRINT USING "#.####"; BP; : PRINT ")"
   NEXT R
   PRINT : PRINT
   PRINT "Other Significant Favored Transitions";
   PRINT "   Significantly Disfavored Transitions": PRINT
   PRINT "(conf. >ca. 0.95 & <20% probability of selection by chance)"
   PRINT "(NB: binomial probabilities between .1 and .2 don't mean much)"
   PRINT
   FOR R = 1 TO N
    FOR C = 1 TO N
     IF EMB$ = "Y" OR EMB$ = "y" THEN
      IF R = C THEN 650
     END IF
     IF C = N3(R) THEN 650
     GOSUB 690
     IF BP > .2 THEN 650
     IF C(R, C) > 0 THEN 630
     PRINT "                              "; F$(R); "  to "; F$(C)
     PRINT "                              ";
     GOTO 640
630   IF C(R, C) < 0 THEN 650
     PRINT F$(R); " to "; F$(C)
640   PRINT "     BP= "; : PRINT USING "#.####"; BP
650  NEXT C
   NEXT R

' calculate desired binomial probabilities for any cell

651 PRINT "Do you want the binomial probability for any cell?"
   PRINT "Type y (lower case) if so"
660 INPUT C$
   IF C$ <> "y" THEN 740
   PRINT "Input ROW # of cell": INPUT R
   PRINT "Input COLUMN # of cell": INPUT C
   PRINT : LPRINT
```

```
   GOSUB 690

' send output to screen if just analyzing probabilities

   IF Z4 <> 1 THEN 670
   PRINT "BINOMIAL PROBABILITY FOR CELL "; R; ","; C; " = "; BP
   GOTO 680
670 LPRINT "BINOMIAL PROBABILITY FOR CELL "; R; ","; C; " = "; BP
680 PRINT "Do you want another one? Type y (lower case) if yes": GOTO 660

' Start of subroutine to calculate summed binomial probabilities, ' from n to N for favored transitions, or n to 0 if disfavored ' n=# observed = A#(R,C); N= max. possible = row total F(R)
' 2600-2740 sum binomial probabilities for at least obs. sucesses ' 2620-2660 calculates factorials for the smaller of (N-n)! & n! ' and for N! divided by the larger of n! and (N-n)!.
' 2690-2730 sum binomial probabilities for each iteration

690  BP = 0:  BPZ = 0
    Y2 = F(R)
    Y1 = A(R, C)
   IF C(R, C) < 0 THEN Y1 = F(R) - A(R, C)
   FOR Z = Y1 TO Y2
    A1 = 0:  A2 = 0
   IF Z = Y2 THEN 700
   FOR J = 1 TO (F(R) - Z)
     A1 = A1 + LOG(F(R) - (J - 1))
     A2 = A2 + LOG(J)
   NEXT J
700  P = B(R, C) / F(R)
   IF C(R, C) > 0 THEN 710
   BPZ = (F(R) - Z) * LOG(P) + Z * LOG(1 - P) + A1 - A2
   GOTO 720
710  BPZ = Z * LOG(P) + (F(R) - Z) * LOG(1 - P) + A1 - A2
720   BP = BP + EXP(BPZ)
   IF BP > (EXP(BPZ) * 1000) THEN 730
  NEXT Z
730 RETURN
740 END
```

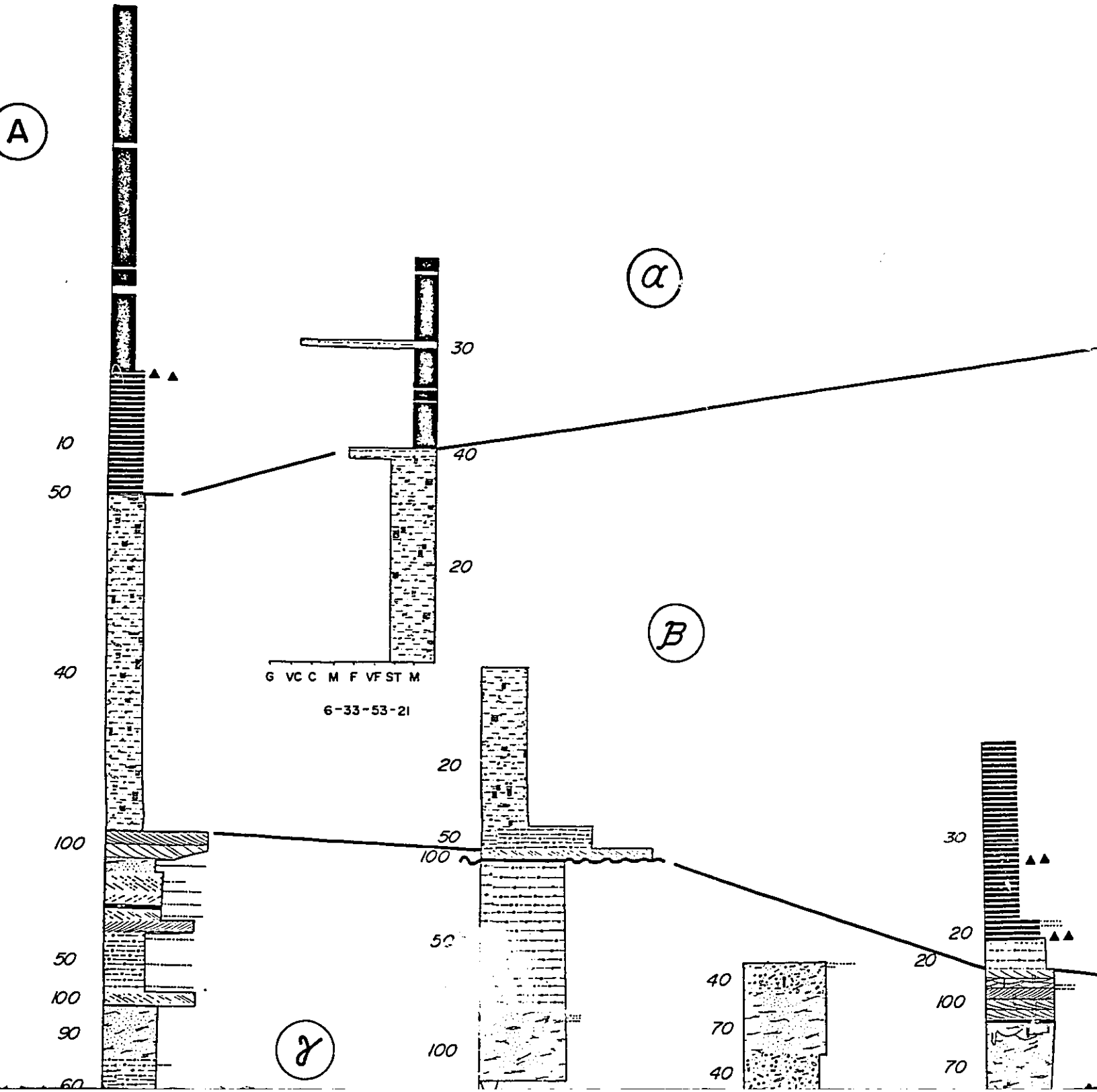
A
α
30
40
20
10
50
40
G VC C M F VF ST M
6-33-53-21
B
20
50
100
100
50
100
γ
40
70
40
30
20
20
100
70

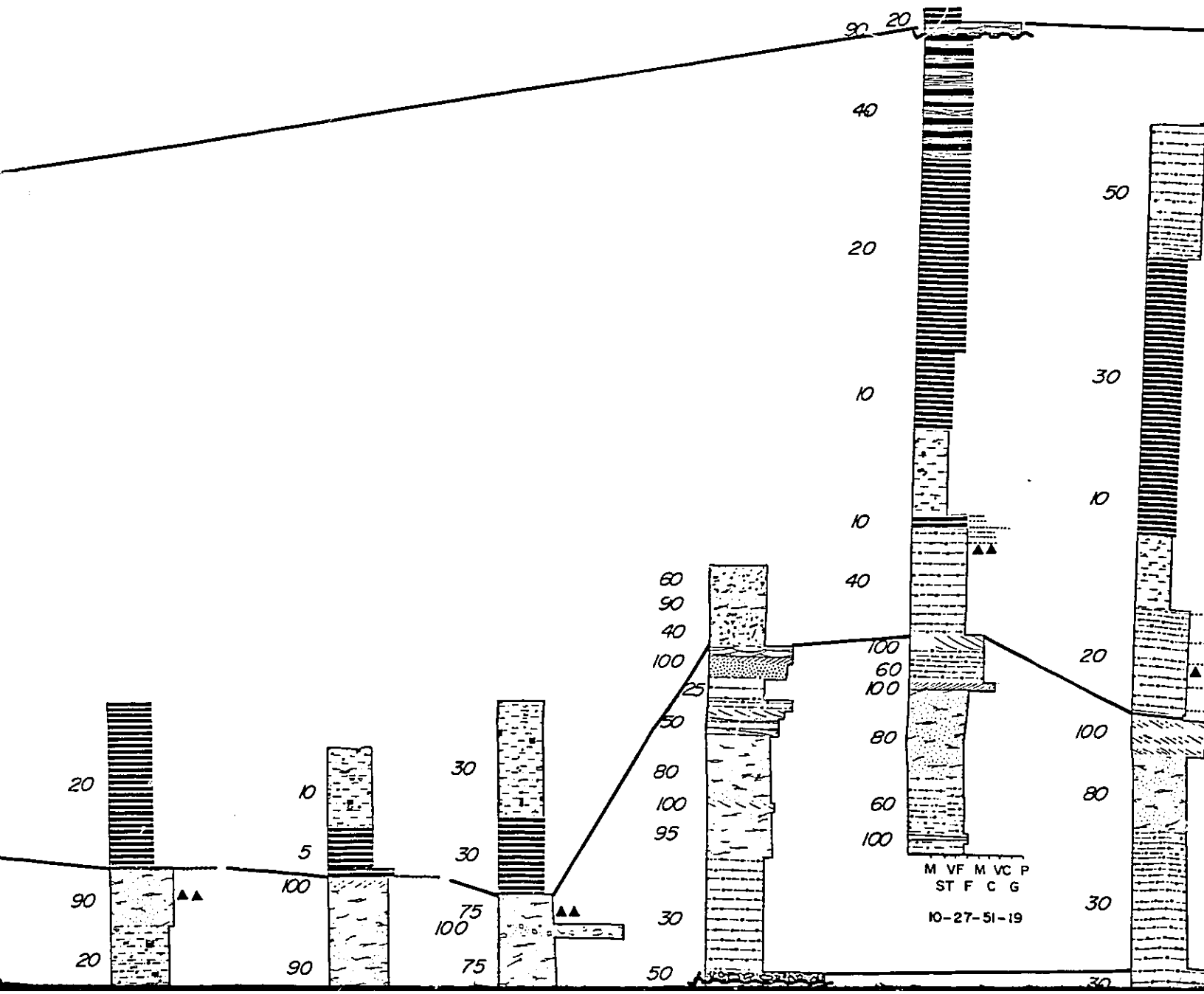
M VF M VC P
ST F C G
10-27-51-19

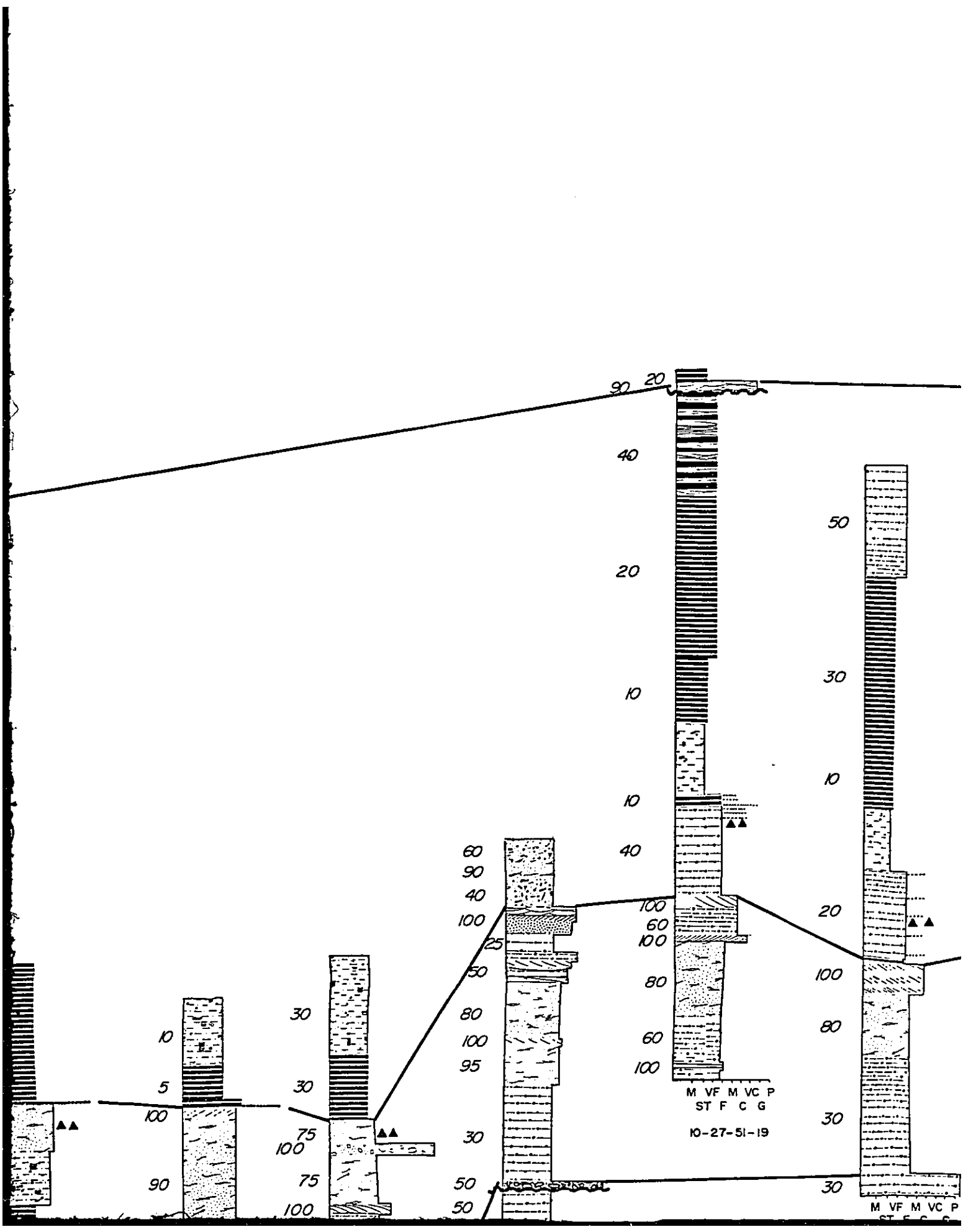
M VF M VC P
ST F C G
10-27-51-19
M VF M VC P

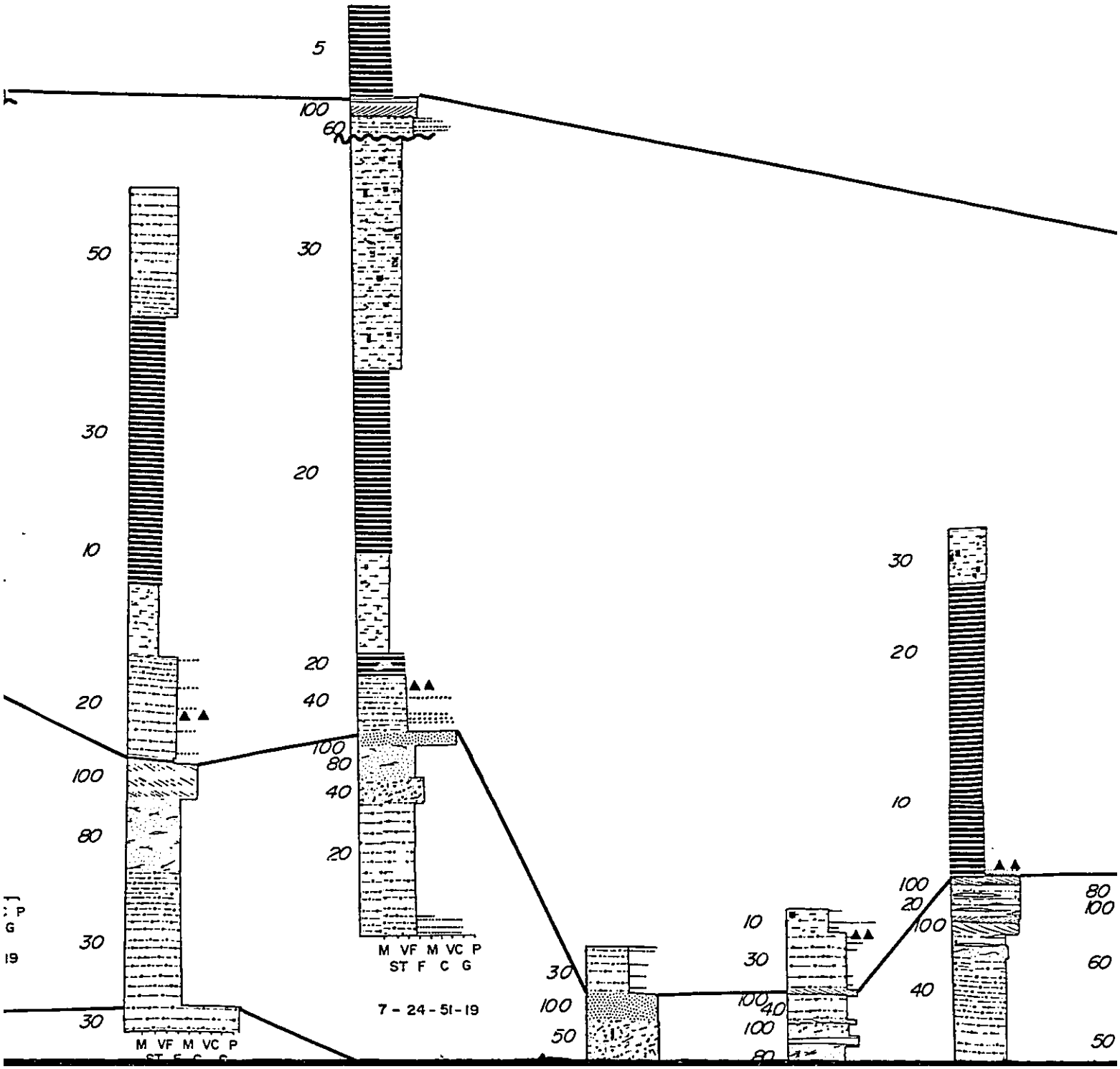
5
100
60
50
30
20
10
20
100
80
30
M VF M VC P
ST F C G
20
40
100
80
40
20
30
100
50
7 - 24 - 51 - 19
10
30
100
40
100
80
30
20
100
20
10
100
80
100
60
40
50

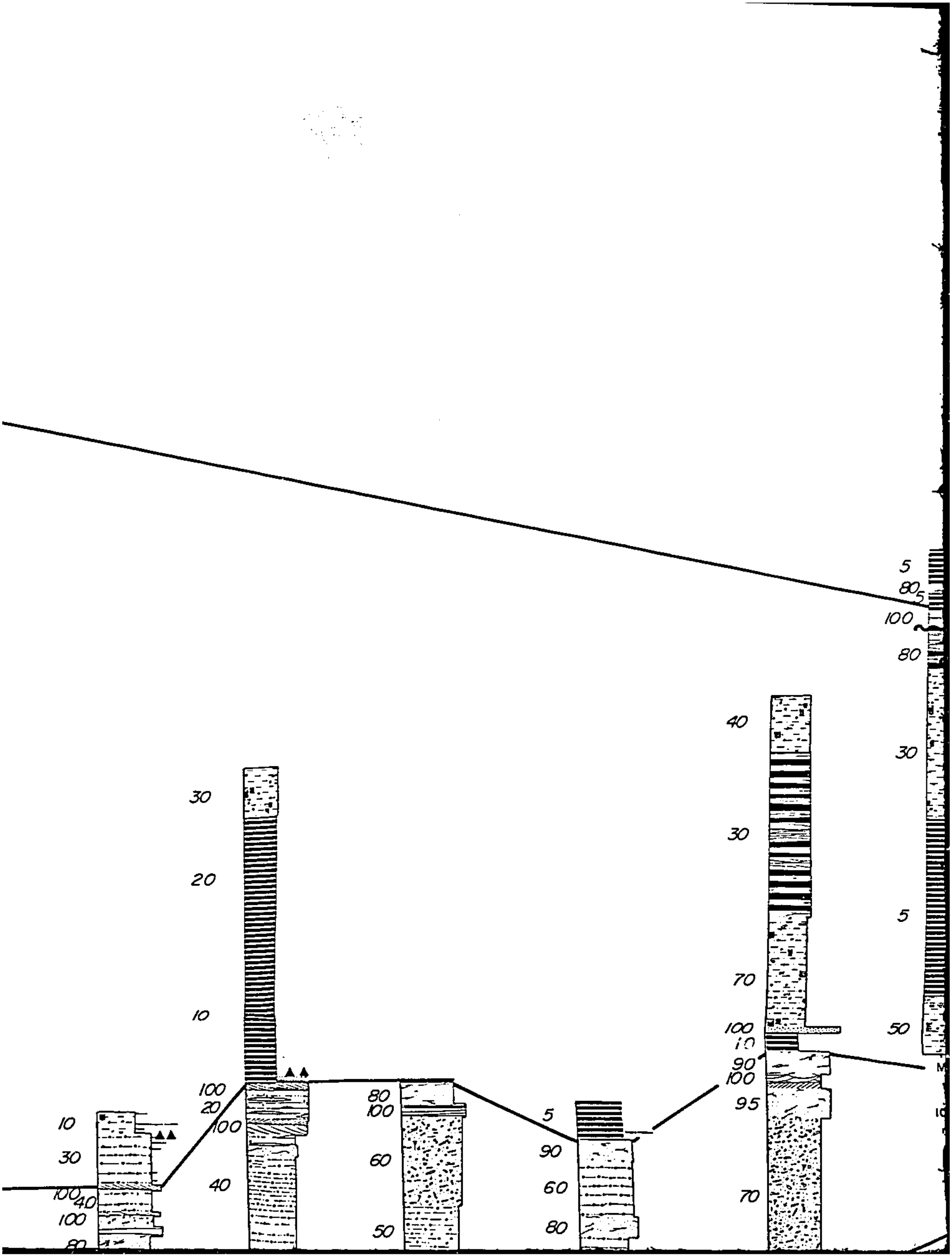

10
30
100
40
100
80
30
20
10
100
20
100
40
80
100
60
50
5
90
60
80
40
30
70
100
10
90
100
95
70
5
80
5
100
80
30
5
50

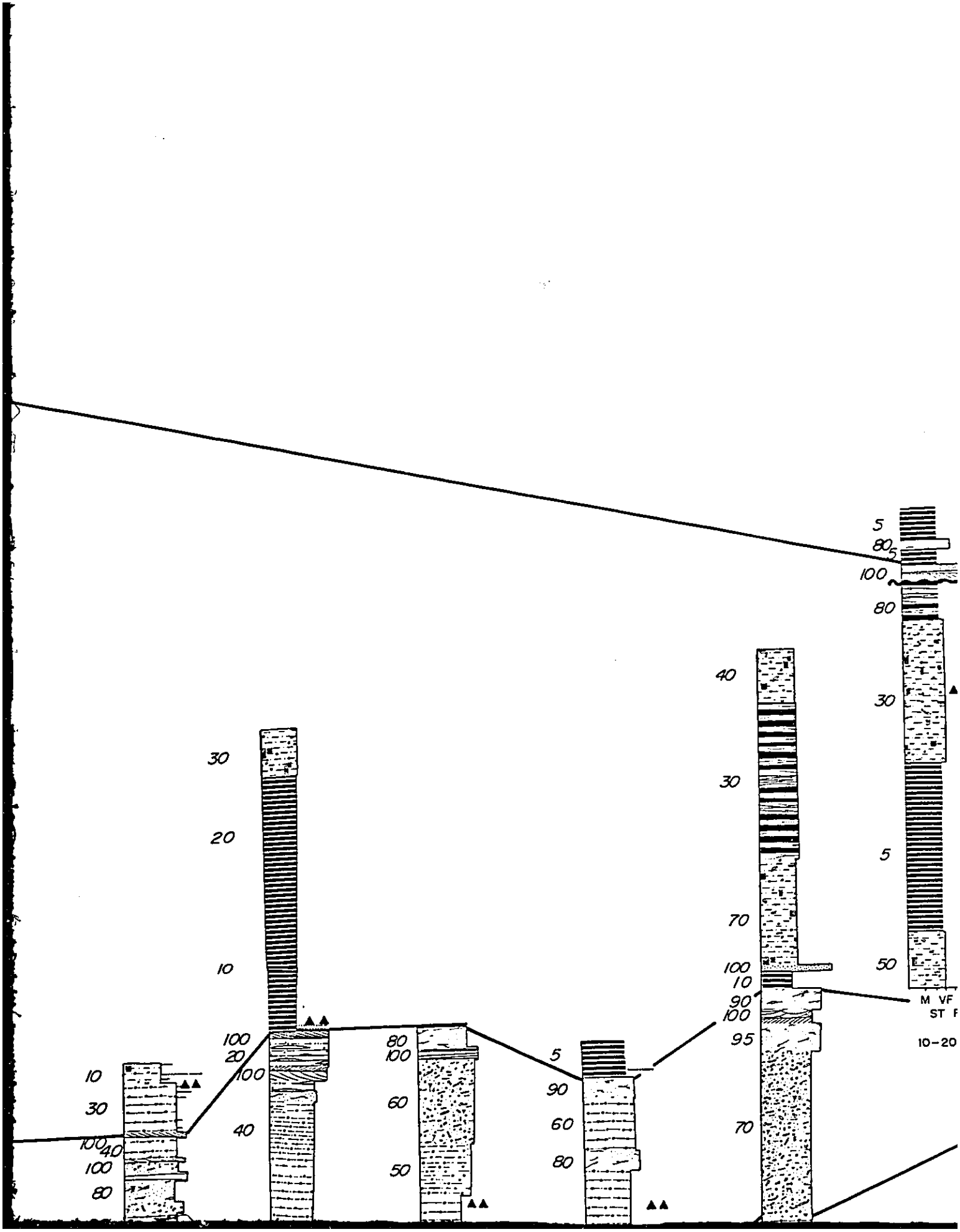
5
80
5
100
80
30
5
50
M VF
ST F
10-20
40
30
70
100
10
90
100
95
70
30
20
10
100
20
100
40
10
30
100
40
100
80
80
100
60
50
5
90
60
80

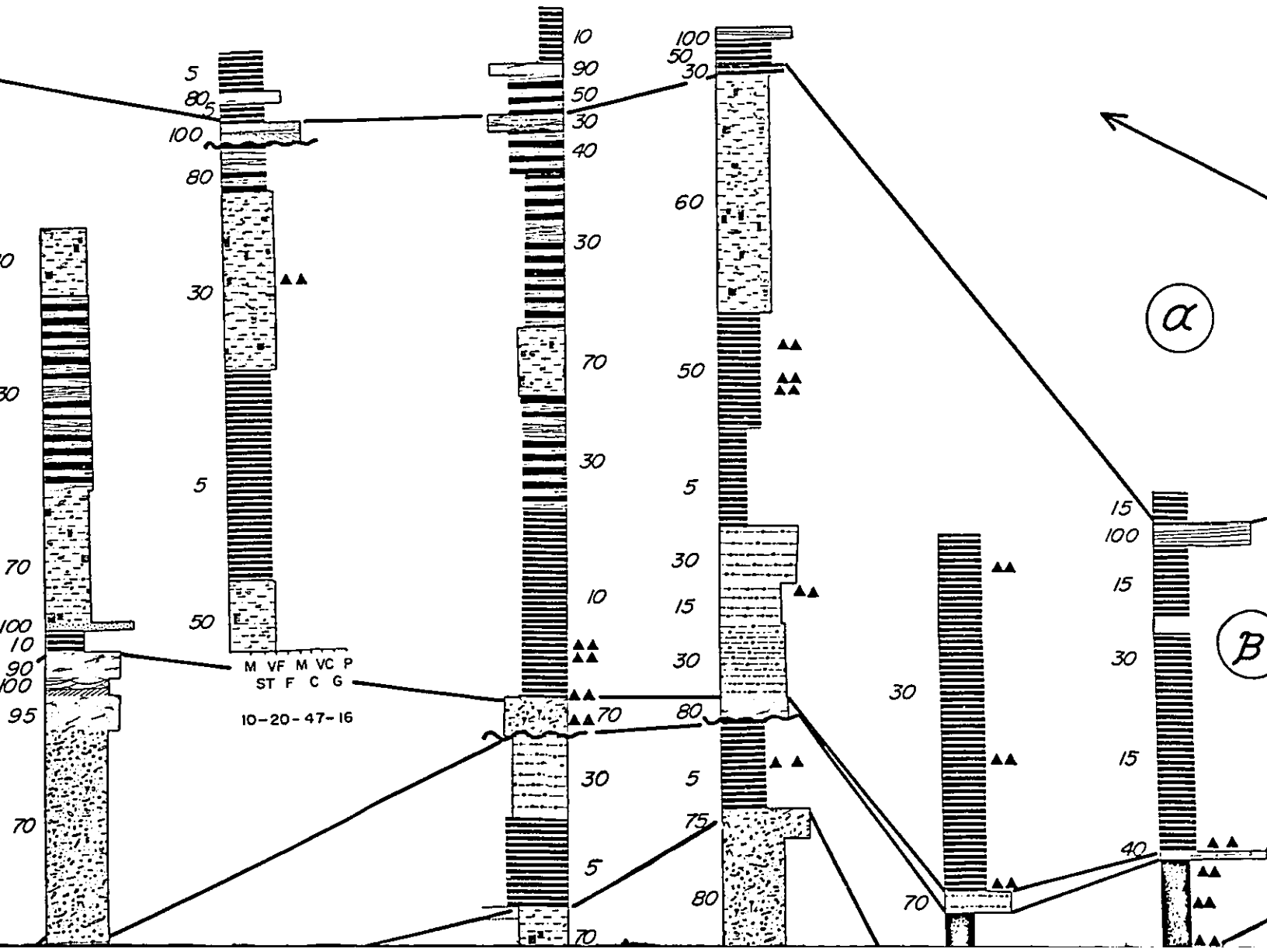
M VF M VC P
ST F C G
10-20-47-16
α
β

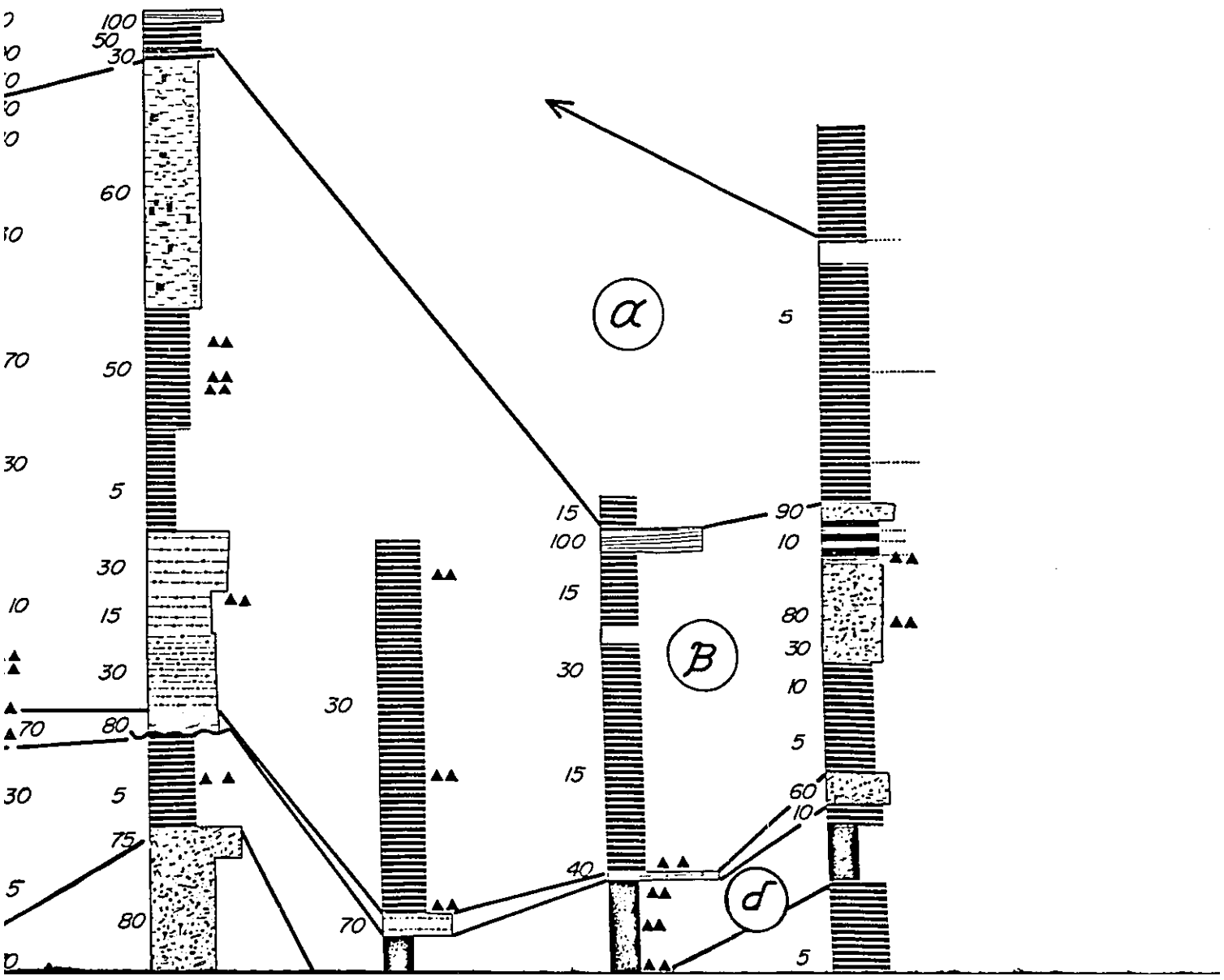
A'
α
β
δ
100
50
30
60
70
50
30
5
30
15
30
70
80
30
5
75
80
15
100
15
30
15
40
70
90
10
80
30
10
5
60
10
5

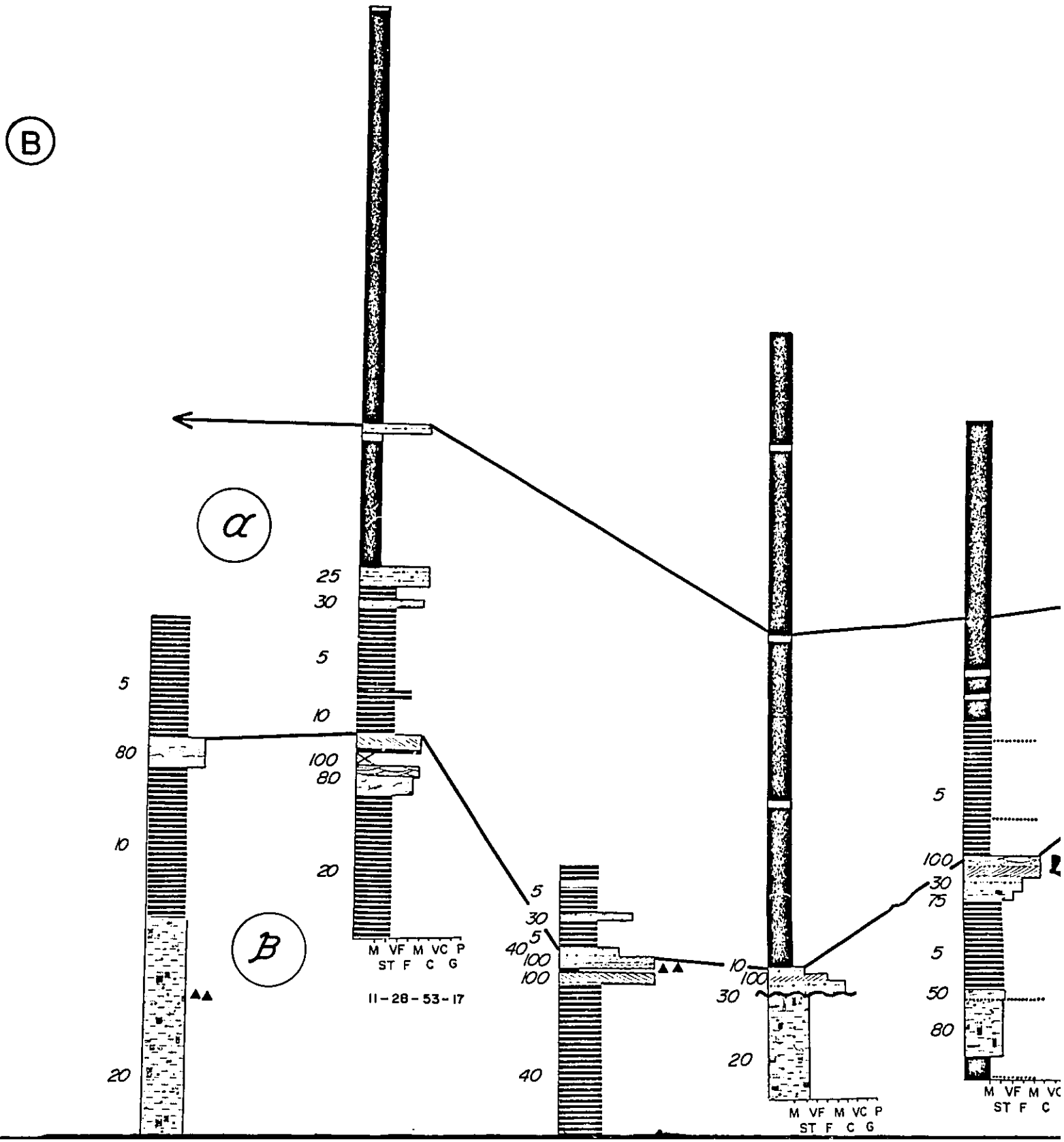
B
α
25
30
5
10
100
80
20
5
80
10
20
B
M VF M VC P
ST F C G
11-28-53-17
5
30
5
40
100
100
40
10
100
30
20
M VF M VC P
ST F C G
5
100
30
75
5
50
80
M VF M VC
ST F C

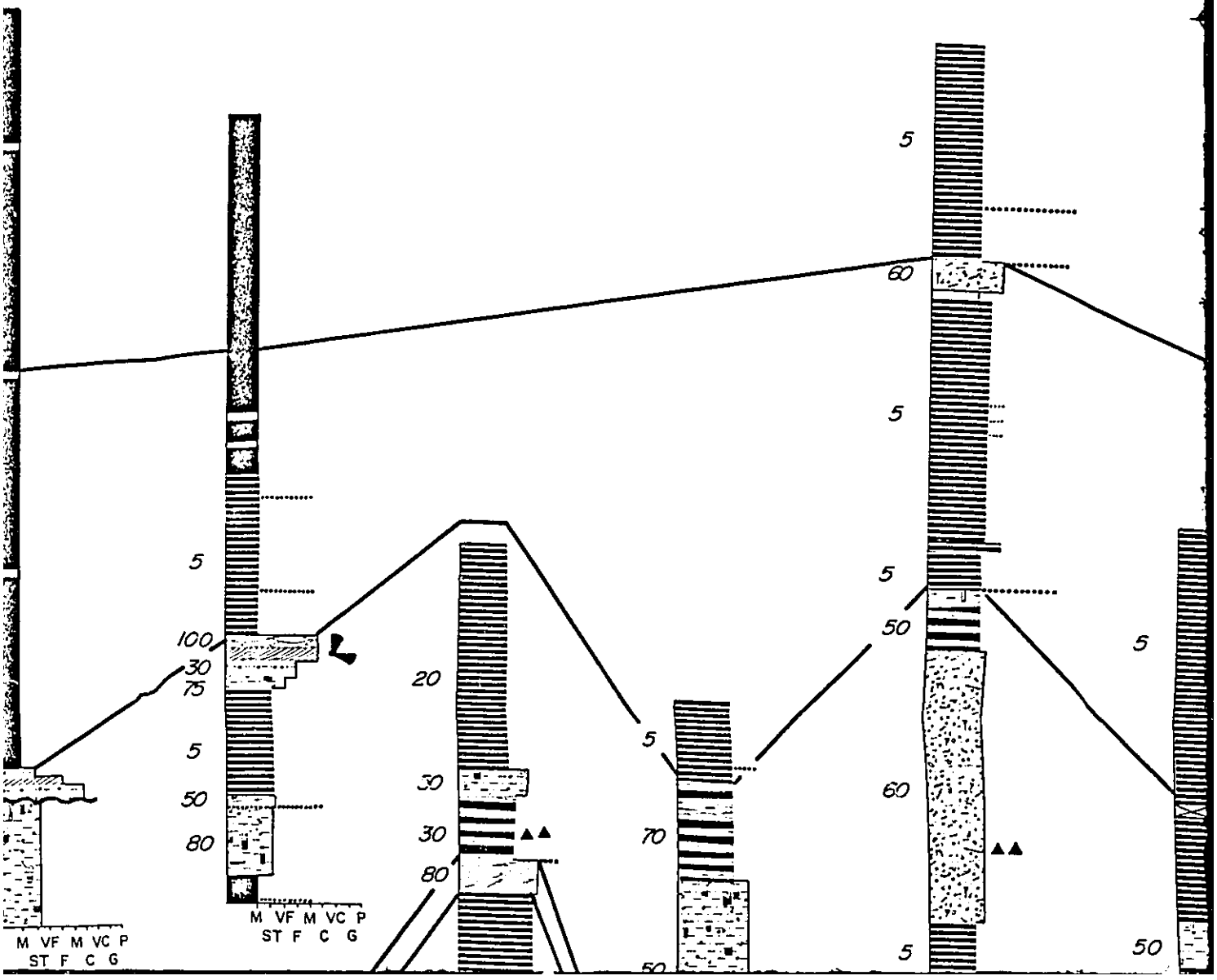
M VF M VC P
ST F C G
M VF M VC P
ST F C G
5
60
5
5
100
30
75
5
50
80
20
30
30
80
5
70
5
50
60
5
5
50

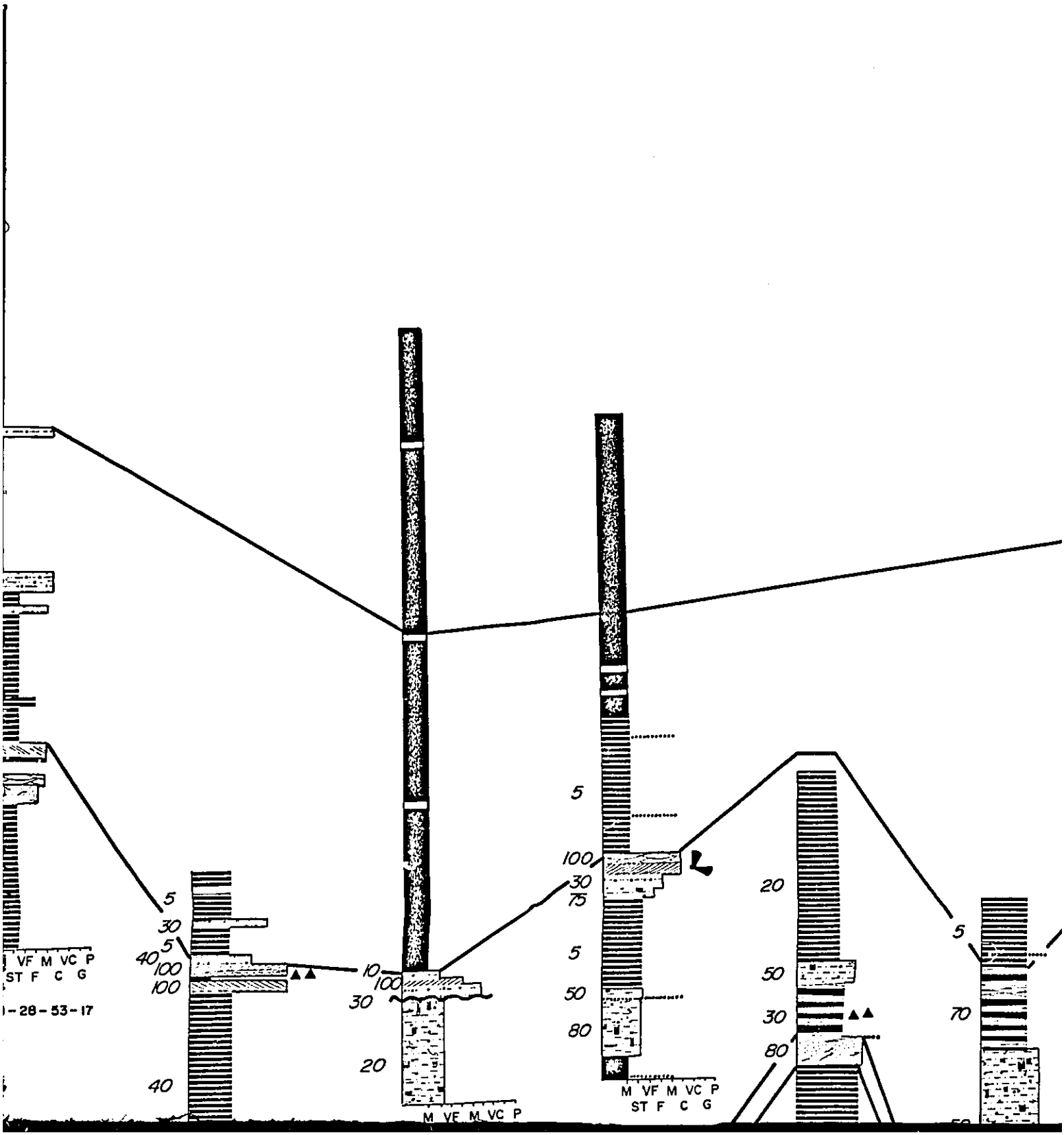
VF M VC P
ST F C G
-28-53-17
5
30
5
40
100
100
40
10
100
30
20
M VF M VC P
5
100
30
75
5
50
80
M VF M VC P
ST F C G
20
50
30
80
5
70

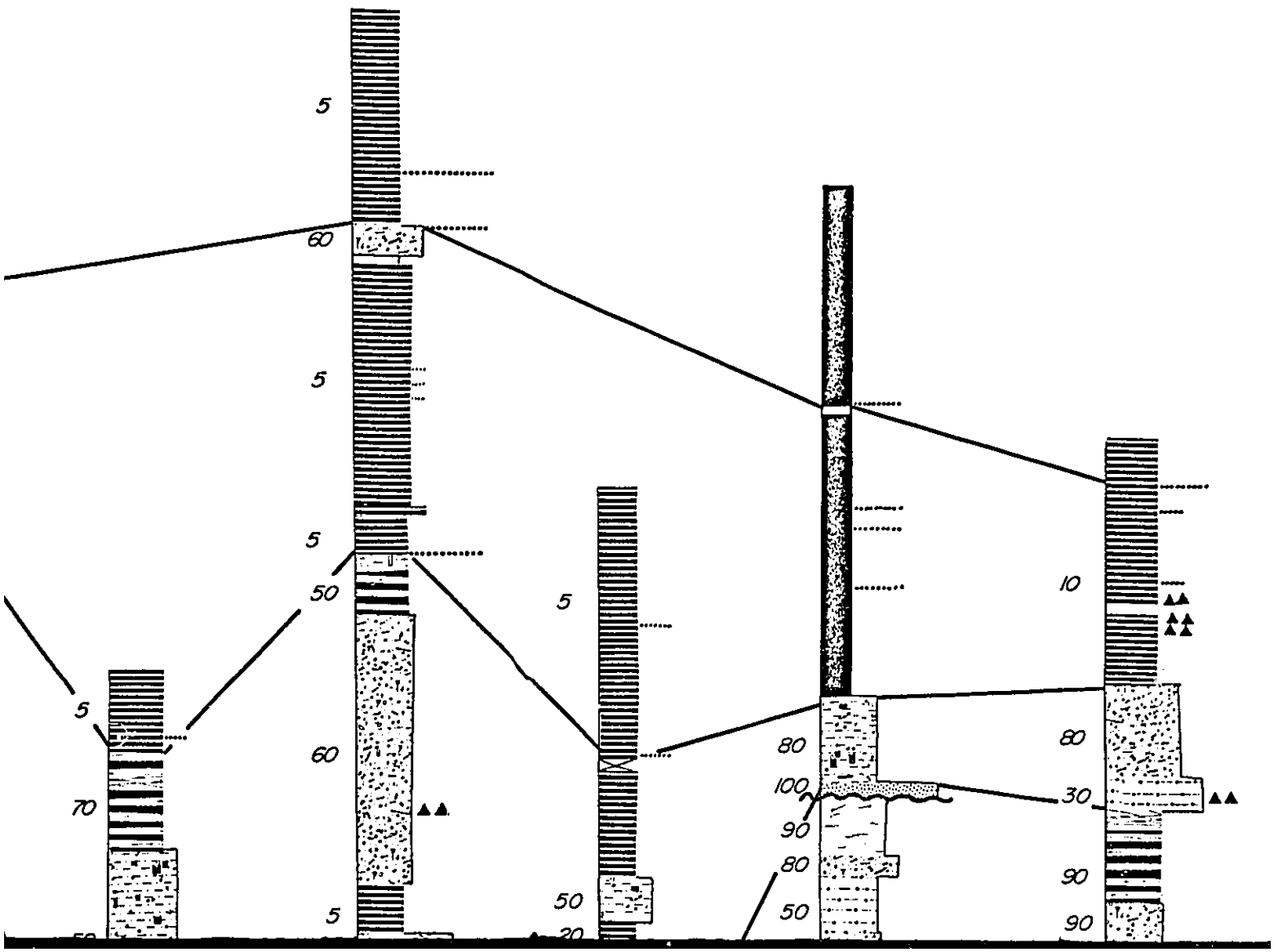
B'
5
60
5
5
50
5
5
60
70
5
50
20
80
100
90
80
50
10
80
30
90
90

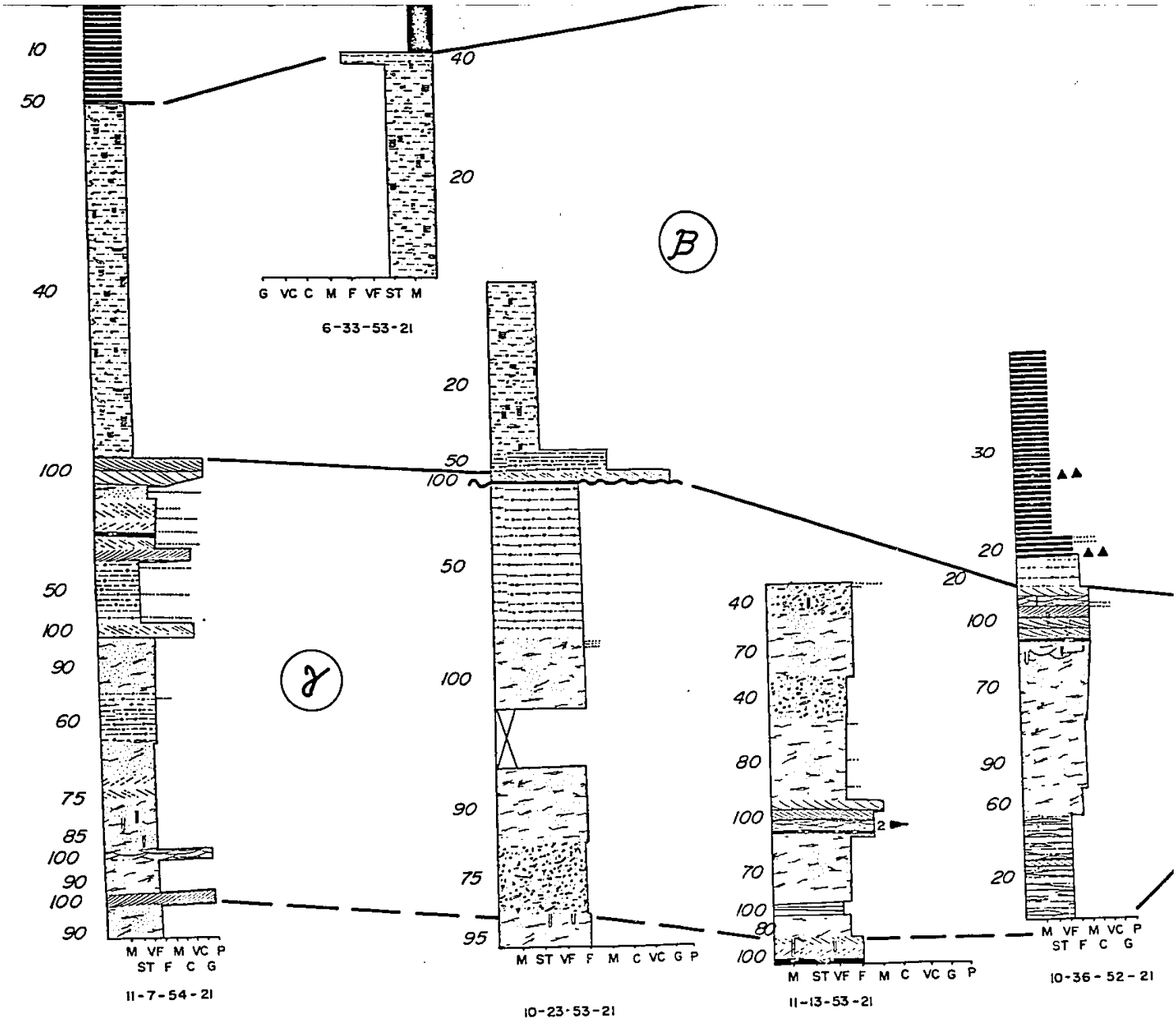

A — A′ CORE CROSS SECTION

no horizontal scale

2 m

▭ = SIDEI

10 = % S

SEQUENCE BOUNDARY

▲▲ = bentonites

= relative p

M VF M VC P
ST F C G

MAXIMUM GRAIN SIZE SCALE

M = mud ST = silt VF = very fine F = fine M = medium C = coarse VC = very coarse G = granules P = pebble

Sand

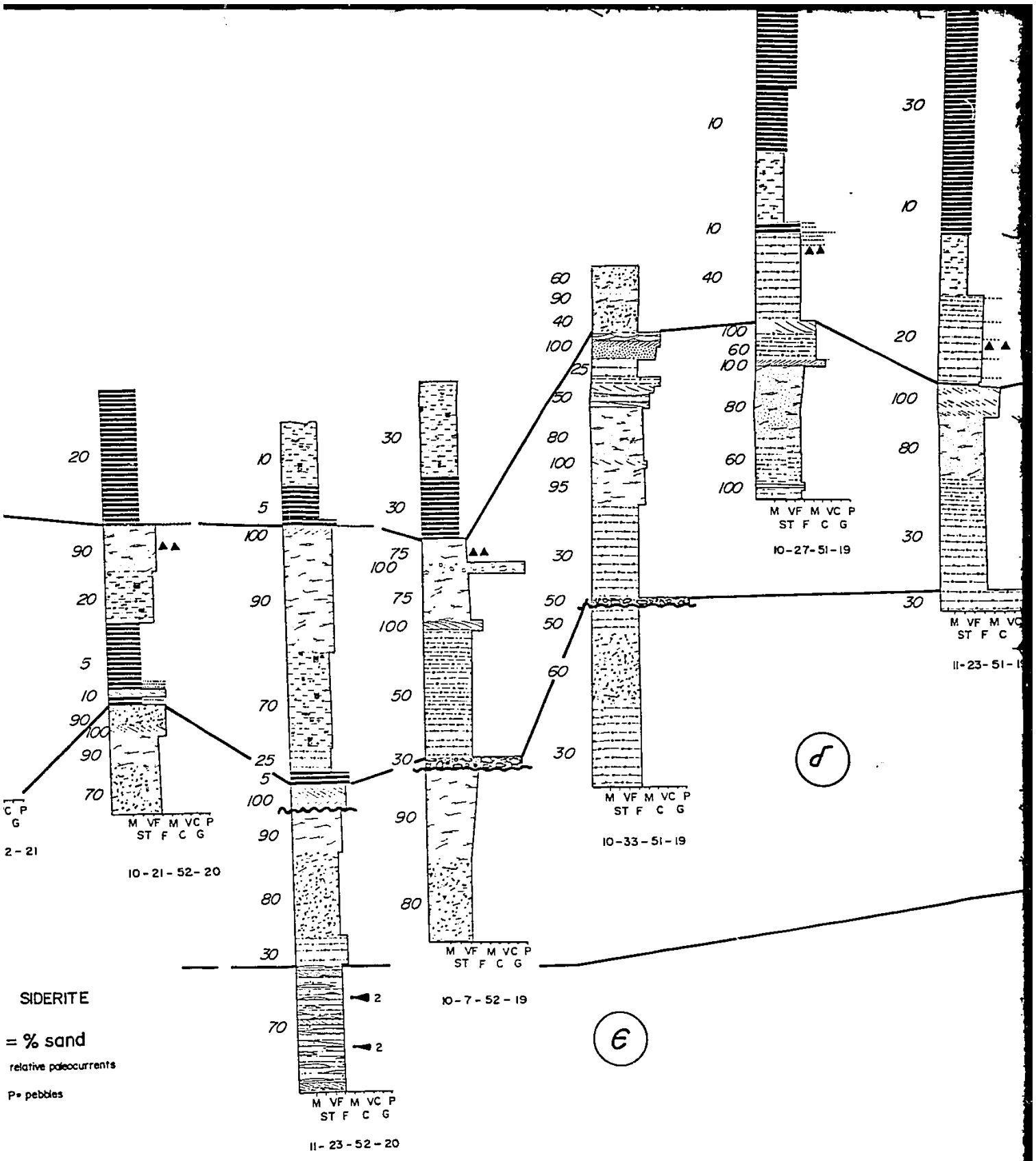
M VF M VC P
ST F C G
10-21-52-20
10-7-52-19
10-33-51-19
10-27-51-19
11-23-52-20
SIDERITE
= % sand
relative paleocurrents
P= pebbles

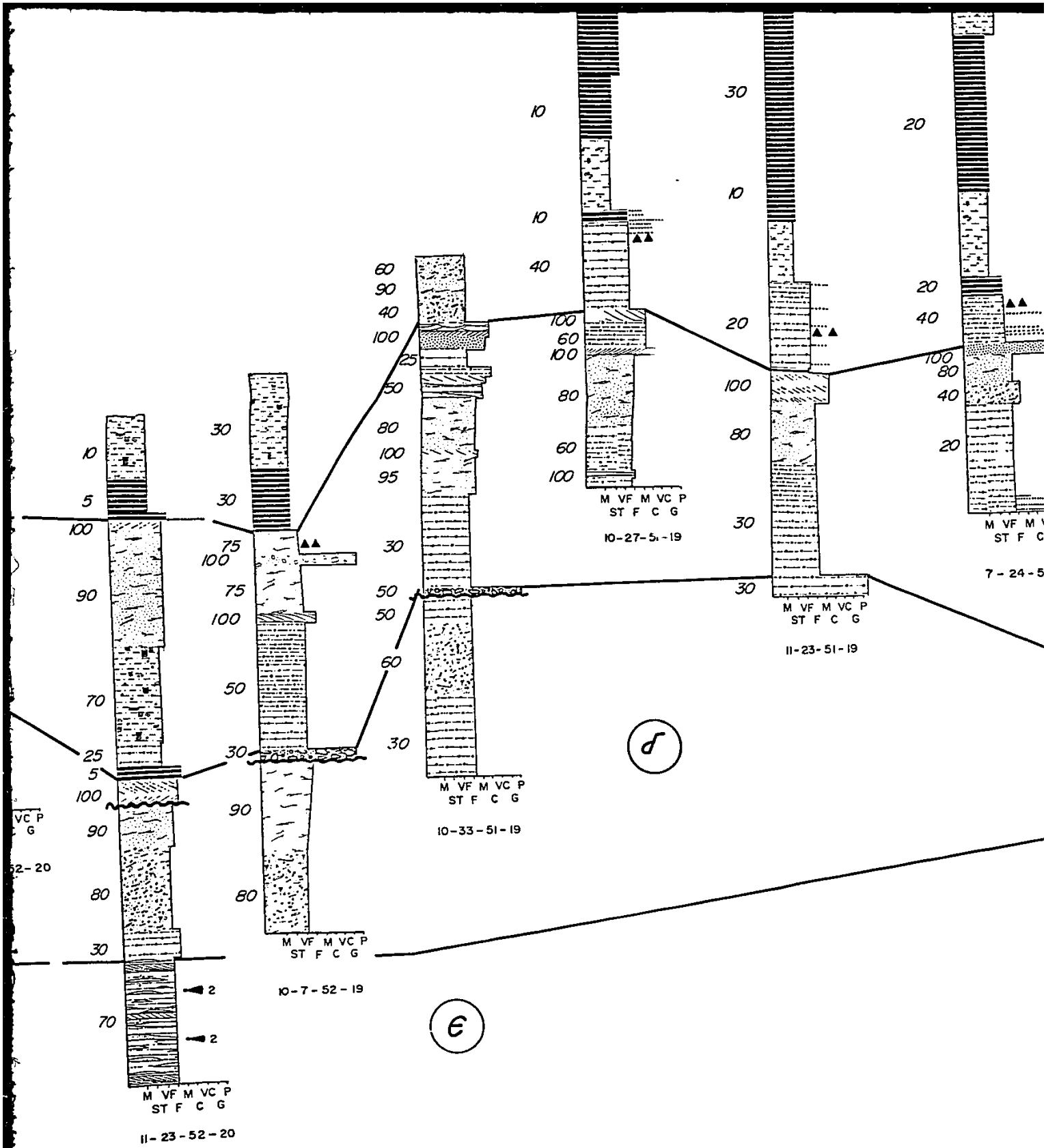
M VF M VC P
ST F C G
11-23-52-20
10-7-52-19
10-33-51-19
10-27-51-19
11-23-51-19
7-24-5
C
D

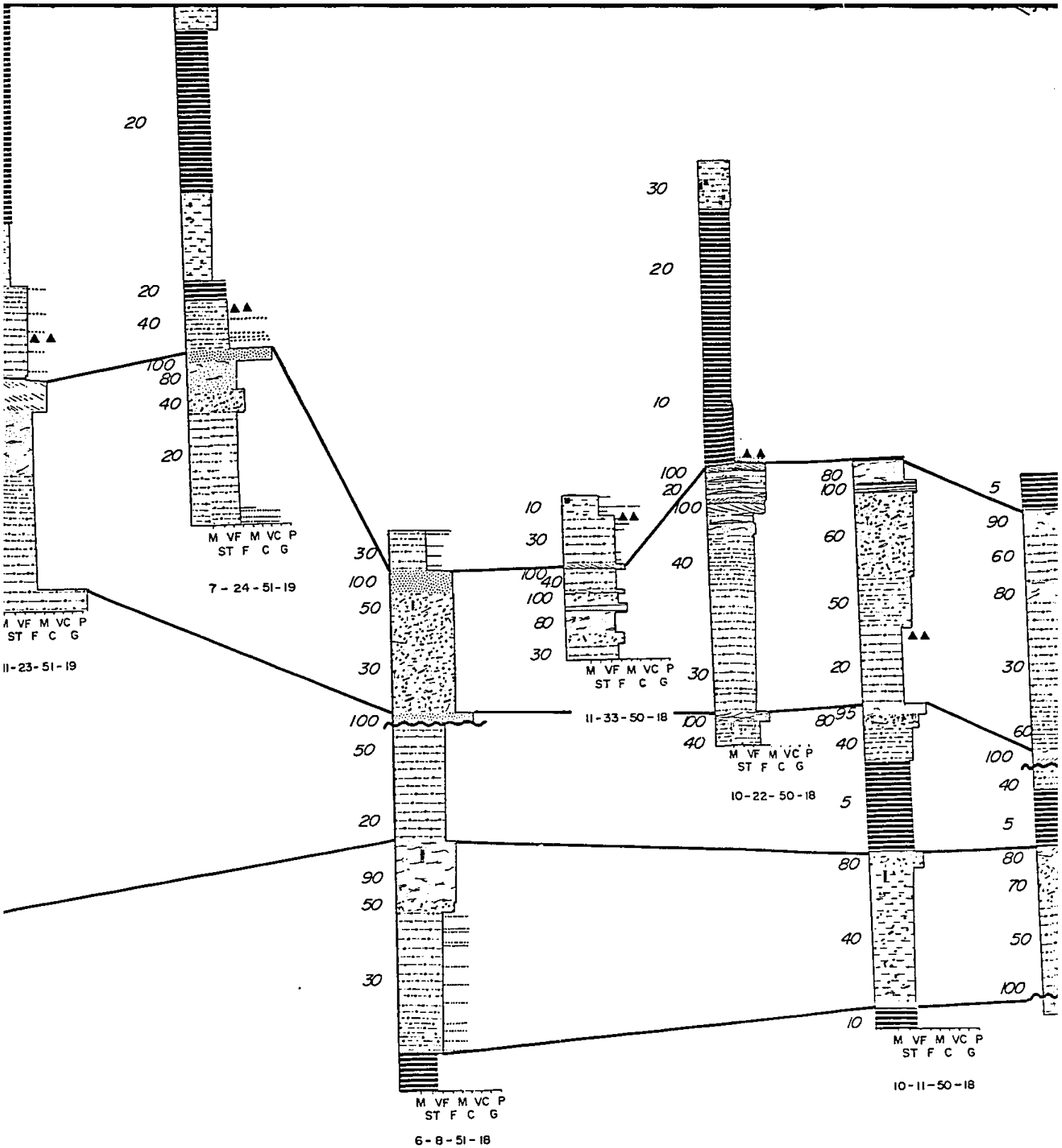
M VF M VC P
ST F C G
11-23-51-19
7-24-51-19
11-33-50-18
10-22-50-18
10-11-50-18
6-8-51-18

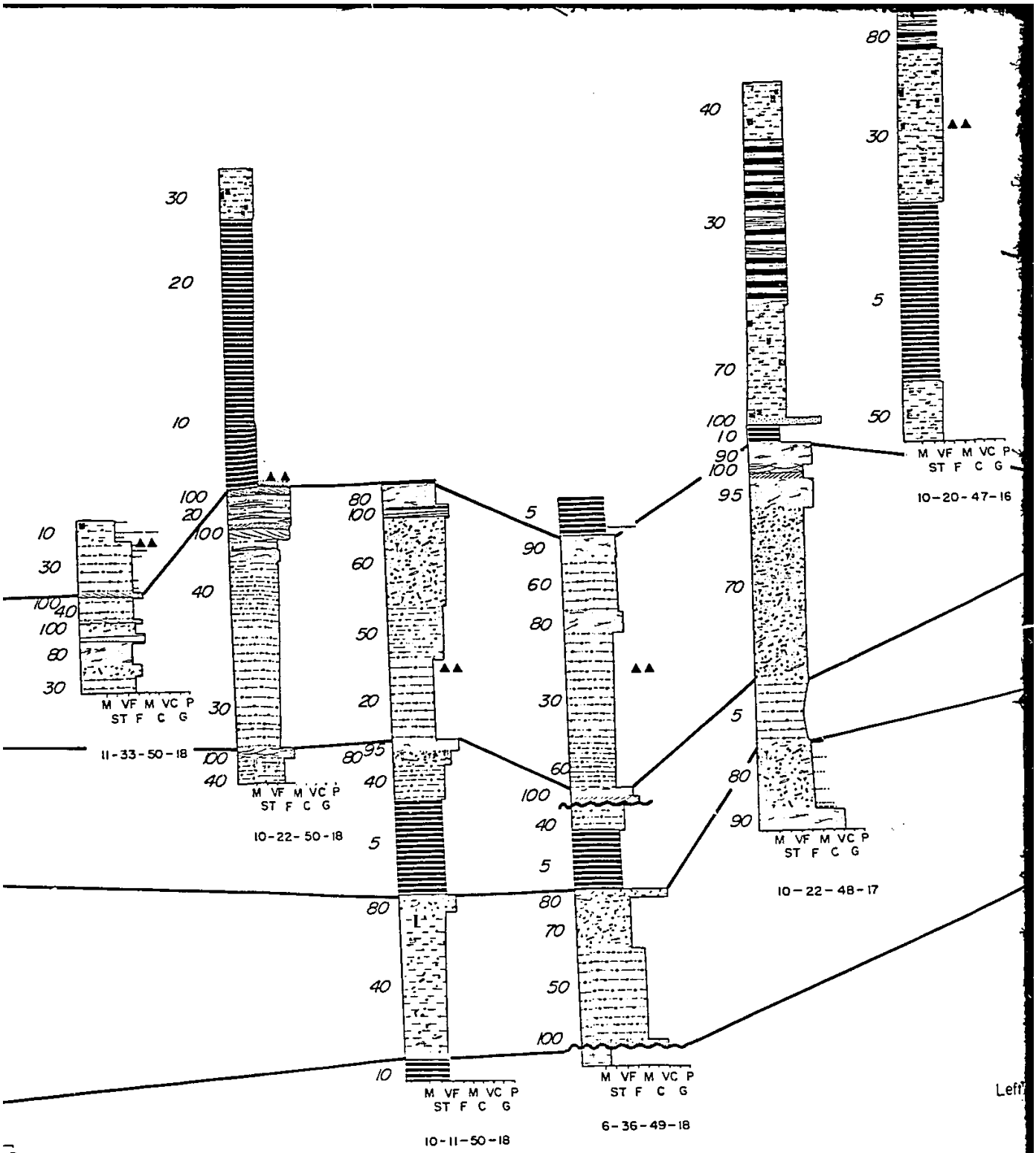
M VF M VC P
ST F C G
11-33-50-18
10-22-50-18
10-11-50-18
6-36-49-18
10-22-48-17
10-20-47-16

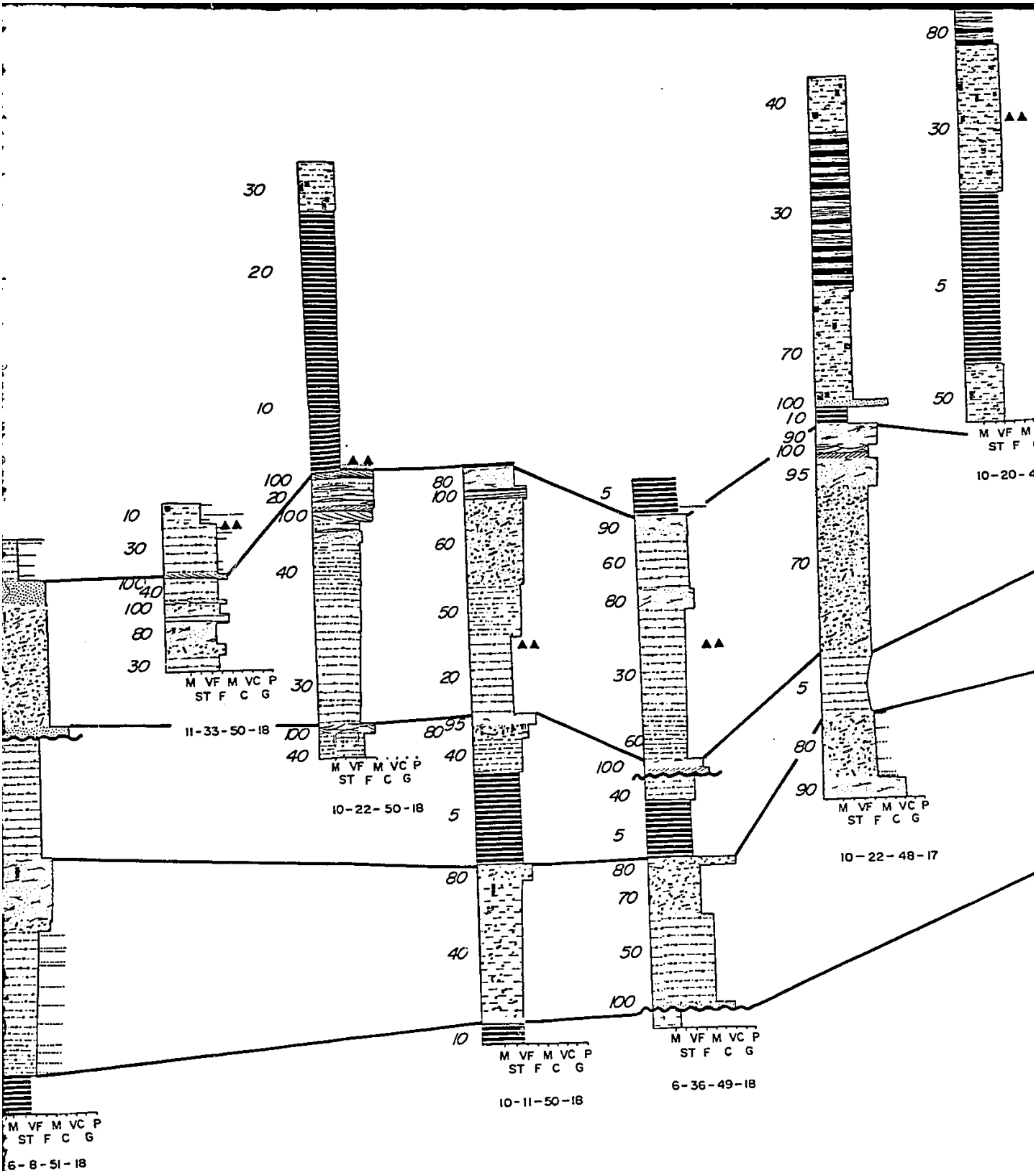
M VF M VC P
ST F C G
11-33-50-18
10-22-50-18
10-11-50-18
6-36-49-18
10-22-48-17
6-8-51-18

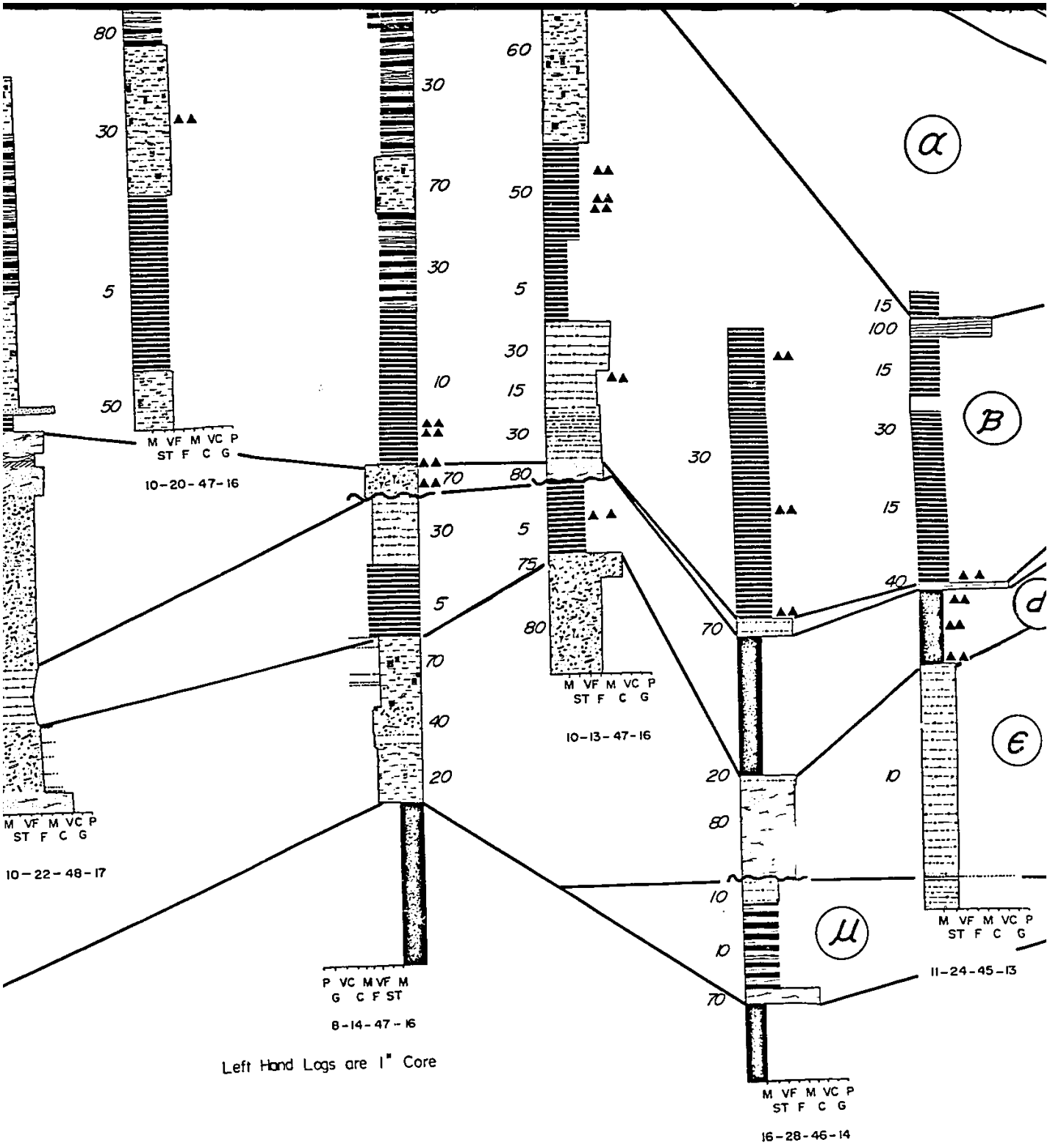
80
30
5
50
M VF M VC P
ST F C G
10-20-47-16
30
70
30
10
70
30
5
70
40
20
M VF M VC P
ST F C G
10-22-48-17
P VC M VF M
G C F ST
8-14-47-16
60
50
5
30
15
30
80
5
75
80
M VF M VC P
ST F C G
10-13-47-16
30
70
20
80
10
10
70
M VF M VC P
ST F C G
16-28-46-14
15
100
15
30
15
40
10
M VF M VC P
ST F C G
11-24-45-13
α
B
d
ε
μ
Left Hand Logs are 1" Core

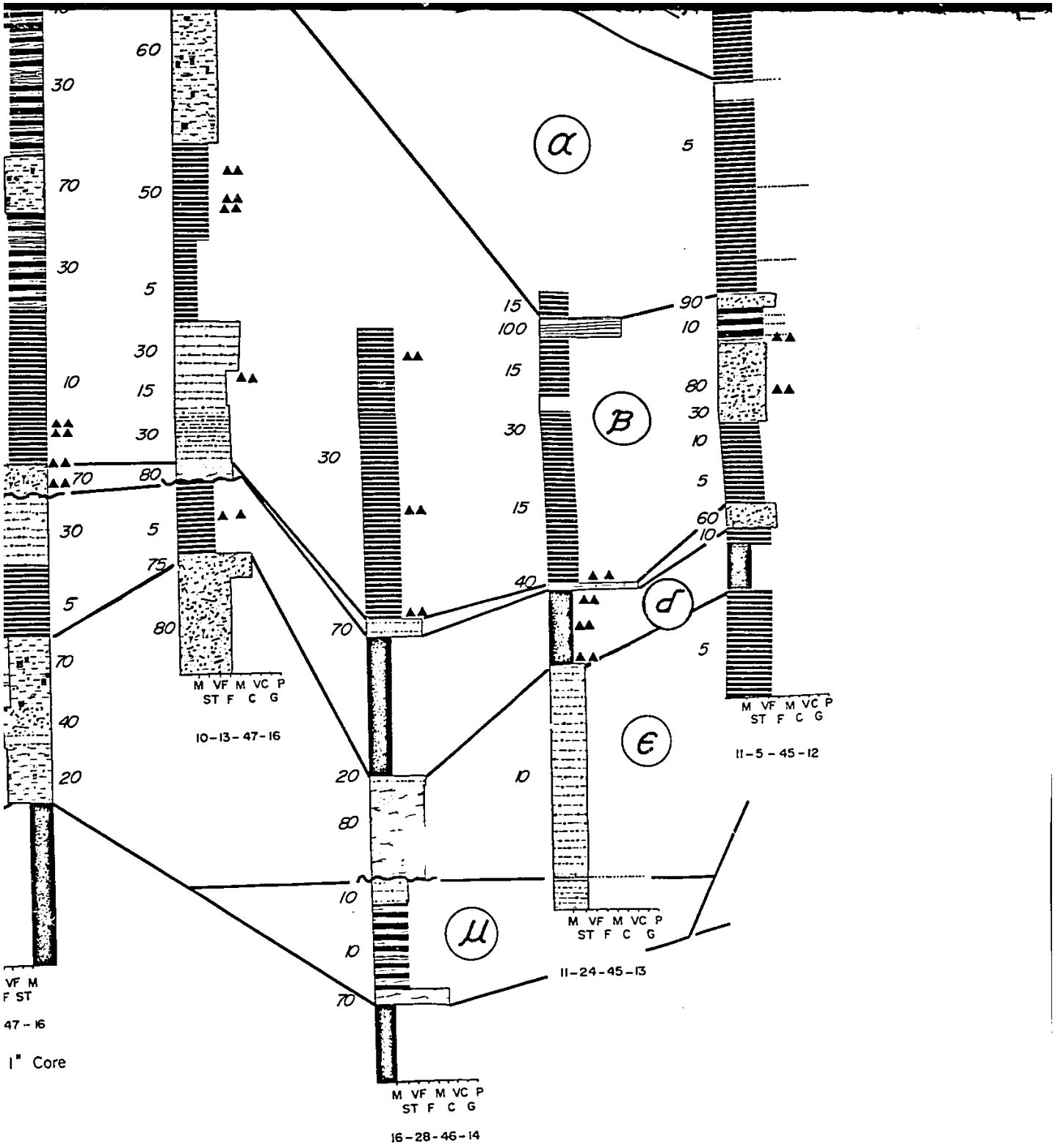
α
β
γ
δ
ε
μ
M VF M VC P
ST F C G
10-13-47-16
11-5-45-12
11-24-45-13
16-28-46-14
VF M
F ST
47-16
1" Core

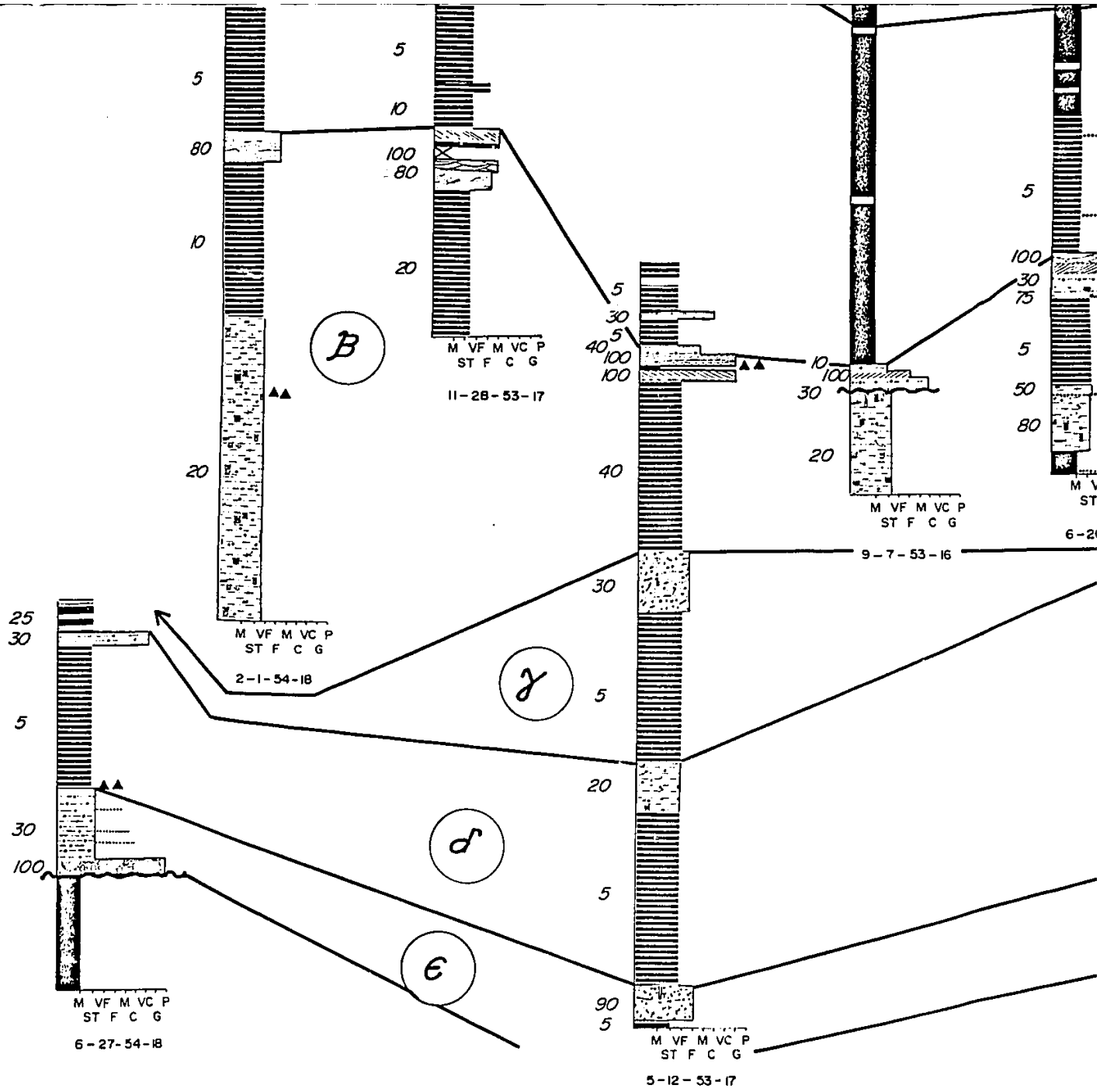
5
80
10
20
B
M VF M VC P
ST F C G
11-28-53-17
5
10
100
80
20
5
30
5
40
100
100
40
10
100
30
20
5
100
30
75
5
50
80
20
M VF M VC P
ST F C G
9-7-53-16
6-2
25
30
5
30
2-1-54-18
γ
5
20
30
100
δ
5
ε
M VF M VC P
ST F C G
6-27-54-18
90
5
M VF M VC P
ST F C G
5-12-53-17

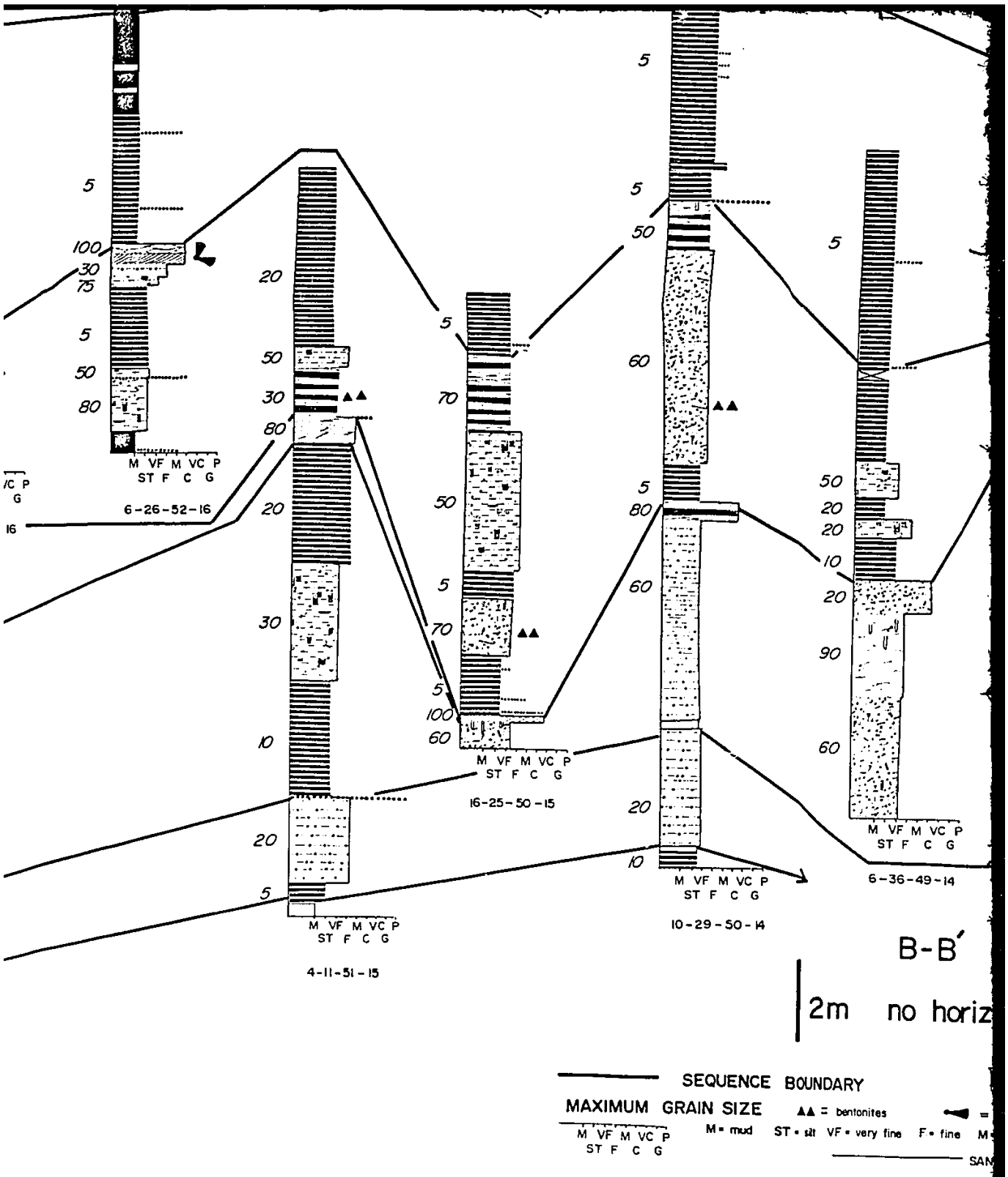
M VF M VC P
ST F C G
6-26-52-16
4-11-51-15
16-25-50-15
10-29-50-14
6-36-49-14
B-B'
2m
no horiz
SEQUENCE BOUNDARY
MAXIMUM GRAIN SIZE
▲▲ = bentonites
M = mud
ST = silt
VF = very fine
F = fine

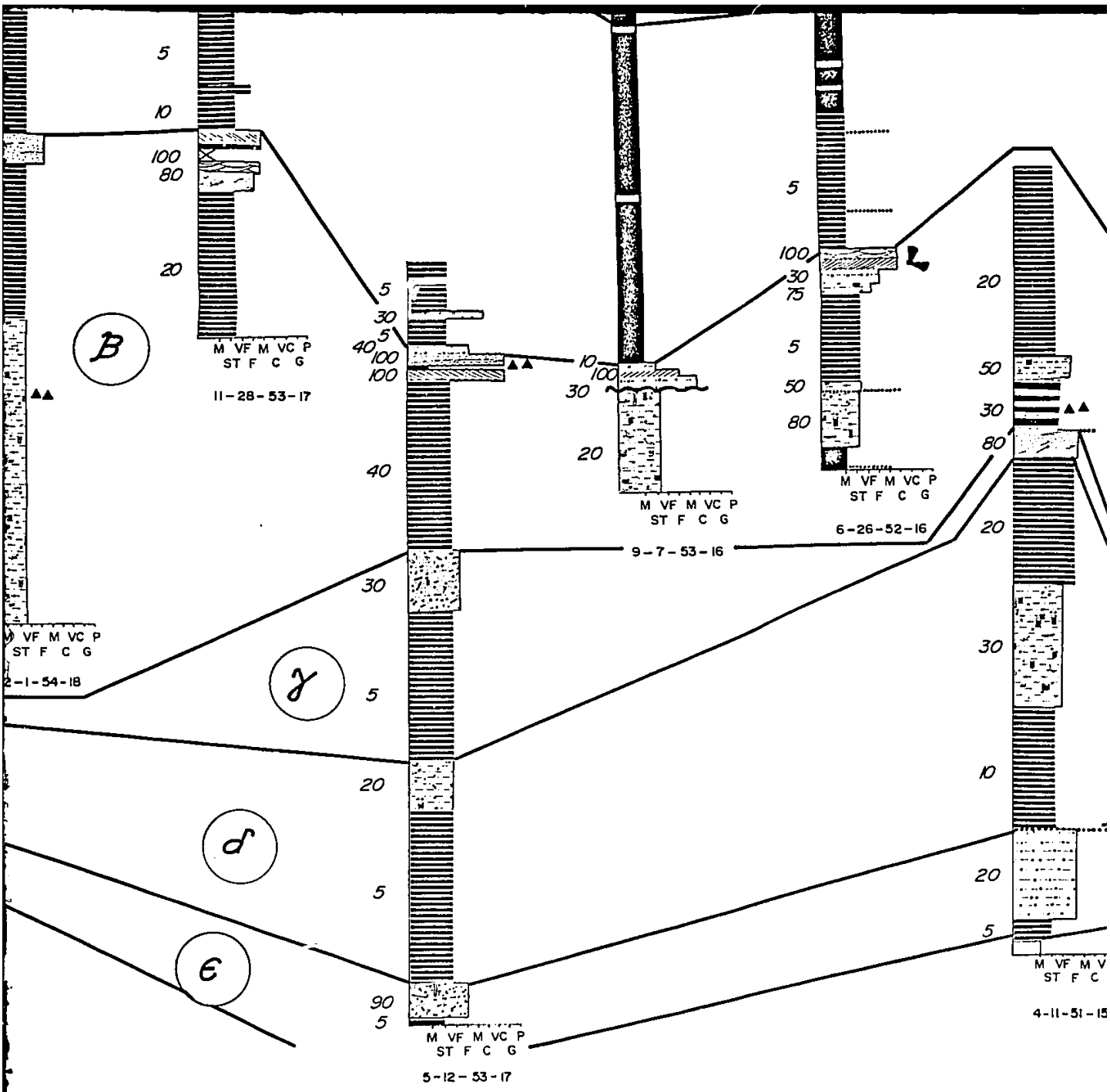
B
γ
δ
ε
M VF M VC P
ST F C G
11-28-53-17
9-7-53-16
6-26-52-16
2-1-54-18
5-12-53-17
4-11-51-15

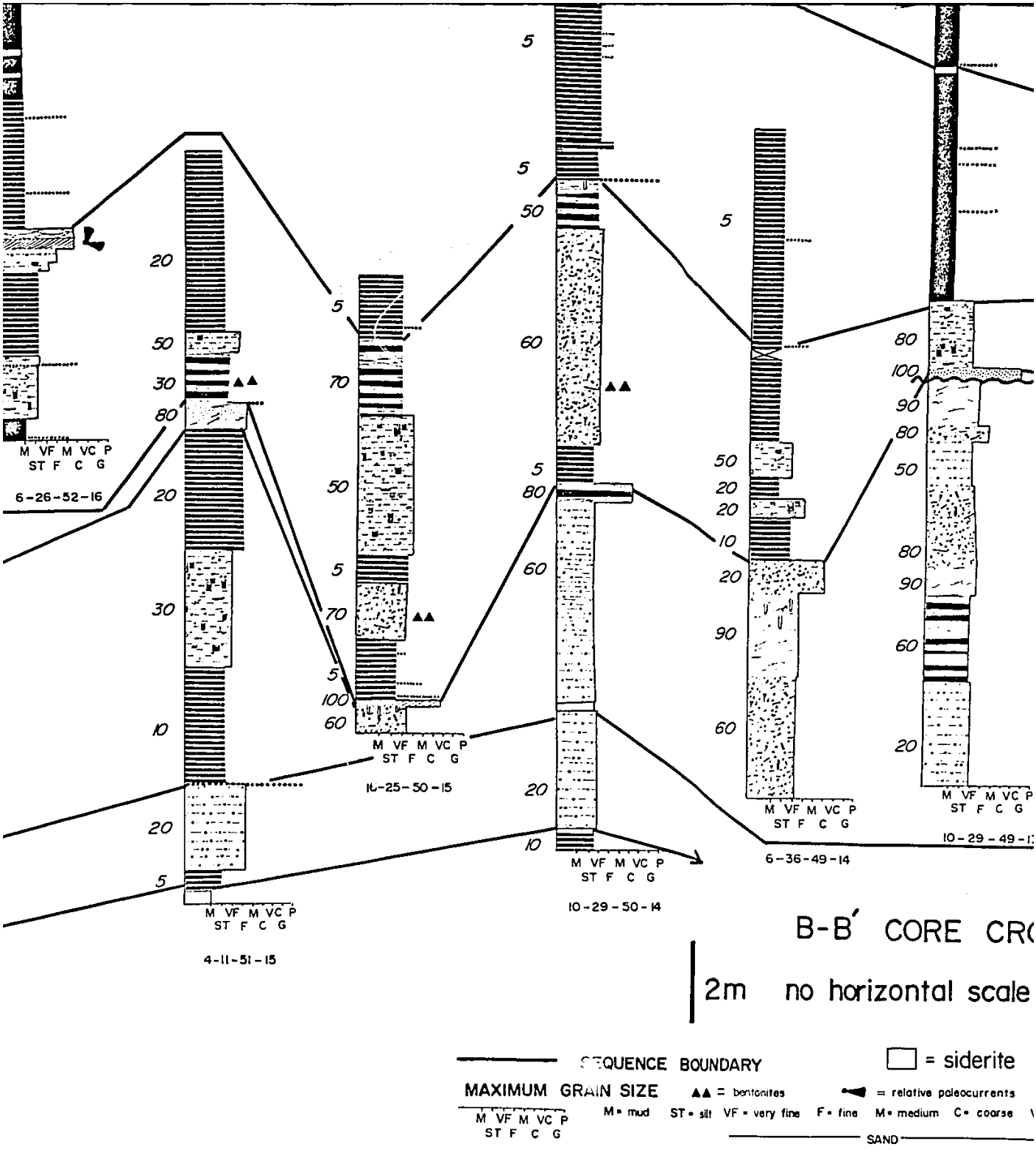
M VF M VC P
ST F C G
6-26-52-16
4-11-51-15
10-25-50-15
10-29-50-14
6-36-49-14
10-29-49-1
B-B' CORE CR(
2m no horizontal scale
SEQUENCE BOUNDARY
= siderite
MAXIMUM GRAIN SIZE
▲▲ = bentonites
= relative paleocurrents
M = mud ST = silt VF = very fine F = fine M = medium C = coarse
SAND

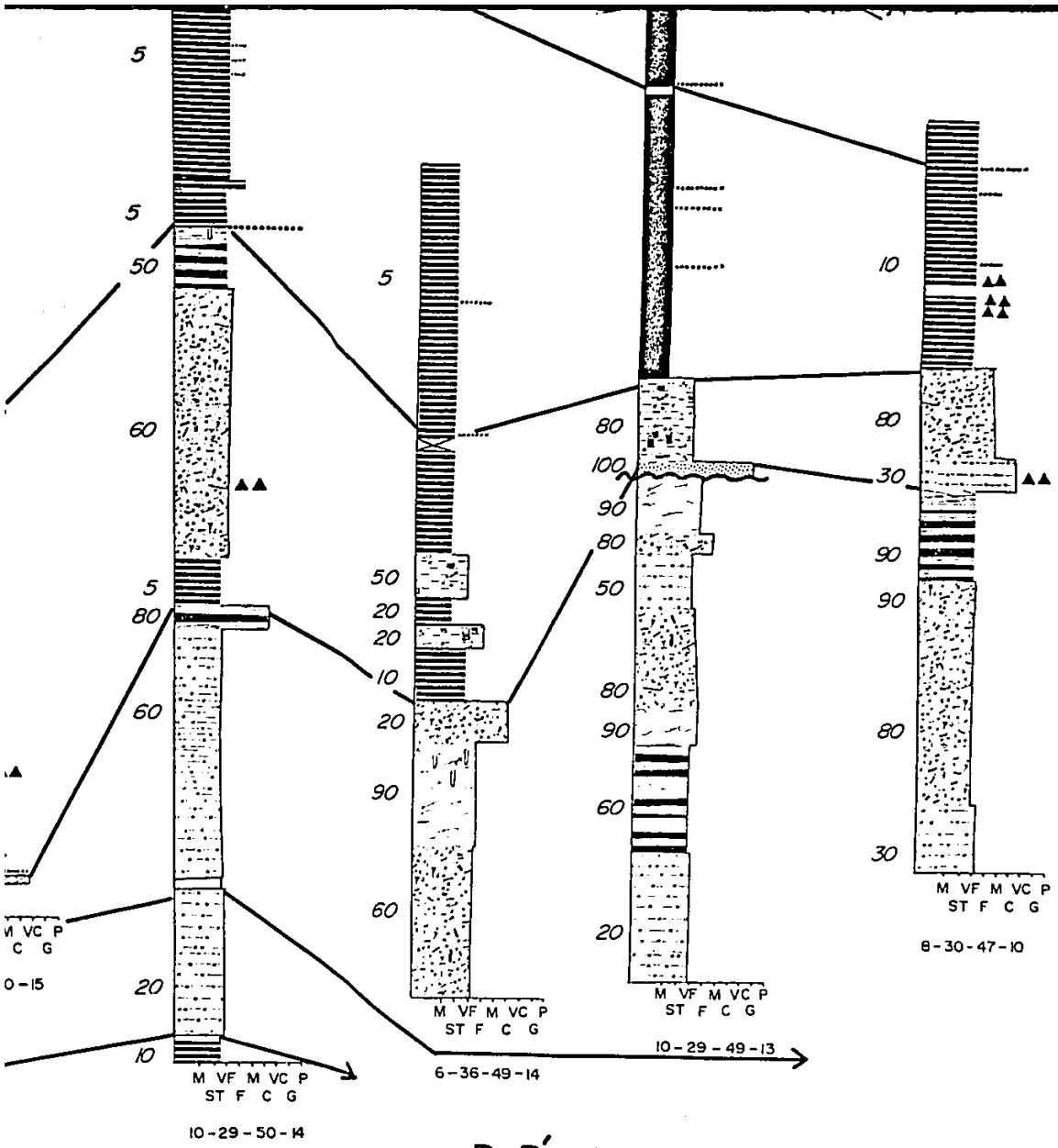

B-B′ CORE CROSS SECTION

2m no horizontal scale

SEQUENCE BOUNDARY

□ = siderite

MAXIMUM GRAIN SIZE

▲▲ = bentonites

= relative paleocurrents

10 = % sand

M VF M VC P
ST F C G

M = mud ST = silt VF = very fine F = fine M = medium C = coarse VC = very coarse G = granules P = pebbles

SAND

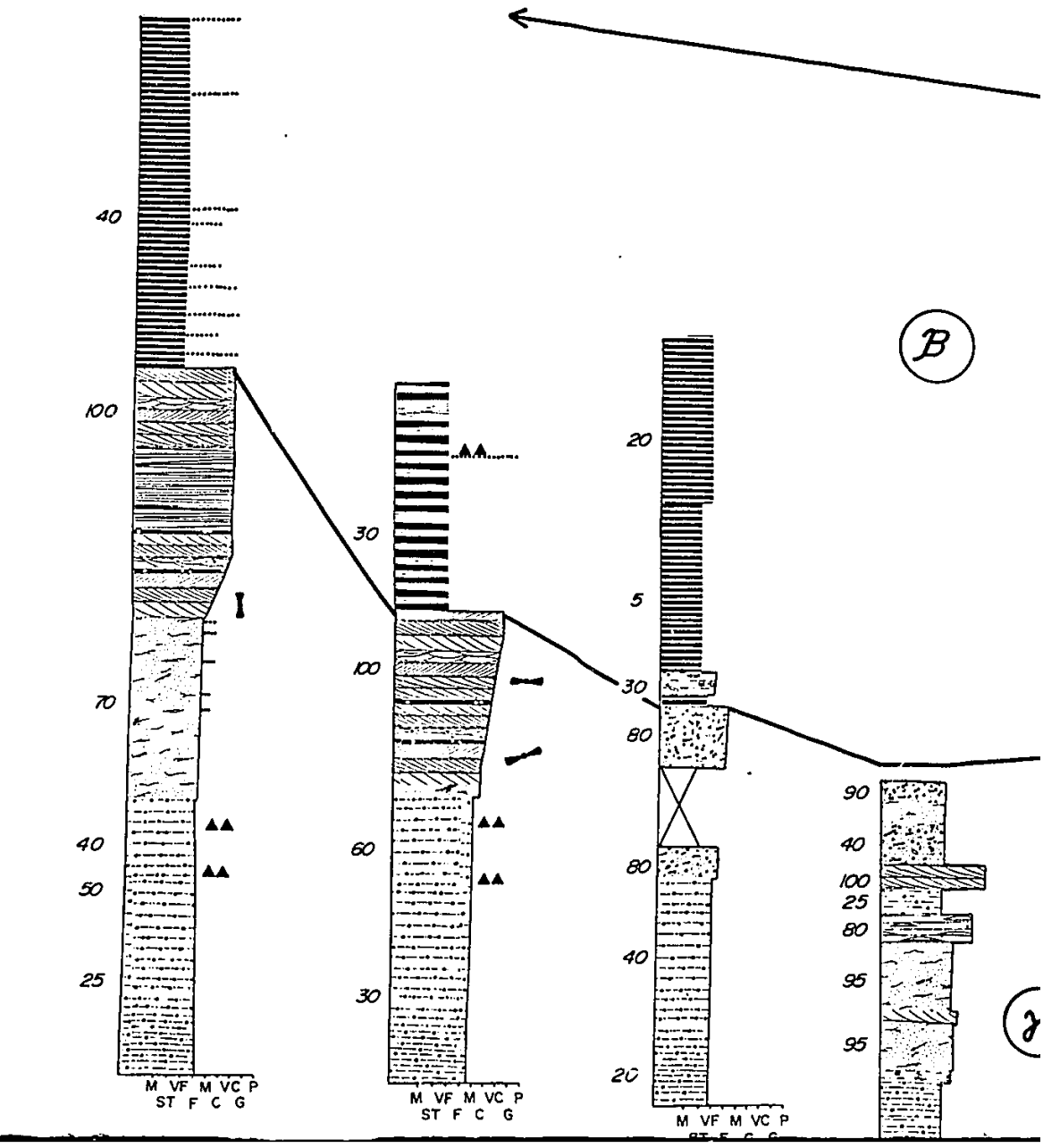
C
B
40
100
70
40
50
25
30
100
60
30
20
5
30
80
80
40
20
90
40
100
25
80
95
95
M VF M VC P
ST F C G

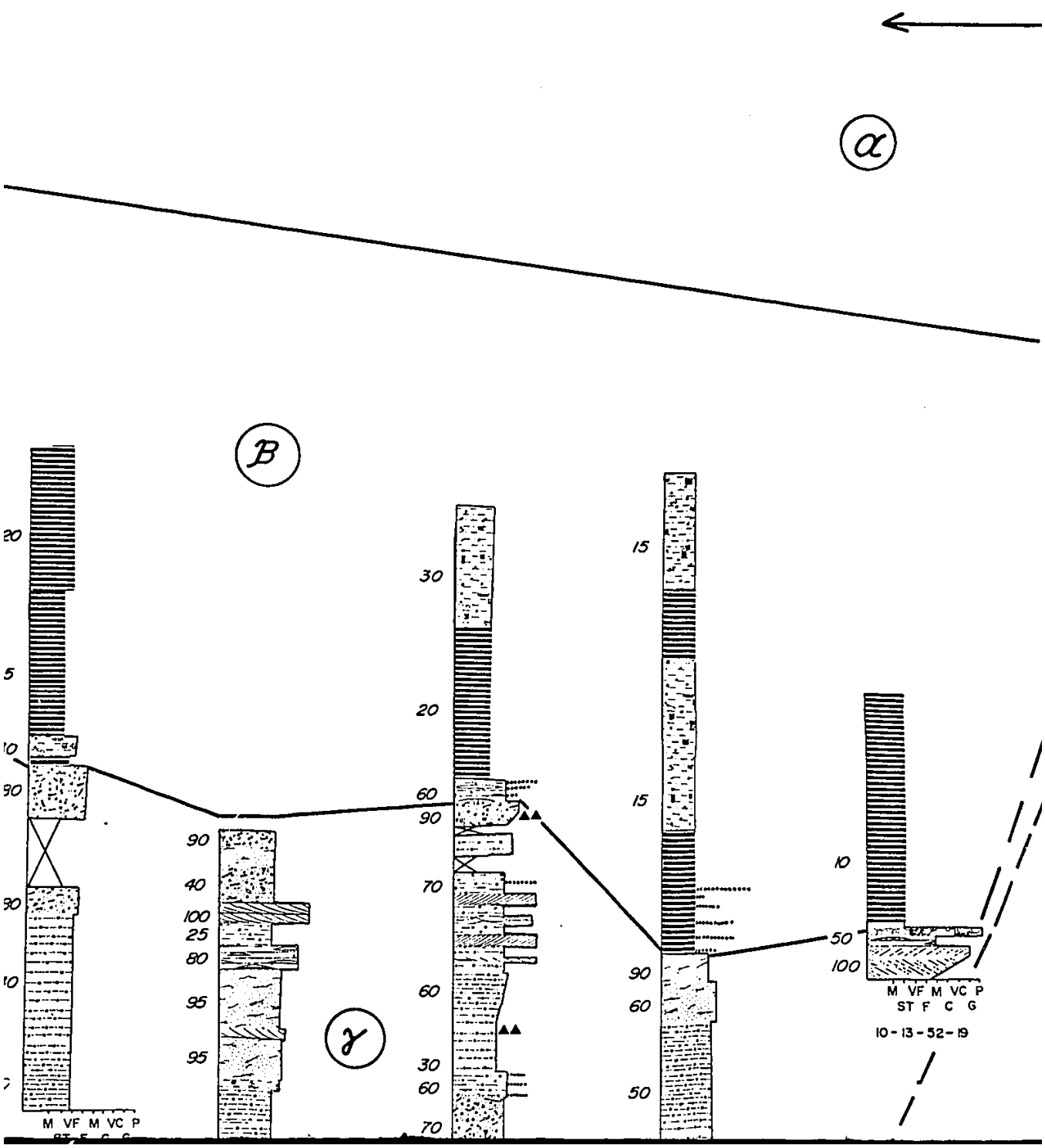
α
β
γ
M VF M VC P
ST F C G
10-13-52-19

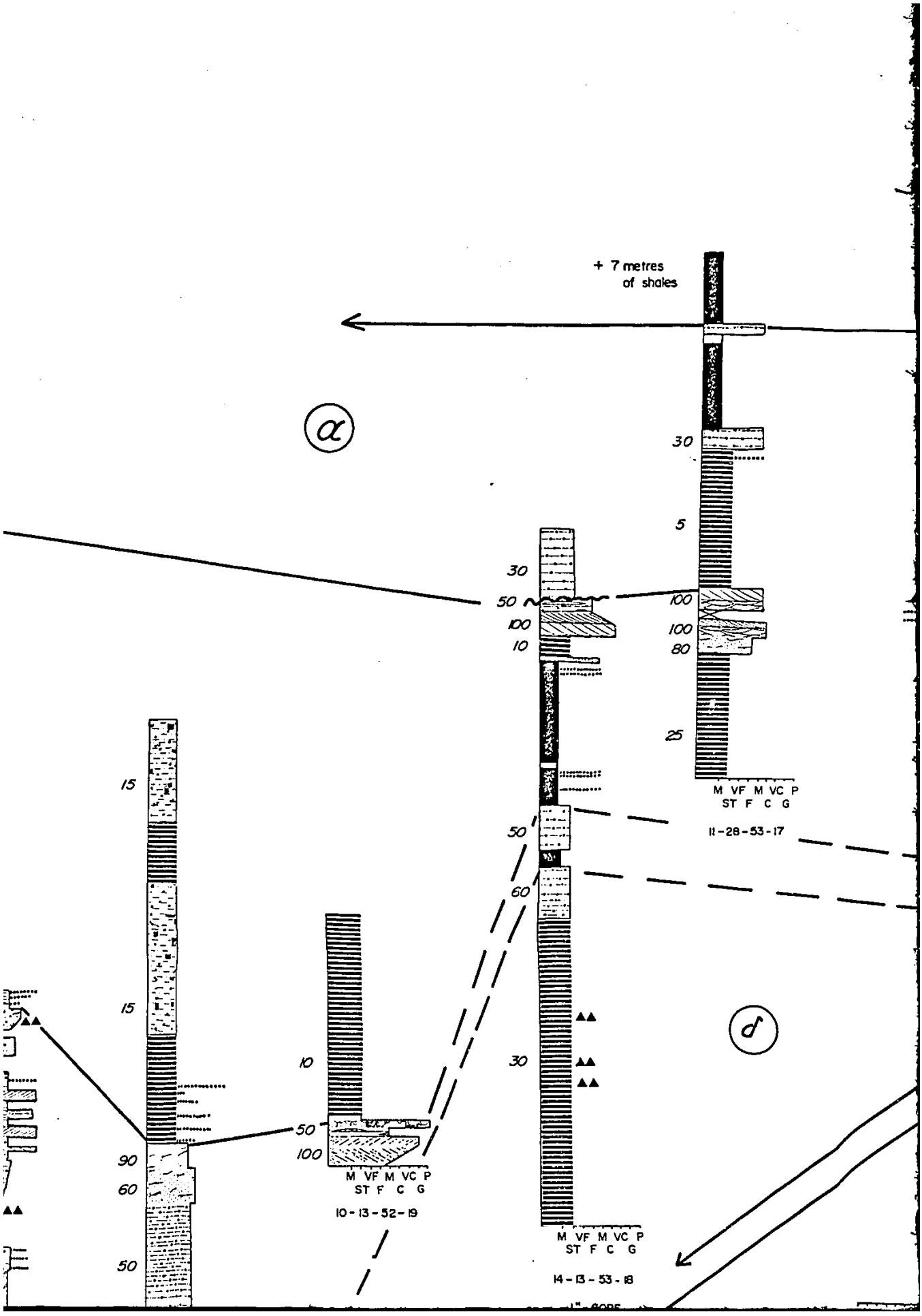
+ 7 metres
of shales
α
30
5
100
100
80
25
M VF M VC P
ST F C G
11-28-53-17
30
50
100
10
50
60
30
15
15
90
60
50
10
50
100
M VF M VC P
ST F C G
10-13-52-19
M VF M VC P
ST F C G
14-13-53-18
δ

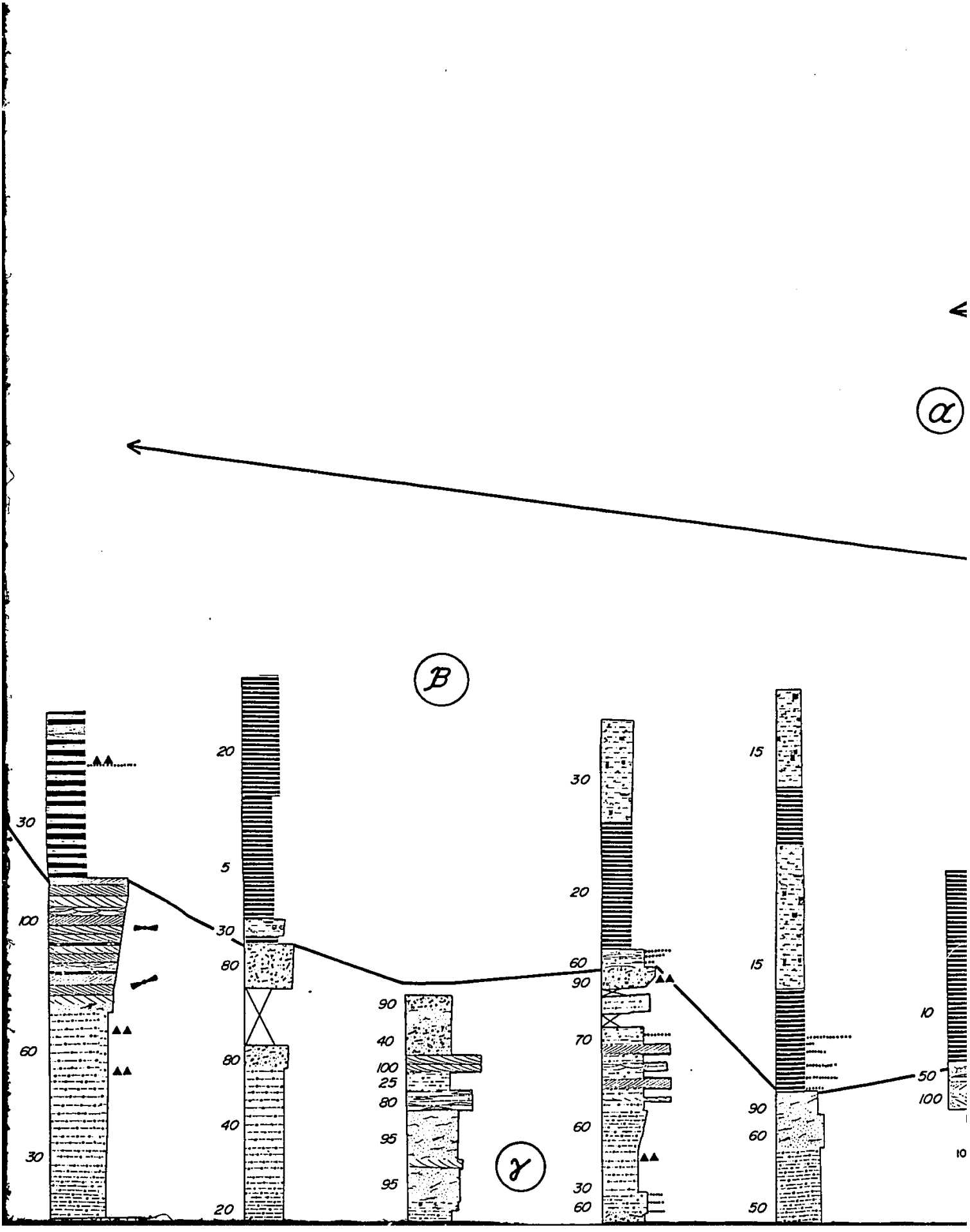
α
β
γ
30
100
60
30
20
5
30
80
80
40
20
90
40
100
25
80
95
95
30
20
60
90
70
60
30
60
15
15
90
60
50
10
50
100
10

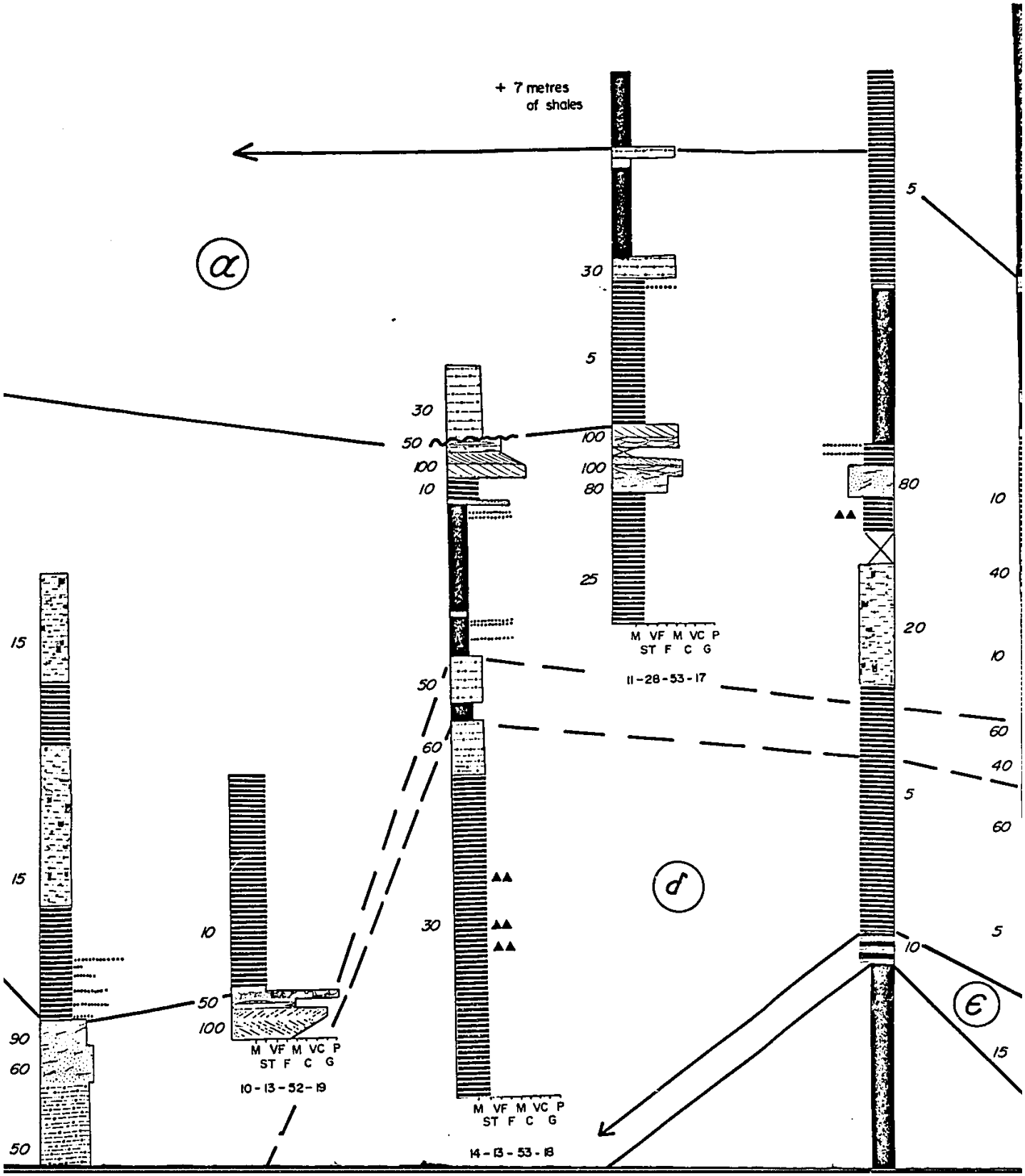
+ 7 metres
of shales
α
30
5
30
50
100
10
100
100
80
25
M VF M VC P
ST F C G
11-28-53-17
80
10
40
20
10
60
40
5
60
15
15
50
60
10
30
d
50
100
M VF M VC P
ST F C G
10-13-52-19
M VF M VC P
ST F C G
14-13-53-18
90
60
50
5
10
15
ε

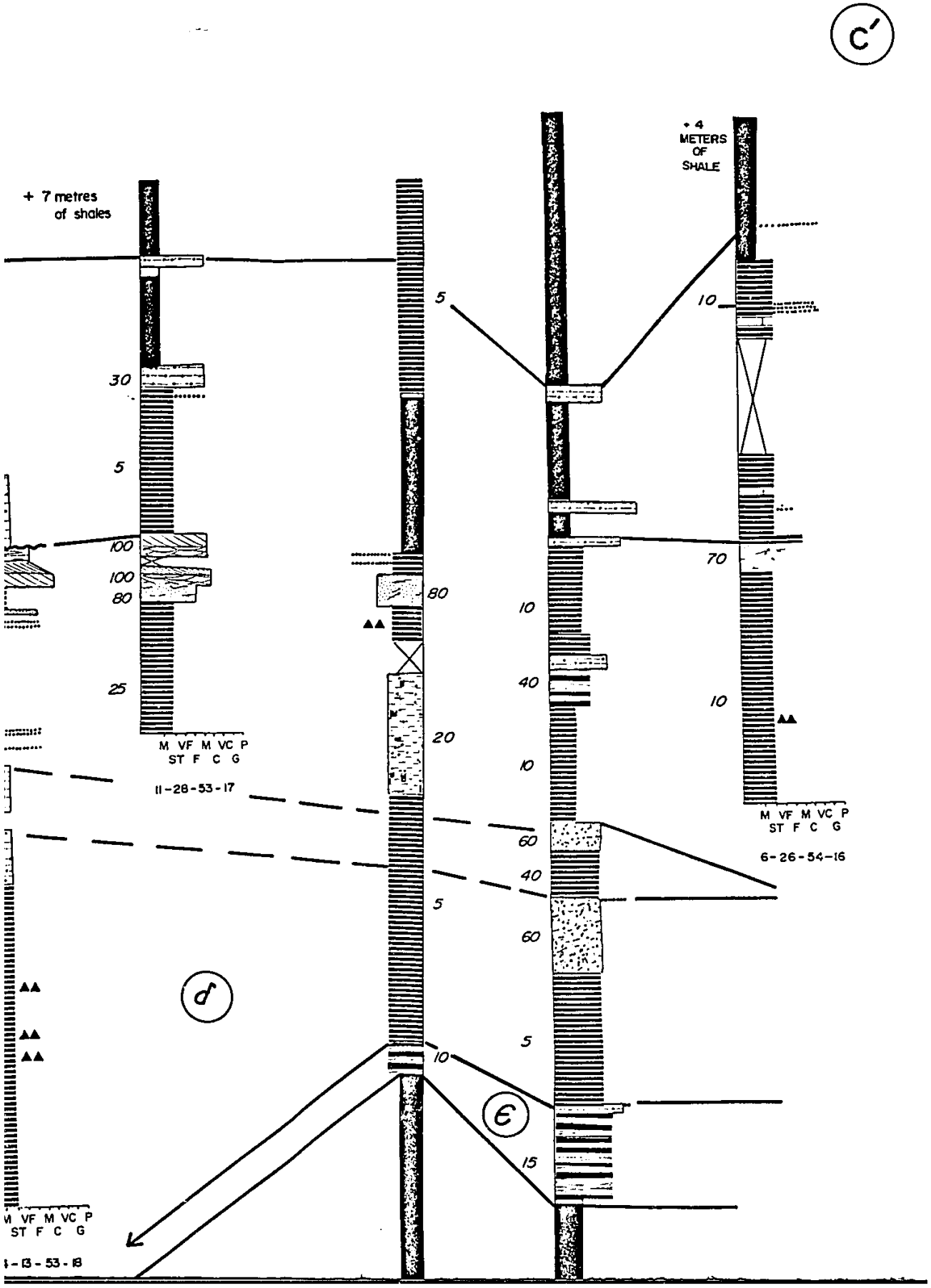
C'
+ 7 metres of shales
+ 4 METERS OF SHALE
30
5
100
100
80
25
80
20
5
10
10
40
10
60
40
60
5
5
10
15
70
10
M VF M VC P
ST F C G
11-28-53-17
6-26-54-16
d
e

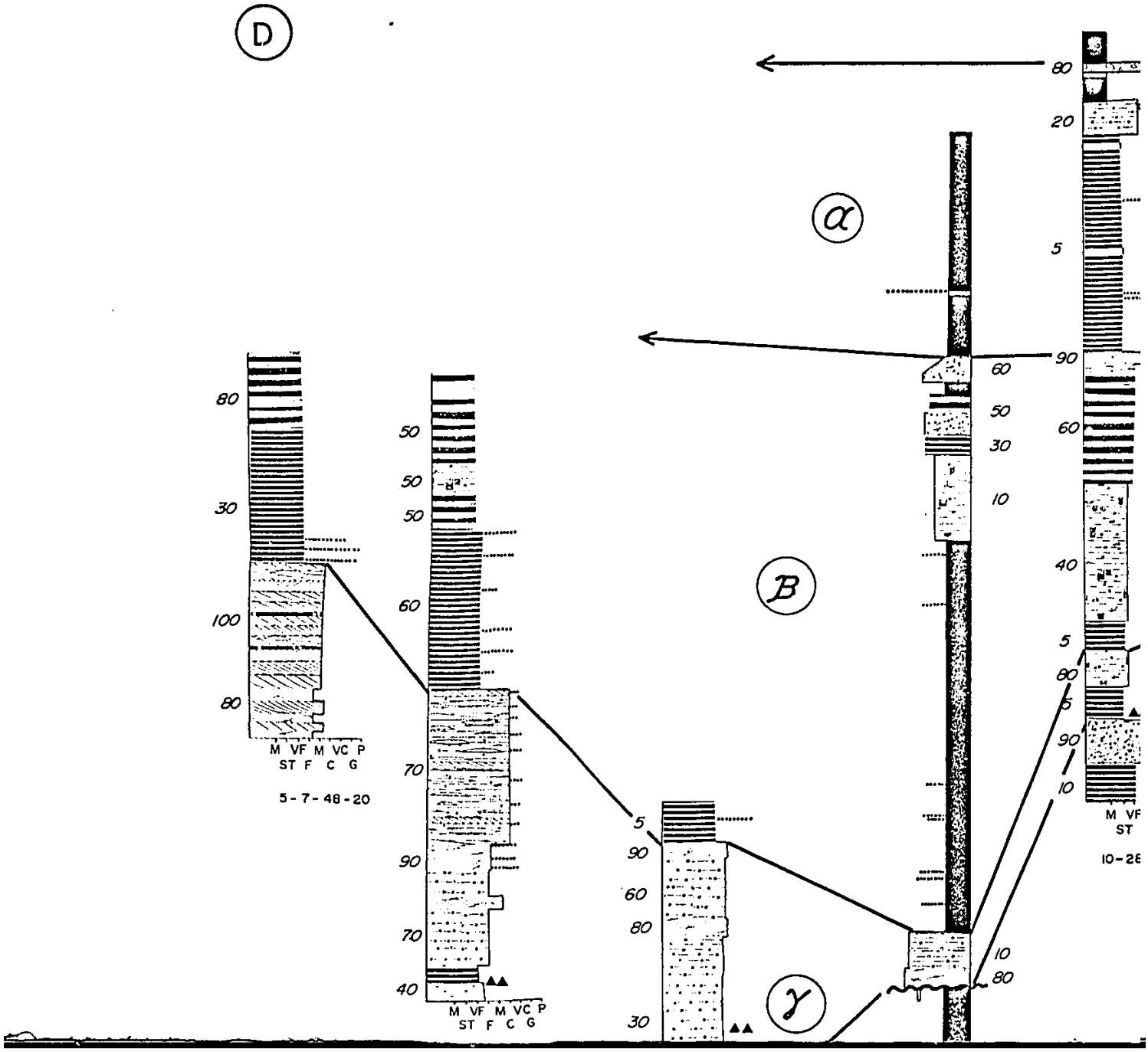
D
α
B
γ
80
30
100
80
M VF M VC P
ST F C G
5-7-48-20
50
50
50
60
70
90
70
40
M VF M VC P
ST F C G
5
90
60
80
30
80
20
5
90
60
50
30
10
10
80
40
5
80
5
90
10
M VF
ST
10-2E

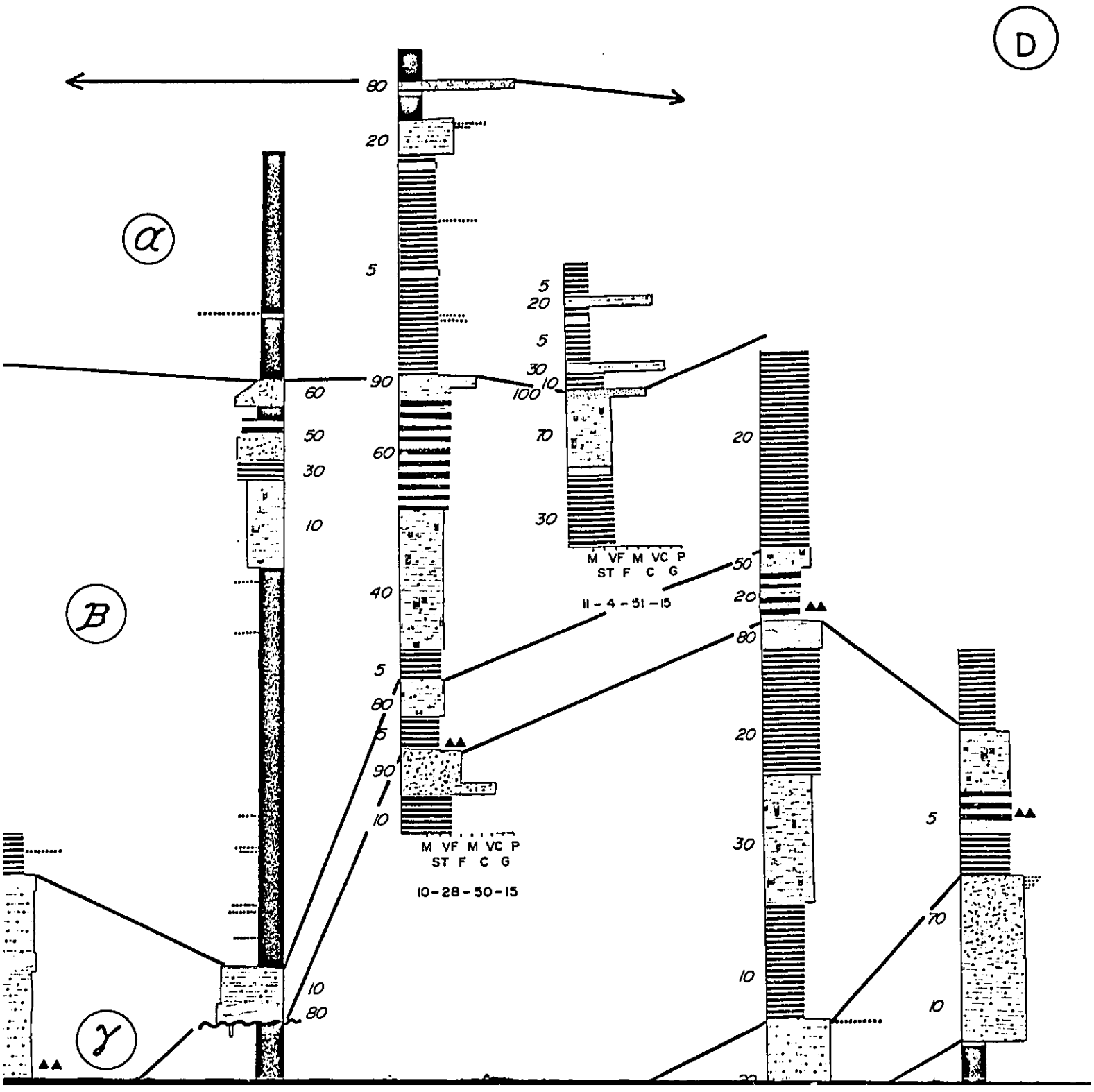
D
α
β
γ
M VF M VC P
ST F C G
10-28-50-15
M VF M VC P
ST F C G
11-4-51-15

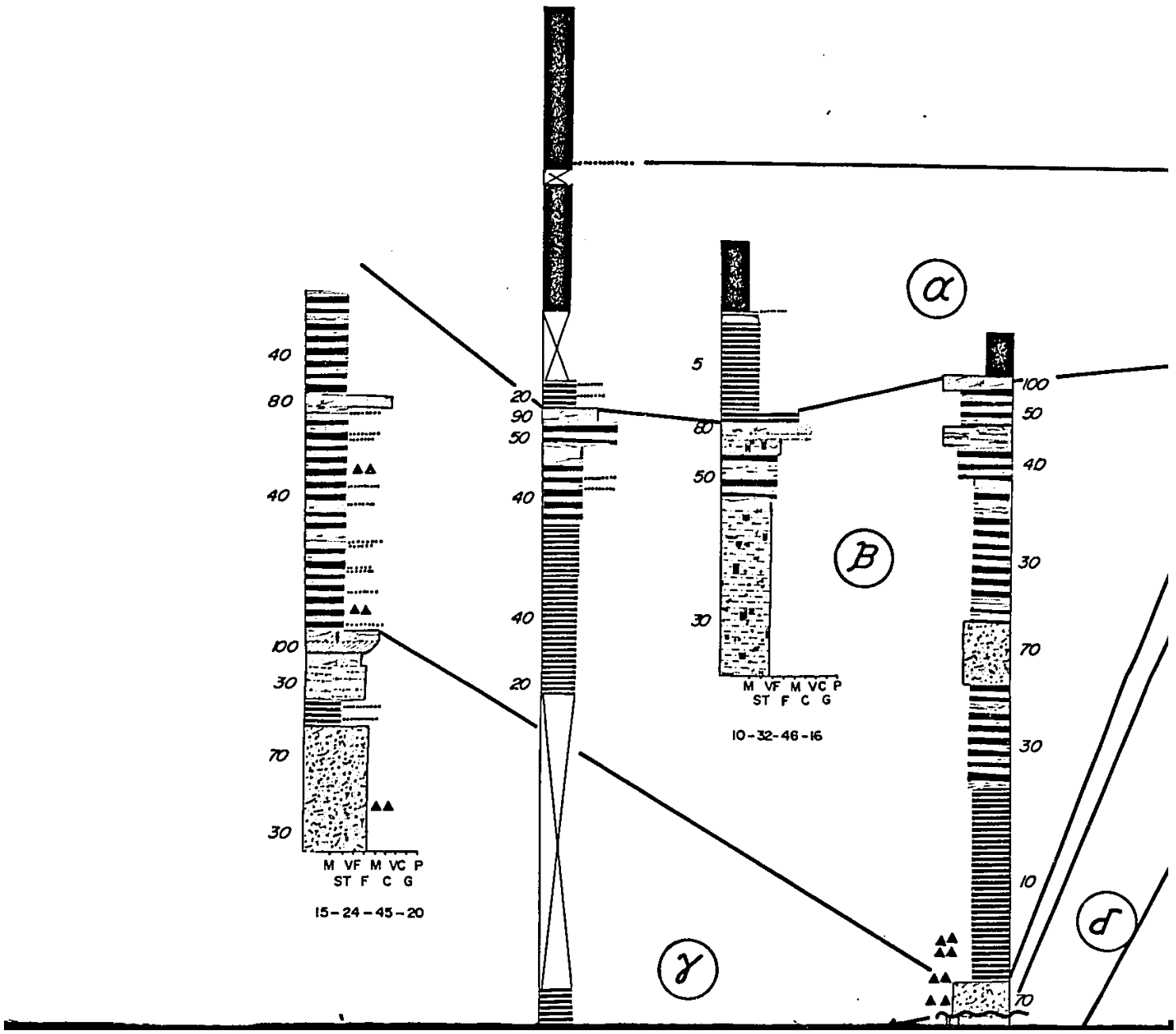
E
40
80
40
100
30
70
30
M VF M VC P
ST F C G
15-24-45-20
20
90
50
40
40
20
5
80
50
30
M VF M VC P
ST F C G
10-32-46-16
α
β
γ
δ
100
50
40
30
70
30
10
70

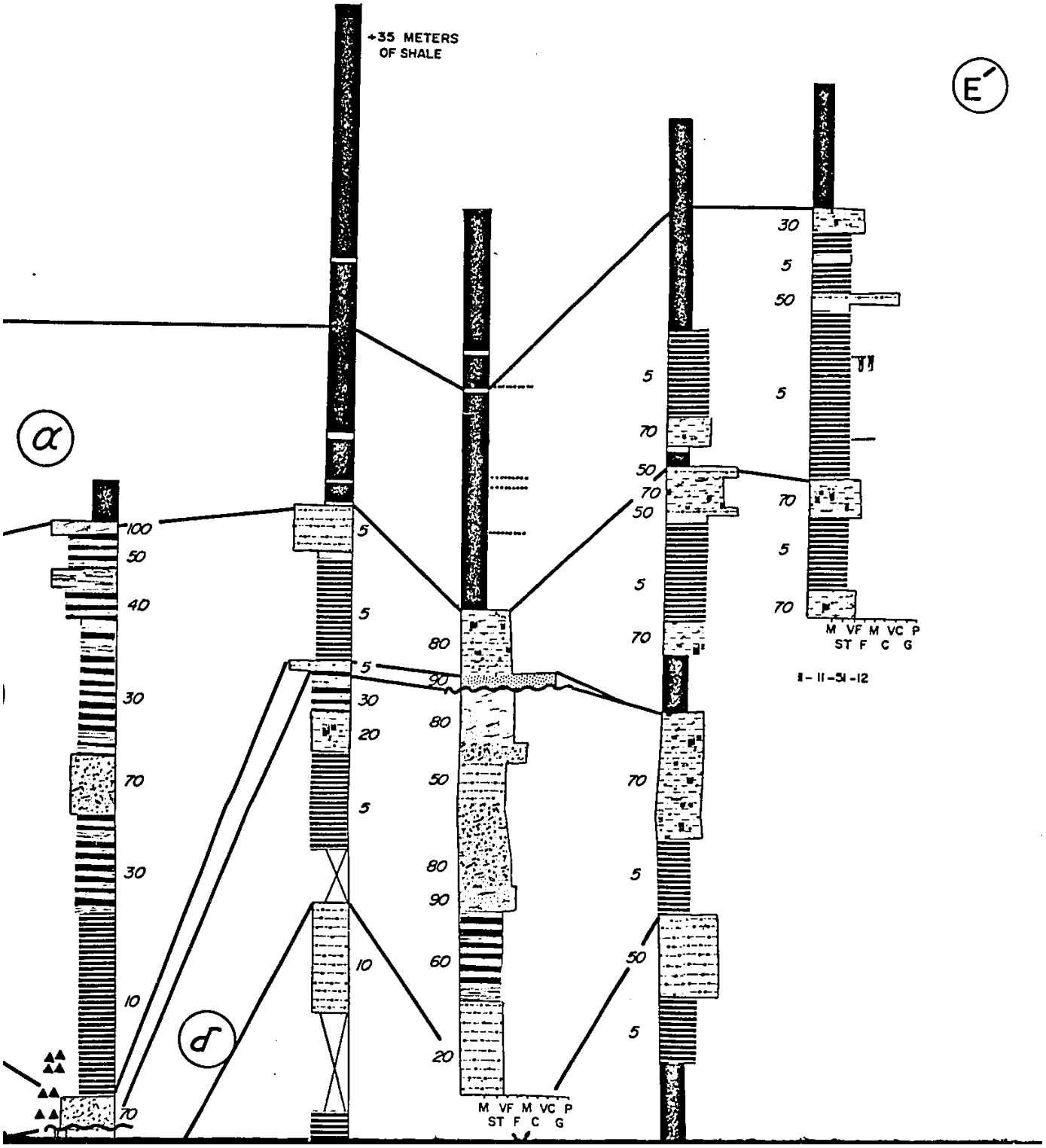
+35 METERS
OF SHALE
α
E'
d
100
50
40
30
70
30
10
70
5
5
5
30
20
5
10
80
90
80
50
80
90
60
20
M VF M VC P
ST F C G
5
70
50
70
50
5
70
5
70
50
5
30
5
50
5
70
5
70
M VF M VC P
ST F C G
II-11-51-12

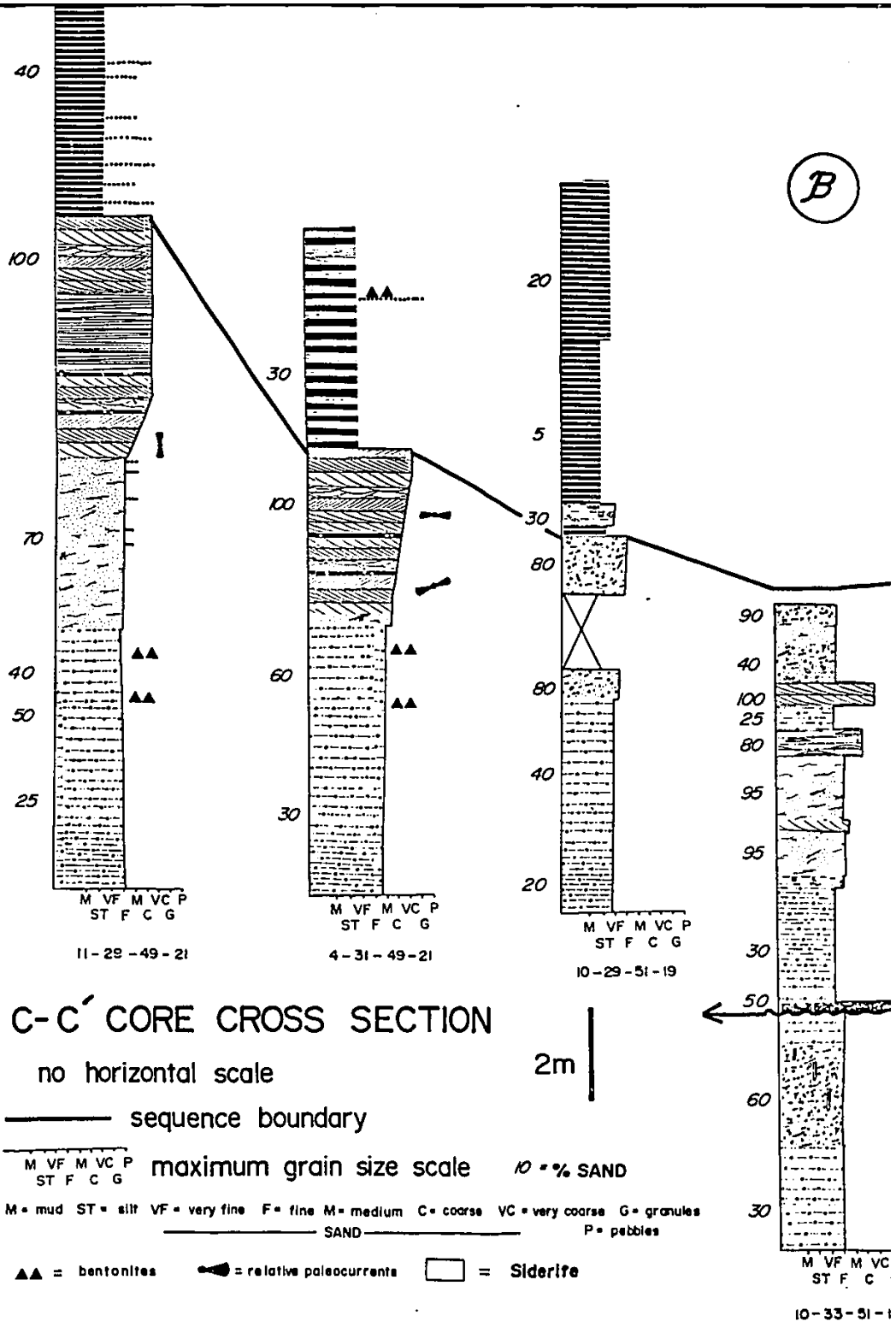
B
40
100
70
40
50
25
M VF M VC P
ST F C G
11-29-49-21
30
100
60
30
4-31-49-21
20
5
30
80
80
40
20
10-29-51-19
90
40
100
25
80
95
95
30
50
60
30
M VF M VC
ST F C
10-33-51-
C-C´ CORE CROSS SECTION
no horizontal scale
2m
sequence boundary
M VF M VC P
ST F C G
maximum grain size scale
10 = % SAND
M = mud ST = silt VF = very fine F = fine M = medium C = coarse VC = very coarse G = granules
SAND
P = pebbles
▲▲ = bentonites
= relative paleocurrents
= Siderite

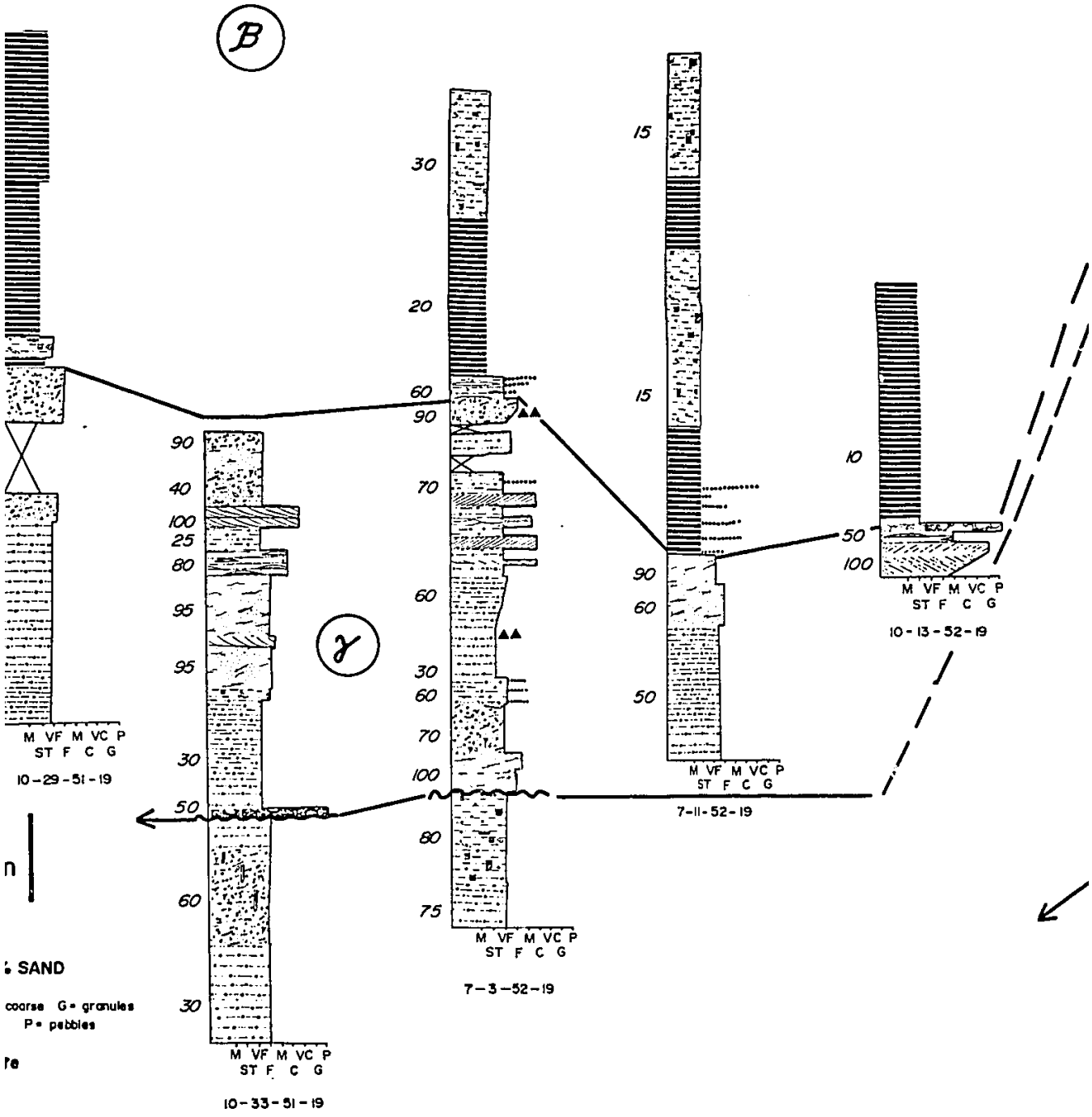
B
γ
30
20
60
90
70
60
30
60
70
100
80
75
90
40
100
25
80
95
95
30
50
60
30
15
15
90
60
50
10
50
100
M VF M VC P
ST F C G
10-29-51-19
10-33-51-19
7-3-52-19
7-11-52-19
10-13-52-19
SAND
coarse G = granules
P = pebbles

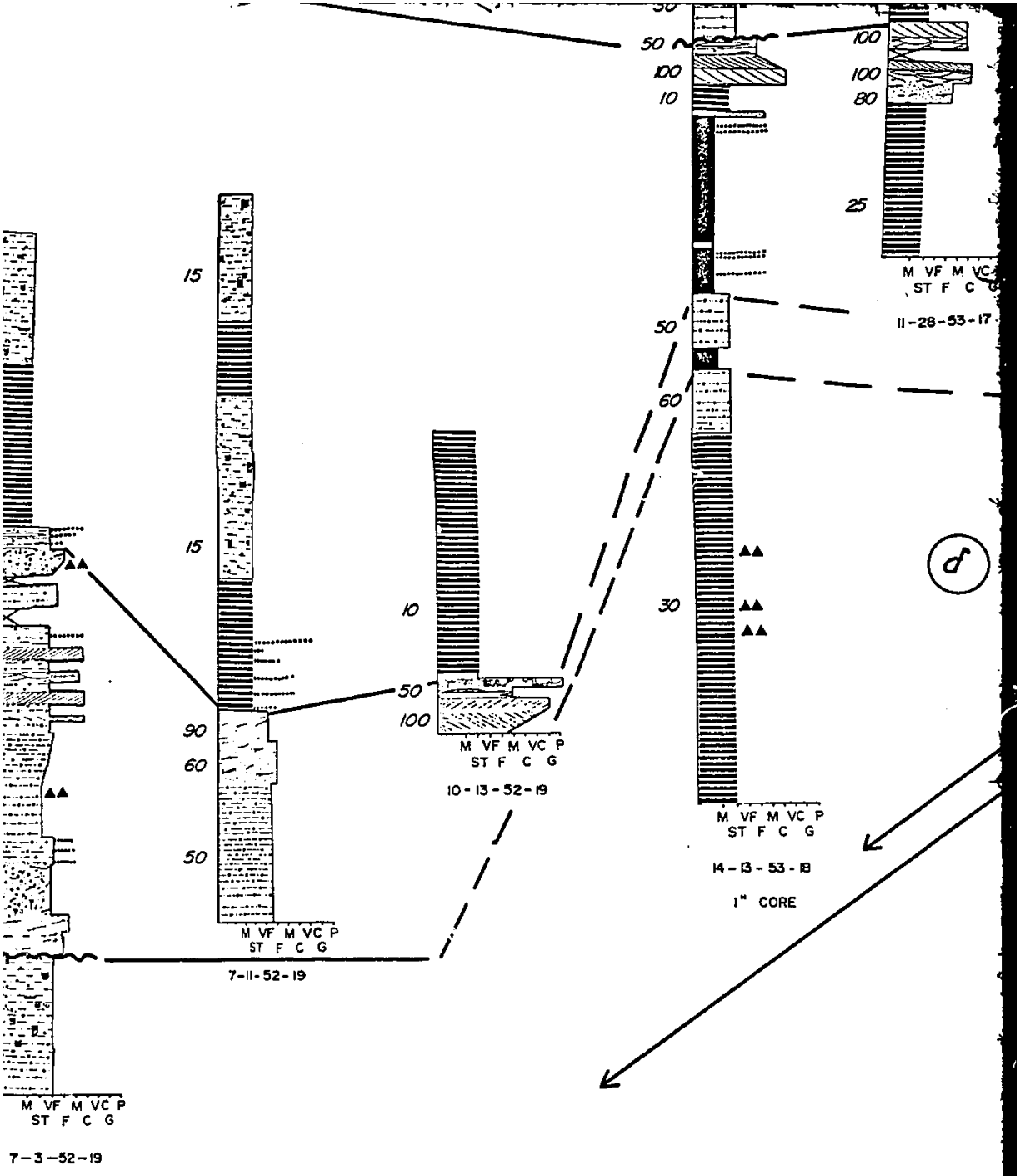
50
100
10
100
100
80
25
M VF M VC P
ST F C G
11-28-53-17
50
60
30
15
15
10
50
100
90
60
50
M VF M VC P
ST F C G
10-13-52-19
14-13-53-18
1" CORE
7-11-52-19
7-3-52-19

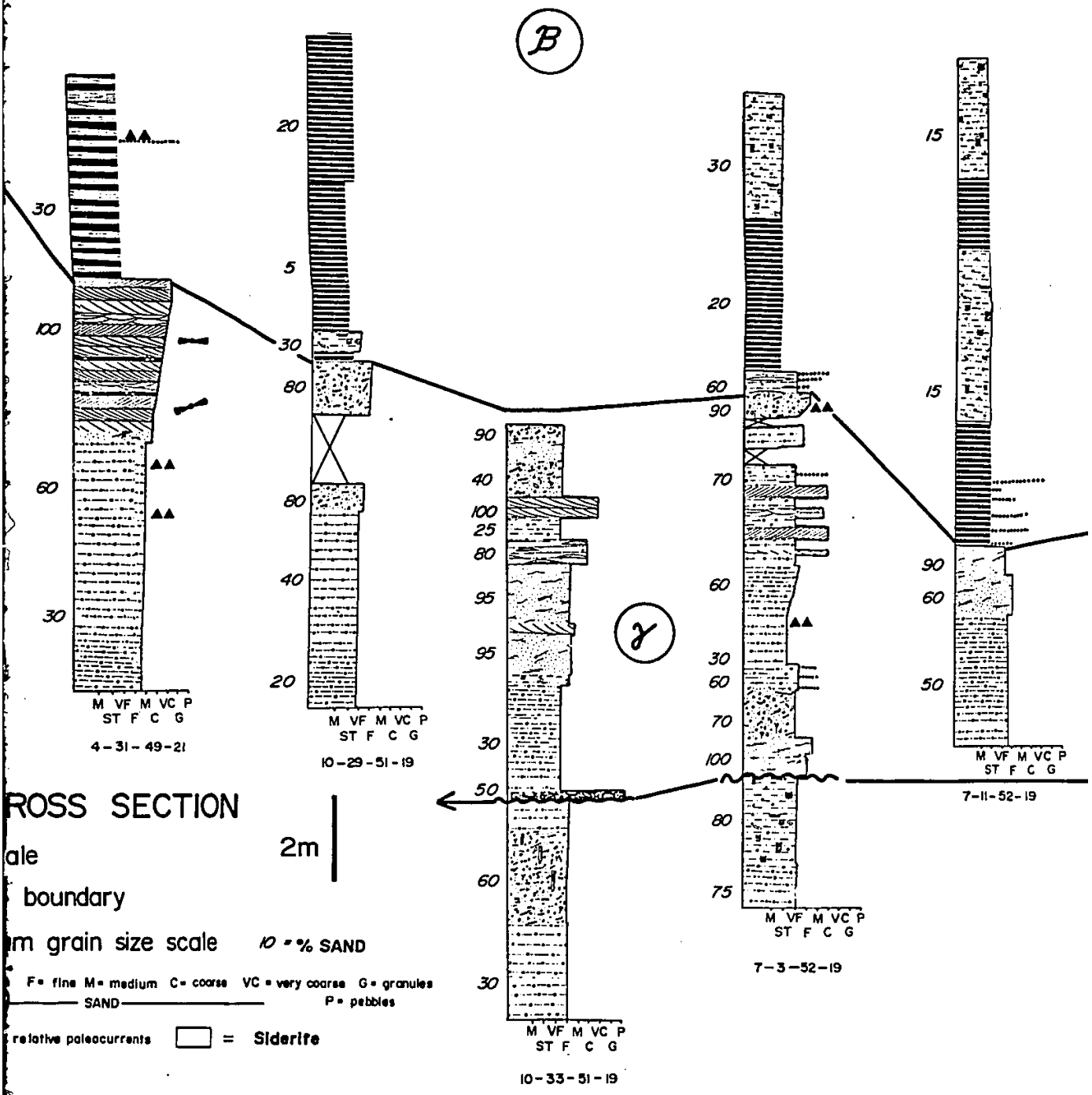
B
γ
30
100
60
30
M VF M VC P
ST F C G
4-31-49-21
20
5
30
80
80
40
20
M VF M VC P
ST F C G
10-29-51-19
90
40
100
25
80
95
95
30
50
60
30
M VF M VC P
ST F C G
10-33-51-19
30
20
60
90
70
60
30
60
70
100
80
75
M VF M VC P
ST F C G
7-3-52-19
15
15
90
60
50
M VF M VC P
ST F C G
7-11-52-19
ROSS SECTION
ale
2m
boundary
m grain size scale
10 = % SAND
F = fine M = medium C = coarse VC = very coarse G = granules
SAND
P = pebbles
relative paleocurrents
= Siderite

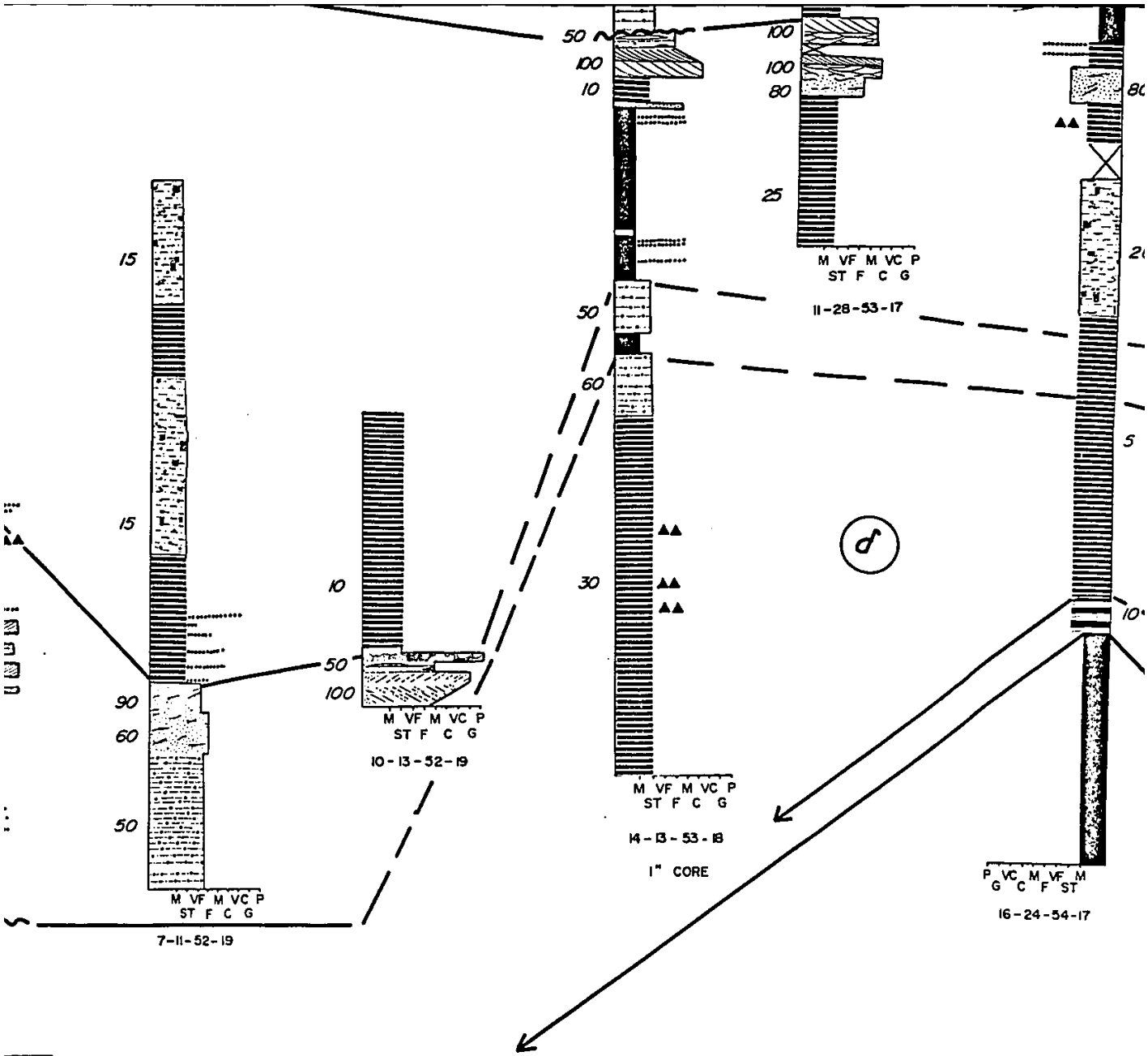
15
15
90
60
50
M VF M VC P
ST F C G
7-11-52-19
10
50
100
M VF M VC P
ST F C G
10-13-52-19
50
100
10
60
30
M VF M VC P
ST F C G
14-13-53-18
1" CORE
100
100
80
25
M VF M VC P
ST F C G
11-28-53-17
80
2
5
10
P VC M VF M
G C F ST
16-24-54-17
d

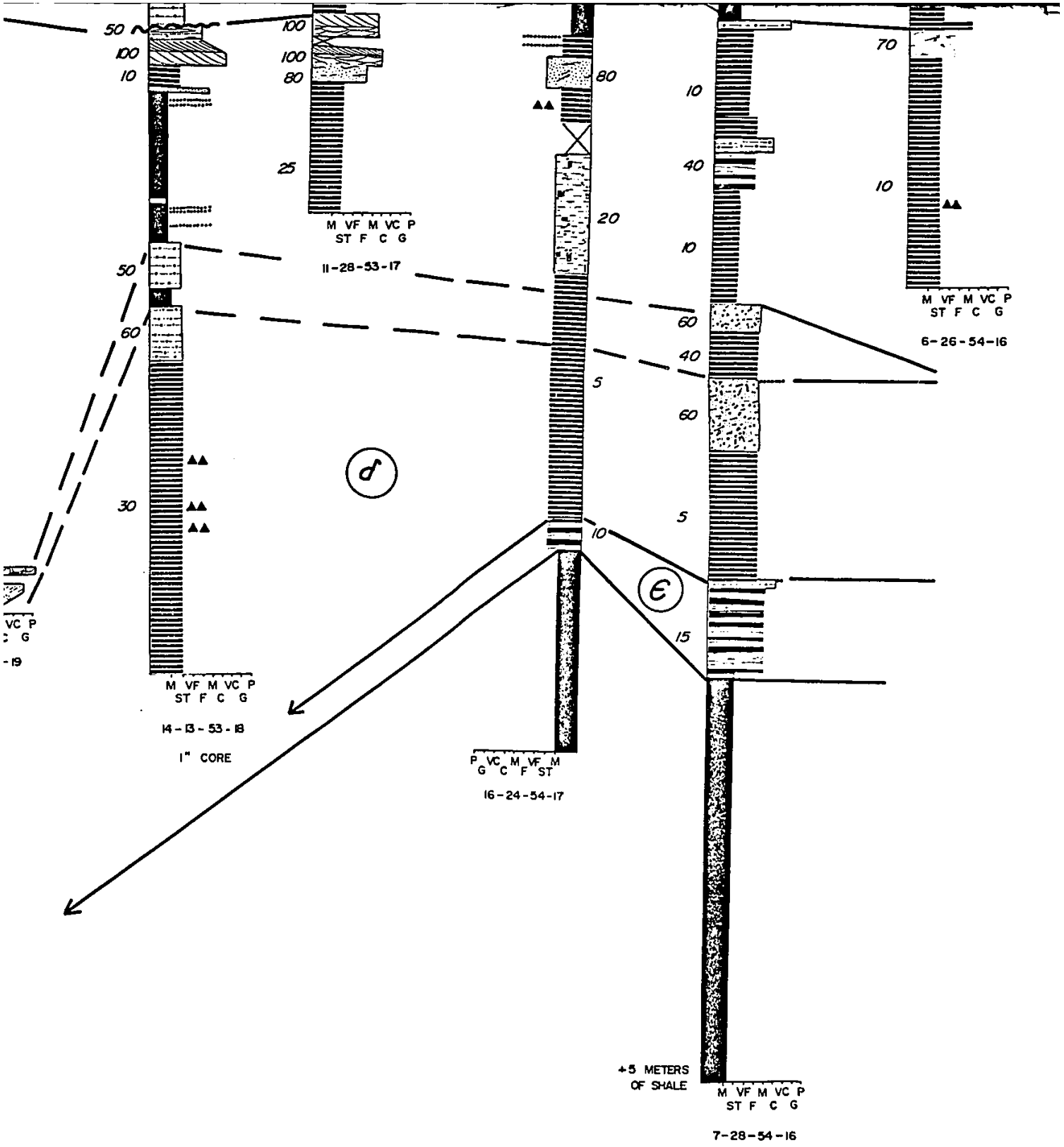
50
100
10
50
60
30
M VF M VC P
ST F C G
14-13-53-18
1" CORE
100
100
80
25
M VF M VC P
ST F C G
11-28-53-17
80
20
5
10
P VC M VF M
G C F ST
16-24-54-17
10
40
10
60
40
60
5
15
+5 METERS
OF SHALE
M VF M VC P
ST F C G
7-28-54-16
70
10
M VF M VC P
ST F C G
6-26-54-16
d
e

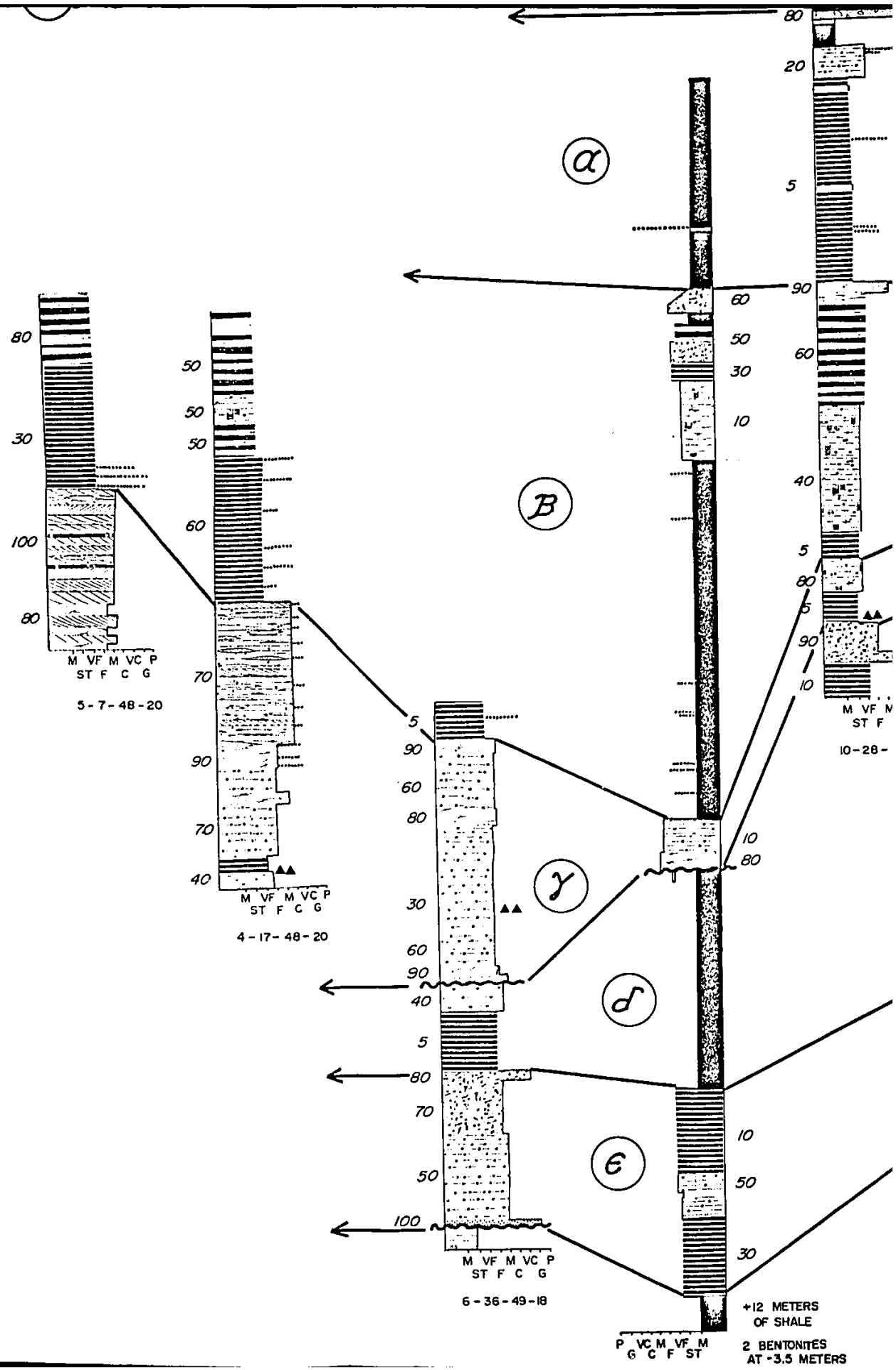
α
B
γ
δ
ε
80
20
5
90
60
50
30
10
40
5
80
5
90
10
M VF M VC P
ST F C G
10-28-
80
30
100
80
M VF M VC P
ST F C G
5-7-48-20
50
50
50
60
70
90
70
40
M VF M VC P
ST F C G
4-17-48-20
5
90
60
80
30
60
90
40
5
80
70
50
100
M VF M VC P
ST F C G
6-36-49-18
10
80
10
50
30
P VC M VF M
G C F ST
+12 METERS
OF SHALE
2 BENTONITES
AT -3.5 METERS

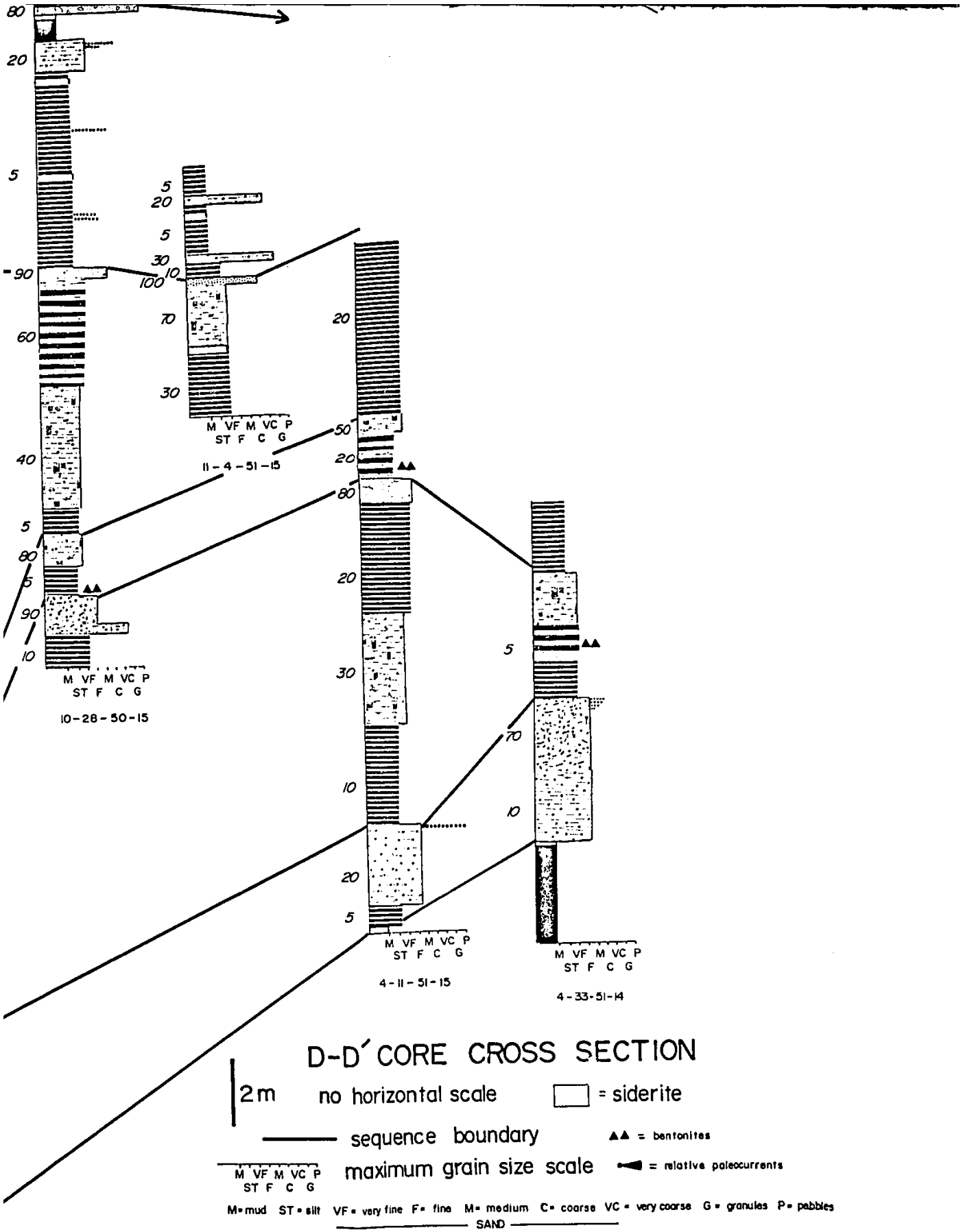

ETERS
HALE

TONITES
.5 METERS

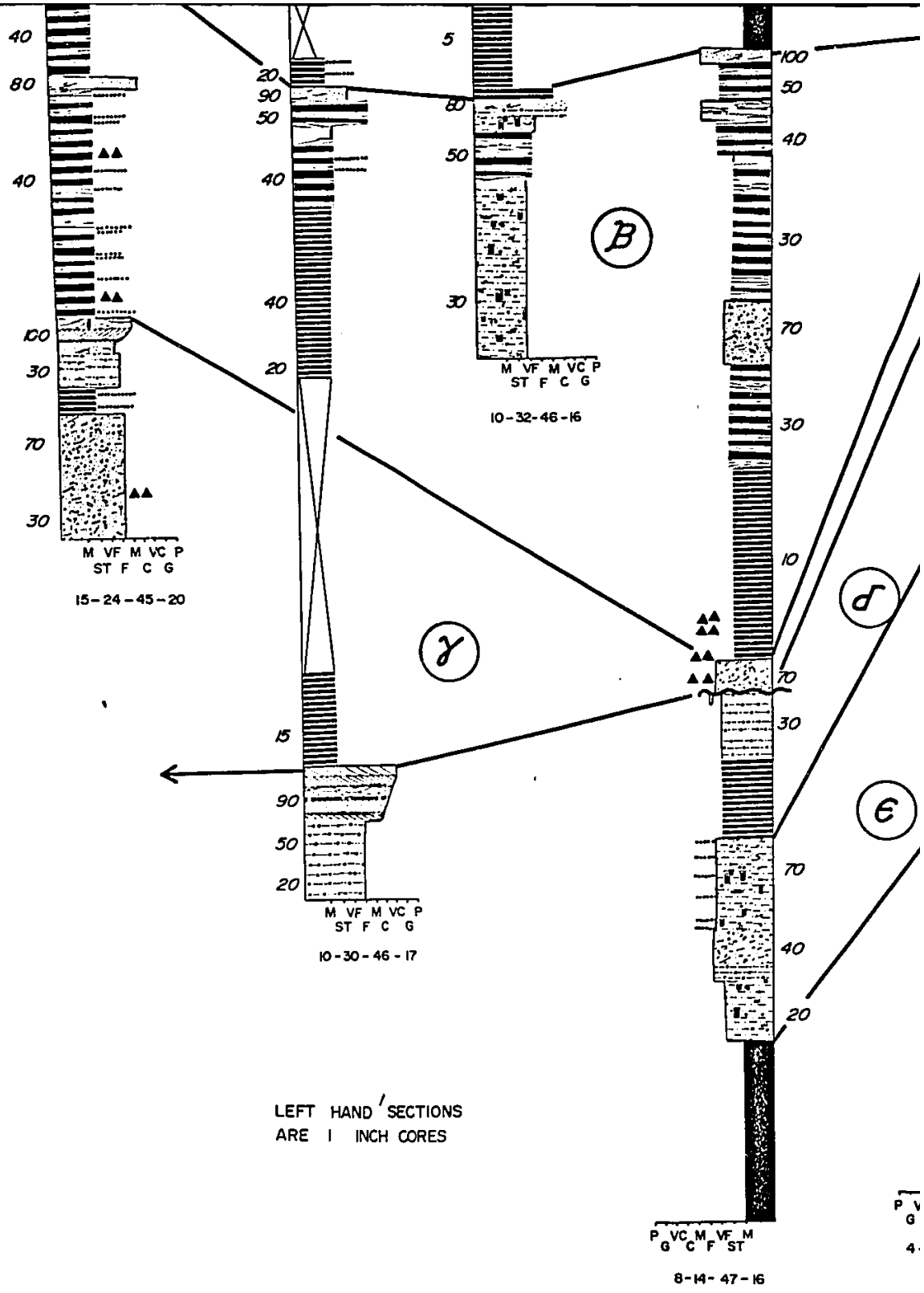
40
80
40
100
30
70
30
M VF M VC P
ST F C G
15-24-45-20
20
90
50
40
40
20
15
90
50
20
M VF M VC P
ST F C G
10-30-46-17
γ
5
80
50
30
M VF M VC P
ST F C G
10-32-46-16
β
100
50
40
30
70
30
10
70
30
70
40
20
P VC M VF M
G C F ST
8-14-47-16
δ
ε
LEFT HAND SECTIONS
ARE 1 INCH CORES

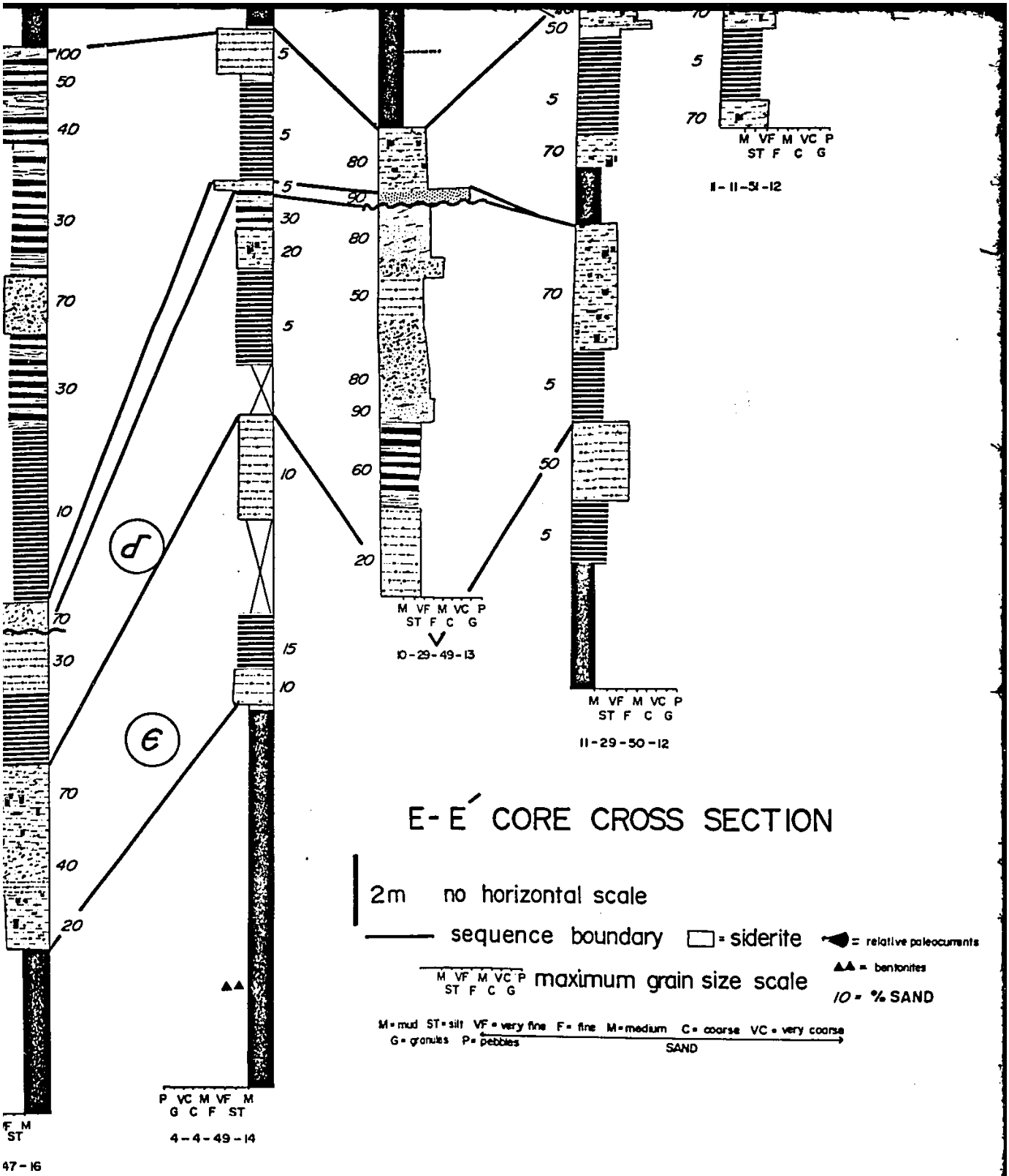
E-E´ CORE CROSS SECTION
2m no horizontal scale
sequence boundary
siderite
relative paleocurrents
bentonites
maximum grain size scale
10 = % SAND
M = mud ST = silt VF = very fine F = fine M = medium C = coarse VC = very coarse
G = granules P = pebbles
SAND
M VF M VC P
ST F C G
P VC M VF M
G C F ST
4-4-49-14
10-29-49-13
11-29-50-12
11-11-51-12
47-16

A-A´

SUMMARY SECTION

CORE

50' 15 m

NO HORIZONTAL SCALE

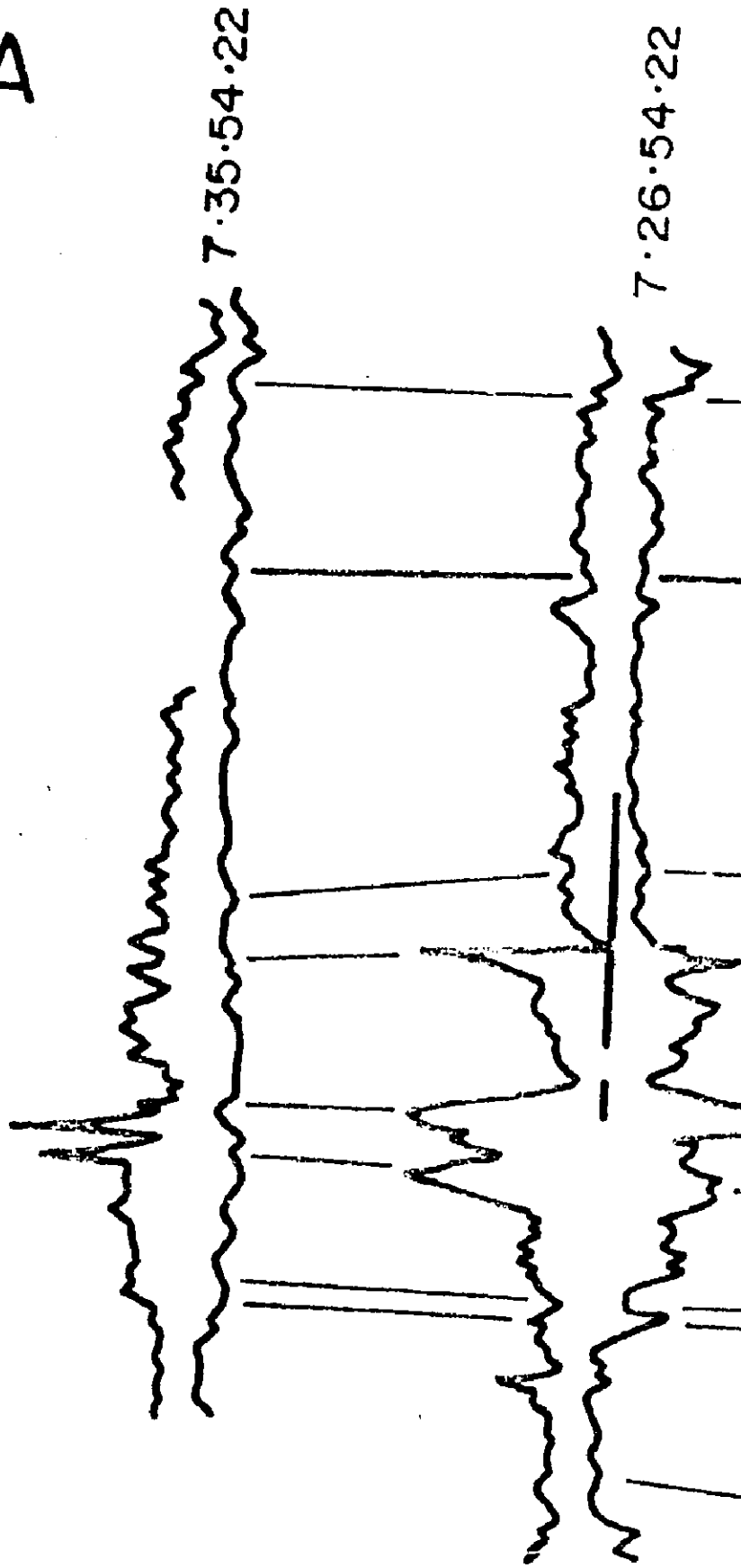

NW

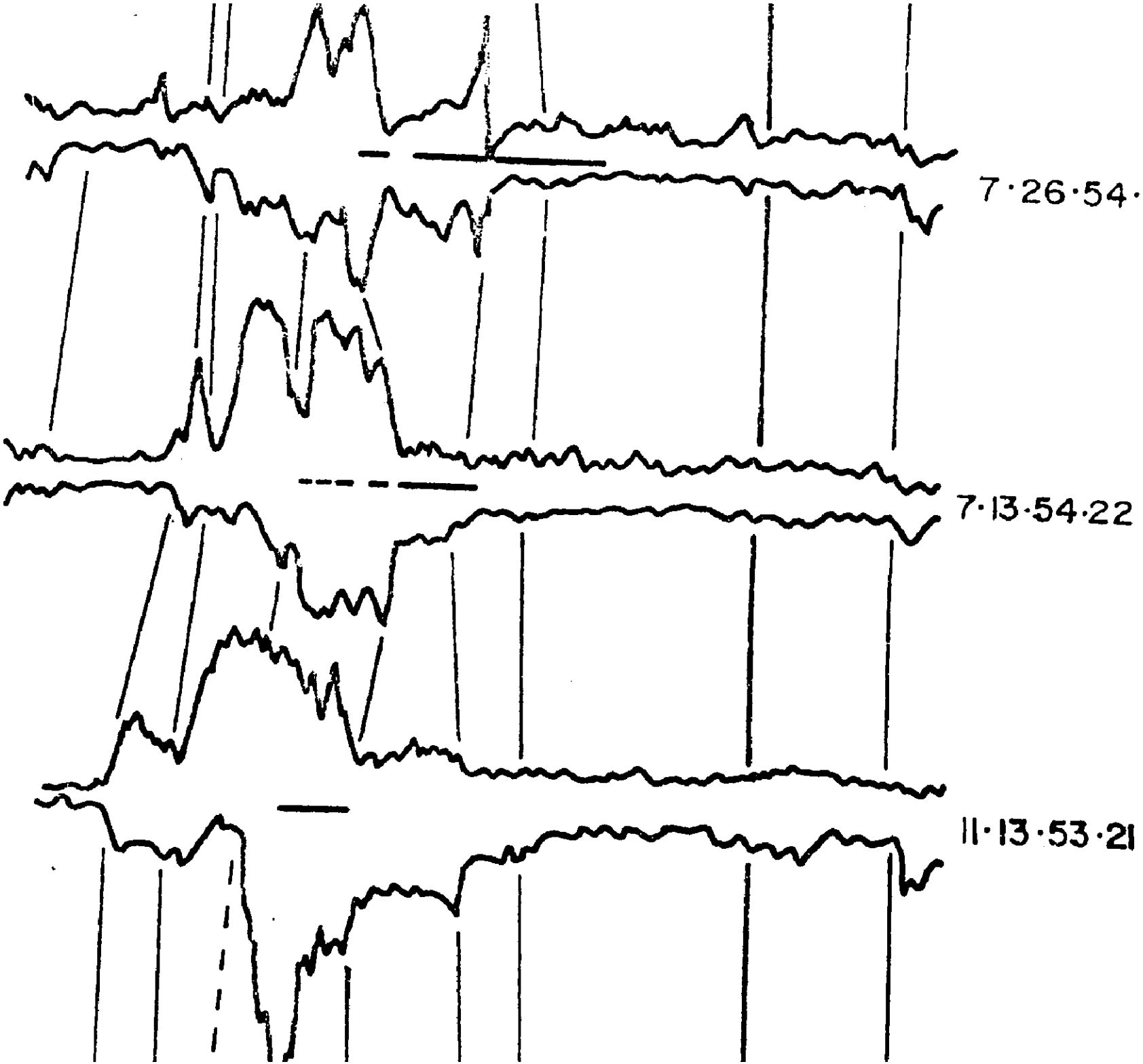
7·26·54·22
7·13·54·22
11·13·53·21

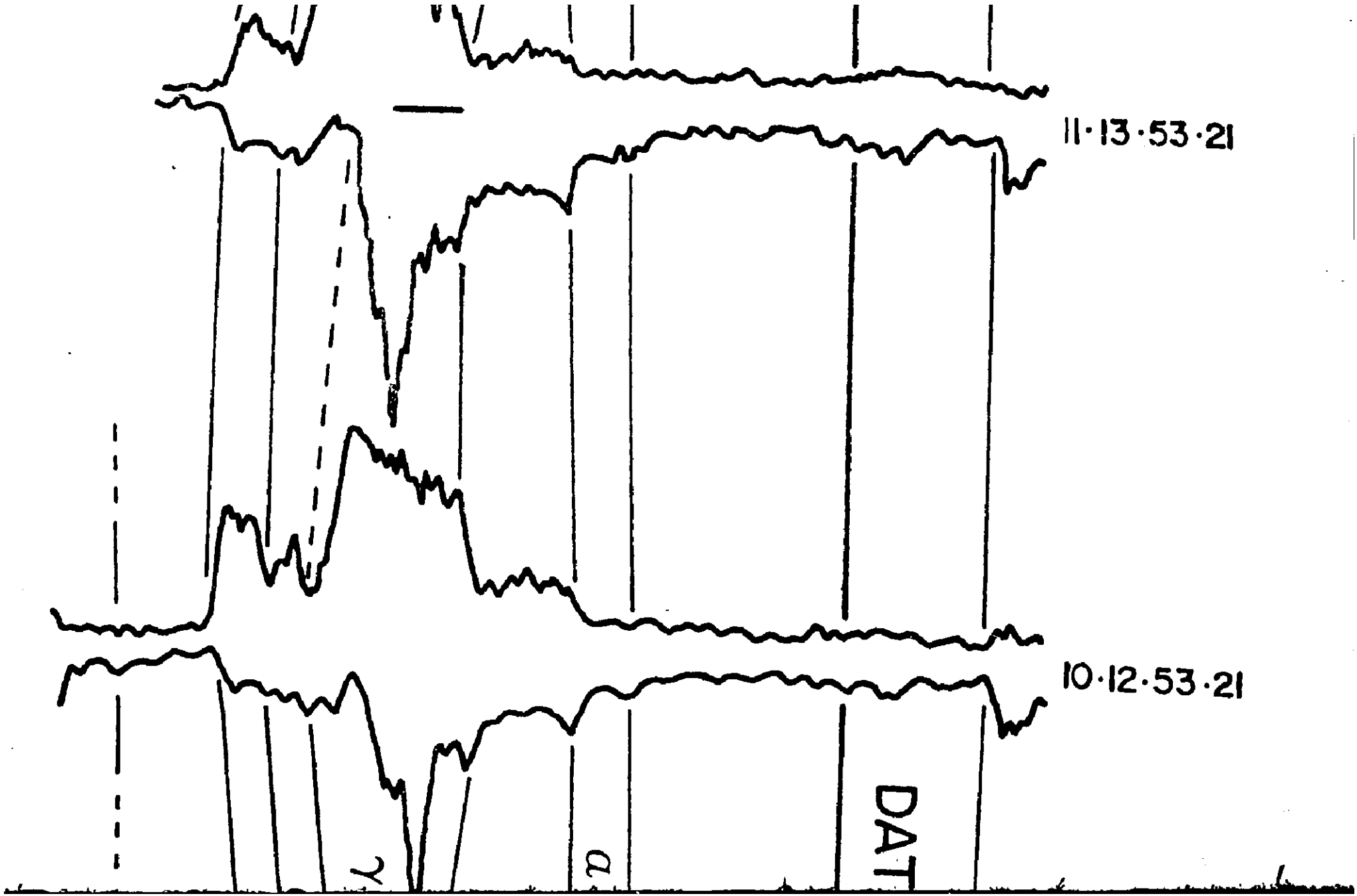
11·13·53·21
10·12·53·21
γ
α
DAT

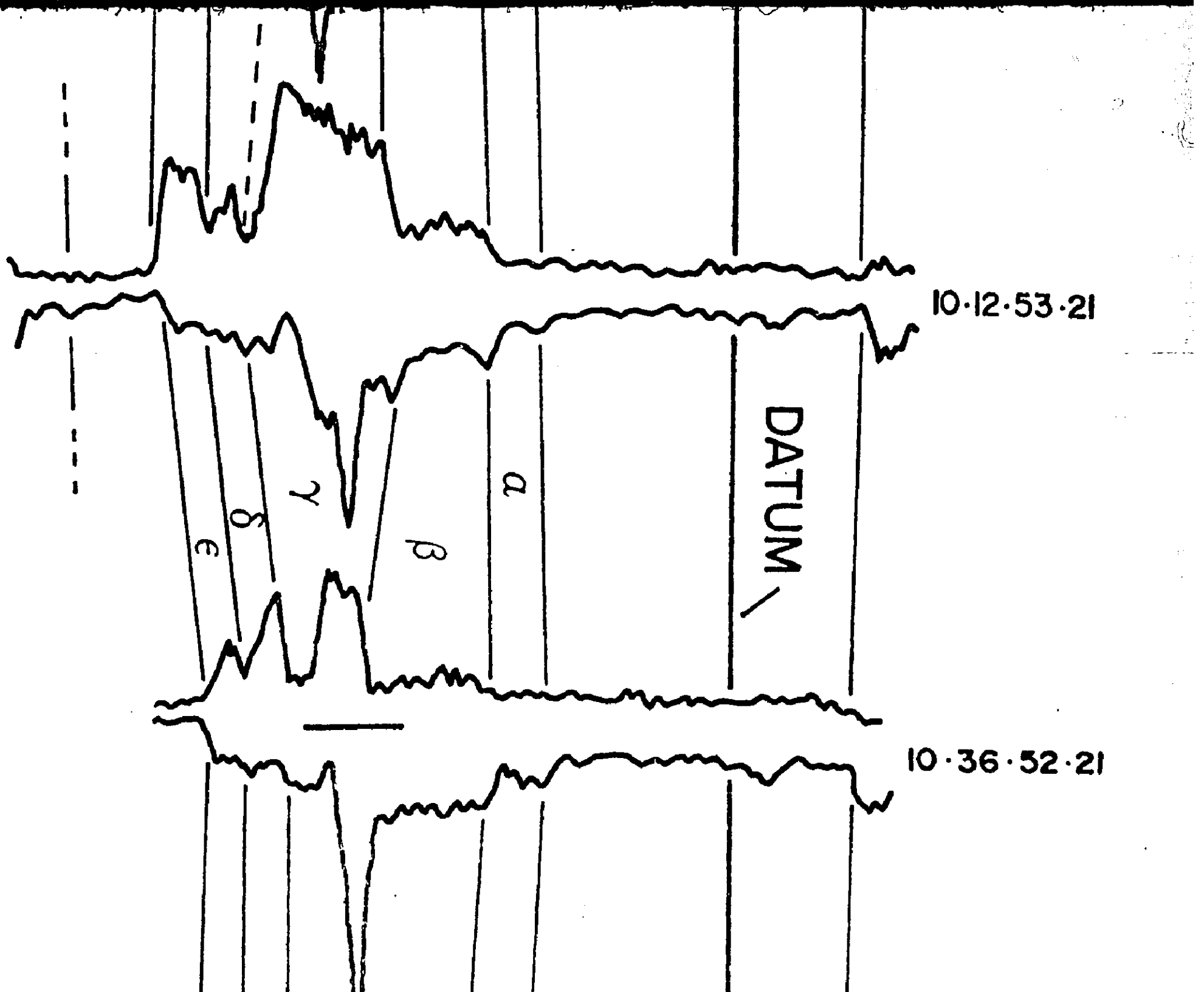
10·12·53·21
DATUM
α
β
γ
δ
ε
10·36·52·21

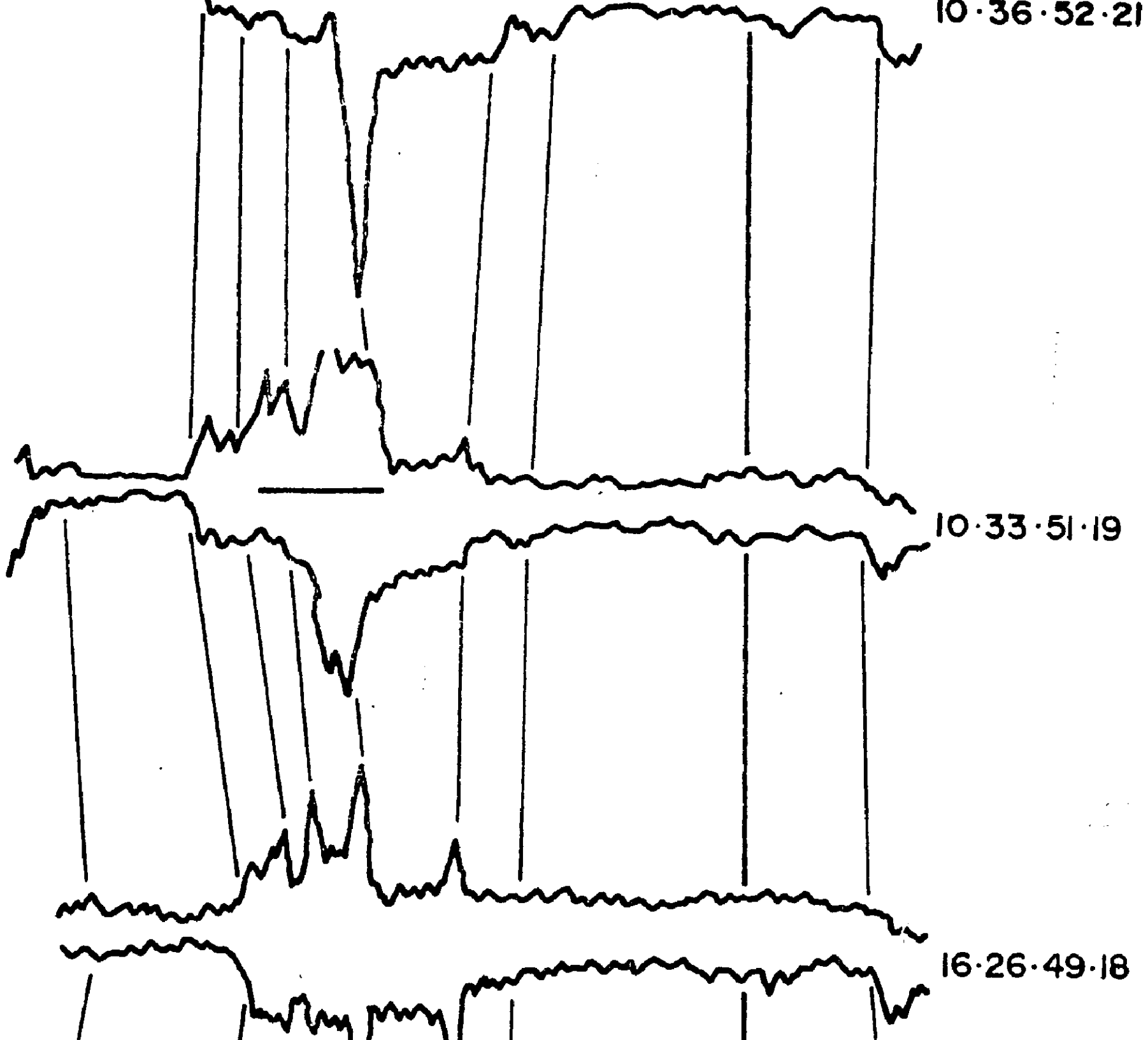
10·36·52·21
10·33·51·19
16·26·49·18

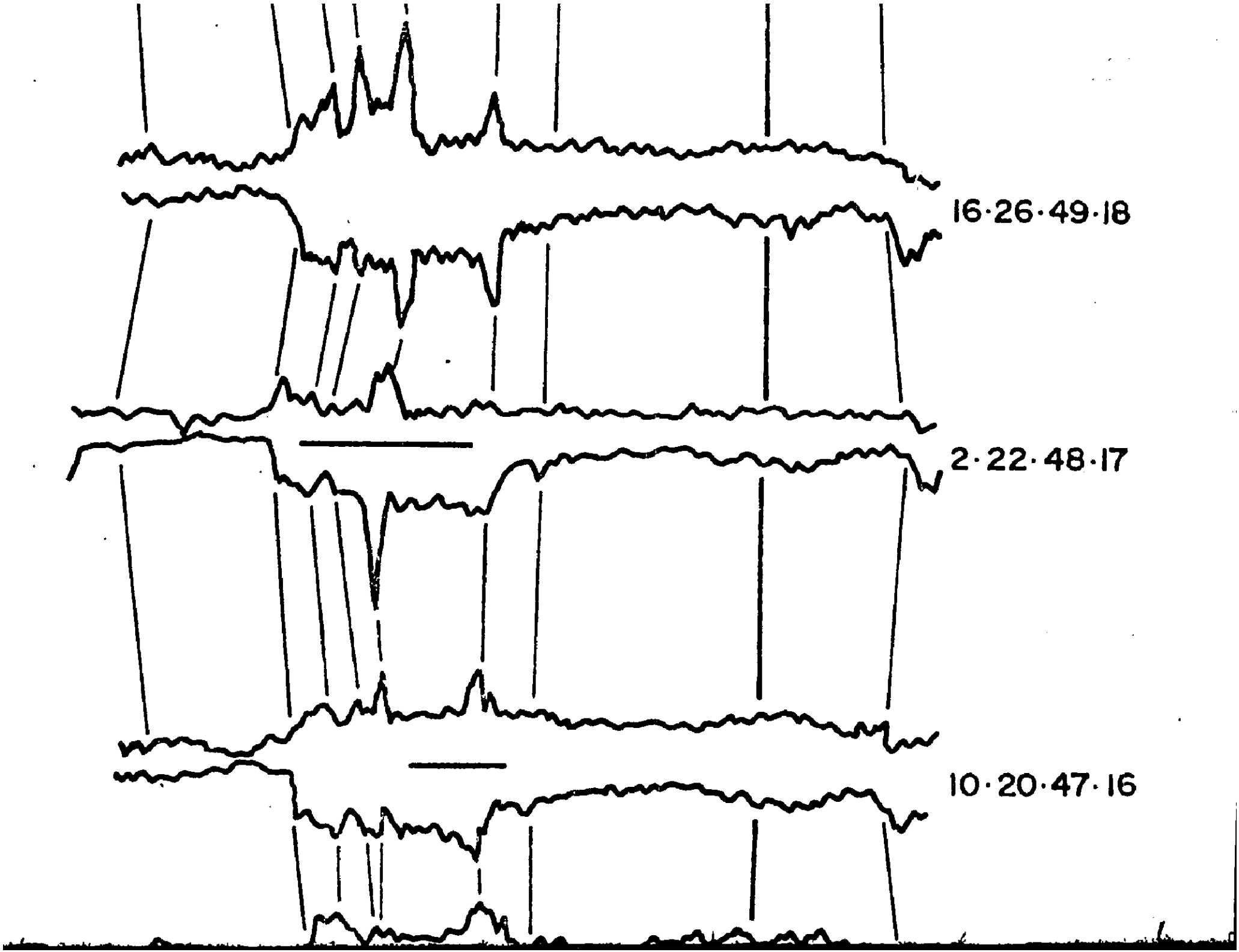
16·26·49·18
2·22·48·17
10·20·47·16

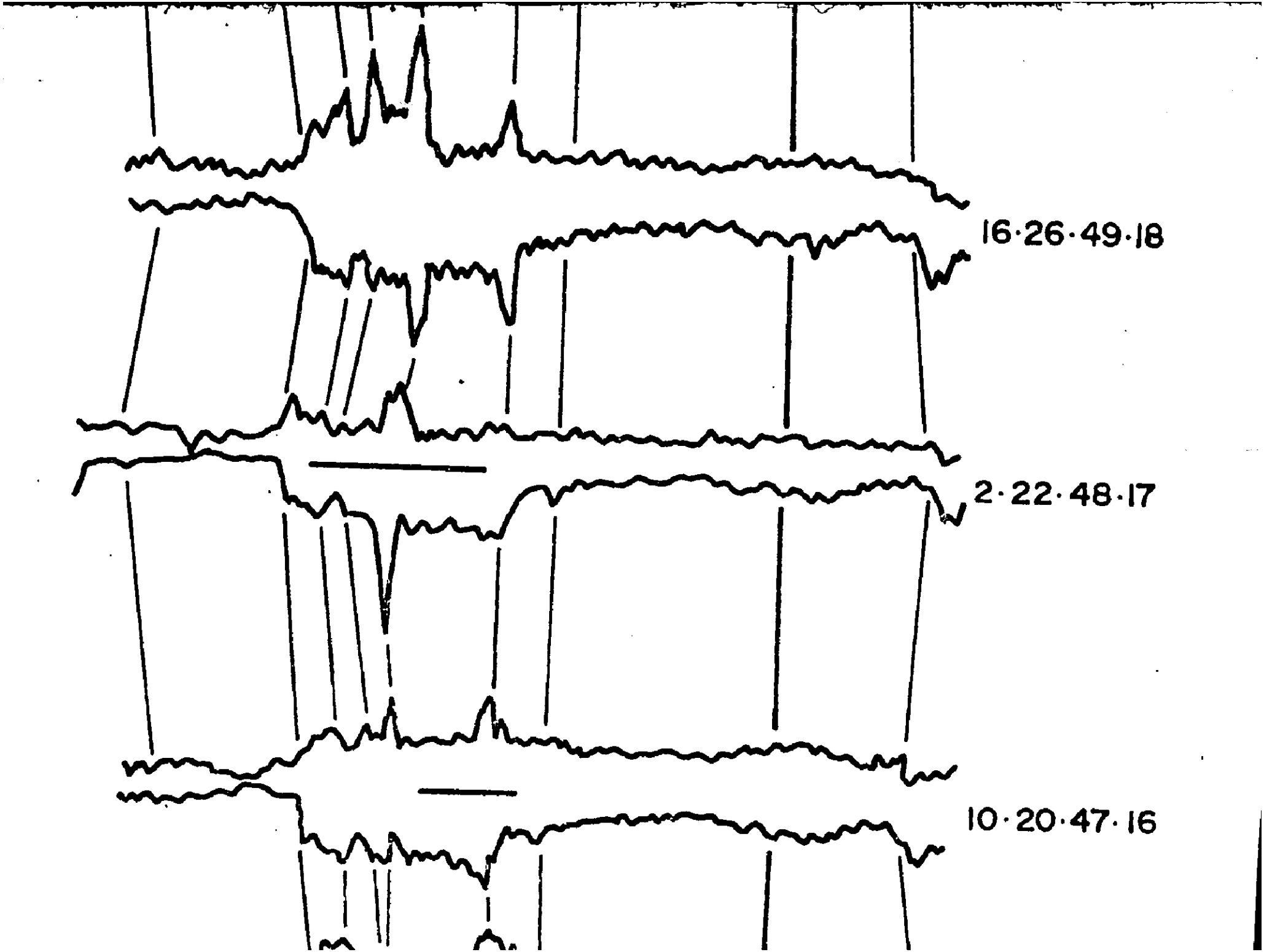
16·26·49·18
2·22·48·17
10·20·47·16

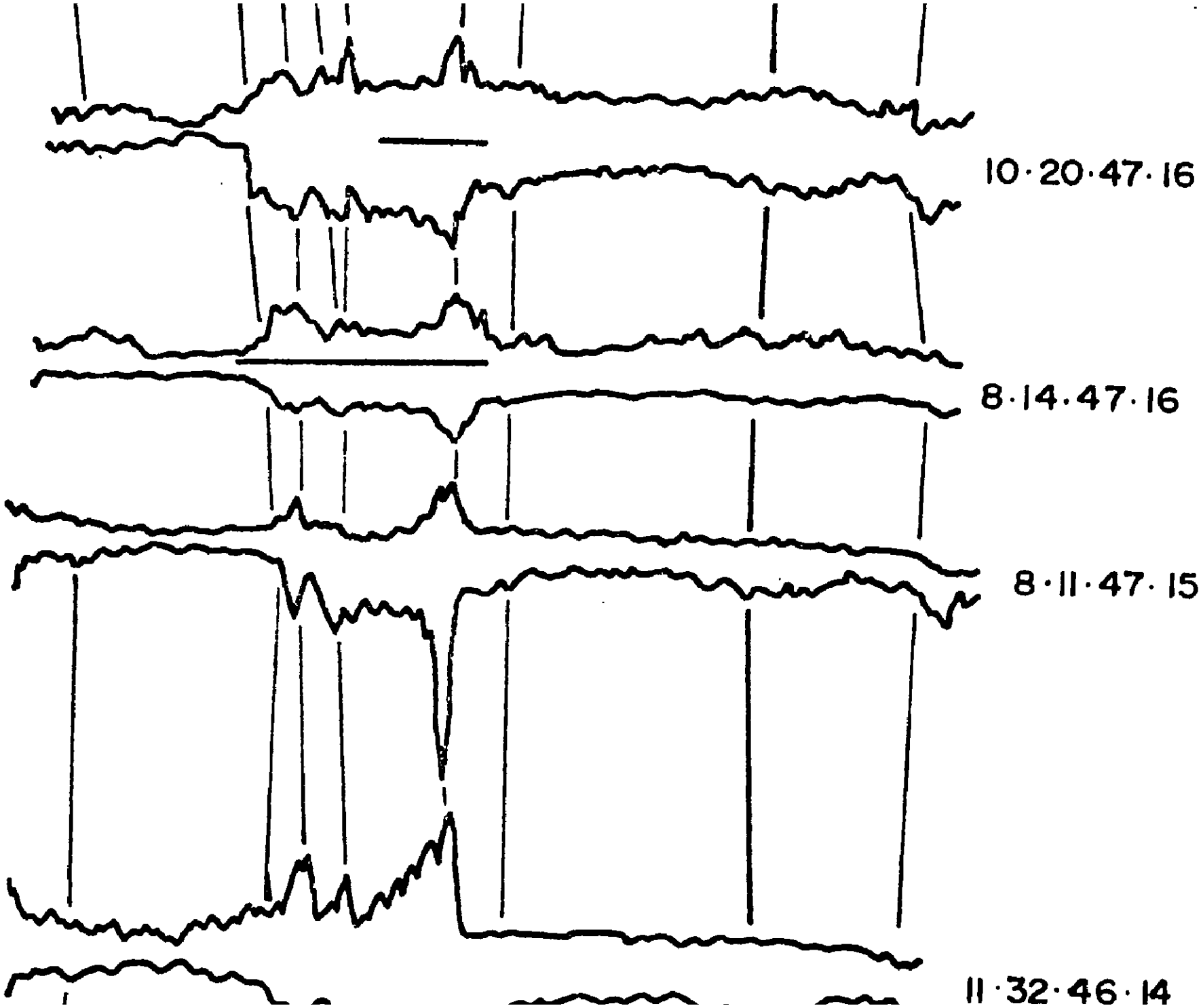
10·20·47·16
8·14·47·16
8·11·47·15
11·32·46·14

11·32·46·14
16·28·46·14
11·24·45·13
A'
a
b
c
α
β
δ
ε
μ
SE

B-B′

SUMMARY SECTION

50' || 15m

NO HORIZONTAL SCALE

| CORE

NW

B

6·27·54·18

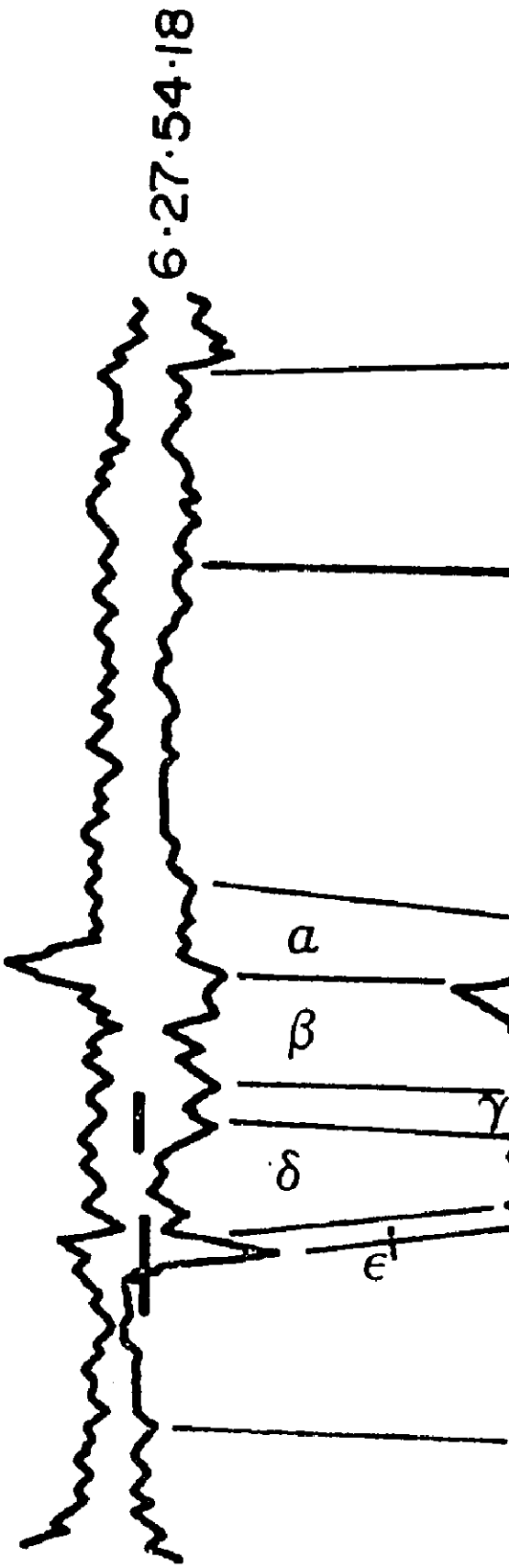

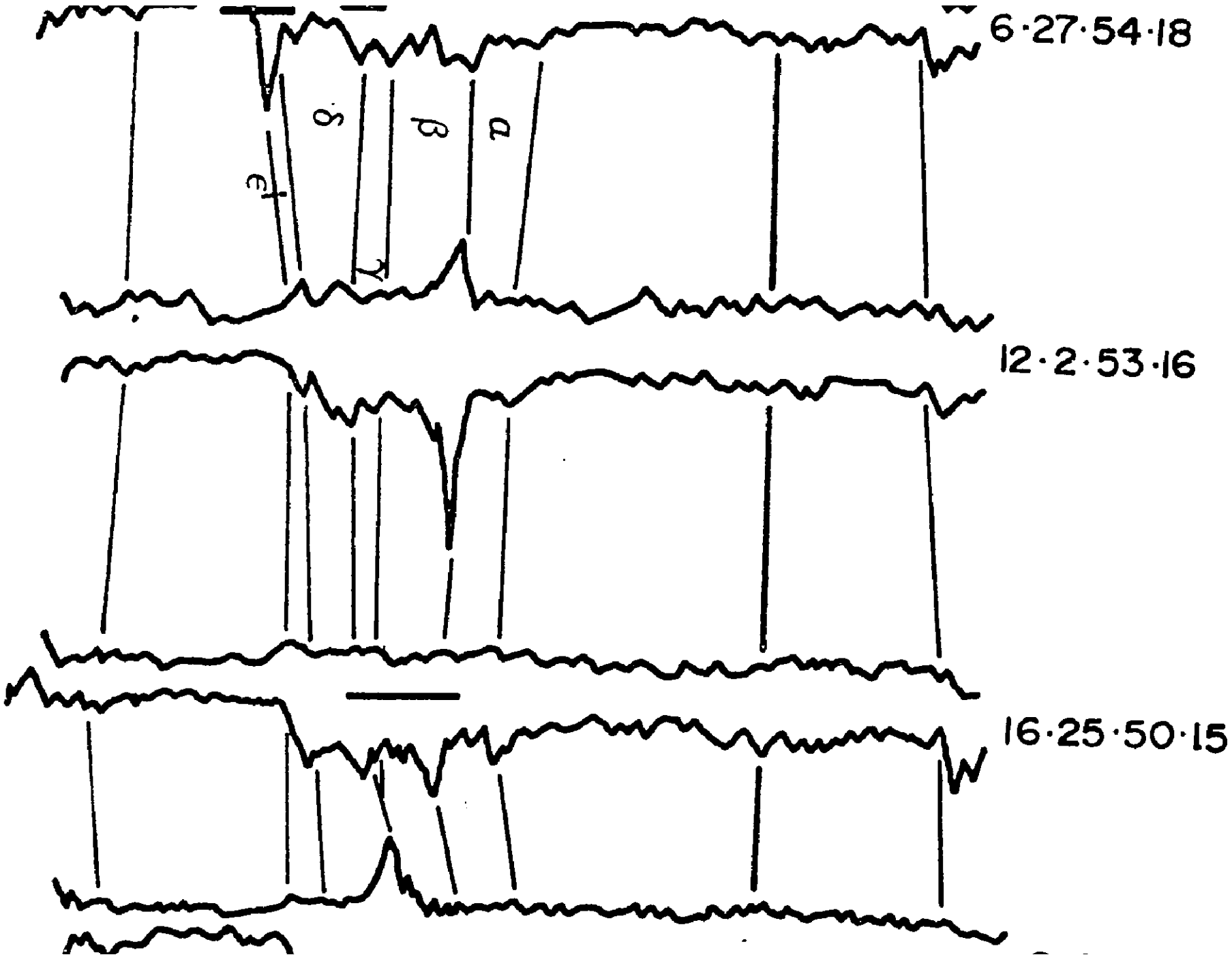
6·27·54·18
12·2·53·16
16·25·50·15
ε
δ
γ
β
α

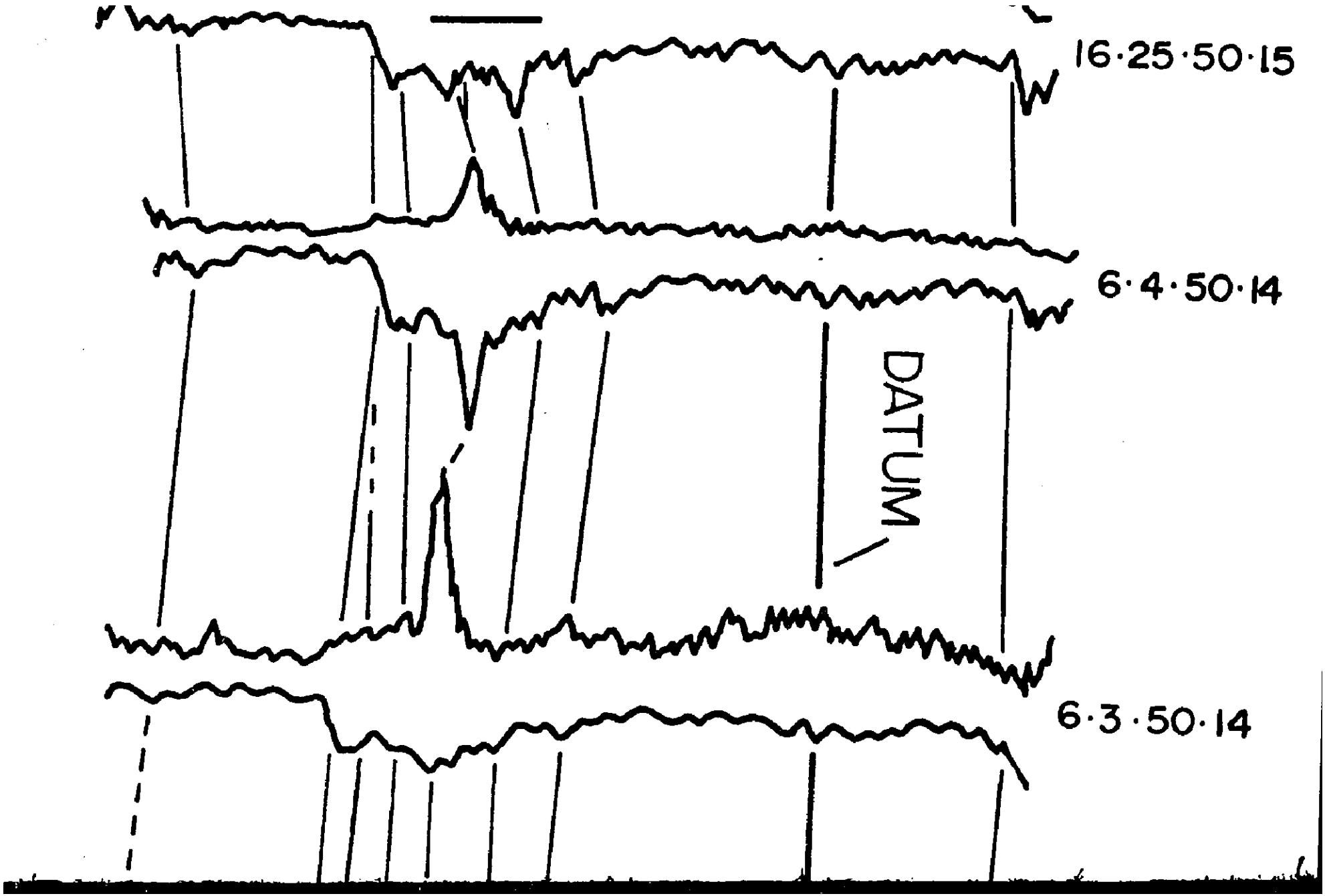
16·25·50·15
6·4·50·14
DATUM
6·3·50·14

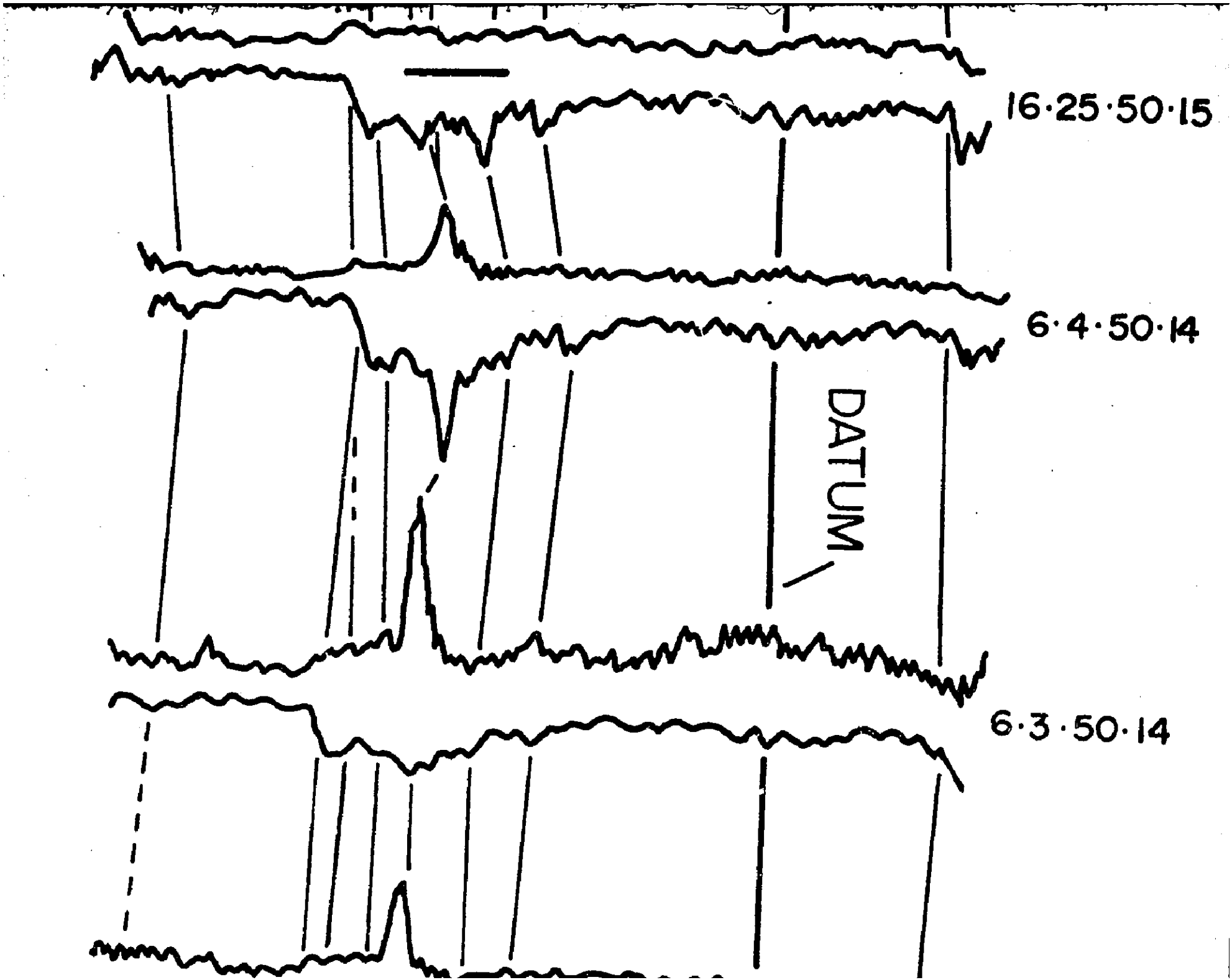
16·25·50·15
6·4·50·14
DATUM
6·3·50·14

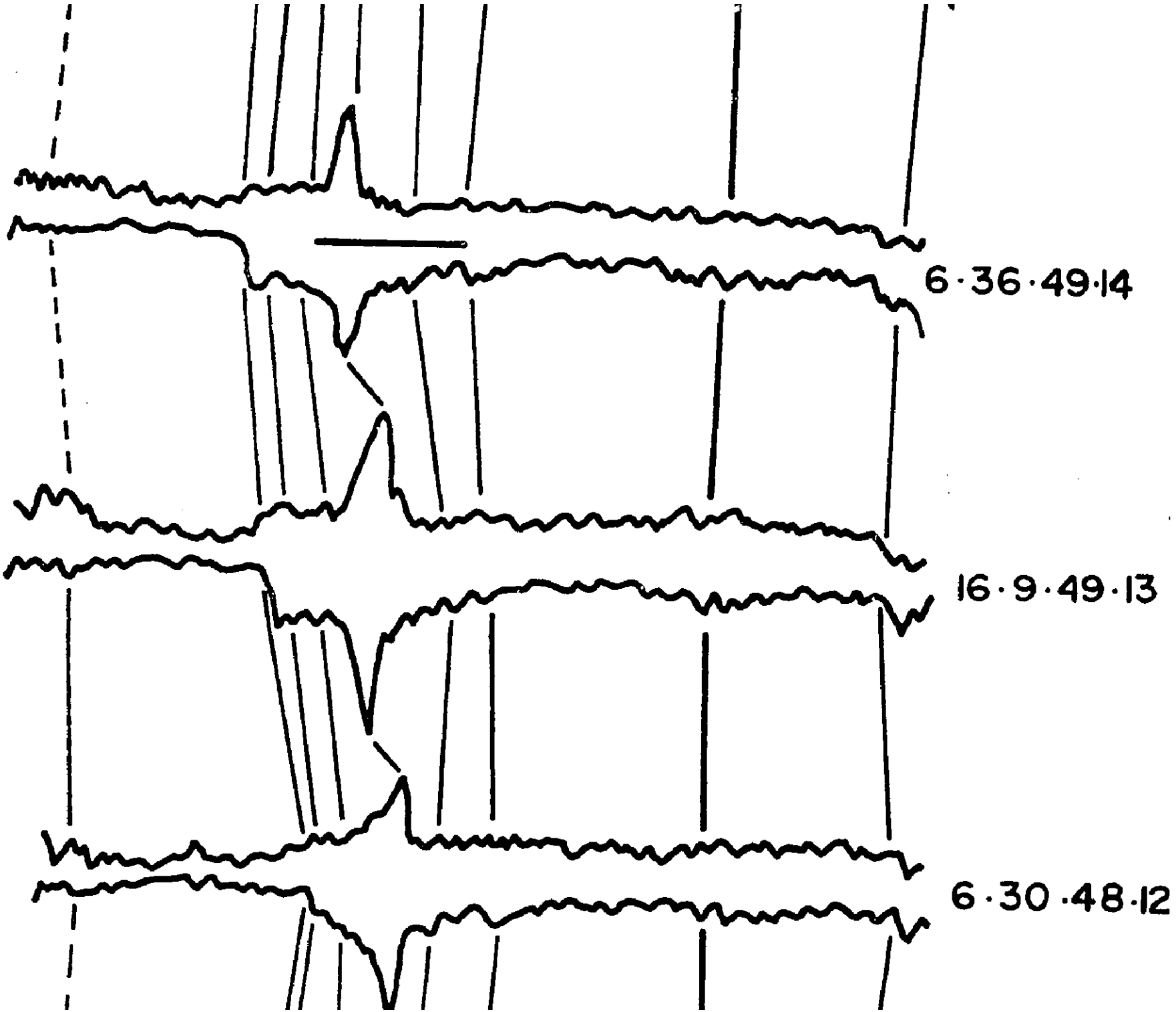
6·36·49·14
16·9·49·13
6·30·48·12

6·30·48·12
16·14·48·12
4·35·46·10
B'
a
b
c
a
β
δ
ϵ
μ
SE

C

C – C´

SUMMARY SECTION

CORE

50' || 15m

NO HORIZONTAL SCALE

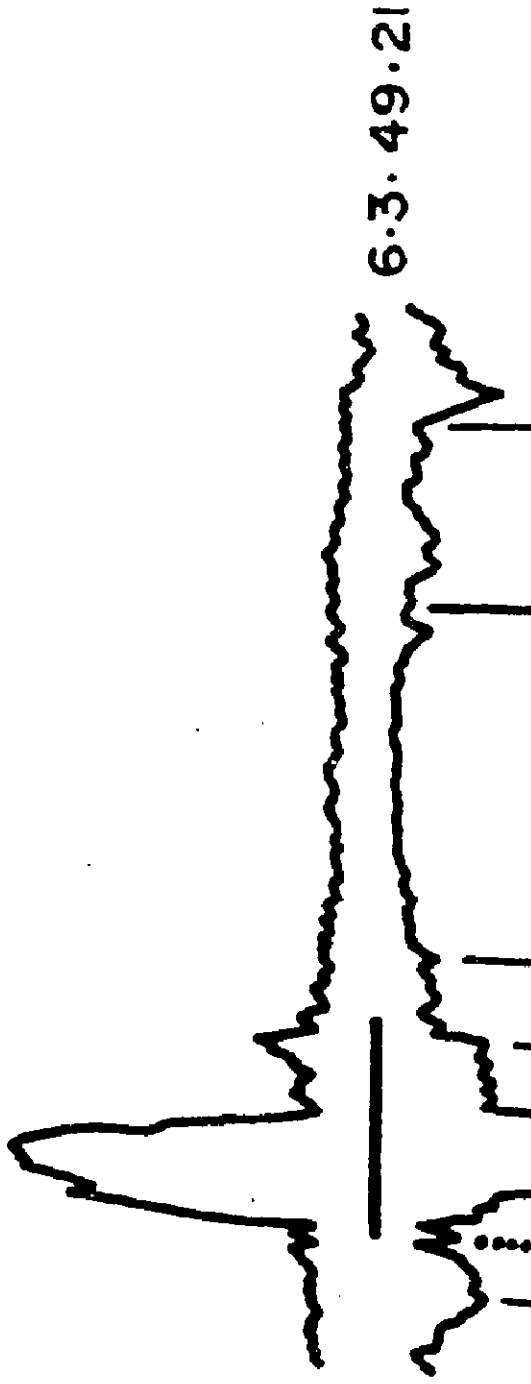

SW

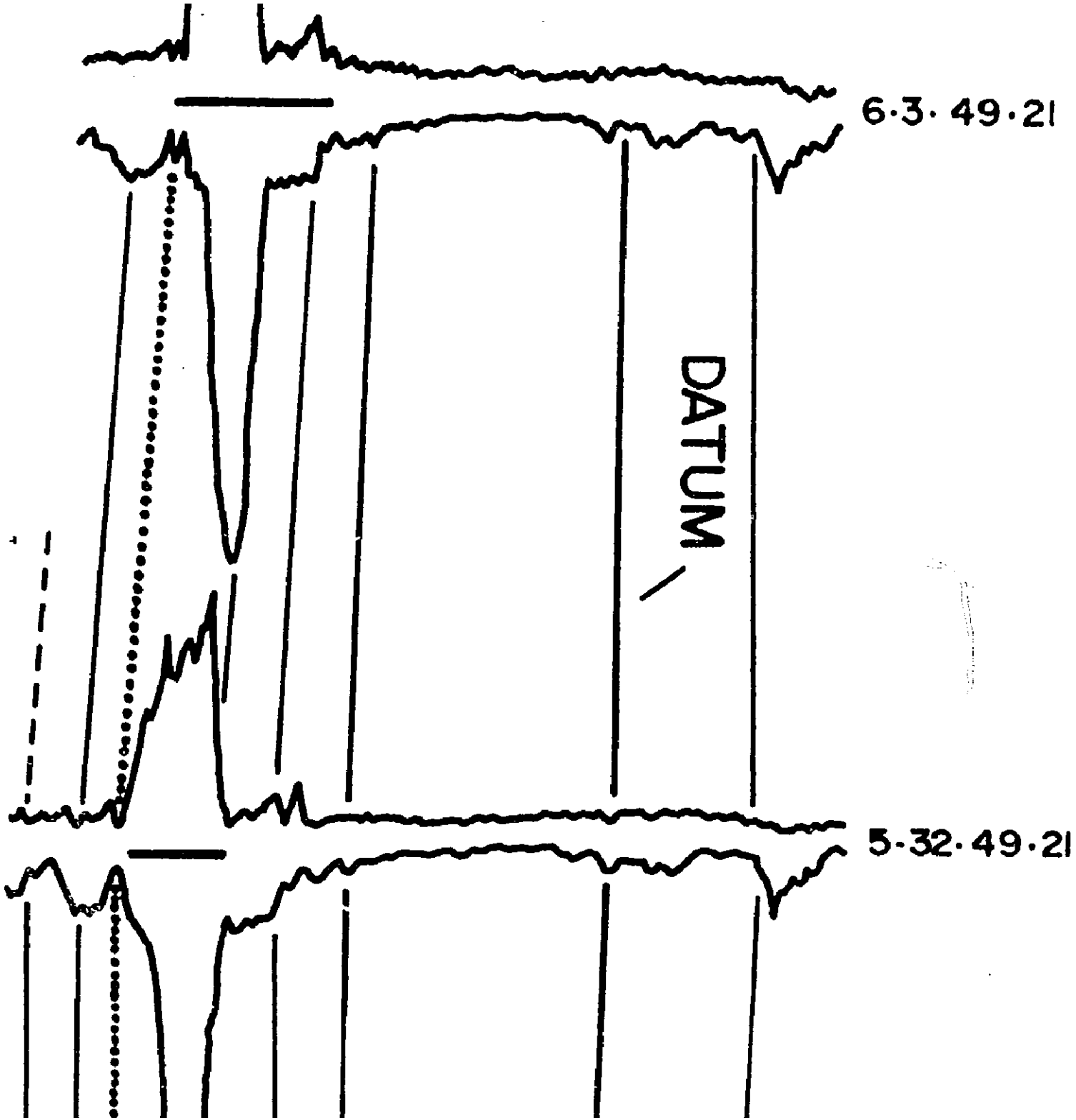
6·3·49·21
DATUM
5·32·49·21

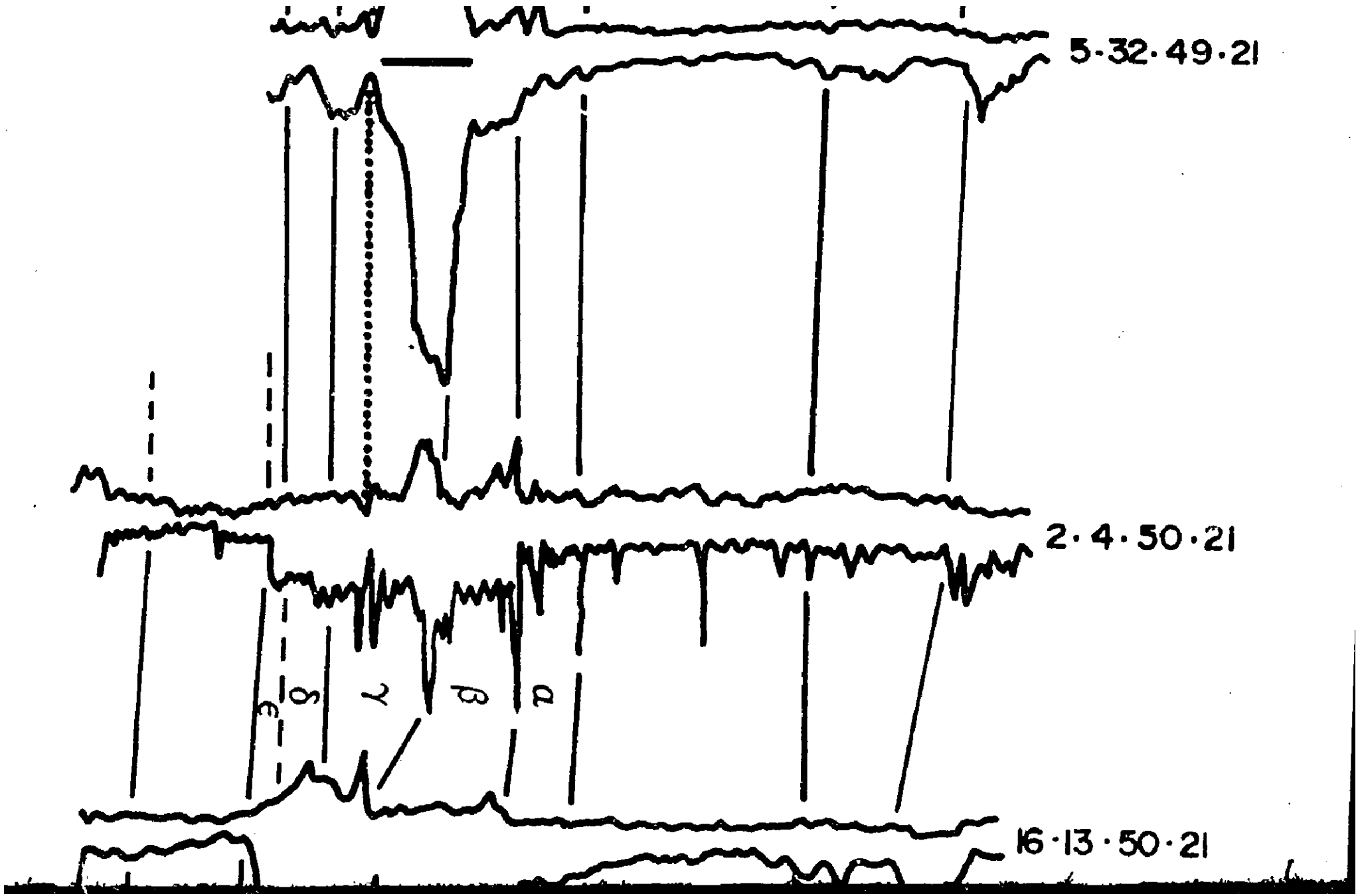
5·32·49·21
2·4·50·21
16·13·50·21
e
δ
γ
β
α

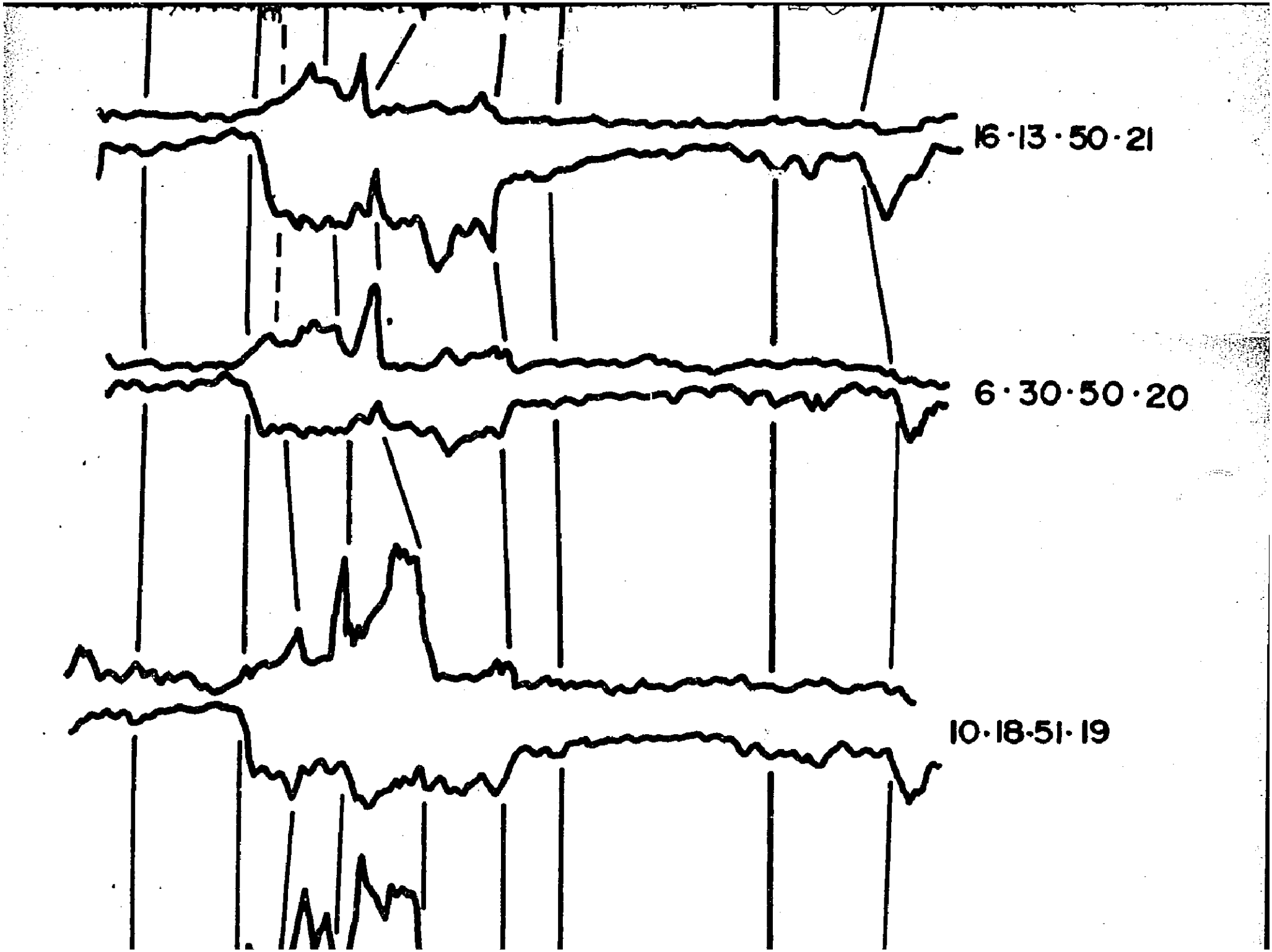
16·13·50·21
6·30·50·20
10·18·51·19

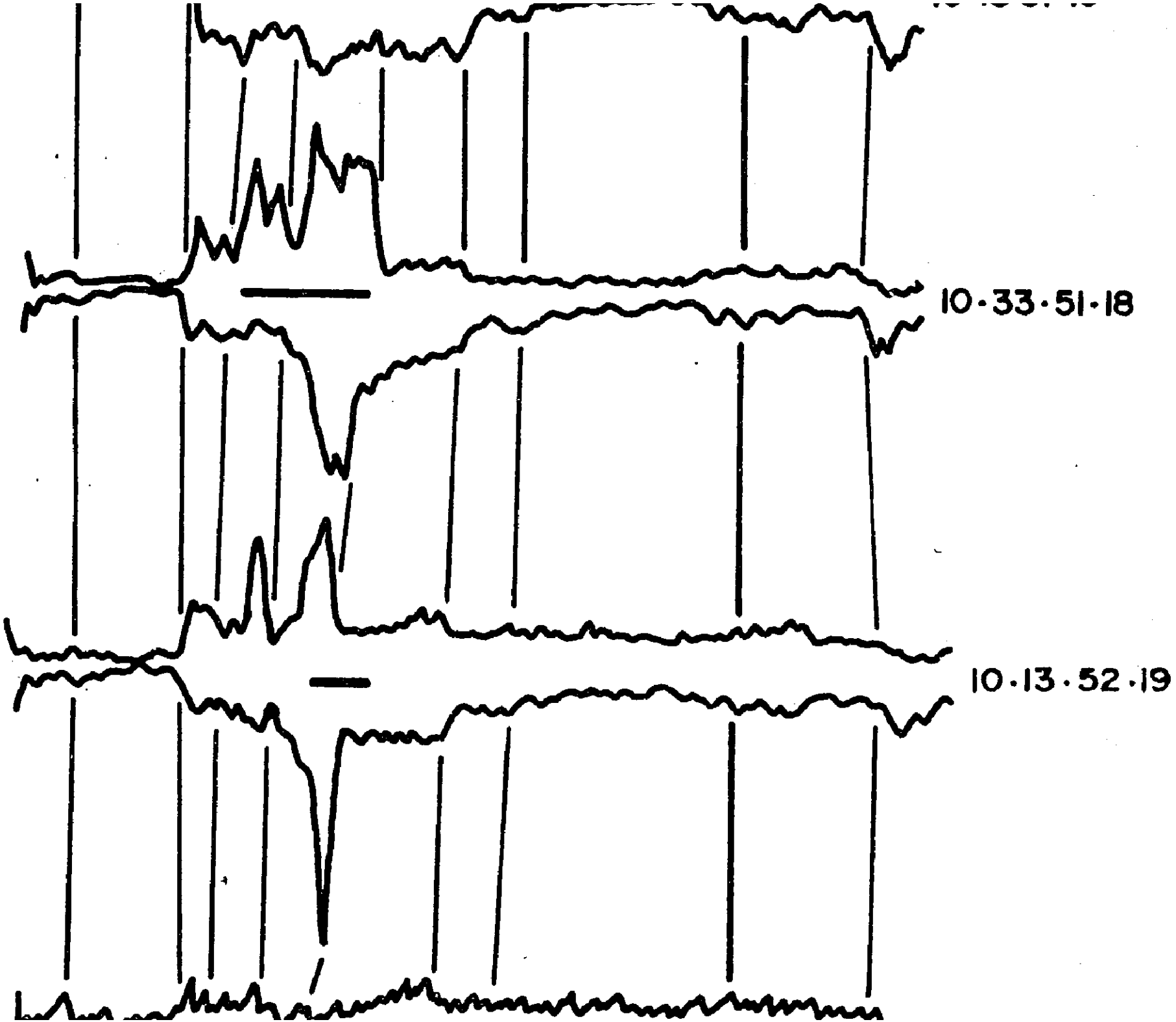
10·33·51·18
10·13·52·19

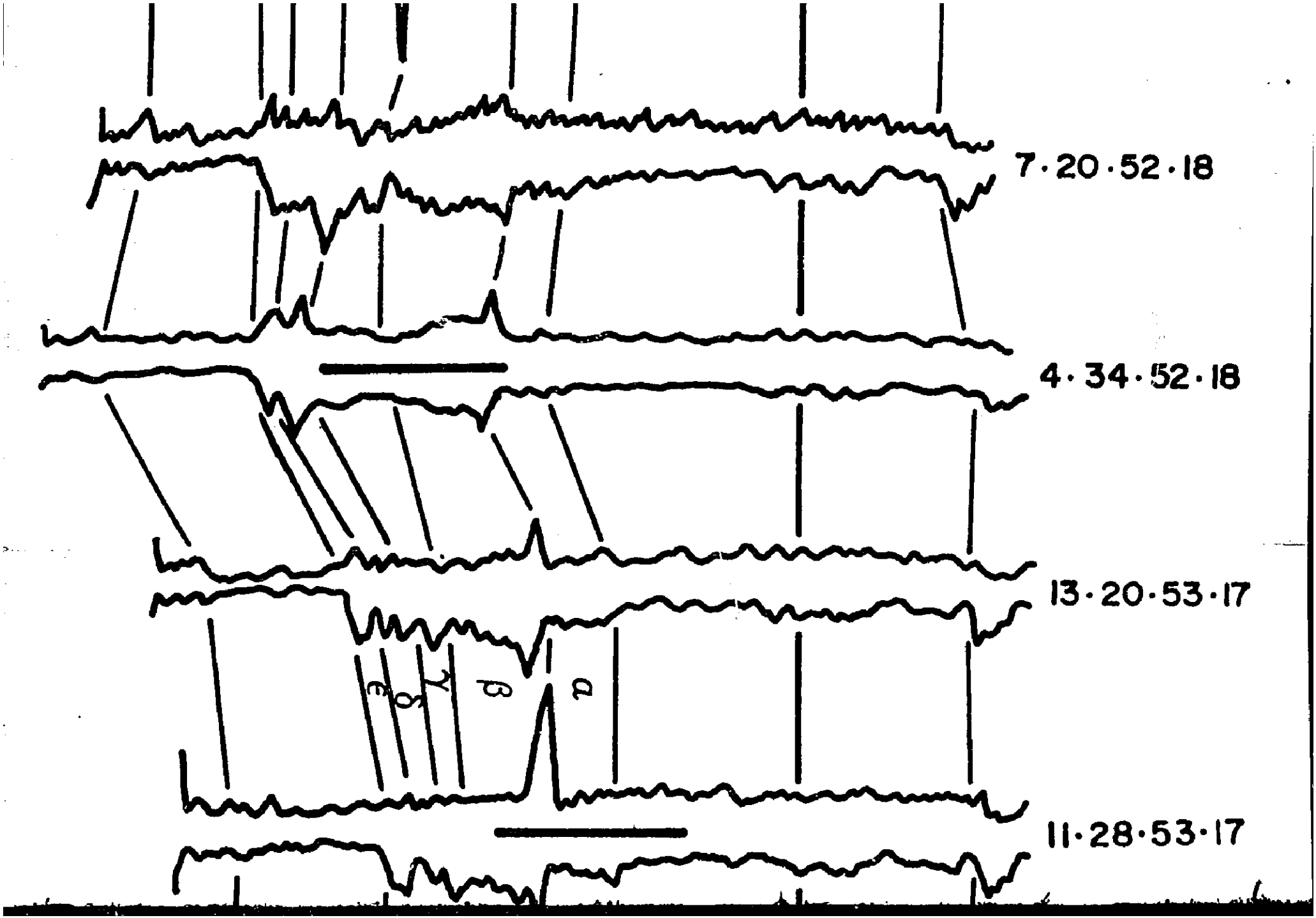
7·20·52·18
4·34·52·18
13·20·53·17
11·28·53·17
ε
δ
γ
β
α

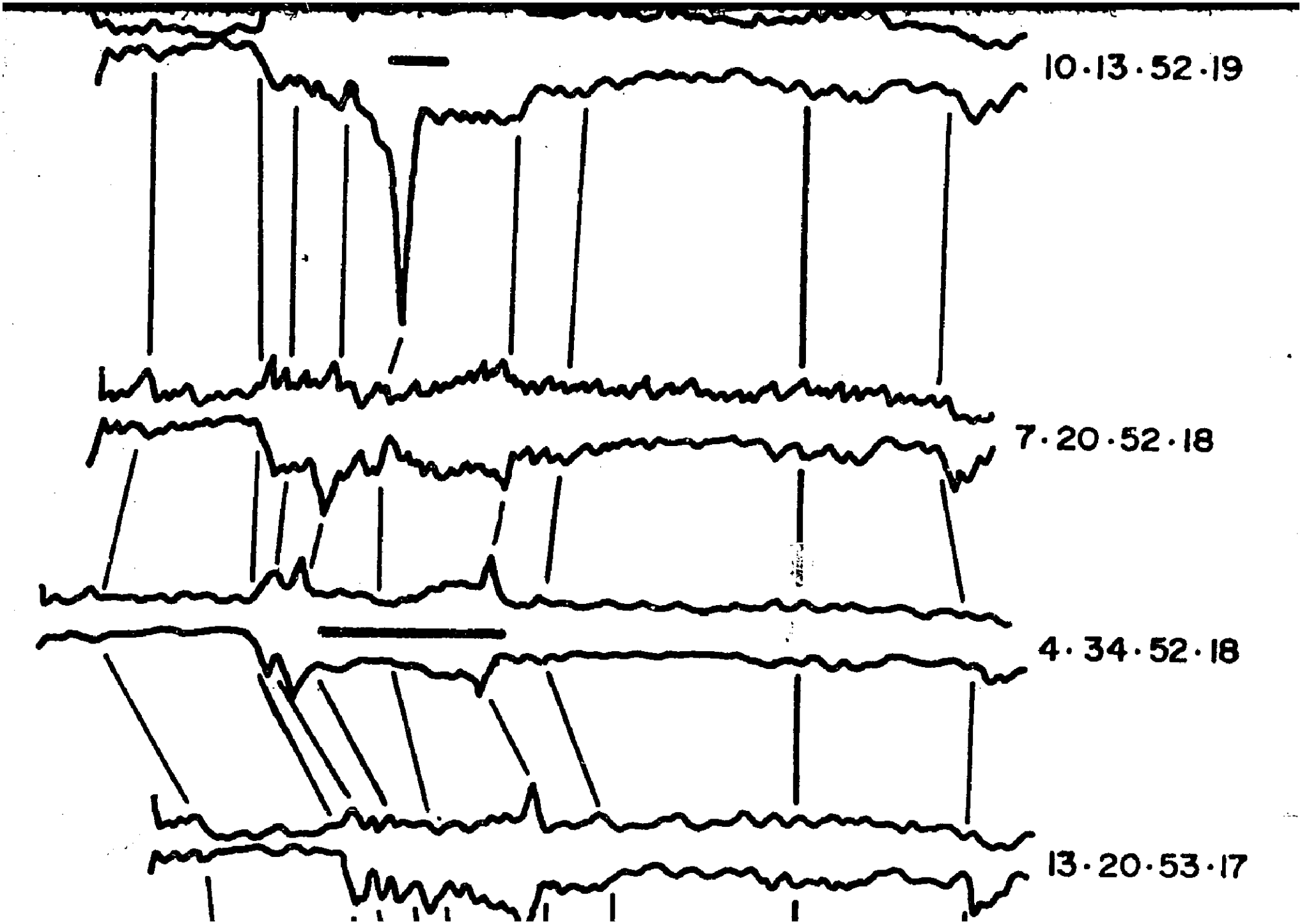
10·13·52·19
7·20·52·18
4·34·52·18
13·20·53·17

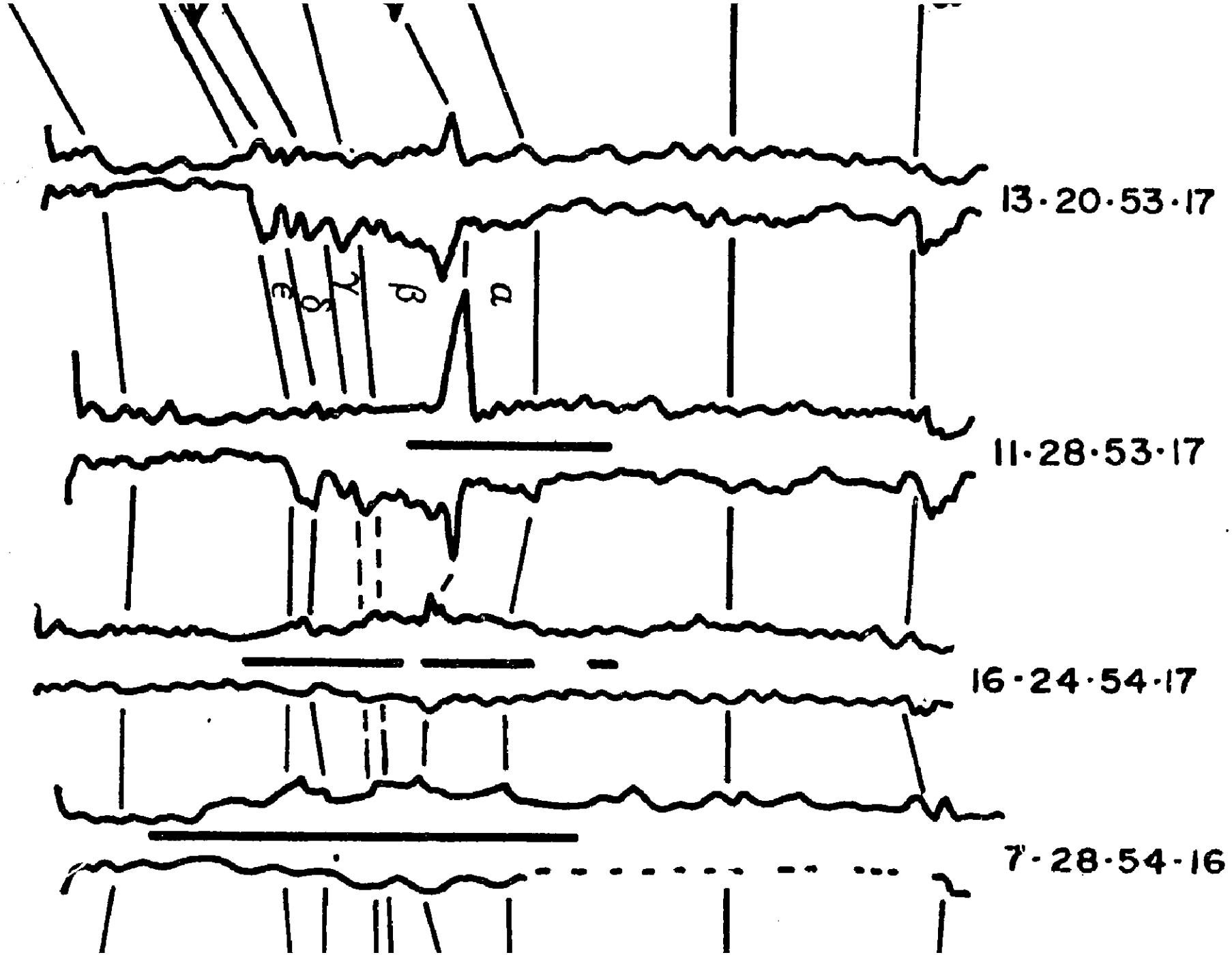
13·20·53·17
11·28·53·17
16·24·54·17
7·28·54·16

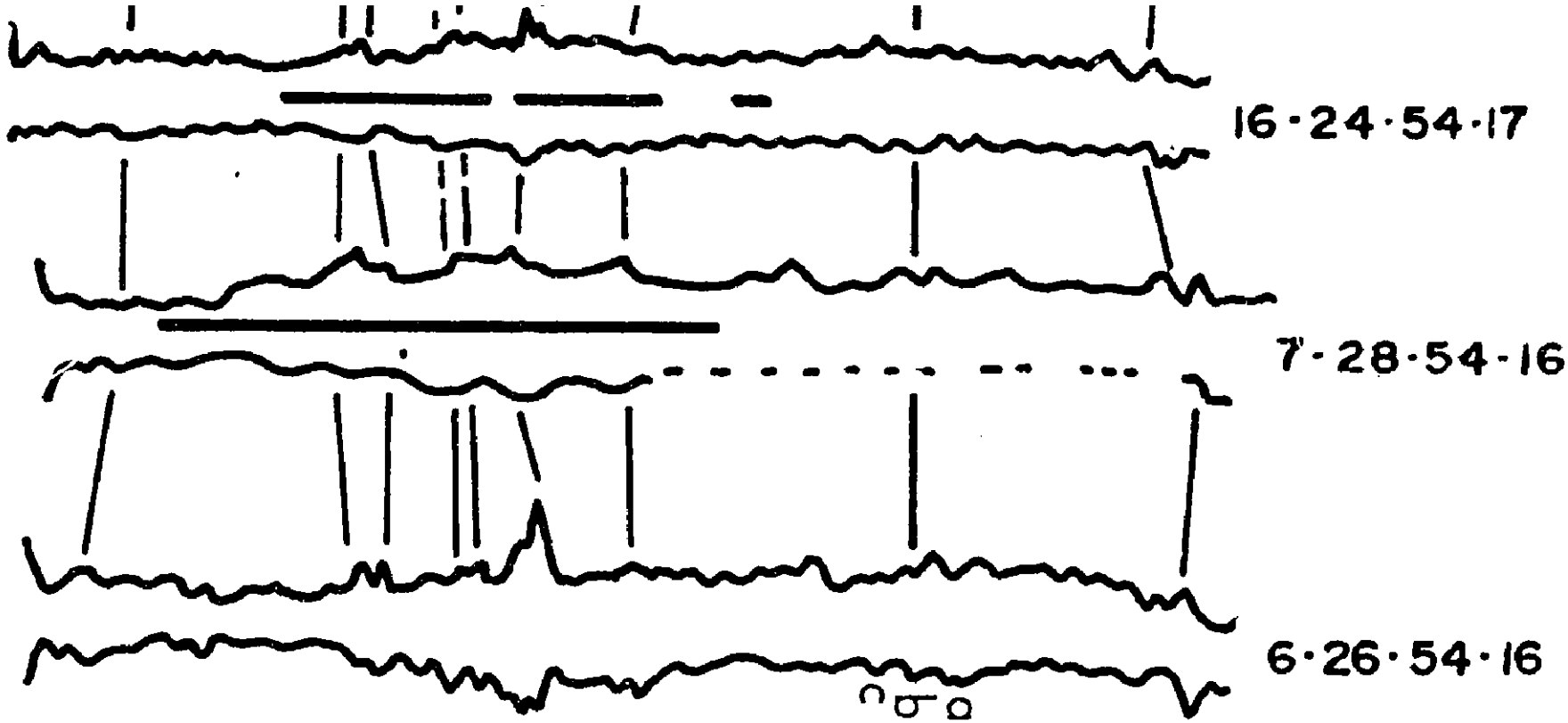

NE

D

D – D′

SUMMARY SECTION

CORE

50' || 15 m

NO HORIZONTAL SCALE

SW

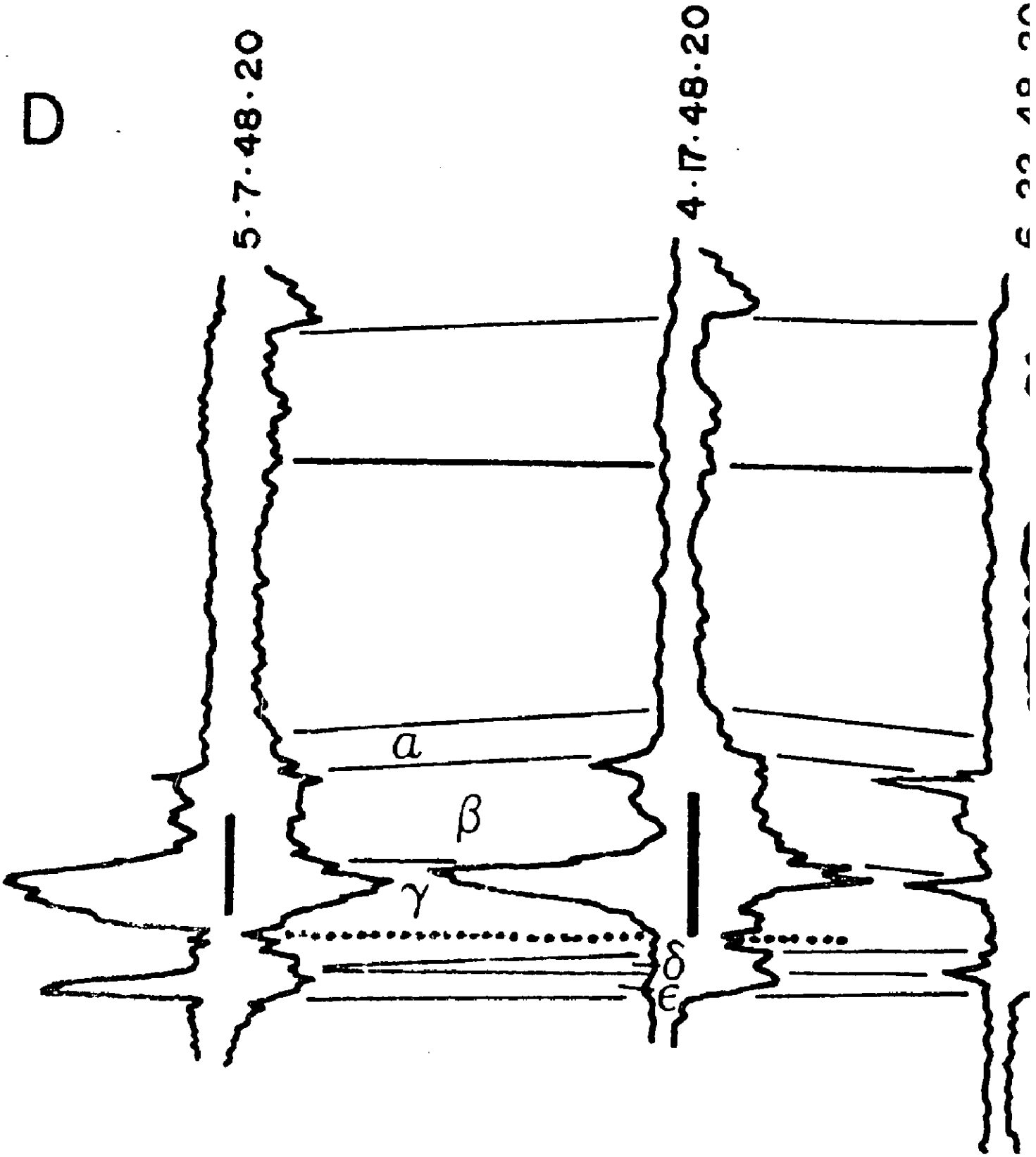

V

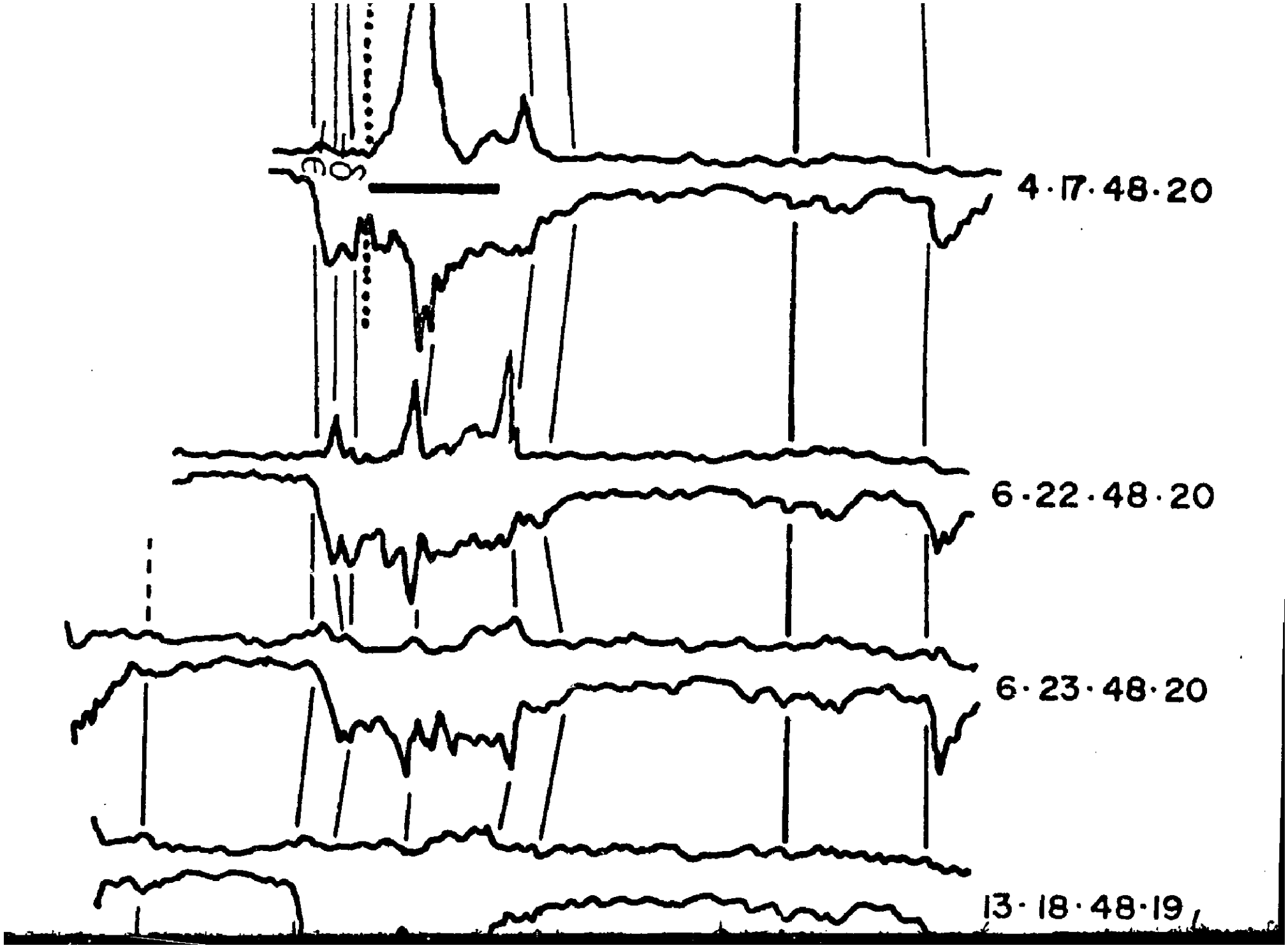
4·17·48·20
6·22·48·20
6·23·48·20
13·18·48·19

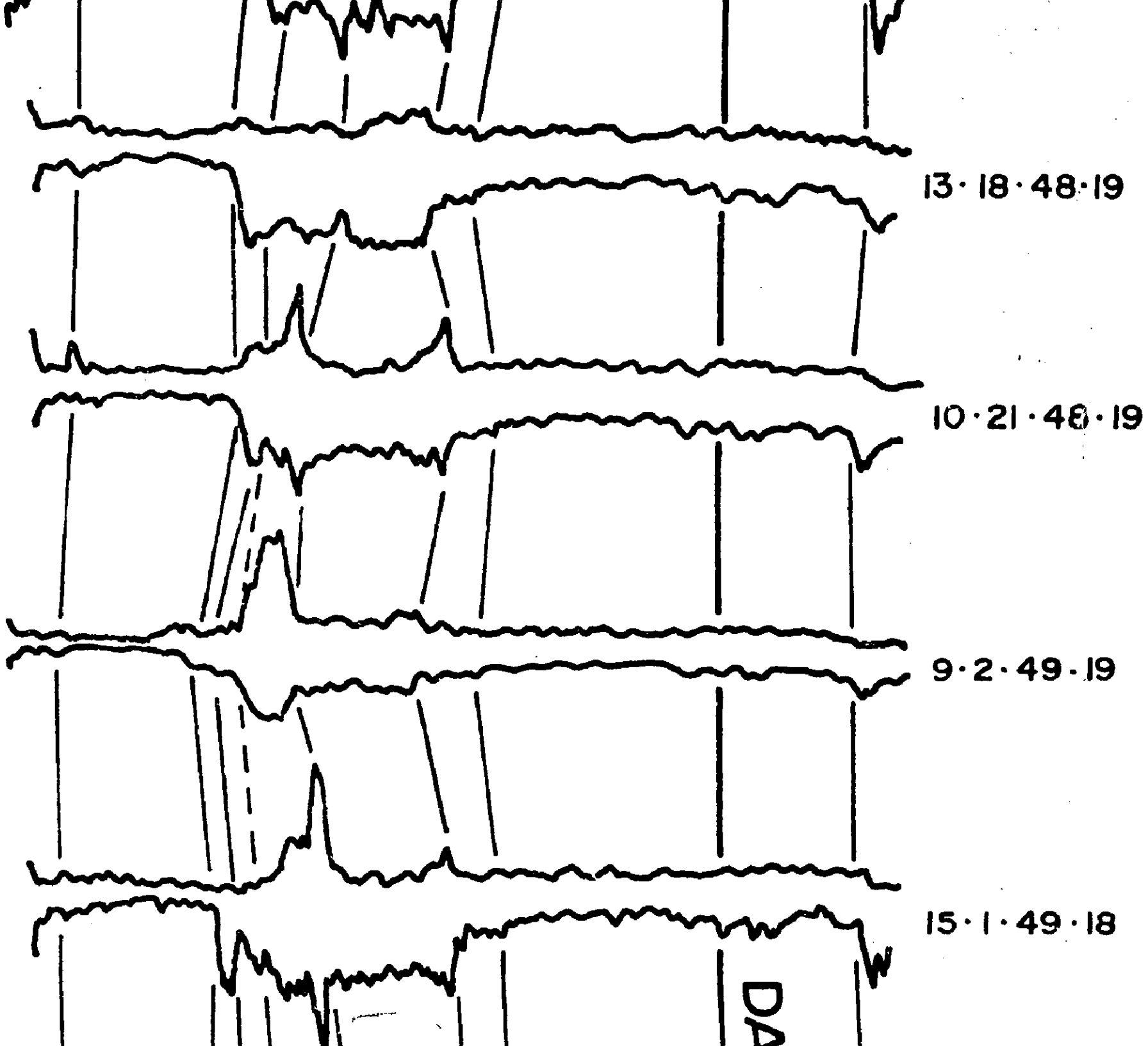
13·18·48·19
10·21·48·19
9·2·49·19
15·1·49·18

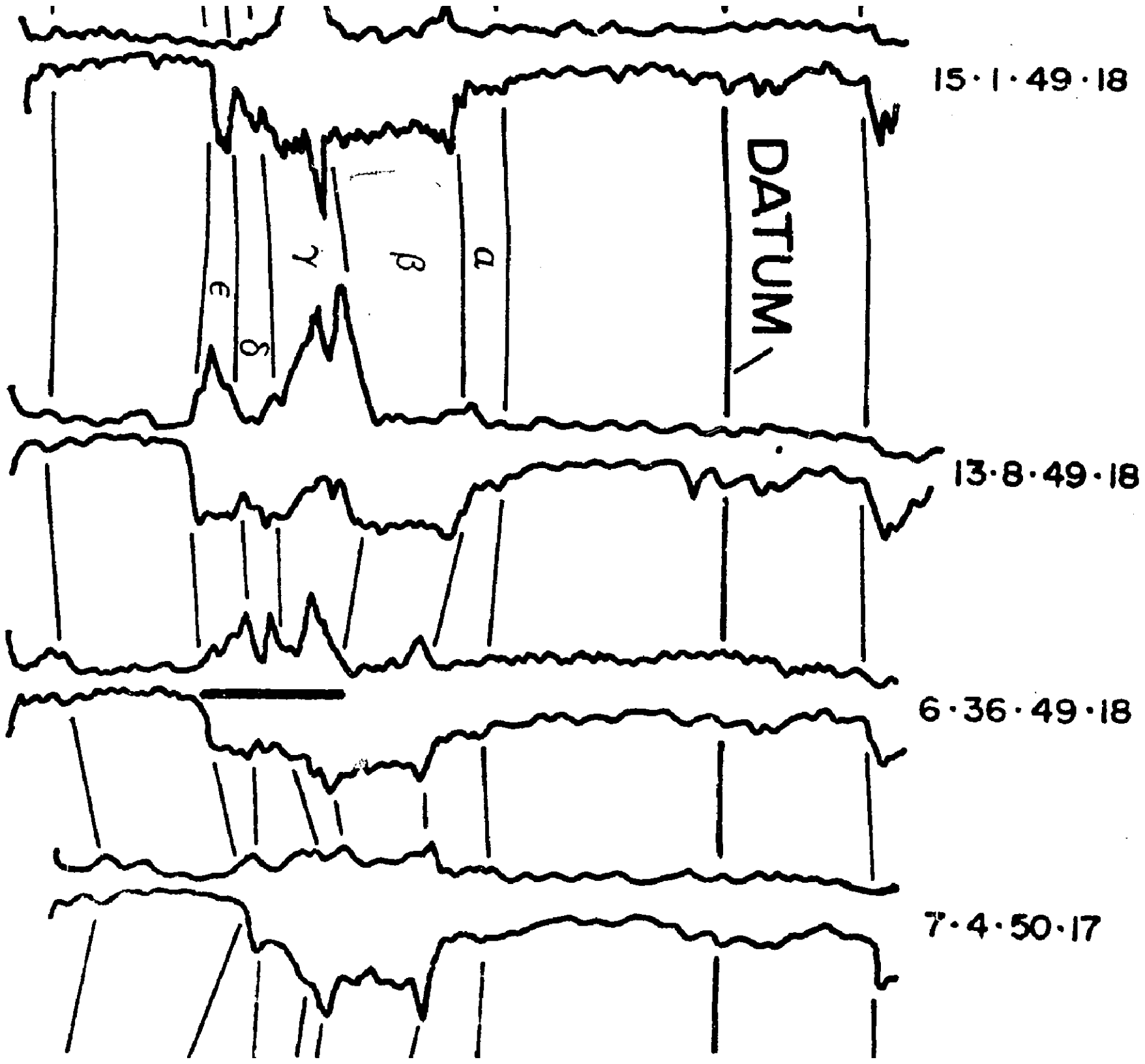
15·1·49·18
DATUM
ε
δ
γ
β
α
13·8·49·18
6·36·49·18
7·4·50·17

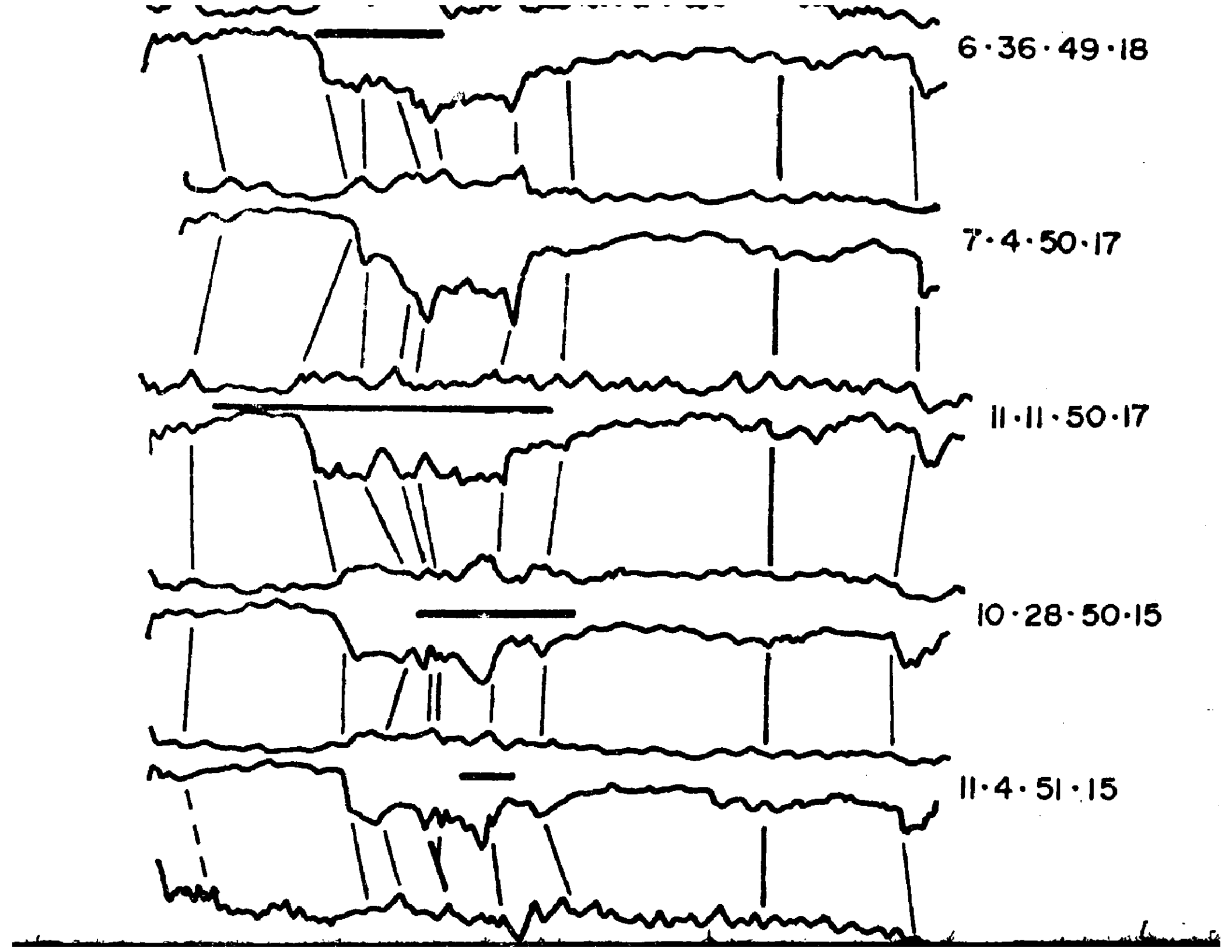
6·36·49·18
7·4·50·17
11·11·50·17
10·28·50·15
11·4·51·15

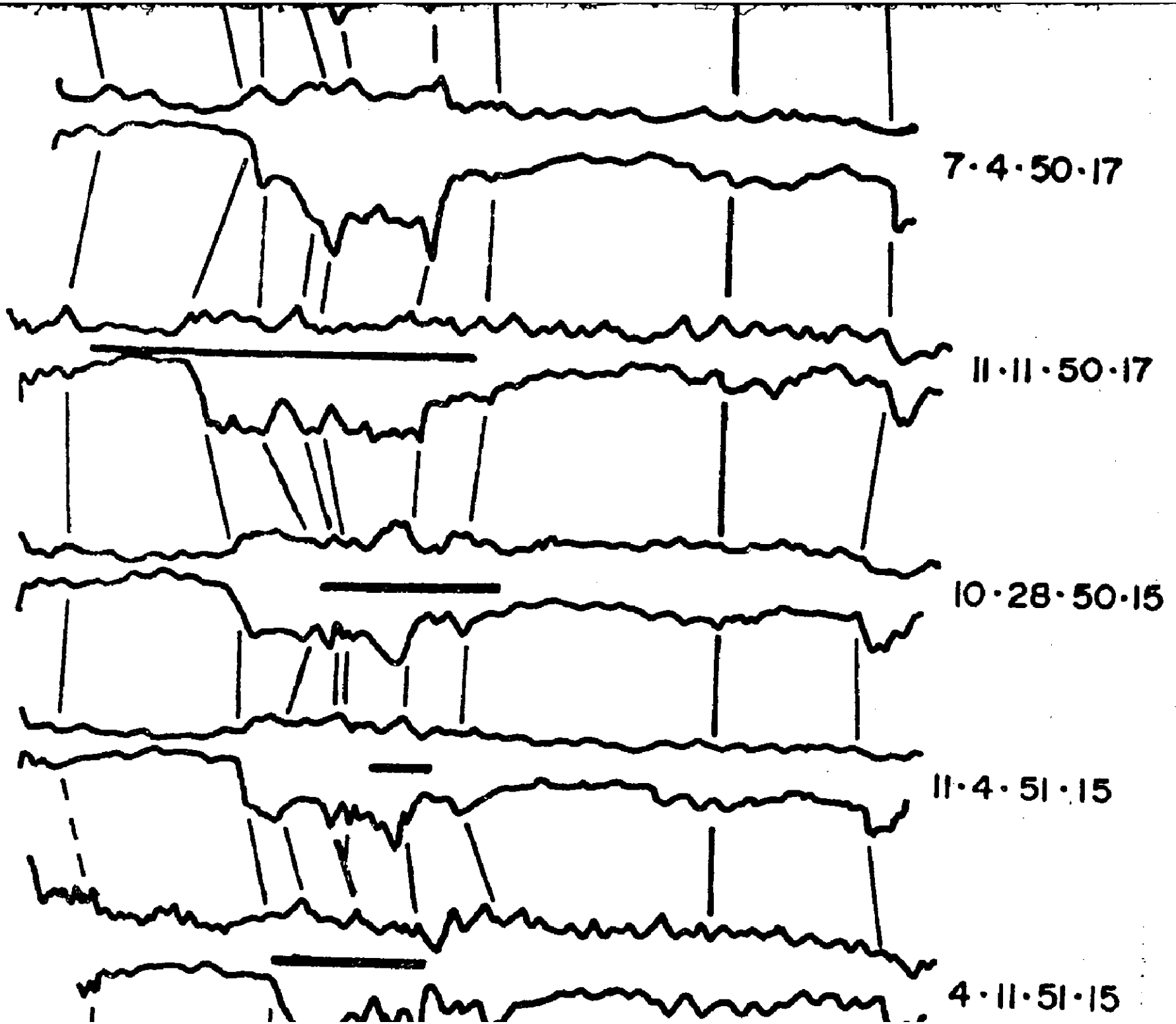
7·4·50·17
11·11·50·17
10·28·50·15
11·4·51·15
4·11·51·15

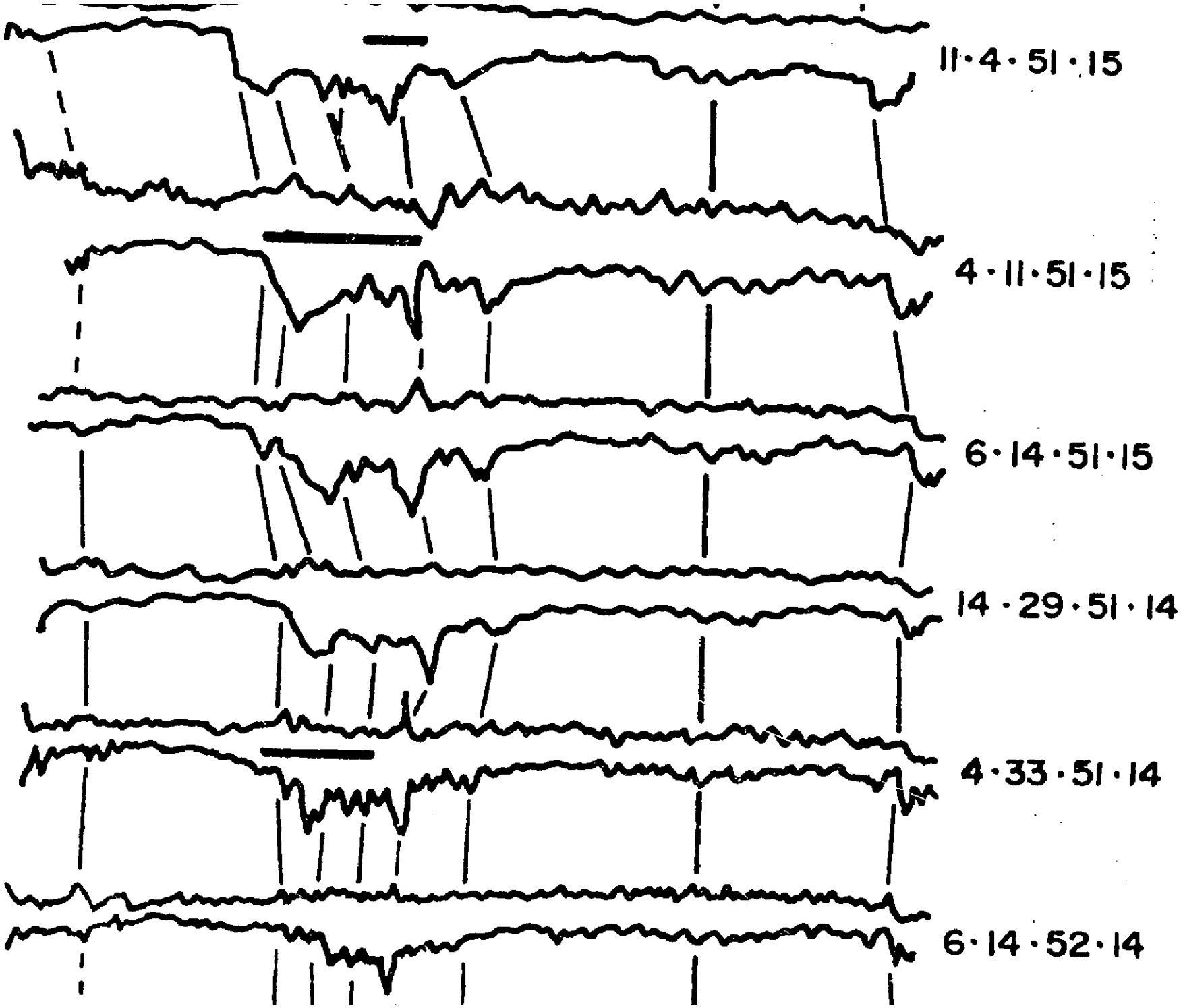
11·4·51·15
4·11·51·15
6·14·51·15
14·29·51·14
4·33·51·14
6·14·52·14

4·33·51·14
6·14·52·14
6·31·52·13
6·8·53·13
6·29·53·12
a
b
c
α
β
γ
δ
ε
D
NE

E-E´ SUMMARY SECTION

CORE

50' || 15 m

NO HORIZONTAL SCALE

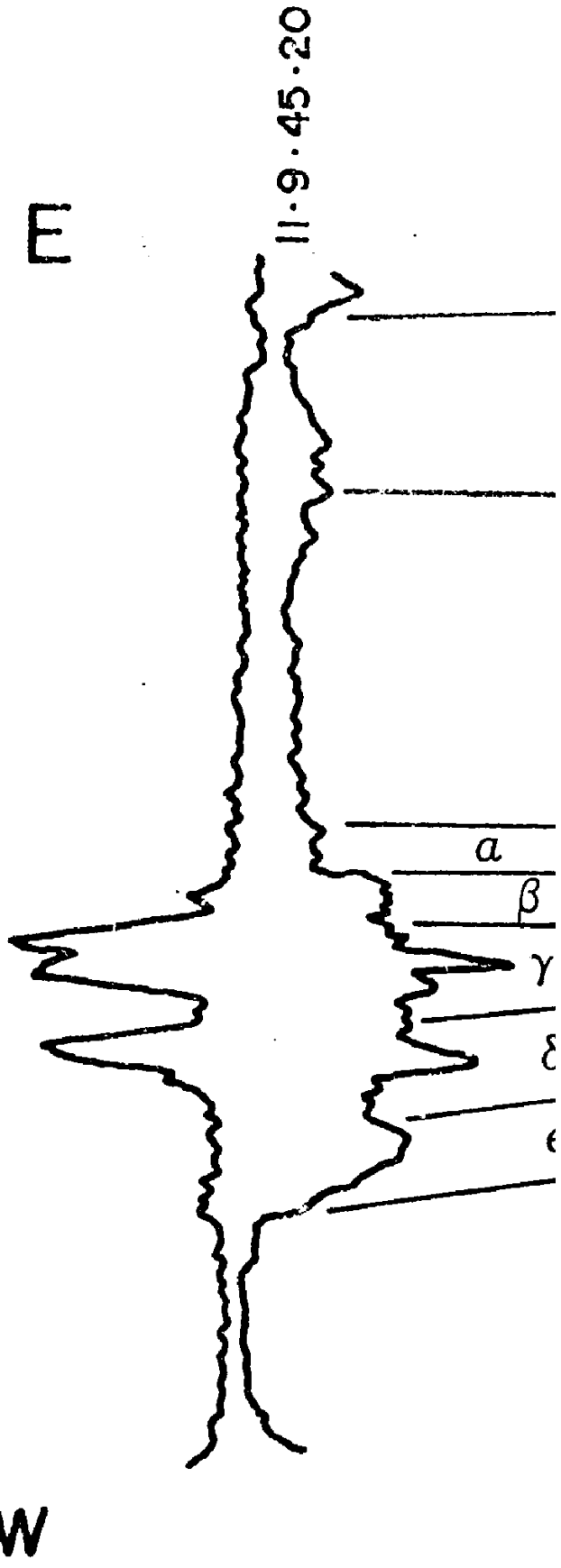

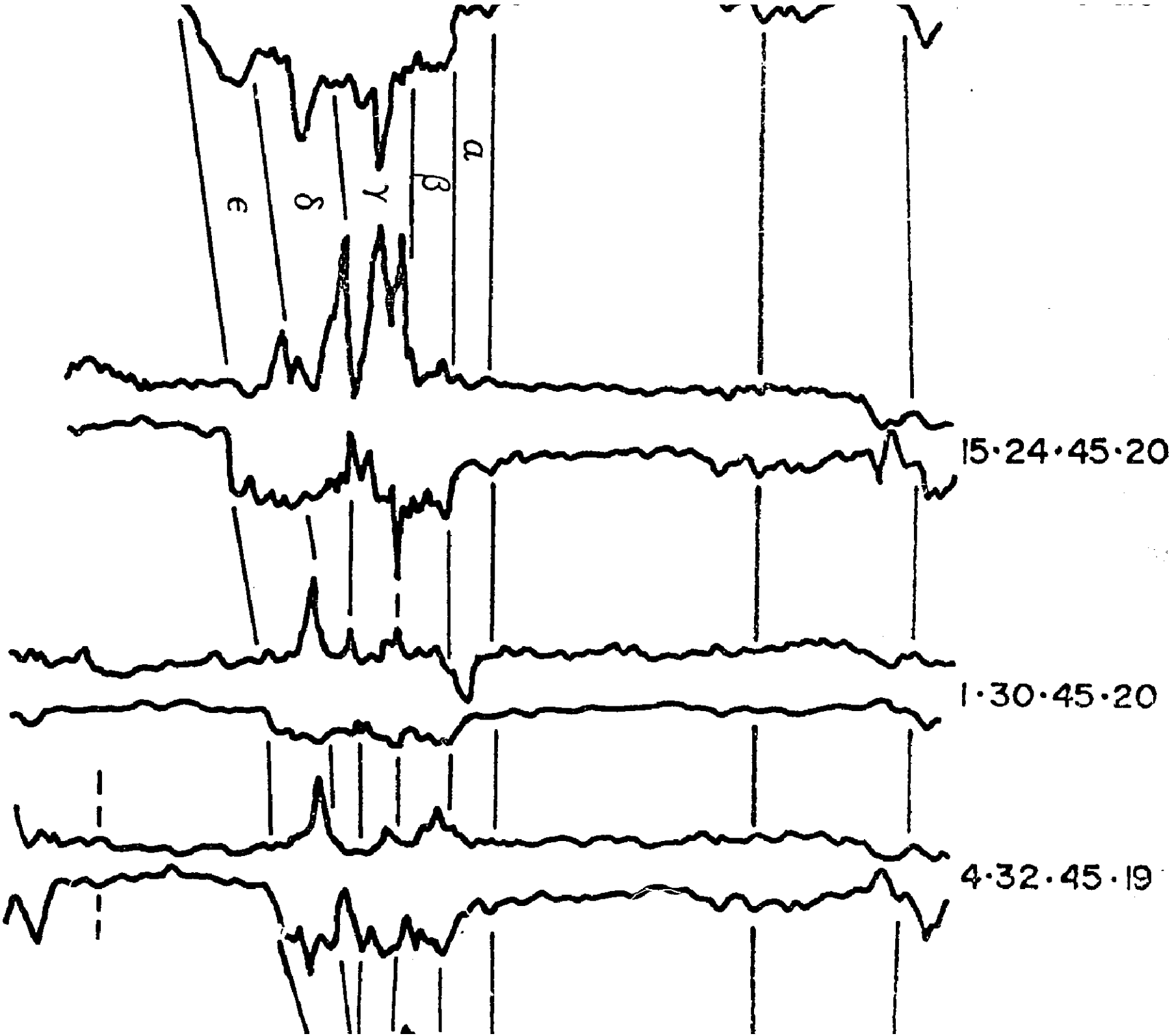
ε
δ
γ
β
α
15·24·45·20
1·30·45·20
4·32·45·19


4·32·45·19
4·34·45·19
7·34·45·19
6·35·45·19
3·36·45·19

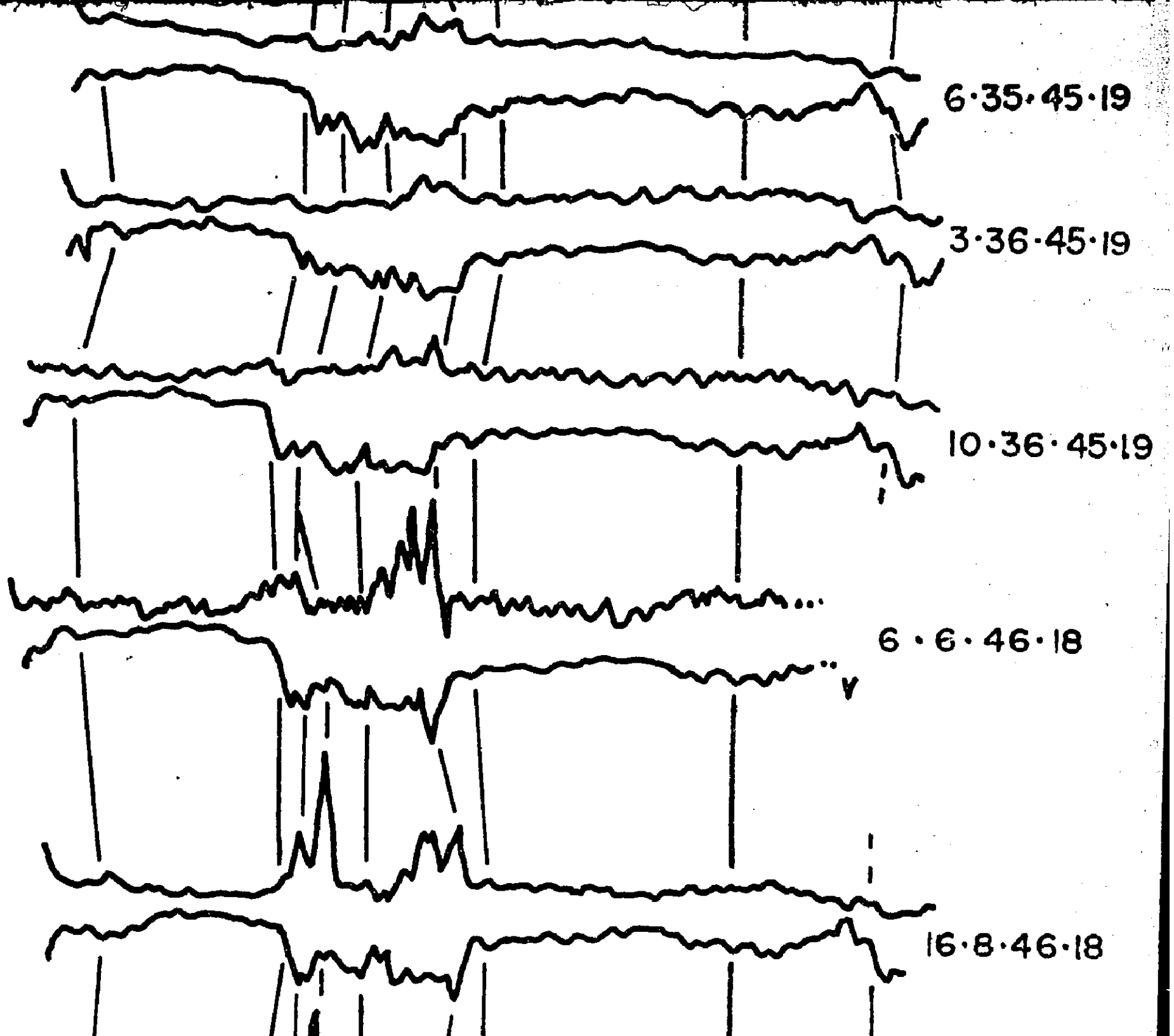
6·35·45·19
3·36·45·19
10·36·45·19
6·6·46·18
16·8·46·18

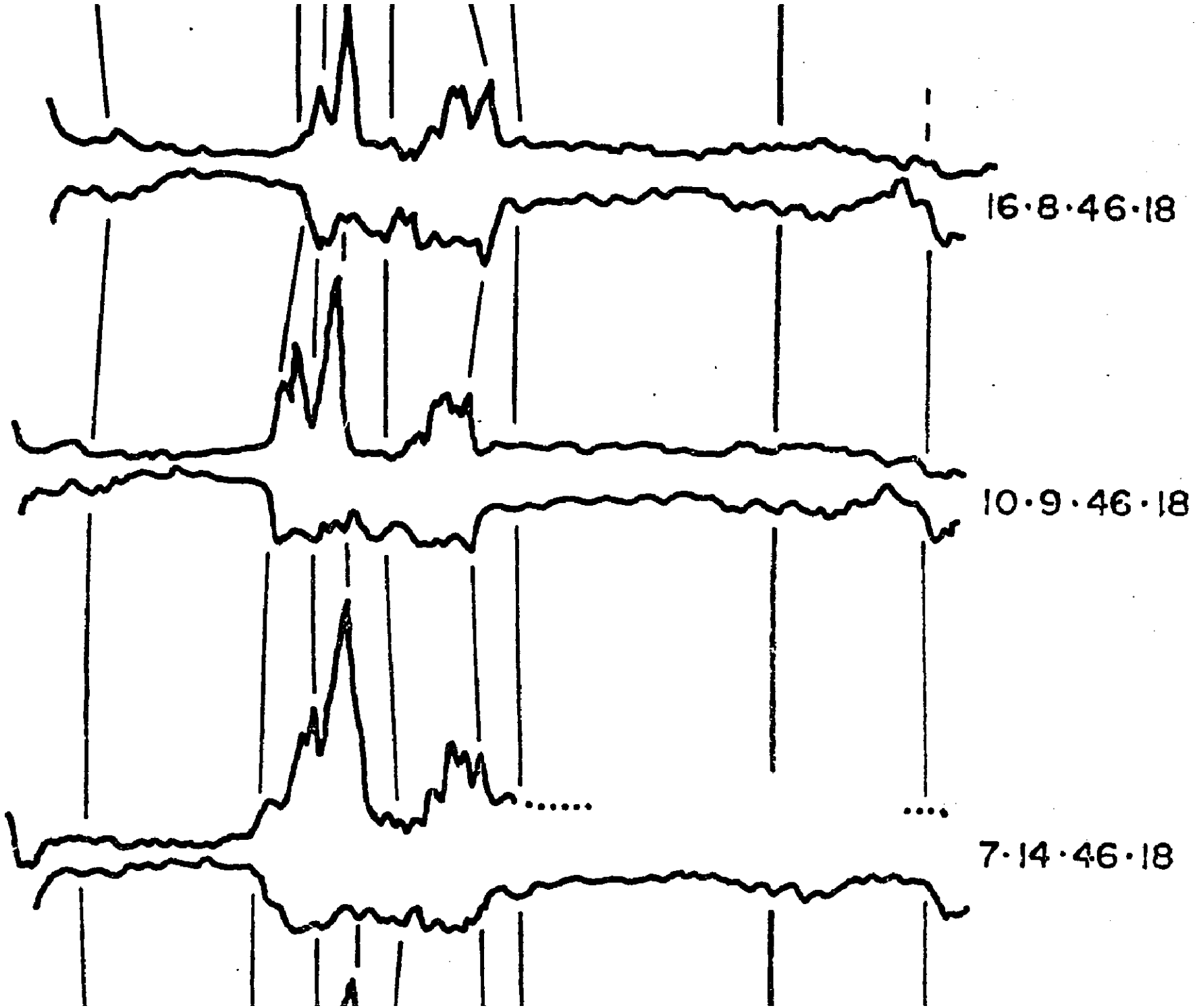
16·8·46·18
10·9·46·18
7·14·46·18

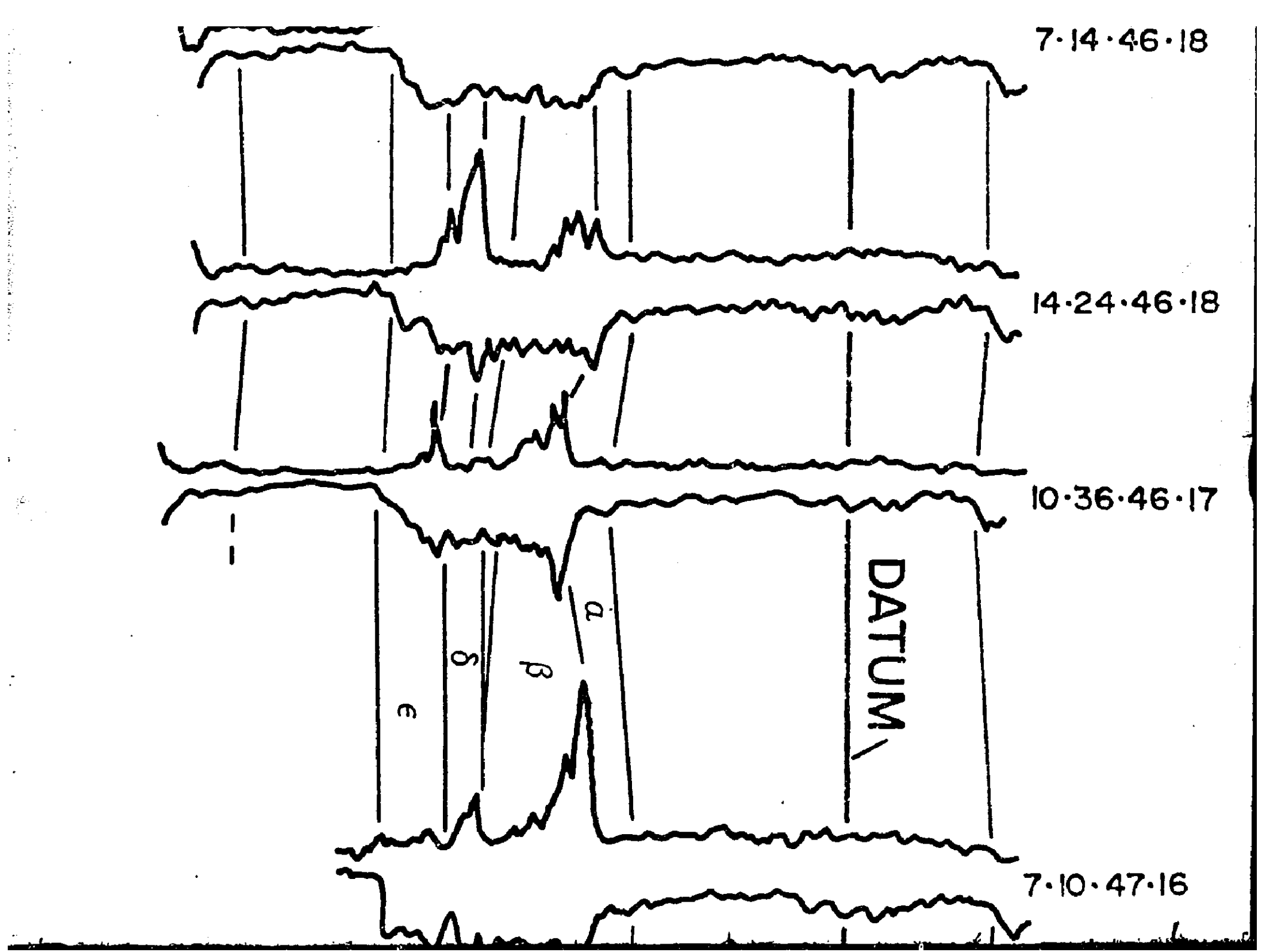
7·14·46·18
14·24·46·18
10·36·46·17
DATUM
α
β
δ
ε
7·10·47·16

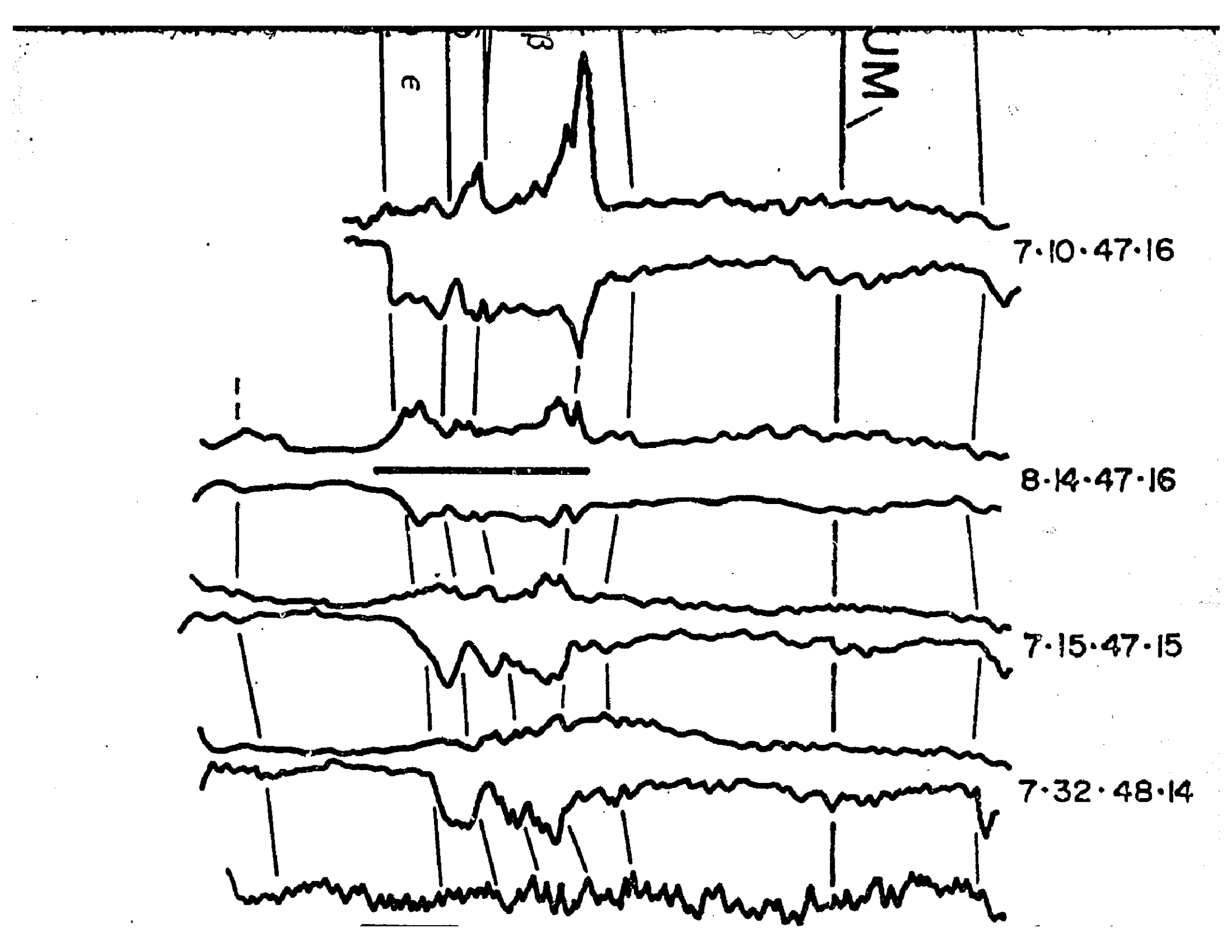
UM
7·10·47·16
8·14·47·16
7·15·47·15
7·32·48·14

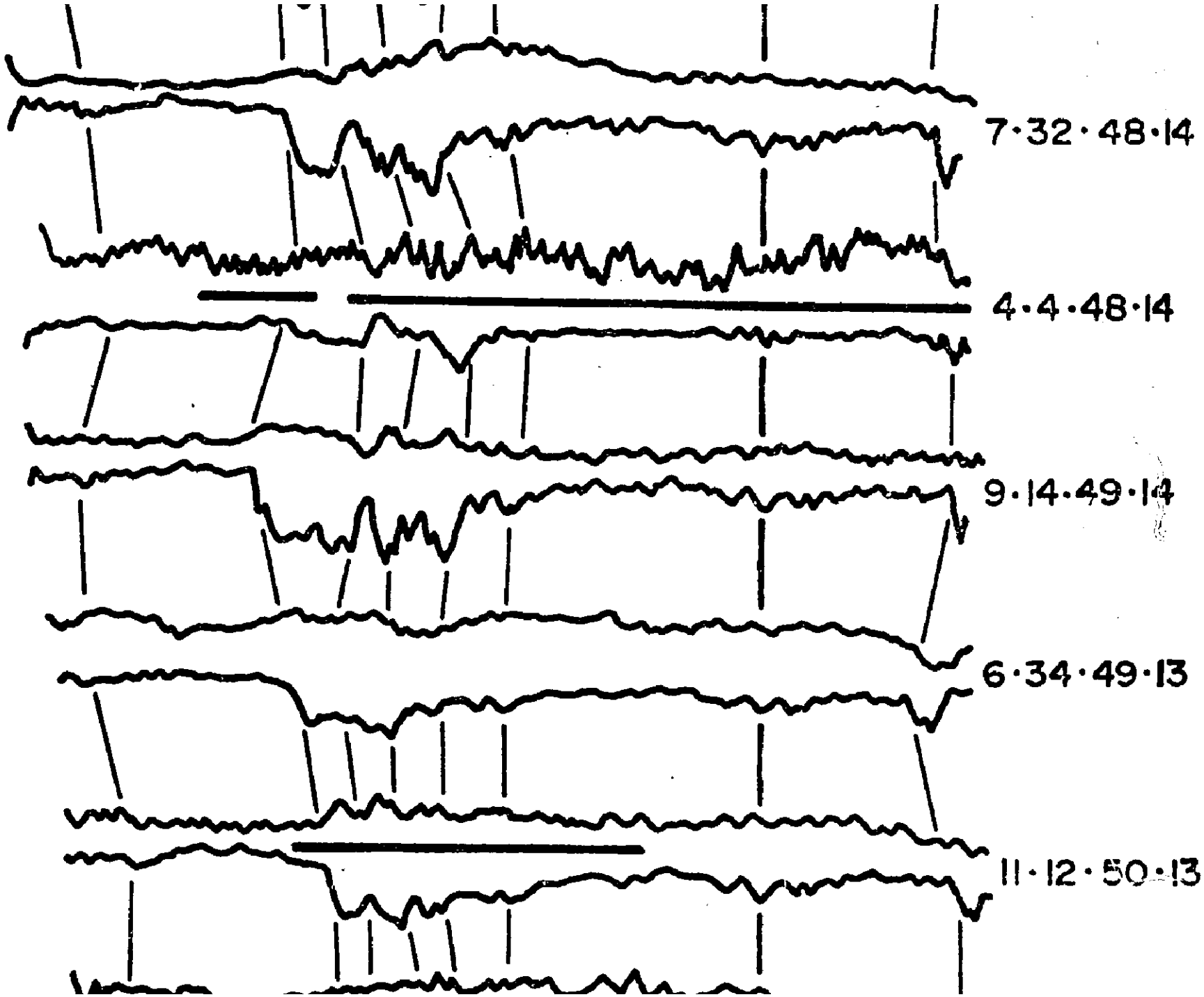
7·32·48·14
4·4·48·14
9·14·49·14
6·34·49·13
11·12·50·13

11-12-50-13
11-11-51-12
11-10-51-11
16-25-51-11
a'
b
c
E'
NE

F

F – F′

SUMMARY SECTION

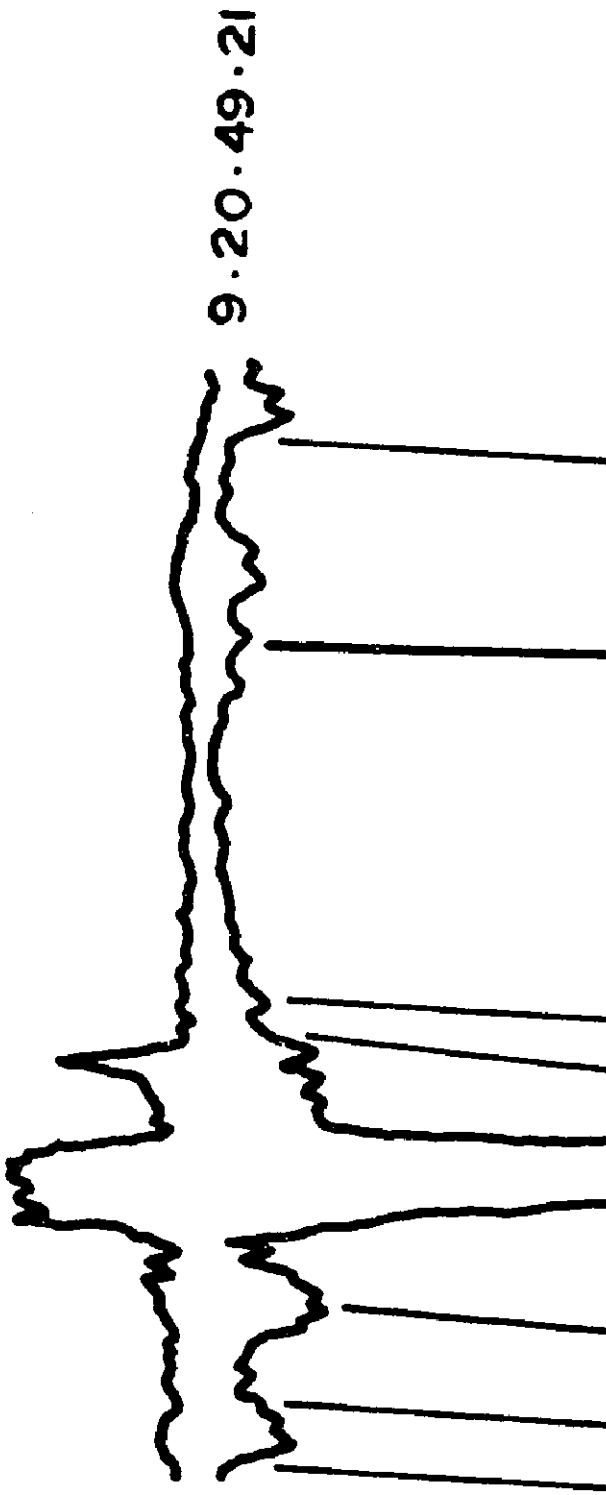

50' 15m

NO HORIZONTAL SCALE

CORE

NW

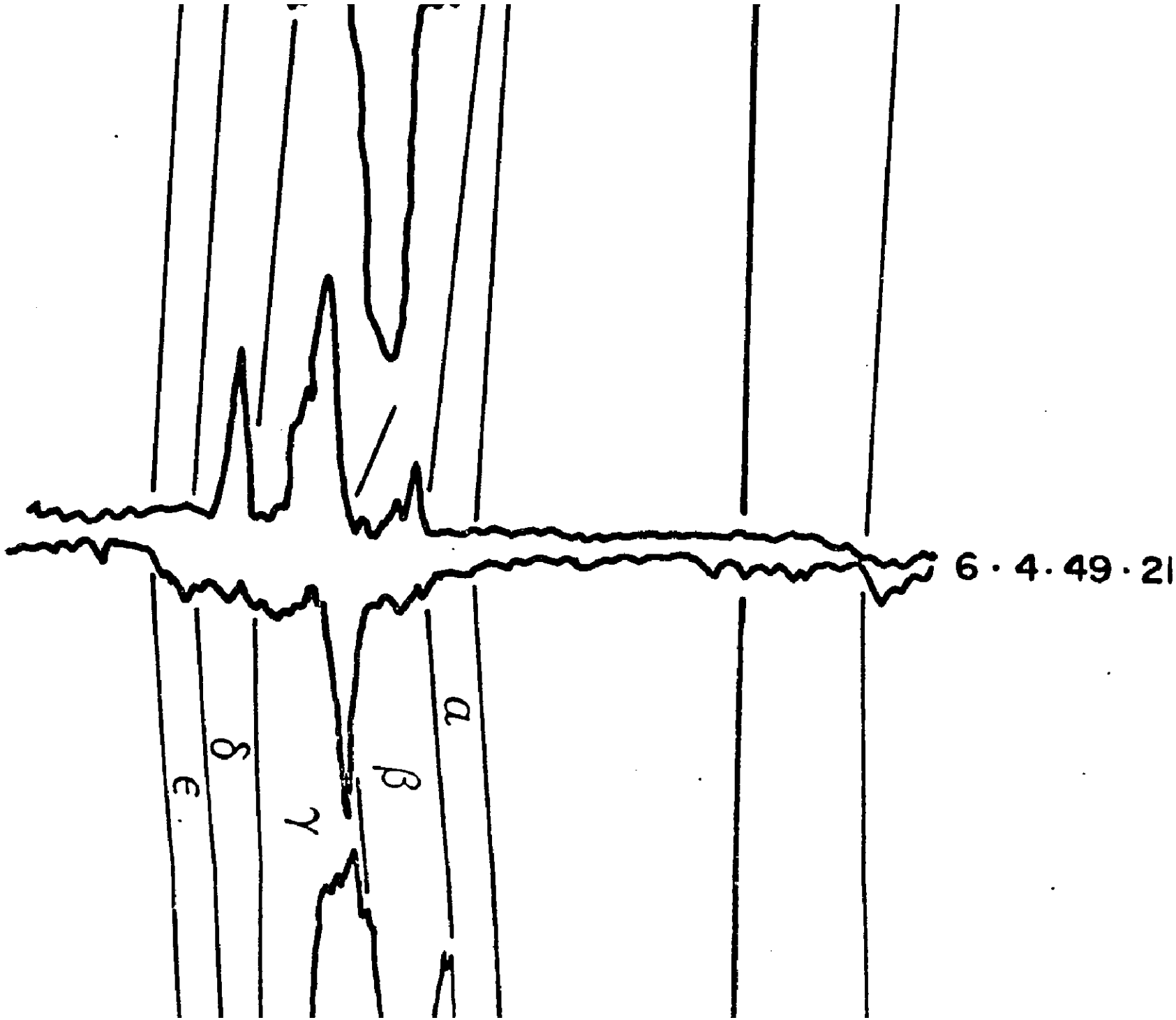
6 · 4 · 49 · 21
ε
δ
γ
β
α

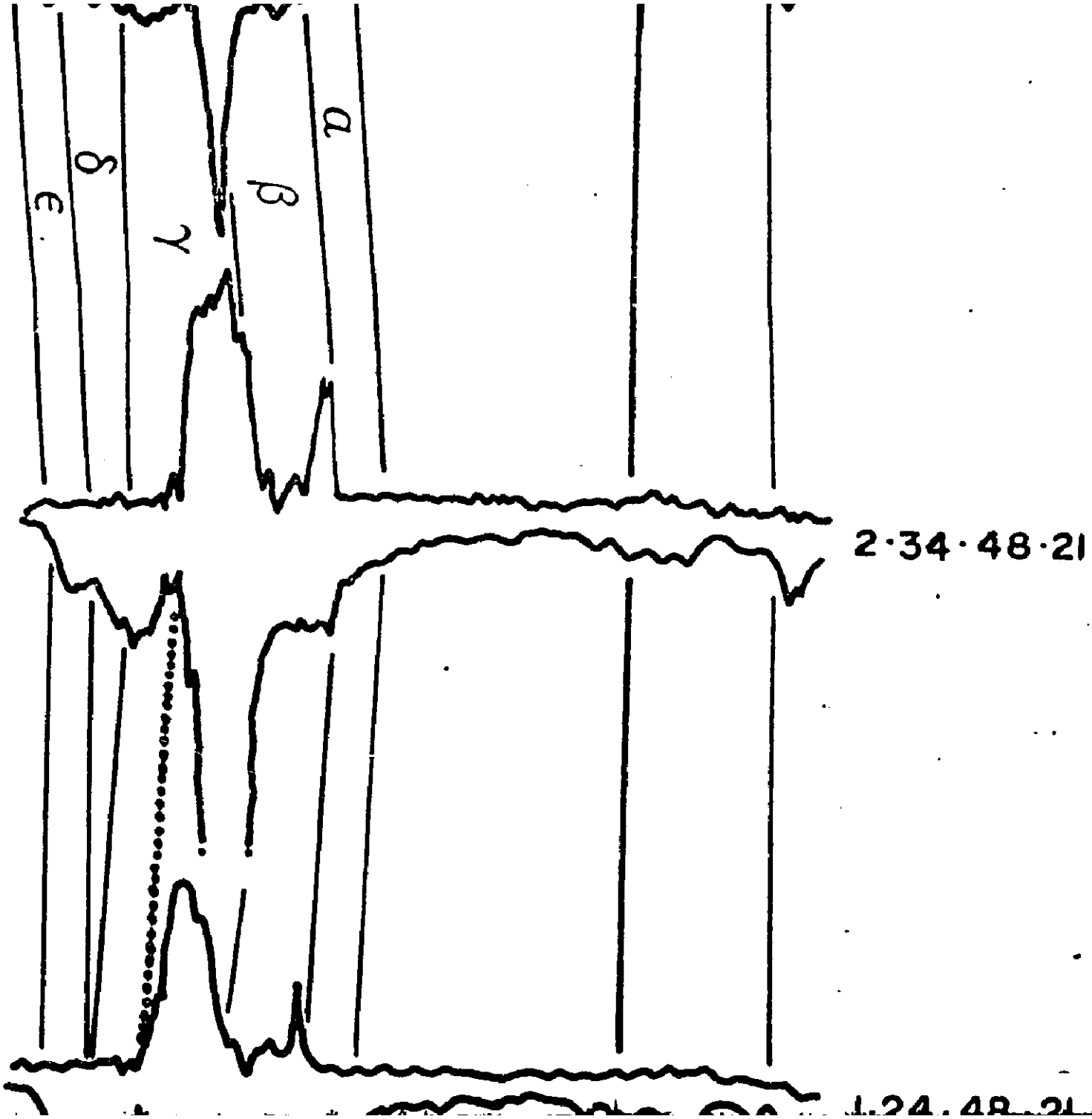
ε
δ
γ
β
α
2·34·48·21
1·24·48·21

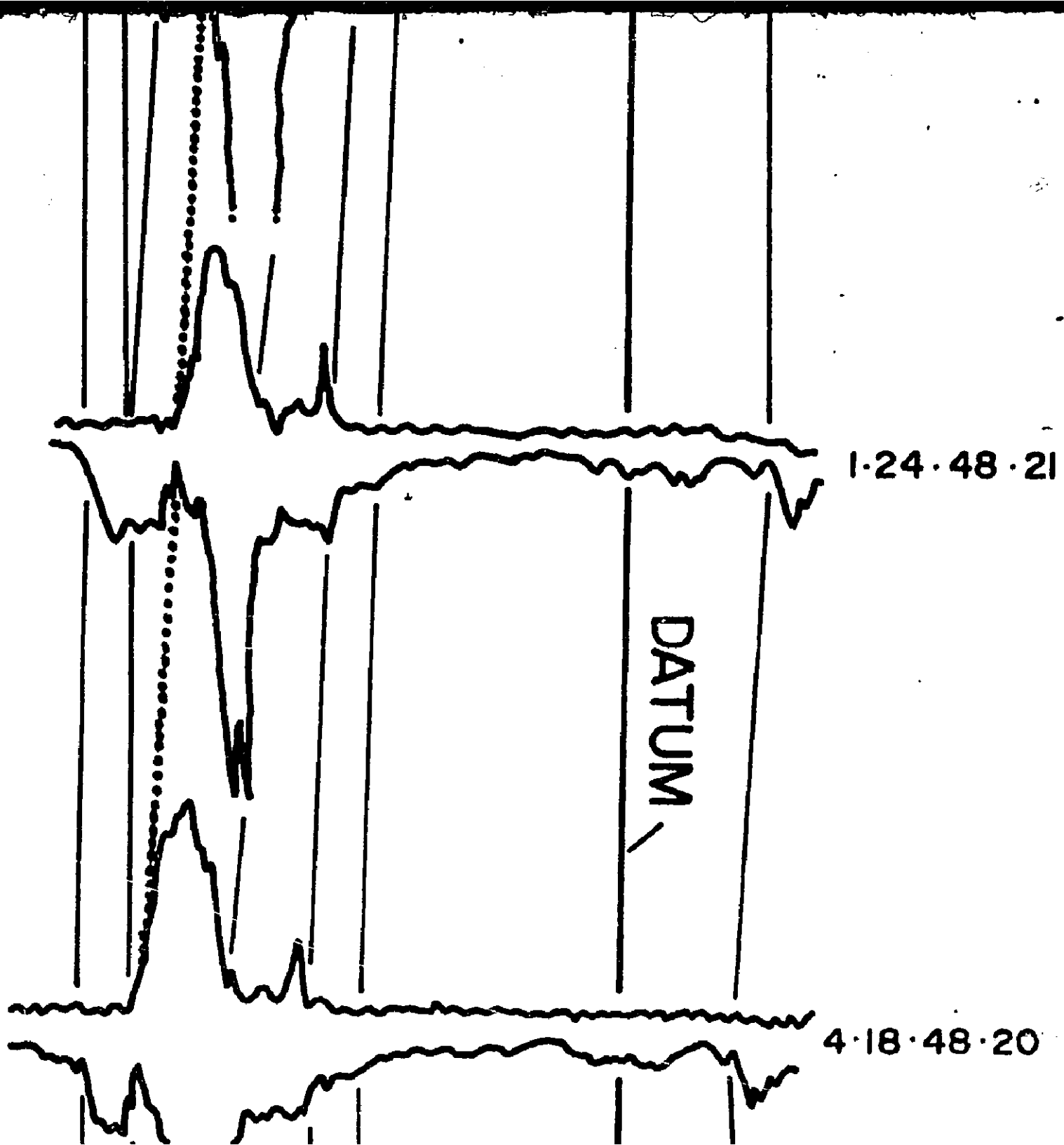
1·24·48·21
DATUM
4·18·48·20

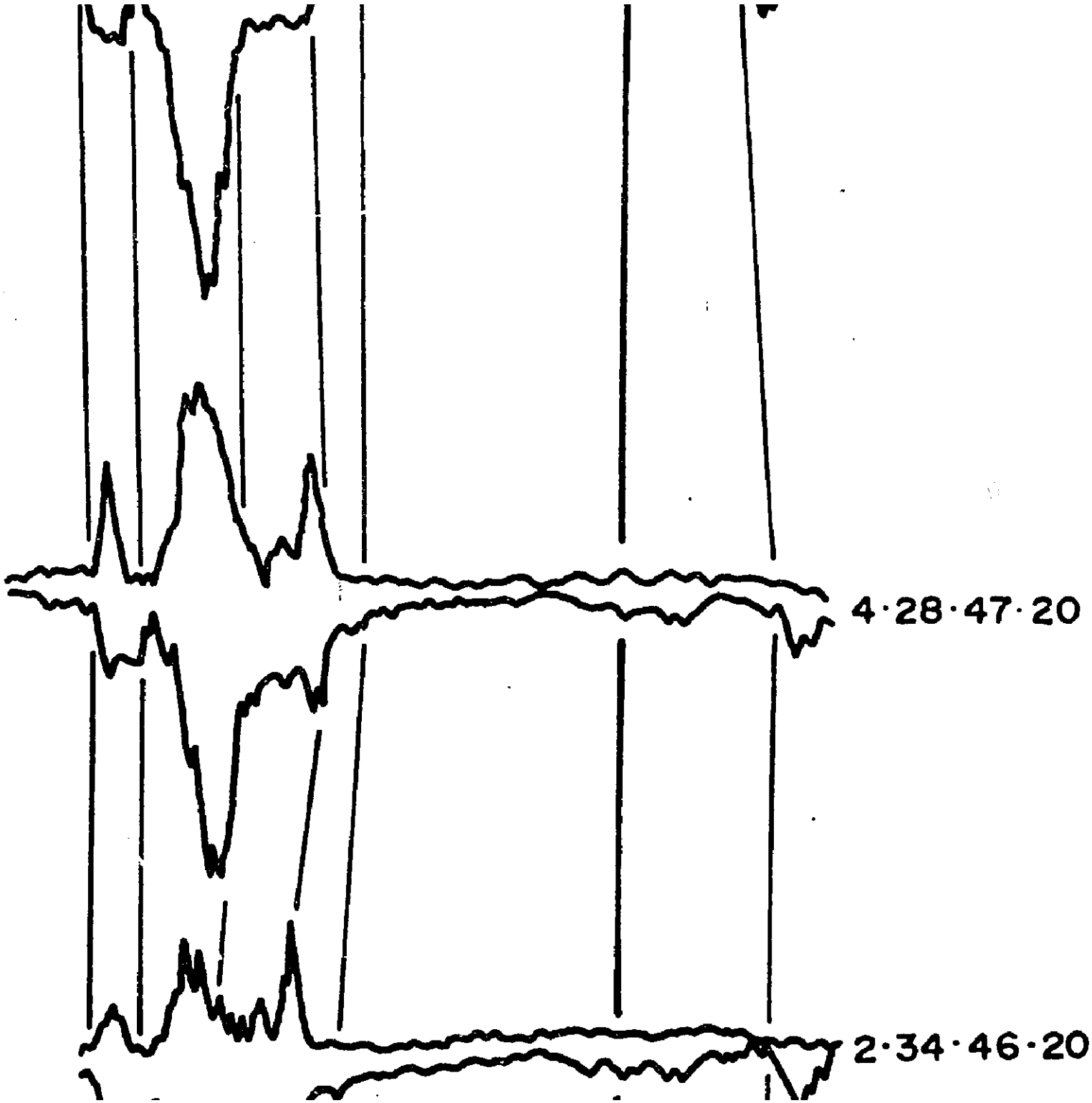
4·28·47·20
2·34·46·20

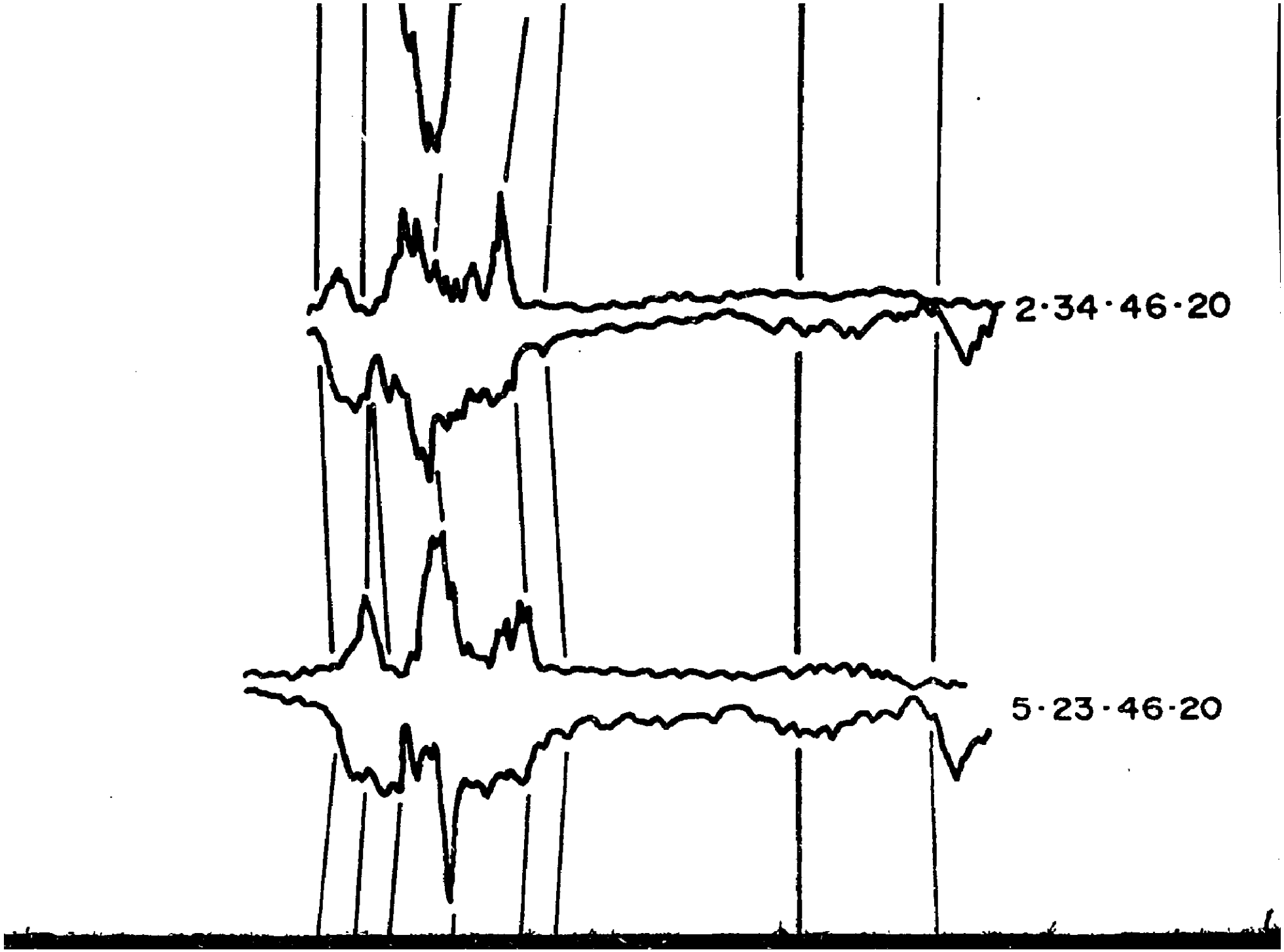
2·34·46·20
5·23·46·20

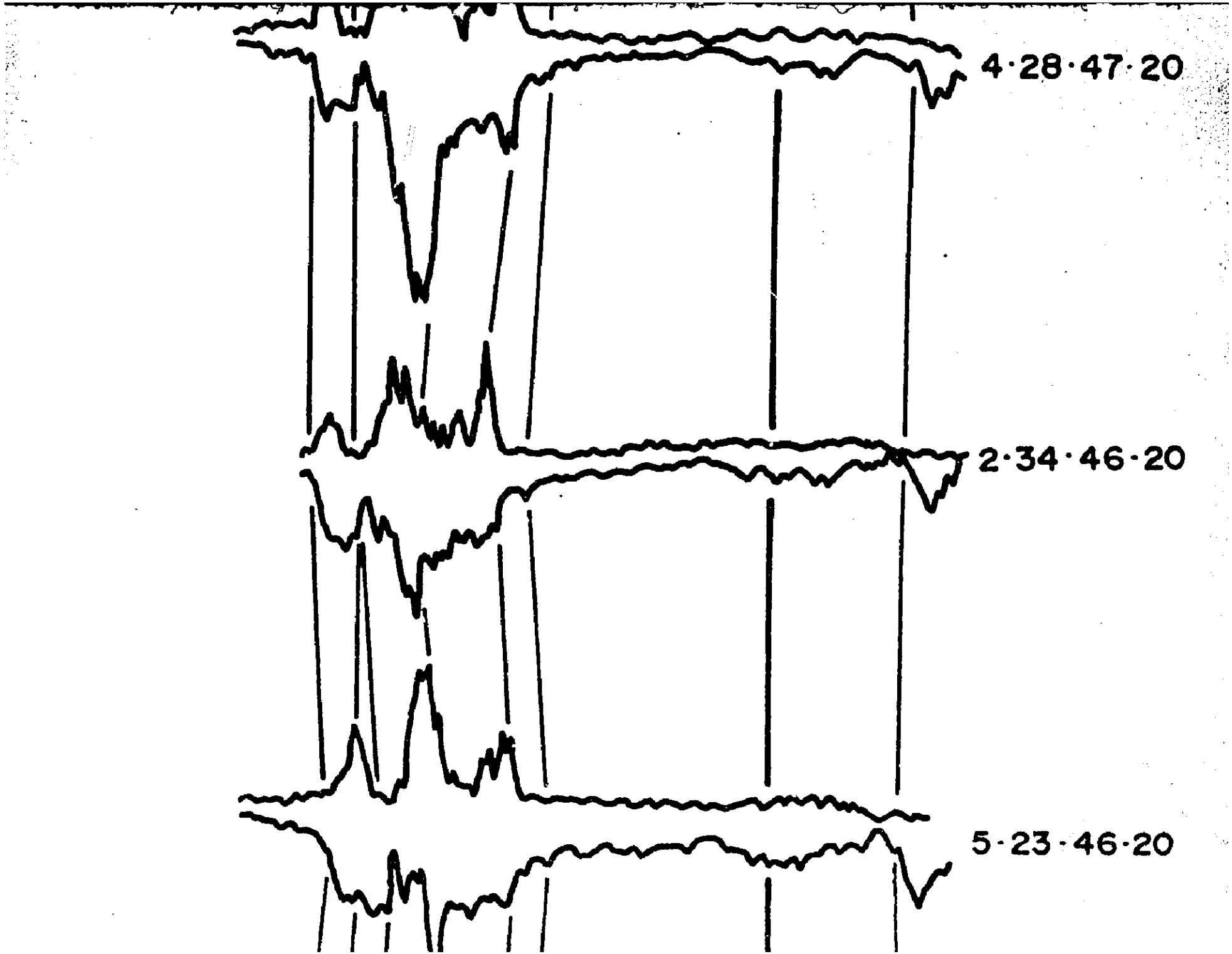
4·28·47·20
2·34·46·20
5·23·46·20

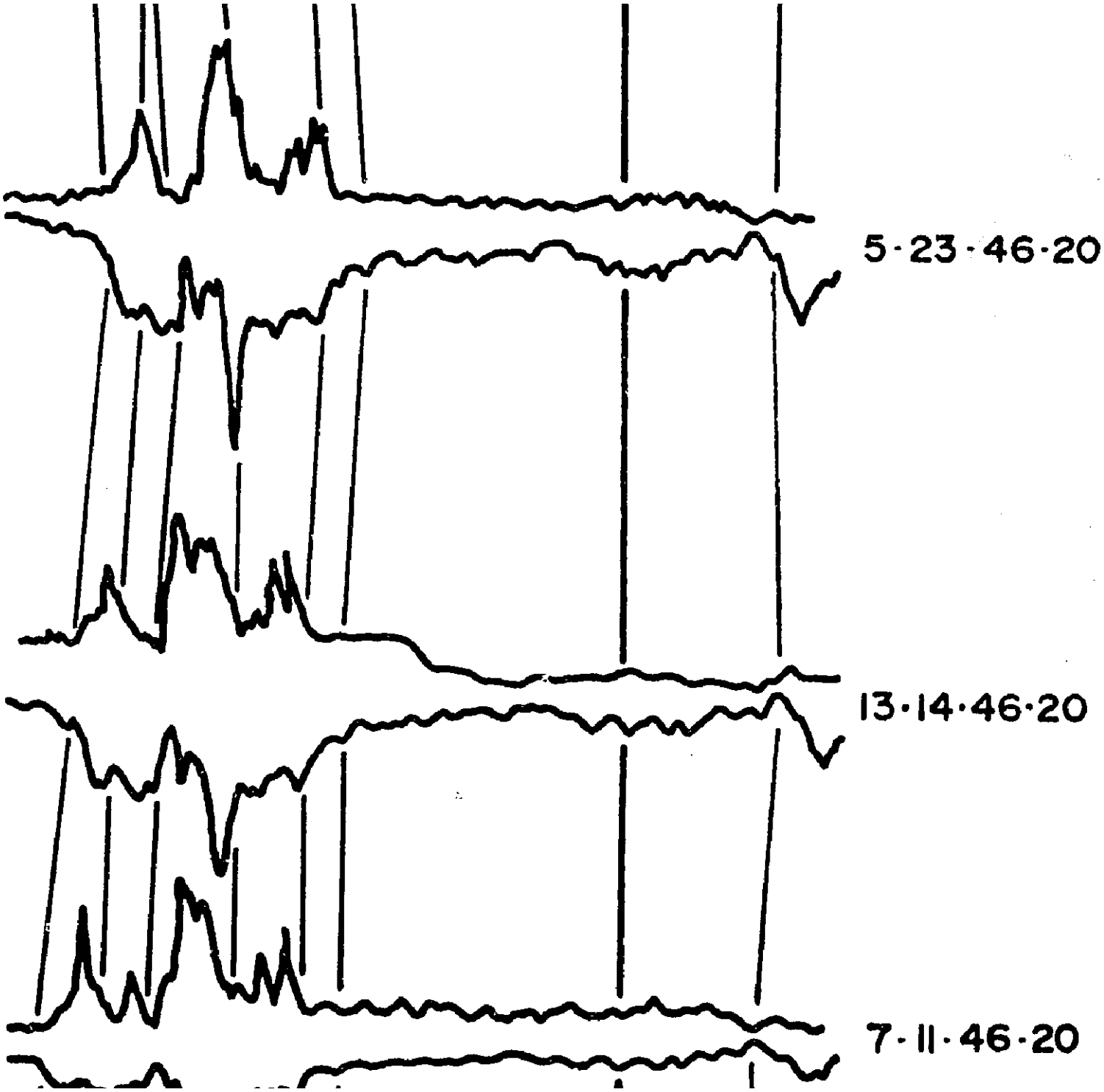
5-23-46-20
13-14-46-20
7-11-46-20

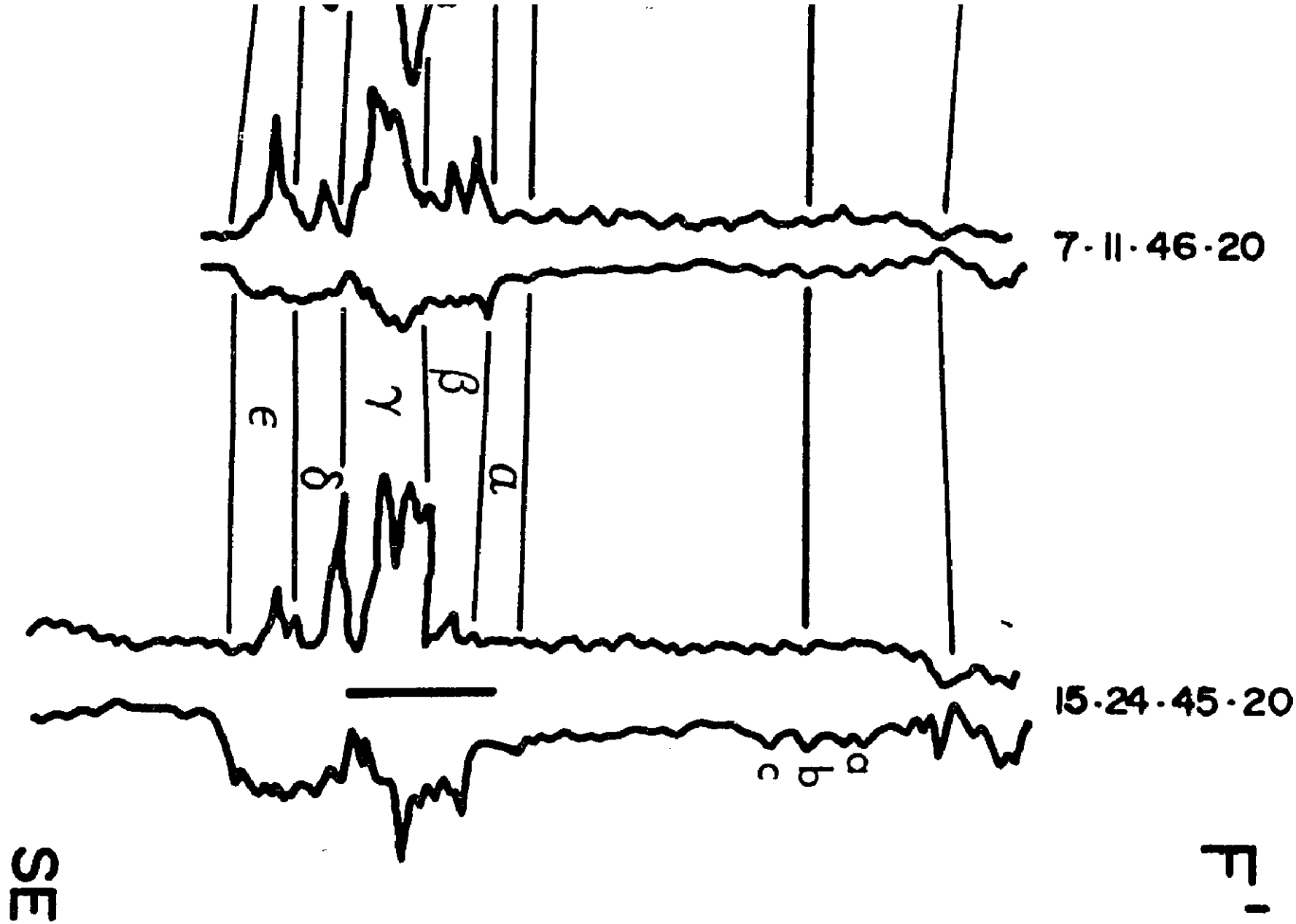
7·11·46·20
15·24·45·20
ε
δ
γ
β
α
c
b
a
SE

G - G'
SUMMARY SECTION

CORE

50' || 15m

NO HORIZONTAL SCALE

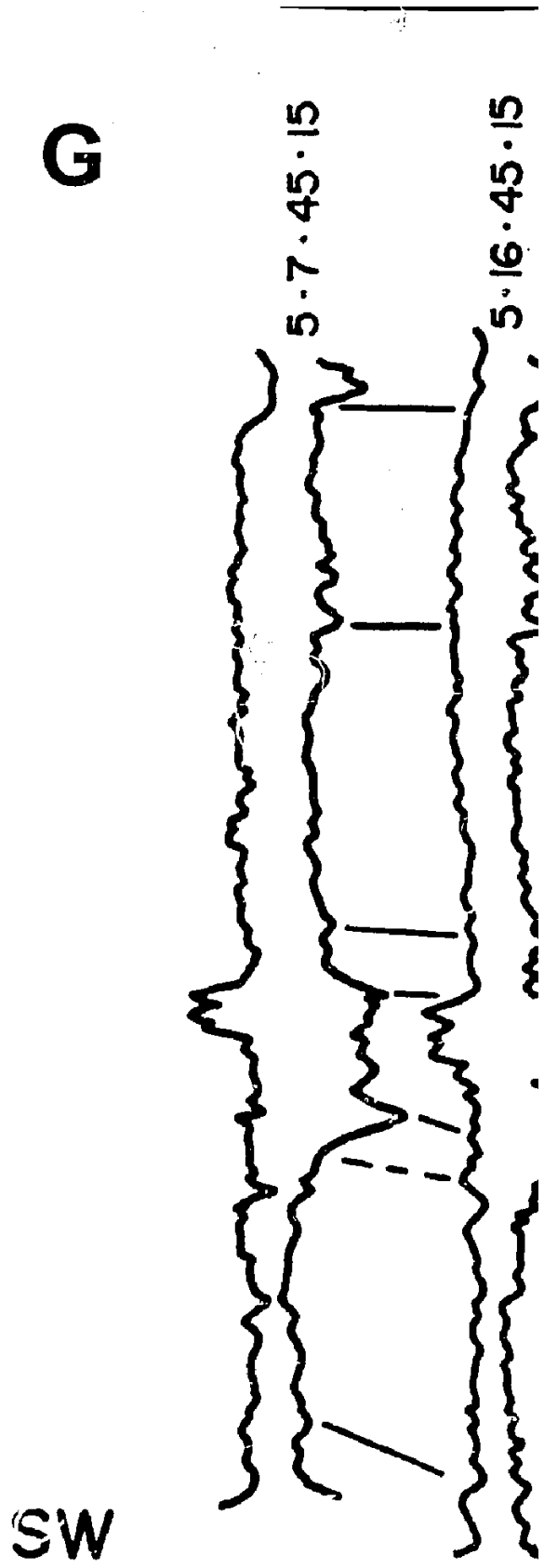

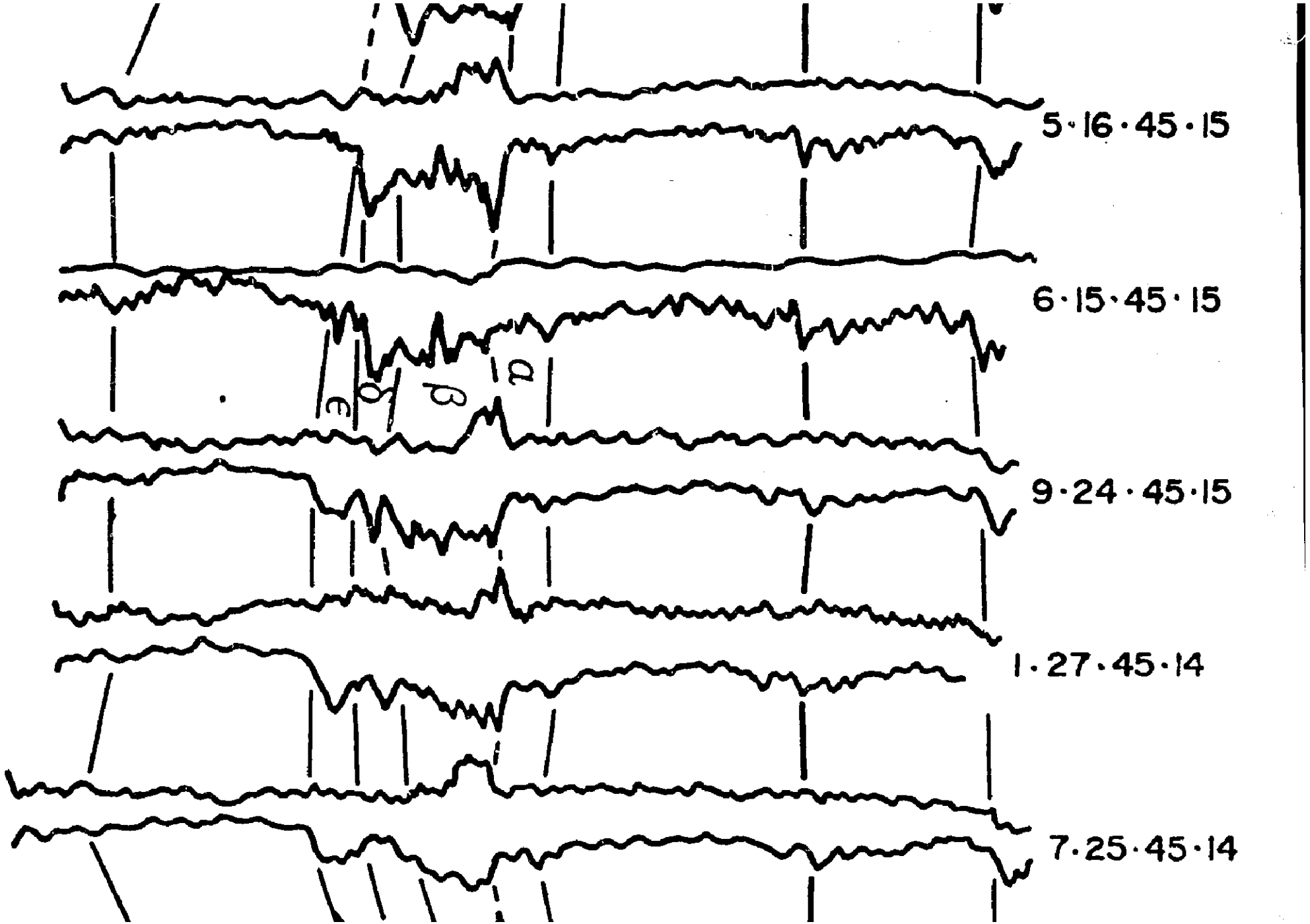
5·16·45·15
6·15·45·15
9·24·45·15
1·27·45·14
7·25·45·14
a
β
γ
δ
ε

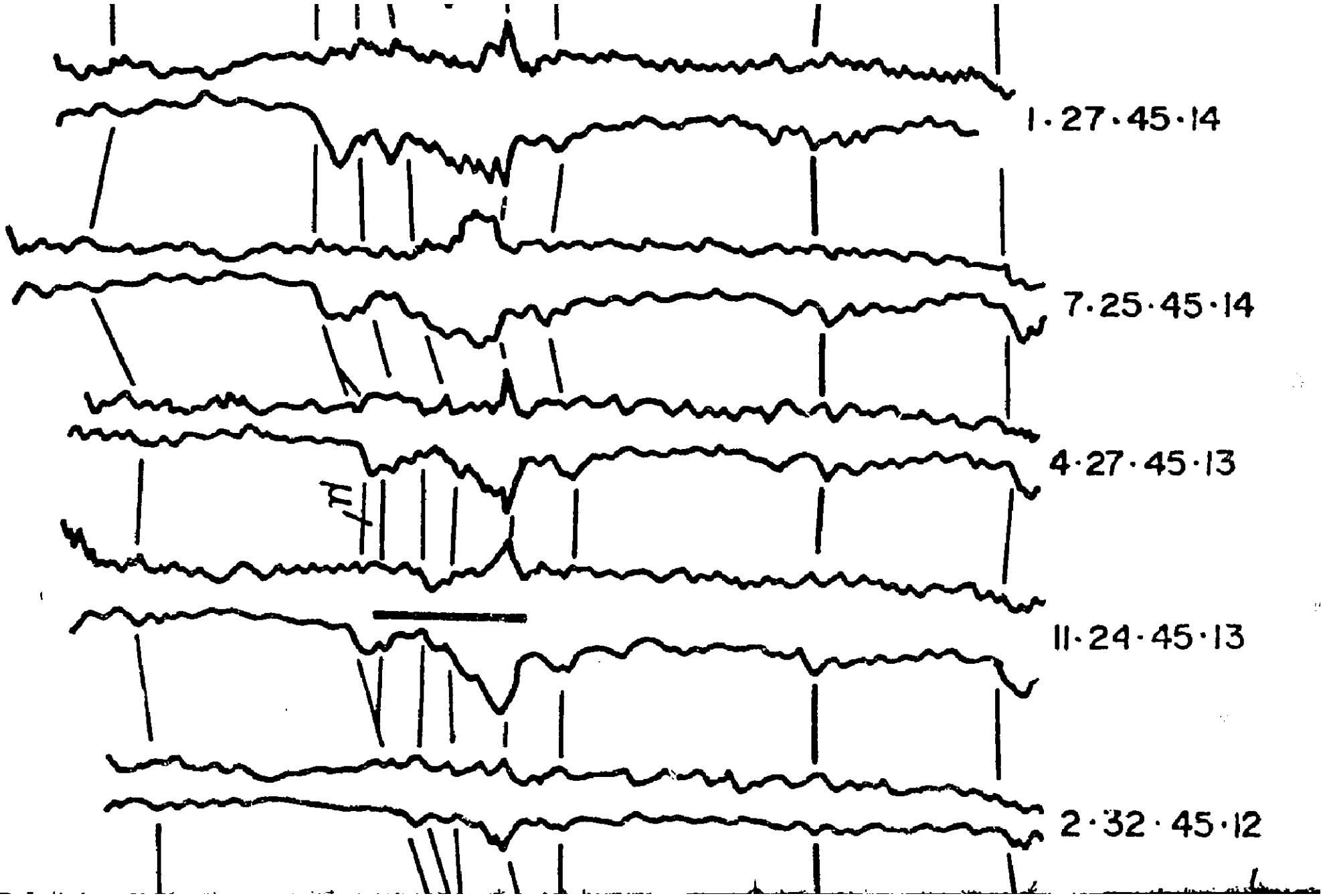
1·27·45·14
7·25·45·14
4·27·45·13
11·24·45·13
2·32·45·12

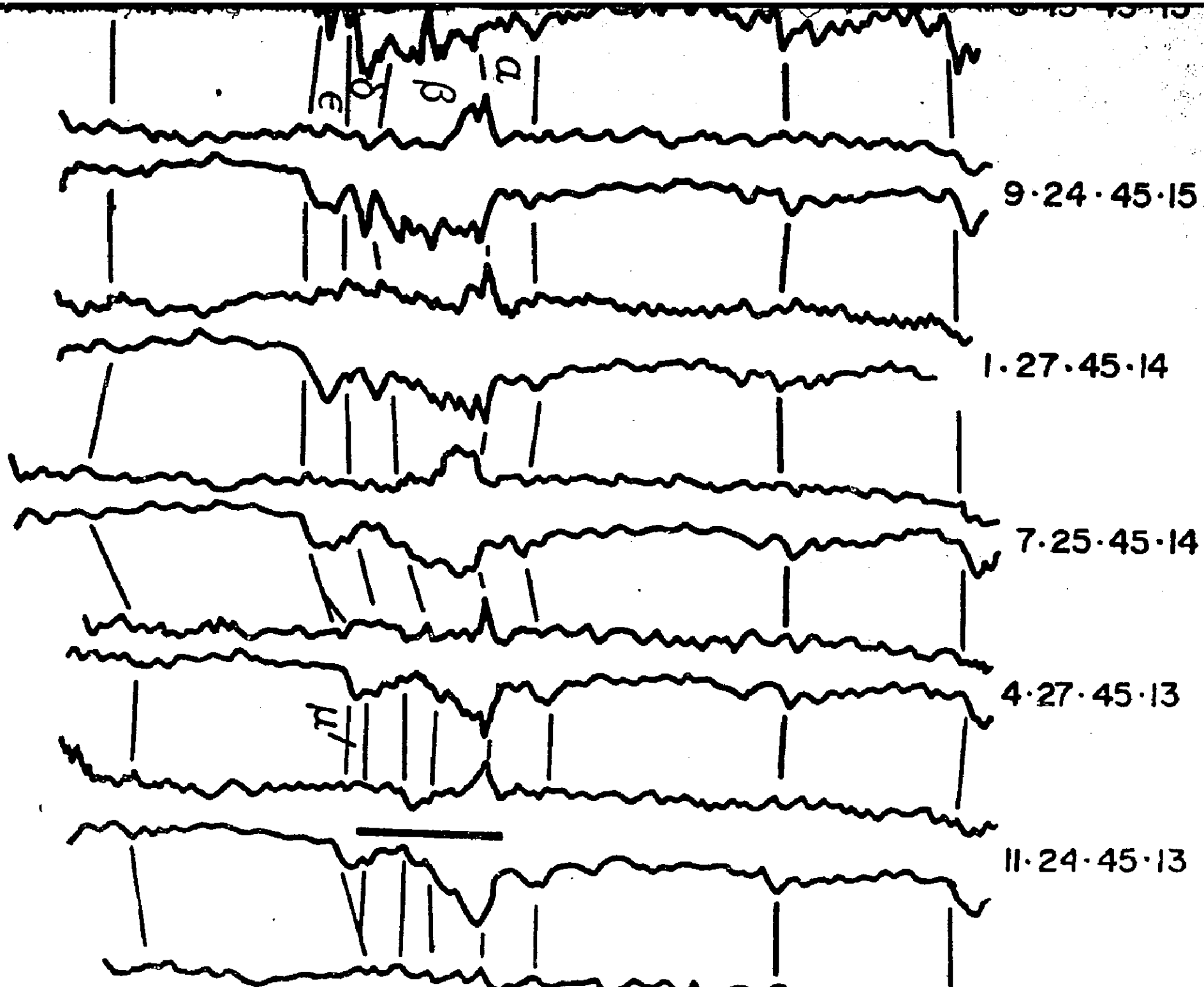
ε
δ
β
a
9·24·45·15
1·27·45·14
7·25·45·14
4·27·45·13
11·24·45·13

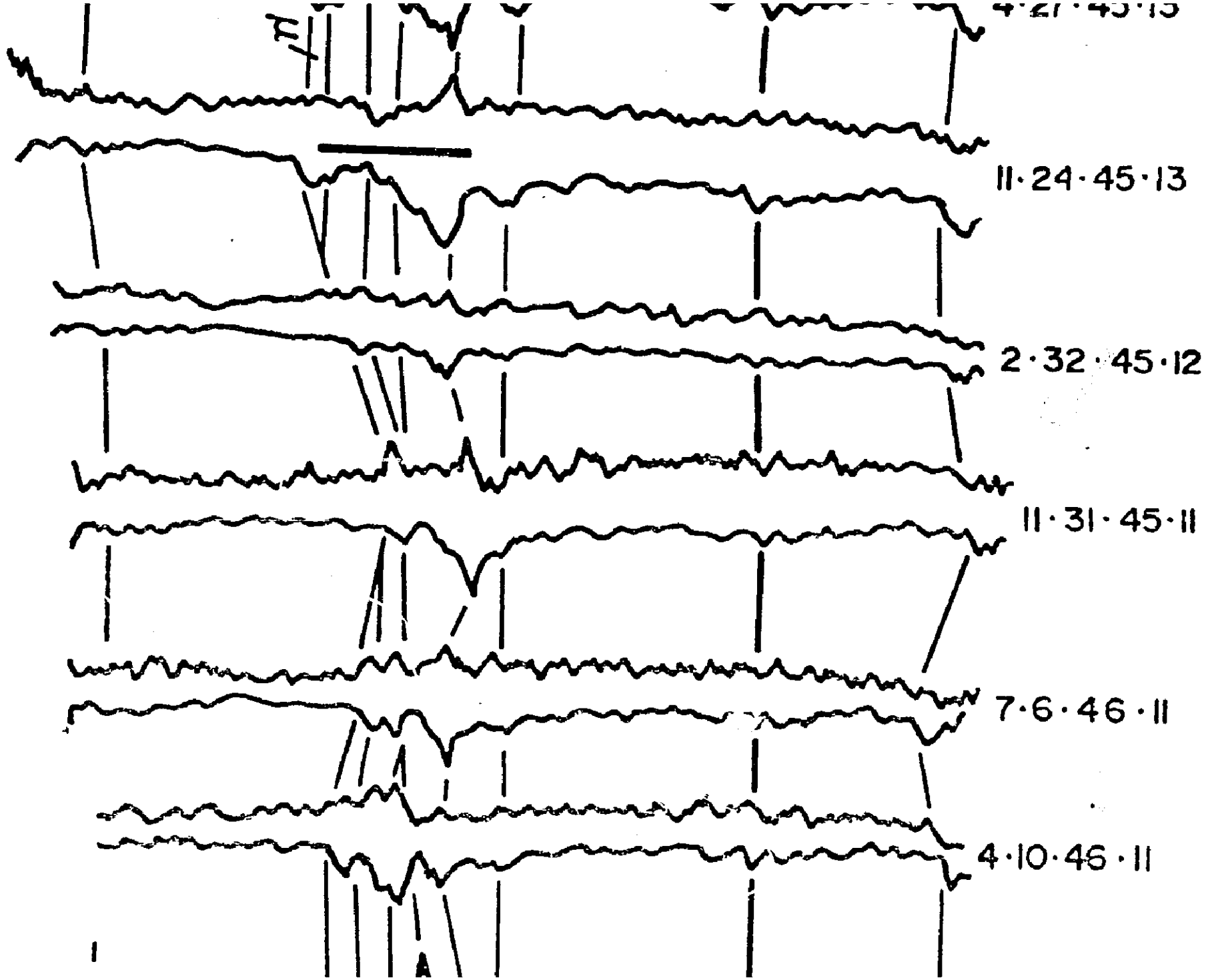
11·24·45·13
2·32·45·12
11·31·45·11
7·6·46·11
4·10·46·11

G'
7·6·46·11
4·10·46·11
7·18·46·10
4·35·46·10
DATUM
a
b
c
α
β
δ
ϵ
μ
NE